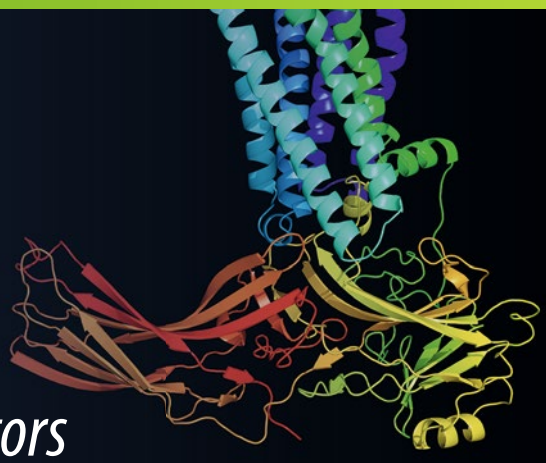
Methods in Molecular Biology 1957

Springer Protocols



Mark G. H. Scott
Stéphane A. Laporte *Editors*

Beta-Arrestins

Methods and Protocols

Humana Press

METHODS IN MOLECULAR BIOLOGY

Series Editor
John M. Walker
School of Life and Medical Sciences
University of Hertfordshire
Hatfield, Hertfordshire, AL10 9AB, UK

For further volumes:
http://www.springer.com/series/7651

Beta-Arrestins

Methods and Protocols

Edited by

Mark G. H. Scott

Institut Cochin, INSERM U1016, Paris, France

CNRS, UMR8104, Paris, France

Université Paris Descartes, Sorbonne Paris Cité, Paris, France

Stéphane A. Laporte

Department of Medicine, Research Institute of the McGill University Health Center (RI-MUHC), McGill University, Montreal, QC, Canada

Department of Pharmacology and Therapeutics, McGill University, Montréal, QC, Canada

Department of Anatomy and Cell Biology, McGill University, Montréal, QC, Canada

RI-MUHC/Glen Site, Montréal, QC, Canada

Humana Press

Editors
Mark G. H. Scott
Institut Cochin
INSERM U1016
Paris, France

CNRS, UMR8104
Paris, France

Université Paris Descartes,
Sorbonne Paris Cité
Paris, France

Stéphane A. Laporte
Department of Medicine, Research Institute of the McGill
University Health Center (RI-MUHC)
McGill University
Montreal, QC, Canada

Department of Pharmacology and Therapeutics
McGill University
Montréal, QC, Canada

Department of Anatomy and Cell Biology
McGill University
Montréal, QC, Canada

RI-MUHC/Glen Site
Montréal, QC, Canada

ISSN 1064-3745 ISSN 1940-6029 (electronic)
Methods in Molecular Biology
ISBN 978-1-4939-9157-0 ISBN 978-1-4939-9158-7 (eBook)
https://doi.org/10.1007/978-1-4939-9158-7

Library of Congress Control Number: 2019935574

© Springer Science+Business Media, LLC, part of Springer Nature 2019
This work is subject to copyright. All rights are reserved by the Publisher, whether the whole or part of the material is concerned, specifically the rights of translation, reprinting, reuse of illustrations, recitation, broadcasting, reproduction on microfilms or in any other physical way, and transmission or information storage and retrieval, electronic adaptation, computer software, or by similar or dissimilar methodology now known or hereafter developed.
The use of general descriptive names, registered names, trademarks, service marks, etc. in this publication does not imply, even in the absence of a specific statement, that such names are exempt from the relevant protective laws and regulations and therefore free for general use.
The publisher, the authors, and the editors are safe to assume that the advice and information in this book are believed to be true and accurate at the date of publication. Neither the publisher nor the authors or the editors give a warranty, express or implied, with respect to the material contained herein or for any errors or omissions that may have been made. The publisher remains neutral with regard to jurisdictional claims in published maps and institutional affiliations.

Cover Caption: This image represents the homology model of AT1R/β-arrestin complex based on the Rhodopsin-arrestin crystal structure (5W0P). This model was graciously provided by Dr. Laporte's student Aaron Cho.

This Humana Press imprint is published by the registered company Springer Science+Business Media, LLC, part of Springer Nature.
The registered company address is: 233 Spring Street, New York, NY 10013, U.S.A.

Preface

The arrestin family is composed of four members: visual arrestin (arrestin-1) and cone arrestin (arrestin-4), which are expressed in the eye, and the ubiquitously expressed β-arrestins (β-arrs), β-arr1 and β-arr2 (also known as arrestin-2 and arrestin-3, respectively). β-arrs were initially appreciated for the roles they play in the desensitization and endocytosis of G protein-coupled receptors (GPCRs), but they are now also known to act as multifunctional adaptor proteins binding many non-receptor protein partners to control a plethora of signalling pathways. β-arrs are therefore key regulators at the crossroads of external cell inputs and functional outputs in cellular processes ranging from gene transcription to cell growth, survival, cytoskeletal regulation, and migration. An increasing number of studies have also highlighted the scaffolding roles β-arrs play in vivo in both physiological and pathological conditions, which open up therapeutic avenues to explore. As our understanding of β-arrs has progressed, multiple new techniques and approaches have been developed to probe β-arr function.

This volume entitled *Beta-Arrestins: Methods and Protocols* provides approaches to study the pleiotropic roles of β-arrs in the control of signal transduction and the subsequent cellular and in vivo consequences that arise. Contributions cover established and cutting-edge techniques to investigate different facets of β-arr function. The chapters are provided in an easy-to-follow format with background information, lists of materials and reagents, step-by-step protocols, and a notes section describing tips and variations on techniques that can be used, as well as potential problems that can arise and how they can be circumvented. A first series of chapters cover various methods, including bioluminescence resonance energy transfer (BRET)-based techniques, to investigate the canonical roles of β-arrs in GPCR regulation and trafficking (Chapters 3–6). A spectrum of methods is next provided to study the scaffolding functions of β-arrs with non-receptor protein partners that influence MAPK activation, cAMP hydrolysis, and cytoskeletal dynamics (Chapters 7–11). In addition, methods to validate β-arr-partner binding interfaces predicted by a docking algorithm (Chapter 12) and methods describing a mathematical framework to dynamically model β-arr-signalling networks (Chapter 13) are included. Methods to perform global proteomic analysis of the β-arr interactome using mass spectrometry are also detailed (Chapter 14). While GPCRs can signal through both G proteins and β-arrs, in some situations, agonists can skew the receptor to preferentially activate one effector in what is termed "ligand bias." A stepwise protocol is provided to analyze bias (Chapter 15). β-arrs have also been shown to play non-canonical roles in the nucleus and in ciliogenesis; methods are furnished to investigate the nucleocytoplasmic trafficking functions of β-arrs (Chapter 16) and to monitor targeting of β-arr2 to the centrosome, basal body, and primary cilium (Chapter 17). The ability of β-arrs to perform such a broad range of functions within cells depends on their capacity to adopt multiple conformations; chapters detailing methods to monitor β-arr conformational rearrangement using a mass spectrometry-based structural assay (Chapter 18) and FlAsH-BRET intramolecular biosensors are provided (Chapter 19). The final chapters cover methods to study the roles of β-arrs in physiopathology, using cellular and in vivo models, in the contexts of host–pathogen interactions (Chapter 20), allergic inflammatory airway disease (Chapter 21), Type 2 diabetes (Chapters 22 and 23), Parkinson's disease (Chapter 24), and cancer (Chapter 25).

It was our goal here to provide a helpful resource to those interested in investigating the function and regulation of β-arrestins. As editors, we express our sincere gratitude to the scientists that have contributed their time, expertise, and enthusiasm in producing chapters for this volume. Clearly, without their valuable input this book would not have been possible.

Paris, France — *Mark G. H. Scott*
Montreal, QC, Canada — *Stéphane A. Laporte*

Contents

Preface . . . . . *v*
Contributors . . . . . *xi*

PART I INTRODUCTION

1 A Brief History of the β-Arrestins 3
Marc G. Caron and Lawrence S. Barak

2 β-Arrestins: Multitask Scaffolds Orchestrating the Where and When in Cell Signalling 9
Stéphane A. Laporte and Mark G. H. Scott

PART II METHODS TO STUDY ROLES OF β-ARRESTINS IN GPCR REGULATION

3 Methods to Monitor the Trafficking of β-Arrestin/G Protein-Coupled Receptor Complexes Using Enhanced Bystander BRET 59
Yubo Cao, Yoon Namkung, and Stéphane A. Laporte

4 Methods to Investigate β-Arrestin-Mediated Regulation of GPCR Function in Human Airway Smooth Muscle 69
Tonio Pera and Raymond B. Penn

5 Measuring Recruitment of β-Arrestin to G Protein-Coupled Heterodimers Using Bioluminescence Resonance Energy Transfer 83
Dany Fillion, Dominic Devost, and Terence E. Hébert

6 Detection of β-Arrestin-Mediated G Protein-Coupled Receptor Ubiquitination Using BRET 93
Karim Nagi and Sudha K. Shenoy

PART III METHODS TO STUDY SCAFFOLDING FUNCTIONS OF β-ARRESTINS

7 Using In Vitro Pull-Down and In-Cell Overexpression Assays to Study Protein Interactions with Arrestin 107
Nicole A. Perry, Xuanzhi Zhan, Eugenia V. Gurevich, T. M. Iverson, and Vsevolod V. Gurevich

8 Methods to Investigate Arrestins in Complex with Phosphodiesterases 121
Amy J. Tibbo, Tara Busiau, and George S. Baillie

9 Methods to Characterize Protein Interactions with β-Arrestin In Cellulo 139
Revu Ann Alexander, Isaure Lot, and Hervé Enslen

10 Methods to Investigate the β-Arrestin-Mediated Control of ARF6 Activation to Regulate Trafficking and Actin Cytoskeleton Remodeling 159
Ricardo Charles, Mohamed Bourmoum, Shirley Campbell, and Audrey Claing

11 Methods to Investigate the Roles of β-Arrestin-Dependent RalGDS Activation in GPCR-Stimulated Membrane Blebbing 169
Stephen S. G. Ferguson

12 Methods to Determine Interaction Interfaces Between β-Arrestins and Their Protein Partners 177
Thomas Bourquard, Astrid Musnier, Aurélie Tréfier, Flavie Landomiel, Thomas Boulo, Eric Reiter, Pascale Crépieux, and Anne Poupon

13 Workflow Description to Dynamically Model β-Arrestin Signaling Networks 195
Romain Yvinec, Mohammed Akli Ayoub, Francesco De Pascali, Pascale Crépieux, Eric Reiter, and Anne Poupon

14 Proteomic Analysis of the β-Arrestin Interactomes 217
Yang Zhao and Kunhong Xiao

Part IV Methods to Analyse Ligand Bias

15 Quantitating Ligand Bias Using the Competitive Model of Ligand Activity 235
Edward L. Stahl, Frederick J. Ehlert, and Laura M. Bohn

Part V Methods to Study β-Arrestin Localization

16 Methods to Investigate the Nucleocytoplasmic Shuttling Properties of β-Arrestins 251
Elodie Blondel-Tepaz, Thomas Guilbert, and Mark G. H. Scott

17 Monitoring β-Arrestin 2 Targeting to the Centrosome, Basal Body, and Primary Cilium by Fluorescence Microscopy 271
Anahi Molla-Herman, Kathryn M. Davis, Kirk Mykytyn, and Alexandre Benmerah

Part VI Methods to Study Conformational Change of β-Arrestin

18 A Mass Spectrometry-Based Structural Assay for Activation-Dependent Conformational Changes in β-Arrestins 293
Yang Zhao and Kunhong Xiao

19 Probing Arrestin Function Using Intramolecular FlAsH-BRET Biosensors 309
Erik G. Strungs, Louis M. Luttrell, and Mi-Hye Lee

Part VII Methods to Study Roles of β-Arrestins in Physiopathology

20 Methods to Study the Roles of β-Arrestins in Meningococcal Signaling 325
Zoé Virion, Stefano Marullo, and Mathieu Coureuil

21 Methods to Investigate the Roles for β-Arrestin-2 in Allergic Inflammatory Airway Disease 335
Akhil Hegde and Julia K. L. Walker

22 Methods to Study Roles of β-Arrestins in the Regulation of Pancreatic β-Cell Function 345
Stéphane Dalle, Safia Costes, Gyslaine Bertrand, and Magalie A. Ravier

23 Methods to Investigate β-Arrestin Function in Metabolic Regulation 365
Bing Luan, Jian Zhao, and Gang Pei

24 Methods to Investigate the Role of β-Arrestin Signaling in Parkinson's Disease 385
Nikhil M. Urs

25 Methods to Investigate β-Arrestin-1/β-Catenin Signaling in Ovarian Cancer Cells 393
Laura Rosanò, Roberta Cianfrocca, and Anna Bagnato

Index *407*

Contributors

Revu Ann Alexander • *Institut Cochin, INSERM U1016, CNRS UMR8104, Université Paris Descartes, Sorbonne Paris Cité, Paris, France*

Mohammed Akli Ayoub • *PRC, INRA, CNRS, IFCE, Université de Tours, Nouzilly, France; Biology Department, College of Science, United Arab Emirates University, Al Ain, United Arab Emirates*

Anna Bagnato • *Preclinical Models and New Therapeutic Agents Unit, IRCCS-Regina Elena National Cancer Institute, Rome, Italy*

George S. Baillie • *Institute of Cardiovascular and Medical Sciences, College of Veterinary, Medical and Life Sciences, University of Glasgow, Glasgow, UK*

Lawrence S. Barak • *Department of Cell Biology, Duke University Medical Center, Durham, NC, USA*

Alexandre Benmerah • *Laboratoire des Maladies Rénales Héréditaires, INSERM U1163, Paris, France; Institut Imagine, Université Paris Descartes, Sorbonne Paris Cité, Paris, France*

Gyslaine Bertrand • *Institut de Génomique Fonctionnelle, CNRS UMR5203, INSERM U1191, Montpellier University, Montpellier, France*

Elodie Blondel-Tepaz • *Institut Cochin, INSERM U1016, Paris, France; CNRS, UMR8104, Paris, France; Université Paris Descartes, Sorbonne Paris Cité, Paris, France*

Laura M. Bohn • *Department of Molecular Medicine, The Scripps Research Institute, Jupiter, FL, USA; Department of Neuroscience, The Scripps Research Institute, Jupiter, FL, USA*

Thomas Boulo • *PRC, INRA, CNRS, Université François Rabelais-Tours, Nouzilly, France*

Mohamed Bourmoum • *Department of Pharmacology and Physiology, Faculty of Medicine, Université de Montréal, Montreal, QC, Canada*

Thomas Bourquard • *PRC, INRA, CNRS, Université François Rabelais-Tours, Nouzilly, France; Department of Human and Molecular Genetics, Baylor College of Medicine, Houston, TX, USA*

Tara Busiau • *Institute of Cardiovascular and Medical Sciences, College of Veterinary, Medical and Life Sciences, University of Glasgow, Glasgow, UK*

Shirley Campbell • *Department of Pharmacology and Physiology, Faculty of Medicine, Université de Montréal, Montreal, QC, Canada*

Yubo Cao • *Department of Pharmacology and Therapeutics, McGill University, Montréal, QC, Canada*

Marc G. Caron • *Department of Cell Biology, Duke University Medical Center, Durham, NC, USA; Department of Neurobiology, Duke University Medical Center, Durham, NC, USA; Department of Medicine, Duke University Medical Center, Durham, NC, USA*

Ricardo Charles • *Department of Pharmacology and Physiology, Faculty of Medicine, Université de Montréal, Montreal, QC, Canada*

Roberta Cianfrocca • *Preclinical Models and New Therapeutic Agents Unit, IRCCS-Regina Elena National Cancer Institute, Rome, Italy*

Audrey Claing • *Department of Pharmacology and Physiology, Faculty of Medicine, Université de Montréal, Montreal, QC, Canada*

Safia Costes • *Institut de Génomique Fonctionnelle, CNRS UMR5203, INSERM U1191, Montpellier University, Montpellier, France*
Mathieu Coureuil • *Institut-Necker-Enfants-Malades, INSERM, Unité U1151, Paris, France; Faculté de Médecine, Université Paris Descartes, Sorbonne Paris Cité, Paris, France*
Pascale Crépieux • *PRC, INRA, CNRS, Université François Rabelais-Tours, Nouzilly, France*
Stéphane Dalle • *Institut de Génomique Fonctionnelle, CNRS UMR5203, INSERM U1191, Montpellier University, Montpellier, France*
Kathryn M. Davis • *Department of Biological Chemistry and Pharmacology, The Ohio State University, Columbus, OH, USA*
Francesco De Pascali • *PRC, INRA, CNRS, IFCE, Université de Tours, Nouzilly, France*
Dominic Devost • *Department of Pharmacology and Therapeutics, McGill University, Montréal, QC, Canada*
Frederick J. Ehlert • *Department of Pharmacology, School of Medicine, University of California, Irvine, Irvine, CA, USA*
Hervé Enslen • *Institut Cochin, INSERM U1016, CNRS UMR8104, Université Paris Descartes, Sorbonne Paris Cité, Paris, France*
Stephen S. G. Ferguson • *Department of Cellular and Molecular Medicine, University of Ottawa Brain and Mind Institute, University of Ottawa, Ottawa, ON, Canada*
Dany Fillion • *Department of Pharmacology and Therapeutics, McGill University, Montré al, QC, Canada*
Thomas Guilbert • *Institut Cochin, INSERM U1016, Paris, France; CNRS, UMR8104, Paris, France; Université Paris Descartes, Sorbonne Paris Cité, Paris, France*
Eugenia V. Gurevich • *Department of Pharmacology, Vanderbilt University, Nashville, TN, USA*
Vsevolod V. Gurevich • *Department of Pharmacology, Vanderbilt University, Nashville, TN, USA*
Terence E. Hébert • *Department of Pharmacology and Therapeutics, McGill University, Montréal, QC, Canada*
Akhil Hegde • *School of Nursing, Duke University Medical Center, Durham, NC, USA*
T. M. Iverson • *Department of Pharmacology, Vanderbilt University, Nashville, TN, USA; Department of Biochemistry, Vanderbilt University, Nashville, TN, USA; Center for Structural Biology, Vanderbilt University, Nashville, TN, USA; Vanderbilt Institute of Chemical Biology, Vanderbilt University, Nashville, TN, USA*
Flavie Landomiel • *PRC, INRA, CNRS, Université François Rabelais-Tours, Nouzilly, France*
Stéphane A. Laporte • *Department of Medicine, Research Institute of the McGill University Health Center (RI-MUHC), McGill University, Montréal, QC, Canada; Department of Pharmacology and Therapeutics, McGill University, Montréal, QC, Canada; Department of Anatomy and Cell Biology, McGill University, Montréal, QC, Canada; RI-MUHC/ Glen Site, Montréal, QC, Canada*
Mi-Hye Lee • *Department of Medicine, Medical University of South Carolina, Charleston, SC, USA*
Isaure Lot • *Institut Cochin, INSERM U1016, CNRS UMR8104, Université Paris Descartes, Sorbonne Paris Cité, Paris, France*
Bing Luan • *Department of Endocrinology, Shanghai Tenth People's Hospital, School of Medicine, Tongji University, Shanghai, China*

Louis M. Luttrell • *Department of Medicine, Medical University of South Carolina, Charleston, SC, USA; Department of Biochemistry and Molecular Biology, Medical University of South Carolina, Charleston, SC, USA*

Stefano Marullo • *Faculté de Médecine, Université Paris Descartes, Sorbonne Paris Cité, Paris, France; Institut Cochin, INSERM, U1016, CNRS UMR 8104, Paris, France*

Anahi Molla-Herman • *Department of Genetics and Developmental Biology, Institut Curie, CNRS-UMR3215, INSERM-U934, Paris, France; CIRB, Collège de France, CNRS-UMR7241, INSERM-U1050, Paris, France*

Astrid Musnier • *PRC, INRA, CNRS, Université François Rabelais-Tours, Nouzilly, France*

Kirk Mykytyn • *Department of Biological Chemistry and Pharmacology, The Ohio State University, Columbus, OH, USA; Neuroscience Research Institute, The Ohio State University, Columbus, OH, USA*

Karim Nagi • *Department of Cell Biology, Duke University Medical Center, Durham, NC, USA; College of Medicine, Member of QU Health, Qatar University, Doha, Qatar*

Yoon Namkung • *Department of Medicine, Research Institute of the McGill University Health Center (RI-MUHC), McGill University, Montréal, QC, Canada*

Gang Pei • *State Key Laboratory of Cell Biology, CAS Center for Excellence in Molecular Cell Science, Shanghai Institute of Biochemistry and Cell Biology, Chinese Academy of Sciences, Shanghai, China; Laboratory of Receptor-Based Bio-Medicine, Shanghai Key Laboratory of Signaling and Disease Research, School of Life Sciences and Technology, Tongji University, Shanghai, China*

Raymond B. Penn • *Division of Pulmonary, Allergy, and Critical Care Medicine, Department of Medicine, Center for Translational Medicine, Jane and Leonard Korman Respiratory Institute, Thomas Jefferson University, Philadelphia, PA, USA*

Tonio Pera • *Division of Pulmonary, Allergy, and Critical Care Medicine, Department of Medicine, Center for Translational Medicine, Jane and Leonard Korman Respiratory Institute, Thomas Jefferson University, Philadelphia, PA, USA*

Nicole A. Perry • *Department of Pharmacology, Vanderbilt University, Nashville, TN, USA*

Anne Poupon • *PRC, INRA, CNRS, Université François Rabelais-Tours, Nouzilly, France*

Magalie A. Ravier • *Institut de Génomique Fonctionnelle, CNRS UMR5203, INSERM U1191, Montpellier University, Montpellier, France*

Eric Reiter • *PRC, INRA, CNRS, Université François Rabelais-Tours, Nouzilly, France*

Laura Rosanò • *Preclinical Models and New Therapeutic Agents Unit, IRCCS-Regina Elena National Cancer Institute, Rome, Italy*

Mark G. H. Scott • *Institut Cochin, INSERM U1016, Paris, France; CNRS, UMR 8104, Paris, France; Université Paris Descartes, Sorbonne Paris Cité, Paris, France*

Sudha K. Shenoy • *Department of Cell Biology, Duke University Medical Center, Durham, NC, USA; Department of Medicine (Cardiology), Duke University Medical Center, Durham, NC, USA*

Edward L. Stahl • *Department of Molecular Medicine, The Scripps Research Institute, Jupiter, FL, USA; Department of Neuroscience, The Scripps Research Institute, Jupiter, FL, USA*

Erik G. Strungs • *Department of Medicine, Medical University of South Carolina, Charleston, SC, USA*

Amy J. Tibbo • *Institute of Cardiovascular and Medical Sciences, College of Veterinary, Medical and Life Sciences, University of Glasgow, Glasgow, UK*

Aurélie Tréfier • *PRC, INRA, CNRS, Université François Rabelais-Tours, Nouzilly, France*

Nikhil M. Urs • *Department of Pharmacology and Therapeutics, University of Florida, Gainesville, FL, USA*

Zoé Virion • *Institut-Necker-Enfants-Malades, INSERM, Unité U1151, Paris, France; Faculté de Médecine, Université Paris Descartes, Sorbonne Paris Cité, Paris, France*

Julia K. L. Walker • *School of Nursing, Duke University Medical Center, Durham, NC, USA; Department of Medicine, Duke University Medical Center, Durham, NC, USA*

Kunhong Xiao • *Department of Pharmacology and Chemical Biology, University of Pittsburgh, Pittsburgh, PA, USA; Vascular Medicine Institute, University of Pittsburgh, Pittsburgh, PA, USA; Biomedical Mass Spectrometry Center, School of Medicine, University of Pittsburgh, Pittsburgh, PA, USA*

Romain Yvinec • *PRC, INRA, CNRS, IFCE, Université de Tours, Nouzilly, France*

Xuanzhi Zhan • *Department of Chemistry, Tennessee Technological University, Cookeville, TN, USA*

Jian Zhao • *Translational Medical Center for Stem Cell Therapy, Shanghai East Hospital, School of Medicine, Tongji University, Shanghai, China*

Yang Zhao • *Department of Pharmacology and Chemical Biology, University of Pittsburgh, Pittsburgh, PA, USA*

Part I

Introduction



Chapter 1

A Brief History of the β-Arrestins

Marc G. Caron and Lawrence S. Barak

Abstract

Arrestins have now been implicated in the actions of virtually every G protein-coupled receptor (GPCR) for which they have been examined. Originally discovered for their role in the turnoff of visual perception, their newly discovered pleotropic functions in the cellular and physiological actions of GPCRs not only illuminate new mechanisms of signal transduction but also offer new avenues for therapeutic utility. Below, in this introductory chapter, we provide a short historical description and synopsis of how arrestins conceptually became associated with the function of GPCRs.

Key words β-Arrestins, GPCR, GPCR kinases, Desensitization, Endocytosis, Signaling selectivity/bias, Therapeutics

1 Historical Perspective of β-Arrestin Biology

Arrestins were first discovered as a major protein component of the retinal photoreceptor region and originally called the "retinal S antigen" for their involvement in uveitis [1]. Subsequent work in the visual system in the early 1980s led to the idea that the protein was involved in the turnoff of light-activated rhodopsin [2]. At that time, the relationship between the visual system machinery and receptors for hormones and neurotransmitters was not yet fully appreciated. This interesting relationship became more obvious with the cloning of the β2-adrenergic receptor (β2AR) in 1986, which revealed that the putative membrane topology of the β2AR was similar to that of rhodopsin [3]. Early biochemical work with photoaffinity labeled and/or purified β2AR had demonstrated that phosphorylation of the β2AR by a kinase distinct from protein kinase A (PKA) might be involved in its desensitization process [4–6]. Subsequently, a purified candidate protein kinase—originally called β2-adrenergic receptor kinase or βARK1, and later renamed G protein-coupled receptor kinase 2 (GRK2)—was isolated from lymphoma cells lacking protein kinase A and shown to inhibit the β2AR activation of G protein [7]. However, as the

Mark G. H. Scott and Stéphane A. Laporte (eds.), *Beta-Arrestins: Methods and Protocols*, Methods in Molecular Biology, vol. 1957, https://doi.org/10.1007/978-1-4939-9158-7_1, © Springer Science+Business Media, LLC, part of Springer Nature 2019

purity of this kinase preparation advanced, its β2AR/G protein uncoupling activity was lost until the reconstituted mix was supplemented with purified retinal S antigen/visual arrestin [7, 8], suggesting a role for an arrestin-like protein in the regulation of non-visual GPCRs. Subsequent work in the field led to the eventual purification and/or cloning of two visual GPCR kinases (GRKs) [9, 10] and five non-visual GRKs [11–15], as well as the genes for two distinct visual arrestins (arrestin 1 and 4) [16, 17] and two non-visual arrestins alternatively referred to as β-arrestin 1 or arrestin 2 and β-arrestin 2 or arrestin 3 [18, 19]. Further investigations established that GRKs and arrestins together were necessary not only to fully modulate the signaling function or "desensitization" of the β2AR but also the signaling function of other GPCRs [20–22]. Moreover, it was established that while these two classes of visual and non-visual accessory proteins display similar functions, specificity of action as well as tissue specificity could be demonstrated [22].

Cellular work in the early 1990s began to investigate other possible roles for the GRK/arrestin modulation of GPCRs. Following on the earlier observations that GPCRs became "desensitized" and internalized following prolonged agonist activation [23, 24], it was demonstrated that desensitized β2AR could co-localize within the same endocytic compartment as the transferrin receptor, suggesting that GPCR internalization might use the same endocytic machinery [25]. This observation was further corroborated when it was revealed that β-arrestin 2 played an essential role in the internalization of the desensitized β2AR, functioning as an adaptor to the endocytic machinery [26, 27]. Interestingly, tagging β-arrestins with GFP provided not only a way to assess GPCR/β-arrestin interactions and trafficking in real time but also a foundation for the development of various cellular reporters widely used today for GPCR ligand screening [28]. Subsequent observations with different GPCRs led to the rather unexpected idea at the time that GPCR/arrestin interaction could initiate intracellular signaling cascades, distinct from the canonical G protein-mediated signals [29, 30]. Eventually, this provocative idea was further supported by the demonstration that a given ligand could bind to a given receptor and act as an agonist at G protein signaling but an antagonist for β-arrestin interactions or vice versa [31, 32].

Finally, the relevance of the visual arrestin/β-arrestin concept was further established by demonstrating an in vivo physiological relevance for GPCR/β-arrestin interactions. Indeed, the absence of β-arrestin 2 in mice markedly enhanced the analgesic effects of the opiate agonist morphine while concomitantly eliminating the development of morphine induced tolerance as well as the life-threatening side effects of decreased respiration and gastrointestinal function [33–35].

To use a colloquial expression, "the rest is history." As is elegantly outlined in this collection of methodological essays, the breadth of techniques presented in this compendium speaks not only to multitude of ways in which GPCR/β-arrestins can be studied in the context of protein/protein interactions but also in the potential functions these interactions can play in the normal and dysfunctional physiological contexts.

2 Implications of β-Arrestin for Improved Therapeutics

Since the early 2000s, the breakthrough resolution of the crystal structure of the prototypical GPCRs like rhodopsin and β2AR [36, 37] as well as complexes of GPCRs with their G protein or β-arrestin signaling partners [38–41] has added an unprecedented level of sophistication in approaches to elucidate GPCR signaling mechanisms and developing new therapies. As case in point, the advent of molecular modeling and docking of millions of chemical structures onto the structure of GPCRs [42] combined with conventional cellular screening platforms has provided exciting new ways to develop novel receptor probes with exquisitely high affinity and specificity [43, 44]. The methodologies described in this collection of papers/essays become crucial for relating the molecular determinants underlying GPCR/β-arrestin interactions to the experimental parameters that define a receptor's signal transduction network. Indeed, one of the most interesting and potentially significant aspects of the GPCR/β-arrestin paradigm is the possibility to selectively target that interaction for therapeutic gain. GPCRs represent a large portion of the therapeutic landscape, but most drugs invariably have untoward side effects. While these unwanted effects have been commonly attributed to the promiscuous interaction of drugs with other GPCRs, a lack of selectivity of these agents for the distinct signaling modes of targeted receptors may significantly contribute to an unnecessary reduction in their therapeutic specificity. Our ability to now develop therapeutic agents that have improved selectivity or bias for either the G protein or β-arrestin signaling pathways is bound to produce better therapies.

Acknowledgments

Work in the Caron/Barak group at Duke University has been supported by grants for the United States National Institutes of Health (5R37-MH073853, 5P30-DA029925, 4U19-MH082441, 1R33CA191198); a gift from the Pall Family Foundation and the Howard Hughes Medical Institutes (1992-2005).

References

1. Dorey C, Faure JP (1977) Isolation and characterization of a retinal antigen inducing experimental autoimmune uveo-retinitis. Ann Immunol (Paris) 128:229–232
2. Pfister C, Chabre M, Plouet J, Tuyen VV, De Kozak Y, Faure JP, Kuhn H (1985) Retinal S antigen identified as the 48K protein regulating light-dependent phosphodiesterase in rods. Science 228:891–893
3. Dixon RA, Kobilka BK, Strader DJ, Benovic JL, Dohlman HG, Frielle T, Bolanowski MA, Bennett CD, Rands E, Diehl RE, Mumford RA, Slater EE, Sigal IS, Caron MG, Lefkowitz RJ, Strader CD (1986) Cloning of the gene and cDNA for mammalian beta-adrenergic receptor and homology with rhodopsin. Nature 321:75–79
4. Stadel JM, Nambi P, Lavin TN, Heald SL, Caron MG, Lefkowitz RJ (1982) Catecholamine-induced desensitization of turkey erythrocyte adenylate cyclase. Structural alterations in the beta-adrenergic receptor revealed by photoaffinity labeling. J Biol Chem 257:9242–9245
5. Stadel JM, Nambi P, Shorr RG, Sawyer DF, Caron MG, Lefkowitz RJ (1983) Catecholamine-induced desensitization of turkey erythrocyte adenylate cyclase is associated with phosphorylation of the beta-adrenergic receptor. Proc Natl Acad Sci U S A 80:3173–3177
6. Strasser RH, Sibley DR, Lefkowitz RJ (1986) A novel catecholamine-activated adenosine cyclic 3′,5′-phosphate independent pathway for beta-adrenergic receptor phosphorylation in wild-type and mutant S49 lymphoma cells: mechanism of homologous desensitization of adenylate cyclase. Biochemistry 25:1371–1377
7. Benovic JL, Strasser RH, Caron MG, Lefkowitz RJ (1986) Beta-adrenergic receptor kinase: identification of a novel protein kinase that phosphorylates the agonist-occupied form of the receptor. Proc Natl Acad Sci U S A 83:2797–2801
8. Benovic JL, Kuhn H, Weyand I, Codina J, Caron MG, Lefkowitz RJ (1987) Functional desensitization of the isolated beta-adrenergic receptor by the beta-adrenergic receptor kinase: potential role of an analog of the retinal protein arrestin (48-kDa protein). Proc Natl Acad Sci U S A 84:8879–8882
9. Lorenz W, Inglese J, Palczewski K, Onorato JJ, Caron MG, Lefkowitz RJ (1991) The receptor kinase family: primary structure of rhodopsin kinase reveals similarities to the beta-adrenergic receptor kinase. Proc Natl Acad Sci U S A 88:8715–8719
10. Weiss ER, Raman D, Shirakawa S, Ducceschi MH, Bertram PT, Wong F, Kraft TW, Osawa S (1998) The cloning of GRK7, a candidate cone opsin kinase, from cone- and rod-dominant mammalian retinas. Mol Vis 4:27–34
11. Benovic JL, DeBlasi A, Stone WC, Caron MG, Lefkowitz RJ (1989) Beta-adrenergic receptor kinase: primary structure delineates a multigene family. Science 246:235–240
12. Boekhoff I, Inglese J, Schleicher S, Koch WJ, Lefkowitz RJ, Breer H (1994) Olfactory desensitization requires membrane targeting of receptor kinase mediated by beta gamma-subunits of heterotrimeric G proteins. J Biol Chem 269:37–40
13. Premont RT, Macrae AD, Stoffel RH, Chung N, Pitcher JA, Ambrose C, Inglese J, MacDonald ME, Lefkowitz RJ (1996) Characterization of the G protein-coupled receptor kinase GRK4. Identification of four splice variants. J Biol Chem 271:6403–6410
14. Kunapuli P, Benovic JL (1993) Cloning and expression of GRK5: a member of the G protein-coupled receptor kinase family. Proc Natl Acad Sci U S A 90:5588–5592
15. Benovic JL, Gomez J (1993) Molecular cloning and expression of GRK6. A new member of the G protein-coupled receptor kinase family. J Biol Chem 268:19521–19527
16. Shinohara T, Dietzschold B, Craft, CM, Wistow G, Early JJ, Donoso LA, Horwitz J, Tao R (1987) Primary and secondary structure of bovine retinal S antigen (48-kDa protein). Proc Natl Acad Sci U S A 84: 6975–6979
17. Craft CM, Whitmore DH (1995) The arrestin superfamily: cone arrestins are a fourth family. FEBS Lett 362: 247–255
18. Parruti G, Peracchia F, Sallese M, Ambrosini G, Masini M, Rotilio D, De Blasi A (1993) Molecular analysis of human beta-arrestin-1: cloning, tissue distribution, and regulation of expression. Identification of two isoforms generated by alternative splicing. J Biol Chem 268:9753–9761
19. Attramadal H, Arriza JL, Aoki C, Dawson TM, Codina J, Kwatra MM, Snyder SH, Caron MG, Lefkowitz RJ (1992) Beta-arrestin2, a novel member of the arrestin/beta-arrestin gene family. J Biol Chem 267:17882–17890
20. Lohse MJ, Andexinger S, Pitcher J, Trukawinski S, Codina J, Faure JP, Caron MG, Lefkowitz RJ (1992) Receptor-specific desensitization with purified proteins. Kinase

dependence and receptor specificity of beta-arrestin and arrestin in the beta 2-adrenergic receptor and rhodopsin systems. J Biol Chem 267:8558–8564

21. Pippig S, Andexinger S, Daniel K, Puzicha M, Caron MG, Lefkowitz RJ, Lohse MJ (1993) Overexpression of beta-arrestin and beta-adrenergic receptor kinase augment desensitization of beta 2-adrenergic receptors. J Biol Chem 268:3201–3208
22. Gurevich VV, Dion SB, Onorato JJ, Ptasienski J, Kim CM, Sterne-Marr R, Hosey MM, Benovic JL (1995) Arrestin interactions with G protein-coupled receptors. Direct binding studies of wild type and mutant arrestins with rhodopsin, beta 2-adrenergic, and m2 muscarinic cholinergic receptors. J Biol Chem 270:720–731
23. Harden TK, Cotton CU, Waldo GL, Lutton JK, Perkins JP (1980) Catecholamine-induced alteration in sedimentation behavior of membrane bound beta-adrenergic receptors. Science 210:441–443
24. Stadel JM, Strulovici B, Nambi P, Lavin TN, Briggs MM, Caron MG, Lefkowitz RJ (1983) Desensitization of the beta-adrenergic receptor of frog erythrocytes. Recovery and characterization of the down-regulated receptors in sequestered vesicles. J Biol Chem 258:3032–3038
25. von Zastrow M, Kobilka BK (1992) Ligand-regulated internalization and recycling of human beta 2-adrenergic receptors between the plasma membrane and endosomes containing transferrin receptors. J Biol Chem 267:3530–3538
26. Ferguson SS, Downey WE 3rd, Colapietro AM, Barak LS, Menard L, Caron MG (1996) Role of beta-arrestin in mediating agonist-promoted G protein-coupled receptor internalization. Science 271:363–366
27. Goodman OB Jr, Krupnick JG, Santini F, Gurevich VV, Penn RB, Gagnon AW, Keen JH, Benovic JL (1996) Beta-arrestin acts as a clathrin adaptor in endocytosis of the beta2-adrenergic receptor. Nature 383:447–450
28. Barak LS, Ferguson SS, Zhang J, Caron MG (1997) A beta-arrestin/green fluorescent protein biosensor for detecting G protein-coupled receptor activation. J Biol Chem 272:27497–27500
29. Luttrell LM, Ferguson SS, Daaka Y, Miller WE, Maudsley S, Della Rocca GJ, Lin F, Kawakatsu H, Owada K, Luttrell DK, Caron MG, Lefkowitz RJ (1999) Beta-arrestin-dependent formation of beta2 adrenergic receptor-Src protein kinase complexes. Science 283:655–661
30. DeFea KA, Zalevsky J, Thoma MS, Dery O, Mullins RD, Bunnett NW (2000) beta-arrestin-dependent endocytosis of proteinase-activated receptor 2 is required for intracellular targeting of activated ERK1/2. J Cell Biol 148:1267–1281
31. Azzi M, Charest PG, Angers S, Rousseau G, Kohout T, Bouvier M, Pineyro G (2003) Beta-arrestin-mediated activation of MAPK by inverse agonists reveals distinct active conformations for G protein-coupled receptors. Proc Natl Acad Sci U S A 100:11406–11411
32. Wei H, Ahn S, Shenoy SK, Karnik SS, Hunyady L, Luttrell LM, Lefkowitz RJ (2003) Independent beta-arrestin 2 and G protein-mediated pathways for angiotensin II activation of extracellular signal-regulated kinases 1 and 2. Proc Natl Acad Sci U S A 100:10782–10787
33. Bohn LM, Lefkowitz RJ, Gainetdinov RR, Peppel K, Caron MG, Lin FT (1999) Enhanced morphine analgesia in mice lacking beta-arrestin 2. Science 286:2495–2498
34. Bohn LM, Gainetdinov RR, Lin FT, Lefkowitz RJ, Caron MG (2000) Mu-opioid receptor desensitization by beta-arrestin-2 determines morphine tolerance but not dependence. Nature 408:720–723
35. Raehal KM, Walker JK, Bohn LM (2005) Morphine side effects in beta-arrestin 2 knockout mice. J Pharmacol Exp Ther 314:1195–1201
36. Palczewski K, Kumasaka T, Hori T, Behnke CA, Motoshima H, Fox BA, Le Trong I, Teller DC, Okada T, Stenkamp RE, Yamamoto M, Miyano M (2000) Crystal structure of rhodopsin: a G protein-coupled receptor. Science 289:739–745
37. Rasmussen SG, Choi HJ, Rosenbaum DM, Kobilka TS, Thian FS, Edwards PC, Burghammer M, Ratnala VR, Sanishvili R, Fischetti RF, Schertler GF, Weis WI, Kobilka BK (2007) Crystal structure of the human beta2 adrenergic G-protein-coupled receptor. Nature 450:383–387
38. Rasmussen SG, DeVree BT, Zou Y, Kruse AC, Chung KY, Kobilka TS, Thian FS, Chae PS, Pardon E, Calinski D, Mathiesen JM, Shah ST, Lyons JA, Caffrey M, Gellman SH, Steyaert J, Skiniotis G, Weis WI, Sunahara RK, Kobilka BK (2011) Crystal structure of the beta2 adrenergic receptor-Gs protein complex. Nature 477:549–555
39. Zhou XE, Gao X, Barty A, Kang Y, He Y, Liu W, Ishchenko A, White TA, Yefanov O, Han GW, Xu Q, de Waal PW, Suino-Powell KM, Boutet S, Williams GJ, Wang M, Li D, Caffrey M, Chapman HN, Spence JC, Fromme P, Weierstall U, Stevens RC,

Cherezov V, Melcher K, Xu HE (2016) X-ray laser diffraction for structure determination of the rhodopsin-arrestin complex. Sci Data 3:160021

40. Komolov KE, Du Y, Duc NM, Betz RM, Rodrigues J, Leib RD, Patra D, Skiniotis G, Adams CM, Dror RO, Chung KY, Kobilka BK, Benovic JL (2017) Structural and Functional Analysis of a beta2-Adrenergic Receptor Complex with GRK5. Cell 169(407–421): e416
41. Cahill TJ 3rd, Thomsen AR, Tarrasch JT, Plouffe B, Nguyen AH, Yang F, Huang LY, Kahsai AW, Bassoni DL, Gavino BJ, Lamerdin JE, Triest S, Shukla AK, Berger B, Little J t, Antar A, Blanc A, Qu CX, Chen X, Kawakami K, Inoue A, Aoki J, Steyaert J, Sun JP, Bouvier M, Skiniotis G, Lefkowitz RJ (2017) Distinct conformations of GPCR-beta-arrestin complexes mediate desensitization, signaling, and endocytosis. Proc Natl Acad Sci U S A 114:2562–2567
42. Shoichet BK, Kobilka BK (2012) Structure-based drug screening for G-protein-coupled receptors. Trends Pharmacol Sci 33:268–272
43. Manglik A, Lin H, Aryal DK, McCorvy JD, Dengler D, Corder G, Levit A, Kling RC, Bernat V, Hubner H, Huang XP, Sassano MF, Giguere PM, Lober S, Da D, Scherrer G, Kobilka BK, Gmeiner P, Roth BL, Shoichet BK (2016) Structure-based discovery of opioid analgesics with reduced side effects. Nature 537:185–190
44. Wang S, Wacker D, Levit A, Che T, Betz RM, McCorvy JD, Venkatakrishnan AJ, Huang XP, Dror RO, Shoichet BK, Roth BL (2017) D4 dopamine receptor high-resolution structures enable the discovery of selective agonists. Science 358:381–386



Chapter 2

β-Arrestins: Multitask Scaffolds Orchestrating the Where and When in Cell Signalling

Stéphane A. Laporte and Mark G. H. Scott

Abstract

The β-arrestins (β-arrs) were initially appreciated for the roles they play in the desensitization and endocytosis of G protein-coupled receptors (GPCRs). They are now also known to act as multifunctional adaptor proteins binding many non-receptor protein partners to control multiple signalling pathways. β-arrs therefore act as key regulatory hubs at the crossroads of external cell inputs and functional outputs in cellular processes ranging from gene transcription to cell growth, survival, cytoskeletal regulation, polarity, and migration. An increasing number of studies have also highlighted the scaffolding roles β-arrs play in vivo in both physiological and pathological conditions, which opens up therapeutic avenues to explore. In this introductory review chapter, we discuss the functional roles that β-arrs exert to control GPCR function, their dynamic scaffolding roles and how this impacts signal transduction events, compartmentalization of β-arrs, how β-arrs are regulated themselves, and how the combination of these events culminates in cellular regulation.

Key words β-Arrestin, GPCR, Desensitization, Endocytosis, Protein scaffolds, Signal transduction, Compartmentalization, Biased signalling

1 Introduction

The arrestin family is composed of four members encompassing visual rod arrestin (arrestin-1) and cone arrestin (arrestin-4), which are expressed in the eye, and the ubiquitously expressed β-arrestins (β-arrs), β-arr1 and β-arr2 (also known as arrestin-2 and arrestin-3, respectively). Visual rod arrestin was first characterized for the role it plays in the desensitization of G protein coupling of the G protein-coupled receptor (GPCR) rhodopsin, thus turning off or "arresting" receptor signalling [1]. β-arrs were subsequently discovered via their sequence homology to visual arrestin and found to desensitize β2-adrenoreceptor (β2-AR)-G protein signalling following ligand-mediated activation [2, 3]. In addition to their role in GPCR desensitization, β-arrs were shown to promote the endocytosis of GPCRs by acting as endocytic adaptors through

Mark G. H. Scott and Stéphane A. Laporte (eds.), *Beta-Arrestins: Methods and Protocols*, Methods in Molecular Biology, vol. 1957, https://doi.org/10.1007/978-1-4939-9158-7_2, © Springer Science+Business Media, LLC, part of Springer Nature 2019

interactions with clathrin and AP-2, hence targeting receptors for internalization [4]. β-arrs are now known to regulate the vast majority of receptors belonging to the GPCR superfamily and demonstrate high species conservation with around 50% sequence homology between vertebrates and invertebrates [5]. More recently, the arrestin clan was extended by the identification of a group of related proteins called arrestin domain-containing proteins or α-arrestins that, despite demonstrating low sequence homology (11–15%) with β-arrs, contain the arrestin structural fold [6, 7]. The functional repertoire that α-arrestins perform is still emerging, but it includes roles in GPCR trafficking and degradation.

In addition to switching off G protein-dependent signalling, β-arrs can also function as dynamic molecular scaffolds to promote alternative signalling pathways downstream of GPCR activation [8]. This is achieved through their remarkable capacity to interact with an ever-expanding list of non-GPCR protein partners coupled with their subcellular trafficking properties, resulting in compartmentalization of signalling complexes [9, 10]. β-arrs also influence signalling downstream of other non-GPCR receptor classes and even provide control on signal transduction pathways independently of receptor input [11–13]. Through these mechanisms β-arrs thus act as regulatory hubs in a diverse array of signalling pathways, including MAPK cascades and the PTEN/PI3K/AKT, Mdm2/p53, and NF-κB pathways with consequences for cell proliferation, survival, and migration [9, 11, 14–16]. While β-arr1 and β-arr2 share 78% sequence homology and many overlapping functions, additional levels of control emanate from discrete molecular differences that result in isoform selective functions on receptor regulation, subcellular trafficking events, and preferential binding to protein binding partners [5].

Here, we discuss the roles that β-arrs play to regulate GPCR desensitization and endocytosis, their dynamic scaffolding functions, roles of compartmentalized pools of β-arrs, how β-arrs are subjected to regulation themselves, and how the association of these events gives rise to cellular outcomes.

2 Roles of β-arrs in GPCR Desensitization

GPCRs are integral membrane proteins containing seven transmembrane domains that represent the largest class of cell surface receptors with around 800 members identified in the human genome [17]. GPCRs bind a diverse array of ligands and are implicated in a wide range of physiological processes and many human diseases. These receptors therefore represent attractive drug targets, and currently around 35% of prescription drugs target GPCRs [17, 18].

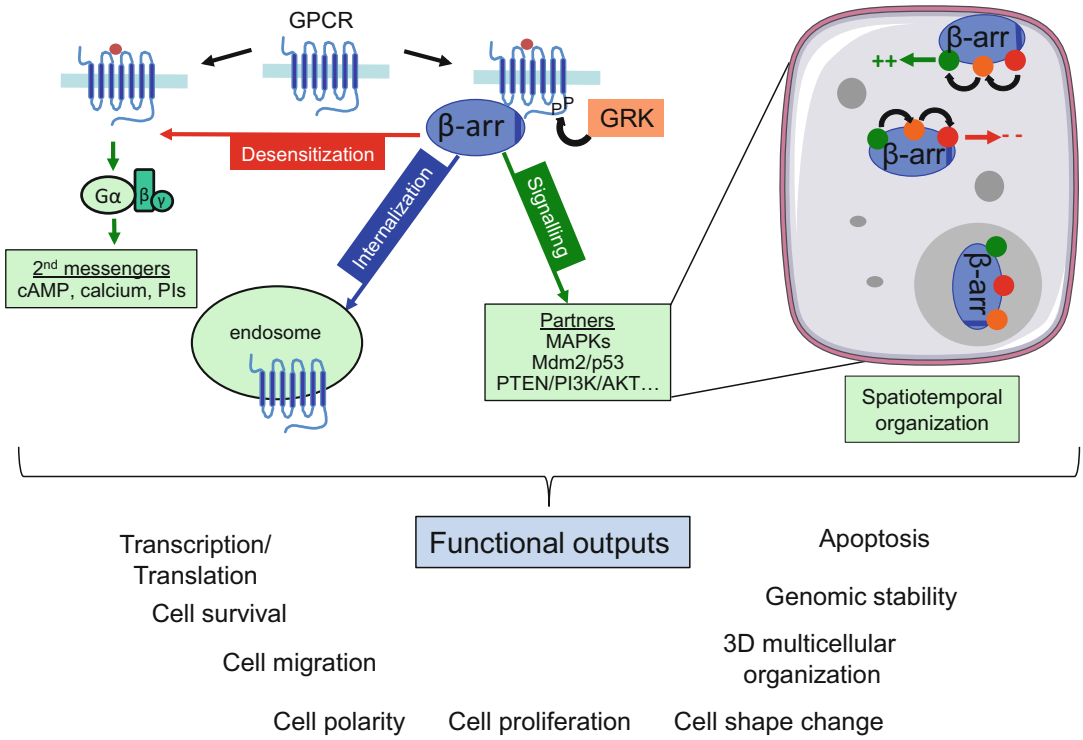


Fig. 1 Roles of β-arrestin in GPCR regulation and cell signalling. Following agonist stimulation of GPCRs, they are rapidly phosphorylated by GRKs. This promotes the translocation of β-arrs from the cytoplasm to the phosphorylated receptors, where β-arrs promote uncoupling of GPCRs from their cognate G proteins in the process of homologous desensitization. β-arrs, via their interactions with clathrin and AP-2, also promote GPCR internalization. Through the capacity of β-arrs to act as protein scaffolds and their ability to dynamically shuttle to different cell compartments, they provide signalling compartmentalization and spatiotemporal organization of the cell. The combination of all these events leads to diverse functional cellular outcomes

Following activation by their cognate ligands, GPCRs undergo a conformational change leading to G protein coupling and activation. Activated G proteins subsequently activate downstream effectors leading to the generation of second messengers including cyclic AMP (cAMP), calcium, and phosphoinositides (Fig. 1). Repeated or prolonged agonist stimulation of GPCRs leads to decreased responsiveness, a process known as desensitization. Homologous desensitization is a two-step process involving first the phosphorylation of agonist-occupied receptors in their intracellular regions (Fig. 1) by G protein-coupled receptor kinases (GRKs). GRKs are a family of serine/threonine kinases composed of seven members [19, 20]. GRK1 and GRK7 expression is confined to the retina, and GRK4 also has a restricted tissue distribution with highest expression in the testes [20]. The other members, GRK2, GRK3, GRK5, and GRK6, are widely expressed and are involved in the phosphorylation of most non-rhodopsin GPCRs.

Subsequent to phosphorylation of GPCRs by GRKs, the second step of homologous desensitization involves the recruitment of β-arrs to the activated receptors. β-arr binding to phosphorylated receptors precludes further GPCR-G protein coupling through steric hindrance, giving rise to desensitization [2, 21] (Fig. 1). β-arr1 and β-arr2 have similar structures, consisting of N- and C-globular domains composed almost completely of antiparallel β sheets that are linked by a hinge region, and a flexible C-terminal tail region [13]. β-arrs regulate the vast majority of GPCRs, indicating that they recognize shared structural elements of the activated receptors belonging to this family.

3 Roles of β-arrs in GPCR Trafficking

The roles that β-arrs play in GPCR regulation were further expanded by the findings that they can interact with proteins playing important roles in endocytosis including clathrin [22], the clathrin adaptor AP-2 [23], and the GTPase ADP-ribosylation factor 6 (ARF6) [24]. Through interactions with these components of the endocytic machinery, β-arrs promote internalization of the majority of GPCRs (Fig. 1). β-arr1 and β-arr2 display differential affinities for different groups of GPCRs. "Class A" receptors, such as the β2-AR, endothelin type A receptor (ET-AR), and the mu opioid receptor (μ-OR), bind β-arr2 with higher affinity than β-arr1 [25]. The interaction is transient with the receptor-β-arr complex dissociating at, or near, the plasma membrane. In contrast, "class B" receptors, such as the angiotensin II type 1AR (AT1R), vasopressin V2 receptor (V2R), and thyrotropin-releasing hormone receptor (TRHR), bind β-arr1 and β-arr2 with similar high affinity, and the interaction is more stable, allowing the receptor-β-arr complex to internalize into endosomes [25]. Clusters of serine and threonine residues found in the carboxy-terminal tails of "class B" receptors promote the increased stability of the GPCR-β-arr interaction [26]. The stability of the receptor-β-arr interaction determines whether the GPCRs undergo rapid recycling ("class A") or slow recycling/endosomal targeting ("class B").

β-arrs can also function as E3 ubiquitin ligase adaptors to play key roles in GPCR trafficking [27]. Prolonged β-arr2 ubiquitination leads to sustained receptor interaction and internalization of the receptor-β-arr2 complex to endosomes [28]. In addition to binding E3 ubiquitin ligases, β-arrs also scaffold deubiquitinases (DUBs). The control of β-arr ubiquitination dynamics comes from reciprocal regulation of β-arr by E3 ubiquitin ligases and DUBs. Ligand-induced ubiquitination of β-arr2 by the E3 ubiquitin ligase Mdm2 is essential for β2-AR endocytosis. β-arr2 also interacts with the DUB ubiquitin-specific protease 33 (USP33) that leads to β-arr2 deubiquitination [29]. The "class A" β2-AR elicits a

conformation of β-arr2 that enhances USP33 binding, whereas "class B" V2R induces a conformation of β-arr2 that promotes dissociation of USP33, allowing sustained ubiquitination [29]. The interplay between Mdm2 and USP33 with β-arr2 thus regulates β-arr2 ubiquitination status and dictates GPCR-β-arr complex trafficking properties. β-arr2 can also recruit the E3 ubiquitin ligase NEDD4 to the β2-AR, following agonist stimulation, which results in receptor ubiquitination, lysosomal targeting, and degradation [30]. Downstream of chemokine receptor CXCR4 activation, β-arr1 interacts with the NEDD4-like E3 ubiquitin ligase AIP4 [31]. This interaction does not appear to be required for internalization but plays a role in endosomal sorting of the receptor into the degradative pathway.

β-arrs have also been implicated in the internalization of other non-GPCR integral membrane proteins. These include promoting endocytosis of VE-cadherin with consequences for endothelial cell permeability [32], mediating internalization of the transient receptor potential ion channel family member TRPV4 to regulate intracellular calcium levels [33], and binding to phosphorylated single transmembrane-spanning type III transforming growth factor-β receptor (TβRIII) leading to internalization of TβRII/TβRIII and downregulation of TGF-β signalling [34]. Taken together, these findings indicate that β-arrs participate in the internalization of diverse integral membrane proteins and therefore play additional non-GPCR cargo trafficking roles.

4 β-Arrs as Signalling Scaffolds

In addition to the roles they play in GPCR desensitization and endocytosis, β-arrs are now known to act as multifunctional scaffold proteins, involved in the regulation of multiple signalling pathways (Fig. 1). β-arr-dependent signalling is often spatiotemporally distinct from that of G protein-dependent signalling, giving rise to a specific array of cellular consequences. Yeast two-hybrid screens and global proteomic analyses using β-arrs as bait have uncovered hundreds of potential non-receptor protein partners [10, 23, 35, 36]. These include non-receptor tyrosine kinases, MAPKs, lipid and protein kinases and phosphatases, E3 ubiquitin ligases and deubiquitinases, enzymes implicated in second messenger control, and proteins implicated in the regulation of the cytoskeleton. For a comprehensive overview of the β-arrestin proteome, readers are referred to recent reviews [9, 11, 13, 15, 37], database mining on the subject [16], and focused chapters on β-arr interactions with subsets of non-receptor partners [4, 14, 27, 38–43]. Clearly, given the relatively small size (45 kDa) and interaction interface of β-arrs, they can only engage a limited number of binding proteins at the same time out of hundreds of potential partners [44]. Therefore,

structural changes in β-arrs, varying affinities for partners and different subcellular pools, likely dictate what subset of partners is bound at any one time. A partial list of β-arr-binding partners with functional validation is shown in Table 1, and these are discussed below.

4.1 Endocytic Partners

4.1.1 Clathrin

Clathrin is a key endocytic protein that is required for the formation of clathrin-coated pits (CCPs), which are essential multi-protein structures required for classical receptor endocytosis [45]. The majority of GPCRs are internalized via targeting to CCPs. β-arrs function as adaptors between GPCRs and CCP components including clathrin [22]. The clathrin-binding site in β-arrs is located in the distal part of the flexible carboxy-terminal tail [46], which is deployed downstream of GPCR activation, following interaction of the phosphate sensor and receptor-appended phosphates. The sequence of the binding site corresponds to the clathrin-binding box motif LϕXϕ[D/E] (ϕ is a bulky hydrophobic amino acid and x is a polar residue), which is found in other clathrin-binding proteins such as AP-2 and epsin [47]. The binding site sequences are 373-LIEFD-377 in human β-arr2 and 376-LIELD-380 in human β-arr1 [46]. Mutation or deletion of these motifs results in impairment of clathrin binding and GPCR endocytosis [46, 48, 49]. The β-arr-binding site in clathrin localizes to residues 89–100 in the N-terminal domain of the clathrin heavy chain [50].

4.1.2 AP-2

The clathrin adaptor AP-2 is another key component of CCPs. AP-2 is a stable heterotetramer composed of α, β2, μ2, and σ2 subunits that function in cargo recruitment to CCPs [47]. The α-adaptin and β2-adaptin subunits contain core, hinge, and appendage domains. The appendage domains act as hubs to bind adaptor proteins. β-arr interacts directly with β2-adaptin through a region in its C-terminal tail in close proximity to the clathrin binding box. Laporte et al. initially demonstrated that R394 and R396 in rat β-arr2 were required for β2-adaptin binding and that a β-arr2 R396A mutant displayed defective recruitment to CCPs following β2-AR stimulation [23, 51]. Subsequent studies using biochemical, fluorescence, and crystallographic studies helped define a β2-adaptin-binding consensus [D/E]xxFxx[F/L]xxxR in β-arrs, epsin, and autosomal recessive hypercholesterolemia protein (ARH) [48, 49, 52, 53]. Of particular interest is that this motif undergoes a β-strand to α-helix transition when bound to β2-adaptin, indicating that a conformational change occurs upon β-arr/β2-adaptin binding. R834, W841, E849, Y888, and E902 were shown to be important residues in β2-adaptin required for β-arr binding [52–54]. A recent study used the coordinates of the β-arr C-terminal peptide/β2-adaptin crystal structure [52] to perform a virtual screen of a small molecule library and identified a compound that selectively inhibits the β-arr/β2-adaptin interaction

Table 1
β-Arrestin-binding partners

Partner	β-Arrestin isoform	Functional effect	References
Endocytosis			
Clathrin heavy chain	β-arr1 & 2	Clathrin-mediated endocytosis of GPCRs	[22, 46]
β2-Adaptin	β-arr1 & 2	Clathrin-mediated endocytosis of GPCRs	[23, 51]
μ-Adaptin	β-arr2 > β-arr1	Increased endocytic efficiency of β-arr2	[56]
ARF6/ARNO	β-arr1 & 2	Endocytosis of GPCRs	[24]
SFK & MAPK pathways			
c-Src	β-arr1 & 2	Activation of ERK1/2; Dynamin phosphorylation; β2-adaptin phosphorylation; GRK2 degradation; Cytoskeletal reorganization that stabilizes meningococcus binding to endothelial cells; Colorectal cancer cell migration and metastasis	[60, 62–66, 164]
cRaf1-MEK1/2-ERK1/2	β-arr1 & 2	Cytoplasmic ERK1/2 activation; Feedback control on β2-AR endocytosis; Cytoskeletal reorganization; Regulation of ERK1/2-dependent transcription; Activation of Mnk1/eIF4E-mediated translation	[36, 42, 68–70, 73, 172]
ASK1-MKK4-JNK3 / MKP7	β-arr2	Activation of JNK3; Nuclear to cytoplasmic relocalization of JNK3; JNK3 de-activation (MKP7)	[12, 35, 76–80]
ASK1-MKK3-p38	β-arr1 & 2	Activation of p38 & enhanced chemotaxis; Actin bundle formation; Behavioural stress	[40, 81, 82]
NF-kB pathway			
IκBα/IKK/NIK	β-arr1 & 2	Inhibition of NF-κB activity (IκBα binding)	[101, 102]
CARMA-3	β-arr2	LPA-mediated activation of NF-κB activity	[104]
p65	β-arr1	ET-1- and BK-mediated activation of NF-κB activity	[105, 106]
PI3K/AKT pathway			
PI3K	β-arr1 & 2	Inhibition of PI3K activity in vitro and downstream of PAR-2; Activation of PI3K downstream of the IGF-1R	[87–89]
PTEN	β-arr1 & 2	Increase PTEN activity/decrease AKT signalling & proliferation; Inhibition of PTEN anti-migratory activity; Regulation of mitotic spindle orientation & 3D multicellular assembly	[97, 98]

(continued)

Table 1
(continued)

Partner	β-Arrestin isoform	Functional effect	References
AKT	β-arr2	Inhibition of AKT signalling affecting dopaminergic neurotransmission and behaviour via an AKT/PP2A scaffold; c-Src/AKT scaffold downstream of the insulin receptor leading to AKT activation and metabolic actions in mice	[92–94]
Second messenger control			
PDE4 cAMP phosphodiesterase	β-arr1 & 2	Increased cAMP degradation at the plasma membrane downstream of β2-AR	[83, 84]
Diacylglycerol kinases	β-arr1 & 2	Increased diacylglycerol degradation at the plasma membrane downstream of M1MR	[85]
E3 ubiquitin ligases & DUBs			
Mdm2	β-arr1 & 2	β-arr2 ubiquitination & increased stabilization of GPCR-arrestin complex; Mdm2 cytoplasmic relocalization/promotes p53-driven apoptosis (β-arr2); Scaffolding of Mdm2/p53 in nucleus promotes p53 degradation & DNA damage (β-arr1)	[28, 107, 109–112]
Parkin	β-arr1 & 2	Promotes β-arr-Mdm2 binding & inhibits β-arr ubiquitination	[114]
Nedd4	β-arr1 & 2	NHE1 ubiquitination & endocytosis (β-arr1); Lysosomal degradation of β2-AR (β-arr2)	[30, 115]
TRAF6	β-arr1 & 2	Prevents TRAF6 autoubiquitination & NF-kB activation	[103]
AIP4	β-arr1	Lysosomal targeting of the CXCR4	[31]
USP33	β-arr2	β-arr2 deubiquitination	[29]
Cytoskeleton			
Ral-GDS	β-arr1 & 2	Chemoattractant-induced cytoskeletal regulation; LPA-induced breast cancer cell migration and invasion	[116, 117]
Filamin A	β-arr1 & 2	Regulation of ERK activation & membrane ruffling	[36]
Cofilin/chronophin/LIM kinase	β-arr1 & 2	Regulation of cofilin activity, actin polymerization & cell migration; Control of NDMA-dependent dendritic spine plasticity; Regulation of δOR function & δOR-dependent behaviours	[121–124]

(continued)

Table 1
(continued)

Partner	β-Arrestin isoform	Functional effect	References
Tubulin; microtubules (MTs)	β-arr1 & 2	ERK1/2 recruitment to MTs resulting in reduced active ERK1/2 levels; Mdm2 recruitment to MTs skewing Mdm2 activity to cytoskeletal-associated substrates	[74]
Rho115RhoGEF	β-arr2	RhoA activation/Focal adhesion formation	[120]
ARHGAP21	β-arr1	RhoA activation/stress fibre formation; Cdc42 activation/3D multicellular assembly	[98, 119]
Oligomerization			
Inositol hexakisphosphate (IP6)	β-arr1 & 2	Homo- and heterooligomerization; β-arr1 cytoplasmic localization; Non-receptor β-arr2 conformational activation; Mdm2 cytoplasmic relocalization/increased p53 activity	[111, 125, 135–138]
Nuclear factors			
Histone acetyltransferase CBP/p300	β-arr1	Histone H4 acetylation & transcription of c-fos/p27	[126]
β-Catenin	β-arr1	Increases β-catenin nuclear accumulation/activity & metastasis	[128]
Androgen Receptor (AR)	β-arr1 & 2	β-arr2 scaffolds Mdm2 to AR promoting its degradation; β-arr1 activates AR leading to prostate tumourigenesis	[130, 131]
HIF-1α	β-arr1	Recruitment of p300 to hypoxia response elements & increased HIF-1 target gene expression for invasion/angiogenesis/metastasis	[132, 133]
YY1	β-arr1	Derepression of cdx4-hox pathway to regulate zebrafish hematopoiesis	[127]
PPARγ	β-arr1	β-arr1 inhibits PPARγ/RXR complex & enhances formation of PPARγ/nuclear receptor corepressor complex; Repression of PPARγ-mediated adipogenesis, inflammatory responses, diet-induced obesity. Improves glucose tolerance and systemic insulin sensitivity	[129]

The table displays a partial list of β-arrestin-binding partners with associated functional effect(s) that have been documented

in cells [55]. This chemical inhibitor, dubbed Barbadin, curbs ligand-induced endocytosis of the β2-AR, V2R, and AT1R but doesn't affect transferrin receptor or AP-2-independent ET-AR internalization. Barbadin inhibits V2R-mediated ERK1/2 activation and cAMP accumulation, highlighting that the β-arr/AP-2 interaction is required for both G protein-dependent and β-arr-dependent signalling [55]. The F54 residue in the N-terminal domain of β-arr2 can also engage the μ-adaptin as an endocytic partner, increasing its endocytic efficiency. β-arr1 does not support the same level of endocytosis due to the presence of a tyrosine residue at the equivalent position and modification by Src [56].

4.1.3 ARF6

Both β-arrs can directly bind the GTPase ARF6 and are found in a complex with ARF6 following β2-AR activation [24, 57]. The C-terminal amino acids 319–418 of β-arr1 contain an ARF6 binding site. β-arr also constitutively binds the ARF GEF, ARNO, that promotes GTP loading of ARF6. The activated ARF6 arising from the β-arr/ARF6/ARNO complex mediates the recruitment of AP-2 and clathrin, promoting receptor endocytosis [58, 59].

4.2 Signalling Partners: Src and MAPK Cascades

4.2.1 Src

The first non-GPCR signalling partner identified for β-arr was Src [60]. β-arr-Src complexes are recruited to agonist-stimulated GPCRs where they can influence downstream ERK1/2 and AKT activation [60–62]. The proline-rich N-terminal domain of β-arr1 contains three P-X-X-P motifs that are implicated in binding to the SH3 domain of Src [60]. A β-arr1 P91G/P121E mutant, with two of the P-X-X-P motifs altered, displays reduced Src binding and inhibits ERK1/2 activation [60]. The interaction also involves additional contact with the catalytic SH1 domain of Src [63]. The β-arr1-Src interaction is regulated by phosphorylation. Phosphorylation of S412 in β-arr1 (absent in β-arr2) inhibits Src binding and ERK1/2 activation [60]. Recruitment of Src to activated GPCR-β-arr complexes also promotes β2-adaptin phosphorylation to regulate the interaction of β-arrs with AP-2 and receptor internalization through CCPs [64, 65]. Another point of feedback for GPCR signalling was shown in a study demonstrating that degradation of GRK2 is regulated in a β-arr- and c-Src-dependent manner [66]. β-arr1-mediated Src activation was also shown to be required for EGFR transactivation, downstream AKT activation, and subsequent migration and metastasis of colorectal carcinoma cells [62]. Cells overexpressing a β-arr1 S412D mutant, which mimics phosphorylated β-arr1 and that displays impaired Src binding, exhibited both decreased cell migration and metastasis compared to cells expressing wild-type β-arr1 that metastasize at a high rate [62].

4.2.2 c-Raf1-MEK1/2-ERK1/2 Cascade

One of the most studied signalling roles of β-arrs is their function as MAPK scaffolds. MAPKs are serine/threonine kinases, which phosphorylate nuclear and cytoplasmic substrates to control a wide range of cellular processes including cell proliferation, differentiation, and apoptosis. The MAPK signalling cassette is composed of a triple kinase module consisting of a MAPK kinase kinase that phosphorylates a MAPK kinase that can then activate the terminal MAPK by dual phosphorylation on threonine and tyrosine residues [67]. β-arrs play a role as MAPK scaffolds to colocalize pathway components for efficient and compartmentalized signalling. They can interact with all three kinases of the ERK1/2 cascade, namely, c-Raf1, MEK1/2, and ERK1/2, to promote ERK1/2 activation downstream of multiple GPCRs [42, 68, 69], and cascade assembly is promoted by GPCR stimulation. Compared to G protein-mediated ERK1/2 activation, which is short-lived, β-arr-mediated ERK1/2 activation displays sustained kinetics with consequences for cell growth, survival, and proliferation [42, 70]. In addition, ERK1/2 is sequestered in the cytoplasm by β-arr where it can phosphorylate cytoplasmic substrates to influence non-transcriptional processes such as GPCR trafficking, cytoskeletal rearrangement/migration, and protein translation [42]. β-arrs therefore direct both the kinetics and subcellular localization of GPCR-triggered ERK1/2 activation.

ERK-2, MEK-1, and c-Raf1 interact with the N- and C-domains of both β-arr1 and β-arr2 suggesting that the interaction interface is large [71]. In spite of this, alanine-scanning mutagenesis enabled the identification of a β-arr1 R307A mutant that displayed impaired c-Raf1 binding and that failed to rescue β2-AR/β-arr1-dependent ERK1/2 activation in β-arr1−/−β-arr2−/− mouse embryonic fibroblasts [72]. In a similar manner, SPOT-immobilized peptide arrays of β-arr1 overlayed with MEK-1, coupled with scanning alanine analysis and mutagenesis, also enabled the identification of a β-arr1D26A/D29A mutant that displayed impaired binding to MEK-1 [73]. ERK1/2-dependent phosphorylation of S412 in the β-arr1D26A/D29A mutant was compromised. A cell-permeable β-arr1/MEK-1 interaction disruptor peptide, based on amino acids 6–29 of β-arr1, also impaired ERK1/2-dependent S412 phosphorylation of β-arr1 and promoted its capacity to interact with c-Src and clathrin, facilitating β2-AR endocytosis [73].

Finally, in addition to promoting receptor-triggered ERK1/2 activation, β-arr is also able to reduce active ERK1/2 levels in certain contexts. This is achieved through β-arr-mediated targeting of ERK to microtubules (MTs) [74]. MT-bound and receptor-bound conformations of β-arrs differ resulting in different subsets of mobilized partners. Whereas c-Raf1 and MEK-1 are recruited to

the receptor-β-arr complex, the upstream kinases c-Raf1 and MEK-1 are not mobilized to MTs by β-arrs resulting in dampened basal ERK1/2 activation [74].

4.2.3 ASK1-MKK4/7-JNK3 Cascade

As with the ERK1/2 signalling cassette, β-arrs bind the triple kinase module of the JNK3 cascade: ASK1, MKK4/MKK7, and JNK3 [35, 41]. β-arr2-mediated JNK3 activation has been demonstrated downstream of the activated AT1R or following overexpression of ASK1 or MKK4 [35, 75]. β-arr2 activates JNK3 through binding to its non-conserved extended N-terminus [76]. β-arr2 in its "basal" conformation binds and redistributes JNK3 from the nucleus to the cytoplasm due to the nuclear export signal in the C-terminal tail of β-arr2 [12, 77]. This suggests that β-arr2 is preloaded with JNK3 when recruited to GPCRs. The N- and C-domains of both β-arrs can interact with ASK1, MKK4, and JNK3 although only β-arr2 promotes efficient pathway activation [71]. Interestingly, the first 25 amino acids in the N-domain of β-arr2 display the highest affinity for JNK3 [78], and remarkably this "mini-scaffold" peptide element can also bind ASK1 and MKK4/7 to promote JNK3 activation in cells [79] providing a tool that forms a platform to modulate JNK signalling.

β-arr2 also binds the phosphatase MKP7, a negative regulator of the JNK3 pathway [80]. MKP7 dephosphorylates JNK3 associated with β-arr2, either following activation by ASK1 overexpression or downstream of AT1R stimulation. Following AT1R activation, MKP7 initially dissociates from β-arr2. MPK7 then later reforms a complex with β-arr2 on endocytic vesicles 30–60 min after initial AT1R activation [80]. β-arr2 therefore dynamically associates with positive and negative regulators of the pathway to control active JNK3 levels.

4.2.4 ASK1-MKK3-p38 Cascade

This MAPK cascade is the least well studied in terms of molecular detail underlying β-arr-dependent scaffolding function, but several studies highlight the importance of β-arrs in regulating p38 function. β-arr2 functions as a MAPK scaffold to activate p38 downstream of CXCR4 stimulation to promote CXC12-induced chemotaxis [81]. An ASK1/p38 complex is recruited to β-arr1-bound MKK3 resulting in p38 activation and actin bundle formation downstream of platelet-activating receptor (PAFR) ligation in neutrophils. This process is required for endosomal scission and PAFR internalization [82]. Activated kappa opioid receptor/β-arr-mediated p38 activation also promotes hypertrophy and proliferation of astrocytes in the spinal cord and brain, and plays an important role in behavioral stress response [40].

4.3 Partners Involved in Second Messenger Control

4.3.1 PDE4 cAMP Phosphodiesterase

Following activation of the β2-AR and Gαs protein coupling, the second messenger adenosine 3′,5′-monophosphate (cAMP) is produced. In addition to the role β-arrs play in desensitization of the β2-AR, it was found that they target the cAMP degradation enzyme PDE4 phosphodiesterase to activated receptors at the plasma membrane [83]. β-arrs thus play a dual role in dampening cAMP/PKA signalling through limiting cAMP production via β2-AR desensitization and also increasing cAMP degradation at the plasma membrane. Both β-arr1 and β-arr2 can form a complex with five members of the PDE4D subfamily. Peptide array technology was used to map the sites on β-arr2 required for binding to PDE4D5 [84]. A zone in the cytoplasmic surface of the β-arr2 N-terminal domain including residues K18, T20, and R26 was required for interaction with the common PDE4D catalytic unit, and R286, D291, and the L215-H220 region in the β-arr2 C-terminal domain were also found to be important for the interaction with PDE4D5.

4.3.2 Diacylglycerol Kinases

Following activation of the muscarinic M1 receptor (M1MR) and Gαq protein coupling, the second messenger diacylglycerol (DAG) is produced from the activation of phospholipase C. Analogous to the situation with dampening β2-AR signalling mentioned above, β-arrs were also found to play a dual role in limiting signalling downstream of the M1MR by both promoting desensitization and also binding and recruiting DAG-degrading enzymes diacylglycerol kinases (DGKs) to the activated receptor at the plasma membrane [85]. Both β-arrs can form complexes with α, β, γ, δ, ε, ζ, and ι isoforms of DGKs, and the interaction requires residues 177–253 corresponding to an outer loop in the C-domain of β-arrs and the Cys-rich domains in DGK.

4.4 PTEN/PI3K/AKT Pathway Partners

4.4.1 PI3K

β-arrs can both positively and negatively regulate the PI3K/AKT signalling pathway depending on the receptor input and scaffolding context [14]. Activation of PI3K promotes increased phosphatidyl-3,4,5-trisphosphate (PIP3) formation. PIP3 acts as a signalling intermediate to recruit a number of proteins, including AKT, to the plasma membrane, by binding their PH domains [86]. Activated AKT subsequently phosphorylates a wide range of substrates, causing their activation or inhibition, and this leads to cell growth, survival, and proliferation. When β-arr1 was reintroduced in β-arr1−/−β-arr2−/− mouse embryonic fibroblasts, it promoted the activation of PI3K downstream of the RTK IGF-1R [87]. This activation occurred independently of classical IRS-mediated tyrosine phosphorylation, indicating that even in the absence of this key insulin signalling hub, β-arr1 is recruited to the IGF-1R where it activates PI3K leading to increased AKT phosphorylation and enhanced protection from apoptosis [87]. β-arrs can also inhibit PI3K: both β-arr1 and β-arr2 can directly inhibit PI3K catalytic subunit activity downstream of the protease-activated receptor-2

(PAR-2) receptor [88]. β-arr1 colocalizes with p85 in pseudopodia, and this association with PI3K may therefore spatially inhibit its activity leading to efficient PAR-2-driven chemotaxis [89].

4.4.2 AKT

β-arrs have been shown to activate AKT downstream of several GPCRs including the PAR-1 receptor [90] and the ghrelin receptor [91]. In the case of the ghrelin receptor, AKT activation occurs through an early Gαi/o-dependent pathway and a late β-arr-dependent pathway, which recruits c-Src and AKT. In a similar fashion, β-arr2 can scaffold c-Src and AKT downstream of the insulin receptor leading to AKT activation, which is important for the metabolic actions of insulin in mice [92]. β-arrs can also recruit protein phosphatases to AKT to modulate signalling. β-arr2 forms a complex with PP2A/AKT and GSK-3β downstream of the activated dopamine D2 receptor resulting in dephosphorylation of AKT at Thr308 and thus increased GSK-3β signalling [93]. This scaffolding function of β-arr2 is important for dopamine-associated behaviors in mice, and lithium, used in the management of psychiatric disorders, disrupts the complex [94]. Activated AT1R also regulates this complex by promoting G protein-independent-mediated phosphorylation of the PP2A inhibitor I2PP2A, which is associated with inhibition of β-arr2-PP2A association leading to increased AKT activation [95].

4.4.3 PTEN

An additional point of impact on the PI3K/AKT pathway occurs via β-arr-mediated regulation of the phosphatase PTEN. PTEN is a non-redundant lipid phosphatase that counteracts the action of PI3K by dephosphorylating PIP3 at position D3 to generate PIP2 [96]. PTEN also possesses phosphatase-independent functions important in the control of cell migration and genomic stability [96]. Both β-arrs bind directly to PTEN and stimulate its catalytic activity in vitro [97]. Downstream of GPCR-induced Gα12/RhoA/ROCK signalling, β-arrs recruit PTEN to the plasma membrane, increase PTEN activity, and thus inhibit AKT activation leading to reduced cell proliferation. β-arrs can also regulate lipid phosphatase-independent functions of PTEN. The C2 membrane-binding domain of PTEN inhibits glioma cell migration. Both β-arrs can bind the C2 domain to disinhibit the anti-migratory effect PTEN and thus promote cell migration [97]. Distinct functional outputs of PTEN signalling are therefore regulated by β-arrs resulting in differential control of cell proliferation and migration.

PTEN regulates 3D glandular morphogenesis by linking juxtamembrane signalling to mitotic spindle machinery. The C2 domain of PTEN targets a signalling complex composed of β-arr1, the Cdc42 GTPase-activating protein, ARHGAP21, and Cdc42 to the plasma membrane [98]. In this complex β-arr1 binds and inhibits ARHGAP21, resulting in activated Cdc42, which controls the orientation of cell division and multicellular assembly in 3D

colorectal cancer model systems [98]. Taken together the above studies indicate bidirectional regulatory cross talk between β-arrs and PTEN with implications for cell proliferation, polarity, and migration.

Interestingly, the interaction between arrestins and PTEN is evolutionarily conserved. The unique arrestin orthologue of *C. elegans* ARR-1 was found in a signalling complex with DAF-18, the PTEN orthologue in this organism, which was implicated in the control of DAF-2 (IGF-1R) signalling and longevity [99].

4.5 NF-κB Pathway Partners

The transcription factor NF-κB controls the expression of multiple genes implicated in the regulation of inflammation, cell proliferation, and survival [100]. NF-κB is bound to the inhibitor of NF-κB (IκB) anchoring it in the cytoplasm in an inactive state. Extracellular stimuli, such as TNFα, promote the phosphorylation and subsequent degradation of IκB, allowing NF-κB to translocate to the nucleus. β-arrs bind multiple proteins in the NF-κB cascade, including IκB, IκB kinase (IKK), NF-κB-inducing kinase (NIK), and TNF receptor-associated factor 6 (TRAF6) [101–103]. Downstream of GPCR activation, β-arrs interact with IκB preventing its phosphorylation and degradation, thus blocking TNFα-induced activation of NF-κB. Deletion mapping studies demonstrated that the N-terminal 60 residues in β-arr2 and the C-terminal 42 residues in IκB are important for the interaction [101]. β-arrs also interact with TRAF6, which is involved in Toll-like receptor (TLR)-interleukin 1 receptor (IL-1R) signalling. The β-arr-TRAF6 interaction blocks TRAF6 autoubiquitination and downstream activation of NF-kB and AP-1 [103].

In addition to the negative effects on the NF-κB pathway mentioned above, β-arrs have also been shown to positively modulate the pathway in other contexts. For example, β-arr2 is found in a complex with caspase recruitment domain and membrane associated guanylate kinase-like domain protein 3 (CARMA-3), which is recruited to lysophosphatidic (LPA) receptors and required for LPA-triggered NF-κB activation [104]. β-arr1 can also form a complex with the p65 subunit of NF-κB to promote endothelin-1 and bradykinin-induced NF-κB activation [105, 106]. Mutation of the nuclear localization signal (NLS) in the N-domain of β-arr1 inhibits its nuclear import and decreases bradykinin-induced NF-κB activation [105].

4.6 E3 Ubiquitin Ligase and Deubiquitinase Partners

4.6.1 Mdm2

The E3 ubiquitin ligase Mdm2 was identified as a β-arr-binding partner in a yeast two-hybrid screen [107]. Mdm2 promotes the transient ubiquitination of β-arr2 following stimulation of the β2-AR, which is important for receptor endocytosis [107]. The ubiquitination is thought to enhance interaction of β-arr with the receptor and also clathrin [28, 29, 107, 108]. β-arrs in the "basal" conformation bind Mdm2 most efficiently [12] suggesting that β-arrs are "preloaded" with Mdm2 when they bind the receptor.

The region between amino acids 383 and 410 in the C-terminus of Mdm2 interacts with the intact N-domain of β-arr2 [109]. Mdm2 demonstrates a predominant nuclear distribution when expressed in cells. Under "basal" conditions coexpression of Mdm2 with β-arr2, which contains a nuclear export signal (NES) in its C-terminal tail and is actively excluded from the nucleus [77, 110], results in the displacement of Mdm2 from the nucleus to the cytoplasm [12, 110, 111]. This Mdm2 delocalization leads to increased p53 stability in the nucleus and p53-dependent cell cycle arrest in G_2/M [111], and enhances p53-mediated apoptosis [109]. In contrast, following chronic stimulation of the β2-AR, nuclear β-arr1 scaffolds Mdm2 to p53, facilitating the ubiquitination and degradation of p53, which compromises genome integrity [112].

4.6.2 Parkin

Mutations in the E3 ubiquitin ligase parkin are associated with familial Parkinson's disease [113]. Both β-arrs bind directly to parkin, which promotes β-arr-Mdm2 interaction via shifting β-arrs to the "basal" conformation favored by Mdm2 [114]. As mentioned above Mdm2 normally promotes ubiquitination of β-arr2. Interestingly, although parkin enhances β-arr-Mdm2 interaction, it also dramatically reduces the ubiquitination status of β-arrs suggesting that parkin conceals lysines on β-arr that are normally targeted by Mdm2 [114]. These findings may have implications for Parkinson's disease.

4.6.3 Nedd4

In contrast to Mdm2, which mediates ubiquitination of β-arr2 following stimulation of the β2-AR, β-arr2-bound Nedd4 directs ubiquitination of the agonist-bound receptor [30]. This E3 ubiquitin ligase adaptor role for β-arr2, in mediating ubiquitination of the β2-AR via Nedd4 recruitment, promotes receptor degradation in the lysosomal compartments. β-arr1-bound Nedd4 can also target other plasma membrane proteins including the Na+/H+ exchanger 1 (NHE1), resulting in increased NHE1 ubiquitination and endocytosis [115].

4.6.4 TRAF6

The E3 ubiquitin ligase TRAF6 mediates TLR-IL-1R signalling and downstream activation of the transcriptional activators NF-κB and AP-1. Following TLR-IL-1R activation, β-arrs directly interact with TRAF6 to inhibit TRAF6 autoubiquitination, thus preventing NF-κB and AP-1 activation [103]. β-arr2−/− mice display higher expression of proinflammatory cytokines following endotoxin treatment. Via the interaction with TRAF6, β-arrs therefore act as negative regulators of innate immunity [103].

4.6.5 AIP4

Downstream of chemokine receptor CXCR4 activation, β-arr1 interacts with the NEDD4-like E3 ubiquitin ligase AIP4 [31]. This interaction does not appear to be required for CXCR4 internalization but plays a role in sorting of the receptor from early endosomes to lysosomes, promoting degradation.

4.6.6 USP33

β-arrs also scaffold DUBs. β-arr ubiquitination dynamics results from reciprocal regulation of β-arr by E3 ubiquitin ligases and DUBs. β-arr2 interacts with the DUB USP33 that leads to β-arr2 deubiquitination [29]. The "class A" β2-AR elicits a conformation of β-arr2 that enhances USP33 binding, whereas "class B" V2R induces a conformation of β-arr2 that promotes dissociation of USP33, allowing sustained ubiquitination [29]. The interplay between Mdm2 and USP33 with β-arr2 thus regulates β-arr2 ubiquitination status and dictates GPCR-β-arr complex trafficking properties.

4.7 Cytoskeletal Partners

Ral is a member of the Ras superfamily of small G protein GTPases and is implicated in the regulation of the cytoskeleton and cell migration. Ral proteins are activated following exchange of bound GDP for GTP. Ral GDP dissociation stimulator (Ral-GDS) is a Ral-specific guanine nucleotide exchange factor (GEF) that can activate RalA. β-arr interacts with Ral-GDS in the cytosol of unstimulated cells [116]. Following formyl-Met-Leu-Phe (fMLP) receptor activation, the β-arr-Ral-GDS complex dissociates, and both β-arr and Ral-GDS translocate to the plasma membrane where Ral is activated leading to cytoskeletal reorganization [116]. β-arr/Ral signalling is also implicated in LPA-induced breast cancer cell migration and invasion, and LPA1R, Ral, and β-arr2 mRNA transcripts are found significantly increased in invasive breast cancers [117].

4.7.1 Ral-GDS

4.7.2 ARHGAP21

Agonist-mediated stimulation of the AT1R leads to β-arr1-mediated small GTPase RhoA activation and stress fiber formation in HEK cells [118]. ARHGAP21 is a GTPase-activating protein (GAP) that regulates both Cdc42 and RhoA. β-arr1 binds directly to ARHGAP21 in a region that traverses the RhoA GAP effector domain [119]. Following AT1R stimulation, the β-arr1-ARHGAP21 complex increases, blocking the GAP domain of

ARHGAP21, which promotes RhoA activity and stress fiber formation [119]. In addition to acting as upstream RhoA regulators, β-arrs can also act as downstream RhoA effectors: downstream of GPCR-induced Gα12/RhoA/ROCK signalling, a β-arr/PTEN complex is enhanced and translocated to the plasma membrane, leading to increased PTEN activity, inhibition of the PI3K/AKT pathway, and reduced cell proliferation [97].

β-arr1 interaction with ARHGAP21 also regulates Cdc42 activity in 3D colorectal cancer cell systems. A juxtamembrane complex containing β-arr1, ARHGAP21, Cdc42, and PTEN promotes Cdc42 activity ensuring correct mitotic spindle orientation and 3D glandular morphogenesis [98].

4.7.3 p115RhoGEF

β-arrs have also been shown to interact with RhoA GEFs to regulate active RhoA levels. Under basal conditions β-arr2 forms a complex with p115RhoGEF in the cytosol of resting cells, where it exerts tonic inhibition of RhoA [120]. Following β2-AR activation, β-arr2 inhibition of RhoA is relieved. In this case β-arr2 and p115RhoGEF translocate to the plasma membrane coinciding with increased RhoA activation and the formation of focal adhesions and stress fibers [120]. These findings therefore indicate that β-arrs can fine-tune cellular RhoA activity via regulation of both RhoA activators (e.g., p115RhoGEF) and inhibitors (e.g., ARHGAP21).

4.7.4 Filamin A

Filamin A (FLNA) is an actin-binding protein that acts as a large scaffolding platform to integrate cell signalling events and cytoskeletal reorganization. It plays a key role in integrin turnover during cell migration. FLNA is a 280 kDa dimer composed of an amino-terminal actin-binding domain; 24 repeat regions, each composed of around 96 amino acids; and 2 hinge regions that provide flexibility to the protein. β-arrs were found to bind the C-terminal domains of FLNA (repeats 22–24) and ERK in the same complex [36]. Downstream of activated AT1R and muscarinic M1 receptor, this complex was found to promote efficient ERK activation and membrane ruffling [36]. Interestingly, RhoA, Rac, Cdc42, and GTP-bound RalA also share the β-arr-binding region in FLNA repeats 22–24, perhaps suggesting that FLNA can help provide spatial control for β-arr-mediated small GTPase regulation events.

4.7.5 Cofilin/Chronophin/LIM Kinase

The GPCR PAR-2 employs the scaffolding function of β-arr for chemotaxis. β-arrs scaffold the actin severing protein cofilin, a key player in the formation of the leading edge in migrating cells through its capacity to bind and sever actin filaments, which can serve as seeds for new actin polymerization [39]. Cofilin activity is regulated by phosphorylation/dephosphorylation cycles. Dephosphorylation on Ser3 by phosphatases such as slingshot and chronophin (CIN) promotes cofilin activation, and phosphorylation on

the same residue by LIM kinase (LIMK) results in cofilin inhibition [39]. In the context of PAR-2-mediated cell migration, cofilin dephosphorylation requires both the activity of chronophin and the inhibition of LIMK activity. β-arrs interact with cofilin, chronophin, and LIMK and colocalize with them in membrane protrusions [121]. This results in the scaffolding of cofilin with its activator chronophin, whereas at the same time β-arr inhibits the inhibitor LIMK [121, 122]. The regulatory role of β-arr on cofilin has also been demonstrated downstream of the NDMA receptor, where it regulates dendritic spine plasticity [123], and the GPCR δOR where it regulates actin polymerization, δOR function, and δOR-dependent behavioral effects [124].

4.7.6 Tubulin

Both β-arrs bind microtubules (MTs) in vitro and in cellulo, with β-arr2 displaying stronger interaction than β-arr1 [74]. The MT-binding site on β-arrs contains the concave sides of the N- and C-domains and displays significant overlap with the receptor-binding site, leaving the interaction sites for non-receptor binding partners accessible. However, the affinity of β-arrs for MTs is substantially lower versus activated GPCRs, resulting in receptors dominating over MTs for β-arr binding. Interestingly, a mutant of β-arr1 with a 7-residue deletion in its interhinge domain connecting the N- and C-domains, resulting in a locked basal conformation, enhances binding to MTs. This suggests that MT-bound and receptor-bound conformations of β-arrs are different. β-arr-mediated targeting of ERK to MTs reduces active ERK levels in contrast to that observed with β-arr-mediated targeting of ERK to receptors, which results in ERK activation [74]. This is likely explained in the subsets of mobilized partners, as the upstream kinases c-Raf1 and MEK-1 are not mobilized to MTs by β-arrs, whereas they are recruited to the receptor-β-arr complex. β-arrs also recruit Mdm2 to MTs and in this case redirect the E3 ubiquitin ligase activity of Mdm2 toward cytoskeletal-associated proteins [74].

4.8 Nuclear Factors

A striking difference between the β-arrs is their distribution within the cell under basal conditions. Whereas β-arr1 is localized between the nucleus and cytoplasm, β-arr2 shows an apparent cytoplasmic distribution at steady state. Both β-arrs are actively imported into the nucleus, but β-arr2 is constitutively exported by a leptomycin B-sensitive pathway due to a nuclear export signal (NES) in its C-terminus that is absent in β-arr1 [77, 110]. This is due to a single amino acid change: L394 in human β-arr2 and Q394 in human β-arr1. Substitution to the corresponding amino acid in the other isoform by mutagenesis (i.e., L394Q in β-arr2 and Q394L in β-arr1) results in "rewiring" of the distribution phenotype, with β-arr2ΔNES(L394Q) accumulating in the nucleus and β-arr1+NES(Q394L) displaying a prominent cytoplasmic

localization [77, 110]. These mutants have proved useful for probing nucleocytoplasmic shuttling and nuclear roles of the β-arrs. The nucleocytoplasmic shuttling function of β-arr2 serves to displace nuclear partners such as Mdm2, JNK3, and β-arr1 from the nucleus to the cytoplasm [77, 110, 125]. A nuclear localization signal (NLS) was also recently characterized in β-arr1 [105], and this isoform has scaffolding roles within the nucleus, some of which are discussed below.

4.8.1 Histone Acetyltransferase p300

The first study describing a nuclear scaffolding role for β-arr1 showed that stimulation of the δ-opioid receptor promoted nuclear accumulation of β-arr1, indicating a potential role as a cytoplasm-nucleus messenger [126]. Nuclear β-arr1 was shown to be enriched at specific promoters, such as p27 and c-fos, where it promotes recruitment of the histone acetyltransferase p300 resulting in enhanced local H4 histone acetylation and p27/c-fos transcription [126]. β-arr1 can therefore play a "go-between" role, linking plasma membrane GPCR signalling to epigenetic control within the nucleus.

4.8.2 Yin Yang 1 (YY1)

The same group subsequently identified a physiological role for nuclear β-arr1 in regulating zebrafish hematopoiesis. The transcription factor cdx4 and its downstream *hox* genes were downregulated following β-arr1 depletion in zebrafish embryos, which failed to undergo hematopoiesis and displayed developmental defects [127]. Mechanistically, β-arr1 binds and sequesters the transcription factor YY1, which relieves polycomb group transcriptional repression of the cdx4-hox pathway.

4.8.3 β-Catenin

β-arr1 can also act as an epigenetic regulator of ET-AR-triggered β-catenin signalling in epithelial ovarian cancer (EOC). ET-AR activation promotes nuclear translocation of β-arr1, which promotes β-catenin binding, enhancing its nuclear accumulation and transcriptional activity [128]. The β-arr1+NES(Q394L) mutant, which is actively pumped out of the nucleus, does not display this effect, indicating the importance of prolonged β-arr1 nuclear transit. The N-terminal domain of β-arr1 is important for β-catenin association. The β-arr1-β-catenin complex promotes histone acetyltransferase p300 recruitment to β-catenin target promoters, including endothelin-1, Axin 2, matrix metalloproteinase 2, and cyclin D1. This enhances H3 and H4 histone acetylation and transcription of these genes important for cell migration, invasion, and epithelial-to-mesenchymal transition [128]. The β-arr1-β-catenin complex is also thought to be important for promoting metastasis in a murine orthotopic model of metastatic human EOC, and human EOC tissues display β-arr1-β-catenin complexes enriched at β-catenin target promoters [128].

4.8.4 Peroxisome Proliferator-Activated Receptor-γ (PPARγ)

A major player in the regulation of adipogenesis and macrophage function is the nuclear receptor PPARγ. β-arr1 inhibits the formation of a PPARγ/9-cis-retinoic acid receptor-α (RXR) complex and enhances the formation of a PPARγ/nuclear receptor corepressor complex [129]. This results in the repression of PPARγ-mediated adipogenesis, inflammatory responses, and diet-induced obesity, and improves glucose tolerance and systemic insulin sensitivity. Residues M255, E256, A258, T261, and A263 in the C-domain of β-arr1 are important for the β-arr1-PPARγ interaction.

4.8.5 Androgen Receptor (AR)

The AR is important in the development and progression of prostate cancer. β-arr1 expression levels correlate with AR expression levels and the AR effector prostate-specific antigen (PSA) in prostate cancer cells [130]. siRNA-induced knockdown of β-arr1 results in decreased binding of AR to androgen response elements and reduced transcription of AR-controlled genes. This in turn results in decreased cell proliferation, prostasphere growth, and invasion, in addition to inhibition of prostate tumor formation, invasion, and distant metastasis.

In contrast to β-arr1, β-arr2 can act as a corepressor of AR signalling. β-arr2 forms a complex with Mdm2 and AR, promoting AR ubiquitination and degradation [131]. In line with this, overexpression of β-arr2 decreased, while siRNA-mediated knockdown of β-arr2 increased androgen-induced PSA gene expression in prostate cancer cell lines. Whether the nucleocytoplasmic role of β-arr2 is required for this effect remains to be determined.

4.8.6 Hypoxia-Inducible Factor (HIF-1)

HIF-1 is a major transcriptional activator of genes implicated in adaptive responses to hypoxia. Enhanced nuclear β-arr1 accumulation and associated HIF-1α-dependent transcription of the angiogenic factor VEGF-A were observed in breast cancer cells during hypoxia [132]. Interestingly, treatment of the breast cancer cells with either thalidomide or imatinib mesylate, which suppresses angiogenesis, promoted nuclear exclusion of β-arr1-HIF-1α complexes, and this was linked to reduced HIF-1-mediated transcription. This indicates that nuclear β-arr1 is required for HIF-1-mediated transcription and demonstrates that agents capable of changing β-arr1 subcellular localization can modify β-arr1-mediated effects in cancer signalling pathways. The scaffold role of nuclear β-arr1 in mediating HIF-1α-induced VEGF expression was also demonstrated downstream of the ET-AR in ovarian cancer cells [133].

Cancer cells undergo metabolic reprogramming, switching from oxidative phosphorylation to aerobic glycolysis, to maintain their high proliferation rate, and HIF-1α is a key regulator in this process. A study using genome-wide mapping of chromatin binding for β-arr1 demonstrated that nuclear β-arr1 supports this metabolic switch in prostate cancer cells through HIF-1α-mediated

transcription, by regulating succinate dehydrogenase A and fumarate hydratase expression [134]. This indicates that β-arr1 may function as a tumor promoter in prostate cancer by influencing metabolic alteration.

4.9 Phosphoinositides

β-arrs also interact with nonprotein partners to influence GPCR trafficking and signal transduction. β-arrs bind several different species of phosphoinositides with different affinities. From highest to lowest affinities, these are IP6 > PIP3 > PIP2 > IP4 > IP3 [4, 135, 136]. The crystal structure of a β-arr1-IP6 complex combined with mutagenesis studies identified two IP6-binding sites: a low affinity site in the N-domain involving amino acids K157, K160, and K161 and a high affinity site in the C-domain involving residues K232, R236, K250, K324, and K326 [137]. IP6 promotes homo-oligomerization of β-arr1, and the IP6-binding sites are also required for hetero-oligomerization of β-arr1 with β-arr2. While mutation of either IP6-binding site in β-arr1 impaired oligomerization, interactions with clathrin, AP-2, and ERK2 were conserved. β-arr1 monomers displayed an enhanced nuclear localization [137]. Combined, this suggests that IP6-binding promotes β-arr1 cytoplasmic oligomerization providing a pool of "inactive" β-arr1, which negatively regulates association with plasma membrane and nuclear protein partners.

In contrast to the situation with β-arr1, β-arr2 oligomers were shown to play an active signalling role [111]. Mutation of the equivalent IP6-binding sites in β-arr2 also provoked a loss in β-arr2 oligomerization. While these mutants retained competence for receptor regulation, their capacity to interact and redirect Mdm2 from the nucleus to the cytoplasm was impaired, resulting in loss of p53-dependent antiproliferative effects of β-arr2 [111]. This indicates that β-arr2 oligomerization coupled with its nucleocytoplasmic shuttling role is required to titrate Mdm2 out of the nucleus. In line with these results of a receptor-independent active signalling role for β-arr2, recent structural data indicate that IP6 acts as a non-receptor activator of β-arr2 [138].

5 Structure and Conformations of β-arrs

The ability of β-arrs to regulate GPCRs and also act as scaffolds for signal transduction pathways lies in their capacity to adopt multiple conformations. β-arr1 and β-arr2 have similar basal structures, consisting of an elongated molecule with N- and C-globular domains composed almost completely of antiparallel β sheets that are linked by a short hinge region, and a flexible C-terminal tail region [13]. Two interdomain interactions are key in stabilizing the protein in the basal state with the C-tail participating in both interactions [13]. These are the "polar core" with a set of buried

polar residues (D26, R169, D290, D297, and R393) and the "three element interaction" involving the β-strand I and α-helix of the N-domain and the C-tail (residues V8, L100, L104, L108, I386, and F388). Interfering with either of these interdomain interactions creates "pre-activated" β-arrs that are more readily activated.

Various studies, using low- [139, 140] and high-resolution structural approaches including the X-ray crystallization structure of β-arr1 bound to a C-terminal phosphopeptide of the V2R, with a stabilizing nanobody for β-arr1, have led to a model of conformational change for arrestins bound to the receptor [141]. The model involves the polar core acting as a phosphate sensor for the phosphorylated C-terminal tail of the receptor. Binding of the phosphorylated receptor tail results in the release of the β-arr C-tail, through disruption of the polar core by binding to positively charged residues, thus destabilizing basal interdomain interactions. This is associated with a marked 20° rotation between the N- and C-domains and exposure of parts of β-arr, including the interhinge domain, and the finger, middle, and lariat loops that act as an activation sensor. Interestingly, the structure of β-arr2 in complex with IP6 also demonstrates these hallmark features of active arrestin with an interdomain rotation and displaced C-tail, indicating a non-receptor activation mode of β-arr2 [138].

Single particle negative-stain electron microscopy has also enabled the visualization of β-arr recruitment by a GPCR and identified two distinct conformational populations: the "partially engaged" complex where β-arr1 associates with the receptor tail only and the "fully engaged" complex where β-arr1 associates with both the receptor tail (through the phosphate sensor) and the receptor transmembrane core (through the activation sensor). This reveals a biphasic mode of GPCR-β-arr interaction. Subsequent studies have revealed that the "tail only" conformation can support both endocytosis and β-arr-dependent signalling, whereas the "fully engaged" conformation is required for desensitization [142–144]. Whereas β-arr and G protein binding to GPCRs are traditionally thought of as mutually exclusive consistent with the "fully engaged" β-arr conformation, the "partially engaged" conformation opened up the possibility of deciphering further insight into GPCR-β-arr complexes. Indeed, a study using single particle negative-stain electron microscopy revealed the formation of a "supercomplex" where a "partially engaged" β-arr1 conformation with the receptor tail resides along with a receptor core interaction with heterotrimeric Gαs proteins [145]. This provides structural insight into the sustained G protein signalling sometimes observed on endosomes from internalized receptors.

It is also possible to monitor dynamic conformational changes in live cells using resonance energy transfer (RET)-based approaches. An intramolecular Rluc-β-arr2-YFP bioluminescence

resonance energy transfer (BRET)-based biosensor [146] and a series of fluorescein arsenical hairpin (FlAsH) binder fluorescence resonance energy transfer (FRET)-based β-arr2 biosensors [147] demonstrated that β-arr2 conformational rearrangement detected by RET changes follows the initial GPCR/β-arr engagement. This agrees with the structural data above that the disruption of the polar core by the phosphorylated GPCR C-terminus drives the basal to active β-arr transition. Use of the FlAsH FRET-based β-arr2 biosensors and also a series of FlAsH-BRET-based β-arr2 biosensors [148], allowing the assessment of β-arr2 conformational rearrangement from multiple perspectives, demonstrated that β-arr2 adopts different conformations downstream of different GPCRs. Furthermore, the FlAsH FRET study demonstrated that downstream of the β2-AR the conformational change of β-arr2 persisted after dissociation from the receptor indicating that β-arr2 remains in an active "effector-competent" conformation [147]. This would permit signal amplification akin to the situation with G protein-mediated signalling. Further data in favor of this "activation at a distance" mechanism comes from a study demonstrating that following dissociation from its activating β1-AR GPCR, β-arr2 robustly accumulates in clathrin-coated structures to activate ERK1/2 signalling [149]. These studies therefore collectively demonstrate that β-arrs adopt receptor type-specific conformations triggered by the different GPCRs to permit appropriate transmission of information flow into the cell.

6 β-arr-Biased Signalling

Following on from the initial findings that β-arrs can act as signal transducers in their own right, independently of G proteins, came the discovery that certain ligands targeting GPCRs can selectively promote either G protein- or β-arr-dependent signalling [150, 151]. It is therefore possible to dissect apart these distinct signalling branches pharmacologically. In contrast then to "unbiased" agonists, which trigger both G protein- and β-arr-mediated signalling, these "biased" agonists preferentially activate either the G protein- or β-arr-mediated pathway leading to "biased" signalling (Fig. 2). This transformed the idea of thinking of GPCRs as linear signalling entities with one active and one inactive conformation, to a scenario where they can adopt multiple different conformations and signalling behaviors [151]. Signalling bias has further additional layers, including coupling of GPCRs to different G proteins, differential phosphorylation of the receptor by GRK family members, and different conformational shifts in β-arrs resulting in varying functional outcomes.

One of the best-studied GPCRs in the investigation of biased signalling is the AT1R. In angiotensin II (AngII), the octapeptide

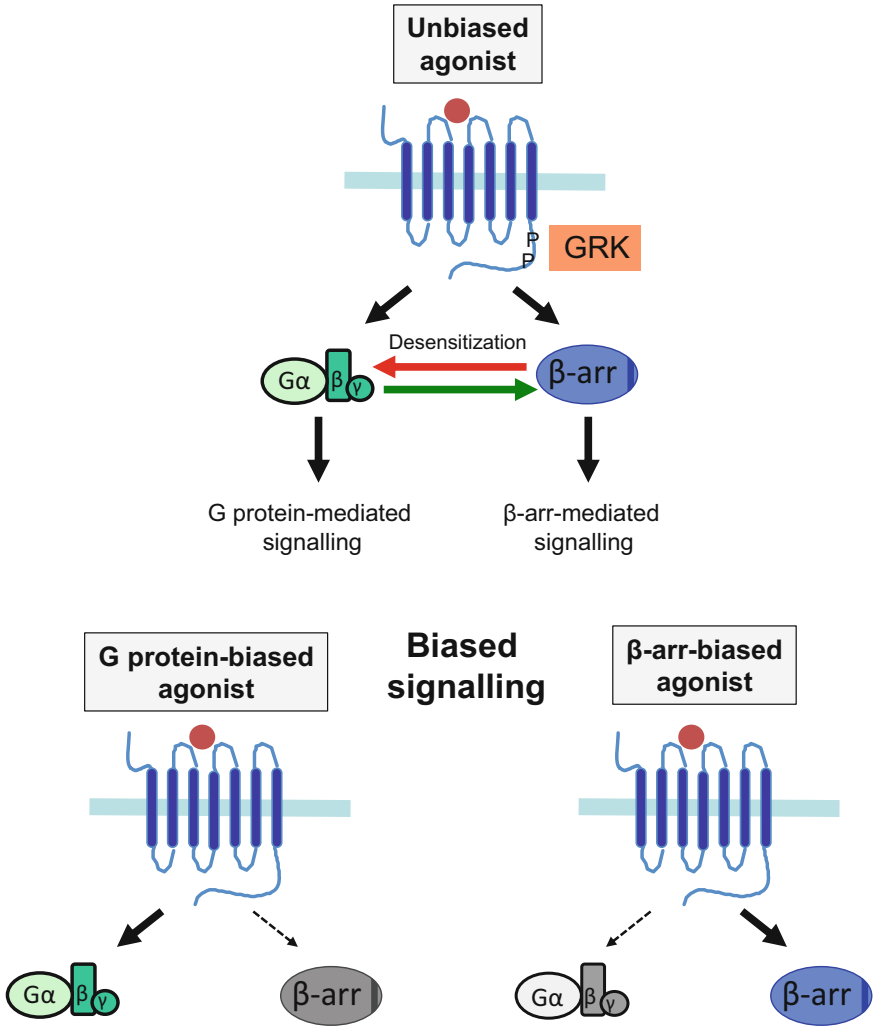


Fig. 2 Different types of biased GPCR signalling. A "classical" balanced agonist triggers both G protein- and β-arr-mediated signalling. β-arr desensitizes G protein coupling, and G proteins can positively impact β-arr-mediated ERK signalling. In the case of biased agonists, the ligand-receptor complex preferentially activates either the G protein- or β-arr-mediated pathway leading to biased signalling. Biases between different G protein-mediated or β-arr-mediated responses may also occur

ligand for the AT1R, Y at position 4 and F at position 8 are important for both AT1R ligand binding and G protein-dependent signalling. Changing the residues at these positions antagonizes G protein-mediated signalling to produce β-arr-biased ligands. An example of a β-arr-biased ligand is SII [(Sar1, Ile4, Ile8)-Ang], where Sar is N-methylglycine. This compound promotes β-arr recruitment to the AT1R and downstream β-arr-dependent ERK signalling [152]. Studies using a series of AngII analogues carrying substitutions at position 8, and either an intramolecular BRET-based double-brilliance β-arr biosensor or intramolecular FlAsH-

BRET β-arr biosensors, demonstrated that the analogues elicited differential conformational signatures in β-arr [148, 153]. GRK classes differentially affected these conformational rearrangements in β-arr, with GRK6 having a greater influence than GRK2. The efficacy of the analogues on ERK1/2 activation correlated with stability of the AT1R-β-arr complexes on endosomes, rather than with the ability of the receptor to recruit β-arr. The analogue-triggered conformational changes in β-arr determined whether the ligand promoted β-arr-dependent cell migration or proliferation [153]. Taken together, these findings indicate that different AngII analogues induce distinct conformational signatures of β-arr that specify divergent functional cell outputs.

Biased ligands of GPCRs may provide an opportunity to skew receptor signalling in a manner that enables the isolation of therapeutic properties from side effects, providing improved drugs. The AngII analogue TRV120027 competitively antagonizes AngII-stimulated G protein signalling but activates β-arr-mediated Src, ERK1/2, and endothelial nitric-oxide synthase phosphorylation, and promotes increased cardiomyocyte contractility in vitro, unlike unbiased antagonists [154]. As with the unbiased antagonists losartan and telmisartan, TRV120027 reduced mean arterial pressure in rats. In contrast, however, to the unbiased antagonists, which decreased cardiac performance, TRV120027 increased cardiac performance and preserved cardiac stroke volume [154]. In a model of heart failure in canines, TRV120027 demonstrated cardiac unloading actions while maintaining renal function, indicating that it may have potential as a novel drug for heart failure treatment [155, 156]. While these preclinical studies hold great promise, the challenge of translating these findings into therapeutic possibilities in humans is highlighted by a recent assessment of the β-arr-biased agonist TRV027, which did not improve clinical status in a phase IIb clinical trial [157].

Many other examples of ligand bias for multiple GPCRs, favoring either G protein- or β-arr-dependent signalling, as well as their therapeutic implications have been documented, and these are discussed elsewhere [150, 158–160]. Despite a large body of work pointing to a role of β-arr as a signalling scaffold in ERK signalling for GPCRs, the concept of β-arr-dependent ERK signalling being completely G protein-independent has also recently been challenged by two studies using genome-edited cells [161, 162]. These studies suggest β-arrs may instead act as "rheostats" downstream of G proteins to shape GPCR-triggered G protein-dependent ERK signalling, thus controlling the intensity, kinetics, and subcellular location of ERK activation. Another recent study also using genome-edited and siRNA approaches has provided insight on β-arr's role in these two pathways, reconciling both their function as regulators of G protein- and β-arr-dependent ERK signalling [163]. This study suggests that β-arrs participate

both in regulation of MAPK activation by Gαs-coupled receptors through dampening the receptor/G protein-dependent response and in the scaffolding of ERK by β-arrs, and that the balance of pathways varies among Gαs-coupled receptors and the β-arr-depleted cells used. Additional studies will be required to further define the contribution of β-arrs in these two signalling pathways leading to MAPK engagement for other GPCRs and for refining how this evolving concept of β-arr-dependent signalling also applies to other β-arr-scaffolding/signalling arms.

In addition to ligand-activated β-arr-biased signalling, the bacterium that causes cerebrospinal meningitis, *Neisseria meningitidis*, can trigger a biased β2-AR/β-arr signalling response in brain endothelial cells [164]. This ultimately leads to the bacterial hijacking of β-arr-binding partners such as c-Src and junctional proteins under the colonies. Cytoskeletal rearrangement driven by β-arr-dependent Src activation secures bacterial adhesion to endothelial cells, and β-arr-mediated mislocalization of junctional proteins leads to the formation of anatomical gaps permitting the bacteria to cross the brain endothelium [164]. Mechanical or osmotic stress of cells can also lead to ligand-independent β-arr-biased signalling downstream of the AT1R [165].

7 β-arr Compartmentalization

Compartmentalization of associated protein partners also provides texture into how β-arrs control signal transduction to orchestrate cellular regulation (Fig. 3). Certain conformations of β-arrs are associated with distinct cellular pools, and localization signals encoded in their primary sequence can also act as "postcodes" to direct subcellular targeting and signalling.

7.1 Cytosolic Pools

Under steady-state conditions, β-arrs are found in the cytosol in the basal conformational state. Several partners demonstrate preference for this conformation including calmodulin, Mdm2, and JNK3 [12, 166] (Fig. 3). The calmodulin-binding site significantly overlaps receptor and MT-binding sites, and basal β-arr can therefore sequester calmodulin (Fig. 3). The β-arr-calmodulin complex likely regulates their availability for other interaction partners [166]. In addition β-arr2 is constitutively ejected from the nucleus via its NES, resulting in cytoplasmic sequestration of nuclear partners such as Mdm2 (Fig. 3) and JNK3 [77, 110, 111]. This changes Mdm2 and JNK3 target profiles with consequences for cytoplasmic and nuclear signalling. In the case of Mdm2, β-arr is considered "preloaded" with the E3 ubiquitin ligase, which helps prime its ubiquitination following β2-AR activation [107]. Finally, the recent structure of β-arr2 in complex with the cytosolic inositol IP6 demonstrates hallmark features of active arrestin with an

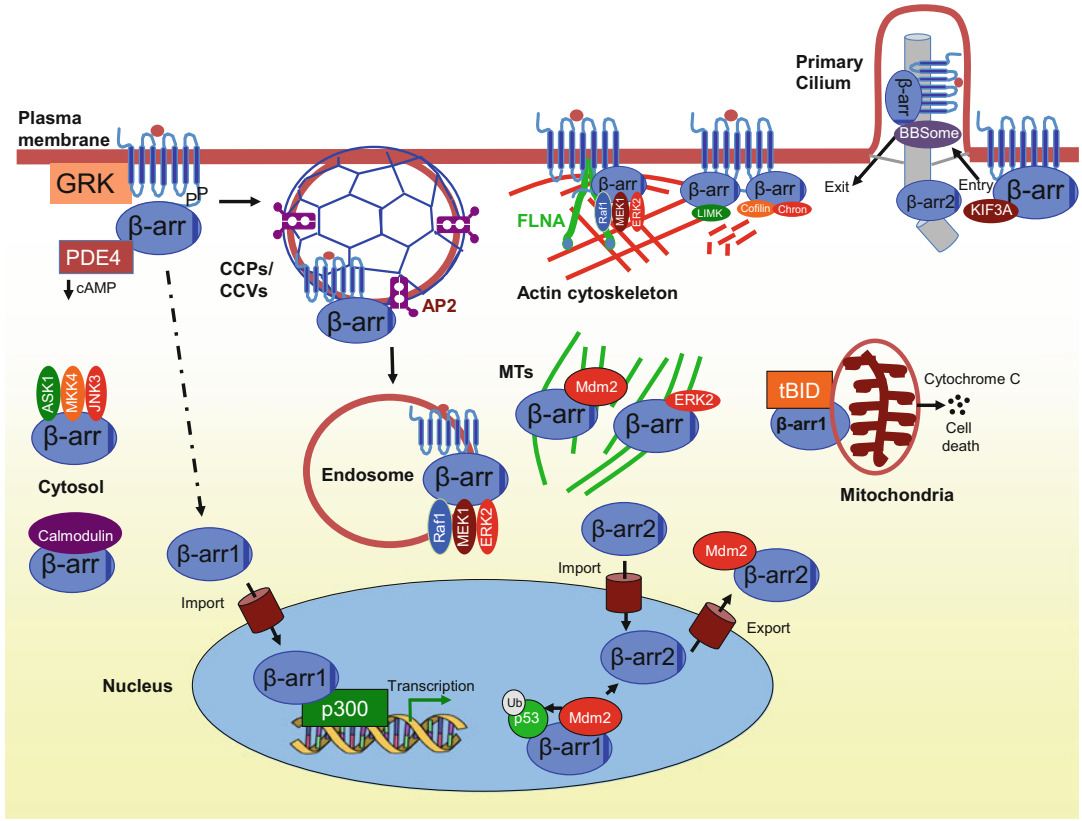


Fig. 3 Subcellular pools of β-arrestins. Calmodulin, Mdm2, and JNK3 bind cytosolic pools of β-arrs. Following phosphorylation of GPCRs by GRKs, β-arrs translocate from the cytoplasm to activated receptors at the plasma membrane, promoting desensitization. They also target PDE4 to the plasma membrane to increase cAMP degradation. Following binding of β-arrs to GPCRs, the β-arr C-terminal tail is deployed, unveiling clathrin and AP-2 binding sites. This permits targeting of the GPCR-β-arr complex to CCPs, which is essential for clathrin-mediated endocytosis. Class B GPCR-β-arr complexes traffic to endosomes and can assemble the Raf1/MEK1/ERK1/2 cassette. This leads to prolonged and spatially cytoplasmic-restricted activated ERK1/2 signalling. β-arrs can interact with the cytoskeletal accessory proteins filamin, involved in MAPK signalling, actin filament bundling, and integrin turnover, and cofilin, implicated in actin filament polymerization/depolymerization, to regulate actin cytoskeleton dynamics. β-arrs bind MTs, and the MT-binding site overlaps the receptor-binding site indicating that they are mutually exclusive. β-arr recruits ERK (but not Raf1 and MEK1) to MTs resulting in dampened basal ERK1/2 activation. β-arrs also target Mdm2 to MTs, and this directs Mdm2 activity toward cytoskeleton-associated proteins. β-arrs can localize in the primary cilium (PC). β-arrs bind KIF3A and transport Smoothened to the PC. β-arrs were also found to be important for activated GPCR retrieval from cilia back into the cell. Both β-arrs are actively imported into the nucleus, but β-arr2 is constitutively exported via its NES. The nucleocytoplasmic shuttling function of β-arr2 displaces nuclear Mdm2 from the nucleus to the cytoplasm. An NLS in β-arr1 promotes nuclear import and scaffolding roles within the nucleus, enhancing recruitment of p300 to specific promoters. Nuclear β-arr1 also scaffolds Mdm2 to p53, facilitating the ubiquitination and degradation of p53. A cleavage fragment β-arr1(1-380), lacking the C-terminal tail, translocates to mitochondria where it binds and cooperates with pro-apoptotic tBID, resulting in increased cytochrome C release and cell death

interdomain rotation and displaced C-tail, indicating a non-receptor activation mode of β-arr2 [138]. This indicates that cytosolic non-receptor-activated conformations of β-arr2 likely exist, and these are capable of β-arr2-dependent JNK3 signalling.

7.2 Plasma Membrane Pools

Plasma membrane-associated pools of β-arrs are involved in GPCR desensitization, targeting receptor toward endocytic pathways, second messenger degradation, and control of signal transduction pathways. Subsequent to phosphorylation of GPCRs by GRKs, β-arrs translocate from the cytoplasm to the activated receptors at the plasma membrane, where β-arr binding to the phosphorylated receptors inhibits GPCR-G protein coupling, giving rise to desensitization [2, 21]. In addition to the roles β-arrs play in GPCR desensitization, they target the cAMP degradation enzyme PDE4 cAMP phosphodiesterase to the activated β2-AR at the plasma membrane, thus increasing cAMP degradation at the plasma membrane (Fig. 3), and in a similar fashion recruit DAG-degrading enzymes diacylglycerol kinases (DGKs) to the activated M1MR receptor at the plasma membrane [83, 85].

Plasma membrane-bound pools of β-arrs are also implicated in RTK transactivation, and β-arr1 is recruited to the IGF-1R where it activates PI3K leading to increased AKT phosphorylation and enhanced protection from apoptosis [87]. β-arrs can also inhibit PI3K at the plasma membrane: both β-arr1 and β-arr2 can directly inhibit PI3K catalytic subunit activity downstream of the PAR-2 receptor [88, 89]. Interplay between β-arrs and PTEN at the plasma membrane also impacts the PI3K/AKT pathway. Following LPA1R activation, β-arr2 and PTEN are co-recruited to the plasma membrane, and PTEN through its lipid phosphatase activity converts the lipid signalling intermediate PIP3 to PIP2 resulting in PI3K/AKT pathway inhibition and decreased cell proliferation [97]. In addition, in colorectal cancer cell systems, the C2 domain of PTEN assembles a signalling complex composed of β-arr1, the Cdc42 GTPase-activating protein, ARHGAP21, and Cdc42 at the plasma membrane, which controls the orientation of cell division and multicellular assembly [98].

7.3 Endocytic Pools

Following binding of β-arrs to GPCRs and disruption of the interdomain interactions, the β-arr C-terminal tail is deployed, unveiling clathrin and AP-2 binding sites [22, 23, 51]. This permits targeting of the GPCR-β-arr complex to pre-existing clathrin-coated pits [167], which is essential for clathrin-mediated endocytosis (Fig. 3). Interestingly, mutants targeting the interdomain interactions can be found constitutively targeted to clathrin-coated pits in the absence of GPCR stimulation [49]. The stability of the receptor-β-arr interaction and β-arr ubiquitination dynamics determine whether the GPCRs undergo rapid recycling ("class A") or slow recycling/endosomal targeting ("class B") [26, 168]. The GPCR-

bound conformation of β-arrs preferentially binds ERK1/2 and c-Raf1 promoting MAPK cassette assembly on endosomes [69] (Fig. 3). This leads to prolonged ERK1/2 signalling and also spatially cytoplasmic-restricted activated ERK, resulting in inhibition of nuclear Elk-1 signalling [169]. The β-arr-associated cytoplasmic pool of activated ERK also influences its phosphorylation by ERK with consequences for clathrin binding and GPCR endocytosis [73, 170].

7.4 Cytoskeletal Pools

Proteomic studies revealed that 15% of the β-arr interactome was made up of cytoskeletal proteins [10]. β-arrs bind constituent proteins of cytoskeleton filaments, cytoskeletal accessory proteins, and motor proteins. This is in line with the roles attributed to β-arrs in cytoskeletal reorganization, cell migration, and metastasis [171]. β-arrs can localize in membrane protrusions and ruffle structures following GPCR activation [36, 172]. They interact with the cytoskeletal accessory proteins filamin, involved in MAPK signalling, actin filament bundling, and integrin turnover, and cofilin, implicated in actin filament polymerization/depolymerization, to regulate actin cytoskeleton dynamics [36, 121] (Fig. 3).

β-arrs also bind MTs, and the MT-binding site overlaps the receptor-binding site indicating that they are mutually exclusive [74]. MT-bound and receptor-bound conformations of β-arrs differ resulting in different subsets of mobilized partners. Whereas c-Raf1, MEK-1, and ERK1/2 are recruited to the receptor-β-arr complex, the upstream kinases c-Raf1 and MEK-1 are not mobilized to MTs by β-arrs, resulting in dampened basal ERK1/2 activation [74] (Fig. 3). β-arrs also target Mdm2 to MTs, and this directs Mdm2 activity toward cytoskeleton-associated proteins, resulting in their increased ubiquitination (Fig. 3). The affinity of β-arrs for MTs is substantially lower versus activated GPCRs, indicating that MT-associated pools can be mobilized to the plasma membrane upon receptor stimulation [74]. Both MT targeting and recruitment of clathrin facilitate focal adhesion disassembly. In this context β-arrs regulate focal adhesion dynamics and thus cell adhesion by providing a molecular link between MTs and clathrin [173]. This property of β-arrs is independent of GPCRs as mutants defective in GPCR regulation have the same effect on focal adhesion dynamics as wild-type β-arrs.

β-arrs have also been found localized in primary cilia (PC), antenna-like sensory/signalling structures at the cell surface of most quiescent cell types that are highly enriched in GPCRs [174, 175]. β-arrs bind KIF3A (Fig. 3), a subunit of the dimeric anterograde intraflagellar transport (IFT) motor kinesin II. Multiple ciliary roles have been attributed to β-arrs including the transport of Smoothened to PC [175] and in ciliogenesis [174]. β-arr2 is exported from cilia via the multimeric BBSome

complex [176], which acts in concert with the IFT to control cargo transport in and out of cilia (Fig. 3). β-arrs were also found to be important for activated GPCR retrieval from cilia back into the cell [177–179] mirroring their function as receptor cargo adaptors in clathrin-mediated endocytosis.

7.5 Nuclear Pools

Both β-arrs are actively imported into the nucleus, but β-arr2 is constitutively exported by a leptomycin B-sensitive pathway due to a NES in its C-terminus that is absent in β-arr1. The nucleocytoplasmic shuttling function of β-arr2 serves to displace nuclear partners such as Mdm2 (Fig. 3), JNK3, and β-arr1 from the nucleus to the cytoplasm [77, 110, 125]. A nuclear localization signal (NLS) has also been characterized in β-arr1 [105], and this isoform has scaffolding roles within the nucleus, notably by promoting recruitment of the histone acetyltransferase p300 to specific promoters (Fig. 3) including c-fos, p27 [126], and β-catenin target promoters [128]. The importance of prolonged β-arr1 nuclear transit is demonstrated by the "rewired" β-arr1+NES(Q394L) mutant, which is actively ejected out of the nucleus and therefore loses the nuclear scaffolding role. β-arr1 can therefore play a "go-between" role, linking plasma receptor signalling to epigenetic control within the nucleus. Interestingly, increased nuclear accumulation of β-arr1 has been observed in lung, breast, and ovarian cancers [14], and nuclear β-arr1 drives a metabolic switch in prostate cancer, through HIF-1α-mediated transcription, favorable for tumor progression [134].

7.6 Mitochondrial Pool

Cytochrome C release from mitochondria promotes caspase-3/7 activation during cell commitment to apoptosis. β-arr1 is cleaved in its C-terminus at caspase cleavage sites (D/VxxD) by caspases during apoptosis [180]. The main cleavage fragment β-arr1 (1-380) translocates to mitochondria where it binds and cooperates with pro-apoptotic tBID resulting in increased cytochrome C release (Fig. 3). A caspase-resistant β-arr1 mutant loses its ability to provide sensitivity to apoptotic stimuli.

8 β-arr Regulation

The expression and function of β-arrs are fine-tuned at transcriptional, posttranscriptional, and posttranslational levels. The combination of these regulatory mechanisms on β-arr levels impacts β-arr actions in trafficking and signalling, giving rise to cellular outcomes.

8.1 Transcriptional Level

β-arr1 and β-arr2 gene expression is differentially regulated by glucocorticoids [181]. Glucocorticoids enhance the expression of β-arr1 and repress the expression of β-arr2 via the recruitment of ligand-activated glucocorticoid receptors (GRs) to conserved and

functional glucocorticoid receptor elements (GREs) localized within introns of the β-arr genes (Fig. 4a, b). While intron 1 in the β-arr1 gene contains a classical GRE that functions as a glucocorticoid-dependent enhancer (Fig. 4a), intron 11 in the β-arr2 gene contains an inverted repeat negative GRE (nGRE) that acts as a glucocorticoid-dependent repressor (Fig. 4b), explaining these differential effects on β-arr1 and β-arr2 expression.

β-arr1 is also a transcriptional target of NF-κB. β-arr1 promoter activity is enhanced following NF-κB activation (Fig. 4a) due to the presence of a conserved κB site, leading to increased β-arr1 expression [182]. β-arr1 then operates a negative feedback loop by interfering with the p50–p65 interaction to decrease NF-κB transcriptional activity in TNF-α-induced cell death.

8.2 Posttranscriptional

MicroRNAs (miRNAs) are a class of small noncoding RNAs containing 18–24 nucleotides. These short RNAs can negatively regulate gene expression by complementary binding to the 3-untranslated region (3′-UTR) of target transcripts, leading to translation inhibition and/or mRNA degradation. One single miRNA may target the expression of many different genes. Conversely, one transcript may be targeted by distinct miRNAs.

Several miRNAs have recently been shown to target β-arrs (Fig. 4a, b): miR-525-3p (targets β-arr1), miR-365, miR-150, and miR-155 (all target β-arr2). Expression of miR-525-3p is increased following ionizing radiation exposure. Downregulation of its direct targets including β-arr1 is required for cell survival following irradiation [183]. Increased expression of miR-365 leads to decreased β-arr2 expression [184]. β-arr2 is an important modulator of morphine tolerance [185], and it was found that miR-365 was robustly decreased in the spinal cord following chronic morphine administration. Downregulation of miR-365 is therefore involved in the development of morphine tolerance through regulation of β-arr2, and increasing miR-365 may provide a potential therapeutic approach to enhance morphine analgesia. MiR-150 is selectively expressed in mature B and T cells and is implicated in the differentiation and activation of immune cells. MiR-150 repressed β-arr2 levels, leading to decreased cytokine production and negative regulation of T-cell function [186]. Finally, β-arr2 is a target for miR-155, and this regulation is important for 5′-azacytizine-induced differentiation of cardiac stem cells into cardiomyocytes [187].

8.3 Posttranslational Modifications

There are multiple posttranslational modifications, including phosphorylation, ubiquitination, SUMOylation, S-nitrosylation, and hydroxylation that control β-arr function in both trafficking and signalling events (Fig. 5). These are described below.

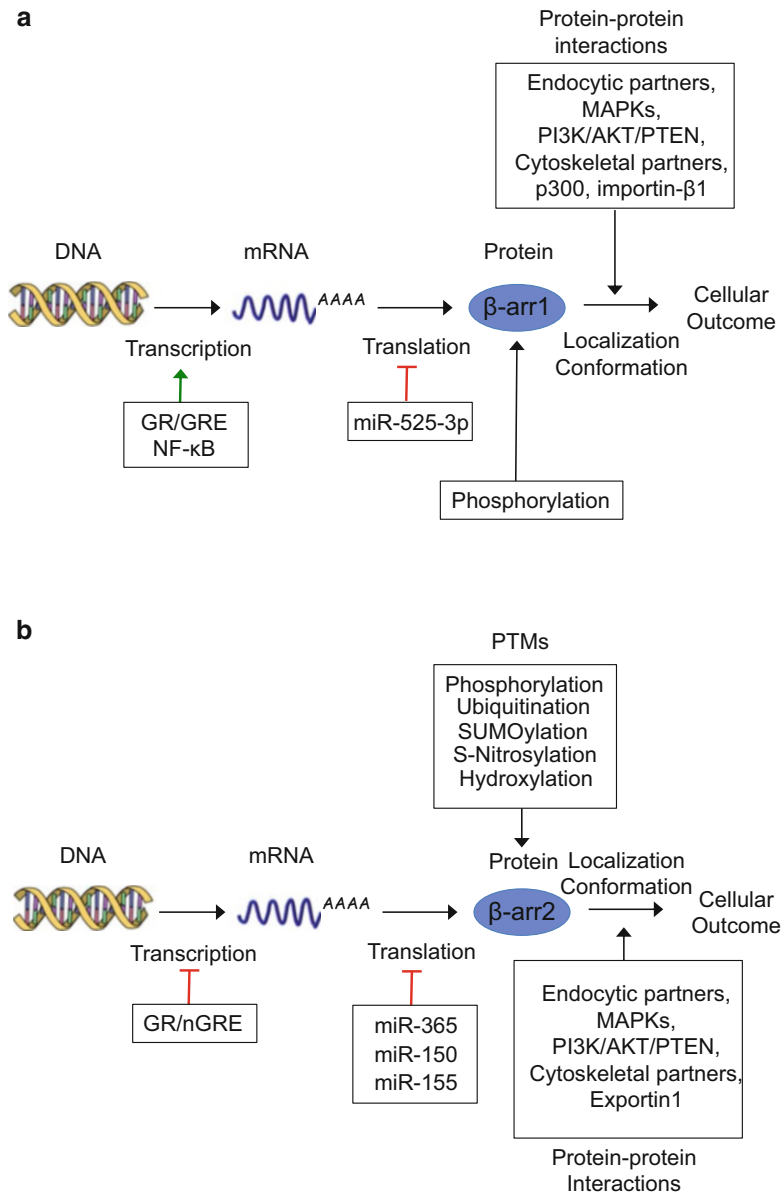


Fig. 4 Control of β-arrestin expression and regulatory posttranslational events dictating cell outcomes. The diagram depicts the different mechanisms by which (**a**) β-arr1 and (**b**) β-arr2 expression are regulated and posttranslational modifications that impact β-arr function. These include positive and negative regulation of *β-arr* mRNA by transcription factors, *β-arr* mRNA degradation and translation repression by miRNAs, and posttranslational modifications, which impact protein function. These events coupled with the resulting scaffolding functions of β-arrs, based on conformation and their subcellular localization, lead to cell outputs

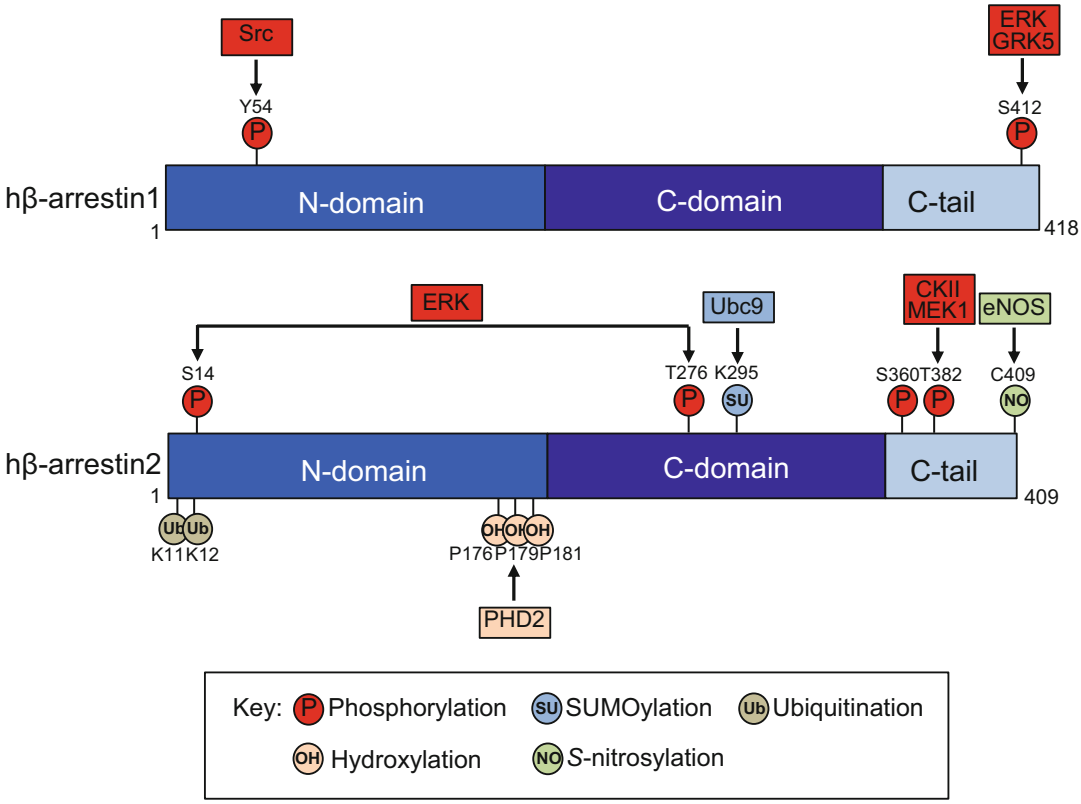


Fig. 5 Posttranslational modifications of β-arrestins. Sites of phosphorylation, ubiquitination, SUMOylation, S-nitrosylation, and hydroxylation on β-arr1 and β-arr2 are indicated. The amino acid numbering is based on the human forms of β-arrs. Enzymes involved in these posttranslational modifications of β-arrs are also shown

8.3.1 Phosphorylation

Both β-arrs are regulated by phosphorylation/dephosphorylation cycles in the carboxy-terminal tails. β-arr1 is constitutively phosphorylated at S412 (which is absent in β-arr2) in the carboxy-terminal tail by ERK1/2 [170] and GRK5 [188] (Fig. 5). Dephosphorylated β-arr1 promotes targeting of the β2-AR to clathrin-coated pits and is also required for maximal c-Src binding and ERK1/2 activation [60]. In contrast, phosphorylation of S412 inhibits β2-AR endocytosis and β-arr1-c-Src interaction leading to dampened ERK1/2 signalling. Colorectal carcinoma cell lines engineered to express a S412D mutant of β-arr1, which mimics phosphorylated β-arr1 and that displays impaired binding to c-Src, exhibit decreased cell migration in vitro and metastasis in vivo compared to β-arr1 wild-type expressing cells that metastasize at a high rate [62]. The phosphorylation of S412 by GRK5 was also proposed to inhibit Src/ERK pathway activation downstream of the 5-HT(4) receptor [188]. In a similar manner, β-arr2 is regulated by a phosphorylation/dephosphorylation mechanism. β-arr2 is constitutively phosphorylated in its carboxy-terminal tail, and dephosphorylation is required for targeting of receptors for

internalization [189]. The phosphorylation sites are however different: S361 (S360 in human sequence) and T383 (T382 in human). Both sites are absent in β-arr1. Phosphorylation at T383 is mediated by casein kinase 2 (Fig. 5) [189], and it was proposed that this posttranslational modification regulates formation of a large β-arr2-containing protein complex [190]. A last point of control on this site is via MEK-1-dependent phosphorylation (Fig. 5), which is required for ERK1/2 recruitment to a 5-HT_{2C} receptor-β-arr complex and ERK1/2 activation [191]. This mode of β-arr-mediated ERK1/2 activation is also found downstream of the β2-AR, FSH, and CXCR4 receptors. Several regulatory phosphorylation events occur outwith the carboxy-terminal tails of β-arrs in the globular N- and C-domains. The first of these is a Src phosphorylation site, Y54 (Fig. 5), in the N-domain of β-arr1 that again is absent in β-arr2 [56]. The Y54 site decreases β-arr1 association with μ-adaptin, and mutation of this site to the residue found in β-arr2 Y54F improves β-arr1-μ-adaptin interaction and the capacity to promote β2-AR internalization. Taken together these data indicate that β-arr2 engages μ-adaptin as an endocytic partner, increasing its endocytic efficiency, and that β-arr1 does not support the same level of endocytosis due to the Y54 residue and modification by Src [56]. β-arr2 can also be phosphorylated by ERK1/2 on S14 and T276 (Fig. 5) [192]. Phosphorylation on these sites by ERK1/2 activation with constitutively active forms of Ras and MEK, as well as via stimulation of receptor tyrosine kinases or GPCRs, promotes intracellular sequestration of a large panel of GPCRs. This leads to global dampening of cell responsiveness with decreased ligand-mediated G protein activation, second messenger generation, and GRK/β-arr recruitment [192]. This mechanism therefore provides key regulatory control on cell receptivity to GPCR stimulation. Another ERK phosphorylation regulatory site is found in the hinge domain of β-arr2 (T178), but not β-arr1, which increases the lifetime of "class B" receptor-β-arrestin complexes in endosomes, and intracellular MAPK signalling [193]. This site, however, seems to be specific to β-arr2 species like in murine, as it is not found in other mammals like the bovine and human.

8.3.2 *Ubiquitination*

β-arrs can undergo covalent modification with ubiquitin (Ub) on lysine residues in the process of ubiquitination. This impacts both GPCR-β-arr trafficking and signalling outputs depending on the relative dynamics of β-arr ubiquitination [194]. "Class B" GPCRs, such as the AT1R and the V2R, which contain clustered phosphorylation sites in the receptor C-tail, elicit prolonged β-arr2 ubiquitination [28]. This leads to sustained receptor interaction and internalization/trafficking of the receptor-β-arr2 complex to endosomes, which is associated with prolonged MAPK activation from these "signalosomes." In contrast to this, "class A" GPCRs such as

the β2-AR that demonstrate a different phosphorylation pattern on the receptor intracellular domains, compared to "class B" receptors, promote transient β-arr2 ubiquitination, leading to transient signalling in the proximity of the plasma membrane. Interestingly, switching the C-tail of the β2-AR with either of the "class B" receptors AT1R or V2R, or fusing Ub directly to the C-terminus of β-arr2, switches transient β2-AR-β-arr complexes to stable "signalosome" complexes that traffic to endosomes [28, 195]. K11 and K12 were found to be essential sites for sustained β-arr2 ubiquitination (Fig. 5) and the formation of stable receptor-β-arr complexes following AngII stimulation of the AT1R [195].

8.3.3 SUMOylation

SUMO (small ubiquitin-like modifier) can also be conjugated to β-arr2 in a process known as SUMOylation. SUMO is covalently attached to lysine residues in a similar fashion to ubiquitination. Whereas ubiquitination is generally associated with protein trafficking or degradation, SUMOylation can affect protein stability, localization, and activity [196]. These alterations in protein function are due to changes in inter- and/or intramolecular protein interactions. In contrast to ubiquitination that does not occur on a defined consensus sequence, SUMOylation can occur on a consensus motif ψ-K-x-D/E (where ψ represents a bulky hydrophobic residue and x represents any amino acid), which provides a recognition site [197] for the sole E2 SUMO-conjugase, Ubc9. The bovine form of β-arr2 was shown to be SUMOylated on two different acceptor sites: one in the C-terminal globular domain (K295) and one in the C-tail (K400). SUMOylation on these sites was shown to be important for β-arr2-AP-2 binding and GPCR internalization [198]. The sequence of the bovine C-tail SUMOylation site is not completely conserved in human β-arr2, which has only K295 as the major SUMO acceptor site [199]. SUMOylation of human β-arr2 on K295 inhibits interaction with TRAF6, allowing TRAF6 oligomerization and autoubiquitination, leading to enhanced TRAF6-mediated NF-κB/AP-1 activation. The SUMO protease SENP1 was also shown to reverse β-arr2 SUMOylation. β-arr2 SUMOylation dynamics therefore regulate β-arr2-mediated IL-1R/TRAF6 signalling. β-arr1 also contains several SUMOylation consensus motifs, but the functional roles of these remain to be determined [194].

8.3.4 Other Posttranslational Modifications

β-arr2 can be S-nitrosylated at C410 (C409 in human β-arr2). Following agonist-mediated activation of the β2-AR, β-arr2 is S-nitrosylated by endothelial NO synthase (eNOS), and this promotes β-arr2 binding to both AP-2 and clathrin leading to enhanced receptor internalization [200]. Finally, β-arr2 has also been shown to be hydroxylated on proline residues P176, P179, and P181 by the enzyme prolyl hydroxylase 2 (PHD2) that is

critical for intracellular oxygen sensing. Hydroxylation on these sites delays β-arr2 recruitment to the membrane, thus inhibiting β2-AR internalization [201].

Continued investigation into how β-arrs are regulated at the transcriptional, posttranscriptional, and posttranslational levels will likely reveal other currently unappreciated mechanisms that impact β-arr-mediated signalling outcomes.

9 β-arr-Dependent Regulation of Physiological and Pathological Processes

β-arr-mediated control of GPCR function, their dynamic compartmentalized scaffolding roles, how β-arr conformation affects cargo binding, and how they are regulated themselves give rise to functional cellular outcomes. These include the regulation of cell proliferation, cell survival, apoptosis, cytoskeletal organization, cell polarity, and cell migration in both normal and pathological contexts [5, 9, 11, 171, 202]. The development of β-arr-deficient mouse models allowed the investigation of the roles of β-arrs in vivo [9, 203, 204]. Mice lacking both β-arrs (β-arr1−/−, β-arr2−/−) display developmental defects: one study demonstrated double deletion to be embryonic lethal [205] and a second study that double deletion neonates display abnormal lung and liver development, correlating with decreased glucocorticoid receptor levels, dying shortly after birth due to respiratory distress [206]. Although the developmental endpoints of the studies differ, they clearly underscore the importance of β-arrs in development.

While β-arr1−/− or β-arr2−/− mice do not display apparent gross phenotypes compared to their wild-type (WT) counterparts, they do display marked differences following challenge with different agents and also, upon closer examination, subtle differences in the absence of pharmacological challenge, including altered bone absorption, body mass, and locomotor activity [204]. In vivo relevance for GPCR-β-arr interaction came from studies using β-arr2−/− mice, which displayed enhanced analgesic effects of the opioid agonist morphine, while at the same time diminishing morphine-induced tolerance, constipation, and respiratory suppression [185, 207, 208]. β-arr2−/− mice have also unveiled positive signalling roles for β-arr2 in vivo. D2 class dopamine receptor-mediated AKT regulation requires the formation of a β-arr2/AKT/PP2A signalling module [93]. β-arr2−/− mice display a decrease in dopamine-dependent behaviors, loss of AKT control by dopamine in the striatum, and inhibition of the dopamine-dependent AKT/PP2A interaction. The β-arr2-dependent assembly of this kinase/phosphatase signalling module is therefore implicated in dopaminergic synaptic transmission. Interestingly, the pharmacological agent lithium used in the

management of psychiatric disorders such as bipolar disorder regulates AKT/GSK3 signalling and related behaviors in mice by disrupting the β-arr2/AKT/PP2A signalling complex [94]. These findings therefore provide proof of principle that alteration of β-arr-dependent signalling can modulate GPCR function in vivo.

In addition to the above studies, β-arrs have been implicated in a wide range of physiological and pathophysiological processes, including the control of cardiac function, allergic asthma, metabolic control, Parkinson's disease, host-pathogen interactions, and cancer. Treatment of β-arr1 KO mice with isoprenaline elicited greater cardiac ejection volumes compared to WT mice, consistent with a role of β-arr1 in the desensitization of the β2-AR [209]. T cells derived from β-arr2 KO mice demonstrate impaired migration in vitro [210]. In a model of allergic asthma, allergen-sensitized β-arr2 KO mice do not accumulate T lymphocytes in their airways nor display inflammatory characteristics of asthma, indicating that β-arr2 represents a potential therapeutic target in the treatment of asthma [211]. Several studies have revealed roles for β-arrs in the control of metabolism including insulin-stimulated Akt activation, insulin sensitivity, pancreatic β-cell function and plasticity, and repression of obesity [92, 129, 212–214]. β-arr2 reverses or protects against L-DOPA-induced dyskenias observed in a mouse model of Parkinson's symptoms [215]. The bacterium that causes cerebrospinal meningitis, *Neisseria meningitidis*, can trigger a biased β2-AR/β-arr signalling pathway in brain endothelial cells [164] leading to the bacterial hijacking of β-arr-binding partners such as c-Src and junctional proteins under the colonies. Cytoskeletal rearrangement driven by β-arr-dependent Src activation secures bacterial adhesion to endothelial cells, and β-arr-mediated mislocalization of junctional proteins leads to the formation of anatomical gaps permitting the bacteria to cross the brain endothelium [164]. Finally, the roles played by β-arrs in various cancer types have also been demonstrated. For example, the interaction between β-arr1 and c-Src was shown to be important for colorectal carcinoma cell migration and metastatic spread to the liver in vivo [62]. Transgenic β-arr1 mice display enhanced tumor progression and angiogenesis [216]. In a murine orthotopic model of metastatic epithelial ovarian cancer, silencing β-arr1 or blocking the ET-AR/β-arr1 signalling program pharmacologically inhibits metastasis [128]. In contrast, depletion of β-arr2 promoted tumor growth and angiogenesis in a murine model of lung cancer, via a CXCR2/NF-κB-mediated mechanism [217]. β-arr2 KO mice were also used to demonstrate that β-arr2 is essential for the initiation and growth of intestinal tumors displaying elevated Wnt pathway activity [218]. Therefore, whereas β-arr1 appears to be more associated with increased cell proliferation, invasion, and metastasis, β-arr2 appears to possess both cancer-promoting and cancer-repressing functions. There have also been several studies that

document changes in expression and/or localization of β-arr1 and β-arr2 in human breast, prostate, lung, and ovary cancers that correlate with clinical outcomes [14].

10 Concluding Remarks

Our understanding of β-arr biology has evolved enormously over the last two decades, with increased appreciation of the roles β-arrs play in cellular regulation, systems biology, and human disease. Investigation using prevailing and novel biochemical, cell biology, biophysical, and structural approaches will provide further discoveries into how these multitask scaffolds achieve their roles. Intracellular targeting of β-arrs using newly developed tools including small molecule compounds, synthetic intrabodies, and aptamers will also provide new opportunities to probe β-arr functions [219]. The study of β-arrs in vivo as positive or negative regulators of physiological and pathological processes, and drug functions, will also provide therapeutic avenues to explore and ultimately help toward developing agents with increased selectivity.

Acknowledgments

Work in the group of Mark G.H. Scott is supported by the Fondation ARC pour la Recherche sur le Cancer, Ligue Contre le Cancer (comité de L'Oise), France-Canada Research Foundation, the Who am I? laboratory of excellence (grant ANR-11-LABX-0071) funded by the "Investments for the Future" program operated by the French National Research Agency (grant ANR-11-IDEX-0005-01), CNRS, and INSERM. Work in the Laporte laboratory is supported by Canadian Institutes of Health Research grants (MOP-74603).

References

1. Pfister C et al (1985) Retinal S antigen identified as the 48K protein regulating light-dependent phosphodiesterase in rods. Science 228(4701):891–893
2. Lohse MJ et al (1990) beta-Arrestin: a protein that regulates beta-adrenergic receptor function. Science 248(4962):1547–1550
3. Attramadal H et al (1992) beta-Arrestin2, a novel member of the arrestin/beta-arrestin gene family. J Biol Chem 267 (25):17882–17890
4. Tian X, Kang DS, Benovic JL (2014) beta-arrestins and G protein-coupled receptor trafficking. Handb Exp Pharmacol 219:173–186
5. Smith JS, Rajagopal S (2016) The beta-arrestins: multifunctional regulators of G protein-coupled receptors. J Biol Chem 291 (17):8969–8977
6. Kang DS, Tian X, Benovic JL (2014) Role of beta-arrestins and arrestin domain-containing proteins in G protein-coupled receptor trafficking. Curr Opin Cell Biol 27:63–71
7. Aubry L, Guetta D, Klein G (2009) The arrestin fold: variations on a theme. Curr Genomics 10(2):133–142
8. Shenoy SK, Lefkowitz RJ (2005) Seven-transmembrane receptor signaling through beta-arrestin. Sci STKE 2005(308):cm10

9. Peterson YK, Luttrell LM (2017) The diverse roles of arrestin scaffolds in G protein-coupled receptor signaling. Pharmacol Rev 69(3):256–297
10. Xiao K et al (2007) Functional specialization of beta-arrestin interactions revealed by proteomic analysis. Proc Natl Acad Sci U S A 104 (29):12011–12016
11. Dewire SM et al (2007) beta-arrestins and cell signaling. Annu Rev Physiol 69:483–510
12. Song X et al (2006) Visual and both non-visual arrestins in their "inactive" conformation bind JNK3 and Mdm2 and relocalize them from the nucleus to the cytoplasm. J Biol Chem 281(30):21491–21499
13. Chen Q, Iverson TM, Gurevich VV (2018) Structural basis of arrestin-dependent signal transduction. Trends Biochem Sci 43 (6):412–423
14. Enslen H, Lima-Fernandes E, Scott MG (2014) Arrestins as regulatory hubs in cancer signalling pathways. Handb Exp Pharmacol 219:405–425
15. Shukla AK, Xiao K, Lefkowitz RJ (2011) Emerging paradigms of beta-arrestin-dependent seven transmembrane receptor signaling. Trends Biochem Sci 36(9):457–469
16. Crepieux P et al (2017) A comprehensive view of the beta-arrestinome. Front Endocrinol 8:32
17. Hauser AS et al (2017) Trends in GPCR drug discovery: new agents, targets and indications. Nat Rev Drug Discov 16(12):829–842
18. Sriram K, Insel PA (2018) G protein-coupled receptors as targets for approved drugs: how many targets and how many drugs? Mol Pharmacol 93(4):251–258
19. Pitcher JA, Freedman NJ, Lefkowitz RJ (1998) G protein-coupled receptor kinases. Annu Rev Biochem 67:653–692
20. Gurevich EV et al (2012) G protein-coupled receptor kinases: more than just kinases and not only for GPCRs. Pharmacol Ther 133 (1):40–69
21. Benovic JL et al (1987) Functional desensitization of the isolated ß-adrenergic receptor by the ß-receptor kinase: potential role of an analog of the retinal protein arrestin (48-kDa protein). Proc Natl Aca Sci U S A 84:8879–8882
22. Goodman OBJ et al (1996) ß-arrestin acts as a clathrin adaptor in endocytosis of the ß2-adrenergic receptor. Nature 383:447–450
23. Laporte SA et al (1999) The beta2-adrenergic receptor/betaarrestin complex recruits the clathrin adaptor AP-2 during endocytosis. Proc Natl Acad Sci U S A 96(7):3712–3717
24. Claing A et al (2001) beta-Arrestin-mediated ADP-ribosylation factor 6 activation and beta 2-adrenergic receptor endocytosis. J Biol Chem 276(45):42509–42513
25. Oakley RH et al (2000) Differential affinities of visual arrestin, beta arrestin1, and beta arrestin2 for G protein-coupled receptors delineate two major classes of receptors. J Biol Chem 275(22):17201–17210
26. Oakley RH et al (2001) Molecular determinants underlying the formation of stable intracellular G protein-coupled receptor-beta-arrestin complexes after receptor endocytosis*. J Biol Chem 276(22):19452–19460
27. Shenoy SK (2014) Arrestin interaction with E3 ubiquitin ligases and deubiquitinases: functional and therapeutic implications. Handb Exp Pharmacol 219:187–203
28. Shenoy SK, Lefkowitz RJ (2003) Trafficking patterns of beta-arrestin and G protein-coupled receptors determined by the kinetics of beta-arrestin deubiquitination. J Biol Chem 278:14498–14506
29. Shenoy SK et al (2009) Beta-arrestin-dependent signaling and trafficking of 7-transmembrane receptors is reciprocally regulated by the deubiquitinase USP33 and the E3 ligase Mdm2. Proc Natl Acad Sci U S A 106(16):6650–6655
30. Shenoy SK et al (2008) Nedd4 mediates agonist-dependent ubiquitination, lysosomal targeting, and degradation of the beta2-adrenergic receptor. J Biol Chem 283 (32):22166–22176
31. Bhandari D et al (2007) Arrestin-2 interacts with the ubiquitin-protein isopeptide ligase atrophin-interacting protein 4 and mediates endosomal sorting of the chemokine receptor CXCR4. J Biol Chem 282(51):36971–36979
32. Gavard J, Gutkind JS (2006) VEGF controls endothelial-cell permeability by promoting the beta-arrestin-dependent endocytosis of VE-cadherin. Nat Cell Biol 8(11):1223–1234
33. Shukla AK et al (2010) Arresting a transient receptor potential (TRP) channel: beta-arrestin 1 mediates ubiquitination and functional down-regulation of TRPV4. J Biol Chem 285(39):30115–30125
34. Chen W et al (2003) Beta-arrestin 2 mediates endocytosis of type III TGF-beta receptor and down-regulation of its signaling. Science 301 (5638):1394–1397
35. McDonald PH et al (2000) Beta-arrestin 2: a receptor-regulated MAPK scaffold for the activation of JNK3. Science 290 (5496):1574–1577

36. Scott MG et al (2006) Cooperative regulation of ERK activation and cell shape change by Filamin A and ß-arrestins. Mol Cell Biol 26:3432–3445
37. DeFea KA (2011) Beta-arrestins as regulators of signal termination and transduction: how do they determine what to scaffold? Cell Signal 23(4):621–629
38. Cameron RT, Baillie GS (2014) Arrestin regulation of small GTPases. Handb Exp Pharmacol 219:375–385
39. McGovern KW, DeFea KA (2014) Molecular mechanisms underlying beta-arrestin-dependent chemotaxis and actin-cytoskeletal reorganization. Handb Exp Pharmacol 219:341–359
40. Chavkin C, Schattauer SS, Levin JR (2014) Arrestin-mediated activation of p38 MAPK: molecular mechanisms and behavioral consequences. Handb Exp Pharmacol 219:281–292
41. Zhan X et al (2014) Arrestin-dependent activation of JNK family kinases. Handb Exp Pharmacol 219:259–280
42. Strungs EG, Luttrell LM (2014) Arrestin-dependent activation of ERK and Src family kinases. Handb Exp Pharmacol 219:225–257
43. Chen Q et al (2014) Self-association of arrestin family members. Handb Exp Pharmacol 219:205–223
44. Gurevich VV, Gurevich EV (2014) Extensive shape shifting underlies functional versatility of arrestins. Curr Opin Cell Biol 27:1–9
45. Kirchhausen T, Owen D, Harrison SC (2014) Molecular structure, function, and dynamics of clathrin-mediated membrane traffic. Cold Spring Harb Perspect Biol 6(5):a016725
46. Krupnick JG et al (1997) Arrestin/clathrin interaction. Localization of the clathrin binding domain of nonvisual arrestins to the carboxy terminus. J Biol Chem 272 (23):15011–15016
47. Owen DJ, Collins BM, Evans PR (2004) Adaptors for clathrin coats: structure and function. Annu Rev Cell Dev Biol 20:153–191
48. Kim YM, Benovic JL (2002) Differential roles of arrestin-2 interaction with clathrin and adaptor protein 2 in G protein-coupled receptor trafficking. J Biol Chem 277 (34):30760–30768
49. Burtey A et al (2007) The conserved isoleucine-valine-phenylalanine motif couples activation state and endocytic functions of beta-arrestins. Traffic 8(7):914–931
50. Goodman OB Jr et al (1997) Arrestin/clathrin interaction. Localization of the arrestin binding locus to the clathrin terminal domain. J Biol Chem 272(23):15017–15022
51. Laporte SA et al (2000) The interaction of beta-arrestin with the AP-2 adaptor is required for the clustering of beta 2-adrenergic receptor into clathrin-coated pits. J Biol Chem 275(30):23120–23126
52. Schmid EM et al (2006) Role of the AP2 beta-appendage hub in recruiting partners for clathrin-coated vesicle assembly. PLoS Biol 4(9):e262
53. Edeling MA et al (2006) Molecular switches involving the AP-2 beta2 appendage regulate endocytic cargo selection and clathrin coat assembly. Dev Cell 10(3):329–342
54. Laporte SA et al (2002) {beta}-arrestin/AP-2 interaction in GPCR internalization: Identification of a {beta}-arrestin binding site in {beta}2-adaptin. J Biol Chem 2:2
55. Beautrait A et al (2017) A new inhibitor of the beta-arrestin/AP2 endocytic complex reveals interplay between GPCR internalization and signalling. Nat Commun 8:15054
56. Marion S et al (2007) N-terminal tyrosine modulation of the endocytic adaptor function of the beta-arrestins. J Biol Chem 282 (26):18937–18944
57. Macia E et al (2012) Arf6 negatively controls the rapid recycling of the beta2 adrenergic receptor. J Cell Sci 125(Pt 17):4026–4035
58. Poupart ME et al (2007) ARF6 regulates angiotensin II type 1 receptor endocytosis by controlling the recruitment of AP-2 and clathrin. Cell Signal 19(11):2370–2378
59. Paleotti O et al (2005) The small G-protein Arf6GTP recruits the AP-2 adaptor complex to membranes. J Biol Chem 280 (22):21661–21666
60. Luttrell LM et al (1999) Beta-arrestin-dependent formation of beta2 adrenergic receptor-Src protein kinase complexes. Science 283 (5402):655–661
61. DeFea KA et al (2000) The proliferative and antiapoptotic effects of substance P are facilitated by formation of a beta -arrestin-dependent scaffolding complex. Proc Natl Acad Sci U S A 97(20):11086–11091
62. Buchanan FG et al (2006) Role of beta-arrestin 1 in the metastatic progression of colorectal cancer. Proc Natl Acad Sci U S A 103(5):1492–1497
63. Miller WE et al (2000) beta-arrestin1 interacts with the catalytic domain of the tyrosine kinase c-SRC. Role of beta-arrestin1-dependent targeting of c-SRC in receptor endocytosis. J Biol Chem 275(15):11312–11319

64. Fessart D et al (2007) Src-dependent phosphorylation of beta2-adaptin dissociates the beta-arrestin-AP-2 complex. J Cell Sci 120 (Pt 10):1723–1732
65. Zimmerman B et al (2009) c-Src-mediated phosphorylation of AP-2 reveals a general mechanism for receptors internalizing through the clathrin pathway. Cell Signal 21 (1):103–110
66. Penela P et al (2001) Beta-arrestin- and c-Src-dependent degradation of G-protein-coupled receptor kinase 2. EMBO J 20 (18):5129–5138
67. Yang SH, Sharrocks AD, Whitmarsh AJ (2013) MAP kinase signalling cascades and transcriptional regulation. Gene 513(1):1–13
68. DeFea KA et al (2000) beta-arrestin-dependent endocytosis of proteinase-activated receptor 2 is required for intracellular targeting of activated ERK1/2. J Cell Biol 148 (6):1267–1281
69. Luttrell LM et al (2001) Activation and targeting of extracellular signal-regulated kinases by beta-arrestin scaffolds. Proc Natl Acad Sci U S A 98(5):2449–2454
70. DeWire SM et al (2008) Beta-arrestin-mediated signaling regulates protein synthesis. J Biol Chem 283(16):10611–10620
71. Song X et al (2009) How does arrestin assemble MAPKs into a signaling complex? J Biol Chem 284(1):685–695
72. Coffa S et al (2011) A single mutation in arrestin-2 prevents ERK1/2 activation by reducing c-Raf1 binding. Biochemistry 50 (32):6951–6958
73. Meng D et al (2009) MEK1 binds directly to betaarrestin1, influencing both its phosphorylation by ERK and the timing of its isoprenaline-stimulated internalization. J Biol Chem 284(17):11425–11435
74. Hanson SM et al (2007) Arrestin mobilizes signaling proteins to the cytoskeleton and redirects their activity. J Mol Biol 368 (2):375–387
75. Miller WE et al (2001) Identification of a motif in the carboxyl terminus of beta -arrestin2 responsible for activation of JNK3. J Biol Chem 276(30):27770–27777
76. Guo C, Whitmarsh AJ (2008) The beta-arrestin-2 scaffold protein promotes c-Jun N-terminal kinase-3 activation by binding to its nonconserved N terminus. J Biol Chem 283(23):15903–15911
77. Scott MG et al (2002) Differential nucleocytoplasmic shuttling of beta-arrestins. Characterization of a leucine-rich nuclear export signal in beta-arrestin2. J Biol Chem 277 (40):37693–37701
78. Zhan X et al (2014) Arrestin-3 binds the MAP kinase JNK3alpha2 via multiple sites on both domains. Cell Signal 26(4):766–776
79. Zhan X et al (2016) Peptide mini-scaffold facilitates JNK3 activation in cells. Sci Rep 6:21025
80. Willoughby EA, Collins MK (2005) Dynamic interaction between the dual specificity phosphatase MKP7 and the JNK3 scaffold protein beta-arrestin 2. J Biol Chem 280 (27):25651–25658
81. Sun Y et al (2002) Beta-arrestin2 is critically involved in CXCR4-mediated chemotaxis, and this is mediated by its enhancement of p38 MAPK activation. J Biol Chem 277:49212–49219
82. McLaughlin NJ et al (2006) Platelet-activating factor-induced clathrin-mediated endocytosis requires beta-arrestin-1 recruitment and activation of the p38 MAPK signalosome at the plasma membrane for actin bundle formation. J Immunol 176 (11):7039–7050
83. Perry SJ et al (2002) Targeting of cyclic AMP degradation to beta 2-adrenergic receptors by beta-arrestins. Science 298(5594):834–836
84. Baillie GS et al (2007) Mapping binding sites for the PDE4D5 cAMP-specific phosphodiesterase to the N- and C-domains of beta-arrestin using spot-immobilized peptide arrays. Biochem J 404(1):71–80
85. Nelson CD et al (2007) Targeting of diacylglycerol degradation to M1 muscarinic receptors by beta-arrestins. Science 315 (5812):663–666
86. Chalhoub N, Baker SJ (2009) PTEN and the PI3-kinase pathway in cancer. Annu Rev Pathol 4:127–150
87. Povsic TJ, Kohout TA, Lefkowitz RJ (2003) Beta-arrestin1 mediates insulin-like growth factor 1 (IGF-1) activation of phosphatidylinositol 3-kinase (PI3K) and anti-apoptosis. J Biol Chem 278(51):51334–51339
88. Wang P et al (2007) Differential regulation of class IA phosphoinositide 3-kinase catalytic subunits p110 alpha and beta by protease-activated receptor 2 and beta-arrestins. Biochem J 408(2):221–230
89. Wang P, DeFea KA (2006) Protease-activated receptor-2 simultaneously directs beta-arrestin-1-dependent inhibition and Galphaq-dependent activation of phosphatidylinositol 3-kinase. Biochemistry 45 (31):9374–9385

90. Goel R et al (2002) alpha-Thrombin induces rapid and sustained Akt phosphorylation by beta-arrestin1-dependent and -independent mechanisms, and only the sustained Akt phosphorylation is essential for G1 phase progression. J Biol Chem 277(21):18640–18648
91. Lodeiro M et al (2009) c-Src regulates Akt signaling in response to ghrelin via beta-arrestin signaling-independent and -dependent mechanisms. PLoS One 4(3):e4686
92. Luan B et al (2009) Deficiency of a beta-arrestin-2 signal complex contributes to insulin resistance. Nature 457(7233):1146–1149
93. Beaulieu JM et al (2005) An Akt/beta-arrestin 2/PP2A signaling complex mediates dopaminergic neurotransmission and behavior. Cell 122(2):261–273
94. Beaulieu JM et al (2008) A beta-arrestin 2 signaling complex mediates lithium action on behavior. Cell 132(1):125–136
95. Kendall RT et al (2011) The beta-arrestin pathway-selective type 1A angiotensin receptor (AT1A) agonist [Sar1,Ile4,Ile8]angiotensin II regulates a robust G protein-independent signaling network. J Biol Chem 286(22):19880–19891
96. Song MS, Salmena L, Pandolfi PP (2012) The functions and regulation of the PTEN tumour suppressor. Nat Rev Mol Cell Biol 13 (5):283–296
97. Lima-Fernandes E et al (2011) Distinct functional outputs of PTEN signalling are controlled by dynamic association with beta-arrestins. EMBO J 30(13):2557–2568
98. Javadi A et al (2017) PTEN controls glandular morphogenesis through a juxtamembrane beta-Arrestin1/ARHGAP21 scaffolding complex. elife 6:e24578
99. Palmitessa A, Benovic JL (2010) Arrestin and the multi-PDZ domain-containing protein MPZ-1 interact with phosphatase and tensin homolog (PTEN) and regulate Caenorhabditis elegans longevity. J Biol Chem 285 (20):15187–15200
100. Karin M, Lin A (2002) NF-kappaB at the crossroads of life and death. Nat Immunol 3 (3):221–227
101. Gao H et al (2004) Identification of beta-arrestin2 as a G protein-coupled receptor-stimulated regulator of NF-kappaB pathways. Mol Cell 14(3):303–317
102. Witherow DS et al (2004) beta-Arrestin inhibits NF-kappaB activity by means of its interaction with the NF-kappaB inhibitor IkappaBalpha. Proc Natl Acad Sci U S A 101 (23):8603–8607
103. Wang Y et al (2006) Association of beta-arrestin and TRAF6 negatively regulates Toll-like receptor-interleukin 1 receptor signaling. Nat Immunol 7(2):139–147
104. Sun J, Lin X (2008) Beta-arrestin 2 is required for lysophosphatidic acid-induced NF-kappaB activation. Proc Natl Acad Sci U S A 105(44):17085–17090
105. Hoeppner CZ, Cheng N, Ye RD (2012) Identification of a nuclear localization sequence in beta-arrestin-1 and its functional implications. J Biol Chem 287 (12):8932–8943
106. Cianfrocca R et al (2014) beta-Arrestin 1 is required for endothelin-1-induced NF-kappaB activation in ovarian cancer cells. Life Sci 118(2):179–184
107. Shenoy SK et al (2001) Regulation of receptor fate by ubiquitination of activated beta 2-adrenergic receptor and beta-arrestin. Science 294(5545):1307–1313
108. Shenoy SK et al (2007) Ubiquitination of beta-arrestin links seven-transmembrane receptor endocytosis and ERK activation. J Biol Chem 282(40):29549–29562
109. Wang P et al (2003) Beta-arrestin 2 functions as a G-protein-coupled receptor-activated regulator of oncoprotein Mdm2. J Biol Chem 278(8):6363–6370
110. Wang P et al (2003) Subcellular localization of beta-arrestins is determined by their intact N domain and the nuclear export signal at the C terminus. J Biol Chem 278:11648–11653
111. Boularan C et al (2007) beta-arrestin 2 oligomerization controls the Mdm2-dependent inhibition of p53. Proc Natl Acad Sci U S A 104(46):18061–18066
112. Hara MR et al (2011) A stress response pathway regulates DNA damage through beta2-adrenoreceptors and beta-arrestin-1. Nature 477(7364):349–353
113. Kitada T et al (1998) Mutations in the parkin gene cause autosomal recessive juvenile parkinsonism. Nature 392(6676):605–608
114. Ahmed MR et al (2011) Ubiquitin ligase parkin promotes Mdm2-arrestin interaction but inhibits arrestin ubiquitination. Biochemistry 50(18):3749–3763
115. Simonin A, Fuster D (2010) Nedd4-1 and beta-arrestin-1 are key regulators of Na+/H+ exchanger 1 ubiquitylation, endocytosis, and function. J Biol Chem 285 (49):38293–38303
116. Bhattacharya M et al (2002) Beta-arrestins regulate a Ral-GDS Ral effector pathway that mediates cytoskeletal reorganization. Nat Cell Biol 4(8):547–555

117. Li TT et al (2009) Beta-arrestin/Ral signaling regulates lysophosphatidic acid-mediated migration and invasion of human breast tumor cells. Mol Cancer Res 7(7):1064–1077
118. Barnes WG et al (2005) beta-Arrestin 1 and Galphaq/11 coordinately activate RhoA and stress fiber formation following receptor stimulation. J Biol Chem 280(9):8041–8050
119. Anthony DF et al (2011) beta-Arrestin 1 inhibits the GTPase-activating protein function of ARHGAP21, promoting activation of RhoA following angiotensin II type 1A receptor stimulation. Mol Cell Biol 31(5):1066–1075
120. Ma X et al (2012) Acute activation of beta2-adrenergic receptor regulates focal adhesions through betaArrestin2- and p115RhoGEF protein-mediated activation of RhoA. J Biol Chem 287(23):18925–18936
121. Zoudilova M et al (2007) Beta-arrestin-dependent regulation of the cofilin pathway downstream of protease-activated receptor-2. J Biol Chem 282(28):20634–20646
122. Zoudilova M et al (2010) beta-Arrestins scaffold cofilin with chronophin to direct localized actin filament severing and membrane protrusions downstream of protease-activated receptor-2. J Biol Chem 285 (19):14318–14329
123. Pontrello CG et al (2012) Cofilin under control of beta-arrestin-2 in NMDA-dependent dendritic spine plasticity, long-term depression (LTD), and learning. Proc Natl Acad Sci U S A 109(7):E442–E451
124. Mittal N et al (2013) Select G-protein-coupled receptors modulate agonist-induced signaling via a ROCK, LIMK, and beta-arrestin 1 pathway. Cell Rep 5(4):1010–1021
125. Storez H et al (2005) Homo- and hetero-oligomerization of beta-arrestins in living cells. J Biol Chem 280(48):40210–40215
126. Kang J et al (2005) A nuclear function of beta-arrestin1 in GPCR signaling: regulation of histone acetylation and gene transcription. Cell 123(5):833–847
127. Yue R et al (2009) Beta-arrestin1 regulates zebrafish hematopoiesis through binding to YY1 and relieving polycomb group repression. Cell 139(3):535–546
128. Rosano L et al (2013) beta-arrestin-1 is a nuclear transcriptional regulator of endothelin-1-induced beta-catenin signaling. Oncogene 32(42):5066–5077
129. Zhuang LN et al (2011) Beta-arrestin-1 protein represses adipogenesis and inflammatory responses through its interaction with peroxisome proliferator-activated receptor-gamma (PPARgamma). J Biol Chem 286 (32):28403–28413
130. Purayil HT et al (2015) Arrestin2 modulates androgen receptor activation. Oncogene 34 (24):3144–3151
131. Lakshmikanthan V et al (2009) Identification of betaArrestin2 as a corepressor of androgen receptor signaling in prostate cancer. Proc Natl Acad Sci U S A 106(23):9379–9384
132. Shenoy SK et al (2012) beta-arrestin1 mediates metastatic growth of breast cancer cells by facilitating HIF-1-dependent VEGF expression. Oncogene 31(3):282–292
133. Cianfrocca R et al (2016) Nuclear beta-arrestin1 is a critical cofactor of hypoxia-inducible factor-1alpha signaling in endothelin-1-induced ovarian tumor progression. Oncotarget 7(14):17790–17804
134. Zecchini V et al (2014) Nuclear ARRB1 induces pseudohypoxia and cellular metabolism reprogramming in prostate cancer. EMBO J 33(12):1365–1382
135. Gaidarov I et al (1999) Arrestin function in G protein-coupled receptor endocytosis requires phosphoinositide binding. EMBO J 18(4):871–881
136. Hanson SM et al (2008) Opposing effects of inositol hexakisphosphate on rod arrestin and arrestin2 self-association. Biochemistry 47 (3):1070–1075
137. Milano SK et al (2006) Nonvisual arrestin oligomerization and cellular localization are regulated by inositol hexakisphosphate binding. J Biol Chem 81:9812–9823
138. Chen Q et al (2017) Structural basis of arrestin-3 activation and signaling. Nat Commun 8(1):1427
139. Xiao K et al (2004) Activation-dependent conformational changes in {beta}-arrestin 2. J Biol Chem 279(53):55744–55753
140. Nobles KN et al (2007) The active conformation of beta-arrestin1: direct evidence for the phosphate sensor in the N-domain and conformational differences in the active states of beta-arrestins1 and −2. J Biol Chem 282 (29):21370–21381
141. Shukla AK et al (2013) Structure of active beta-arrestin-1 bound to a G-protein-coupled receptor phosphopeptide. Nature 497 (7447):137–141
142. Cahill TJ 3rd et al (2017) Distinct conformations of GPCR-beta-arrestin complexes mediate desensitization, signaling, and endocytosis. Proc Natl Acad Sci U S A 114 (10):2562–2567
143. Kumari P et al (2017) Core engagement with beta-arrestin is dispensable for agonist-

induced vasopressin receptor endocytosis and ERK activation. Mol Biol Cell 28 (8):1003–1010

144. Ranjan R et al (2017) Novel Structural Insights into GPCR-beta-Arrestin Interaction and Signaling. Trends Cell Biol 27 (11):851–862
145. Thomsen ARB et al (2016) GPCR-G protein-beta-arrestin super-complex mediates sustained G protein signaling. Cell 166 (4):907–919
146. Charest PG, Terrillon S, Bouvier M (2005) Monitoring agonist-promoted conformational changes of beta-arrestin in living cells by intramolecular BRET. EMBO Rep 6 (4):334–340
147. Nuber S et al (2016) beta-Arrestin biosensors reveal a rapid, receptor-dependent activation/deactivation cycle. Nature 531 (7596):661–664
148. Lee MH et al (2016) The conformational signature of beta-arrestin2 predicts its trafficking and signalling functions. Nature 531 (7596):665–668
149. Eichel K, Jullie D, von Zastrow M (2016) beta-Arrestin drives MAP kinase signalling from clathrin-coated structures after GPCR dissociation. Nat Cell Biol 18(3):303–310
150. Reiter E et al (2012) Molecular mechanism of beta-arrestin-biased agonism at seven-transmembrane receptors. Annu Rev Pharmacol Toxicol 52:179–197
151. Smith JS, Lefkowitz RJ, Rajagopal S (2018) Biased signalling: from simple switches to allosteric microprocessors. Nat Rev Drug Discov 17(4):243–260
152. Ahn S et al (2004) Differential kinetic and spatial patterns of beta-arrestin and G protein-mediated ERK activation by the angiotensin II receptor. J Biol Chem 279 (34):35518–35525
153. Zimmerman B et al (2012) Differential beta-arrestin-dependent conformational signaling and cellular responses revealed by angiotensin analogs. Sci Signal 5(221):ra33
154. Violin JD et al (2010) Selectively engaging beta-arrestins at the angiotensin II type 1 receptor reduces blood pressure and increases cardiac performance. J Pharmacol Exp Ther 335(3):572–579
155. Boerrigter G et al (2011) Cardiorenal actions of TRV120027, a novel ss-arrestin-biased ligand at the angiotensin II type I receptor, in healthy and heart failure canines: a novel therapeutic strategy for acute heart failure. Circ Heart Fail 4(6):770–778
156. Boerrigter G et al (2012) TRV120027, a novel beta-arrestin biased ligand at the angiotensin II type I receptor, unloads the heart and maintains renal function when added to furosemide in experimental heart failure. Circ Heart Fail 5(5):627–634
157. Pang PS et al (2017) Biased ligand of the angiotensin II type 1 receptor in patients with acute heart failure: a randomized, double-blind, placebo-controlled, phase IIB, dose ranging trial (BLAST-AHF). Eur Heart J 38(30):2364–2373
158. Luttrell LM, Kenakin TP (2011) Refining efficacy: allosterism and bias in G protein-coupled receptor signaling. Methods Mol Biol 756:3–35
159. Whalen EJ, Rajagopal S, Lefkowitz RJ (2011) Therapeutic potential of beta-arrestin- and G protein-biased agonists. Trends Mol Med 17 (3):126–139
160. Rankovic Z, Brust TF, Bohn LM (2016) Biased agonism: An emerging paradigm in GPCR drug discovery. Bioorg Med Chem Lett 26(2):241–250
161. O'Hayre M et al (2017) Genetic evidence that beta-arrestins are dispensable for the initiation of beta2-adrenergic receptor signaling to ERK. Sci Signal 10(484):eaal3395
162. Grundmann M et al (2018) Lack of beta-arrestin signaling in the absence of active G proteins. Nat Commun 9(1):341
163. Luttrell LM et al (2018) Manifold roles of beta-arrestins in GPCR signaling elucidated with siRNA and CRISPR/Cas9. Sci Signal 11(549):eaat7650
164. Coureuil M et al (2010) Meningococcus Hijacks a beta2-adrenoceptor/beta-Arrestin pathway to cross brain microvasculature endothelium. Cell 143(7):1149–1160
165. Rakesh K et al (2010) beta-Arrestin-biased agonism of the angiotensin receptor induced by mechanical stress. Sci Signal 3(125):ra46
166. Wu N et al (2006) Arrestin binding to calmodulin: a direct interaction between two ubiquitous signaling proteins. J Mol Biol 364(5):955–963
167. Scott MG et al (2002) Recruitment of activated G protein-coupled receptors to pre-existing clathrin-coated pits in living cells. J Biol Chem 277(5):3552–3559
168. Shenoy SK (2014) Deubiquitinases and their emerging roles in beta-arrestin-mediated signaling. Methods Enzymol 535:351–370
169. Tohgo A et al (2002) {beta}arrestin scaffolding of the ERK cascade enhances cytosolic ERK activity but inhibits ERK mediated transcription following angiotensin AT1a

receptor stimulation. J Biol Chem 98 (change):9429–9436

170. Lin FT et al (1999) Feedback regulation of beta-arrestin1 function by extracellular signal-regulated kinases. J Biol Chem 274 (23):15971–15974
171. DeFea KA (2007) Stop that cell! Beta-arrestin-dependent chemotaxis: a tale of localized actin assembly and receptor desensitization. Annu Rev Physiol 69:535–560
172. Ge L et al (2004) Constitutive protease-activated receptor-2-mediated migration of MDA MB-231 breast cancer cells requires both beta-arrestin-1 and -2. J Biol Chem 279(53):55419–55424
173. Cleghorn WM et al (2015) Arrestins regulate cell spreading and motility via focal adhesion dynamics. Mol Biol Cell 26(4):622–635
174. Molla-Herman A et al (2008) Targeting of beta-arrestin2 to the centrosome and primary cilium: role in cell proliferation control. PLoS One 3(11):e3728
175. Kovacs JJ et al (2008) Beta-arrestin-mediated localization of smoothened to the primary cilium. Science 320(5884):1777–1781
176. Mick DU et al (2015) Proteomics of primary cilia by proximity labeling. Dev Cell 35 (4):497–512
177. Pal K et al (2016) Smoothened determines beta-arrestin-mediated removal of the G protein-coupled receptor Gpr161 from the primary cilium. J Cell Biol 212(7):861–875
178. Green JA et al (2016) Recruitment of beta-arrestin into neuronal cilia modulates somatostatin receptor subtype 3 ciliary localization. Mol Cell Biol 36(1):223–235
179. Nager AR et al (2017) An actin network dispatches ciliary GPCRs into extracellular vesicles to modulate signaling. Cell 168 (1-2):252–263 e14
180. Kook S et al (2014) Caspase-cleaved arrestin-2 and BID cooperatively facilitate cytochrome C release and cell death. Cell Death Differ 21 (1):172–184
181. Oakley RH, Revollo J, Cidlowski JA (2012) Glucocorticoids regulate arrestin gene expression and redirect the signaling profile of G protein-coupled receptors. Proc Natl Acad Sci U S A 109(43):17591–17596
182. Li J et al (2018) NF-kappaB directly regulates beta-arrestin-1 expression and forms a negative feedback circuit in TNF-alpha-induced cell death. FASEB J 32(8):4096–4106. p. fj201700642RRR
183. Kraemer A et al (2013) Cell survival following radiation exposure requires miR-525-3p mediated suppression of ARRB1 and TXN1. PLoS One 8(10):e77484
184. Wang J et al (2016) miR-365 targets beta-arrestin 2 to reverse morphine tolerance in rats. Sci Rep 6:38285
185. Bohn LM et al (1999) Enhanced morphine analgesia in mice lacking beta-arrestin 2. Science 286(5449):2495–2498
186. Sang W et al (2016) MiR-150 impairs inflammatory cytokine production by targeting ARRB-2 after blocking CD28/B7 costimulatory pathway. Immunol Lett 172:1–10
187. Zhao J et al (2014) beta-arrestin2/miR-155/GSK3beta regulates transition of 5-′-azacytizine-induced Sca-1-positive cells to cardiomyocytes. J Cell Mol Med 18 (8):1562–1570
188. Barthet G et al (2009) Beta-arrestin1 phosphorylation by GRK5 regulates G protein-independent 5-HT4 receptor signalling. EMBO J 28(18):2706–2718
189. Lin FT et al (2002) Phosphorylation of beta-arrestin2 regulates its function in internalization of beta(2)-adrenergic receptors. Biochemistry 41(34):10692–10699
190. Kim YM et al (2002) Regulation of arrestin-3 phosphorylation by casein kinase II. J Biol Chem 277(19):16837–16846
191. Cassier E et al (2017) Phosphorylation of beta-arrestin2 at Thr383 by MEK underlies beta-arrestin-dependent activation of Erk1/2 by GPCRs. elife 6:e23777
192. Paradis JS et al (2015) Receptor sequestration in response to beta-arrestin-2 phosphorylation by ERK1/2 governs steady-state levels of GPCR cell-surface expression. Proc Natl Acad Sci U S A 112(37):E5160–E5168
193. Khoury E et al (2014) Differential regulation of endosomal GPCR/beta-arrestin complexes and trafficking by MAPK. J Biol Chem 289(34):23302–23317
194. Shenoy SK, Lefkowitz RJ (2011) beta-Arrestin-mediated receptor trafficking and signal transduction. Trends Pharmacol Sci 32(9):521–533
195. Shenoy SK, Lefkowitz RJ (2005) Receptor-specific ubiquitination of beta-arrestin directs assembly and targeting of seven-transmembrane receptor signalosomes. J Biol Chem 280(15):15315–15324
196. Flotho A, Melchior F (2013) Sumoylation: a regulatory protein modification in health and disease. Annu Rev Biochem 82:357–385
197. Rodriguez MS, Dargemont C, Hay RT (2001) SUMO-1 conjugation in vivo requires both a consensus modification motif and

nuclear targeting. J Biol Chem 276 (16):12654–12659

198. Wyatt D et al (2011) Small ubiquitin-like modifier modification of arrestin-3 regulates receptor trafficking. J Biol Chem 286 (5):3884–3893
199. Xiao N et al (2015) SUMOylation attenuates human beta-arrestin 2 inhibition of IL-1R/TRAF6 signaling. J Biol Chem 290 (4):1927–1935
200. Ozawa K et al (2008) S-nitrosylation of beta-arrestin regulates beta-adrenergic receptor trafficking. Mol Cell 31(3):395–405
201. Yan B et al (2011) Prolyl hydroxylase 2: a novel regulator of beta2 -adrenoceptor internalization. J Cell Mol Med 15 (12):2712–2722
202. Min J, Defea K (2011) beta-arrestin-dependent actin reorganization: bringing the right players together at the leading edge. Mol Pharmacol 80(5):760–768
203. Premont RT, Gainetdinov RR (2007) Physiological roles of G protein-coupled receptor kinases and arrestins. Annu Rev Physiol 69:511–534
204. Schmid CL, Bohn LM (2009) Physiological and pharmacological implications of beta-arrestin regulation. Pharmacol Ther 121 (3):285–293
205. Kohout TA et al (2001) beta-Arrestin 1 and 2 differentially regulate heptahelical receptor signaling and trafficking. Proc Natl Acad Sci U S A 98(4):1601–1606
206. Zhang M et al (2011) Disruption of beta-arrestins blocks glucocorticoid receptor and severely retards lung and liver development in mice. Mech Dev 128(7-10):368–375
207. Bohn LM et al (2000) Mu-opioid receptor desensitization by beta-arrestin-2 determines morphine tolerance but not dependence. Nature 408(6813):720–723
208. Raehal KM, Walker JK, Bohn LM (2005) Morphine side effects in beta-arrestin 2 knockout mice. J Pharmacol Exp Ther 314 (3):1195–1201
209. Conner DA et al (1997) beta-Arrestin1 knockout mice appear normal but demonstrate altered cardiac responses to beta-adrenergic stimulation. Circ Res 81 (6):1021–1026
210. Fong AM et al (2002) Defective lymphocyte chemotaxis in beta-arrestin2- and GRK6-deficient mice. Proc Natl Acad Sci U S A 99 (11):7478–7483
211. Walker JK et al (2003) Beta-arrestin-2 regulates the development of allergic asthma. J Clin Invest 112(4):566–574
212. Zhuang LN et al (2011) Beta-arrestin-1 protein represses diet-induced obesity. J Biol Chem 286(32):28396–28402
213. Ravier MA et al (2014) beta-Arrestin2 plays a key role in the modulation of the pancreatic beta cell mass in mice. Diabetologia 57 (3):532–541
214. Zhu L et al (2017) beta-arrestin-2 is an essential regulator of pancreatic beta-cell function under physiological and pathophysiological conditions. Nat Commun 8:14295
215. Urs NM et al (2015) Targeting beta-arrestin2 in the treatment of L-DOPA-induced dyskinesia in Parkinson's disease. Proc Natl Acad Sci U S A 112(19):E2517–E2526
216. Zou L et al (2008) Rapid xenograft tumor progression in beta-arrestin1 transgenic mice due to enhanced tumor angiogenesis. FASEB J 22(2):355–364
217. Raghuwanshi SK et al (2008) Depletion of beta-arrestin-2 promotes tumor growth and angiogenesis in a murine model of lung cancer. J Immunol 180(8):5699–5706
218. Bonnans C et al (2012) Essential requirement for beta-arrestin2 in mouse intestinal tumors with elevated Wnt signaling. Proc Natl Acad Sci U S A 109(8):3047–3052
219. Chaturvedi M et al (2018) Emerging paradigm of intracellular targeting of G protein-coupled receptors. Trends Biochem Sci 43 (7):533–546

Part II

Methods to Study Roles of β-Arrestins in GPCR Regulation



Chapter 3

Methods to Monitor the Trafficking of β-Arrestin/G Protein-Coupled Receptor Complexes Using Enhanced Bystander BRET

Yubo Cao, Yoon Namkung, and Stéphane A. Laporte

Abstract

β-Arrestins are adaptors that regulate the signaling and trafficking of G protein-coupled receptors (GPCRs). Bioluminescence resonance energy transfer (BRET) is a sensitive and versatile method for real-time monitoring of protein-protein interactions and protein kinesis within live cells, such as the recruitment of β-arrestins to activated receptors at the plasma membrane (PM) and the trafficking of GPCR/β-arrestin complexes to endosomes. Trafficking of receptor/β-arrestin complexes can be assessed by BRET through tagging β-arrestins with the donor luciferase from *Renilla reniformis* (Rluc) and anchoring the acceptor green fluorescent protein from the same species (rGFP) in distinct cell compartments (e.g., PM or endosomes) to generate highly efficient bystander BRET (referred to as enhanced bystander BRET (EbBRET)) upon re-localization of β-arrestins to these compartments following receptor activation. Here, we outline the protocol for quantitatively monitoring β-arrestin recruitment to agonist-activated Angiotensin II type 1 receptor (AT1R) and β2-adrenergic receptor (β2AR) at the PM and the trafficking of receptor/β-arrestin complexes into endosomes using EbBRET-based biosensors.

Key words G protein-coupled receptors (GPCRs), β-Arrestin, Plasma membrane (PM), Endosomes, Internalization, Endocytosis, Trafficking, BRET, EbBRET, Angiotensin II type 1 receptor (AT1R), β2-Adrenergic receptor (β2AR)

1 Introduction

β-Arrestins (β-arrestin 1 and 2, also referred to as arrestin 2 and 3, respectively) are adaptor proteins involved in the desensitization, internalization, and signaling of G protein-coupled receptors (GPCRs) [1, 2]. They control the initial steps of endocytosis at the plasma membrane (PM) by linking agonist-activated receptors to elements of the clathrin coat and differentially regulate intracellular receptor trafficking and recycling to the PM by either co-trafficking or not with receptors into early endosomes. β-arrestins are homogenously localized in the cytosol (β-arrestin 1 is also found in nucleus), but upon GPCR stimulation, they

Mark G. H. Scott and Stéphane A. Laporte (eds.), *Beta-Arrestins: Methods and Protocols*, Methods in Molecular Biology, vol. 1957, https://doi.org/10.1007/978-1-4939-9158-7_3, © Springer Science+Business Media, LLC, part of Springer Nature 2019

rapidly translocate to the PM where they interact with activated receptors. Receptors categorized as class A GPCRs (including β2-adrenergic receptor (β2AR), α1b-adrenergic receptor, μ-opioid receptor, endothelin ETA receptor, and dopamine D1A receptor) form transient receptor/β-arrestin complexes that dissociate at, or near, the PM after internalization of receptors through clathrin-coated pits [3]. In such cases, receptors traffic to early endosomes free of β-arrestins, where they can recycle more rapidly to the PM. For class B GPCRs (including Angiotensin II type 1 receptor (AT1R), neurotensin receptor 1, and vasopressin V2 receptor), β-arrestins bind activated receptors with higher affinity at the PM and form more stable complexes that internalize into endosomes, thereby delaying and/or preventing receptor recycling to the PM [3].

Bioluminescence resonance energy transfer (BRET) is achieved through the transfer of energy from a bioluminescent donor enzyme (e.g., luciferase) to a complementary fluorophore acceptor (e.g., GFP) following substrate oxidation. Protein-protein interactions, such as GPCR interactions with their cognate effectors (e.g., G protein and β-arrestins), can be monitored using BRET by fusing each protein of interest with either the donor or the acceptor [4, 5]. In such cases, the efficiency of energy transfer is highly dependent on the distance between the RLuc and GFP moieties, when interacting proteins containing each entity are either functionally associating or dissociating from each other. BRET signals can also emanate from random collisions (also referred to as bystander BRET) when RLuc and GFP are present in close proximity and in sufficiently high concentrations relative to each other, such as when proteins re-colocalize in the same bidimensional membrane compartment [4]. Bystander BRET has been used to study receptor trafficking to and from the PM, as well as their targeting to specialized intracellular compartments [6, 7]. We use the highly dynamic BRET-based biosensors (referred to as "enhanced bystander BRET" or "EbBRET") that employ the highly efficient natural BRET pair of Rluc and rGFP from *Renilla reniformis* to study the trafficking of receptor/β-arrestin complexes [7, 8].

Here, we describe two pairs of EbBRET biosensors that allow for the live cell monitoring of β-arrestin 1 and 2 trafficking to and from the PM, as well as their trafficking to endosomes upon ligand-induced GPCR activation. We use the two prototypical class A and B GPCRs, β2AR and AT1R, respectively, to describe protocols to detect receptor-mediated β-arrestin translocation at the PM following receptor activation and the internalization of receptor/β-arrestin into endosomes. This is achieved by expressing RlucII-tagged β-arrestins (β-arrestin 1- or 2-RlucII) with either PM-localized rGFP (rGFP-CAAX) or endosomally localized rGFP (rGFP-FYVE) in cells. Such methods can be used to study the

engagement of β-arrestins by different receptors and ligands, as well as for studying the kinesis of other GPCRs/β-arrestin complexes within live cells, and can also be adapted to vet GPCRs endocytosis from the PM and their internalization into endosomes (e.g., using receptor-tagged RlucII) [7].

2 Materials

2.1 DNA Constructs

AT1R, β2AR, rGFP-CAAX, rGFP-FYVE [7], β-arrestin1-RlucII [9], β-arrestin2-RlucII [10], and pcDNA3.1 (Invitrogen) (*see* **Note 1**).

2.2 Cell Culture and Transfection

All media and buffers should be sterile.

1. Tissue culture plates (100 mm dishes).
2. HEK 293 cells (ATCC) (*see* **Note 2**).
3. Media: minimum essential media (MEM) supplemented with 10% FBS, 5 mM L-glutamine, 20 μg/mL gentamicin (*see* **Note 3**).
4. Calcium phosphate solution: 2.5 M $CaCl_2$ in deionized water.
5. 2× HBS buffer: 50 mM HEPES, 280 mM NaCl, 1.5 mM Na_2HPO_4, pH 7.1 (adjusted using NaOH) in deionized water.
6. Poly-L-ornithine: 15 μg/mL in deionized water.
7. Cell culture grade trypsin-EDTA.
8. Phosphate-buffered saline (PBS)-EDTA: 5 mM EDTA in PBS.
9. Tyrode's buffer: 140 mM NaCl, 2.7 mM KCl, 1 mM $CaCl_2$, 12 mM $NaHCO_3$, 5.6 mM D-glucose, 0.5 mM $MgCl_2$, 0.37 mM NaH_2PO_4, 25 mM HEPES (pH 7.4, adjusted using NaOH) in deionized water.

2.3 BRET

1. Tissue culture grade white 96-well flat bottom plates.
2. Ligands: angiotensin II (AngII) and isoproterenol (ISO) or appropriate ligands of interest for these receptors or other GPCRs. ISO is prepared by diluting 2.47 mg in 1 mL of Tyrode's buffer, which will give a stock solution of 10 mM. AngII is prepared as a stock solution of 1 mM in water, by dissolving 1.05 mg in 1 mL (*see* **Note 4**). Serial dilutions of each ligand can then be made using Tyrode's buffer.
3. Coelenterazine 400a (#340, Nanolight technology).
4. Microplate reader (*see* **Note 5**).

3 Methods

3.1 Cell Culture and Transfection

1. HEK 293 cells should be grown to confluency in MEM/10% FBS at 37 °C in 5% CO_2 and 90% humidity.
2. On day 1, trypsinize cells and seed them at a density of ~7.5×10^5 cells per 100 mm dish.
3. After 24 h (day 2), transfect cells with cDNAs for AT1R or β_2AR and β-arrestin1-RlucII or β-arrestin2-RlucII, with the appropriate EbBRET acceptor (e.g., rGFP-CAAX or rGFP-FYVE) using a calcium phosphate co-precipitation method. For each transfection in 100 mm dish, we use 1 μg of receptor cDNA with 120 ng of β-arrestin-RlucII and 480 ng of rGFP-CAAX or rGFP-FYVE DNAs. Adjust total DNA amount to 12 μg with pcDNA3.1 in a total volume of 450 μL of sterile deionized water in a 14 mL round bottom tube. Next, add 50 μL of 2.5 M $CaCl_2$, followed by dropwise addition of 500 μL of 2× HBS (*see* **Note 6**). The transfection solution should be gently mixed and then evenly added dropwise over the cells in the 100 mm dish within 5 min of the DNA-salt complex formation (*see* **Note 7**).
4. Meanwhile, coat 96-well plates with 55 μL/well of poly-L-ornithine and leave overnight at 37 °C in 5% CO_2 and 90% humidity (*see* **Note 8**).
5. The following day (day 3), aspirate media from transfected 100 mm dishes and replace with fresh MEM/10% FBS.
6. Four hours later, aspirate media and replace with 2 mL of PBS-EDTA for 5 min to allow cells to detach (*see* **Note 9**).
7. Add 6 mL Tyrode's buffer into 100 mm dish and pipette up and down to detach cells (*see* **Note 10**).
8. Transfer detached cells into 15 mL conical tubes.
9. Centrifuge cells at low speed (1.0×10^3 rpm) for 5 min.
10. Meanwhile, aspirate the poly-L-ornithine solution from 96-well plates and wash with 200 μL/well of sterile water. Let wells air-dry.
11. Aspirate the supernatant from centrifuged cells, leaving a small residual volume in order to avoid losing the pelleted cells.
12. Resuspend cells in 6 mL of MEM/10% FBS and count them using a hemocytometer (*see* **Note 11**).
13. Seed around 2.5×10^4/100 μL cells per well in the poly-L-ornithine-coated 96-well plates (*see* **Note 12**).
14. Incubate cells overnight at 37 °C in 5% CO_2 and 90% humidity, and proceed with the desired experimental modality (*see* below, Subheadings 3.2, 3.3, and 3.4).

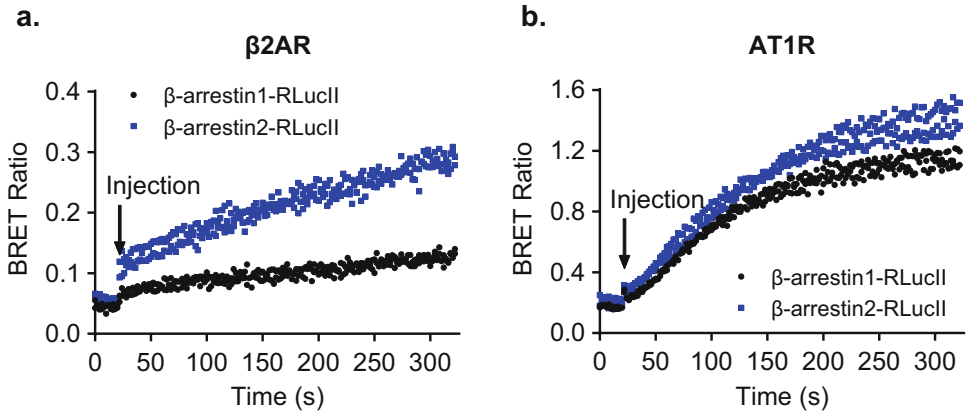


Fig. 1 Kinetics of agonist-induced recruitment of β-arrestins to the PM as measured by EbBRET. HEK 293 cells were transfected with receptors, rGFP-CAAX, and β-arrestin1-RLucII or β-arrestin2-RlucII. (**a**) Following 10 μM ISO stimulation, the β2AR, a classical class A GPCR, favors a better recruitment of β-arrestin2-RLucII than of β-arrestin1-RLucII to the PM and thus generates greater BRET signals with β-arrestin2. (**b**) The AT1R, a classical class B GPCR, recruits both β-arrestin1-RLucII and β-arrestin2-RLucII to the PM efficiently following 100 nM AngII stimulation and generates similar BRET signals. Data represent duplicate BRET ratios at each time point from a representative experiment

3.2 BRET Kinetics with Ligand Injection

1. For measuring kinetics of β-arrestin recruitment at the PM, ligands can be injected into the wells, and BRET measurements can be recorded every 2 s for up to 5–10 min (Fig. 1).
2. On day 4, aspirate media from the 96-well plate and wash wells with 150 μL/well Tyrode's buffer, which has been warmed at room temperature (*see* **Note 13**). After washing the cells, add 80 μL/well of Tyrode's buffer and starve cells for 1 h at room temperature.
3. Turn on the microplate reader and set filters to BRET2, and set protocol to take measurements every 2 s for 20 s before and 300 s after ligand injection (*see* **Note 14**). Set ligand injection volume to 10 μL.
4. Ten minutes prior to reading the 96-well plate, make 10× ligand dilutions: AngII (1 μM) and ISO (100 μM) (*see* **Note 4**).
5. Prepare a 10× (50 μM) Coelenterazine 400a solution in Tyrode's buffer from 5 mM stock, and 3–4 min before BRET measurements, add 10 μL/well of Coelenterazine 400a (final concentration of 5 μM) (*see* **Note 15**).
6. Read the 96-well plate in microplate reader and record values for 410 nm (RLucII) and 515 nm (rGFP).
7. Analyze data. The intensity of the acceptor emission (rGFP) relative to the donor emission (RlucII) is used to calculate the efficiency of energy transfer, which is determined ratiometrically (e.g., BRET ratio) by dividing the rGFP values by the RLucII ones (rGFP/RlucII).

3.3 Fixed Time Course BRET Measurements

1. Alternatively, on day 4, aspirate media from the 96-well plate and wash wells with 150 μL/well of pre-warmed Tyrode's buffer as described in Subheading 3.2, **step 2**.
2. Add 90 μL/well of pre-warmed Tyrode's buffer and starve cells for 1 h at 37 °C in an incubator or a water bath.
3. Turn on the BRET microplate reader, set emission filters to BRET2, and set platform temperature to 37 °C (*see* **Note 14**).
4. Ten minutes prior to running the experiment, make 10× ligand dilutions as in Subheading 3.2, **step 4**.
5. For the β-arrestin recruitment to receptors at the PM assay (Fig. 2), add 10 μL of 10× ligand solution on cells in a countdown manner, starting with the longest time of stimulation (i.e., 45 min) and subsequently adding the ligands for the desired incubation time points (i.e., 30, 20, 15, 10, 5, and 2 min). For the zero time point, add Tyrode's buffer to cells at the same time as the longest time of agonist stimulation (i.e., 45 min). For β-arrestin trafficking to receptors in endosomes assay (Fig. 3), ligands or Tyrode's buffer are added in a similar manner for periods of 90, 60, 45, 30, 20, 10, 5, and 2 min.
6. Prepare and add Coelenterazine 400a solution as in Subheading 3.2, **step 5** (*see* **Notes 15** and **16**).
7. Read the 96-well plate in microplate reader and record values for 410 nm (RLucII) and 515 nm (rGFP).
8. Analyze data as in Subheading 3.2, **step 7**.

3.4 BRET Dose Responses

1. Alternatively, on day 4, for obtaining a dose-response curve at a desired time point, BRET responses can be measured at different log10 concentrations of agonist (Fig. 4).
2. After washing the cells with Tyrode's buffer as previously described in Subheading 3.2, **step 2**, add 80 μL/well of Tyrode's buffer and starve cells for 1 h at room temperature (*see* **Note 17**).
3. Turn on the microplate reader and set filters to BRET2 (*see* **Note 14**).
4. Make serial dilutions of 10× ligand concentrations from 10^{-11} to 10^{-4} M for AngII and 10^{-10} to 10^{-3} M for ISO, spanning every log10.
5. Add 10 μL/well of Coelenterazine 400a 1 min before ligand stimulation.
6. Stimulate with each ligand dilution, 2 min before reading the 96-well plate (*see* **Note 18**).
7. Read the 96-well plate using microplate reader.
8. Analyze data as previously described in Subheading 3.2, **step 7**.

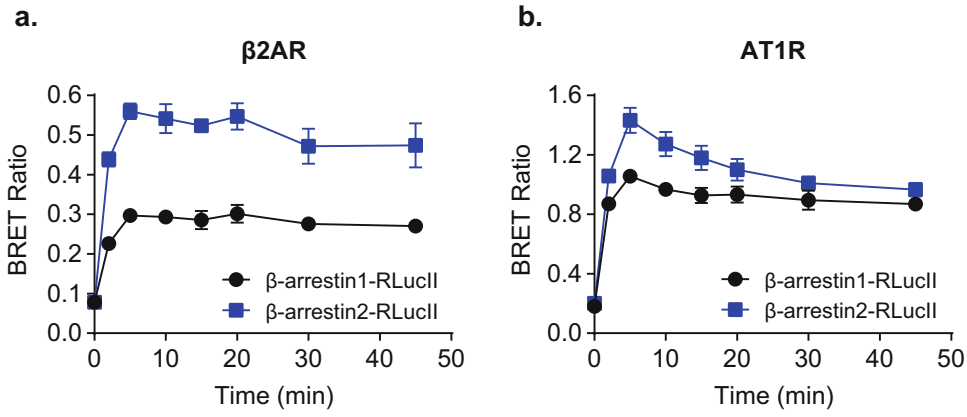


Fig. 2 Time course of agonist-induced recruitment of β-arrestins to receptors at the PM as measured by EbBRET. HEK 293 cells were transfected with receptors, rGFP-CAAX, and β-arrestin1-RLucII or β-arrestin2-RlucII. (**a**) The β2AR, a classical class A GPCR, favors a better recruitment to the PM of β-arrestin2-RLucII and thus generates a greater BRET signal than β-arrestin1-RLucII following 10 μM ISO stimulation. (**b**) The AT1R, a classical class B GPCR, recruits both β-arrestin1-RLucII and β-arrestin2-RLucII to the PM to generate BRET responses almost as efficiently following 100 nM AngII stimulation. Data represent the mean ± s.e.m. from three independent experiments

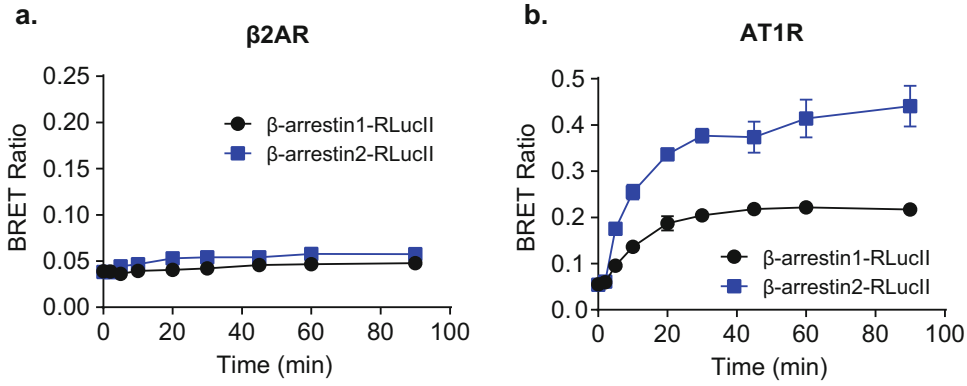


Fig. 3 Time course of agonist-induced trafficking of β-arrestins to receptors in the endosomes as measured by EbBRET. HEK 293 cells were transfected with receptors, rGFP-FYVE, and β-arrestin1-RLucII or β-arrestin2-RlucII. (**a**) The β2AR, a classical class A GPCR, does not promote the re-localization of β-arrestin1-RLucII or β-arrestin2-RLucII into endosomes, and BRET signals therefore do not change from basal following 10 μM ISO stimulation. (**b**) The AT1R, a classical class B GPCR, induces both β-arrestin1-RLucII and β-arrestin2-RLucII accumulation into endosomes and BRET signals following 100 nM AngII stimulation. BRET signals obtained are greater with β-arrestin2-RLucII than with β-arrestin1-RlucII. Data represent the mean ± s.e.m. from three independent experiments

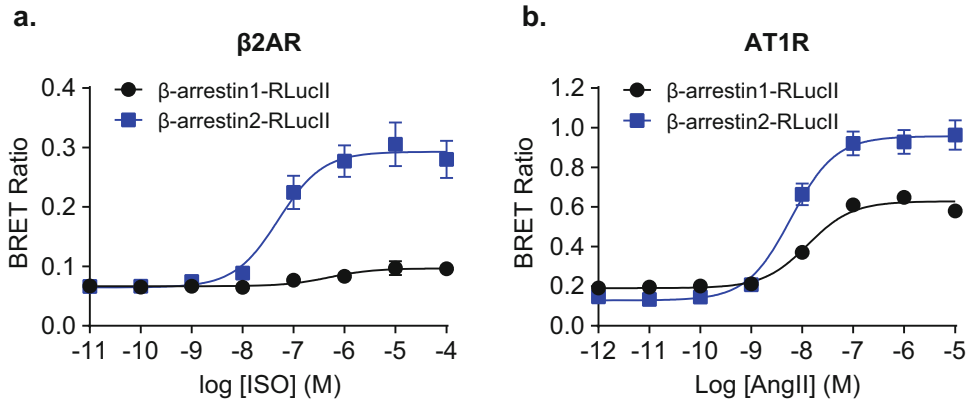


Fig. 4 Concentration-response curve of agonist-induced recruitment of β-arrestins to the PM as measured by EbBRET. HEK 293 cells were transfected with receptors, rGFP-CAAX, and β-arrestin1-RLucII or β-arrestin2-RlucII. (**a**) The β2AR, a classical class A GPCR, favors the recruitment of β-arrestin2-RLucII to the PM and a BRET signal in a concentration-dependent manner following ISO stimulation. β-Arrestin1-RLucII is less well recruited to the PM than β-arrestin2-RLucII, as seen by the lower efficacy of BRET signal obtained at high ISO concentrations. (**b**) The AT1R, a classical class B GPCR, recruits both β-arrestin1-RLucII and β-arrestin2-RLucII to the PM in a AngII concentration-dependent manner. In these conditions, β-arrestin2-RLucII also generates a better BRET signal than β-arrestin1-RLucII following maximal AT1R stimulation. Data represent the mean ± s.e.m. from three independent experiments

4 Notes

1. Any empty mammalian expressing vectors, other than pcDNA3.1, can also be used as carrier DNA.
2. Other mammalian cell lines, such as COS-7 and CHO, can also be used. In such cases, amounts of DNA and transfection method should be optimized for each cell line.
3. We usually purchase sterile MEM, but if it is prepared from powder, the solution should be sterilized by filtration using a 0.22 μm filter. This also applies for all the other solutions.
4. ISO should always be prepared fresh from powder, while AngII can be prepared as a stock solution of 1 mM and store at −80 °C until needed.
5. We use a Synergy II plate reader (BioTek®), with filter sets: 410/80 nm and 515/30 nm for detecting RlucII and rGFP signals, respectively. Other microplate readers, such the Victor X (PerkinElmer) or Mithras LB940 (Berthold Technologies), with similar filter sets can also be used. For BRET kinetic measurements, an injector is required.
6. The HBS should be added slowly and dropwise over a span of 1 min. Formation of DNA-salt complexes and transfection efficiency may vary depending on how HBS is added.

7. After adding the transfection solution, avoid shaking the dish as it might disturb the even distribution of DNA-salt complexes on cells. The calcium phosphate co-precipitation method works well for HEK 293 cells, however, if using other cell lines such as COS or CHO cells, other transfection reagents such as lipofectamine should be considered.
8. Make sure poly-L-ornithine covers the entire bottom surface of the wells. If using other cell types that are more adherent, such as CHO cells, this step can be omitted.
9. Pre-warmed PBS-EDTA facilitates the detachment of cells. Do not incubate with PBS-EDTA for more than 5 min, as it will reduce the cell viability.
10. Volume of Tyrode's buffer should be at least three times that of PBS-EDTA to neutralize the effect of EDTA. Cells should visibly detach as you wash the 100 mm plate with Tyrode's buffer.
11. Resuspending in 6 mL MEM/10% FBS should yield approximately 2.5×10^4 cells/100 μL. One 100 mm dish should provide enough cells to seed half of a 96-well plate.
12. We normally prepare triplicate wells for each concentration or time point to be tested.
13. Be careful while washing cells, as they may detach.
14. For BRET2, set emission filters at 410/80 nm and 515/30 nm and make measurements for 0.5 s in each channel for each well.
15. We usually make a 5 mM Coelenterazine 400a stock solution using NanoFuel Solvent (Nanolight Technology). If using ethanol as the solvent, the stock solution should be made at 2.5 mM. The stock solution should be protected with foil, because Coelenterazine is light sensitive. The 10× solution needs to be prepared just before adding it to cells, because it rapidly oxidizes in aqueous environments.
16. Coelenterazine 400a should be added 3–4 min before reading the time points at the end of the countdown. For instance, for the 45-min time point, add Coelenterazine 400 after 41–42 min of ligand stimulation; for the 30-minute time point, add it after 26–27 min, and so forth. For the shorter time stimulation with ligand, like the 2-min time point, add Coelenterazine 400a 1–2 min before adding the ligand, while for the 5-min time point, Coelenterazine 400a should be added 1–2 min after ligand addition.
17. These experiments are conducted at room temperature to minimize the effect of internalization of receptors from the PM.
18. Aim to stimulate half of the 96-well plate within 2 min to minimize the effects of internalization and read half of the

96-well plate in order to match the speed at which the BRET machine reads each well. Start stimulation from lowest to highest ligand concentration and switch pipette tips when going back to the lowest concentration.

Acknowledgments

This work was supported by Canadian Institutes of Health Research grants to SAL.

References

1. Claing A, Laporte SA, Caron MG, Lefkowitz RJ (2002) Endocytosis of G protein-coupled receptors: roles of G protein-coupled receptor kinases and ß-arrestin proteins. Prog Neurobiol 66(2):61–79
2. Shenoy SK, Lefkowitz RJ (2011) β-Arrestin-mediated receptor trafficking and signal transduction. Trends Pharmacol Sci 32(9):521–533
3. Oakley RH, Laporte SA, Holt JA, Caron MG, Barak LS (2000) Differential affinities of visual arrestin, beta arrestin1, and beta arrestin2 for G protein-coupled receptors delineate two major classes of receptors. J Biol Chem 275 (22):17201–17210
4. Marullo S, Bouvier M (2007) Resonance energy transfer approaches in molecular pharmacology and beyond. Trends Pharmacol Sci 28(8):362–365
5. Salahpour A, Espinoza S, Masri B, Lam V, Barak LS, Gainetdinov RR (2012) BRET biosensors to study GPCR biology, pharmacology, and signal transduction. Front Endocrinol 3 (105):1–9
6. Lan TH, Liu Q, Li C, Wu G, Lambert NA (2012) Sensitive and high resolution localization and tracking of membrane proteins in live cells with BRET. Traffic 13(11):1450–1456
7. Namkung Y, Le Gouill C, Lukashova V, Kobayashi H, Hogue M, Khoury E, Song M, Bouvier M, Laporte SA (2016) Monitoring G protein-coupled receptor and ß-arrestin trafficking in live cells using enhanced bystander BRET. Nat Commun 7:12178
8. Molinari P, Casella I, Costa T (2008) Functional complementation of high-efficiency resonance energy transfer: a new tool for the study of protein binding interactions in living cells. Biochem J 409(1):251–261
9. Zimmerman B, Beautrait A, Aguila B, Charles R, Escher E, Claing A, Bouvier M, Laporte SA (2012) Differential β-arrestin-dependent conformational signaling and cellular responses revealed by angiotensin analogs. Sci Signal 5(221):ra33
10. Quoyer J, Janz JM, Luo J, Ren Y, Armando S, Lukashova V, Benovic JL, Carlson KE, Hunt SW, Bouvier M (2013) Pepducin targeting the CXC chemokine receptor type 4 acts as a biased agonist favoring activation of the inhibitory G protein. Proc Natl Acad Sci U S A 110(52): E5088–E5097



Chapter 4

Methods to Investigate β-Arrestin-Mediated Regulation of GPCR Function in Human Airway Smooth Muscle

Tonio Pera and Raymond B. Penn

Abstract

Arrestin proteins were originally characterized as regulators of GPCR desensitization, and that function alone was sufficient to promote extreme interest in their study. It is now appreciated that arrestins also function as mediators of GPCR trafficking and G protein-independent signaling. This latter function places them as prominent players in the emerging field of qualitative signaling, which promises to launch a new area of pharmacology that defines ligands with selectivity/bias toward either G protein-dependent or -independent signaling. To meet the demands of research into arrestin function, methodology has evolved accordingly over the last three decades since the discovery of the arrestin family. Herein we describe state-of-the-art approaches for studying the role of arrestins (β-arrestin1 *aka* arrestin 2, β-arrestin2 *aka* arrestin 3) in GPCR function in a primary cell type, cultured airway smooth muscle cells.

Key words Arrestin, siRNA, Transfection, Infection, β2-Adrenoceptor, Muscarinic acetylcholine receptor

1 Introduction

Arrestin proteins were originally characterized as regulators of GPCR desensitization, and that function alone was sufficient to promote extreme interest in their study. It is now appreciated that arrestins also function as mediators of GPCR recycling and G protein-independent signaling. This latter function places them as prominent players in the emerging field of qualitative signaling, which promises to launch a new area of pharmacology that defines ligands with selectivity/bias toward either G protein-dependent or G protein-independent signaling. To meet the demands of research into arrestin function, methodology has evolved accordingly over the last three decades since the discovery of the arrestin family.

Early studies of nonvisual arrestins were limited primarily to overexpression of arrestins or dominant-negative arrestin mutants, in cellular expression systems such as COS or HEK293 cells. However, the advent of si/sh RNA methodology, as well as genetic

Mark G. H. Scott and Stéphane A. Laporte (eds.), *Beta-Arrestins: Methods and Protocols*, Methods in Molecular Biology, vol. 1957, https://doi.org/10.1007/978-1-4939-9158-7_4, © Springer Science+Business Media, LLC, part of Springer Nature 2019

strategies in mice, has provided more powerful approaches capable of greater insight into the role of arrestins in physiologically relevant systems. Herein we describe state-of-the-art approaches for studying the role of arrestins in GPCR function in a primary cell type, the airway smooth muscle (ASM) cells. Generation of cultures of human and murine ASM cells have been previously detailed [1, 2].

2 Materials

2.1 Cell Culture Media

1. ASM cell culture growth media (maintenance). Complete Ham's F-12 media with antibiotics: Ham's F-12 nutrient mix (500 mL) containing 10% FBS (50 mL of invitrogen 10437028), 50,000 units penicillin/50,000 μg streptomycin (P/S) (5 mL of invitrogen 15140122), L-glutamine (5 mL), 12.5 mL of 1 M HEPES, 6 mL of 1 M NaOH, and 850 μL of 1 M $CaCl_2$.
2. Complete Ham's F-12 media *without antibiotics* for ASM cultures subject to transient transfection/virus infection: Ham's F-12 Nutrient Mix (500 mL) containing 10% FBS, L-glutamine (5 mL), 12.5 mL of 1 M HEPES, 6 mL of 1 M NaOH, and 850 μL of 1 M $CaCl_2$.
3. Complete DMEM media for virus generation: DMEM high glucose (500 mL) containing 10% FBS and P/S.
4. DMEM media no P/S for virus generation: DMEM high glucose (500 mL) with 10% FBS only.
5. Plain DMEM media for virus generation: DMEM high glucose (500 mL) with no additions.
6. Serum-free media for terminal experiments: Ham's F-12: Ham's F-12 Nutrient Mix (500 mL) containing L-glutamine (5 mL), 12.5 mL of 1 M HEPES; 4 mL of 1 M NaOH, P/S, and 794 μL of 1 M $CaCl_2$ insulin/transferrin (IT)-supplemented media are made by adding 5 ng/mL of insulin and 5 ng/mL of transferrin to serum-free Ham's F-12. Alternatively, serum-free Ham's F-12 can be supplemented with 0.1% bovine serum albumin (BSA) (30% sterile BSA stock solution).

2.2 ASM Cell Culture

1. 60 mm and 100 mm cell culture dishes.
2. ASM cell culture growth media (maintenance) (*see* Subheading 2.1, **item 1**).
3. Phosphate-buffered saline (PBS): 8.1 mM Na_2PO_4, 1.47 mM KH_2PO_4, 137 mM NaCl, and 2.7 mM KCl, pH 7.4.
4. Trypsin (0.5% trypsin, 1 mM EDTA).

5. Micropipette (2–20, 20–200, 200–1000 μL).
6. Serological pipette (2, 5, 10, 25 mL).
7. Phase contrast and/or fluorescence microscope (Nikon Eclipse E800 fluorescence microscope; Plan-Apo 60 × 1.40 NA oil immersion objective; QED Camera software).
8. Antibiotics for plasmid expression selection (G418 or hygromycin, e.g., depending on the plasmid resistance cassette).
9. Water bath at 37 °C.

2.3 Plasmid Transfection

1. Fugene HD reagent (Promega E2311) (*see* **Note 1**).
2. DNA plasmids (ARR2-GFP, ARR3-GFP, and ARR2(R169E)-GFP) as per [3] (*see* **Note 2**).
3. OptiMEM media.

2.4 siRNA Transfection

1. Nuclease-free water.
2. siRNA buffer: 60 mM KCl, 6 mM HEPES, pH 7.5, and 0.2 mM $MgCl_2$ (prepared from 5× stock with nuclease-free water; 1 part 5× siRNA buffer + 4 parts nuclease-free water; store at 4 °C).
3. Cell culture media (Ham's F-12; without additives).
4. β-arrestin1 siRNA (Dharmacon Cat no. L-011971), β-arrestin2 siRNA (Dharmacon Cat no. L-007292) (*see* **Note 3**).
5. DharmaFECT1 (Dharmacon).
6. Cell culture media (Complete Ham's F-12 media and plain DMEM).
7. 1.5 mL Eppendorf tubes.
8. Table top centrifuge.

2.5 Retrovirus Generation

1. Complete DMEM media.
2. DMEM media without P/S.
3. Plain DMEM media.
4. Fugene HD (*see* Subheading 2.3, **item 1**).
5. 0.45 μm PVDF filter unit.
6. Complete Ham's F-12 media with antibiotics.
7. Complete Ham's F-12 media *without antibiotics.*
8. Polybrene—supplied as 10 mg/mL.
9. G418 sulfate—(500 mg/mL) (*see* **Note 4**).
10. GP2-293 packaging cells.

2.6 Immunoblotting, Second Messenger Assays, mRNA Isolation, and Migration Assays

1. Radioimmunoprecipitation assay (RIPA) buffer (25 mM Tris–HCl, pH 7.6, 150 mM NaCl, 1% NP-40, 1% sodium deoxycholate, 0.1% SDS) with protease and phosphatase inhibitor cocktail.
2. Gel electrophoresis and transfer equipment (Biorad).
3. Criterion midi 10% polyacrylamide gels (Biorad).
4. Nitrocellulose blotting membrane.
5. LiCOR blocking buffer (LiCOR).
6. Anti-β-arrestin1/2 rabbit mAb (1:1000; Cell Signaling Technology).
7. LiCOR IRDye secondary anti-rabbit Ab (1:10,000; LiCOR).
8. Protein Simple Wes apparatus (Protein Simple).
9. Protein Simple Wes electrophoresis kit (Protein Simple).
10. Applied Biosystems cAMP-Screen system (Thermo Fisher).
11. CyQuant NF cell proliferation assay kit (Thermo Fisher).
12. TRIzol reagent.
13. mRNA column isolation kit.
14. Boyden chamber fitted with an 8 μm pore membrane.

3 Methods

3.1 Molecular Strategies: Overexpression of Wild-Type or Dominant-Negative Arrestins

The methodology described here is similar to that previously used by us (*see* **Note 5**).

1. Aspirate media from a 100 mm dish of near-confluent (~3×10^6 cells/dish) ASM cells.
2. Wash cells twice with 37 °C calcium-free PBS and add 2 mL trypsin; incubate at 37 °C until cells detach (1–2 min).
3. Resuspend cells in serum-containing media and plate cells in a 60 mm cell culture dish at a density of 12,500 cells/cm^2 so as to achieve ~50% confluence the next day.
4. Twenty-four (24) h after plating cells (now at ~50% confluence), re-feed cells with serum-containing media (3 mL for a 60 mm dish) lacking antibiotics.
5. Pipette 300 μL of OptiMEM into a 1.5 mL tube.
6. Add 6 μg of DNA (encoding arrestin isoforms or mutants) to the tube and resuspend gently by pipetting.
7. Add 18 μL of Fugene HD to the tube; resuspend gently by pipetting.
8. Incubate for 10 min (*see* **Note 6**).
9. Add dropwise to the cells.

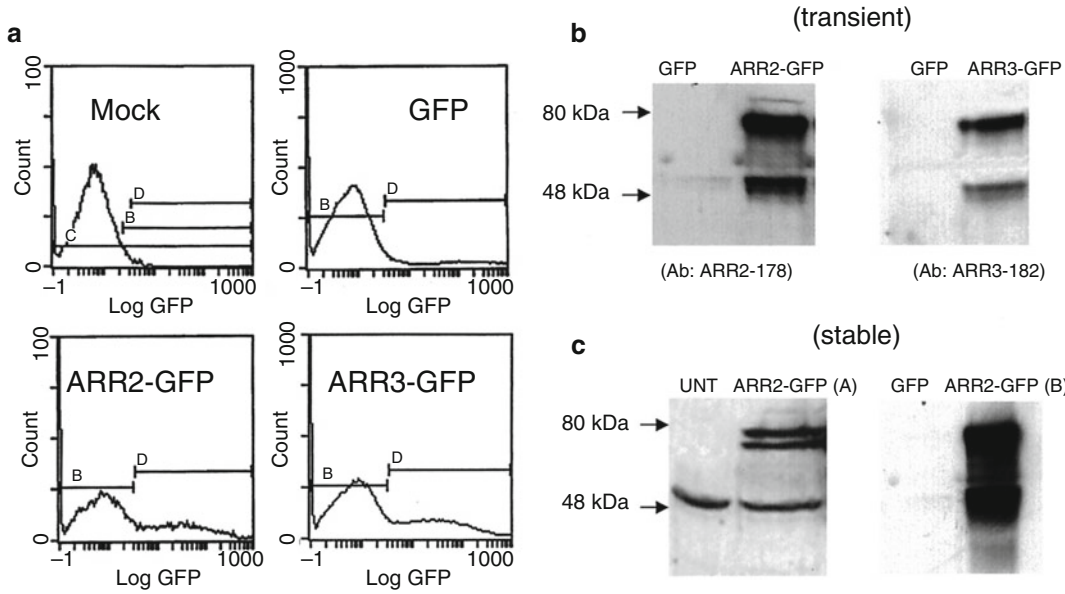


Fig. 1 Expression of arrestin-GFP chimeras in transient and stably transfected human ASM cells. (**a**) HASM cells were transfected with pcDNA3 vector (*Mock*), pEGFPN1 (*GFP*), ARR2-GFP, or ARR3-GFP and analyzed for fluorescence using a Coulter Epics Elite ESP Flow Cytometer. The population of cells exhibiting fluorescence greater than that established in mock-transfected cells (autofluorescence) was sorted and subsequently plated for analysis of arrestin expression, receptor-mediated cAMP production, or agonist-dependent ARR2-GFP localization. (**b**) Populations of ARR2-GFP- or ARR3-GFP-expressing cells isolated by FACS were plated onto 12-well plates. Four days later cells were harvested, and ARR2-GFP and ARR3-GFP expressions were assessed by immunoblotting using the polyclonal antibodies 178 (specific for arrestin-2) and 182 (specific for arrestin-3). (**c**) Two separate lines expressing ARR2-GFP were also established by selection with G418, with one line expressing a low level of ARR2-GFP (ARR2-GFP(A); ~three- to fourfold of endogenous arrestin-2 observed in untranslated cells (*UNT*)) and another line expressing a high level of ARR2-GFP (ARR2-GFP(B); >100-fold of endogenous arrestin-2). Different lengths of autoradiograph exposure account for differences in intensity of bands representing endogenous arrestin-2. From Penn et al. *J. Biol. Chem.* 2001;276:32648–32656

10. Assess the expression of arrestins by visualization of GFP (*see* **Note 7**) or by immunoblot analysis; and/or add selection agents 48 h post-transfection to select for stable expression of arrestins (*see* **Note 8**).
11. Addition of antibiotics is optional at this stage.
12. Harvest cells and replate them for specific experiments (Fig. 1).

3.2 Molecular Strategies: Arrestin Knockdown Using Transient siRNA Transfection

The strategy described below results in robust knockdown of β-arrestins (*see* **Note 9**).

1. As per Subheading 3.1 methods, passage ASM cells the day prior into 60 mm dishes to achieve ~50% confluence the day of siRNA transfection.
2. Warm up all buffers and media to 37 °C in a water bath.

3. Re-feed plated cells with complete Ham's F-12 media prior to preparing transfection reagents (3 mL per 60 mm dish).
4. Resuspend lyophilized siRNA to 100 μM in 1× siRNA buffer. Vortex at the lowest speed or shake lightly by hand to resuspend. Spin the tube down briefly using a tabletop centrifuge at a low speed (100 rcf; ≤1 min).
5. Prepare three 1.5 mL tubes per siRNA used.
6. Fill first tube with 100 μL of 1× siRNA buffer.
7. Fill second and third tubes with 100 μL plain DMEM cell culture media.
8. Add 2 μL of 100 μM siRNA solution to the first tube.
9. Transfer the contents of the first tube to the second tube.
10. Add 6 μL of DharmaFECT to the third tube.
11. Incubate for 5 min at RT.
12. Transfer the contents of the second tube to the third tube.
13. Incubate for 20 min at RT.
14. Add the entire contents of the third tube, dropwise, to the cell culture dish.
15. Assess the effect of protein knockdown 72–96 h post-transfection by immunoblotting.
16. The procedure can be scaled up or down for other size cell culture dishes (Fig. 2).

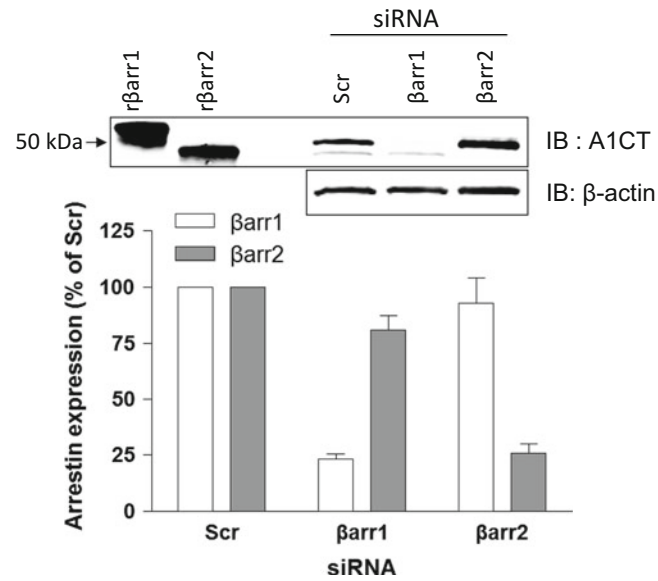


Fig. 2 β-arrestin1 and β-arrestin2 expression in human ASM cultures treated with scrambled (SCR), βarr1, or βarr2 siRNA. Values are means ± SEM from nine experiments. From Pera et al. *FASEB J,* 2015, 10:4227–4235

3.3 Molecular Strategies: Stable Arrestin Knockdown, Using a Retrovirus-Mediated Approach

1. For retrovirus generation, thaw GP2-293 packaging cells and plate into a 10-cm dish containing 10 mL *complete* DMEM media.
2. Change cell media to fresh complete DMEM the day after thawing. Depending on the freezing of the cells, there may be many dead/floating cells. Do not discard the plate, just continue to change the media every few days until cells recover, and start to grow. Be careful not to overgrow cells or plate them at a very low density as they will not behave properly.
3. When cells are confluent, they should be split ~1:4 into new 10 cm dishes. They usually need to be split 2–3 times per week.
4. When ready to make virus (day 1), split the packaging cells 1:10–12 (assuming a fully or nearly confluent 10 cm dish) into new 10 cm dishes.
5. On day 2 (transfection day), check to see that cells are ~30% confluent (*see* **Note 10**). *Change media to DMEM no P/S (10 mL) prior to transfection.*
6. Transfect the packaging cells using Fugene HD.
   (a) Per 10 cm plate/construct—In a sterile Eppendorf tube (in hood), add 5 μg of retroviral vector construct and 5 μg of the helper plasmid (pVSVG) to 485 μL of plain DMEM media (*see* **Note 11**).
   (b) Add 15 μL of Fugene HD to the media/DNA mixture. Make sure to add the Fugene HD directly to the media without touching the plastic of the tube!!
   (c) Mix thoroughly and incubate for 15 min at room temperature.
   (d) Add mixture to the 10 cm dish (containing DMEM *no P/S* media).
7. Eighteen to twenty-four hours (18–24 h) later (on day 3) change media to 10 mL of *complete* DMEM. Incubate the culture for another 48 h to allow viral titer to increase.
8. On day 5, collect the supernatant containing the virus. Filter through a 0.45 μm PVDF filter into a sterile 50 mL conical tube. Virus can be used to infect target cells immediately; if not, freeze filtered virus in the conical tube at −80 °C.
9. Twenty-four hours (24 h) prior to infection, plate ASM cells at a density of 12,500 cells/cm^2 into 10 cm dishes in 10 mL of *complete* F-12; this should achieve ~50% confluence the next day.
10. Obtain filtered virus just harvested from packaging cells (or thaw out the frozen virus at 37 °C; *see* **Note 12**).
11. On day of infection, prepare *F-12 NO P/S* media containing 8 μg/mL polybrene. Aspirate media from the target cells, and

add 5 mL of the media/polybrene mixture to each 10 cm dish of target cells.

12. Add 5 mL of the appropriate, previously prepared virus per dish. Virus amounts may vary, but the logic here is to use one half volume of fresh media (so cells stay fed and happy) plus one half volume of virus which should be of sufficient titer to infect cells. Incubate cells at 37 °C.
13. After 24 h incubation with virus, remove virus-containing media and replace with fresh *complete* F-12 media.
14. The next day (48 h post-virus addition):
    (a) For transient expression, cells can be plated for experiments in complete F-12 media.
    (b) For stable expression, change media to complete F-12 *containing 250 μg/mL G418* (250 μL of 500 mg/mL G418 solution per bottle complete F-12). Cells will select/die off over the next 7–14 days. If virus expresses a fluorescent protein, this can be used to monitor selection/infection efficiency. Change media to fresh F-12/G418 every 3–4 days. Once cells are confluent/no longer dying off, pass into a 15 cm dish to expand and/or plate for experiments.
15. For infection of lung tissue ex vivo that contains ASM (either isolated airways or precision cut lung slices in culture, from either mice or humans), the tissue infection is performed using lentivirus (*see* **Note 13**) as per Morgan et al. [4]. The virus titer, and duration of virus exposure, may need to be empirically determined for each tissue culture and each virus preparation.

3.4 Signaling, Functional Experiments in ASM Using Transfected/Infected ASM Cultures

1. Plating of cells for terminal experiments: After transient transfection or stable line generation, cells are plated at a density of 25,000 cells/cm^2 in either 96-, 24-, 12-, or 6-well plates (day 0) (*see* **Note 14**).
2. Cells are re-fed with complete F-12 media on day 3.
3. On day 6, cells (which should be ~95% confluent) are then washed once with sterile room temperature PBS and re-fed with serum-free media. Twenty-four hours (24 h) later (day 7, if re-fed with F-12 media containing 0.1% BSA, or 48 later, if re-fed IT media) cells are stimulated for signaling or functional experiments.
    (a) Stimulation of ASM cells for signaling analyses: wash cells with room temperature PBS and re-feed plain Ham's F12 (*see* **Note 15**).
    (b) When ready to stimulate cells with the appropriate agonist, add reagents and place culture dish in either a 37 °C water bath (for experiments of 1 h duration or less) or

return to the 37 °C incubator (for experiments of >1 h duration).

(c) Upon conclusion of stimulation, wash cells in ice-cold PBS twice, then lyse with appropriate lysis buffer for specific experiment as described previously in [5–9].

4. For analysis of cAMP accumulation, we use the Applied Biosystems cAMP-Screen system [10]; lyse cells with manufacturer provided lysis buffer and perform assay according to manufacturer's instructions.
5. For immunoblot analysis, we use standard SDS-PAGE and the Li-Cor Odyssey system as per [5]; lyse cells in RIPA buffer with protease and phosphatase inhibitor cocktail. Perform SDS-PAGE gel electrophoresis and transfer proteins onto nitrocellulose membranes; block with LiCOR blocking buffer (1 h at RT), and incubate membrane with anti-β-arrestin1/2 rabbit mAb (1 h at RT); incubate with secondary IRDye (1 h at RT), and perform detection and quantification as per [5], with discrimination of isoform based on protein size. *See* **Note 16** for protein detection using the ProteinSimple Wes system.
6. For immunoblot analysis of ASM cells, the current antibody of choice that we use is anti-β-arrestin1/2 rabbit mAb (1:1000, Cell Signaling Technology), with discrimination of isoform based on size.
7. For immunocytochemistry of ASM cells and immunohistochemistry of ASM tissue, no commercially available antibody has been validated (*see* **Note 17**).
8. For analysis of ASM growth, we use the CyQuant assay as per [9] plate cells in a 96-well plate (1×10^4 cells per well) and maintain in complete Ham's F-12 medium supplemented with 10% FBS. After 24 h, switch to serum-free IT media, and treat with stimuli for 72 h; aspirate media, and add manufacturer-provided assay buffer containing CyQuant dye; incubate for 30 min (RT), and measure fluorescence intensity as per the manufacturer's instructions.
9. For analysis of mRNA abundance regulation by quantitative PCR, we lyse the cells in TRIzol and isolate mRNA using a column-based mRNA isolation kit. cDNA generation and quantitative PCR are performed as per [8].
10. To assess single cell contractility of ASM cells, we use magnetic twisting cytometry (MTC). Dynamic changes in cell stiffness are measured as an indicator of contraction of isolated ASM cells using the MTC technique as per [8]. Briefly Arg-Gly-Asp (RGD)-coated ferrimagnetic microbeads bound to adherent cells are magnetized horizontally and then twisted in a vertically aligned homogeneous magnetic field that was varying

sinusoidally in time. This sinusoidal twisting magnetic field caused both a rotation and a pivoting displacement of the bead: such forced bead motions are, in turn, impeded by internal stresses developed by the cell. Lateral bead displacements in response to the resulting oscillatory torque is detected with a spatial resolution of ~5 nanometer (nm), and the ratio of specific torque to bead displacements is computed and expressed as the cell stiffness in units of Pascal (Pa) per nm. For each individual ASM cell, baseline stiffness is measured for the first 60 s, and changes in cell stiffness in response to agonists are measured continuously for the next 240 s. Given this technique requires expensive equipment, software, and considerable expertise, it is typically performed by one of only a handful of labs throughout the world, in a collaborative manner.

11. For cell migration assays, cells are trypsinized and resuspended in serum-free media supplemented with BSA. Cells (5×10^4) are then placed into the upper wells of a Boyden chamber, fitted with an 8 μm pore membrane. Agonists or vehicle in serum-free media supplemented with BSA are added to the lower chambers. Cells in the Boyden chamber are incubated for 4 h at 37 °C in a 5% CO_2 incubator. Nonmigrated cells are scraped off. The membrane is then fixed and stained, and the cells are counted as per [6].

4 Notes

1. Other transfection reagents are likely effective. As with any transfection reagents, their efficacy and toxicity should be empirically determined for the specific cell type and protocol employed.
2. Constructs encoding ARR2-GFP, ARR3-GFP, and ARR2 (R169E)-GFP were generated by polymerase chain reaction amplification of the open reading frames of bovine ARR2, ARR3, and ARR2R169E (all previously cloned into pcDNA3) and cloning in pEGFPN1 (CLONTECH, Palo Alto, CA) such that the C-terminal GFP sequence was in frame to generate the intended chimera. Design of dominant-negative arrestin constructs were based on and validated by studies from the Gurevich [11] and Lefkowitz labs [12].
3. siRNA are ON-TARGETplus SMARTpool oligos (Dharmacon, Lafayette, CO, USA), representing a combination of siRNA empirically established to selectively target human β-arrestin1 or β-arrestin2. Single-specific siRNAs targeting β-arrestin1 (5′-AAAGCCUUCUGCGCGGAGAAU-3′) or

β-arrestin2 (5′-AAGGACCGCAAAGUGUUUGUG-3′) are also effective [13].

4. Dissolve contents of bottle (5 g) in 10 mL dH_2O, and filter through a 0.22 μm filter. Aliquot into individual Eppendorf tubes and freeze at −20 °C until needed.
5. This methodology is similar to that employed in Penn et al. *J Biol Chem* 2001 [3], the original study assessing the effect of arrestin overexpression on signaling of multiple endogenously expressed Gs-coupled GCPRs (β2-adrenoceptor, EP2/4 receptors, and A2b adenosine receptor) in human ASM. Our early studies on arrestins in ASM, performed prior to the successful application of antisense or si/sh RNA knockdown strategies, employed overexpression of wild-type or dominant-negative arrestin mutants in order to assess which GPCRs in ASM might be susceptible to arrestin-mediated regulation. Although this strategy suffers from the inherent limitation of overexpression strategies (e.g., protein-protein interactions and events occurring solely as a result of supraphysiological expression of a protein), later studies that involved knockdown or knockout of endogenous arrestins would both clarify the physiological role of arrestins and reveal those spurious effects conferred by arrestin overexpression. Our laboratory prefers to use a transfecting scrambled siRNA oligonucleotide to generate control cells. However, comparison of cells transfected with scrambled siRNA oligonucleotides with those (sham) transfected with oligonucleotide vehicle suggest no differences in GPCR signaling or function between these two control lines (Penn, unpublished data).
6. For Fugene HD it is important not to incubate for too long (max 10 min); transfection efficiency may drop with increasing incubation times.
7. The strategy of expressing arrestin constructs as GFP chimeras was based on: (1) the ability to easily detect GFP and confirm efficiency of transfection/infection, (2) enabling the option to sort GFP+ cells to further achieve a greater % of cells expressing the recombinant arrestin, and (3) the experimental control and ease of interpretation provided by the use of control cells transfected/infected with GFP alone. Transfection efficiency with this method 48 h after transfection of primary ASM culture using Fugene HD can range from 40 to 75%.
8. For stable expression, strategies employing retroviral or lentiviral infection (with selection, following the protocol below for stable shRNA expression) are preferable to transient transfection followed by selection. This is due to the greater efficiency of expression/integration that occurs with virus-mediated infection, enabling a greater number of cells to survive

selection which in turn allows for a more rapid expansion of cells expressing the construct of interest.

9. In our hands, this method results in typically ≥75% knockdown of β-arrestin1 or β-arrestin2. Dual knockdown can be achieved with similar efficiency. In ASM cells this level of knockdown was shown to increase isoproterenol-induced cAMP response by 50% post-β-arrestin2 knockdown, whereas β-arrestin1 knockdown resulted in a 30% decrease of methacholine-induced calcium mobilization [7].
10. If there are too few cells, they will not produce enough virus. If cells are too dense, they will overgrow before the virus is ready.
11. Our lab has used multiple viral vectors to generate virus to infect ASM successfully. The choice of vector may depend on the ease of cloning the desired DNA into the vector, the need for co-expressing a fluorescent protein, or the type of selection required. The majority of viral preparations have used the pLNCX2 retroviral vector, which we have employed with great success [4].
12. This procedure is for unconcentrated virus. The amount of virus added per dish may vary if it is concentrated (or cells other than HASM are used) and should be empirically determined before starting. Aim to end with 10 mL of media/polybrene/virus per 10 cm dish.
13. Infection of ASM cells with lentivirus, enabling the expression of either recombinant protein or shRNA, follows a similar protocol with the preparation of lentivirus differing as per [4]. As with retrovirus, each lentivirus preparation requires empirical assessment of the amount of virus that produces optimal expression/knockdown with minimal toxicity.
14. Typically, optimal (highest) expression of arrestin recombinant proteins expressed via transient transfection occurs 48–72 h post-transfection, whereas the highest level of arrestin isoform knockdown occurs at 96 h post-transient transfection. Pre-treatments, serum starvation, and cell cycle arrest steps for various functional assays should be timed accordingly, if optimal expression/knockdown is desired.
15. For select acute signaling experiments, such as assessing short duration treatment effects on intracellular cAMP accumulation or phosphoprotein induction, cells can be refed PBS (with Ca^{2+} and Mg^{2+}). Solubility of stimuli in media/buffer is a factor to consider. If pre-treating cells with reagents, return cells to 37 °C incubator.
16. Protein Simple Wes is a fully automated capillary electrophoresis apparatus used for immunodetection of (phospho-)proteins [14]. After stimulation cells are washed with ice-cold PBS and

lysed in RIPA buffer, and lysates are loaded on manufacturer-provided plates and run in the Wes apparatus according to manufacturer's instructions. Data are analyzed using manufacturer-provided software as per [10].

17. Few published studies exist in which endogenous arrestins are detected using either immunocytochemistry or immunohistochemistry for any cell type or tissue. Overwhelmingly, the consensus among labs known for studying arrestins is that immunocytochemical and immunohistochemical detection of endogenous arrestins requires affinity-purified arrestin antibodies produced in academic labs.

Acknowledgment

Studies in the Penn and Pera labs are supported by NIH grants HL58506, HL136209, HL114471, and AI110007 (RBP) and HL140064 (TP).

References

1. Deshpande DA, Pascual RM, Wang SW, Eckman DM, Riemer EC, Funk CD, Penn RB (2007) PKC-dependent regulation of the receptor locus dominates functional consequences of cysteinyl leukotriene type 1 receptor activation. FASEB J 21(10):2335–2342
2. Panettieri RA, Murray RK, DePalo LR, Yadvish PA, Kotlikoff MI (1989) A human smooth muscle cell line that retains physiological responsiveness. Am J Physiol Cell Physiol 256 (25):C329–C335
3. Penn RB, Pascual RM, Kim Y-M, Mundell SJ, Krymskaya VP, Panettieri RA Jr, Benovic JL (2001) Arrestin specificity for G protein-coupled receptors in human airway smooth muscle. J Biol Chem 276:32648–32656
4. Morgan SJ, Deshpande DA, Tiegs BC, Misior AM, Yan H, Hershfeld AV, Rich TC, Panettieri RA, An SS, Penn RB (2014) Beta-agonist-mediated relaxation of airway smooth muscle is protein kinase A-dependent. J Biol Chem 289(33):23065–23074
5. Billington CK, Kong KC, Bhattacharyya R, Wedegaertner PB, Panettieri RA, Chan TO, Penn RB (2005) Cooperative regulation of p70S6 kinase by receptor tyrosine kinases and G protein-coupled receptors augments airway smooth muscle growth. Biochemistry 44:14595–14605
6. Goncharova EA, Goncharov DA, Zhao H, Penn RB, Krymskaya VP, Panettieri RA Jr (2012) beta2-adrenergic receptor agonists modulate human airway smooth muscle cell migration via vasodilator-stimulated Phosphoprotein. Am J Respir Cell Mol Biol 46 (1):48–54
7. Pera T, Hegde A, Deshpande DA, Morgan SJ, Tiegs BC, Theriot BS, Choi YH, Walker JK, Penn RB (2015) Specificity of arrestin subtypes in regulating airway smooth muscle G protein-coupled receptor signaling and function. FASEB J 29(10):4227–4235
8. Saxena H, Deshpande D, Tiegs B, Yan H, Battafarano R, Burrows W, Damera G, Panettieri R, Dubose JT, An S, Penn R (2012) The GPCR OGR1 (GPR68) mediates diverse signalling and contraction of airway smooth muscle in response to small reductions in extracellular pH. Br J Pharmacol 166 (3):981–990
9. Sharma P, Panebra A, Pera T, Tiegs BC, Hershfeld A, Kenyon LC, Deshpande DA (2016) Antimitogenic effect of bitter taste receptor agonists on airway smooth muscle cells. Am J Physiol Lung Cell Mol Physiol 310(4):L365–L376
10. Pera T, Deshpande DA, Ippolito M, Wang B, Gavrila MJ, Nayak AP, Tompkins E, Farrell E, Kroeze WK, Roth BL, Panettieri RAJ, Benovic JL, An SS, Dulin NO, Penn RB (2017) Biased signaling of the proton-sensing receptor OGR1 by benzodiazepines. FASEB J 32 (2):862–874. In press

11. Kovoor A, Celver J, Abdryashitov RI, Chavkin C, Gurevich VV (1999) Targeted construction of phosphorylation-independent beta-arrestin mutants with constitutive activity in cells. J Biol Chem 274(11):6831–6834
12. Attramadal H, Arriza JL, Aoki C, Dawson TM, Codina J, Kwatra MM, Snyder SH, Caron MG, Lefkowitz RJ (1992) Beta-arrestin2, a novel member of the arrestin/beta-arrestin gene family. J Biol Chem 267(25):17882–17890
13. Ahn S, Nelson CD, Garrison TR, Miller WE, Lefkowitz RJ (2003) Desensitization, internalization, and signaling functions of beta-arrestins demonstrated by RNA interference. Proc Natl Acad Sci U S A 100(4):1740–1744
14. Harris VM (2015) Protein detection by simple western™ analysis. In: Kurien BT, Scofield RH (eds) Western blotting: methods and protocols. Springer, New York, NY, pp 465–468



Chapter 5

Measuring Recruitment of β-Arrestin to G Protein-Coupled Heterodimers Using Bioluminescence Resonance Energy Transfer

Dany Fillion, Dominic Devost, and Terence E. Hébert

Abstract

Initially identified as monomers, G protein-coupled receptors (GPCRs) can also form functional dimers that act as distinct signalling hubs for the integration of cellular signalling. We previously found that the angiotensin II (Ang II) type 1 receptor (AT1R) and the prostaglandin F2α (PGF2α) receptor (FP), both important in the control of smooth muscle contractility, form such a functional heterodimeric complex in HEK 293 and vascular smooth muscle cells (Goupil et al., J Biol Chem 290:3137–3148, 2015; Sleno et al., J Biol Chem 292:12139–12152, 2017). In addition to canonical G protein coupling, GPCRs recruit and engage β-arrestin-dependent pathways. Using BRET-based biosensors, we demonstrate how to assess recruitment of β-arrestin-1 and -2 to AT1R and the AT1R/FP dimer in response to Ang II. Surprisingly, β-arrestin-1 and -2 were recruited to the dimer, in response to PGF2α as well, even though FP alone cannot recruit either β-arrestin-1 and -2.

Key words GPCRs, G protein-coupled receptors, Heterodimerization, Bioluminescence resonance energy transfer, BRET, β-arrestin recruitment

1 Introduction

GPCR dimers remain a source of both excitement and skepticism in the field. We previously found that the AT1R and FP formed a functional heterodimeric complex in HEK 293 and vascular smooth muscle cells [1, 2]. Since the discovery that GABA-B receptors were obligate heterodimers in 1998–1999 (and other class C GPCRs since), many researchers became interested in how such heterodimers might generally affect ligand specificity, allostery, and downstream signalling outputs from GPCRs. This research area remains lively, but apart from the certainty regarding class C GPCRs, dimers of class A GPCRs remain an area of contentious study [3–7]. Interested readers are directed to several comprehensive reviews [8–11]. Potentially, GPCR heterodimers can have distinct pharmacological and signalling properties that can

Mark G. H. Scott and Stéphane A. Laporte (eds.), *Beta-Arrestins: Methods and Protocols*, Methods in Molecular Biology, vol. 1957, https://doi.org/10.1007/978-1-4939-9158-7_5, © Springer Science+Business Media, LLC, part of Springer Nature 2019

be assayed by classical biochemical methods or by using resonance energy transfer (RET)-based approaches. Here, we review a simple BRET-based β-arrestin recruitment assay based on other studies [12–15] that can be used to demonstrate distinct patterns of signalling when GPCRs form heterodimers.

2 Materials

2.1 Cell Culture and Transfection

1. Tissue culture-treated T75 flasks and 12-well plates.
2. Cell culture incubator fixed at 37 °C, 100% humidity, and 5% final CO_2.
3. Tissue culture hood.
4. HEK 293 cells.
5. Culture media composed of Dulbecco's modified Eagle's medium (DMEM) high glucose supplemented with 5% (v/v) fetal bovine serum (FBS) and 1% (v/v) penicillin/streptomycin (P/S) (Wisent, cat.no 450-201-EL).
6. Trypsinization solution: 0.25% trypsin/2.21 mM EDTA tetrasodium (Wisent).
7. Mycoplasma testing kit (MycoAlertTM from Lonza (Rockland, MD, USA)).
8. Cell transfection reagent Lipofectamine® 2000.
9. DNA constructs: pcDNA3.1(−) empty vector. The βArr1-RlucII and βArr2-RlucII plasmids have been described previously [16, 17]. pcDNA3.1/SP-FLAG-hAT1R-WT and pcDNA3.1/SP-HA-hFP-WT have been described previously [1]. pcDNA3.1/SP-FLAG-hAT_1R-KPVAT-Venus (AT_1R-Venus) and pcDNA3.1/SP-HA-hFP-KPVAT-Venus (FP-Venus) plasmids were generated by PCR and contain a signal peptide (SP), a peptide Tag (FLAG and HA), a peptide linker (KPVAT), and a yellow fluorescent protein (Venus, details are available upon request).

2.2 Bioluminescence Resonance Energy Transfer (BRET)

1. Ligand solutions: Angiotensin II (Ang II, dissolved in water) and PGF2α (dissolved in pure ethanol) both at 1 mM are freshly diluted in Krebs buffer to 5 μM.
2. Sterile solution of 0.1 mg/mL poly-L-ornithine hydrobromide prepared in phosphate-buffered saline.
3. 30 μM coelenterazine h solution: stock solution of 1 mM coelenterazine h prepared in pure ethanol is freshly diluted in Kreb's solution (*see* below) to 30 μM. The solution is prepared in a dark tube to protect from light.

4. White 96-well plates were from Costar® #3917, Corning, NY, USA, and were coated with poly-L-ornithine hydrobromide (*see* above).
5. Kreb's buffer: 146 mM NaCl, 4.2 mM KCl, 0.5 mM $MgCl_2$, 1 mM $CaCl_2$, 5.9 mM glucose, and 10 mM HEPES pH 7.4, 0.1% (v/v) glucose.
6. Either a TriStar^2 LB 942 multimode microplate reader from Berthold Technologies Inc. (Bad Wildbad, 75323, Germany) equipped with the predetermined BRET1 filter pair F485/F530 or a VICTOR X-light multilabel plate reader from Perkin Elmer Inc. (Waltham, MA, USA) equipped with the predetermined BRET1 filter pair F460/F535 were used to measure BRET ratios. Other instruments can be adapted accordingly.
7. GraphPad PRISM software v6.0 (La Jolla, CA, USA).

3 Methods

3.1 Cell Culture and Transient Transfection

1. HEK 293 cells are cultured in 75 cm^2 plastic flasks containing culture media. Cells are grown in a controlled, humidified environment maintained at 37 °C and 5% CO_2 atmosphere until a confluency of 80–100% was reached.
2. For transfection, cells are trypsinized, and 125,000 cells/well in 1 mL of the same fresh media are seeded into 12-well plates. Cells are left in a cell culture incubator overnight.
3. Twenty-four hours later, media from the plate is replaced by 1 mL/well of culture media without penicillin/streptomycin and transfected with the appropriate plasmids.
4. Here, cells are transfected with plasmids coding for (Venus-tagged or not) AT_1R (0.3 μg/well), (Venus-tagged or not) FP (0.1 μg/well), and the sensors (βArr1/2-RlucII (0.0025–0.025 μg/well), along with pcDNA3.1(−) for a total of 1.0 μg per well using Lipofectamine® 2000 (2.5 μL (Lipofectamine 2000):1 μg (DNA) ratio), following the manufacturer's instructions.
5. Twenty-four hours post-transfection, the cells are trypsinized, and 40,000–50,000 cells/well are transferred into white 96-well plates previously coated with poly-L-ornithine hydrobromide (50 μL of poly-L-ornithine hydrobromide solution is added to each well and left overnight in the tissue culture incubator; then wells are washed with sterile water). Cells were left in a cell culture incubator for another 24 h before performing the experiments (*see* **Note 1**).

1. For BRET experiments, energy-donor proteins were fused to *Renilla* luciferase (Rluc) II, and energy-acceptor proteins were

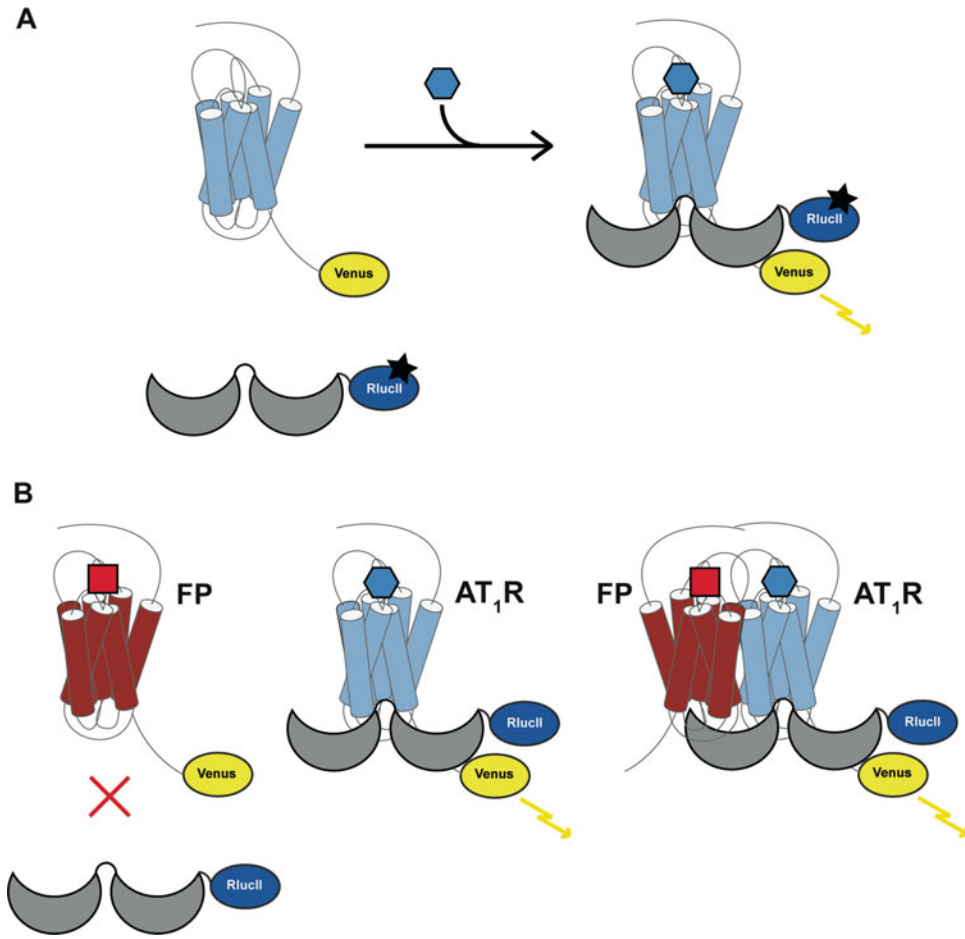


Fig. 1 *Assay design*. (**a**) Schematic showing the principle of β-arrestin recruitment in response to ligand stimulation by tagging the receptor at the C-terminus with Venus or another GFP variant and β-arrestin1/2 with RlucII. (**b**) Different configurations of the assay-AT1R-Venus/βArr2-RlucII, FP-Venus/βArr2-RlucII, or AT1R-Venus/WT-FP/βArr2-RlucII

3.2 Bioluminescence Resonance Energy Transfer (BRET)

fused to the yellow florescent protein (Venus). In all experiments, coelenterazine h was used as the Rluc/RlucII substrate to generate light with a maximal emission peak at 480 nm, allowing YFP excitation. The assay design is shown in Fig. 1a. AT1R-Venus or FP-Venus were expressed alone with βArr1/2-RlucII, or both receptors were expressed together with only one of them tagged with Venus, along with βArr1/2-RlucII (Fig. 1b).

2. A typical experiment was carried out as follows: transfected cells from a white 96-well plate were carefully washed once with 150 μL of Kreb's buffer at room temperature. The buffer was removed by aspiration, and 95 μL/well of the same buffer was

added to the cells. The plate was then protected from light, and the cells were incubated for 1 h at 37 °C.

3. During this time, the plate reader is allowed to reach 37 °C and programmed to collect luminescence in such a way that it can complete the BRET ratio measurements of a whole 96-well plate in 2 min. This corresponds to a luminescence collection time of 330 ms/filter (TriStar^2 LB 942 equipped with the predetermined BRET1 filter pair F485/F530) or 200 msec/filter (VICTOR X-light equipped with the predetermined BRET1 filter pair F460/F535) (*see* **Notes 2** and **3**). The coelenterazine h, Ang II, and PGF2α (see below) are also prepared fresh and protected from direct light, just before being used.
4. *Addition of coelenterazine h substrate*: following 1 h of incubation in BRET buffer, 25 μL/well of a 30 μM coelenterazine h solution (for a final concentration of 5 μM) is sequentially added to the cells, so it takes 2 min to fill the entire 96-well plate.
5. Measurement of basal, unstimulated BRET ratios: luminescence and fluorescence is then immediately measured with the plate reader over a period of 10 min (plate reader is set to measure five cycles).
6. Stimulation of the cells: upon completion of basal reading, the 96-well plate is rapidly removed from the plate reader, and 30 μL/well of either vehicle (Kreb's buffer) or 5 μM ligand (Ang II or PGF2α, for a final concentration of 1 μM in 150 μL) is sequentially added to the cells, so, again, it takes 2 min to fill up the entire 96-well plate.
7. Measurement of ligand-induced, stimulated BRET ratios: luminescence and fluorescence is then immediately measured over a period of 90 min (plate reader is set to measure 45 cycles).

3.3 BRET Data Analysis

1. BRET ratio is calculated as BRET = $\lambda_{530 \text{ or } 535}/\lambda_{485 \text{ or } 460}$ and ligand-induced BRET changes as ΔBRET = $\text{BRET}_{\text{Ligand}} - \text{BRET}_{\text{Vehicle}}$. Conditions associated with ligand and vehicle should all be conducted in triplicate (i.e., 3 wells each), and averaged data is generally used in all calculations. BRET data integrates the area under the curve (*see* **Note 4**).
2. Statistical analysis and curve fitting can be carried out using the software GraphPad.
3. ΔBRET data can be fitted to curves using nonlinear regression and a one-phase exponential dissociation decay with a least squares method.
4. As discussed above (Fig. 1), used a BRET-based approach to examine in live cells and in real-time the recruitment of βArr1/

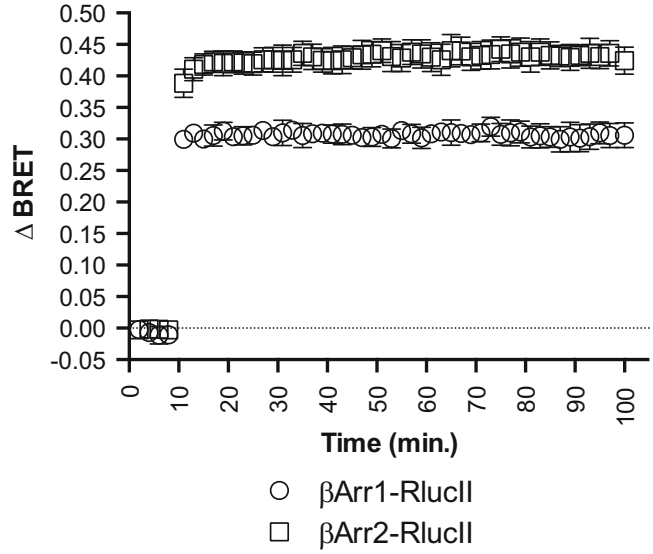


Fig. 2 *AngII-induced recruitment of βArr1/2 to AT1R.* AngII (1 μM) induces rapid and sustained recruitment of βArr1-RlucII (○) and to a larger extent βArr2-RlucII (□) to AT_1R-Venus when expressed alone. Data represent mean ± s.e.m. of independent experiments performed in triplicate ($n = 3–4$)

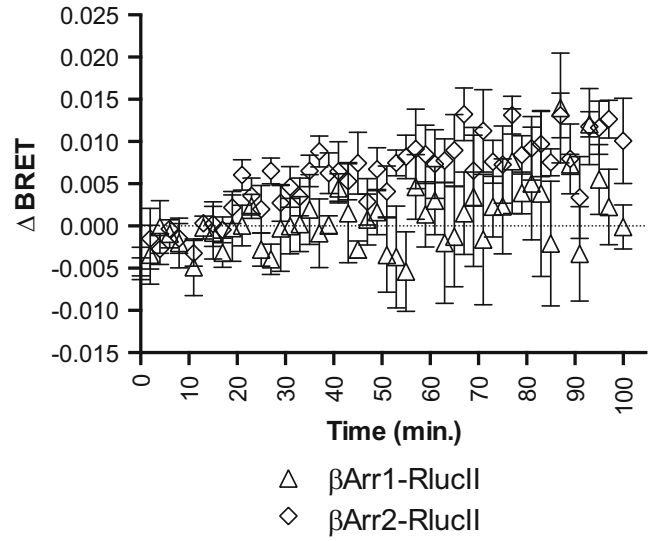


Fig. 3 *PGF2α-induced recruitment of βArr1/2 to FP.* PGF2α (1 μM) induced a much lower recruitment of βArr1-RlucII (△) and βArr2-RlucII (◇) to FP-Venus when expressed alone. Data represent mean ± s.e.m. of independent experiments performed in triplicate ($n = 4–7$)

2-RlucII to AT1R-Venus alone, FP-Venus alone, and the AT1R/FP dimer where Venus was fused to either AT1R or FP. As shown in Fig. 2, Ang II stimulation induces a rapid and

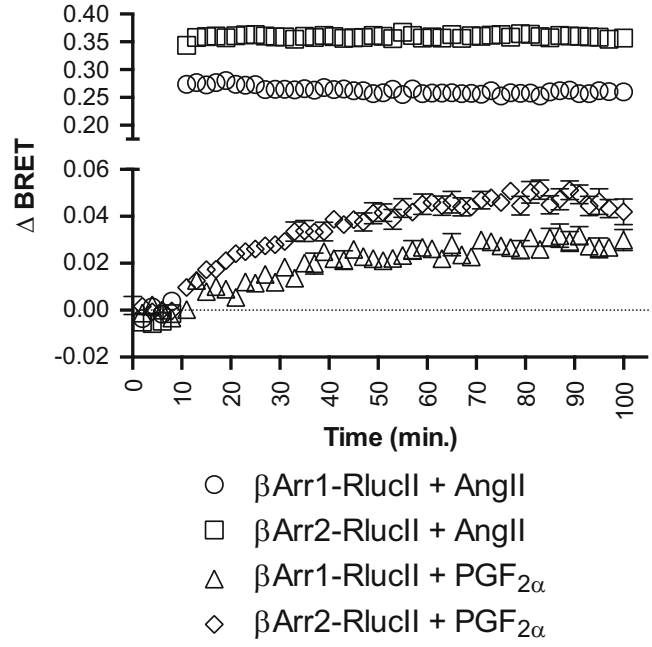


Fig. 4 *Ang II- and PGF2α-induced recruitment of βArr1/2 to the AT1R/FP dimer.* Ang II (1 μM) induces a rapid and sustained recruitment of βArr1-RlucII (○) and βArr2-RlucII (□) to the AT1R-Venus/FP-WT dimer but to a lower extent as compared to AT_1R alone. However, PGF2α also induced recruitment of βArr1-RlucII (△) and βArr2-RlucII (◇) to the dimer. Data represent mean ± s.e.m. of independent experiments performed in triplicate ($n = 8–15$)

sustained βArr1/2-Rluc recruitment to AT1R-Venus alone, typical for a class-B interaction with arrestin [18]. PGF2α stimulation does not induce any recruitment of βArr1/2-Rluc to FP alone (Fig. 3), consistent with the evidence that FP does not recruit β-arrestin in response to ligand stimulation [1]. The responses are also specific since no recruitment is detected when AT1R alone or FP alone are stimulated with their non-cognate ligands (data not shown) or when βArr1/2-RlucII are transfected alone (*see* **Note 5**).

5. However, the picture changes when the two receptors are co-expressed. In this experiment, we used AT1R-Venus along with untagged FP and βArr1/2-RlucII. Stimulation of the AT1R-Venus/FP-WT dimer shows robust βArr1/2-RlucII recruitment in response to Ang II, with similar kinetics as when AT1R-Venus is expressed alone (Fig. 4). Interestingly, PGF2α also induces prolonged βArr1/2-Rluc recruitment to the AT_1R-Venus/FP-WT dimer, but the kinetics are slower, and the extent of recruitment is reduced compared to Ang II, suggesting that the dimer conveys a new role for FP in recruiting β-arrestin, distinct from when it is expressed alone. Taken

together, the sensitivity, coupled with the versatility and high-throughput amenability, of BRET-based approaches described here represent powerful tools to tease out allosteric regulation and biased signalling events specific to GPCR heterodimers.

4 Notes

1. Mycoplasma testing is carried out periodically on all cell lines using the MycoAlert™ kit.
2. Other plate readers can be used for measuring BRET–but it is helpful if they have injectors to capture kinetic information following ligand addition.
3. Experiments in 96-well plates can be carried out according to two different schemes: plate-mode or well-mode. In plate-mode, steps in each experiment are conducted on the 96-well plate as a whole. A strict 2-min interval is applied to each of the four following steps such that each well of the 96-well plate is processed in an identical fashion throughout the experiment:
   - Addition of coelenterazine h substrate for light generation (using a repeater pipette).
   - Measurement of the BRET ratios before Ang II or PGF2α stimulation (i.e., BRET measurement of basal, unstimulated cells).
   - Stimulation of the cells with either vehicle, Ang II or PGF2α (using a multichannel pipette).
   - Measurement of the BRET ratios after Ang II or PGF2α stimulation (i.e., BRET measurement of ligand-induced, stimulated cells).

   Alternatively, in well-mode, the same experimental steps are conducted on each plate well separately, and no common time interval is applied to all these steps. For more information on plate-mode and well-mode operations, readers are encouraged to consult the relevant documentation from 96-well plate reader manufacturers.
4. BRET kinetic traces are shown as a direct kinetic plot of BRET signals, where the *X*-axis represents time and the *Y*-axis represents ΔBRET. BRET signals area under the curve ($\Delta BRET_{AUC}$) are shown as column bars integrating all the area under the curve delimiting by kinetic traces.
5. As a control for BRET specificity, ligand-induced recruitment of βArr2-RlucII to the AT1R-Venus/FP-WT dimer can also be titrated by increasing AT1R-WT co-expression to disrupt the reporting dimer response to PGF2α, to demonstrate the specificity of the AT1R-Venus/FP-WT dimer formation for the asymmetric recruitment of βArr2 mediated by FP.

Acknowledgments

This work was supported by funding from the Canadian Institutes for Health Research and the Ferring Foundation. We also thank Dr. Nicolas Audet (McGill University, Montréal) for useful discussions regarding statistical analysis.

References

1. Goupil E, Fillion D, Clement S, Luo X, Devost D, Sleno R, Petrin D, Saragovi HU, Thorin E, Laporte SA, Hébert TE (2015) Angiotensin II type I and prostaglandin F2α receptors cooperatively modulate signaling in vascular smooth muscle cells. J Biol Chem 290:3137–3148
2. Sleno R, Devost D, Petrin D, Zhang A, Bourque K, Shinjo Y, Aoki J, Inoue A, Hebert TE (2017) Conformational biosensors reveal allosteric interactions between heterodimeric AT1 angiotensin and prostaglandin F2α receptors. J Biol Chem 292:12139–12152
3. Franco R, Martinez-Pinilla E, Lanciego JL, Navarro G (2016) Basic pharmacological and structural evidence for class A G-protein-coupled receptor heterodimerization. Front Pharmacol 7:76
4. Ferre S, Casado V, Devi LA, Filizola M, Jockers R, Lohse MJ, Milligan G, Pin JP, Guitart X (2014) G protein-coupled receptor oligomerization revisited: functional and pharmacological perspectives. Pharmacol Rev 66:413–434
5. Gomes I, Ayoub MA, Fujita W, Jaeger WC, Pfleger KD, Devi LA (2016) G protein-coupled receptor heteromers. Annu Rev Pharmacol Toxicol 56:403–425
6. Smith NJ, Milligan G (2010) Allostery at G protein-coupled receptor homo- and heteromers: uncharted pharmacological landscapes. Pharmacol Rev 62(4):701–725
7. Kleinau G, Muller A, Biebermann H (2016) Oligomerization of GPCRs involved in endocrine regulation. J Mol Endocrinol 57(1): R59–R80
8. Bouvier M, Hebert TE (2014) Rebuttal from Michel Bouvier and Terence E. Hebert. J Physiol 592(12):2447
9. Bouvier M, Hebert TE (2014) CrossTalk proposal: weighing the evidence for Class A GPCR dimers, the evidence favours dimers. J Physiol 592(12):2439–2441
10. Lambert NA, Javitch JA (2014) CrossTalk opposing view: Weighing the evidence for class A GPCR dimers, the jury is still out. J Physiol 592(12):2443–2445
11. Lambert NA, Javitch JA (2014) Rebuttal from Nevin A. Lambert and Jonathan A. Javitch. J Physiol 592(12):2449
12. Bosma R, Moritani R, Leurs R, Vischer HF (2016) BRET-based β-arrestin2 recruitment to the histamine H1 receptor for investigating antihistamine binding kinetics. Pharmacol Res 111:679–687
13. Bonneterre J, Montpas N, Boularan C, Gales C, Heveker N (2016) Analysis of arrestin recruitment to chemokine receptors by bioluminescence resonance energy transfer. Methods Enzymol 570:131–153
14. Donthamsetti P, Quejada JR, Javitch JA, Gurevich VV, Lambert NA (2015) Using bioluminescence resonance energy transfer (BRET) to characterize agonist-induced arrestin recruitment to modified and unmodified G protein-coupled receptors. Curr Protoc Pharmacol 70 (2):14 11–14 14
15. Namkung Y, Le Gouill C, Lukashova V, Kobayashi H, Hogue M, Khoury E, Song M, Bouvier M, Laporte SA (2016) Monitoring G protein-coupled receptor and β-arrestin trafficking in live cells using enhanced bystander BRET. Nat Commun 7:12178
16. Quoyer J, Janz JM, Luo J, Ren Y, Armando S, Lukashova V, Benovic JL, Carlson KE, Hunt SW 3rd, Bouvier M (2013) Pepducin targeting the C-X-C chemokine receptor type 4 acts as a biased agonist favoring activation of the inhibitory G protein. Proc Natl Acad Sci U S A 110: E5088–E5097
17. Zimmerman B, Beautrait A, Aguila B, Charles R, Escher E, Claing A, Bouvier M, Laporte SA (2012) Differential β-arrestin-dependent conformational signaling and cellular responses revealed by angiotensin analogs. Sci Signal 5:ra33
18. Leonard AP, Appleton KM, Luttrell LM, Peterson YK (2013) A high-content, live-cell, and real-time approach to the quantitation of ligand-induced β-Arrestin2 and Class A/Class B GPCR mobilization. Microsc Microanal 19 (1):150–170



Chapter 6

Detection of β-Arrestin-Mediated G Protein-Coupled Receptor Ubiquitination Using BRET

Karim Nagi and Sudha K. Shenoy

Abstract

Ubiquitination of G protein-coupled receptors (GPCRs) is an important dynamic posttranslational modification that has been linked to the intracellular trafficking of internalized GPCRs to lysosomes. Ubiquitination of GPCRs is mediated by specific E3 ubiquitin ligases that are scaffolded by the adaptor proteins called β-arrestins. Traditionally, detection of GPCR ubiquitination is achieved by using ubiquitin antibodies to Western blot immunoprecipitates of detergent-solubilized GPCRs expressed in heterologous cells. However, studies have also shown that bioluminescence resonance energy transfer (BRET)-based techniques can reveal ubiquitination of GPCRs in intact cells and in real time. This chapter describes a step-by-step protocol to evaluate ubiquitination of GPCRs using the BRET methodology.

Key words GPCR, Arrestin, Ubiquitination, BRET, Ubiquitin, Titration, Adrenergic receptor

1 Introduction

G protein-coupled receptors (GPCRs) represent the superfamily of seven-transmembrane cell-surface receptors that respond to a wide variety of extracellular stimuli (photons, hormones, chemicals, etc.) and transduce signaling to affect cellular responses. GPCR signaling governs many aspects of mammalian physiology ranging from vision, olfaction, cardiovascular homeostasis to reproduction and behavior. Hence GPCRs have been center stage for pharmaceutical drug development, and about 35% of prescription drugs are compounds that intercept or modulate GPCR activation [1–3].

Upon agonist stimulation, GPCRs undergo conformational changes that lead to their cytosolic domain phosphorylation by distinct G protein-coupled receptor kinases (GRKs). Phosphorylation of GPCRs initiates the activation and engagement of the cytosolic adaptors belonging to the small family of four arrestin proteins (arrestins 1–4) [4, 5]. β-arrestin1 (also called arrestin2) and β-arrestin2 (also called arrestin3) are the non-visual arrestins that are ubiquitously expressed and display high-affinity association

Mark G. H. Scott and Stéphane A. Laporte (eds.), *Beta-Arrestins: Methods and Protocols*, Methods in Molecular Biology, vol. 1957, https://doi.org/10.1007/978-1-4939-9158-7_6, © Springer Science+Business Media, LLC, part of Springer Nature 2019

with phosphorylated GPCRs and promote desensitization of a vast majority of GPCRs. In addition to being endocytic adaptors, [6, 7] arrestins also act as adaptors that recruit components of the ubiquitination machinery to promote ubiquitination of GPCRs [5, 8–12]. Ubiquitination of GPCRs promotes their degradation in the lysosomes and prevents recycling of internalized GPCRs [10, 12, 13]. Activated β-arrestins are also ubiquitinated, which promotes β-arrestin's association with internalized GPCRs, endocytic proteins as well as with signaling kinases [9].

Ubiquitination is a covalent modification in which one or multiple ubiquitin (Ub) molecules (~8 kDa) are appended to lysines in the substrate protein through an isopeptide bond between the carboxyl terminus of Ub and the epsilon amino group of lysine within the substrate protein or in Ub [14]. Accordingly ubiquitination alters the molecular mass of substrate proteins by 8 kDa (single or monoubiquitination) or multiples of 8 (multi-mono-ubiquitination and polyubiquitination) when more Ub molecules are involved. The traditional method of detecting substrate-specific ubiquitination in vivo is to immunoprecipitate the substrate protein from solubilized extracts of tissues or cultured cells, elute and resolve the isolated protein complex on SDS-PAGE, and perform serial Western blotting: first with Ub IgGs that detect monoubiquitination as well as polyubiquitination on substrates and next with substrate-specific IgG [15, 16]. In general, multiple ubiquitination renders the modified protein to appear as a smear or ladder of protein bands when resolved by SDS-PAGE. The ratio of high molecular weight ubiquitinated substrates to unmodified substrate band is generally used as a measure of ubiquitination. The major disadvantages of this methodology are (a) the substrate-specific IgGs may have low sensitivity to ubiquitinated species preventing a total overlap between the signals detected by ubiquitin IgG and substrate-specific IgG; (b) the ubiquitinated substrate can be rapidly degraded by the 26S proteasomes, and an inhibitor of the proteasomal subunit(s) may be required to detect ubiquitinated substrates [17]; and (c) ubiquitination is a dynamic modification and is rapidly reversed by deubiquitinating enzymes [18]. Hence the inhibition of deubiquitinating enzymes might be necessary to detect ubiquitinated species. Therefore, the ubiquitination status of a protein will depend upon its interaction with the elements of both ubiquitination/deubiquitination machinery at any given time and can be elusive to detection after cell lysis and subsequent processing.

Bouvier and colleagues pioneered the use of bioluminescence resonance energy transfer (BRET)-based methods to detect ubiquitination of β-arrestins in intact cells and in real time [19]. This proximity-based methodology consists of detecting, in real time, the occurrence of a resonance energy transfer between a luminescent donor and a fluorescent acceptor protein that is less than 100Å

(10 nm) apart. In this chapter, we describe a BRET-based protocol to detect energy transfer (interaction) between the BRET donor GPCR molecule that is fused to luciferase (β2-adrenergic receptor (β2AR) or the vasopressin V2 receptor (V2R)) and the BRET acceptor ubiquitin molecule that is fused to a fluorescent protein. The assay described could be used as an indicator of the ubiquitination status of each GPCR assayed (β2AR and V2R) and easily adapted to define ubiquitination of other GPCRs or substrate proteins in living cells.

One of the crucial steps in performing a BRET assay is finding the optimal expression level of both BRET partners that enables the optimal and specific BRET signal. These optimal conditions could be experimentally determined by generating a BRET titration curve in which cells are transfected with a constant amount of the BRET donor and increasing amounts of the BRET acceptor [20]. If the interaction is specific, the ratio of the energy emitted by the fluorescent partner over the energy emitted by the luminescent partner (BRET ratio) should increase hyperbolically until it reaches saturation. However, in the case of non-specific interaction resulting from random molecular collisions, the titration curve shows a minimal BRET transfer that progresses linearly over the same levels of donor/acceptor expression [21, 22].

The BRET titration curves obtained for the β2AR and V2R with eYFP-Ub are shown in Fig. 1. For the V2R, the conditions of stimulation used (2 h of AVP) showed a significant increase in BRET than in cells with no agonist treatment; however, similar agonist treatment of the β2AR (2 h of Iso treatment) did not produce any detectable agonist-induced increase in BRET. The failure to detect agonist-induced ubiquitination of the β2AR (which is mostly polyubiquitination [13, 23–27]) by the BRET approach could be attributed to various reasons. Because polyubiquitin chain formation can quench BRET signals, the assay requires the use of Ub in which the two lysines that form polyubiquitin chains, namely, lysines 48 and 63, are mutated [19]. Additionally because overexpression of exogenous Ub can heighten basal ubiquitination signals, prior assays that demonstrated agonist-induced ubiquitination [13, 23–27] did not employ overexpression of ubiquitin. Nonetheless, the titration analysis shown in Fig. 1 shows that GPCR ubiquitination can be detected as a specific BRET signal. Additionally, the BRET between β2AR-Rluc2 and eYFP-Ub is significantly decreased in HEK-293 cells in which β-arrestin1 and β-arrestin2 have been deleted by genome editing [28, 29] (Fig. 2). These results demonstrate that BRET assays can be used for detecting basal and/or agonist-induced ubiquitination of GPCRs and also support the previous findings that β-arrestins can serve as adaptors for promoting ubiquitination of the β2AR [23].

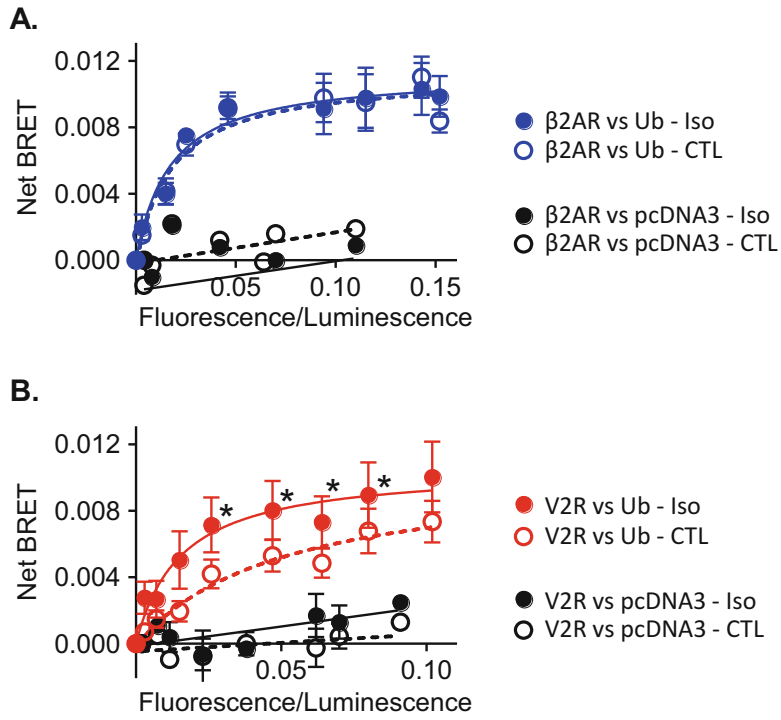


Fig. 1 BRET titration curves of GPCR interaction with ubiquitin. BRET signal was measured in HEK293T cells transiently transfected with a fixed amount (50 ng) of either (**a**) β_2AR-Rluc2 or (**b**) V2R-Rluc2 and increasing amounts **(**0–800 ng**)** of eYFP-Ub. Cells were serum starved for 1 h then stimulated (filled circles) or not (open circles) with Iso (1 μM, **a**) or AVP (100 nM, **b**) for 2 h. The spontaneous, hyperbolic BRET curves produced by these transfections indicate the occurrence of a constitutive and specific interaction between the receptors and the ubiquitin protein (GPCR ubiquitination). In contrast, HEK293T cells transiently transfected with similar donor/acceptor DNA amounts, but by substituting the ubiquitin protein with a vector eYFP construct produces a minimal BRET transfer without displaying any saturable kinetics. Results correspond to mean ± SEM of six independent experiments performed in duplicate. *Iso* isoproterenol, *AVP* arginine vasopressin, *CTL* control vehicle treated. *$p < 0.01$, Two-way ANOVA, Holm-Sidak's multiple comparison V2R vs Ub, AVP compared with V2R vs Ub, CTL

2 Materials

2.1 Cell Culture

1. Human embryonic kidney 293 cells (HEK293T).
2. HEK-293 parental cells and β-arrestin1 and β-arrestin2 double-knockout cells obtained by CRISPR-Cas9 genome editing [28, 29].
3. Complete culture medium: Dulbecco's Modification of Eagle's medium (DMEM) with 4.5 g/L glucose, L-glutamine, and sodium pyruvate), supplemented with 10% (v/v) of fetal

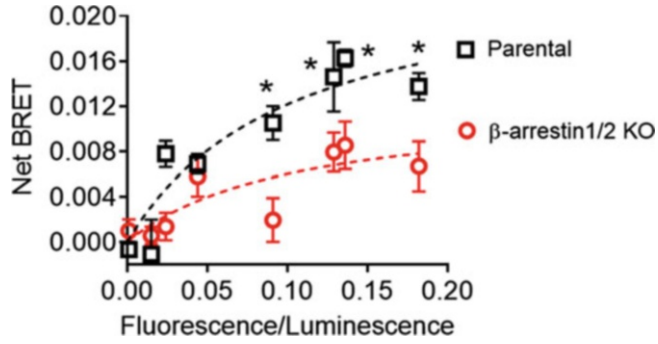


Fig. 2 GPCR ubiquitination in WT and β-arrestin1/2 KO cells. BRET assay shown in Fig. 1a was repeated in two separate HEK-293T cell lines, namely, wild type or parental cells and β-arrestin1/2 KO cells generated by CRISPR-Cas9 genome editing. *$p < 0.01$, Two-way ANOVA, Holm-Sidak's multiple comparison

bovine serum (FBS) and 1% (v/v) of Antibiotic-Antimycotic (100×) (Gibco, cat. no. 15240062) solution (*see* **Note 1**).

4. Trypsin/EDTA solution: 0.05% trypsin, 1× EDTA, and phenol red.
5. Phosphate-buffered saline (PBS) calcium- and magnesium-free (stored at room temperature).
6. Six-well plates or 35 mm cell culture dishes (same surface area).

2.2 Transfection

1. 2.5 M calcium chloride is filter sterilized in a tissue culture hood and stored at 4 °C.
2. 2× HEPES-buffered saline (2× HBS) solution composed of 280 mM sodium chloride, 50 mM HEPES, 12 mM glucose, 10 mM potassium chloride, and 2 mM sodium phosphate dibasic. The pH of the final solution is adjusted to 7.1, and then solution is filter sterilized in a tissue culture hood (*see* **Note 2**).
3. Ub cDNA fused at its N-terminus with the enhanced yellow fluorescent protein eYFP (eYFP-ubiquitin, acceptor BRET partner) and mutated (K48R, K63R) to avoid the formation of poly(eYFP-Ub) chains [19].
4. Human β2AR fused at its C-terminus to a mutant form of the *Renilla* Luciferase (Rluc2) that increases its bioluminescence by multiple times compared to the native Rluc protein [30] (β2AR-Rluc2, donor BRET partner).
5. Human V2R fused at its C-terminus to Rluc2 (V2R-Rluc2, donor BRET partner) [31]. The β2AR or V2R could be easily replaced with other cDNA to study the ubiquitination of any other GPCR or substrate protein of interest.
6. Empty vector such as pcDNA3.1 or any other cloning vector that has been used as the backbone to construct donor and

acceptor plasmids. This vector is used to compensate for differences in DNA amounts transfected.

7. Sterile 1.5 mL microfuge tubes.

2.3 Transfer of Cells into 96 Well Plates

1. Poly-D-lysine powder (Sigma) dissolved in sterile deionized water to a final concentration of 0.1 mg/mL and stored at 4 °C.
2. Phosphate-buffered saline (PBS) calcium- and magnesium-free.
3. Trypsin/EDTA solution: 0.05% trypsin, 1× EDTA, and phenol red.
4. Phenol red-free medium, such as clear MEM solution supplemented with 2% (v/v) of FBS, 2 mM HEPES, and 2 mM Glutamax. If media containing phenol red is used, assure elimination of the phenol red substance on the fourth day of the experiment (*see* **Note 3**).
5. Tissue culture treated white and clear-bottom 96-well plate.
6. 15 mL Falcon tubes.

2.4 BRET Assay

1. Serum-free version of the clear MEM solution mixture used during the transfer step.
2. Hanks' Balanced Salt Solution (HBSS).
3. White adhesive seal to cover the bottom of the 96-well plate.
4. Luciferase substrate, coelenterazine *h* (Promega, Madison, WI) dissolved in anhydrous ethyl alcohol to reach a final concentration of 1 mM (stored at −20 °C). Coelenterazine *h* is light sensitive and should be protected from light at all times.
5. Synergy Neo2 plate reader driven by Gen5 Software to obtain BRET measurements (*see* **Note 4**).
6. GraphPad Prism software version 7.0 (La Jolla, CA) for data analyses.

3 Methods

In this section, we present a step-by-step approach that generates BRET titration curve(s) between GPCR-Rluc2 and eYFP-Ub.

3.1 Cell Culture and Transfection

On day 1 of the experimental procedure, pre-warm complete culture medium, Trypsin/EDTA solution, and PBS in a 37 °C bath before proceeding with subculturing cells.

1. In a tissue culture hood, HEK293T cells that are cultured in 100 mm culture dishes are washed with 5 mL PBS. Next, 1 mL

of Trypsin/EDTA solution is added for 2–5 min to detach cells (*see* **Note 5**).

2. Add 5 mL of complete culture medium to inactivate Trypsin. Detach cells, and transfer them in and out of the pipette tip until no lumps of cells are visible.
3. Transfer cells into a 15 mL Falcon tube, and then proceed for cell counting. Culture 6×10^5 cells in each well of the six-well plate with 2 mL of complete culture medium, such that they reach 40–50% confluence on the next day. Cells are incubated at 37 °C with humidified, 5% CO_2 atmosphere.

3.2 Transfection

On day 2 of the experimental procedure, cells are transfected with equal amounts of DNA using calcium phosphate precipitation method. To ensure that the BRET assay measures interactions that mimic physiological conditions, a low amount of the donor protein is transfected (equal or even lower levels than its endogenous partner). Once the titration analyses of the donor/acceptor pair are obtained, the transfection conditions of the first saturating point could subsequently be used to perform other BRET characterization assays like kinetic measurements and dose-response curves.

For the donor/acceptor titration analyses, plates are transected with a fixed amount of plasmid encoding the BRET donor partner (β2AR-Rluc2 or V2R-Rluc2: 50 ng) and increasing amounts of the BRET acceptor partner (eYFP-Ub: 0, 17, 50, ... 800 ng). To ensure that an equal amount of total DNA is transfected in each plate, decreasing concentrations of the empty vector are also transfected. Transfection should be carried out in a tissue culture hood under sterile conditions using the following steps:

1. Place cDNAs encoding the desired constructs in autoclaved 1.5 mL microfuge tubes.
2. Dilute cDNAs in sterile deionized water for a final volume of 110 μL followed by gentle mixing.
3. Add dropwise 15 μL of 2.5 M calcium chloride to the diluted DNA followed again by gentle mixing.
4. Add dropwise 125 μL of 2× HBS, and mix by bubbling air inside the DNA solution with the P1000 pipette for 15–20 times.
5. Add dropwise the 250 μL transfection mixture to cells by trying to cover the entire culture area, and then return cells to the incubator (37 °C; 5% CO_2).

3.3 Transfer of Cells into 96 Well Plates

On day 3 of the experimental procedure, pre-warm Poly-D-lysine, PBS, Trypsin/EDTA, and supplemented clear MEM solutions at 37 °C.

1. Coat the white and clear-bottom 96-well plates by adding 100 μL of Poly-D-lysine into each well using a multichannel pipette. Rock the plate gently to ensure even coating of the culture surface, and then place it in the incubator (37 °C; 5% CO_2) for 10–20 min.
2. Do not discard the Poly-D-lysine solution after its use since it could be reused several times. Therefore, retrieve the Poly-D-lysine from wells, and then store it at 4 °C.
3. Wash the wells immediately after Poly-D-lysine removal with 100 μL PBS, then aspirate the PBS solution from wells, and keep the plates in the tissue culture hood to dry.
4. Meanwhile, wash six-well plates with 2 mL of PBS. Then, add 0.5 mL of the Trypsin/EDTA solution in each well, and place the plates in the incubator (37 °C, 5% CO_2) for 2–5 min.
5. Add 2.5 mL of clear MEM solution in each well of the six-well plates.
6. Gently detach cells, and transfer them into separate 15 mL Falcon tubes, one tube for each transfection condition.
7. Centrifuge the tubes for 5 min at 500 × *g* in a bench-top centrifuge pellet the cells.
8. Remove the media from the tubes, and then resuspend the cells with 800 μL of clear MEM solution.
9. Cell counting for each tube should then be performed, and cell concentrations are adjusted to one million cells/mL.
10. Place 100,000 cells/well (100 μL) of cell suspensions in 96-well plates according to the experimental design. In addition, place 100 μL of cells of each transfection condition in white and clear-bottom 96-well plates uncoated with Poly-D-lysine (*see* **Note 6**).
11. Keep Poly-D-lysine coated and uncoated plates in the incubator (37 °C, 5% CO_2) until next day (12–24 h).

3.4 BRET Assay and Data Analysis

On day 4 of the experimental procedure, pre-warm serum-free MEM, HBSS solutions, and adjust the plate reader heating system to 37 °C. Using the Gen5 software, design and optimize protocols to perform BRET, total fluorescence, and total luminescence measurements as described below.

1. In the Poly-D-lysine coated 96-well plate, serum starve the cells by removing the media and adding 90 μL of the serum-free version of the clear MEM solution mixture to each well. The plate is then placed in the incubator (37 °C; 5% CO_2) for 60 min.
2. After completing the previous step, stimulate the cells with the cognate agonist (isoproterenol or vasopressin) or vehicle dissolved in serum-free clear MEM for desired time at 37 °C.

3. Remove the media, add 90 μL of HBSS to each well, and then prepare the plate for BRET readings by covering the bottom with a white adhesive seal.
4. Dilute the coelenterazine *h* substrate with HBSS to a final concentration of 50 μM. Immediately after preparation, add 10 μL of the diluted coelenterazine *h* to each well (final concentration of 5 μM/well), and keep the plate in the dark for 5 min, and then measure BRET luminescence and BRET fluorescence simultaneously (*see* **Note 7**). In the Synergy Neo2 plate reader, BRET measurements are detected using a filter cube #117 (excitation at 460 ± 20 nm and emission at 540 ± 12.5 nm).
5. In the 96-well plate uncoated with Poly-D-lysine, proceed for total fluorescence and total luminescence measurements. Begin by measuring the total fluorescence amount in each well at settings that allow adequate excitation/emission by eYFP (*see* **Note 8**). In the Synergy Neo2 plate reader, the total light emitted by eYFP is detected with a filter cube #111 (excitation at 485 ± 10 nm and emission at 528 ± 10 nm) (*see* **Note 9**).
6. Using the same 96-well plate, proceed for total luminescence detection after covering the bottom with a white adhesive seal. For that purpose, add 10 μL of the coelenterazine *h* substrate for a final concentration of 5 μM/well (as described in Subheading 3.4, **step 4**), keep the plate in the dark at room temperature for 10 min, and then read the total luminescence produced by the luciferase substrate using a protocol that measures total luminescence readings. In the Synergy Neo2 plate reader, total luminescence is detected with a filter cube #114 (detecting the standard luminescence without the selection of any filter) (*see* **Note 9**).
7. As shown in Figs. 1 and 2, the deduced NET BRET ratio for each transfection condition mentioned in Subheading 3.2 is plotted against corresponding total luminescence/total fluorescence.

4 Notes

1. DMEM and Antibiotic-Antimycotic used for cell culture purpose are stored at 4 °C. FBS is aliquoted in 50 mL tubes and stored at −20 °C.
2. 2× HBS solution could be stored in aliquots at −20 °C. However, once thawed, store the 2× HBS solution at 4 °C.
3. It is preferable to use phenol red-free media in this step of the study. However, if media with phenol red or any other colored media is used, it is recommended to wash cells three times with

warm PBS or HBSS before starting the BRET assay on the fourth day of the experiment. Coloration in the media may not change luciferase activity but can change light emission and reduce energy transfer between BRET pairs [32].

4. BRET measurements could be done in any plate reader that contains filters that could detect the light emitted by the BRET donor following the addition of the luciferase substrate (emission peak at 480 nm) as well as the light emitted by the BRET acceptor excited by the energy produced by the BRET donor (emission peak at 530 nm).
5. To allow adherent cell dissociation from culture dishes using trypsin, complete culture media should be removed then cells washed with sterile PBS. This washing is essential to eliminate any trace of FBS that contains protease inhibitors that could prevent the trypsinization process.
6. Plate coating with Poly-D-lysine could disturb the total fluorescence measurement. For that reason, uncoated plates will be used to assess total fluorescence and total luminescence measurements.
7. The BRET signal generated by each sample is determined by calculating the ratio (BRET ratio) of the light emitted by YFP (BRET fluorescence) over the light emitted by Rluc2 (BRET luminescence). These values are then corrected by subtracting the background signal (BRET ratio detected in cells expressing only the donor BRET partner) from the BRET ratio detected in cells coexpressing both donor and acceptor constructs (NET BRET).
8. Total fluorescence measurement should be performed without the addition of coelenterazine *h* since luciferase substrate addition will initiate the energy transfer reaction which will activate the fluorescent BRET partner and, therefore, distort the total fluorescence values.
9. To calculate the specific fluorescence and luminescence values produced in each sample, correct the data obtained in **steps 5** and **6** of the BRET assay by subtracting the corresponding background value detected in untransfected cells.

Acknowledgments

We thank Drs. Michel Bouvier, Marc Caron, and Stéphane Laporte for providing plasmid constructs. We thank Dr. Asuka Inoue for providing β-arrestin1/β-arrestin2 double-knockout HEK-293T cells.

References

1. Lefkowitz RJ (2004) Historical review: a brief history and personal retrospective of seven-transmembrane receptors. Trends Pharmacol Sci 25(8):413–422. https://doi.org/10.1016/j.tips.2004.06.006
2. Kobilka BK (2011) Structural insights into adrenergic receptor function and pharmacology. Trends Pharmacol Sci 32(4):213–218. https://doi.org/10.1016/j.tips.2011.02.005
3. Santos R, Ursu O, Gaulton A, Bento AP, Donadi RS, Bologa CG, Karlsson A, Al-Lazikani B, Hersey A, Oprea TI, Overington JP (2017) A comprehensive map of molecular drug targets. Nat Rev Drug Discov 16(1):19–34. https://doi.org/10.1038/nrd.2016.230
4. DeWire SM, Ahn S, Lefkowitz RJ, Shenoy SK (2007) Beta-arrestins and cell signaling. Annu Rev Physiol 69:483–510. https://doi.org/10.1146/annurev.ph.69.013107.100021
5. Tian X, Kang DS, Benovic JL (2014) beta-arrestins and G protein-coupled receptor trafficking. Handb Exp Pharmacol 219:173–186. https://doi.org/10.1007/978-3-642-41199-1_9
6. Kang DS, Tian X, Benovic JL (2014) Role of beta-arrestins and arrestin domain-containing proteins in G protein-coupled receptor trafficking. Curr Opin Cell Biol 27:63–71. https://doi.org/10.1016/j.ceb.2013.11.005
7. Claing A, Laporte SA, Caron MG, Lefkowitz RJ (2002) Endocytosis of G protein-coupled receptors: roles of G protein-coupled receptor kinases and beta-arrestin proteins. Prog Neurobiol 66(2):61–79
8. Jean-Charles PY, Freedman NJ, Shenoy SK (2016) Chapter nine–cellular roles of beta-arrestins as substrates and adaptors of ubiquitination and deubiquitination. Prog Mol Biol Transl Sci 141:339–369. https://doi.org/10.1016/bs.pmbts.2016.04.003
9. Jean-Charles PY, Rajiv V, Shenoy SK (2016) Ubiquitin-related roles of beta-arrestins in endocytic trafficking and signal transduction. J Cell Physiol 231(10):2071–2080. https://doi.org/10.1002/jcp.25317
10. Jean-Charles PY, Snyder JC, Shenoy SK (2016) Chapter one–ubiquitination and deubiquitination of G protein-coupled receptors. Prog Mol Biol Transl Sci 141:1–55. https://doi.org/10.1016/bs.pmbts.2016.05.001
11. Shenoy SK, Lefkowitz RJ (2011) beta-Arrestin-mediated receptor trafficking and signal transduction. Trends Pharmacol Sci 32(9):521–533. https://doi.org/10.1016/j.tips.2011.05.002
12. Shenoy SK, McDonald PH, Kohout TA, Lefkowitz RJ (2001) Regulation of receptor fate by ubiquitination of activated beta 2-adrenergic receptor and beta-arrestin. Science 294(5545):1307–1313. https://doi.org/10.1126/science.1063866
13. Berthouze M, Venkataramanan V, Li Y, Shenoy SK (2009) The deubiquitinases USP33 and USP20 coordinate beta2 adrenergic receptor recycling and resensitization. EMBO J 28(12):1684–1696. https://doi.org/10.1038/emboj.2009.128
14. Hershko A, Ciechanover A (1998) The ubiquitin system. Annu Rev Biochem 67:425–479. https://doi.org/10.1146/annurev.biochem.67.1.425
15. Haas AL, Bright PM (1985) The immunochemical detection and quantitation of intracellular ubiquitin-protein conjugates. J Biol Chem 260(23):12464–12473
16. Mimnaugh EG, Neckers LM (2005) Measuring ubiquitin conjugation in cells. Methods Mol Biol 301:223–241. https://doi.org/10.1385/1-59259-895-1:223
17. Tawa NEJ, Odessey R, Goldberg AL (1997) Inhibitors of the proteasome reduce the accelerated proteolysis in atrophying rat skeletal muscles. J Clin Invest 100(1):197–203. https://doi.org/10.1172/JCI119513
18. Wilkinson KD (2009) DUBs at a glance. J Cell Sci 122(Pt 14):2325–2329. https://doi.org/10.1242/jcs.041046
19. Perroy J, Pontier S, Charest PG, Aubry M, Bouvier M (2004) Real-time monitoring of ubiquitination in living cells by BRET. Nat Methods 1(3):203–208. https://doi.org/10.1038/nmeth722
20. Audet N, Pineyro G (2011) Using BRET to detect ligand-specific conformational changes in preformed signalling complexes. Methods Mol Biol 756:149–163. https://doi.org/10.1007/978-1-61779-160-4_7
21. Nagi K, Charfi I, Pineyro G (2015) Kir3 channels undergo arrestin-dependant internalization following delta opioid receptor activation. Cell Mol Life Sci 72(18):3543–3557. https://doi.org/10.1007/s00018-015-1899-x
22. Richard-Lalonde M, Nagi K, Audet N, Sleno R, Amraei M, Hogue M, Balboni G, Schiller PW, Bouvier M, Hebert TE, Pineyro G (2013) Conformational dynamics of Kir3.1/Kir3.2 channel activation via delta-opioid

receptors. Mol Pharmacol 83(2):416–428. https://doi.org/10.1124/mol.112.081950

23. Han SO, Kommaddi RP, Shenoy SK (2013) Distinct roles for beta-arrestin2 and arrestin-domain-containing proteins in beta2 adrenergic receptor trafficking. EMBO Rep 14 (2):164–171. https://doi.org/10.1038/embor.2012.187
24. Han SO, Xiao K, Kim J, Wu JH, Wisler JW, Nakamura N, Freedman NJ, Shenoy SK (2012) MARCH2 promotes endocytosis and lysosomal sorting of carvedilol-bound beta (2)-adrenergic receptors. J Cell Biol 199 (5):817–830. https://doi.org/10.1083/jcb.201208192
25. Kommaddi RP, Jean-Charles PY, Shenoy SK (2015) Phosphorylation of the deubiquitinase USP20 by protein kinase A regulates post-endocytic trafficking of beta2 adrenergic receptors to autophagosomes during physiological stress. J Biol Chem 290(14):8888–8903. https://doi.org/10.1074/jbc.M114.630541
26. Shenoy SK, Xiao K, Venkataramanan V, Snyder PM, Freedman NJ, Weissman AM (2008) Nedd4 mediates agonist-dependent ubiquitination, lysosomal targeting, and degradation of the beta2-adrenergic receptor. J Biol Chem 283(32):22166–22176. https://doi.org/10.1074/jbc.M709668200
27. Xiao K, Shenoy SK (2011) Beta2-adrenergic receptor lysosomal trafficking is regulated by ubiquitination of lysyl residues in two distinct receptor domains. J Biol Chem 286 (14):12785–12795. https://doi.org/10.1074/jbc.M110.203091
28. Alvarez-Curto E, Inoue A, Jenkins L, Raihan SZ, Prihandoko R, Tobin AB, Milligan G (2016) Targeted elimination of G proteins and arrestins defines their specific contributions to both intensity and duration of G protein-coupled receptor signaling. J Biol Chem 291(53):27147–27159. https://doi.org/10.1074/jbc.M116.754887
29. Schrage R, Schmitz AL, Gaffal E, Annala S, Kehraus S, Wenzel D, Bullesbach KM, Bald T, Inoue A, Shinjo Y, Galandrin S, Shridhar N, Hesse M, Grundmann M, Merten N, Charpentier TH, Martz M, Butcher AJ, Slodczyk T, Armando S, Effern M, Namkung Y, Jenkins L, Horn V, Stossel A, Dargatz H, Tietze D, Imhof D, Gales C, Drewke C, Muller CE, Holzel M, Milligan G, Tobin AB, Gomeza J, Dohlman HG, Sondek J, Harden TK, Bouvier M, Laporte SA, Aoki J, Fleischmann BK, Mohr K, Konig GM, Tuting T, Kostenis E (2015) The experimental power of FR900359 to study Gq-regulated biological processes. Nat Commun 6:10156. https://doi.org/10.1038/ncomms10156
30. Loening AM, Fenn TD, Wu AM, Gambhir SS (2006) Consensus guided mutagenesis of Renilla luciferase yields enhanced stability and light output. Protein Eng Des Sel 19 (9):391–400. https://doi.org/10.1093/protein/gzl023
31. Namkung Y, Le Gouill C, Lukashova V, Kobayashi H, Hogue M, Khoury E, Song M, Bouvier M, Laporte SA (2016) Monitoring G protein-coupled receptor and beta-arrestin trafficking in live cells using enhanced bystander BRET. Nat Commun 7:12178. https://doi.org/10.1038/ncomms12178
32. Couturier C, Deprez B (2012) Setting up a bioluminescence resonance energy transfer high throughput screening assay to search for protein/protein interaction inhibitors in mammalian cells. Front Endocrinol (Lausanne) 3:100. https://doi.org/10.3389/fendo.2012.00100

Part III

Methods to Study Scaffolding Functions of β-Arrestins



Chapter 7

Using In Vitro Pull-Down and In-Cell Overexpression Assays to Study Protein Interactions with Arrestin

Nicole A. Perry, Xuanzhi Zhan, Eugenia V. Gurevich, T. M. Iverson, and Vsevolod V. Gurevich

Abstract

Nonvisual arrestins (arrestin-2/arrestin-3) interact with hundreds of G protein-coupled receptor (GPCR) subtypes and dozens of non-receptor signaling proteins. Here we describe the methods used to identify the interaction sites of arrestin-binding partners on arrestin-3 and the use of monofunctional individual arrestin-3 elements in cells. Our in vitro pull-down assay with purified proteins demonstrates that relatively few elements in arrestin engage each partner, whereas cell-based functional assays indicate that certain arrestin elements devoid of other functionalities can perform individual functions in living cells.

Key words Arrestin, MAPK, Protein-protein interactions, JNK3 activation

1 Introduction

Mammals have only two nonvisual arrestins (arrestin-2 and arrestin-3, aka β-arrestin1 and β-arrestin2) [1], both of which demonstrate an amazing versatility: they interact with hundreds of GPCR subtypes and also numerous non-receptor signaling proteins [2]. The rich multifunctionality of these ~45 kDa proteins raises questions as to where these different partners bind and how many proteins can be brought together by a single arrestin molecule simultaneously. It also creates practical problems in studying biological functions of arrestins; for example, conventional protein overexpression or knockdown in the case of arrestins affects numerous cellular processes, resulting in pleiotropic effects [3]. One could envision an alternative approach using comprehensive mutagenesis of every residue in a ~400 amino acid protein to identify binding sites for interacting partners [4], but it is hardly practical to test dozens of distinct functions of hundreds of mutants. In addition, protein-protein interactions are often mediated by groups of residues, and mutation in any single residue might not affect an

Mark G. H. Scott and Stéphane A. Laporte (eds.), *Beta-Arrestins: Methods and Protocols*, Methods in Molecular Biology, vol. 1957, https://doi.org/10.1007/978-1-4939-9158-7_7, © Springer Science+Business Media, LLC, part of Springer Nature 2019

interaction significantly. There are a few known exceptions in arrestins, where one- or two-point mutations significantly changed receptor preference [5, 6], the binding of MEK1 [7], or c-Raf1 [8], but as a rule, greater perturbations are necessary.

If protein binding is mediated primarily through peptide-based interactions, one possible approach in the identification of elements involved in binding a partner is via separation of the protein in question into a series of peptides and identification of those elements that still bind a partner. This approach was used successfully to identify three arrestin-3-derived peptides that can interact with JNK3 [9]; however, this is not to suggest that other secondary elements in the intact structure do not play a role in the interaction. Interestingly, a 25-residue peptide termed T1A was found to bind JNK3 and each of the upstream kinases in the ASK1-MKK4/7-JNK3 cascade and facilitate JNK3 activation in cells, making it the smallest MAPK scaffold identified so far [10]. Here we describe two critical methods used in these studies: an in vitro pull-down with purified proteins that unambiguously shows that an interaction is direct and a cell-based functional assay, demonstrating the biological relevance of the interactions detected in vitro. Together, these techniques provide a powerful depiction of how arrestin interacts with downstream effectors.

1.1 In Vitro Pull-Down

The in vitro pull-down described here can be used to verify any protein-protein interaction when the proteins in question can be isolated with relatively high purity. The simplest way to perform this experiment is to have usable tags on both proteins (maltose-binding protein/MBP, glutathione S-transferase/GST, His, etc.), so that the pull-down can be performed both ways. If a protein can be expressed as a fusion with one of these tags, it is amenable to this technique and can provide convincing evidence for a direct interaction.

The main advantage of an in vitro pull-down with purified proteins is that any interaction detected by this method is direct, meaning that it does not require helpers and/or intermediaries. The limitations are mostly related to the affinity of the interaction: only relatively high-affinity interactions survive several washes necessary to remove non-specifically bound proteins. This affinity could also be impacted by the addition of another partner protein or cofactor; for example, ATP interaction with a protein kinase could change the kinase's affinity for an interacting partner. Another drawback is that investigated proteins must be expressed and purified and need tags suitable for pull-down. Lastly, as far as scaffolding proteins are involved, their expression level determines the binding outcome; at higher than optimal concentrations, scaffolds suppress signaling in cells and in vitro [11, 12]. An overview of the in vitro pull-down method is provided (Fig. 1).

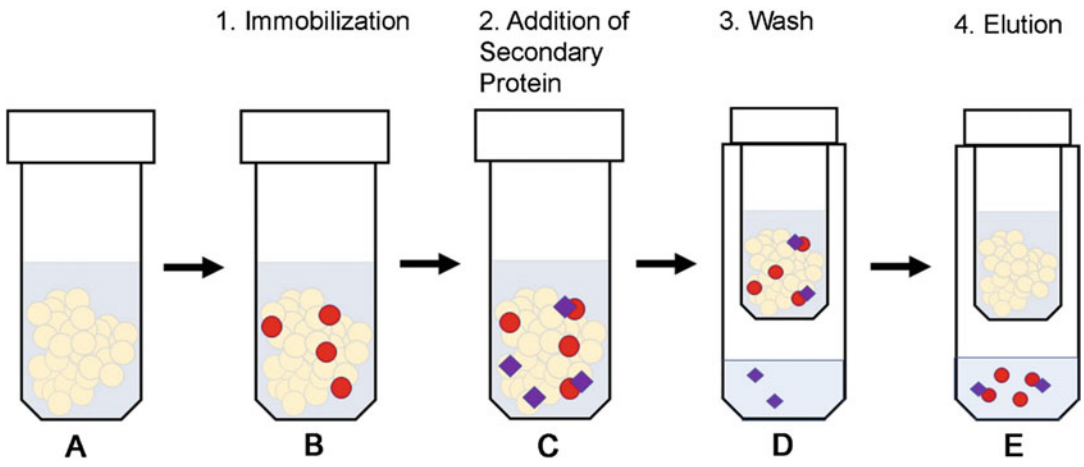


Fig. 1 Schematic overview of the in vitro pull-down assay. This is described as a pull-down for a protein with an MBP affinity tag, but the procedure can be easily modified for a protein with any type of affinity tag. (**a**) Prepare MBP affinity resin (or an alternative resin appropriate for the tag) by washing the suspension in Wash buffer A. (**b**) Immobilize MBP-fused proteins on the resin by incubating for 1 h with gentle rotation at 4 °C. (**c**) Add the secondary protein (either tagged, or for which a validated commercial antibody is available) to the mixture, and incubate for an additional 2 h with gentle rotation at 4 °C. (**d**) Wash each sample three times quickly with Wash buffer B. This will remove any non-specific interactions. (**e**) Elute the bound proteins using buffer containing 50 mM maltose or an alternative appropriate elution buffer for proteins with other tags. The eluate is then analyzed by both Coomassie (to control even bait protein loading) and Western blot (to assess binding)

1.2 Cell-Based Activation

The cell-based activation or phosphorylation assay is suitable when the protein in question facilitates or suppresses the activation or phosphorylation of other proteins, which can be easily assessed experimentally. Here we present ASK1-dependent JNK3 phosphorylation as an example, but similar assays can show the effect of the protein of interest on other processes, such as MKK4- or MKK7-dependent JNK1/2/3 phosphorylation [13]. When the interaction is studied in a cellular context, one can also use co-immunoprecipitation as an alternative approach [14].

The main advantage of cell-based assays is that they demonstrate how the process occurs in an intact living cell. The main disadvantage is that one can never be sure whether additional proteins and/or metabolites are involved. Below is a schematic of the cell-based assay for detection of phosphorylated JNK3 in the presence of HA-ASK1, HA-JNK3, and GFP-tagged arrestins (Fig. 2). Our laboratory is specifically interested in JNK3 for its interaction with arrestin-3 and its role in neuronal apoptosis; however, this setup can be used to detect any arrestin-dependent activation, such as the other JNK isoforms, other MAP kinases, etc.

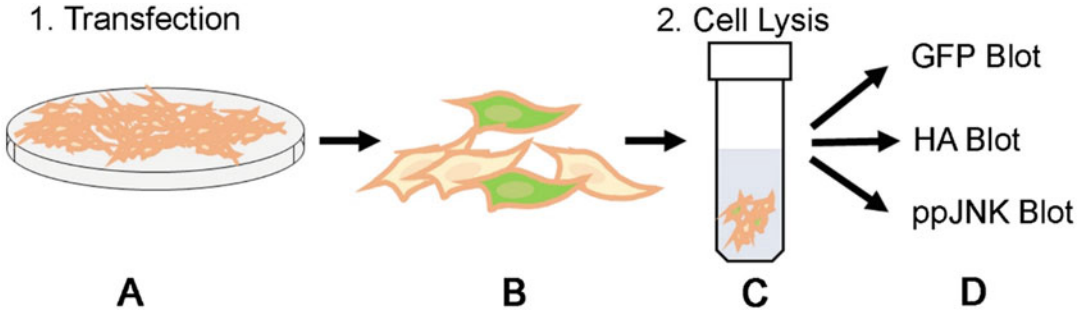


Fig. 2 Schematic overview of the in-cell assay. (**a**) Transfect the cells at 90–100% confluency with HA-ASK1, HA-JNK3, and the appropriate Venus-arrestin construct. (**b**) Allow 48 h for protein expression with serum starvation overnight before the assay. The cells can be monitored using a fluorescent microscope. Cells that have been transfected will glow green because of the Venus (GFP) transfection. (**c**) Lyse the cells to release the protein using the lysis buffer described below. (**d**) Run a Western blot for arrestin expression (GFP), ASK1 and JNK3 expression (HA), and ppJNK

2 Materials

Solutions were prepared using double-distilled water and commercially available reagents. Unless otherwise stated, reagents were prepared and stored at room temperature. The listed antibodies were selected due to widespread use in our laboratory, but primary antibodies will depend on the proteins being tested. It is recommended to follow proper waste disposal for all materials.

2.1 In Vitro Pull-Down Assay

2.1.1 MBP-Fusion Protein Expression

1. Lysis buffer: 50 mM Tris–HCl, pH 8.0, 5 mM EGTA, 2 mM benzamidine (BA), protease inhibitor cocktail (Sigma-Aldrich, Product #P2714).
2. Equilibration buffer: 20 mM Tris–HCl, pH 7.5, 150 mM NaCl, 2 mM BA.
3. Elution buffer: 20 mM Tris–HCl, pH 7.5, 150 mM NaCl, 2 mM BA, and 50 mM maltose.
4. Sonicator, Fisher Scientific, Model 505.
5. MBPTrap HP 5 mL column, GE Healthcare Life Sciences (Product code: 28918779).
6. PD-10 desalting column with Sephadex G-25 resin from GE Healthcare Life Sciences.
7. AKTA protein purification chromatography systems, GE Healthcare Life Sciences.

2.1.2 In Vitro Pull-Down

1. Ultrafree®-MC DV centrifugal filters, Durapore® PVDF 0.65 μm.
2. Amylose resin: Stored in 20% ethanol, New England Biolabs Inc. (#E8021S, store at 4 °C).

3. Wash buffer A: 20 mM Tris–HCl, pH 7.5, and 150 mM NaCl.
4. Wash buffer B: 50 mM HEPES, pH 7.3, and 150 mM NaCl.
5. Elution buffer: 50 mM HEPES, pH 7.3, 150 mM NaCl, 50 mM maltose.

2.1.3 SDS Polyacrylamide Gel

1. Resolving gel buffer: 1.5 M Tris–HCl buffer, pH 8.8.
2. Stacking gel buffer: 0.5 M Tris–HCl buffer, pH 6.8.
3. Thirty percent acrylamide/bis solution 29:1: 3.3% cross-linker.
4. Ammonium persulfate: 10% solution in water.
5. *N,N,N,N′*-tetramethylethylenediamine (TEMED).
6. SDS solution 10% (w/v).
7. SDS-PAGE running buffer: TG-SDS 10× concentrate.
8. Sample buffer, Laemmli (2×) concentrate (store at −20 °C).
9. Bio-Safe Coomassie G-250 stain.

2.1.4 Immunoblotting

1. Transfer buffer: TG 10× concentrate with 15% methanol.
2. Immobilon-P transfer membrane (Merck Millipore Ltd.).
3. Blocking solution: 5% milk (w/v) in Tris-buffered saline and 0.05% Tween 20 (TBS-T) or 2% bovine serum albumin in TBS-T.
4. SuperSignal® West Pico Luminol/enhancer solution and stable peroxide solution.
5. Premium X-ray film.

2.1.5 Antibodies

1. SAPK/JNK and phospho-JNK rabbit (Cell Signaling, 1:1000 dilution, #9252P, #9251).
2. HA Rabbit (Cell Signaling, 1:1000 dilution, #3724).
3. GFP Mouse (Cell Signaling, 1:1000 dilution, #2526) (used for Venus constructs).
4. Secondary antibodies: Peroxidase-conjugated affiniPure goat anti-mouse IgG and anti-rabbit (Jackson Immuno Research Laboratories Inc., 1:10,000 dilution, store at −20 °C).

2.2 In-Cell Activation Assay

2.2.1 Cell Types

1. COS7 African green monkey cells (ATCC).
2. HEK 293 cells (ATCC).

2.2.2 Transfection

1. Transfection reagent: Trans-Hi™ Reagent (FormuMax, Lot 1029) or Lipofectamine® 2000 (Invitrogen by Life Technologies, Ref #11668-019).

2. Media: DMEM (1×) + GlutaMAX™-1, 4.5 g/L D-glucose, 110 mg/L sodium pyruvate, supplemented with 10% fetal bovine serum, and 5% penicillin/streptomycin.
3. 0.05% Trypsin-EDTA (1×).
4. Corning® 100 mm × 20 mm style dish, cell culture treated.
5. Disposable six-well plate.

2.2.3 Cell Lysis

1. Lysis buffer: 50 mM Tris–HCl, pH 7.5, 2 mM EDTA, 250 mM NaCl, 10% glycerol, 0.5% NP-40, 20 mM NaF, 1 mM Na_3VO_4, 10 mM N-ethylmaleimide, 1 mM PMSF, 2 mM benzamide.
2. Phosphate-buffered saline (PBS).
3. Corning™ Falcon™ cell scrapers.

3 Methods

3.1 In Vitro Pull-Down Assay

3.1.1 Expression and Purification of Arrestins

We recently described in detail methods used for the expression and purification of untagged arrestins in *E. coli* [15]. Purification of MBP-tagged arrestin-3 and MBP fusions of arrestin-3-derived peptides was described in [9] and is detailed below.

3.1.2 Expression of MBP-Fusion Proteins

1. Express MBP-fusion proteins in *E. coli* (BL21-codon plus (DE3)-RIL). Inoculate cells in a 500 mL flask (100 mL LB) from a single colony or glycerol stock, and grow overnight at 30 °C at 205 rpm.
2. Use around 10–20 mL of the overnight culture to inoculate each of the four 1-L cultures (in 2 L flasks), and grow the cultures at 30 °C at 205 rpm to an optical density between 0.6 and 0.7 (approximately 3 h postinoculation). Remove the flasks from the shaker, and chill in an ice water bath for 20–30 min (*see* **Note 1a**).
3. Induce the cultures with 1 mM isopropyl β-D-thiogalactoside for an additional 5–6 h at 30 °C followed by centrifugation (15 min, 6000 rpm (4,031 rcf)). Freeze the pellets at −80 °C (*see* **Note 1b**).
4. Thaw protein pellets on ice, and resuspend in lysis buffer (approximately 30 mL per 1 L culture). Add a small amount of lysozyme to the suspension, and incubate on ice for 40 min.
5. Sonicate the suspension at 75% max amplitude for 2 min (5 s on, 10 s off). Incubate the lysate with 25 μL DNase I and 2 mM $MgCl_2$ for 30 min (*see* **Note 1c**).
6. Centrifuge the lysate for 1 h at 18,000 rpm (38,360 rcf) (Sorvall SS-34 rotor in RC 5B plus centrifuge). Filter the

supernatant through a 0.45 μM filter before loading on the MBP column.

7. Wash the MBP-trap column with five column volumes of equilibration buffer before loading the lysate. Filter the lysate, and load on the column at 3 mL/min (check system pressure to ensure that the column is not over-pressurized). After the entire lysate enters the column, wash the system with equilibration buffer until the UV absorption returns to baseline. Use a gradient elution (100% elution buffer, 0–50 mM maltose, flow rate 2 mL/min, 25 min) to elute the MBP-fusion protein off the column. This should result in a symmetric peak. Collect the fractions, and analyze the protein using SDS-PAGE (*see* **Note 1d**).
8. Pool the fractions containing the correct MBP-fusion protein, and concentrate to an appropriate volume for a PD-10 desalting column (less than 2.5 mL) (*see* **Note 1e**). Equilibrate the column by washing four times in equilibration buffer (approximately 25 mL buffer). This can be accomplished by gravity flow or by low-speed centrifugation (1000 × *g*). Apply 2.5 mL of protein sample to the column (add buffer if the sample is less than 2.5 mL), and allow the sample to completely enter the column bed. Discard all flow through. Elute the sample with 3.5 mL of buffer solution and concentrate as necessary. This step removes maltose from the protein sample.

3.1.3 Immobilization of MBP-Fusion Proteins

1. Remove MBP-fusion proteins and the protein being assayed as a potential-binding partner from the −80 °C freezer. Allow the proteins to thaw on ice before proceeding to the next step (*see* **Note 1f**).
2. Remove amylose resin from the 4 °C fridge, and shake at low speed for gentle resuspension. Allotting 25 μL resin per sample condition, cut the tip of a plastic pipette, and remove enough resin for each sample condition plus one additional (*see* **Note 1g**). Add 1 mL of Wash buffer A to the microcentrifuge tube containing the resin, and centrifuge at low speed (around 3200 rpm (1,147 rcf)) for 30 s. Repeat three times. Remove the supernatant without disturbing the resin, leaving enough volume to distribute 25 μL of resin per sample. Using a cut plastic pipette tip, resuspend the resin and aliquot to microcentrifuge tubes.
3. To immobilize the MBP-fusion proteins on the amylose resin, distribute 5–10 μg of an individual MBP-fusion construct diluted to 25 μL in Wash buffer A to one of the microcentrifuge tubes containing amylose resin. Incubate the proteins at 4 °C for 1 h using gentle rotation (*see* **Notes 1h** and **1i**).

3.1.4 Addition of Secondary Protein

1. Add 5–10 μg of the prey protein to a total volume of 50 μL in Wash buffer A. For consistency, calculate the volume of protein and buffer needed for one sample, and multiply these values by the number of samples plus one additional to generate a master mix. From the master mix, distribute 50 μL to each microcentrifuge tube containing an immobilized MBP-fusion construct. Incubate for 2 h at 4 °C with gentle rotation.

3.1.5 Elution

1. Prior to removing samples from the 4 °C incubation, prepare a series of tubes for washing and elution. Label an Ultrafree centrifugal filter for each sample, in addition to a microcentrifuge tube with the cap removed and a microcentrifuge tube labeled to hold the final eluted sample. Place the centrifugal filter and the microcentrifuge tube with the cap removed into a 4 °C centrifuge to cool before adding the samples.
2. Remove the samples from the 4 °C fridge and place on ice. Transfer each sample into a centrifugal filter using a cut plastic pipette tip. Centrifuge the samples at 3200 rpm for 20 s.
3. Add 300 μL of Wash buffer B directly to each sample, and centrifuge at 3200 rpm for 20 s. Quickly remove the centrifugal filter, and place into the microcentrifuge tube with the cap removed (*see* **Note 1j**). Proceed with two additional 300 μL washes in Wash buffer B at 3200 rpm for 20 s.
4. Move the centrifugal filters into the final microcentrifuge tube, and add 100 μL elution buffer to each sample. Incubate at 4 °C for 5 min with gentle rotation. Elute the samples by centrifugation at 4 °C for 1 min at 3200 rpm.

3.1.6 Methanol Precipitation

1. Add 1 mL of 100% methanol to each microcentrifuge tube containing eluted sample. Centrifuge the samples at high speed (around 12,000–14,000 rpm (16,000–21,952 rcf)) for 10 min. Discard the supernatant, and let the samples air-dry for 30 min or until droplets are no longer visible (*see* **Note 1k**).
2. Resuspend in 30 μL SDS loading buffer with dye. Make sure to wash the sides of the tube up to 1 mL. Vortex each sample, and centrifuge the samples in preparation for SDS-PAGE.

3.1.7 SDS-PAGE and Western Analysis

1. Prepare two 10% SDS-PAGE gels (4% stacking). Run 12 μL of sample on a gel for Coomassie staining to verify equal loading of the MBP-fusion constructs on the amylose resin (Fig. 3 top panel). Run 8 μL of sample on another gel for Western blotting to assess protein interaction (Fig. 3 lower panel).
2. Use a primary antibody against the prey protein when performing the Western analysis. This will inform whether a protein interaction occurred.

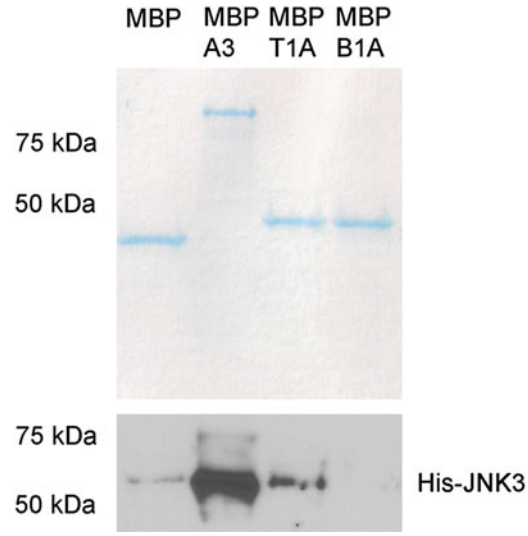


Fig. 3 Representative Coomassie gel and Western blot for an MBP pull-down using His-JNK3 as prey protein. The Coomassie gel is used to assess even loading of the MBP-fusion constructs, while the Western blot to show relative binding of His-JNK3 (A3, arrestin3; T1A, first 25 amino acids of arrestin-3; B1A, first 25 amino acids of arrestin-2)

3.2 In-Cell Activation Assay

All cell culture experiments were performed in the class II laminar flow hood until the cell lysis step. Make sure to maintain lab etiquette when working with cells—clean all materials with 70% ethanol before entering the hood space; wear gloves and a lab coat.

3.2.1 Cell Seeding and Transfection

1. Grow COS7 African green monkey cells in DMEM solution containing 10% FBS and 5% penicillin/streptomycin at 37 °C and 5% CO_2. Other cell lines can be used depending on the system being tested.
2. Remove cells from 10 cm plates using 2.5 mL 0.05% trypsin (~3–5 min), and seed into six-well plates at a density that ensures 90–95% confluency within 24 h (approximately 50,000 cells/mL) (*see* **Note 2a**).
3. After 24 h, replace the cell media with serum-free media, and transfect the cells with pcDNA3-HA-ASK1 (0.4 μg), pcDNA3-HA-JNK3α2 (0.2 μg), and pcDNA3-Venus-arrestin constructs (0.2–0.6 μg) at a 1:2 ratio of DNA:Lipofectamine 2000 (*see* **Note 2b**). The μg amounts of pcDNA3-Venus-arrestin constructs were previously optimized using Western analysis of different transfected amounts (*see* **Note 2c**). Equalize the DNA amounts using an empty pcDNA3 vector. After 5–6 h, replace the serum-free media with DMEM solution containing 10% FBS and 5% penicillin/streptomycin.

4. The night before cell lysis (approximately 12 h), replace the media with serum-free media to exclude any possible receptor stimulation from factors in the serum.

3.2.2 Cell Lysis

1. Forty-eight hours post-transfection, remove the cells from incubation, and wash three times with 1 mL cold phosphate-buffered saline (PBS). Place the cells on ice, and incubate with 1 mL phosphatase inhibitors (20 mM NaF and 1 mM Na_3VO_4) in PBS for 15 min prior to complete lysis (*see* **Note 2d**).
2. After treatment with phosphatase inhibitors, wash the cells twice with 1 mL cold PBS. Prepare lysis buffer and keep on ice. Add PMSF and BA to the lysis buffer immediately prior to adding the buffer to the cells (*see* **Note 2e**). Add 100 μL of lysis buffer to each well, and incubate the plate for 10 min on ice with gentle rotation.
3. Mechanically remove cells from the wells using a cell scraper, and resuspend by pipetting (*see* **Note 2f**). Remove the solutions from each well, and transfer to a 1.5 mL centrifuge tube. Centrifuge the cells for 10 min (4 °C, microcentrifuge at maximum speed) to pellet the debris, and take the top 80% of the lysate for analysis.
4. Measure protein concentration using a Bradford assay (or any alternative method). The yields typically range between 0.5 and 2 mg/mL (*see* **Note 2g**).

3.2.3 Gel Electrophoresis

1. Prepare samples for gel electrophoresis by combining 10 μL of 2× Laemmli buffer with the correct amount of protein for visualization by Western-ppJNK3 blot (8.5 μg), HA blot (5 μg), and Venus blot (1 μg) (*see* **Note 2h**). Boil the samples for 2–3 min to ensure that the proteins will enter the gel.
2. Prepare a 10% SDS-PAGE gel (4% stacking) for each respective blot (ppJNK3 blot (Fig. 4 upper panel), HA blot (Fig. 4 middle panel), and Venus/GFP blot (Fig. 4 lower panel). Load samples into wells at 80 mV for 15 min, and then run at 150 mV for another 45 min–1 h (until the dye front is close to the bottom of the gel).

3.2.4 Transfer and Visualization

1. Remove gels from their casing after electrophoresis, and transfer to PDVF membrane for 45 min (100 V). After transfer, block the membranes with 5% milk (w/v) in TBS-T for 1 h (alternatively, you can use a 5% milk/2% BSA in TBS-T combination for enhanced blocking). Wash the membranes five times for 5 min in TBS-T before overnight incubation with the corresponding primary antibody (*see* **Note 2i**).
2. The next morning, wash the membranes five times for 5 min in TBS-T, and then incubate with HRP-conjugated secondary

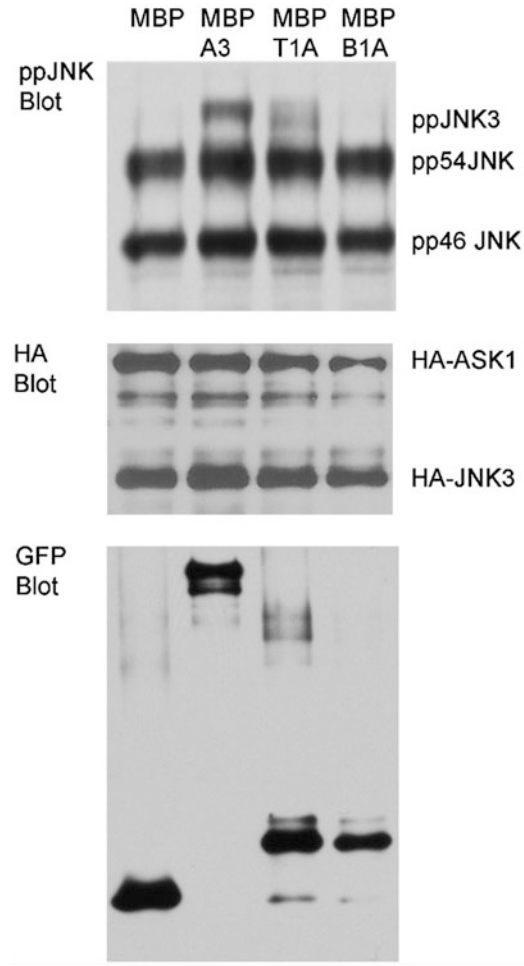


Fig. 4 Representative Western blots for antibodies against ppJNK, HA, and GFP. The HA and GFP blots are used to confirm equal protein expression following transfection. The top band of the ppJNK blot represents ppJNK3, while the other bands are isoforms of ppJNK1/2 (pp54 JNK and pp46JNK). Quantification was performed on ppJNK3 bands and compared across Venus fusion constructs (not shown)

antibodies for 1 h. Detect bands by X-ray film using enhanced chemiluminescence (or an alternative method if you prefer). Perform densitometric quantification to assess the difference in ppJNK3 levels (*see* **Note 2j**).

4 Notes

1. In vitro pull-down assay.

(a) Chilling the flasks slows down cell growth prior to lowering the temperature for induction. This promotes proper folding of the protein.

(b) Can be stored at −80 °C after this step for several weeks.

(c) DNAse I treatment reduces the viscosity and helps with filtration of the lysate during later steps.

(d) Boil the samples at 100 °C for 5 min to make it easier for loading the gel. This helps if you have a lot of protein in the sample.

(e) Alternatives to the PD-10 desalting column include the HiTrap desalting column available from GE or buffer exchange using a concentrator with the correct cutoff to retain your protein of interest.

(f) Limit the number of times that you thaw a protein by freezing your samples in small aliquots.

(g) Cutting the pipette tip ensures successful pipetting of the resin.

(h) Be careful not to agitate the resin as it will stick to the walls of the tube and cannot be recovered.

(i) Optimization may be required when loading the MBP-fusion proteins onto the amylose resin. This is because some protein samples are cleaner than others, and competing proteins might reduce the binding.

(j) The washing step must be performed quickly to minimize change in equilibrium between the bound and unbound state. To assist in this, try not to process more than ten samples at a time.

(k) Methanol will prevent dissolution of the sample proteins in SDS-PAGE buffer.

2. In-cell activation assay.

(a) A 12-well plate can also be used, as this will typically yield enough protein for measurement. The greater the confluency of your cells prior to transfection, the greater the chance of cell survival. Transfection reagent and DNA are toxic to the cells.

(b) Lipofectamine 2000 is more effective for transfection with high DNA, while other transfection agents, such as TransHi, are more effective with lower DNA amounts.

(c) Obtaining an even transfection of the pcDNA3-Venus-arrestin constructs is one of the more difficult aspects of this assay. Perform a titration using different μg amounts of each construct prior to experimentation to balance the constructs.

(d) This prevents the removal of phosphate groups from modified proteins in the cell lysate.

(e) These reagents are not stable over a prolonged period. Make sure to add them directly prior to administering the lysis buffer to the cells.

(f) Complete lysis is important for extraction of all the protein in the cell. Make sure to scrape the cells off so that you do not have any remaining on the dish.

(g) Low yields may indicate high cell death. Revisit the transfection amounts, and monitor your cell population over the 48 h, if you encounter this issue.

(h) These values are experimentally determined. If there is no detectable signal, increase the amounts used for Western analysis. Alternatively, if the signal is too high, decrease the amounts used for analysis.

(i) It is important to wash the milk away completely if the primary antibody solution is to be frozen and reused.

(j) Our preferred software package is Quantity One 1-D Analysis Software from Bio-Rad.

Acknowledgments

This work was supported by NIH R01 grants EY011500, GM109955 and GM077561 (the latter two were merged into R35 GM122491) (VVG), NS065868 and DA030103 (EVG), GM120569 (TMI), R21grant DA DA043680 (TMI/VVG), and an AHA Predoctoral Fellowship 16PRE30180007 (NAP).

References

1. Gurevich EV, Gurevich VV (2006) Arrestins are ubiquitous regulators of cellular signaling pathways. Genome Biol 7:236
2. Xiao K, McClatchy DB, Shukla AK, Zhao Y, Chen M, Shenoy SK, Yates JR, Lefkowitz RJ (2007) Functional specialization of beta-arrestin interactions revealed by proteomic analysis. Proc Natl Acad Sci U S A 104:12011–12016
3. Gurevich VV, Gurevich EV (2015) Analyzing the roles of multi-functional proteins in cells: the case of arrestins and GRKs. Crit Rev Biochem Mol Biol 50:440–452
4. Ostermaier MK, Peterhans C, Jaussi R, Deupi X, Standfuss J (2014) Functional map of arrestin-1 at single amino acid resolution. Proc Natl Acad Sci U S A 111:1825–1830
5. Gimenez LE, Babilon S, Wanka L, Beck-Sickinger AG, Gurevich VV (2014) Mutations in arrestin-3 differentially affect binding to neuropeptide Y receptor subtypes. Cell Signal 26:1523–1531
6. Gimenez LE, Vishnivetskiy SA, Baameur F, Gurevich VV (2012) Manipulation of very few receptor discriminator residues greatly enhances receptor specificity of non-visual arrestins. J Biol Chem 287:29495–29505
7. Meng D, Lynch MJ, Huston E, Beyermann M, Eichhorst J, Adams DR, Klusmann E, Houslay MD, Baillie GS (2009) MEK1 binds directly to betaarrestin1, influencing both its phosphorylation by ERK and the timing of its isoprenaline-stimulated internalization. J Biol Chem 284:11425–11435

8. Coffa S, Breitman M, Spiller BW, Gurevich VV (2011) A single mutation in arrestin-2 prevents ERK1/2 activation by reducing c-Raf1 binding. Biochemistry 50:6951–6958
9. Zhan X, Perez A, Gimenez LE, Vishnivetskiy SA, Gurevich VV (2014) Arrestin-3 binds the MAP kinase JNK3α2 via multiple sites on both domains. Cell Signal 26:766–776
10. Zhan X, Stoy H, Kaoud TS, Perry NA, Chen Q, Perez A, Els-Heindl S, Slagis JV, Iverson TM, Beck-Sickinger AG, Gurevich EV, Dalby KN, Gurevich VV (2016) Peptide mini-scaffold facilitates JNK3 activation in cells. Sci Rep 6:21025
11. Kook S, Zhan X, Kaoud TS, Dalby KN, Gurevich VV, Gurevich EV (2013) Arrestin-3 binds c-Jun N-terminal kinase 1 (JNK1) and JNK2 and facilitates the activation of these ubiquitous JNK isoforms in cells via scaffolding. J Biol Chem 288:37332–37342
12. Zhan X, Kaoud TS, Dalby KN, Gurevich VV (2011) Nonvisual arrestins function as simple scaffolds assembling the MKK4-JNK3alpha2 signaling complex. Biochemistry 50:10520–10529
13. Zhan X, Kook S, Kaoud TS, Dalby KN, Gurevich EV, Gurevich VV (2015) Arrestin-3-dependent activation of c-Jun N-terminal kinases (JNKs). Curr Protoc Pharmacol 68:1–26
14. Seo J, Tsakem EL, Breitman M, Gurevich VV (2011) Identification of arrestin-3-specific residues necessary for JNK3 activation. J Biol Chem 286:27894–27901
15. Vishnivetskiy SA, Zhan X, Chen Q, Iverson TM, Gurevich VV (2014) Arrestin expression in E. coli and purification. Curr Protoc Pharmacol 67:2.11.11–2.11.19



Chapter 8

Methods to Investigate Arrestins in Complex with Phosphodiesterases

Amy J. Tibbo, Tara Busiau, and George S. Baillie

Abstract

The many functions of β-arrestin proteins in the desensitization of G-protein-coupled receptors have been well characterized; however, the discovery that this scaffold protein could actually recruit phosphodiesterases (PDEs) to the site of cAMP synthesis changed the way researchers thought about the static nature of precisely localized cAMP hydrolysis by anchored PDEs. Before this discovery, the compartmentalization of cAMP gradients formed by the activation of specific receptors was generally understood to be underpinned by highly localized pools of specific PDEs that were anchored by large static anchors such as A-kinase-anchoring proteins (AKAPs). Such anchors acted to position cAMP effector proteins such as protein kinase A (PKA) and exchange protein directly activated by cAMP (EPAC) in places that would allow cAMP concentrations to breach their activation threshold only when a specific receptor activation occurred. In this arrangement PDEs acted as local "sinks" for cAMP and this enforced receptor-specific function by allowing the correct activation of a distinct pool of cAMP effectors in precise localizations. The discovery that β-arrestin could shuttle cAMP hydrolyzing activity to the membrane shortly after receptor activation added to the complexity of this process by restricting cAMP diffusion into the cell interior for some receptors. This chapter describes the methods used to identify, confirm, and test the function of PDE-β-arrestin complexes.

Key words PDE, Arrestin, cAMP, PKA

1 Introduction

β-Arrestins are versatile signalling proteins that are involved in many vital cellular processes and are important intermediates in the promotion and inhibition of cell signalling cascades. The variety of β-arrestin orchestrated processes stems from the ability of the scaffold to physically interact with hundreds of other proteins. As these β-arrestin-interacting proteins are often enzymes or receptors, the spatial and temporal control of β-arrestin signalling complexes is crucial for coordinated and functional intra-cell communication. One complex that is transiently assembled by β-arrestin following receptor activation is the β-arrestin-phosphodiesterase type 4 (PDE4)-receptor complex that promotes desensitization of Gs-coupled receptor signalling almost immediately after

Mark G. H. Scott and Stéphane A. Laporte (eds.), *Beta-Arrestins: Methods and Protocols*, Methods in Molecular Biology, vol. 1957, https://doi.org/10.1007/978-1-4939-9158-7_8, © Springer Science+Business Media, LLC, part of Springer Nature 2019

ligand binding. Recruitment of PDE4-β-arrestin to activated receptors serves as a "double-whammy" to desensitize the receptor by concomitantly unhooking the receptor from its associated G protein while delivering active cAMP hydrolysis to the region where cAMP is synthesized. Analysis of the β-arrestin-PDE4 complex uncovered that one of the many (approx. 25) PDE4 isoforms was bound preferentially to β-arrestin by virtue of an extended binding site in the PDEs unique N-terminal targeting region. The PDE4 of choice for β-arrestin is PDE4D5, a long form member of the PDE4D subfamily. This chapter details the methods used to identify, characterize, and verify the unique β-arrestin binding site on PDE4D5.

2 Materials

2.1 Cell Lines and Bacterial Cells

1. Human embryonic kidney—293 (HEK293).
2. HEK293 cell lines stably over expressing FLAG-tagged β_2AR-GFP (HEK-B2 cells).
3. BL21 (DE3) codon plus chemically competent cells (Agilent, 50-125-011).

2.2 Plasmids for Transfection

1. β-Arrestin 2 with a C-terminal FLAG epitope tag, cloned into pcDNA3 backbone.
2. Wild-type PDE4D5 with a VSV epitope tag.
3. β-Arrestin binding-defective PDE4D5 (E27A) with a VSV epitope.
4. RACK-1 binding-defective (L29/30A) PDE4D5 with a VSV epitope.
5. UIM-disrupted (E721A:E722A:E723A) PDE4D5 with a VSV epitope.

2.3 Cell Culture and Transfection

1. HEK293 cells are maintained in Minimum Essential Medium (MEM, Sigma) which was supplemented with 5% L-glutamine and 10% Newborn calf serum.
2. Cultures are incubated at 37 °C with 5% CO_2/95% air and allowed to become 60–80% confluent prior to transfection.
3. Transfections of PDE4D isoforms and β-arrestin (*see* Subheading 2.2) are performed using Lipofectamine reagent (Life Technologies) adhering to the manufacturer's protocol.
4. Stable cell lines expressing the various constructs are made by diluting cells 2 days after transfection into MEM medium, which is supplemented with 1 mg/mL Geneticin sulfate (Life Technology Inc.).

2.4 Cell Harvesting and Sample Preparation

1. KHEM buffer: 50 mM KCl, 50 mM Hepes pH 7.4, 10 mM EGTA, and 1.92 mM $MgCl_2$.
2. 3 T3 lysis buffer: 25 mM Hepes, pH 7.5, 5 mM EDTA, 50 mM NaCl, 50 mM NaF, 30 mM sodium pyrophosphate, and 10% (v/v) glycerol.
3. 2× Laemmli buffer: 4% SDS, 20% glycerol, 10% 2-mercaptoethanol, 0.004% bromophenol blue, and 0.125 M Tris–HCl, pH approx. 6.8. Recommended usage: add 1 volume gel loading solution to 1 volume sample and mix well.
4. 5× Laemmli buffer: 10% SDS, 50% glycerol, 0.1% bromophenol blue, 30 mM dithiothreitol (DTT), 300 mM Tris–HCl, pH approx. 6.8. Recommended usage: add 1 volume gel loading solution to 4 volume sample and mix well.

2.5 Immunoprecipitation (IP)

1. Polyclonal antibody against β-arrestin (A1CT) or antiserum suitable volume that is determined to immunoprecipitate all β_2AR.
2. Tris-buffered saline (TBS) buffer: 50 mM Tris–HCl pH 7.5, 150 mM NaCl.
3. Protein A Sepharose™ Fast Flow (GE Healthcare, 17127901). Volumes given are for one IP sample: add 30 μL of TBS washed beads per IP.
4. Anti-VSV-Glycoprotein-Agarose beads (Sigma, A1970-1ML).

2.6 Western Blotting

1. Precast NuPAGE™ 4–12% Bis–Tris Gel (Invitrogen) was used in this instance. If precast gels are not available, SDS gels can be made the following way (Table 1):
   (a) For each gel, you will require: a short plate, a spacer plate, a comb, with your required number of wells and a rack to hold the plates.
   (b) Layer the two plates together, remembering to keep the spacers on the inside. Make sure the bottom edges of both

Table 1
% Acrylamide running gel volumes

	7.5% gel	10% gel	12.5% gel	15% gel	18% gel
ddH_2O	2.81 mL	250 mL	2.19 mL	1.88 mL	1.50 mL
40% acrylamide/bis stock	0.94 mL	1.25 mL	1.56 mL	1.88 mL	2.25 mL
1.5 M Tris, pH 8.8	1.25 mL	1.25 mL	1.25 mL	1.25 mL	1.25 mL
10% ammonium persulfate	50 μL	50 μL	50 μL	50 μL	50 μL
TEMED	5 μL	5 μL	5 μL	5 μL	5 μL
TOTAL Volume	5 mL	5 mL	5 mL	5 mL	5 mL

Depending on the size of the protein of interest the correct % of acrylamide gel is made using the volumes noted

plates are pressed firmly against the bottom of the rack to ensure there are not leakages. This seal can be tested by the addition of a small volume of water and observing if any leaks are present.

(c) Pour and set the separating gel.

Based on the size of the protein of interest, calculate the % gel required (Table 1).

(d) Take care to avoid air bubbles, as this will hinder the polymerization. After adding the TEMED, the gel will begin to set, so work quickly to pipette the mixture between the two cassettes.

(e) Add a layer of water to the gel to create a level top of the gel. Allow 10–15 min for the gel to set.

(f) Pour and set the stacking gel: For a single 1 mm gel ~1.2 mL is required (Table 2).

(g) Add stacking gel until the level rises to the top of the short cassette. Again, ensure there are no bubbles in gel before adding the comb with determined number of wells.

(h) Leave to set for ~10–15 min. Once the stacking gel has set, remove comb. The cast gels can be stored at 4 °C horizontally for 1 week.

2. NuPAGE SDS MOPS running buffer [20×] (Life technologies; NP0001). Volumes given are for one gel tank: 50 mL of 20× MOPS running buffer with 950 mL dH_2O (Table 2).
3. Precision Plus Protein™ Standards All Blue (Bio-Rad, 161-0373). Load 2 μL of protein ladder per gel.
4. XCell II blotting module (Invitrogen) was used in this instance. The transfer cassette was assembled as described in Fig. 1.

Table 2
Stacking gel

Volume	
ddH_2O	3.13 mL
40% acrylamide/bis stock	0.62 mL
1.5 M Tris, pH 6.8	1.25 mL
10% ammonium persulfate	50 μL
TEMED	5 μL
TOTAL	5 mL

5mL of stacking buffer is made using the noted volumes. For a 1mM thick gel ~1.2 mL is needed and can be made by adjusting the volumes noted. Stacking gel will set quickly in smaller volumes so should be made just before using

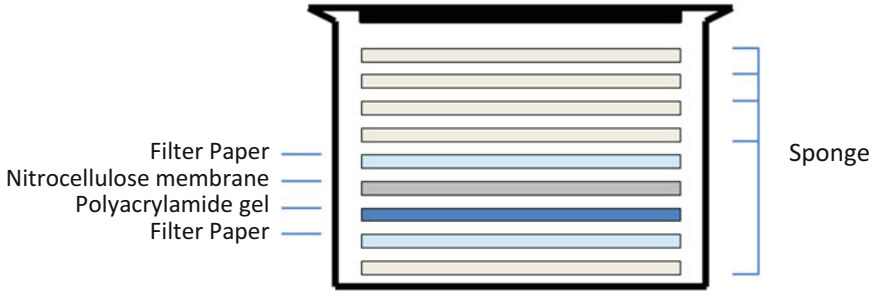


Fig. 1 Diagrammatic representation of a XCell II blotting module (Invitrogen). The polyacrylamide gel is sandwiched between filter paper and a nitrocellulose membrane. Sponge pads for XCell II (Invitrogen) are layered to create a tight seal when the module is added to the Invitrogen NuPAGE Novex gel system

5. NuPAGE Transfer Buffer [20×] (Life Technologies; NP0006-1). Volumes given are for one gel tank: 200 mL methanol and 50 mL transfer buffer, and bring volume up to 1 L with dH_2O.
6. 10× TBST: 20 mM Tris–Cl, pH 7.6, 150 mM NaCl, 0.1% Tween 20. Use as a 1× solution by diluting 100 mL of the 10× solution in 900 mL of dH_2O.
7. Five percent (w/v) nonfat dry milk (Marvel) blocking solution in 1× TBST. Volumes given are for one membrane: weigh out 0.5 g of nonfat dry milk and dissolve in 10 mL of 1× TBST.
8. Five percent (w/v) bovine serum albumin (BSA) blocking solution in 1× TBST. Volumes are given for one membrane: weigh out 0.5 g of BSA and dissolve in 10 mL of 1× TBST.
9. Primary antibodies: sheep PDE4D commissioned by the Scottish Antibody Production Unit, mouse VSV antibody (Abcam, ab50549), mouse monoclonal Ub(P4D1) (SantaCruz, sc-8017).
10. Secondary antibodies for infrared analysis: Donkey anti-goat (Li-Cor, 925-32214) and donkey anti-mouse (Li-Cor, 925-68072).
11. Secondary antibodies for electrochemiluminescence (ECL): Sheep anti-mouse (GE Healthcare, NA931-1ML) and donkey anti-sheep IgG (Invitrogen, A16041).
12. Pierce™ ECL Western Blotting Substrate (Thermo Fisher Scientific, 32106).
13. X-ray film (Carestream, FMXOB0101824).
14. Odyssey Infrared Imaging System (LI-COR Biosciences, UK).
15. Image Studio Lite (LI-COR Biosciences, software version 5.x).
16. ImageJ (https://imagej.nih.gov/ij/).

2.7 Purification of Recombinant Protein

1. BL21 (DE3) transformed *Escherichia coli* with either human β-arrestin 1 or β-arrestin 2 with an N-terminal GST fusion (pGEX-β-arrestin 1, pGEXβ-arrestin 2).

2. Lysogeny broth (LB): in a starting volume of 850 mL of dH_2O, dissolve the following: 10 g bacto-tryptone, 5 g yeast extract, 10 g sodium chloride. Adjust the pH to 7.5 with sodium hydroxide. Adjust volume to 1 L, and autoclave.
3. 100 mg/mL ampicillin is required for bacterial culturing. Added in a 1:1000 dilution.
4. 1 M Isopropyl β-D-1-thiogalactopyranoside (IPTG): dissolve 2.38 g of IPTG in 10 mL of sterile dH_2O. Sterilize by passing through a 0.22 μm filter.
5. GST lysis buffer: 50 mM Tris–HCl, pH 8, 100 mM NaCl, 10 mM β-mercaptoethanol, and 1 tablet of complete protease inhibitor mixture per 50 mL of buffer.
6. Tris–HCl wash buffer: 50 mM Tris–HCl, pH 8.0.
7. GST elution buffer: 10 mM glutathione, 50 mM Tris–HCl, pH 8.0, and 1 tablet of complete protease inhibitor mixture per 50 mL of buffer.
8. Glutathione Sepharose beads (GE Healthcare, 17075601).
9. Dialysis buffer: 100 mM NaCl, 50 mM Tris–HCl; pH 8.0, 5% glycerol, 5 mM DTT.
10. Slide-A-Lyzer™ Dialysis Cassettes (Thermo Scientific, 66380).
11. Bovine serum albumin (BSA) (Sigma, A9647-10G). Recommended use: prepare a 1 mg/mL stock in dH_2O.
12. Ninety-six flat bottom welled plate (Corning, CLS3842-100EA).
13. Bio-Rad Protein Assay Dye Reagent Concentrate (Bio-Rad, 500-0006). Recommended use: dilute 5 mL of the dye in 20 mL of dH_2O. Add 200 μL of the diluted dye to each well in order to determine protein concentration.

2.8 SPOT Synthesis and Peptide Array

1. Peptide array libraries were produced by automatic SPOT synthesis as described previously [1, 2]. Peptides were synthesized on continuous cellulose membrane supports on Whatman 50 cellulose membranes using Fmoc (9-fluorenylmethoxycarbonyl) chemistry with the AutoSpot-Robot ASS 222 (INTAVIS Bioanalytical Instruments).
2. Purified recombinant GST and β-arrestin 1/2-GST.
3. Primary antibody: GST rabbit polyclonal antibody (abcm; ab19256).
4. Secondary antibody: Anti-rabbit IgG (whole molecule)–peroxidase antibody produced in goat (Sigma, A0545-1ML).

2.9 Verification of PDE4D5 Ubiquitination

1. PolyFect transfection reagent (Qiagen, 301105).
2. Mdm2 small interfering RNA (Qiagen).

3. Primary antibody: mouse VSV antibody (Abcam, ab50549), mouse monoclonal UbP4D1 (Santa Cruz, sc-8017), mouse monoclonal Mdm2 (Santa Cruz, sc-56154).
4. Secondary antibody: Sheep anti-mouse (GE Healthcare, NA931-1ML).
5. ECL Western Blotting Substrates (Thermo Scientific, 32106).
6. Purified Mdm2 used for the in vitro ubiquitination assay was provided by Prof. R. Hay (University of Dundee, UK).
7. HEK293 cells stably expressing the ß$_2$ adrenoreceptor were gifted by Dr. R. J. Lefkowitz (Duke University, USA).

3 Methods

3.1 Background

3.1.1 Verification of Interaction Between PDE4 and β-Arrestin by Immune-Purification [3–5]

The original interaction between β-arrestin and PDE4 was discovered using a yeast-2 hybrid screen by the Lefkowitz lab [6] and will not be described here. Initial validation of the interaction was done using co-immunoprecipitation experiments. The purpose of immunoprecipitation is to allow the detection and quantification of a selected protein or proteins from a particular sample. Immunoprecipitation (IP) is widely used to isolate tagged proteins along with interacting proteins in order to study the protein–protein interactions of that complex in vivo. Many protein–protein interactions that exist within cells still remain stable after cell lysis, meaning it is possible to immunoprecipitate one protein possibly along with its interacting proteins [3]. In order to study the protein–protein interactions of two proteins of interest, it is more common to use co-immunoprecipitation (Co-IP) [3]. Cells are lysed in the same manner for each protocol with immunoprecipitated proteins being separated by dodecyl sulfate-polyacrylamide gel electrophoresis (SDS-PAGE) and co-immunoprecipitated proteins being detected through Western blotting with antibodies that are specific to either the protein of interest or its tag [3]. Through this procedure, proteins are separated by weight as they are run through a SDS-PAGE electrophoresis. The advantage of using IP over more traditional methods of immunoblotting is that it provides the ability to analyze the immune response of proteins in their endogenous form [4].

3.1.2 Delineation of β-Arrestin Binding Sites on PDE4D5

The phosphodiesterase superfamily consists of 11 different PDE families (PDEs 1 through 11), and the PDE4 family itself consists of over 25 isoforms encoded by 4 different genes (PDE4 A, B, C, and D). Much of the PDE4 sequence is conserved between isoforms; however, each isoform has its own unique N-terminal region that has been deemed the targeting sequence, which serves to localize each isoform in specific cellular locations. Early work

using yeast-2 hybrid analysis identified the N-terminal region of PDE4D5 as the preferred binding site for β-arrestin. Exact delineation of essential binding sites on PDE4D5 was carried out using peptide array technology. The protocols for which are detailed below.

3.1.3 Verification of PDE4D5 Ubiquitination Via Kit, Peptide Array, and Mutant PDE4D5 [7–9]

Ubiquitination was examined in two main methods:

1. Using an ubiquitin assay kit and cell lysates in vitro *(ab13946)*. This method was performed using a kit and following manufacturer's protocol so will not be described here.
2. Using a PDE4D5 peptide array analysis in vivo.

The in vivo experiments consist of five major protocol steps:

1. Cellular transfection with PDE4D isoforms and mutants. The constructs used are noted in Section 2.2 and the Transfection protocol is outlined in Section 2.3
2. Cell lysis using 3T3-lysis buffer.
3. Immunopurification of VSV-tagged PDE4D constructs.
4. Immunoblotting for ubiquitinated species.
5. Imaging and analysis.

For in vitro analysis, the main steps in the protocol are either:

1. The generation of thioester-linked ubiquitin conjugation enzymes (E2s) using the ubiquitination assay kit.
2. Immunoprecipitation of ubiquitinated proteins.
3. Western blotting using ubiquitin-specific antibody.

Or:

1. Production of scanning peptide array for full length of PDE4D5.
2. Overlay of recombinant purified glutathione *S*-transferase-Mdm2.
3. Anti-ubiquitin antibody incubation and secondary incubation with HRP conjugated antibody ECL imaging.

3.2 Methods

3.2.1 Preparation of Samples for Immunoprecipitation

1. HEK293 and HEK293 cell lines stably overexpressing FLAG-tagged β2AR-GFP (HEK-B2 cells) are washed three times in ice-cold KHEM buffer.
2. 300 μL of ice-cold 3T3 lysis buffer is added to cells and incubated for 10 min on ice (*see* **Note 1**).
3. Harvested cells are added to fresh 1.5 mL Eppendorf tube before centrifugation at 13,000 × *g* for 10 min in a table top centrifuge. A low-speed pellet (P1) and supernatant (S1) fractions are produced. The supernatant is transferred to fresh Eppendorf tube and the pellet is discarded.

4. S1 fraction is centrifuged at 100,000 × *g* for 30 min to yield a high-speed pellet (P2) and supernatant (S2) fraction.

3.2.2 Immunoprecipitation of Endogenous and Overexpressing β-Arrestins and PDE4D Isoforms

1. Immunoprecipitation of endogenous or overexpressing β-arrestin is performed by preclearing the S2 fraction (500 μg of protein) with 50 μL of KHEM-washed Protein A beads (*see* **Note 2**).
2. 5 μL of polyclonal antibody against β-arrestin (A1CT) or 5 μL of anti serum, or a suitable volume that is determined to immunoprecipitate all β_2AR, is added, and incubate tubes at 4 °C with end over end mixing for 1 h.
3. 30 μL of Protein A Sepharose beads are added to the mix.
4. Tubes are incubated for a further 2 h at 4 °C with constant agitation before centrifuging them at 1300 × *g* for 3 min to allow beads to pellet.
5. Supernatant is removed, and beads are washed three times in KHEM buffer through centrifugation with aspiration of the supernatant required between each wash.
6. 40 μL of 2× Laemmli buffer is added to pelleted beads and boiled 5 min at 100 °C (*see* **Note 3**).
7. 20 μL of the immunoprecipitates and control lysates are run on SDS-PAGE gels.

3.2.3 SDS Polyacrylamide Gel and Immunoblotting

1. Proteins are separated by molecular weight using the Invitrogen NuPAGE Novex gel system (*see* Subheading 2.6) (*see* **Note 4**).
2. 20 μL of protein immunoprecipitation samples are then loaded on 4–12% Bis–Tris NuPAGE gels along with the Protein Standard (*see* **Note 5**).
3. Gel electrophoresis is performed at 200 mV for approximately 45 min or until bands have reached the bottom of the gel.
4. Prepare 1× transfer buffer by diluting 50 mL of 20× buffer in 950 mL of dH_2O.
5. Remove polyacrylamide gel from its plastic casing, layer between filter papers and a nitrocellulose membrane, that have been wet in 1× transfer buffer, as noted in Fig. 1. Sponges soaked in 1× transfer buffer are added to fill the XCell® blotting apparatus (*see* **Notes 4**–**8**).
6. Resolved proteins are electro-transferred onto a nitrocellulose membrane using the XCell II blotting module (Invitrogen) submerged in transfer buffer (NuPAGE) for 2 h at 30 mV or 10 mV overnight. The successful transfer is marked by the transfer of the pre-stained molecular ladder onto the nitrocellulose membrane.

7. The nitrocellulose membrane is then removed from the blotting apparatus and blocked in either 5% (w/v) nonfat dry milk in 1× TBST or 5% BSA (w/v) in 1× TBST for 1 h at room temperature with gentle agitation.
8. Add an appropriate primary antibody to the membrane. In this instance, a PDE4D monoclonal antibody was used in a 1:1000 dilution in 1× TBST in either 1% BSA or 1% (w/v) nonfat dry milk. Incubate membranes for a minimum of 4 h at room temperature. An overnight incubation at 4 °C is favorable (*see* **Note 9**).
9. Membranes are washed three times for 10 min in 1× TBST with agitation.
10. An appropriate amount of secondary antibody is diluted 1:5000 in either 1% BSA or 1% (w/v) nonfat dry milk in 1× TBST. If the membrane is to be visualized using the Odyssey Infrared Imaging, a fluorescent secondary antibody must be used. If the membrane is to be visualized using electrochemiluminescence (ECL), a secondary antibody containing horseradish peroxidase (HRP) must be used. Membranes are incubated in the dark for 1 h at room temperature with constant agitation.
11. Membranes are then washed three times in 1× TBST for 10 min each wash.

3.2.4 Analysis

1. If an Odyssey Infrared Imaging System is being utilized, then membranes can be visualized at this stage (Fig. 2).
2. If ECL is being utilized, then membranes are blotted for 5 min in a 1:1 ratio of Detection Reagent 1-Peroxidase Solution and Detection Reagent 2-Luminol Enhancer Solution Membranes can then be developed with ECL.
3. Quantification of protein can be performed using Image Studio or ImageJ software.
4. Membranes can be stored after imaging in 1× TBST at 4 °C.

3.2.5 Expression of Glutathione S-Transferase (GST) Fusion Proteins in E. coli [1, 10, 11] (see ***Note 10–24****)*

1. Prepare LB as a standard media for growth of *Escherichia coli*. Supplement autoclaved LB with 100 mg/mL of ampicillin. Dilute ampicillin to a working concentration of 100 μg/mL.
2. Inoculate starter cultures, individually, with either human β-arrestin 1 or β-arrestin 2 with an N-terminal GST fusion (pGEX β-arrestin 1, pGEX β-arrestin 2) BL21(DE3) transformed *E. coli* in 25 mL of LB with ampicillin. Allow to grow overnight at 225 rpm, 37 °C.
3. The following day, inoculate 500 mL of fresh LB with ampicillin with 10 mL of the starter culture. Allow to grow at 225 rpm, 37 °C, until it reaches an approximate OD_{600} of 0.6–0.7.

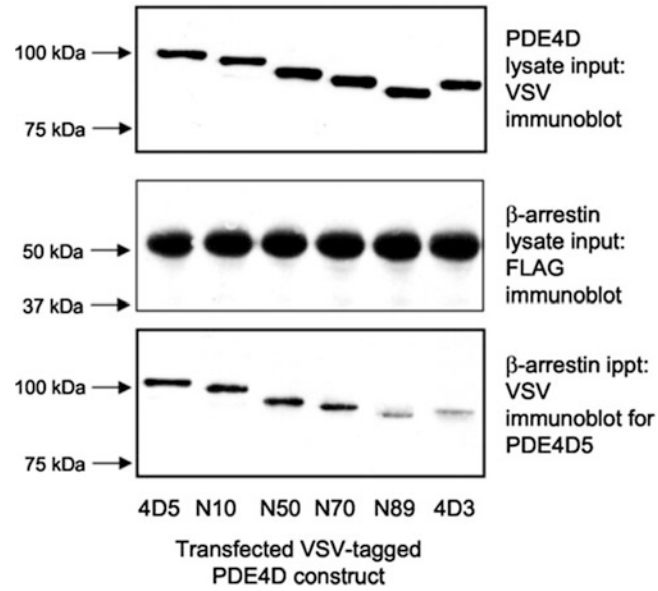


Fig. 2 Example of a Complete Immunoprecipitation. The co-immunoprecipitation of PDE4D5 and β-arrestin to determine interaction sites. This figure shows the co-immunoprecipitation results using an anti-FLAG antibody on cell lysates from HEK293 cells that were double transfected with both FLAG-β-arrestin-2 and a VSV-tagged PDE4D constructs. Membranes were then blotted with an anti-VSV antibody in order to detect PDE4D. To confirm that the levels of loaded β-arrestin onto the gel were identical, membranes were blotted with anti-FLAG antibody. This figure was originally published in Bolger et al. [5]

4. When the correct absorbance is reached, induce cultures with 500 μL of 1 M IPTG, in order to obtain a final concentration of 1 mM. Allow to grow for a further 4 h at 225 rpm, 30 °C.
5. Harvest the induced cultures by centrifugation at 6000 × *g* for 10 min at 4 °C. Discard supernatant and freeze the pellet overnight at −80 °C.
6. Resuspend frozen pellets in 10 mL of GST lysis buffer containing complete protease inhibitor.
7. Sonicate the resuspended pellets three times for 5 min at maximal setting, resting on ice for 5 min between each sonication.
8. Remove cell debris by centrifugation, 27,000 × *g* for 20 min at 4 °C.
9. During centrifugation, wash 1 mL of Glutathione Sepharose beads with 2 mL of GST lysis buffer, three times for 5 min at 500 × *g*, 4 °C.

10. Collect cleared supernatants, and incubate with 1 mL of the washed beads overnight on an orbital shaker at 4 °C.
11. Collect beads the following day by centrifugation, 500 × *g* for 5 min, 4 °C.
12. Wash beads three times for 5 min at 500 × *g*, 4 °C, with ice-cold GST lysis buffer.
13. Wash beads three times for 5 min at 500 × *g*, 4 °C with ice-cold Tris–HCl wash buffer.
14. Incubate beads with 1 mL of the GST elution buffer for 10 min on ice, and collect the eluate by centrifugation at 500 × *g*, 4 °C.
15. Repeat elution a further five times.
16. Check protein concentration of eluates using a standard Bradford assay.
17. Pool eluates, and dialyze proteins overnight in dialysis buffer, at 4 °C, using the correct Slide-A-Lyzer™ Dialysis Cassettes (Thermo Scientific).
18. Perform dialysis on the purified protein twice more the following day.
19. Collect purified fusion protein and check concentration using a standard Bradford assay.
20. Store at −80 °C until required.

*3.2.6 Peptide Array Overlay Experiments with GST-Fusion Proteins [1] (See **Notes 25–29**)*

1. Peptide array libraries were produced by automatic SPOT synthesis as described previously [1, 2, 12].
2. A library of overlapping peptides (25-mers), each shifted by five amino acids (Fig. 3) across the entire sequence of PDE4D5, was immobilized on cellulose membranes.
3. Wet cellulose membranes for 5 min with 1× TBST in a container.



Fig. 3 Example peptide array design. Overlapping peptides, each shifted by 5 amino acids, are spotted across Whatman 50 cellulose membrane. This figure was originally published in Bolger et al. [1]

4. Remove TBST and block membranes with 5 mL of 5% nonfat dry milk for 1 h at room temperature on a shaker.
5. While the membranes are blocking, dilute the recombinant proteins to 10 μg/mL in 2.5 mL of 1% nonfat dry milk. Keep samples on ice until needed.
6. Blot PDE4D5 membranes with either GST or recombinant β-arrestin 1/2-GST at room temperature for 4 h with gentle shaking.
7. Wash the membranes three times the following day with 2.5 mL of TBST.
8. During the washes, dilute GST antibody 1:1000 in 1% milk.
9. After the final wash, incubate each membrane with 2.5 mL of the appropriate antibody for 4 h at room temperature, gently shaking.
10. Wash the membranes three times with 2.5 mL of 1× TBST.
11. During the washes, dilute secondary anti-rabbit HRP antibody at a 1:5000 in 1% nonfat dry milk.
12. After the final wash, incubate each membrane with 2.5 mL of secondary antibody for 1 h at room temperature, gently shaking.
13. Wash the membranes three times in 1× TBST.
14. Prepare Pierce ECL Western blotting reagent by mixing the Detection Reagent 1-Peroxidase Solution and Detection Reagent 2-Luminol Enhancer Solution Membranes in a 1:1 ratio.
15. Drain excess reagent. Cover blot with a clear plastic sheet protector or clear plastic wrap.
16. Expose blot to X-ray film for various times in order to see dark spots. Dark spots signify positive interactions between PDE4D5 and β-arrestin 1/2-GST (Fig. 4).

3.2.7 Cell Culture and Transfection

1. HEK293 B2 cells, which are a stable cell line overexpressing GFP-tagged β2-adrenoreceptor, are maintained in Dulbecco's Minimum Essential Medium Media (DMEM) supplemented with 1% L-glutamine, 1% penicillin/streptomycin and 10% fetal bovine serum (FBS) with flasks kept in 37 °C with 5% CO_2 [9].
2. HEK239 B2 cells are seeded at ~6×10^6 cells in a 10 cm dish 24 h prior to transfections.
3. Once cells reach 60–80% confluency, they are transiently transfected with one of the following VSV epitope-tagged constructs:
   (a) Wild-type PDE4D5.
   (b) β-Arrestin binding-defective PDE4D5 (E27A),

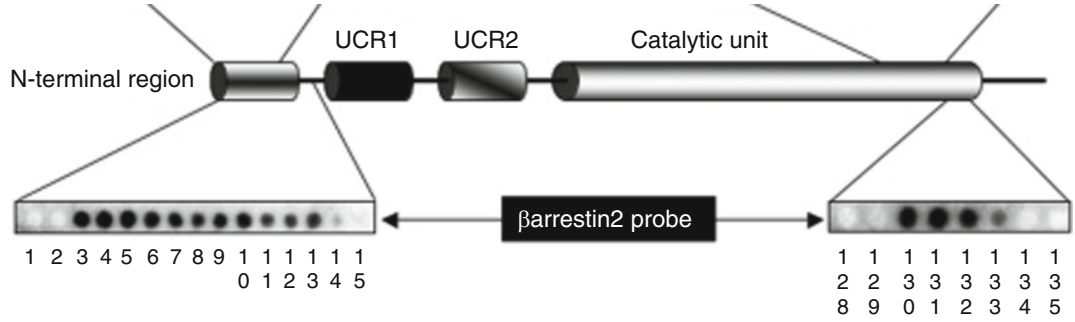


Fig. 4 Example of peptide array overlay experiment. Full-length PDE4D5 was spotted in overlapping 25-mer peptides as described previously. A dark spot, which is not present in the control condition, indicates positive binding *between β-arrestin 2 and the* peptides. Noninteracting peptides leave blank (white) spots. This figure was originally published in Bolger et al. [1]

(c) RACK-1 binding-defective (L29/30A) PDE4D5.

(d) UIM-disrupted (E721A:E722A:E723A) PDE4D5

Transfections are carried out using PolyFect transfection reagent (Qiagen) according to the manufacturers' instructions [7].

4. After transfection, cells were returned to 37 °C with 5% CO_2 for 48 h [8].

3.2.8 In Vivo Assay to Determine the Ubiquitination of PDE4D5

1. Forty-eight hours after transfection cells are either challenged with 10 μM isoprenaline, a nonselective β-adrenoreceptor agonist for determined periods of time, or left untreated.
2. Harvest the cells as previously mentioned in Subheading 3.2.1.
3. Following the immunopurification protocol, previously mentioned in Subheading 3.2.2. Ubiquitin conjugates were immunopurified using VSV-agarose beads. Any ubiquitinated species was then detected by immunoblotting using UbP4D1 antibody. Follow the IP protocol mentioned in Subheading 3.2.2, **step 2** to pull down ubiquitinated conjugates.
4. PDE4D5 levels of expression were examined through Westernblotting protocol, outlined in section 2.6, using VSV antibody and ECL detection methods.

4 Notes

1. If required, a stronger buffer such as RIPA (10 mM Tris–Cl pH 8.0; 1 mM EDTA; 1% Triton X-100; 0.1% sodium deoxycholate; 1% SDS; 140 mM NaCl and 1 mM PMSF) can be used on the cell debris or in place of the initial lysis buffer.
2. Protocol was carried out for FLAG-tagged β-arrestin constructs. However, the lysates were precleared with

VSV-agarose beads, and immunopurification is carried out using FLAG-tagged agarose beads.

3. When removing immunoprecipitated lysates, it is recommended to use a gel loading tip in order to reduce the risk of pipetting up any of the agarose beads, as this can affect protein separation.
4. Precast gels were used in this instance. If precast gels are not available, SDS gels can be made (*see* Subheading 2.6).
5. When handling SDS-PAGE gels, always wear gloves to avoid any exposure to unpolymerized polyacrylamide, as it is a neurotoxin.
6. Make sure all components used when transferring proteins from SDS-PAGE gel to nitrocellulose membrane remain wet at all times.
7. The orientation of the gel when placed into the cassette will directly relate to the orientation of the transfer so it is important to note this.
8. When closing the transfer cassette, ensure there are no air bubbles between any of the layers, as this will impede the protein transfer.
9. When incubating the cellulose membrane with protein, primary antibody, or secondary antibody, seal the membranes in individual plastic bags.
10. Take a sample of the culture and elutions during each stage of the purification. These samples will be used for quality control purposes at the end of the procedure.
11. Check OD every 30 min. Once it reaches an OD600 of 0.3, check every 15 min.
12. Work around a flame to keep the bacterial culture as sterile as possible.
13. Allow the temperature of the shaker to drop to 30 °C. If the cultures are left to be induced above 30 °C, the protein will become insoluble.
14. Once harvested, keep all samples on ice.
15. Transfer resuspended pellets into 50 mL falcon tubes to facilitate later stages of the protocol.
16. Submerge sonicator probe to the bottom of the falcon tube in order to avoid frothing of the lysate.
17. Cut the end of the pipette tip to easily pipette 1 mL of beads.
18. After the final wash, remove the maximum amount of the wash from the beads using a gel loading tip. Resuspend the beads in 1 mL of the resuspension buffer prior to use in order to create a bead slurry.

19. Wrap the lid of the 50 mL falcon tube with parafilm in order to avoid spillages overnight.
20. Keep resuspension buffer on ice during use.
21. If some of the beads have been pipetted with eluate, spin down the Eppendorf tube containing the protein at 700 × g for 5 min at 4 °C. Transfer the eluted protein into a fresh 1.5 mL Eppendorf using a gel loading tip to avoid pipetting the beads again.
22. Pre-chill 3 L of water prior to preparing the dialysis buffer.
23. Use 3 L of dialysis buffer per dialysis cassette. If dialyzing multiple cassettes, prepare individual dialysis buffers for each cassette.
24. When finished, run all quality control samples on a SDS-PAGE gel, and use for a Western blot. Blot for the epitope-tagged protein, as well as for the purified untagged protein of interest, in order to ensure that the protein has been purified.
25. When incubating the cellulose membrane with protein, primary antibody, or secondary antibody, seal the membranes in individual plastic bags. This will avoid contamination of the control condition with the experimental condition and vice versa.
26. Ensure that all the air bubbles are removed from the bag prior to sealing. This will ensure that the membrane is efficiently probed with the antibody or protein..
27. The recombinant GST serves as a control. If the same dark spot appears on the membrane probed with GST and recombinant GST protein, this indicates that GST binds non-specifically.
28. Wash the membranes in separate containers after the 4-h protein incubation. This will avoid contamination between the control and experimental condition by excess unbound proteins.
29. Draining the excess ECL reagent will reduce the amount of background detected.

Acknowledgments

This work was supported by MRC (Medical Research Council) grant G8604010, by NIH (National Institutes of Health) Grant R01-GM58553, by Deutsche Forschungsgemeinschaft grant Kl1415/2, and by European Union Grant QLK3-CT-2002-02149. We also thank Dr. David Adams (Department of Chemistry, Heriot-Watt University, Edinburgh, UK) for helpful comments on this work. We thank Haoyan Zhang for preparation of numerous plasmids.

References

1. Bolger GB, Baillie GS, Li X, Lynch MJ, Herzyk P, Mohamed A, Mitchell LH, McCahill A, Hundsrucker C, Klussmann E et al (2006) Scanning peptide array analyses identify overlapping binding sites for the signalling scaffold proteins, beta-arrestin and RACK1, in cAMP-specific phosphodiesterase PDE4D5. Biochem J 398:23–36
2. Frank R (2002) The SPOT-synthesis technique. Synthetic peptide arrays on membrane supports--principles and applications. J Immunol Methods 267:13–26
3. Sambrook J, Russell D (2006) Identification of associated proteins by coimmunoprecipitation. CSH Protoc 2006:pdb.prot3898
4. Walker J (2005) The proteomics protocols handbook. Humana Press, Totowa, N.J
5. Bolger G, McCahill A, Huston E, Cheung Y, McSorley T, Baillie G, Houslay M (2003) The unique amino-terminal region of the PDE4D5 cAMP phosphodiesterase isoform confers preferential interaction with β-arrestins. J Biol Chem 278:49230–49238
6. Baillie GS, Sood A, McPhee I, Gall I, Perry SJ, Lefkowitz RJ, Houslay M (2003) β-Arrestin-mediated PDE4 cAMP phosphodiesterase recruitment regulates β-adrenoceptor switching from Gs to Gi. Proc Natl Acad Sci U S A 100:940–945
7. Li X, Baillie G, Houslay M (2009) Mdm2 directs the ubiquitination of β-arrestin-sequestered cAMP phosphodiesterase-4D5. J Biol Chem 284:21776–21776
8. Beavo J, Brunton L (2002) Cyclic nucleotide research—still expanding after half a century. Nat Rev Mol Cell Biol 3:710–718
9. McLean A, Milligan G (2000) Ligand regulation of green fluorescent protein-tagged forms of the human β1- and β2-adrenoceptors; comparisons with the unmodified receptors. Br J Pharmacol 130:1825–1832
10. Yarwood SJ, Steele MR, Scotland G, Houslay MD, Bolger GB (1999) The RACK1 signaling scaffold protein selectively interacts with the cAMP-specific phosphodiesterase PDE4D5 isoform. J Biol Chem 274:14909–14917
11. Harper S, Speicher DW (2011) Purification of proteins fused to glutathione S-transferase. Methods Mol Biol 681:259–280
12. Kramer A, Schneider-Mergener J (1998) Synthesis and screening of peptide libraries on continuous cellulose membrane supports. Methods Mol Biol 87:25–39



Chapter 9

Methods to Characterize Protein Interactions with β-Arrestin In Cellulo

Revu Ann Alexander, Isaure Lot, and Hervé Enslen

Abstract

β-Arrestins 1 and 2 (β-arr1 and β-arr2) are ubiquitous proteins with common and distinct functions. They were initially identified as proteins recruited to stimulated G protein-coupled receptors (GPCRs), regulating their desensitization and internalization. The discovery that β-arrs could also interact with more than 400 non-GPCR protein partners brought to light their central roles as multifunctional scaffold proteins regulating multiple signalling pathways from the plasma membrane to the nucleus, downstream of GPCRs or independently from these receptors. Through the regulation of the activities and subcellular localization of their binding partners, β-arrs control various cell processes such as proliferation, cytoskeletal rearrangement, cell motility, and apoptosis. Thus, the identification of β-arrs binding partners and the characterization of their mode of interaction in cells are central to the understanding of their function. Here we provide methods to explore the molecular interaction of β-arrs with other proteins in cellulo.

Key words β-Arrestin, Scaffold, GST pull-down, Co-immunoprecipitation, Yeast two hybrid, Bioluminescence resonance energy transfer (BRET)

1 Introduction

The two non-visual arrestins, β-arrestins 1 and 2 (β-arr1 and β-arr2) are ubiquitously expressed scaffold proteins with no catalytic activity that regulate a vast array of cellular processes from the cell surface to the nucleus [1]. β-arrs were originally identified as negative regulators of GPCR function [2]. Indeed the binding of β-arrs to the phosphorylated active form of these receptors functionally uncouples them from cognate G proteins in a process called desensitization [3] and the simultaneous interaction of β-arrs with both clathrin and the adaptor protein 2 (AP-2) [4] promotes the internalization of activated GPCRs, decreasing their concentration at the cell surface [5]. Besides clathrin and AP-2, many other non-GPCR protein partners of β-arrs were identified in subsequent studies using various approaches [6, 7]. Immunoprecipitations of epitope-tagged β-arrs combined with high-throughput mass

Mark G. H. Scott and Stéphane A. Laporte (eds.), *Beta-Arrestins: Methods and Protocols*, Methods in Molecular Biology, vol. 1957, https://doi.org/10.1007/978-1-4939-9158-7_9, © Springer Science+Business Media, LLC, part of Springer Nature 2019

spectrometry revealed a few hundred potential partners depending on experimental conditions [8], and new ones are also regularly identified [9–15]. These β-arr partners, localized in different cell compartments, include protein kinases such as Src, PI3K-Akt, MAP kinases and components of their activating modules, as well as other enzymes such as phosphatases, E3 ubiquitin ligases and deubiquitinases. Other types of proteins like regulators of small GTPases, ion exchangers, cytoskeletal proteins, nuclear proteins, and transcription factors are also interacting with β-arrs [8, 16, 17]. Although some of these proteins remain to be fully confirmed as β-arr protein partners and their mode of interaction (e.g., direct/indirect, regulated) with β-arr1 and/or β-arr2 further characterized [16], it is nonetheless established that β-arrs are essential scaffold proteins that organize signalling networks in different locations within the cell, dynamically regulating the activities and/or the subcellular localization of their binding partners. Thus, through their central roles in signal transduction, β-arrs control a broad range of cellular functions such as proliferation, cytoskeletal rearrangement, cell motility and apoptosis in a GPCR-dependent or GPCR-independent manner [6, 18]. Importantly, changes in β-arr expression and localization have been correlated with various pathological situations and diseases such as inflammation [19], addiction [20] and cancer [1], attesting for their critical physiological roles.

As cellular functions regulated by β-arrs depend on their association with other protein partners, it is critical to be able to study these interactions in cells. In this chapter we provide detailed biochemical and biophysical protocols to investigate interactions of proteins with β-arrs in cells using yeast two-hybrid, co-immunoprecipitation, GST-β-arr pull-down and bioluminescence resonance energy transfer (BRET) assays.

2 Materials

2.1 Cell Lines and Yeast Strain

1. Human embryonic kidney 293T (HEK-293T) cell line (ATCC).
2. *Saccharomyces cerevisiae* HF7c yeast strain (Feilotter 1994) (*see* **Note 1**).

2.2 Plasmids

1. Plasmids used for the yeast two-hybrid assay: pGBT9 (tryptophan, Trp, auxotrophic marker) and pGAD-GH (leucine, Leu, auxotrophic marker) coding for the GAL4 DNA binding domain (GAL4-BD) and the GAL4 transactivation domain (Gal4-AD), respectively. The cDNAs of β-arr (β-arr1 and/or β-arr2) are cloned in pGBT9 and putative binding partner in pGAD-GH plasmid (or vice versa), so that the GAL4 DNA binding or transactivation domains are at the N-terminal ends.

2. Plasmids encoding human β-arr2 and Src, used for the co-immunoprecipitation experiment: pCMVTag2B-Flag-β-arr2, pcDNA3.1-Src, pcDNA3.1, and pCMVTag2B (*see* **Note 2**).
3. Plasmids used for the GST-β-arr pull-down assay: cDNAs of β-arr1 or β-arr2 have been cloned in frame, downstream of the GST coding sequence, in the pGEX-4T3 expression vector (pGEX-4T3-β-arr), to produce GST-β-arr fusion protein (*see* **Note 3**). The empty pGEX-4T3 vector is used to produce GST protein.
4. Plasmids used for the BRET saturation assays: GFP10-fusion protein (acceptor) and Rluc2-fusion protein (donor) inserted into pcDNA3.1 plasmids (*see* **Note 4**).

2.3 Cell Culture and Transfection

1. Complete Dulbecco's modified Eagle's medium (DMEM), 4.5 g/L glucose, 4 mM glutamine and 1 mM pyruvate, supplemented with 10% fetal bovine serum, 100 U/mL penicillin and 0.1 mg/mL streptomycin.
2. Trypsin-EDTA solution (0.05%).
3. OptiMEM.
4. Six-well and 10 cm plates for cell culture, white opaque 96-well microplates: sterile and tissue culture treated (PerkinElmer OptiplateTM-96HB or equivalent).
5. GeneJuice transfection agent (Novagen) is used as transfecting reagent for HEK-293T cells.

2.4 Yeast Two-Hybrid Assay

1. Dextrose solution, 10% (5× solution): prepare in dH_2O, filter sterilize, and store at 4 °C.
2. YPD media: make YP media (2% w/v peptone and 1% w/v yeast extract) in dH_2O and autoclave. Add one volume of filtered sterilized 5× dextrose solution to four volumes of YP media to make up the YPD media containing 2% dextrose. Store at 4 °C.
3. Dropout base synthetic defined medium (DOB) and double or triple dropout Complete Supplement Mixture (CSM), CSM-Leu-Trp and CSM-Leu-Trp-His (MP Biomedicals).
4. Agar plates:
   (a) YPD plates: YPD supplemented with 2% (w/v) agar.
   (b) CSM-Leu-Trp and CSM-Leu-Trp-His selective plates: 2.7% (v/v) DOB medium, 0.064% CSM-Leu-Trp or 0.062% CSM-Leu-Trp-His, and 3% agar in dH_2O. Autoclave and pour plates once the temperature comes down to 55 °C.
5. Salmon sperm DNA (10 mg/mL) as carrier DNA.

6. PEG-4000, 50%: dissolve 50 g PEG-4000 in 50 mL dH_2O and add dH_2O to 100 mL. Filter sterilize and store at room temperature.
7. Lithium buffer: 0.1 M lithium acetate (LiAc), 10 mM Tris-Base, 1 mM EDTA, pH 7.5. Sterilize and store at room temperature.
8. Lithium acetate/PEG-4000: to 1 mL of lithium buffer, pH 7.5, add 9 mL of 50% PEG-4000 and vortex to mix properly. Prepare fresh for each experiment.
9. DMSO: cell culture grade.

2.5 Mammalian Cell Lysis

1. Phosphate buffered saline 1× without calcium (DPBS).
2. Lysis buffer, pH 7.4: 1% Triton X-100, 150 mM NaCl, 20 mM Tris-Base, 0.05% (v/v) Tween20, 1 mM sodium orthovanadate, 10 mM NaF and Protease Inhibitor Cocktail (Roche) (*see* **Notes 5** and **6**).
3. Pierce BCA Protein Assay Kit.
4. Laemmli buffer, 5×: 250 mM Tris-Base, pH 6.8, 50% glycerol, 10% SDS, 0.1 g/mL bromophenol blue, 10% β-mercaptoethanol. Store aliquots at −20 °C.

2.6 Co-Immunoprecipitation and Western Blots

1. EZview Red anti-Flag M2 affinity gel (Sigma-Aldrich).
2. Lysis buffer (as described in Subheading 2.5, **item 2**) supplemented with 2% BSA.
3. High-salt lysis buffer: lysis buffer (Subheading 2.5, **item 2**) supplemented with 150 mM NaCl (300 mM final).
4. PageRuler Plus Prestained Protein Ladder.
5. Protran nitrocellulose membranes.
6. Primary antibodies: rabbit antibodies against the Flag peptide (Cell Signaling Technology) and Src (Santa Cruz Biotechnology).
7. Secondary antibody: TrueBlot anti-rabbit IgG HRP (Rockland).
8. Pierce ECL western blotting substrate.
9. Antibody stripping buffer.
10. Chemiluminescent Imager LAS-3000 (Fuji Lifesciences).

2.7 GST-β-Arr Pull-Down from Cell Lysate

1. One Shot BL21(DE3)pLysS bacteria.
2. Luria-Bertani (LB) liquid media: 0.5% (w/v) yeast extract, 1% NaCl, 1% tryptone in dH_2O.
3. Isopropyl β-D-1-thiogalactopyranoside (IPTG, 100 mM), dioxane-free in dH_2O, filter sterilize. Store aliquots at −20 °C.
4. Phosphate buffered saline (PBS, 1×): sterile.

5. Glutathione Sepharose-4B beads.
6. Bacteria lysis buffer, pH 7.4: 20 mM Tris-Base, 1 M NaCl, 0.2 mM ethylenediaminetetraacetic acid (EDTA), 0.2 mM ethylene glycol-bis(2-aminoethylether)-*N*,*N*,*N*′,*N*′-tetraacetic acid (EGTA), 1 mM dithiothreitol (DTT), Protease Inhibitor Cocktail (Roche). The lysis buffer is prepared without DTT, filter sterilized, and stored at 4 °C. DTT should be added fresh before the start of the procedure.
7. NaCl, 1 M with protease inhibitors.
8. PBS 1× with protease inhibitors.

2.8 BRET2 Saturation Assay

1. Poly-L-ornithine. Dissolve poly-L-ornithine in dH_2O to a final concentration of 1.5 mg/mL (50×). Filter sterilize, aliquot, and freeze at −20 °C.
2. Six-well plates for cell culture, white opaque sterile, and tissue culture treated 96-well microplates for BRET (PerkinElmer OptiplateTM-96HB or equivalent).
3. Phosphate buffered saline (PBS, 1×) with $CaCl_2$ and $MgCl_2$.
4. Hanks buffered salt solution (HBSS, 1×) containing $CaCl_2$ and $MgCl_2$.
5. Coelenterazine 400a (DeepBlueC™), 1 mM: dissolve 500 μg of Coelenterazine 400a (Interchim) in 1.27 mL of ethanol. Store at −20 °C in opaque microcentrifuge tubes.
6. Multimode microplate reader, Mithras LB943 (Berthold) or equivalent.

3 Methods

3.1 Yeast Two-Hybrid Assay

Two-hybrid assays use transcription as a read-out to study protein–-protein interactions in eukaryotic cells. They take advantage of the fact that transcription factors are composed of two distinct domains, the DNA binding domain (BD) and the transcription-activating domain (AD), which are independently nonfunctional but can reconstitute transcription activity when in close proximity to one another even if not covalently associated. In the yeast two-hybrid system, the use of independent fusion proteins including these separate domains (BD and AD) generates an active transcription factor initiating transcription of reporter genes integrated in the yeast genome, if the proteins fused to each domain interact. Nutritional markers allowing yeast to grow on medium lacking histidine and enzymatic reporter (β-galactosidase) are used for such analysis [21]. Yeast two-hybrid assays have been used to identify and characterize new β-arr protein partners [12, 22]. We describe here such an approach successfully used in this context.

3.1.1 Yeast Transformation

1. Inoculate 50 mL of complete YPD medium with HF7c yeast from a YPD agar plate (*see* **Note 7**), and incubate overnight at 30 °C with agitation (180 rpm).
2. Dilute the saturated overnight culture to an OD_{600} of 0.2 in 100 mL of complete YPD medium (*see* **Note 8**).
3. Incubate the diluted culture at 30 °C (180 rpm) until the OD_{600} is 0.5–0.6 (usually 2–3 h) indicating log-phase growth, which is critical for successful yeast transformation.
4. Transfer the culture into 50 mL tubes, and centrifuge at 700 × *g* for 5 min at room temperature (RT).
5. Discard supernatants and wash the yeast pellets with 50 mL dH_2O.
6. Centrifuge at 700 × *g* for 5 min at RT to remove dH_2O.
7. Resuspend/pool the yeast pellet in 2 mL lithium buffer.
8. Incubate the yeast at 30 °C (180 rpm) for 60 min; the competent cells should be used for transformation within an hour.
9. Boil salmon sperm DNA for 5 min at 100 °C and quickly chill in ice. Denaturation of DNA promotes transformation efficiency.
10. In a 2 mL Eppendorf tube, assemble the transformation mix in the following order: add 500 ng of pGBT9 and 500 ng of pGAD-GH plasmids, 100 μL of competent yeast cells, 100 μg of denatured salmon sperm DNA (10 μL of 10 mg/mL stock), and 600 μL lithium acetate/PEG-4000 solution. Multiple transformations can be carried in parallel using different combinations of the pGBT9 and pGAD-GH control plasmids and pGBT9 and pGAD-GH plasmids encoding the fused proteins, to test for specificity.
11. Vortex the Eppendorf tube twice 5 s, and incubate at 30 °C for 30 min.
12. Add DMSO to a final concentration of 10%, and mix immediately by inverting the tube 2–3 times.
13. Heat shock cells at 42 °C for 15 min.
14. Place cells on ice for 2 min.
15. Centrifuge the tube at 12,000 rpm in a microcentrifuge for 20 s at RT.
16. Discard the supernatant and wash the cells with 500 μL YPD medium.
17. Centrifuge the cells at 12,000 rpm in a microcentrifuge for 20 s at RT.
18. Discard the supernatant, resuspend cells in 100 μL YPD medium, and spread the whole content on a CSM-Leu-Trp selective plate.
19. Incubate plates at 30 °C until colonies appear (2–3 days).

3.1.2 Histidine Auxotrophy to Test for Interaction

1. Pick 3–4 colonies per transformation using a sterile pipette tip or toothpick, and streak a patch (1.5 cm × 0.5 cm) for each one onto a fresh CSM-Leu-Trp selective plate. Incubate the plate at 30 °C for 2 days (*see* **Note 9**).
2. For the replica plating, place a sterile velveteen cloth on a replica block, and secure it using the lock to create an even surface (*see* **Note 10**).
3. Place the CSM-Leu-Trp selective plate with the yeast patches on the velveteen square, and press gently but firmly. An impression of the yeast patches should be observed (*see* **Note 11**).
4. In the following order, inoculate a CSM-Leu-Trp-His selective plate, and a CSM-Leu-Trp selective plate onto the velvet cloth, and incubate the plates at 30 °C.
5. Monitor yeast growth over the next couple of days. Growth of yeast transformed with pGBT9 and pGAD-GH plasmids expressing β-arr and its putative binding partner fused to GAL4-BD and Gal4-AD on the CSM-Leu-Trp-His selective plate and no growth of yeast transformed with the other plasmid combinations indicate specific interaction between β-arr and the other protein (*see* **Notes 12** and **13**).

3.2 Transfection and Cell Lysate Preparation for Co-Immunoprecipitation and GST Pull-Down

1. Seed HEK-293T cells at a density of 0.5–1 × 10^6 cells per 10 cm tissue culture plate. The cells are incubated overnight, in a cell culture incubator at 37 °C in a humidified atmosphere of 95% air and 5% CO_2.
2. The next day, cells should be about 60% confluent and ready for transfection using the GeneJuice reagent (3 μL/μg of DNA). For the β-arr2/Src co-immunoprecipitation experiment described below (Subheading 3.3), HEK-293T cells are transfected with 1 μg of plasmid encoding Flag-tagged β-arr2 and/or 0.5 μg of plasmid encoding untagged Src, empty pcDNA3.1, and pCMVTag2B plasmids being used to keep the amount of transfected plasmid DNA constant in the control conditions (Flag-β-arr2 alone, Src alone, and no Flag-β-arr2 or Src). The transfection conditions (amount of each plasmid DNA and ratio of GeneJuice/DNA) should be determined empirically for each new experimental setup and potential β-arr protein partner (*see* **Note 14**).
3. Transfected cells are incubated for 60 h at 37 °C in the cell incubator.
4. For lysis of transfected cells, place the 10 cm dishes on ice, aspirate the media, and wash the dishes once with 10 mL of ice-cold PBS. For all subsequent steps, the plates and lysates should be kept on ice.

5. Add 750 μL of ice-cold lysis buffer per plate, swirl the plates so that the buffer covers the whole surface, scrape the cells on ice with a cell scraper, and collect the lysates in Eppendorf tubes. For cells more difficult to lyse, the collected extracts can be incubated on a rotating wheel at 4 °C for 15 min, or the plates can be incubated with the lysis buffer on a rotating platform at 4 °C for 15 min before the cells can be scraped and collected.
6. Centrifuge at 13,000 rpm in a microcentrifuge for 15 min at 4 °C to pellet cell debris.
7. Transfer the supernatants to new Eppendorf tubes, and determine the protein concentration using the Pierce BCA Protein Assay Kit.

3.3 Co-Immunoprecipitation

Immunoprecipitation, which is the isolation of a target protein bound to an antibody from unbound proteins in a cell or tissue lysates, allows the identification of proteins engaged in a stable interaction with the immunoprecipitated target. This approach can be used to characterize molecular complexes with β-arrs [9–12, 14, 15, 22]. Here, starting from the HEK-293T cell lysates prepared above, we use antibodies directed against the Flag epitope and immobilized on gel to show that transfected Src is co-immunoprecipitated with transfected Flag-β-arr2.

1. 15 μL of EZview Red anti-Flag M2 affinity gel (*see* **Note 15**) is used per IP. Calculate the amount of gel needed for the total number of IP +1 more (here 5). Wash the gel two times with a volume of ice-cold lysis buffer equivalent to three volumes of gel. Centrifuge the beads at 4000 rpm in a microcentrifuge for 4 min at 4 °C. Aspirate the supernatant between each wash.
2. After the second wash, centrifugation, and aspiration of the supernatant, incubate the anti-Flag M2 affinity gel with 500 μL of ice-cold lysis buffer containing 2% BSA on a rotating wheel for 3 h at 4 °C to reduce nonspecific binding.
3. During **step 2**, set aside one 50 μg cell lysate aliquot (15–20 μL) of each condition, prepared in Subheading 3.2, in a new Eppendorf tube. Add 10 μL of 5× Laemmli buffer and adjust the volume to 50 μL with lysis buffer (*see* **Note 16**). Boil the sample for 5 min at 100 °C and centrifuge it at 13,000 rpm in a microcentrifuge for 1 min at RT. The samples are ready to be loaded on a gel or stored at −20 °C (*see* **Note 17**).
4. After 3 h, centrifuge the anti-Flag M2 affinity gel at 4000 rpm, 4 min (4 °C) in a microcentrifuge. Aspirate the supernatant, and wash the gel with ice-cold lysis buffer, centrifuge, aspirate the supernatant, and add ice-cold lysis buffer again.
5. Before centrifugation, aliquot on ice the washed saturated gel into a number of Eppendorfs corresponding to the number of IP (for this experiment 4). Centrifuge 4 min at 4000 rpm (4 °C) in a microcentrifuge, and aspirate the supernatant.

6. Add 500 μg of each cell extract to different Eppendorf tubes containing the anti-Flag M2 affinity gel, adjust the volume to 500 μL with ice-cold lysis buffer, and incubate overnight on a rotating wheel at 4 °C to immunoprecipitate the Flag-tagged β-arr.
7. The next day, centrifuge the samples 4 min at 4000 rpm (4 °C) in a microcentrifuge, and discard the cell lysate (*see* **Note 18**).
8. Wash samples twice with 750 μL of ice-cold high-salt lysis buffer, followed by two washes with 750 μL ice-cold lysis buffer. For each wash, samples can be incubated at 4 °C for 5 min on a rotating wheel to decrease nonspecific binding. Centrifuge 4 min at 4000 rpm (4 °C) in a microcentrifuge after each wash, and aspirate the supernatant. Transfer the third washes to new Eppendorf tubes before centrifugation.
9. After the last centrifugation, aspirate the supernatants, and add 50 μL of 1–3× Laemmli buffer at RT (prepared by diluting the 5× stock with lysis buffer) to the anti-Flag M2 affinity gel. Vortex rapidly and boil immediately at 100 °C for 5 min. Centrifuge the samples at 13,000 rpm in a microcentrifuge for 5 min at RT.
10. Load immunopurified samples on a 12% SDS-PAGE gel along with the whole cell extract prepared in Subheading 3.3, **step 3** and the molecular markers. Run the gel, and transfer the resolved proteins on a nitrocellulose membrane.
11. Western blots are performed with antibodies directed against the Flag epitope (2368, 1:1000) and Src (sc-18, 1:1000). The co-immunoprecipitated protein (here Src) is blotted first and the immunoprecipitated one (here β-arr2), after stripping of the membrane for 15 min with antibody stripping buffer. After incubation with secondary antibodies (*see* **Note 19**), develop the WB immunoreaction with ECL using films or an appropriate chemiluminescent imager.

Figure 1 shows a co-immunoprecipitation experiment where non-tagged Src transfected in HEK-293T cells is specifically co-immunoprecipitated with Flag-β-arr2 using the protocol described above.

3.4 GST-βarr Pull-Down

GST pull-down assay is a method closely related to co-immunoprecipitation. The difference in this assay is that the GST-tagged bait protein replaces antibodies and the isolation of the complex is performed through affinity chromatography. In the case of the identification of protein partners of β-arrs [15, 23, 24], GST-β-arr recombinant proteins are prepared in bacteria before being used for the pull-down assay. A simple procedure for this approach is described below.

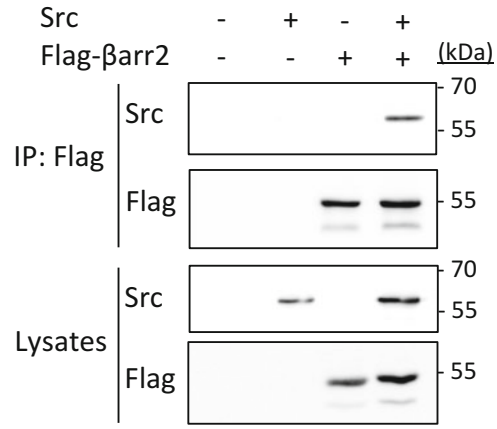


Fig. 1 Co-immunoprecipitation of Src and β-arr2. HEK-293T cells were transfected with Flag-β-arr2 and Src or the corresponding empty pcDNA3.1 vector as indicated. Immunoprecipitations of Flag-β-arr2 were performed with anti-Flag (IP: Flag) antibodies and immunoblotted with anti-Src and anti-Flag antibodies. Immunoblotting of the cell lysate used for the immunoprecipitation experiment is shown

3.4.1 GST and GST-β-Arr-Fusion Protein Induction in Bacteria

1. Transform BL21(DE3)pLysS bacteria separately with pGEX-4T3 plasmid DNA encoding GST or with pGEX-4T3-β-arr vector encoding GST-β-arr. Plate each transformed bacteria on a LB agar plate containing ampicillin, and incubate at 37 °C overnight.
2. Inoculate a single bacterial colony of each transformation into 5 mL of LB (with ampicillin), and grow cells for 6 h at 37 °C (180 rpm).
3. Transfer 250 μL of each bacterial culture into 20 mL of fresh LB media (with ampicillin) in a conical flask, and grow cells overnight at 37 °C with agitation (180 rpm).
4. Transfer 10 mL of each saturated bacterial culture into 100 mL of fresh LB media with ampicillin (1:10) in a flask, and agitate (180 rpm) at 37 °C, until the OD_{600} reaches 0.6–0.8 (approximately 60 min).
5. For GST induction, add IPTG to a final concentration of 0.1 mM, and agitate at 37 °C for 4 h. Add IPTG to a final concentration of 0.1 mM to induce the expression of GST-β-arr1 and 1 mM to induce GST-β-arr2. Agitate cells at 110 rpm for 16 h at 20 °C (*see* **Note 20**).
6. Centrifuge the bacterial cultures in 50 mL conical tubes at 2000 × *g* for 15 min.
7. Wash the bacterial pellets with 10 mL of PBS, and centrifuge at 2000 × *g* for 10 min.

8. Discard the PBS and proceed on ice for the next steps. The bacterial pellets can also be frozen at this step and stored at −80 °C.

3.4.2 Preparation of Glutathione Sepharose Beads

This part of the procedure can be performed during the centrifugation described in Subheading 3.4.1, **step 6** or during the one from Subheading 3.4.3, **step 3**.

1. Prepare a 1:1 mix containing 200 μL of glutathione Sepharose beads and 200 μL sterile PBS per pull-down to be performed.
2. Wash the beads three times with 1 mL of ice-cold 1 M NaCl containing protease inhibitors in a microcentrifuge at 7000 rpm for 30 s at 4 °C.
3. Wash the beads three times with 1 mL of ice-cold sterile PBS with protease inhibitors (centrifuge at 7000 rpm for 30 s at 4 °C in a microcentrifuge).
4. Remove the supernatant and suspend the 200 μL beads (1:1) with 200 μL of sterile PBS.
5. Divide the beads equally into four Eppendorf tubes and keep them on ice. Two Eppendorf tubes with washed beads will be used for GST purification and the two others for GST-β-arr (*see* Subheading 3.4.3, **step 5**).

3.4.3 Purification of GST and GST-Tagged Fusion Protein

1. Resuspend each bacterial pellet in 2 mL of ice-cold bacterial lysis buffer, and transfer to 15 mL conical tubes.
2. Sonicate the bacterial lysates three times (15 s), with a 2 min incubation on ice between each sonication.
3. Transfer to 2 mL Eppendorf tubes, and centrifuge the bacterial lysates for 20 min at 12,000 rpm (4 °C) in a microcentrifuge.
4. Take a 4 μL aliquot of each clarified bacterial lysate, mix it with 16 μL of lysis buffer and 5 μL of 5× Laemmli buffer, and boil the samples for 5 min at 100 °C. Freeze the samples (*see* **Note 21**).
5. Divide each clarified bacterial lysate in two, and transfer to two Eppendorf tubes containing the glutathione Sepharose beads prepared in Subheading 3.4.2.
6. Incubate the tubes for 4 h at 4 °C on a rotating wheel.
7. Centrifuge the tubes at 7000 rpm for 30 s at 4 °C in a microcentrifuge, and remove the lysates (supernatant) that can be kept separately at 4 °C after removing 4 μL aliquots of each as in Subheading 3.4.3, **step 4** (*see* **Note 21**).
8. Wash the beads three times with 1 mL of ice-cold 1 M NaCl with protease inhibitors. Each wash is performed for 5 min at 4 °C on a rotating wheel. Centrifuge the samples at 7000 rpm for 30 s (4 °C) in a microcentrifuge between each wash.

9. Wash the beads three times, as indicated in the previous step, with 1 mL of ice-cold sterile PBS containing protease inhibitors. Following the first wash, transfer the beads to new tubes.
10. After the final wash, resuspend the beads in 100 μL of sterile PBS, and keep them at 4 °C (*see* **Note 22**).
11. Take small aliquots of each set of beads, and mix them with lysis buffer and Laemmli buffer (final concentration 1×). Boil samples for 5 min at 100 °C.
12. Run these samples on a SDS-PAGE gel along with BSA standards ranging from 0.2 μg to 10 μg in 1× Laemmli buffer.
13. By Coomassie Brilliant Blue staining of the gel, determine the concentration of GST and GST-β-arr proteins by comparing the intensity of the colored GST-β-arr to that of the different BSA samples. The GST-bound beads aliquots may need to be diluted to evaluate the GST concentration by comparison to the GST-β-arr bound to the beads.

3.4.4 GST Pull-Down Assay

1. To reduce nonspecific binding to the beads, the cell lysate to be used for the pull-down can be precleared. Fresh glutathione beads are equilibrated by two successive washes with four volumes of mammalian cell lysis buffer (*see* Subheading 2.5.) and centrifugation at 4000 rpm for 4 min at 4 °C in a microcentrifuge. After the second wash, the beads are suspended 1:1 with lysis buffer.
2. Preclear two 100–500 μg lysate aliquots from cells transfected with DNA plasmid encoding the potential β-arr protein partner to be tested and prepared as in Subheading 3.2 (*see* **Note 23**), by adding 50 μL of equilibrated Glutathione Sepharose beads to each aliquot.
3. Rotate the Eppendorf tubes for 2 h at 4 °C on a rotating wheel.
4. Centrifuge at 13,000 rpm for 5 min at 4 °C in a microcentrifuge, and transfer the cell lysates to new tubes.
5. Add 5 μg of GST-bound beads to one precleared sample (negative control) and 5 μg of GST-β-arr1- or GST-β-arr2-bound beads to the other one. Rotate the tubes from 2 h to overnight at 4 °C on a rotating wheel (*see* **Note 24**).
6. Wash the beads twice with high-salt cold mammalian cell lysis buffer (Subheading 2.6, same volume as cell lysate), and centrifuge them at 4000 rpm for 4 min at 4 °C in a microcentrifuge after each wash.
7. Wash the beads twice with ice-cold lysis buffer (Subheading 2.5, same volume as cell lysate), and centrifuge again at 4000 rpm for 4 min at 4 °C in a microcentrifuge.

8. Add ice-cold lysis buffer to the beads, and transfer the mix to new Eppendorf tubes before centrifuging them at 4000 rpm for 4 min at 4 °C in a microcentrifuge.
9. After removing the supernatant, add 50 μL of 2× Laemmli buffer to the beads.
10. Boil the samples at 100 °C for 5 min, and centrifuge the beads at 13,000 rpm for 5 min in a microcentrifuge.
11. Transfer the supernatant to fresh Eppendorf tubes, and proceed to load the samples on SDS-PAGE gels. Perform a western blot with appropriate antibodies. Specificity of interactions is demonstrated by the pull-down of the protein partner with GST-β-arr, but not with GST.

3.5 BRET2 Saturation Assay

Bioluminescence resonance energy transfer (BRET), a non-radiative energy transfer, measures the dynamics of protein–-protein interactions in intact live cells when the two proteins of interest are fused to a luminescent energy donor and to a fluorescent acceptor molecule. Resonance energy transfer depends both on the proximity between the two proteins (less than 10 nm) and on the spatial orientation of the donor and acceptor in fusion with each protein [25]. BRET monitors changes in the light emission ratios between acceptor and donor. In the presence of its substrate, *Renilla* luciferase (Rluc, the energy donor) emits light that excites a green fluorescent protein (GFP) variant (the energy acceptor), which in turn emits light. The Rluc substrate is cell permeable and can be directly added to the cell culture supernatant; hence, no excitation of the donor is required. Different types of BRET technique can be used depending on donor/acceptor pair combinations and the Rluc substrate [26–28]. BRET has been used to study β-arr interactions with GPCRs and other types of proteins [29–31]. To characterize β-arr interaction with other proteins, we have recently used BRET2. In this approach there is large separation between the emission peak of the energy donor RLuc2 (~400–410 nm), a variant of Rluc with increased bioluminescence [26, 32], and the one of the energy acceptor GFP10 (~515 nm) [28] ensuring a high signal-to-noise ratio and detection of small BRET changes. In BRET saturation assays, constant amounts of donor-fused proteins are transfected with increasing concentrations of acceptor-fused protein. In case of specific interaction, BRET ratios will increase with GFP10 concentration up to a plateau when all donor molecules (Rluc2) are saturated by excess GFP10 acceptor molecules and a hyperbolic curve with an asymptote is observed. In the case of nonspecific interactions, BRET ratios will continue to increase with increasing concentration of acceptor proteins resulting in a linear curve.

3.5.1 Cell Preparation and Data Acquisition

1. HEK-293T cells are seeded in 6-well plates at a density of 2.5×10^5 cells per well and incubate for 24 h in a cell culture incubator at 37 °C in a humidified atmosphere of 95% air and 5% CO_2.
2. Transfect cells with a constant amount of plasmid DNA comprising a fixed quantity of plasmid encoding the Rluc2-fusion protein (donor) in the presence or absence of increasing concentrations of GFP10-fusion protein (acceptor) plasmid in different wells (*see* **Note 25**).
3. After 24 h, aspirate media and wash the cells once with PBS.
4. Add 200 μL of trypsin-EDTA to each well of the 6-well plates. Transfer plates to the incubator for 30–60 s, allowing the cells to detach.
5. Add 2 mL of pre-warm complete DMEM media in each well, and resuspend the cells with a pipette.
6. Seed 20,000 cells (100–150 μL) per well on poly-L-ornithine-coated 96-well microplates (*see* **Note 26**), and allow the cells to attach overnight in a 37 °C incubator. Cells from each donor/acceptor plasmid transfection ratio should be distributed into three separate wells for multiple readings of the same condition.
7. Aspirate the media, wash the 96-well microplate once with 100 μL HBSS per well and add 90 μL of the same buffer (*see* **Note 27**).
8. The lid from the microplate is removed and the microplate transferred into a microplate reader. The fluorescence of the acceptor-fusion protein is measured using a 405 ± 5 nm excitation filter to verify that it is expressed in increasing quantities.
9. Add 10 μL of 25 μM Coelenterazine 400a working solution, prepared in HBSS, to each well (final concentration 2.5 μM) using a repeating pipette. Incubate the plate in the dark at room temperature for 30–45 s (*see* **Note 28**).
10. Rluc2 luminescence and GFP10 fluorescence measurements are performed sequentially for each well using 410 ± 40 nm and 515 ± 20 nm emission filters, respectively. Measurements are repeated three to six times for each well in order to get average values.

3.5.2 BRET Calculation

1. BRET ratios are calculated as the ratio of GFP10 fluorescence over Rluc2 luminescence signals.
2. For each well the average fluorescence and luminescence signals are calculated from the 3–6 measurements, and the corresponding BRET ratio is established.

3. The average background BRET ratio from the triplicates of cells transfected with only the donor DNA plasmid is calculated.
4. Subtract the background BRET value from the BRET ratio of each well, and calculate the average net BRET ratio for triplicates corresponding to each donor/acceptor plasmid transfection ratio.
5. The net BRET ratios are multiplied by 1000 and expressed as mBRET values, which is an arbitrary value.
6. Subtract background GFP10 fluorescence, the average fluorescence measurements of triplicate cells transfected with only the donor plasmid, from all other samples to obtain the net GFP10 fluorescence values.
7. Calculate the average of the net GFP10 fluorescence values over Rluc2 luminescence signals for each sample.
8. Saturation assay curves are obtained by plotting the net BRET ratios as a function of the average net GFP10 fluorescence over Rluc2 luminescence.
9. If specific interactions, hyperbolic BRET-donor saturation curves are expected. The $Bret_{max}$ is the maximal BRET value corresponding to the saturation of BRET donors by BRET acceptors. The curves are fitted using a nonlinear regression equation assuming a single binding site using GraphPad prism to calculate $BRET_{50}$ values, which is the BRET value corresponding to 50% saturation of BRET donors; it reflects the relative affinity of β-arr for its protein partner.

4 Notes

1. In this strain either the intact GAL1 upstream activating sequence (UAS), containing four GAL4-binding sites, or an artificially constructed UAS consisting of three copies of the consensus binding site, drives the expression of two reporter genes, *HIS3* and *LacZ*, respectively [33]. HF7c is thus auxotrophic for histidine. The replacement of the HIS3 promoter by the GAL1 promoter is responsible for a tighter regulation of the HIS3 reporter gene. The low number of GAL4-binding sites (as opposed to, e.g., eight in the L410 yeast strain) also decreases the possibility of false positive signals.
2. Plasmids coding for β-arr and/or the potential protein partner fused to other tag peptides (myc, HA) or proteins (GFP) can be used for transfection and co-immunoprecipitation experiments.
3. A recognition site for a protease is encoded by the linker sequence between the cDNAs coding for the GST tag and

the protein of interest. It can be used to cleave GST from the GST-fusion protein, if needed. pGEX-4T3-β-arr vector has a thrombin cleavage site between the GST and β-arr proteins. Various pGEX vectors containing different protease recognition sites (thrombin, Factor Xa, PreScission Protease) are available (GE Healthcare Life Sciences).

4. The plasmids encoding N- and C-terminal fusion of β-arr1, β-arr2, and β-arr putative partners with GFP10 or Rluc2 should be engineered and initially tested to find the most efficient pair for BRET.
5. 2× lysis buffer without sodium orthovanadate, 10 mM NaF, and protease inhibitors can be prepared and stored at −20 °C. On the day of the experiment, thaw the required amount of 2× lysis buffer, dilute it to 1×, and supplement it with 1 mM sodium orthovanadate, 10 mM NaF, and protease inhibitors.
6. Other lysis buffers can be used for cell lysis and β-arr co-immunoprecipitation experiments [12, 22].
7. Streak HF7c yeast on a YPD agar plate, and incubate cells at 30 °C until colonies have grown, and store the plate at 4 °C. Pick a colony to inoculate YPD media. Yeast YPD agar plate should not be kept more than 2 weeks at 4 °C.
8. Eighteen to twenty transformations can be carried out from 100 mL of yeast culture media. Scaling up or down the transformation can be done at this step depending on the number of transformations needed.
9. It is recommended not to make more than 14–16 patches per plate. A patching grid can be used to orient the plate and to prevent cross-contaminations.
10. The velveteen squares are reusable. They should be washed and autoclaved between each use.
11. Label the top of the master and replica plates, so you keep the same orientation.
12. Make sure that the last plate that is inoculated is the CSM-Leu-Trp selective plate in which all the patches will grow. This ensures that failure of growth on the CSM-Leu-Trp-His selective plate is not due to poor transfer from the velveteen cloth.
13. β-Gal assay can be run in parallel to confirm the results obtained with the auxotrophic assay as previously described [34].
14. We use 1 μg of plasmid encoding β-arr; the amount of plasmid encoding the putative partner can vary from 0.5 to 2 μg. Preliminary experiments should be performed by western blot of the cell lysates with the appropriate antibodies to ensure that the same amount of each protein is expressed in each condition.

15. The EZview Red anti-Flag M2 affinity gel is composed of agarose with a covalently attached mouse monoclonal antibody directed against the Flag epitope. Its use shortens the immunoprecipitation procedure compared to the classical one using free primary antibody and binding to protein A and/or G beads. The red color of the gel also facilitates its visualization during the procedure. If primary antibodies are used instead of affinity gels, they can be added at a ratio of 1:100 (v/v) for co-immunoprecipitations. For primary antibodies targeting protein tags such as Flag, HA, and GFP, 1–2.5 μg of antibodies is used per IP.
16. Other final volumes can be chosen depending on the protein concentration of the cell lysates and the type of volume that can be loaded on the SDS-PAGE gel used; the final Laemmli buffer should in any case be 1×.
17. These samples are important to control the expression levels of the transfected proteins in the lysates.
18. After IP, the supernatants can be conserved to check by western blot for immunodepletion of Flag-β-arr in comparison with the cell extract before IP.
19. Because Src and β-arr2 run very close to immunoglobulin (IgG) heavy and light chains, HRP-conjugated secondary antibodies that do not recognize IgG (TrueBlot anti-rabbit IgG HRP, 18-8816-33, 1:1000) are used.
20. When purifying a new GST-fusion protein, a small-scale pilot experiment can be carried out with increasing concentration of IPTG from 0.1 mM to 1 mM to determine the best concentration to induce protein expression. The induction time is variable depending on the protein fused to GST. GST and most GST-fusion protein induction requires only 4 h at 37 °C. For GST-β-arr1 and GST-β-arr2, the induction temperature is lowered to 20 °C with a longer induction duration, as GST-β-arr localizes to inclusion bodies at 37 °C, resulting in low yield.
21. Aliquots of the clarified bacterial lysate can be collected before and after incubation with the beads and run on a SDS-PAGE gel to determine binding efficiency. The supernatants from the first incubation with beads can be conserved and incubated again with fresh glutathione beads, if the binding to the beads is low.
22. The beads with the immobilized GST or GST-fusion proteins can be stored at 4 °C and used during 7–10 days. Sodium azide can be added to a final concentration of 0.05% in the bead suspension to prevent bacterial growth.
23. If the protein to be pulled down is endogenously expressed, use 750 μg to 1 mg of cell lysate.

24. When GST is used as a negative control for the GST-β-arr proteins, make sure that the bead volumes are the same. GST- or GST-β-arr-bound beads can be saturated with 5% BSA overnight to reduce background.
25. GeneJuice (3 μL/μg DNA) is used to transfect the cells. The total amount of transfected DNA (around 1 μg) is maintained constant by adding appropriate amounts of the corresponding empty DNA vector (e.g., pCDNA3.1). The level of the BRET donor (Rluc2-fusion protein) used for saturation assays should correspond to the lowest amount of protein required to obtain a detectable and robust Rluc2 signal (e.g., a minimum of 100,000 light units with a 1 s integration time using a Mithras plate reader), ideally close to the endogenous expression of the protein fused to Rluc2. Preliminary transfection experiments with increasing concentrations of the BRET-donor DNA plasmid followed by Rluc2 measurements should be performed to determine the amount to be used for BRET (usually 1–100 ng). Western blot of the samples will also indicate its level of expression compared to the endogenous protein. The BRET-acceptor DNA plasmid is usually transfected within a range of 10 ng to 1 μg. The expression of the Rluc2-fusion protein must be equivalent in all conditions with a ±20% variability tolerated. Conditions with a negative acceptor-fusion protein should also be included in the saturation assay to demonstrate specificity of the generated BRET. This protein should be expressed in the same cell compartment as the protein of interest.
26. Microplates are coated with poly-L-ornithine (a synthetic positively charged amino acid) to enhance the adherence of HEK cells. Dilute poly-L-ornithine to a final concentration of 30 μg/mL with dH_2O. Coat the 96-well microplate with 100 μL of this diluted poly-L-ornithine per well. Leave the plate in the incubator at 37 °C for 15 min to 2 h. Aspirate the poly-L-ornithine, wash once with 1× PBS and air-dry the plate. Poly-L-ornithine-coated microplates can be stored at RT for a few days.
27. BRET measurements are carried in colorless HBSS or PBS buffer as phenol red interferes with the assay.
28. The 25 μM working solution of Coelenterazine 400a is always prepared fresh, as it is susceptible to oxidation.

References

1. Enslen H, Lima-Fernandes E, Scott MG (2014) Arrestins as regulatory hubs in cancer signalling pathways. Handb Exp Pharmacol 219:405–425
2. Lefkowitz RJ (2013) A brief history of G-protein coupled receptors (Nobel lecture). Angew Chem Int Ed Engl 52(25):6366–6378

3. Rajagopal S, Shenoy SK (2018) GPCR desensitization: acute and prolonged phases. Cell Signal 41:9–16
4. Laporte SA, Oakley RH, Zhang J, Holt JA, Ferguson SS, Caron MG, Barak LS (1999) The β2-adrenergic receptor/β-arrestin complex recruits the clathrin adaptor AP-2 during endocytosis. Proc Natl Acad Sci U S A 96 (7):3712–3717
5. Pavlos NJ, Friedman PA (2017) GPCR signaling and trafficking: the long and short of it. Trends Endocrinol Metab 28(3):213–226
6. DeWire SM, Ahn S, Lefkowitz RJ, Shenoy SK (2007) β-arrestins and cell signaling. Annu Rev Physiol 69:483–510
7. Gurevich EV, Gurevich VV (2006) Arrestins: ubiquitous regulators of cellular signaling pathways. Genome Biol 7(9):236
8. Xiao K, McClatchy DB, Shukla AK, Zhao Y, Chen M, Shenoy SK, Yates JR 3rd, Lefkowitz RJ (2007) Functional specialization of β-arrestin interactions revealed by proteomic analysis. Proc Natl Acad Sci U S A 104 (29):12011–12016
9. Jean-Charles PY, Zhang L, Wu JH, Han SO, Brian L, Freedman NJ, Shenoy SK (2016) Ubiquitin-specific protease 20 regulates the reciprocal functions of β-arrestin2 in toll-like receptor 4-promoted nuclear factor kappaB (NFkappaB) activation. J Biol Chem 291 (14):7450–7464
10. Klenk C, Vetter T, Zurn A, Vilardaga JP, Friedman PA, Wang B, Lohse MJ (2010) Formation of a ternary complex among NHERF1, β-arrestin, and parathyroid hormone receptor. J Biol Chem 285(39):30355–30362
11. Kook S, Zhan X, Kaoud TS, Dalby KN, Gurevich VV, Gurevich EV (2013) Arrestin-3 binds c-Jun N-terminal kinase 1 (JNK1) and JNK2 and facilitates the activation of these ubiquitous JNK isoforms in cells via scaffolding. J Biol Chem 288(52):37332–37342
12. Lima-Fernandes E, Enslen H, Camand E, Kotelevets L, Boularan C, Achour L, Benmerah A, Gibson LC, Baillie GS, Pitcher JA, Chastre E, Etienne-Manneville S, Marullo S, Scott MG (2011) Distinct functional outputs of PTEN signalling are controlled by dynamic association with β-arrestins. EMBO J 30(13):2557–2568
13. Nishida M, Ogushi M, Suda R, Toyotaka M, Saiki S, Kitajima N, Nakaya M, Kim KM, Ide T, Sato Y, Inoue K, Kurose H (2011) Heterologous down-regulation of angiotensin type 1 receptors by purinergic P2Y2 receptor stimulation through S-nitrosylation of NF-kappaB. Proc Natl Acad Sci U S A 108(16):6662–6667
14. Thathiah A, Horre K, Snellinx A, Vandewyer E, Huang Y, Ciesielska M, De Kloe G, Munck S, De Strooper B (2013) β-arrestin 2 regulates Ab generation and γ-secretase activity in Alzheimer's disease. Nat Med 19(1):43–49
15. Trefier A, Musnier A, Landomiel F, Bourquard T, Boulo T, Ayoub MA, Leon K, Bruneau G, Chevalier M, Durand G, Blache MC, Inoue A, Fontaine J, Gauthier C, Tesseraud S, Reiter E, Poupon A, Crepieux P (2018) G protein-dependent signaling triggers a β-arrestin-scaffolded p70S6K/rpS6 module that controls 5'TOP mRNA translation. FASEB J 32(3):1154–1169
16. Crepieux P, Poupon A, Langonne-Gallay N, Reiter E, Delgado J, Schaefer MH, Bourquard T, Serrano L, Kiel C (2017) A comprehensive view of the β-Arrestinome. Front Endocrinol (Lausanne) 8:32
17. Peterson YK, Luttrell LM (2017) The diverse roles of Arrestin scaffolds in G protein-coupled receptor signaling. Pharmacol Rev 69 (3):256–297
18. DeFea KA (2007) Stop that cell! β-arrestin-dependent chemotaxis: a tale of localized actin assembly and receptor desensitization. Annu Rev Physiol 69:535–560
19. Sharma D, Parameswaran N (2015) Multifaceted role of β-arrestins in inflammation and disease. Genes Immun 16(8):576
20. Porter-Stransky KA, Weinshenker D (2017) Arresting the development of addiction: the role of β-Arrestin 2 in drug abuse. J Pharmacol Exp Ther 361(3):341–348
21. Stephens DJ, Banting G (2000) The use of yeast two-hybrid screens in studies of protein: protein interactions involved in trafficking. Traffic 1(10):763–768
22. Scott MG, Pierotti V, Storez H, Lindberg E, Thuret A, Muntaner O, Labbe-Jullie C, Pitcher JA, Marullo S (2006) Cooperative regulation of extracellular signal-regulated kinase activation and cell shape change by filamin a and β-arrestins. Mol Cell Biol 26(9):3432–3445
23. Beaulieu JM, Sotnikova TD, Marion S, Lefkowitz RJ, Gainetdinov RR, Caron MG (2005) An Akt/β-arrestin 2/PP2A signaling complex mediates dopaminergic neurotransmission and behavior. Cell 122(2):261–273
24. Macia E, Partisani M, Paleotti O, Luton F, Franco M (2012) Arf6 negatively controls the rapid recycling of the β2-adrenergic receptor. J Cell Sci 125(Pt 17):4026–4035
25. Marullo S, Bouvier M (2007) Resonance energy transfer approaches in molecular pharmacology and beyond. Trends Pharmacol Sci 28(8):362–365

26. Breton B, Sauvageau E, Zhou J, Bonin H, Le Gouill C, Bouvier M (2010) Multiplexing of multicolor bioluminescence resonance energy transfer. Biophys J 99(12):4037–4046
27. Coriano C, Powell E, Xu W (2016) Monitoring ligand-activated protein-protein interactions using bioluminescent resonance energy transfer (BRET) assay. Methods Mol Biol 1473:3–15
28. Pfleger KD, Eidne KA (2006) Illuminating insights into protein-protein interactions using bioluminescence resonance energy transfer (BRET). Nat Methods 3(3):165–174
29. Beautrait A, Paradis JS, Zimmerman B, Giubilaro J, Nikolajev L, Armando S, Kobayashi H, Yamani L, Namkung Y, Heydenreich FM, Khoury E, Audet M, Roux PP, Veprintsev DB, Laporte SA, Bouvier M (2017) A new inhibitor of the β-arrestin/AP2 endocytic complex reveals interplay between GPCR internalization and signalling. Nat Commun 8:15054
30. Breitman M, Kook S, Gimenez LE, Lizama BN, Palazzo MC, Gurevich EV, Gurevich VV (2012) Silent scaffolds: inhibition of c-Jun N-terminal kinase 3 activity in cell by dominant-negative arrestin-3 mutant. J Biol Chem 287(23):19653–19664
31. Paradis JS, Ly S, Blondel-Tepaz E, Galan JA, Beautrait A, Scott MG, Enslen H, Marullo S, Roux PP, Bouvier M (2015) Receptor sequestration in response to β-arrestin-2 phosphorylation by ERK1/2 governs steady-state levels of GPCR cell-surface expression. Proc Natl Acad Sci U S A 112(37):E5160–E5168
32. Loening AM, Fenn TD, Wu AM, Gambhir SS (2006) Consensus guided mutagenesis of Renilla luciferase yields enhanced stability and light output. Protein Eng Des Sel 19 (9):391–400
33. Van Criekinge W, Beyaert R (1999) Yeast two-hybrid: state of the art. Biol Proced Online 2(1):1–38
34. Scott MG, Le Rouzic E, Perianin A, Pierotti V, Enslen H, Benichou S, Marullo S, Benmerah A (2002) Differential nucleocytoplasmic shuttling of b-arrestins. Characterization of a leucine-rich nuclear export signal in β-arrestin2. J Biol Chem 277(40):37693–37701



Chapter 10

Methods to Investigate the β-Arrestin-Mediated Control of ARF6 Activation to Regulate Trafficking and Actin Cytoskeleton Remodeling

Ricardo Charles, Mohamed Bourmoum, Shirley Campbell, and Audrey Claing

Abstract

ADP-ribosylation factors (ARF) are GTPases that act to control the activation of numerous signaling events and cellular responses. The ARF6 isoform, present at the plasma membrane, can be activated by the angiotensin II type 1 receptor (AT_1R), a process dependent upon β-arrestin recruitment to the activated receptor. Here, we describe classical methods used to assess β-arrestin-dependent activation of ARF6 following agonist stimulation of cells. In addition, because ARF6 and β-arrestin can form a complex, we describe the procedures used to detect the interaction of β-arrestin with this GTPase.

Key words β-Arrestin interacting partner, ADP-ribosylation factor, GST-pulldown, GGA3, Co-immunoprecipitation

1 Introduction

ARF proteins are small monomeric proteins of the Ras superfamily. Six isoforms have been identified, and according to their homology and roles, ARF1 to ARF6 are subdivided into three different classes (I, ARF1 and ARF2; II, ARF3, ARF4, and ARF5; III, ARF6). The best characterized isoforms are ARF1 and ARF6. The former has been shown to localize primarily at the Golgi and regulate vesicle formation, while the latter is only present at the plasma membrane. In some specific cell types, ARF1 can also be found at the cell surface [1–5]. ARF6 activation is triggered by agonist stimulation of G protein-coupled receptors (GPCRs) to regulate the formation of clathrin-coated pits and subsequent internalization of receptors [6]. The activation of ARF also leads to remodeling of the actin cytoskeleton, a process that most often results in cell migration [1, 7]. In addition, ARF6 can be found in complex with β-arrestin upon agonist stimulation [7, 8]. Here, we describe how to assess

Mark G. H. Scott and Stéphane A. Laporte (eds.), *Beta-Arrestins: Methods and Protocols*, Methods in Molecular Biology, vol. 1957, https://doi.org/10.1007/978-1-4939-9158-7_10, © Springer Science+Business Media, LLC, part of Springer Nature 2019

the activity of ARF GTPases in cells that have been previously used to demonstrate the close link between β-arrestin and ARF. Those are HEK 293 cells that stably express the angiotensin II (Ang II) type 1 receptor (AT_1R) or vascular smooth muscle cells (VSMC) that endogenously express this receptor.

Assays developed to detect small GTP-binding protein activation involved the design of glutathione *S*-transferase (GST) fusion proteins of specific key domains of effectors [9]. For ARF, the Golgi-localized, gamma-adaptin ear-containing, ARF-binding (GGA) family of proteins represents the effectors of choice, since these proteins selectively interact with GTP-bound ARF to regulate vesicle trafficking [10, 11]. The most classical approach to assess ARF activation remains the use of a GST fusion containing the VHS domain (derived from its occurrence in **V**PS-27, **H**rs, and **S**TAM) and GAT domain, which is the ARF-binding domain of GGA3. The importance of β-arrestin in assessing ARF activation following GPCR stimulation has been done by knocking down the expression of β-arrestin 1 and/or 2 by RNA interference or by overexpressing mutant forms of the proteins. Furthermore, the impact of β-arrestin or ARF activation can also be supported by the fact that these proteins can be found in complex. We also describe here the methods to detect a complex between β-arrestin 2 and ARF6, in cells.

2 Materials

2.1 Cell Culture and Transfection

1. CO_2 incubator set at 37 °C, 5% CO_2.
2. Biological hood.
3. 10-cm cell culture dishes.
4. HEK293 or vascular smooth muscle cells (VSMC).
5. Eagle's minimal essential medium (EMEM) or Dulbecco's modified Eagle's medium (DMEM).
6. Fetal bovine serum (FBS).
7. Penicillin/streptomycin.
8. β-Arrestin 1 siRNA (5′-AAAGCCUUCUGCGCGGAGAAU-3′), β-arrestin 2 siRNA (5′-AAG-GACCGCAAAGUGUUU-GUG-3′), and non-targeting siRNA.
9. Lipofectamine 2000.
10. Opti-MEM.
11. β-Arrestin cDNA, HA-ARF6 cDNA, and an empty expression vector (e.g., pRK5) (can be provided upon request).
12. 2.5 M $CaCl_2$.

13. HBS 2× (1 l): 11.92 g HEPES, 16.37 g NaCl, 0.2129 g Na_2HPO_4. Adjust pH to 7.1, complete to 1 l with deionized H_2O, and filter sterilize. Aliquot and store at −20 °C.

2.2 Preparation of GST-GGA3

1. Ice bucket filled with ice flakes.
2. Incubator shaker set at 37 °C, 200 rpm.
3. Rotation shaker at 4 °C.
4. Lysogeny broth (LB) culture medium.
5. BL21 bacteria transformed with a pGEX vector expressing GST-GGA3 (vector can be obtained upon request).
6. Ampicillin (100 mg/ml).
7. Isopropyl β-D-1-thiogalactopyranoside (IPTG, 100 mM).
8. Refrigerated centrifuge with a rotor supporting 250 ml bottles or larger.
9. NETN buffer (500 ml): 10 ml of 1 M Tris-Base (pH 8), 1 ml of 0.5 M EDTA (pH 8), 10 ml of 5 M NaCl, 0.5% NP-40, 1 mM DTT, 0.5 mg/ml BSA.
10. Protease and phosphatase inhibitors final concentrations: 23.44 μg/ml leupeptin, 0.76 nM aprotinin, 1.45 μM pepstatin A, 1 mM benzamidine, 1 mM PMSF, 200 μM sodium orthovanadate.
11. Lysosyme (from chicken egg white).
12. Sonicator (with a 3 mm probe).
13. Refrigerated benchtop centrifuge (with a capacity of 10,000 × *g*).
14. Glutathione Sepharose 4B 50% bead slurry, prepared according to manufacturer's instructions.
15. Lysis buffer E (500 ml): 50 mM Tris–HCl, 1% NP-40, 137 mM NaCl, 10% glycerol, 5 mM $MgCl_2$, 20 mM NaF, 1 mM NaPPi, 1 mM Na_3VO_4, pH solution to 7.4.
16. Coomassie Blue staining solution: 50% MeOH, 10% acetic acid, 0.25% Coomassie Blue (Brillant Blue R-250).
17. Coomassie Blue destaining solution: 10% MeOH, 5% acetic acid.

2.3 ARF6 Activation Assay and Immunoprecipitation

1. Ice bucket filled with ice flakes.
2. Benchtop vacuum system used for aspiration of cell media.
3. Eppendorf tubes.
4. Cell scrapers.
5. Refrigerated benchtop centrifuge (with a capacity of 10,000 × *g*).
6. BCA Protein assay Kit (ThermoFisher).

7. SDS sample buffer (4× stock, 100 ml): 10 ml of 1 M Tris–HCl (pH 6.8), 1% β-mercaptoethanol, 4 g SDS, 0.2 g bromophenol blue, 20 ml glycerol, completed with dH_2O.
8. Protease and phosphatase inhibitors final concentrations: 23.44 μg/ml leupeptin, 0.76 nM aprotinin, 1.45 μM pepstatin A, 1 mM benzamidine, 1 mM PMSF, 200 μM sodium orthovanadate.
9. Rotation shaker at 4 °C.

2.3.1 ARF6 Activation Assay

1. Prepared GST-GGA3 bead slurry (*see* Subheadings 2.2 and 3.2).
2. Lysis buffer E (500 ml): 50 mM Tris–HCl, 1% NP-40, 137 mM NaCl, 10% glycerol, 5 mM $MgCl_2$, 20 mM NaF, 1 mM NaPPi, 1 mM Na_3VO_4, pH solution to 7.4.

2.3.2 Immunoprecipitation

1. Rat anti-HA antibody (clone 3F10) (Roche Applied Science).
2. Protein G-plus agarose beads (Santa Cruz).
3. TGH buffer (1 l): 50 mM NaCl, 50 mM HEPES (pH 7.3), 5 mM EDTA, 10% glycerol, 1% Triton.

2.4 Sodium Dodecyl Sulfate Polyacrylamide Gel Electrophoresis (SDS-PAGE) and Western Blot (WB)

All buffers are prepared with deionized H_2O.

1. Running buffer 10× (1 l): 30.28 g Tris-Base, 144.13 g glycine, 10 g SDS (prepare 2 l of 1× buffer by diluting 200 ml of 10× in 1800 ml H_2O).
2. Transfer buffer 10× (1 l): 30.28 g Tris-Base, 144.13 g glycine (prepare 2 l of 1× buffer by diluting 200 ml of 10× in 1400 ml H_2O and 400 ml of MeOH).
3. TBS 10× (2 l): 200 ml of 1 M Tris–HCl (pH 8), 176 g NaCl, complete with H_2O.
4. TGH buffer (1 l): 50 mM NaCl, 50 mM HEPES, pH 7.3, 5 mM EDTA, 10% glycerol, 1% Triton.
5. TBS-Tween (TBS-T, 2 l): dilute 200 ml of TBS 10× in 1800 ml H_2O, and add 2 ml of Tween-20.
6. Blocking solution (2%): Dilute 2 g of bovine serum albumin (BSA) in 100 ml of TBS-T.
7. Separating gel buffer (1 l): 1.5 M Tris–HCl, 0.4% SDS, pH solution to 8.8.
8. Stacking gel buffer (1 l): 0.5 M Tris–HCl, 0.4% SDS, pH solution to 6.8.
9. Per 10 ml of separating gel (14%): 3.90 ml H_2O, 3.5 ml polyacrylamide solution 40%, 2.5 ml separating gel buffer, 100 μl ammonium persulfate 10%, add 8 μl TEMED last (makes enough separating gel for 1 gel).

10. Per 10 ml of stacking gel (5%): 7.4 ml H_2O, 1240 μl polyacrylamide solution 40%, 1260 μl stacking gel buffer, 100 μl ammonium persulfate 10%, add 10 μl TEMED last (makes enough stacking gel for 4 gels).
11. BioRad Mini Trans-Blot Cell.
12. BioRad Criterion blotter.
13. Mouse anti-HA (12CA5) antibody (Abcam) (1:1000): Dilute 5 μl of antibody in 5 ml of blocking solution.
14. Mouse anti-β-arrestin 2 (H9) antibody (Santa Cruz) (1:500): Dilute 10 μl in 5 ml of blocking solution.
15. HRP-conjugated secondary antibodies (R&D).
16. Nitrocellulose membranes (BioRad).
17. ECL (enhanced chemiluminescence) solutions (GE Healthcare).
18. X-ray films if film developer is used (Harvard Apparatus Canada).
19. Gel imaging system (GE mini LAS) or film developer.
20. ImageJ software (NIH).

3 Methods

3.1 Transfections of HEK 293 and Vascular Smooth Muscle Cells (VSMC) with siRNA or cDNA to Assess β-Arrestin-Dependent Activation of ARF6

1. Cells are seeded into 10 cm tissue culture dishes at 50% confluency and maintained at 37 °C in 5% CO_2. HEK293 cells are grown in EMEM, and VSMC are grown in DMEM. For both cell types, add 10% FBS and P/S (1%) for better growth and bacteria control.
2. One day before the transfection, change media for fresh culture media. Do not add antibiotics at this point because it may promote cell death during the transfection process.
3. For β-arrestin siRNAs transfection, perform the following under a biological hood: Add 20 nM of either control or β-arrestin siRNAs to 250 μl of Opti-MEM in a sterile tube. In another sterile tube, add 3 μl of Lipofectamine 2000 to 250 μl of Opti-MEM, and wait for 5 min. Mix gently together the contents of both tubes three to four times and incubate for 20 min at room temperature. Using a pipette, add the mix onto the cells, drop by drop. Mix gently by tilting the tissue culture dish.
4. For β-arrestin cDNA wild type and mutant constructs, use the classical calcium phosphate transfection approach. First, add 3 μg of cDNA to a tube and complete to a volume of 450 μl with sterile water. Next, add 50 μl of 2.5 M $CaCl_2$ drop by drop, and gently mix with the DNA by pipetting. Lastly,

carefully add 500 μl of HBS 2×, drop by drop, by gently swirling the tube between each drop. Gently mix by pipetting three to four times, and transfer onto cells drop by drop using a pipette. Change media after 4 h.

5. For co-immunoprecipitation experiments, co-transfect cells with both β-arrestin cDNA (3 μg) and HA-ARF6 (3.5 μg) as in **step 4**.

3.2 Preparation of GST-GGA3 Fusion Protein for Assessment of GTP-Bound ARF

1. Inoculate 3 ml of LB plus 3 μl of 100 mg/ml ampicillin stock (100 μg/ml final concentration) with a loop of GST-GGA3 bacterial stock, and incubate at 37 °C overnight in an incubation shaker (200 rpm).
2. Dilute the culture in 250 ml of LB plus 250 μl of 100 mg/ml ampicillin stock (100 μg/ml final concentration). Let the bacterial cells grow at 37 °C until OD is between 0.6 and 0.8.
3. Add 250 μl of 100 mM IPTG stock (100 μM final concentration), and incubate 2–3 h at 30 °C.
4. Centrifuge bacteria at 8000 × *g* for 10 min at 4 °C.
   *Next steps should be performed on ice.
5. Resuspend bacterial pellet with 12 ml of NETN buffer.
6. Aliquot (2 ml) bacteria suspension in 15 ml tubes, snap-freeze and store at −80 °C until the day before the experiment.
7. The day before the experiment, thaw one tube of GST-GGA3 slowly in a tube of cold water on ice. Add equal volume of NETN buffer plus PMSF, aprotinin, and leupeptin (*see* **Note 1**).
8. When completely thawed, add lysozyme and invert six to eight times. Leave on ice for 15 min.
9. Sonicate for 20 s, twice, at 30% amplitude. Let rest on ice 30 s between sonication.
10. Transfer the lysed bacteria to cold Eppendorf tubes, and centrifuge at 10,000 × *g* in a microcentrifuge for 15 min at 4 °C.
11. Transfer the supernatant into a clean tube, and add 300 μl of glutathione Sepharose 4B beads. Agitate at 4 °C overnight on a rotation shaker.
12. The day of the experiment, centrifuge at 500 × *g* for 1 min at 4 °C to pellet the beads, and wash three times with 5 ml of lysis buffer E (*see* below).
13. Add 3 ml of lysis buffer E plus protease inhibitors and store at 4 °C.
14. To assess the quality of the GST-GGA3, run an aliquot (approximately 15 μl) of GST-GGA3 on a 14% polyacrylamide gel, next to GST-only control. To reveal the protein bands, incubate gel for 5 min in 100 ml of Coomassie Blue staining

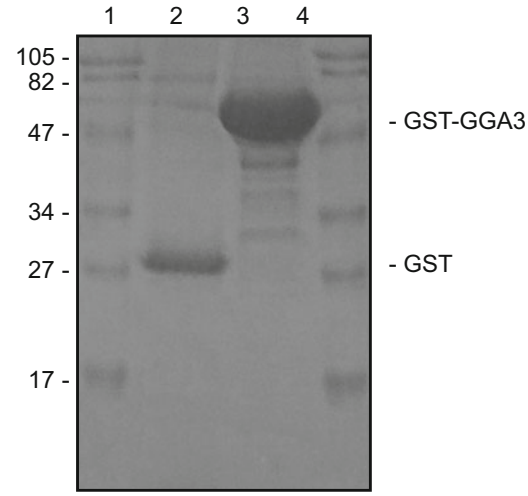


Fig. 1 Polyacrylamide gel stained with Coomassie Blue was used to assess GST-fusion protein production. *Lanes 1 and 4* show prestained SDS-PAGE standards. *Lane 2* shows 30 μl of GST, and *lane 3* shows 30 μl of GST-GGA3, both eluted from Glutathione Sepharose 4B beads

solution, followed by incubation in 100 ml of Coomassie Blue destaining solution. The GST-GGA3 band should begin to be visible after 1 h, and the Coomassie-stained gel should be clear after a 24-h incubation in the destaining solution (*see* Fig. 1).

3.3 Activation of ARF GTPases

1. Seed control and siRNA/cDNA (if assessment of β-arrestin-dependent activation of ARF6 is studied) transfected cells into 10 cm dishes to obtain 80% confluency the next day.
2. Serum starve cells (*see* **Note 2**) for 4 h (HEK 293) or 24 h (VSMC), and stimulate cells, at 37 °C, with either vehicle or agonist for short time periods (0, 1, 2, 5, 15, 30, and 60 min).
3. Place plates on ice to stop the ARF activation process. Quickly remove the media by aspiration, and add 300 μl of lysis buffer E containing protease inhibitors. Harvest cells by scraping, and transfer lysates into cold Eppendorf tubes. All samples must stay on ice during the procedure.
4. Spin all samples for 10 min at 10,000 × *g* in a refrigerated centrifuge (4 °C). Transfer supernatant into a new tube and discard the pellet. Remove 2 μl of each sample for protein quantification using the BCA Protein Assay Kit following the manufacturer's instructions. Maintain all samples on ice.
5. Remove 10% of each sample (equal protein quantities between samples) and add them to separate tubes. Denature proteins into 10 μl of SDS sample buffer containing 1% β-mercaptoethanol by heating each sample at 65 °C for

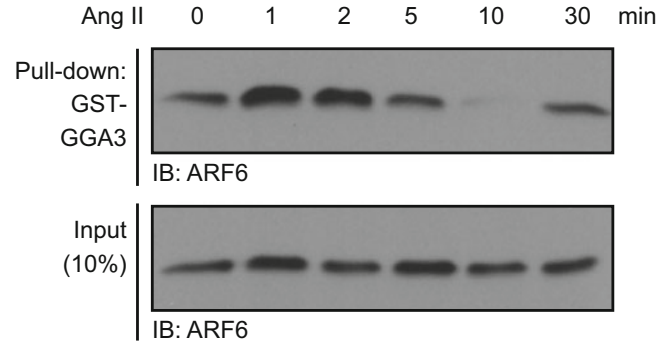


Fig. 2 Western blots of a typical GST-GGA3 pulldown experiment to assay ARF6 activation. HEK293 cells expressing the AT1R were stimulated with Ang II (1 μM) at the indicated times. The *upper* panel shows active ARF6 eluted from Glutathione Sepharose 4B beads that were conjugated with GST-GGA3. The *lower* panel shows the quantity of ARF6 present in an input from the total cell lysate

15 min. Spin samples at 500 × *g* for 1 min. These samples will be used as inputs to assess total ARF6 levels.

6. Equal amounts of protein will be used from the remainder of each sample for the pulldown of ARF6-GTP. Rapidly, add 60 μl of GST-GGA3 fusion protein coupled to glutathione Sepharose 4B beads, and rotate at 4 °C for 1 h on a rotation shaker.
7. Pellet the GST-GGA3 beads with a centrifugation at 500 × *g* for 1 min at 4 °C, and wash three times with 200 μl of lysis buffer E.
8. Elute proteins into 20 μl of SDS sample buffer containing 1% β-mercaptoethanol by heating the sample at 65 °C for 15 min. Spin samples at 500 × *g* for 1 min (*see* **Note 3**).
9. Run pulldown and input samples onto a 14% SDS-PAGE gels next to a molecular weight marker (*see* Fig. 2).

3.4 Cellular Co-Immunoprecipitation of β-Arrestin and ARF Proteins

1. Seed cells transfected with β-arrestin and HA-ARF6 into a 10 cm dish, overnight.
2. The next day, leave cell untreated or treat them with Ang II (100 nM) or the appropriate agonist of the receptor of choice for different time, to allow the β-arrestin/ARF6 complex to form. Then, place plates on ice, aspirate media, rinse once with ice-cold PBS, and add 200 μl TGH buffer supplemented with protease inhibitors and 1 mM Na_3VO_4. Harvest cells into a cold Eppendorf tube.
3. Spin all samples for 10 min at 10,000 × *g* in a refrigerated centrifuge (4 °C). Transfer supernatant into a new tube and discard the pellet. Determine protein concentration in samples using a BCA protein assay. Maintain all samples on ice.

4. Remove 10% of each sample (equal protein quantities between samples), and add them to separate tubes. Denature proteins into 10 μl of SDS sample buffer containing 1% β-mercaptoethanol by heating to 65 °C for 15 min. Spin samples at 500 × *g* for 1 min. These samples will be used as inputs to assess total HA-ARF6 levels.
5. Equal amounts of protein will be used from the remainder of each sample for the immunoprecipitation of HA-ARF6. Add 3 μl of anti-HA antibody (3F10) to each sample, and incubate for 2 h at 4 °C with agitation.
6. Add 30 μl of protein G-plus agarose beads (50% slurry) to each sample, and continue incubation for 2 more hours.
7. Spin samples at 500 × *g* for 2 min. Remove supernatant and wash beads with TGH lysis buffer. Repeat the procedure twice.
8. Elute proteins using 20 μl of SDS sample buffer containing 1% β-mercaptoethanol by heating to 65 °C for 5 min (*see* **Note 3**).
9. Run samples on SDS-PAGE as described in Subheading 3.5.

3.5 SDS-PAGE and WB

3.5.1 SDS-PAGE

1. Separate proteins with electrophoresis in 1× running buffer using a BioRad Mini Trans-Blot Cell, and transfer onto nitrocellulose membranes in 1× transfer buffer using a BioRad Criterion blotter.

3.5.2 WB

These steps are performed under constant agitation on a rocker. Antibody concentrations used are antibody specific.

1. After transfer, rinse membranes twice with TBS-T for 5 min, and then block membranes from non-specific antibody binding by incubating them into TBS-T containing 2% BSA (w/v) for 60 min at room temperature.
2. Rinse membranes once with TBS-T for 5 min, and then incubate the membrane with primary antibody (mouse anti-HA (12CA5) for ARF6 and mouse anti-β-arrestin 2) diluted in 10 ml TBS-T at 4 °C, overnight.
3. Rinse membranes with TBS-T for 5 min, repeat twice.
4. Incubate membranes with an appropriate HRP-conjugated secondary antibody diluted in TBS-T for 45 min at room temperature.
5. Rinse membranes with TBS-T for 5 min, repeat twice.
6. Reveal proteins by incubating membranes with a chemiluminescent HRP substrate, as indicated in the manufacturer's instruction book.
7. Use a Gel Imaging system to detect the enhanced chemiluminescence (ECL) signal, or expose membranes with X-ray films in the dark room in a film developer.

4 Notes

1. Place a 50-ml conical tube on ice, fill it with water containing ice, and place the bacteria tube in it to thaw slowly.
2. In certain cell lines, serum starvation can induce stress, which can increase the basal levels of ARF6 activation. Adding L-ascorbic acid (250 μg/ml) to your serum starvation media can help reduce high basal levels of ARF6 activation induced by stress.
3. Samples can be frozen at this step.

Acknowledgments

This work was supported by the Canadian Institutes of Health Research (MOP-79470 and MOP-106596 to AC).

References

1. Boulay PL, Cotton M, Melancon P, Claing A (2008) ADP-ribosylation factor 1 controls the activation of the phosphatidylinositol 3-kinase pathway to regulate epidermal growth factor-dependent growth and migration of breast cancer cells. J Biol Chem 283(52):36425–36434
2. Hashimoto S, Hirose M, Hashimoto A, Morishige M, Yamada A, Hosaka H, Akagi K, Ogawa E, Oneyama C, Agatsuma T, Okada M, Kobayashi H, Wada H, Nakano H, Ikegami T, Nakagawa A, Sabe H (2006) Targeting AMAP1 and cortactin binding bearing an atypical src homology 3/proline interface for prevention of breast cancer invasion and metastasis. Proc Natl Acad Sci U S A 103 (18):7036–7041
3. Galas MC, Helms JB, Vitale N, Thierse D, Aunis D, Bader MF (1997) Regulated exocytosis in chromaffin cells. A potential role for a secretory granule-associated ARF6 protein. J Biol Chem 272(5):2788–2793
4. Mitchell R, Robertson DN, Holland PJ, Collins D, Lutz EM, Johnson MS (2003) ADP-ribosylation factor-dependent phospholipase D activation by the M3 muscarinic receptor. J Biol Chem 278(36):33818–33830
5. Cohen LA, Honda A, Varnai P, Brown FD, Balla T, Donaldson JG (2007) Active Arf6 recruits ARNO/cytohesin GEFs to the PM by binding their PH domains. Mol Biol Cell 18 (6):2244–2253
6. Poupart ME, Fessart D, Cotton M, Laporte SA, Claing A (2007) ARF6 regulates angiotensin II type 1 receptor endocytosis by controlling the recruitment of AP-2 and clathrin. Cell Signal 19(11):2370–2378
7. Charles R, Namkung Y, Cotton M, Laporte SA, Claing A (2015) Betaarrestin-mediated angiotensin II signaling controls the activation of ARF6 and endocytosis in migration of vascular smooth muscle cells. J Biol Chem 291 (8):3967–3981
8. Claing A, Chen W, Miller WE, Vitale N, Moss J, Premont RT, Lefkowitz RJ (2001) Beta arrestin-mediated ARF6 activation and beta2-adrenergic receptor endocytosis. J Biol Chem 276(45):42509–42513
9. Benard V, Bohl BP, Bokoch GM (1999) Characterization of rac and cdc42 activation in chemoattractant-stimulated human neutrophils using a novel assay for active GTPases. J Biol Chem 274(19):13198–13204
10. Boman AL, Zhang C, Zhu X, Kahn RA (2000) A family of ADP-ribosylation factor effectors that can alter membrane transport through the trans-Golgi. Mol Biol Cell 11 (4):1241–1255
11. Dell'Angelica EC, Puertollano R, Mullins C, Aguilar RC, Vargas JD, Hartnell LM, Bonifacino JS (2000) GGAs: a family of ADP ribosylation factor-binding proteins related to adaptors and associated with the Golgi complex. J Cell Biol 149(1):81–94



Chapter 11

Methods to Investigate the Roles of β-Arrestin-Dependent RalGDS Activation in GPCR-Stimulated Membrane Blebbing

Stephen S. G. Ferguson

Abstract

G protein-coupled receptors (GPCRs) comprise the largest family of integral membrane proteins, which in addition to signaling via heterotrimeric G proteins can activate small G proteins both directly and indirectly. The activation of a variety of GPCRs leads to the translocation of Ral GDP dissociation stimulator (RalGDS) to the plasma membrane, where it functions as a guanine nucleotide exchange factor of RalA to promote membrane blebbing. The translocation of RalGDS is β-arrestin-dependent and can be inhibited by either the expression of the β-arrestin1 amino-terminal domain or the expression of RalGDS clone 284 (amino acid residues 616–768 of RalGDS). We describe here a methodology for assessing GPCR-dependent stimulation of RalGDS plasma membrane translocation.

Key words β-Arrestin, RalGDS, Green fluorescent protein, G protein-coupled receptor, Confocal microscopy, Translocation, Membrane blebbing, Agonist, Antagonist, Plasma membrane

1 Introduction

G protein-coupled receptors (GPCRs) are coupled to the activation of a diverse array of signal transduction pathways by functioning as guanine nucleotide exchange factors (GEFs) for heterotrimeric G proteins to regulate cellular activity [1]. It is well known that GPCRs signal via Ras and Rho following the activation of heterotrimeric G proteins [2]. However, GPCRs can also regulate the activity of small G proteins via their direct association or via intermediary signaling proteins such as β-arrestins [3–9]. In particular, there is evidence that GPCRs can function directly as GEFs for small G proteins and that β-arrestin proteins can interact with both ADP ribosylation factor nucleotide-binding site opener (ARNO) and Ral GDP dissociation stimulator (RalGDS) and function to regulate the small GTPases Arf6 and RalA [3–5].

The family of small G proteins is comprised of over 100 members that can be categorized into 5 subfamilies: Ras family GTPases (e.g., Ras, Rap, and Ral), Rho family GTPases (Rho, Rac, and

Mark G. H. Scott and Stéphane A. Laporte (eds.), *Beta-Arrestins: Methods and Protocols*, Methods in Molecular Biology, vol. 1957, https://doi.org/10.1007/978-1-4939-9158-7_11, © Springer Science+Business Media, LLC, part of Springer Nature 2019

cdc42), Arf family GTPases (Arfs 1–6, Arls 1–7, and Sar), Rab family GTPases (>60 members, e.g., Rab5), and Ran family GTPases [10]. In general, Ras family GTPases regulate gene transcription, but Ral proteins have been shown to contribute to the reorganization of the actin cytoskeleton resulting in membrane ruffling and blebbing involved in cell migration [11–13]. In the case of the angiotensin II type 1A receptor ($AT_{1A}R$), the activation of membrane ruffling and blebbing may be important for the process of vascular remodeling in hypertension and atherosclerosis [14, 15].

RalGDS is a highly specific GEF for RalA and RalB where it functions to promote the exchange of GDP for GTP [16, 17]. RalGDS is a cytosolic protein and must translocate to the plasma membrane in order to function as a GEF for Ral proteins. RalA is activated in response to the activation of both the formyl-met-leu-phe receptor and $AT_{1A}R$ in a RalGDS and β-arrestin-dependent manner [3, 18]. In the absence of receptor activation, RalGDS is localized to the cytosol in a complex with β-arrestin, but following agonist activation RalGDS rapidly translocates with β-arrestin to the plasma membrane where it is released to activate Ral. The translocation of RalGDS to the plasma membrane can be inhibited by either the expression of the β-arrestin1 amino-terminal domain (amino acid residues 1–154) or the expression of RalGDS clone 284 (amino acid residues 616–768 of RalGDS). The current chapter describes methodology for assessing RalGDS membrane translocation in response to GPCR activation, as well as a method to inhibit translocation and subsequently inhibit membrane blebbing.

2 Materials

2.1 Cell Culture

1. Human embryonic kidney (HEK 293) cells.
2. Minimal essential medium (MEM).
3. Fetal bovine serum (FBS).
4. 0.25% Trypsin-EDTA.
5. Gentamicin.
6. Phosphate buffered saline (PBS): 137 mM NaCl, 2.7 mM KCl, 10 mM Na_2PO_4, pH 7.4.
7. T175 tissue culture flasks.
8. 100 mm tissue culture dish.
9. 35 mm dishes containing 1-cm centered sealed glass coverslip.
10. Hanks Buffered Saline Solution (HBSS): 1.2 mM KH_2PO_4, 5 mM $NaHCO_3$, 20 mM HEPES, 11 mM glucose, 116 mM NaCl, 4.7 mM KCl, 1.2 mM $MgSO_4$, 2.5 mM $CaCl_2$.

11. 0.2-μM bottle top filters.
12. 10-, 25- and 50-ml sterile plastic serological pipettes.
13. Type 1 collagen from calf skin (Sigma).

2.2 Transfection

1. Distilled water.
2. 2.5 M $CaCl_2$.
3. 2× HEPES-balanced salt solution (HeBS): 16.4 g NaCl (380 mM final), 11.9 g HEPES (50 mM final), 0.21 g Na_2HPO_4 (1.5 mM final), 800 ml H_2O. Titrate to exactly pH 7.05 with 5 N NaOH, add H_2O to 1 l. Store at −20 °C in 50 ml aliquots.
4. Falcon 2063 tubes.
5. 1-ml sterile plastic serological pipettes.
6. RalGDS-eGFP plasmid cDNA and β-Arr1N construct (available upon request) [3].

2.3 Microscopy

1. Leica SP8 laser scanning confocal microscope or equivalent instrument.
2. Zeiss 63× 1.4 numerical aperture oil immersion lens or equivalent to allow detection of eGFP. Laser excitation at 488 nm and 515–540 nm emission filter set.
3. 35 mm glass coverslip bottomed (Martek).

3 Methods

3.1 Cell Culture

1. *Day 1*: The media is aspirated from stock cultures of human embryonic kidney HEK 293 cells grown to 95% confluency in T175 cell culture flasks (*see* **Notes 1** and **2**). The cells are then washed two times with PBS, subsequently treated with 4 ml of 0.25% Trypsin-EDTA for 1 min, and then gently resuspended in at least one equal volume of MEM containing 10% FBS and 50 μg/μl gentamicin. The cells are counted using a hemocytometer and reseeded at a density of 2×10^6 HEK 293 cells per 100 mm tissue culture dishes in a final volume of 10 ml of MEM containing 10% fetal bovine serum (FBS) and 50 μg/ml gentamicin.
2. *Day 2*: HEK 293 cells cultured in 100 mm dishes are transfected by calcium phosphate precipitation as outlined in Subheading 2.2 and then maintained overnight at 37 °C in a humidified atmosphere of 95% air, 5% CO_2.
3. *Day 3*: 15–18 h after transfection, the culture media is exchanged for 10 ml of fresh MEM containing 10% FBS and 50 μg/ml gentamicin. Six to eight (6–8) hours after changing the media, the 100 mm cell culture dishes are washed two times

with 5 ml of PBS, subsequently treated with 2 ml of 0.05% trypsin for 1 min, and then gently resuspended in 10 ml of MEM containing 10% FBS and 50 μg/ml gentamicin. 2 ml of the suspension is reseeded in 35 mm glass coverslip-bottomed culture dishes that were pretreated for 5 min with 1 ml of collagen solution, and then washed two times with 2 ml of PBS (*see* **Note 3**). The cells are allowed to recover overnight. This should result in cultures that are 40–50% confluent (*see* **Note 4**).

4. *Day 4*: The cell culture media in the 35 mm culture dishes is exchanged for 1 ml of HBSS (pre-warmed at 37 °C) prior to experimentation.

3.2 Transfection

1. 1 μg of pEGFP-C1-RalGDS cDNA (RalGDS-GFP) and 5 μg of plasmid cDNA encoding the receptor protein (e.g., $AT_{1A}R$) along with either 5 μg of either empty plasmid, β-Arr1N (N-terminal amino acid residues 1–154 of β-arrestin1), or RalGDS clone 284 (amino acid residues 616–768 of RalGDS) are pipetted into the bottom of a Falcon 2063 tube (*see* **Notes 5** and **6).**
2. 450 μl of sterile distilled water is added to the plasmid cDNA.
3. 50 μl of 2.5 M $CaCl_2$ is added and the solution mixed by vortexing for 5 s.
4. 500 μl of 2× HeBS is added drop by drop using a 1 ml serological pipette and is thoroughly mixed using the pipette.
5. The mixture containing the plasmid cDNA is then carefully administered drop by drop across the surface of the 100 mm cell culture dish. The drops are applied 1 to 1½ in. (2.5 to 4 cm) above the surface of the liquid.
6. The cells are then cultured overnight at 37 °C in a humidified atmosphere of 95% air, 5% CO_2. The next morning, the cells are washed with fresh MEM containing 10% MEM and reseeded 24 h later into 35 mm glass coverslip-bottomed culture dishes (Matek).

3.3 Microscopy

1. 35 mm glass coverslip-bottomed culture dishes containing HEK 293 cells transfected with receptor and RalGDS-GFP are placed on the microscope stage of a laser scanning confocal microscope (e.g., Leica SP8) (*see* **Note 7**).
2. The cells are imaged using a 63× 1.4 numerical aperture oil immersion lens and focused using transmitted light.
3. It is desirable to obtain a field of RalGDS-GFP transfected cells using the fluorescent microscope prior to switching to laser scanning mode. Healthy HEK 293 cells take on a flat irregular shape; RalGDS-GFP should be localized to the cytoplasm of

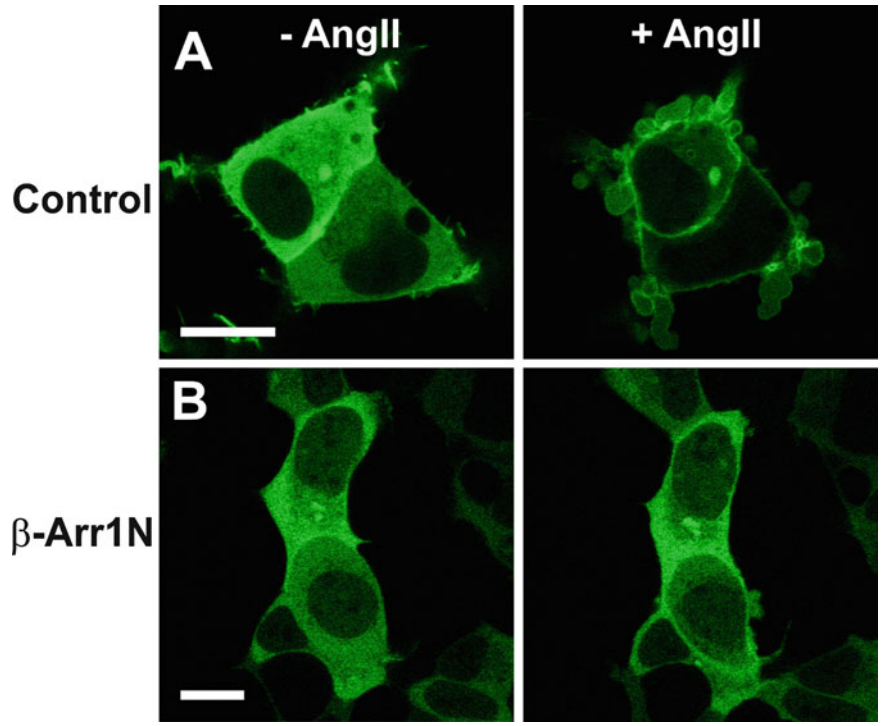


Fig. 1 Effect of $AT_{1A}R$ agonist activation (100 nM, Angiotensin, AngII) for 2 min on RalGDS subcellular localization in (**a**) the absence or (**b**) presence of β-arrestin1N expression. Scale bars, 10 μm

the cell and excluded from the nucleus. A cell with a defined plasma membrane and large cytoplasm should be chosen for imaging. The most desirable image plane is through the center of the cell since this will provide the best definition of the plasma membrane and cytosolic compartments of the cell (Fig. 1).

4. The laser scanning mode can be used to zoom in on the field of cells. A zoom function of no more than four times should be employed. The pinhole should be set to unity. The quality of the image can be increased both by reducing the pixel scan rate of the laser and by increasing the number of image frames that are integrated to provide an image. We find that a pixel scan rate of 2.24–4.48 μs combined with the integration of 8 image frames provides a desirable confocal image every 15–30 s. The laser excitation should be set at 488 nm and the emission filter set to 515–540 nm. Laser power is an issue since GFP is readily bleached. Therefore, the lowest possible laser power should be employed, usually 1–2%.
5. Images should be acquired every 15–30 s. A time series of images can be obtained using the time series software available in the microscope software package. One or two control

images of the cell should be obtained prior to the addition of agonist. Agonist can be applied to the cell culture dish in a 100 μl volume at a final concentration that will maximally activate the cell surface GPCRs (*see* **Note 8**).

3.4 Data Analysis

Data can be analyzed using the Leica software package or other publicly or commercially available software packages provided with available confocal microscopes. Images should be exported into Adobe Photoshop for data presentation.

4 Notes

1. All liquid media should be filter sterilized using 0.2-μm bottle top filters, and all tissue culture glassware must be autoclaved before use. Sterile technique should be followed at all times.
2. Lab stocks of HEK 293 cells seeded in T175 tissue culture flasks containing 15 ml MEM with 10% FBS and 50 μg/ml gentamicin are maintained at 37 °C in a humidified atmosphere of 95% air, 5% CO_2.
3. Stock cultures should be seeded with 2×10^6 HEK 293 cells. The media should be replaced every 3–4 days and cultures split and reseeded in new flasks once a week.
4. The treatment of the 35-mm glass coverslip-bottomed culture dishes with collagen facilitates the attachment of cells to the glass coverslip and avoids detachment of cells during experimentation.
5. It is useful that cells be evenly distributed at a confluence of no more than 40–50% for RalGDS-GFP translocation experiments.
6. Good receptor expression is essential for effective RalGDS-GFP translocation. Expression levels of greater than 1 pmol/mg of total protein are desirable. However, for many receptors translocation can be detected a much lower expression levels. RalGDS-GFP expression should be low.
7. Alternative methods of cell transfection such as Lipofectamine can also be utilized. However, in our experience, the calcium phosphate precipitation method for cell transfection provides a simple cost-effective method for transfecting HEK 293 cells with a co-transfection efficiency that ranges between 50–80%.
8. A microscope equipped with a heated stage, environmental control chamber or perfusion chamber is desirable. The heated stage and environmental control chamber allow cell cultures to be maintained at optimal temperatures. Cell cultures do not need to be maintained at 37 °C for these experiments, and it may be desirable under some conditions to lower temperatures

to slow the translocation process. A cell perfusion chamber should be used if either agonist dose-response curves are desired or the experiment requires changes in drug treatment (e.g., agonist recovery or antagonist treatment).

References

1. Ferguson SSG (2001) Evolving concepts in G protein-coupled receptor endocytosis: the role in receptor desensitization and signaling. Pharmacol Rev 53:1–24
2. Bhattacharya M, Babwah AV, Ferguson SSG (2004) Small G protein-coupled receptors. Biochem Soc Trans 32:1040–1044
3. Bhattacharya M, Anborgh PH, Babwah AV, Dale LB, Dobransky T, Benovic JL, Feldman RD, Verdi JM, Rylett RJ, Ferguson SSG (2002) β-Arrestin regulates a RalGDS-Ral effector pathway mediating cytoskeletal reorganization. Nat Cell Biol 4:547–555
4. Claing A, Chen W, Miller WE, Vitale N, Moss J, Premont RT, Lefkowitz RJ (2001) J Biol Chem 276:42509–42513
5. Seachrist JL, Laporte SA, Dale LB, Babwah AV, Caron MG, Anborgh PH, Ferguson SSG (2002) Rab5 association with the angiotensin II type 1A receptor promotes Rab5 GTP-binding and vesicular fusion. J Biol Chem 277:679–685
6. Mitchell R, McCulloch D, Lutz E, Johnson M, MacKenzie C, Fennell M, Fink G, Zhou W, Sealfon SC (1998) Rhodopsin-family receptors associate with small G proteins to activate phospholipase D. Nature 392:411–414
7. Mukherjee S, Gurevich VV, Jones JC, Casanova JE, Frank SR, Maizels ET, Bader MF, Kahn RA, Palczewski K, Aktories K, Hunzicker-Dunn M (2000) The ADP ribosylation factor nucleotide exchange factor ARNO promotes beta-arrestin release necessary for luteinizing hormone/choriogonadotropin receptor desensitization. Proc Natl Acad Sci U S A 97:5901–5906
8. Koch T, Brandenburg LO, Schulz S, Liang Y, Klein J, Hollt V (2003) ADP-ribosylation factor-dependent phospholipase D2 activation is required for agonist-induced mu-opioid receptor endocytosis. J Biol Chem 278:9979–9985
9. Mukherjee S, Casanova JE, Hunzicker-Dunn M (2001) Desensitization of the luteinizing hormone/choriogonadotropin receptor in ovarian follicular membranes is inhibited by catalytically inactive ARNO(+). J Biol Chem 276:6524–6528
10. Takai Y, Sasaki T, Matozaki T (2001) Small GTP-binding proteins. Physiol Rev 81:153–208
11. Feig LA (2003) Ral-GTPases: approaching their 15 minutes of fame. Trends Cell Biol 13:419–425
12. Charras GT (2008) A short history of blebbing. J Microsc 231:466–478
13. Chhabra ES, Higgs HN (2007) The many faces of actin: matching assembly factors with cellular structures. Nat Cell Biol 9:1110–1121
14. Touyz RM, Schiffrin EL (2000) Signal transduction mechanisms mediating the physiological and pathophysiological actions of angiotensin II in vascular smooth muscle cells. Pharmacol Rev 52:639–672
15. Weir MR, Dzau VJ (1999) The renin-angiotensin-aldosterone system: a specific target for hypertension management. Am J Hypertens 12:205S–213S
16. Albright CF, Giddings BW, Liu J, Vito M, Weinberg RA (1993) Characterization of a guanine nucleotide dissociation stimulator for a ras-related GTPase. EMBO J 12:339–347
17. Matsubara K, Kishida S, Matsuura Y, Kitayama H, Noda M, Kikuchi A (1999) Plasma membrane recruitment of RalGDS is critical for Ras-dependent Ral activation. Oncogene 18:1303–1312
18. Godin C, Ferguson SSG (2010) Angiotensin II type 1 receptor activation induces membrane blebbing by coupling to RhoA, rho kinase and myosin light chain kinase. Mol Pharmacol 77:903–911



Chapter 12

Methods to Determine Interaction Interfaces Between β-Arrestins and Their Protein Partners

Thomas Bourquard, Astrid Musnier, Aurélie Tréfier, Flavie Landomiel, Thomas Boulo, Eric Reiter, Pascale Crépieux, and Anne Poupon

Abstract

β-arrestins are so-called hub proteins: they make complexes with many different partners, assembling functional complexes, and thereby fulfilling their biological function. The importance of this process in G protein-coupled receptor (GPCR) signalling has been fully demonstrated for many different receptors. For direct interactions, determining the interface regions, on β-arrestins and on the partners, is crucial for understanding the function of the complex. Indeed, this brings information on which proteins can interact simultaneously with β-arrestins, or, on the contrary, which partners are exclusive. We present here a method in two steps: protein–protein docking allows finding a limited number of peptides predicted to be involved in the interaction, and then experimental approaches that might be used for validating the prediction.

Key words Protein complex, β-arrestin partners, Interface region, Protein–protein docking

1 Introduction

β-arrestins play key roles in G protein-coupled receptor (GPCR) signalling through their interactions with hundreds of proteins [1]. Characterizing the interaction regions between β-arrestins and their partners is an important step in the understanding of the functional roles of these interactions. In particular, it allows determining the partners that are in competition with each other (XOR) and those whose interactions are compatible (AND) and can thus bind simultaneously on a single β-arrestin molecule [2]. This knowledge can lead to the understanding of how different signalling pathways can be triggered simultaneously, or on the contrary compete each other [3, 4], or how mutations in one partner can affect to various extents its different partners [5, 6].

The gold standard in interface determination is the determination of complex 3D structures, either by crystallography or using NMR. However, this represents a lot of work and requires the production of both proteins at high yield. Moreover, in the case

Mark G. H. Scott and Stéphane A. Laporte (eds.), *Beta-Arrestins: Methods and Protocols*, Methods in Molecular Biology, vol. 1957, https://doi.org/10.1007/978-1-4939-9158-7_12, © Springer Science+Business Media, LLC, part of Springer Nature 2019

of signalling proteins, such as β-arrestins and their partners, the affinities are generally low, and stabilizing the complex can be tricky. Aside from the 3D structure, a widely used experimental method is to evaluate the binding between one partner and mutants of the other one, either in terms of affinity or in terms or relative binding as compared to the wild type. However, single mutations, especially alanine mutations, can lead to undetectable modulation of the affinity, although they affect amino acids involved in the interaction. Moreover, the throughput of such a method is very low. A higher throughput can be achieved using peptide array-based methods [7–9], in which overlapping peptides of one partner are arrayed on solid support and exposed to the second partner. This can be followed by alanine scanning of positive peptides to refine the interaction map. Recently, mass spectrometry-based approaches have been developed [10, 11]. The principle is to submit the complex either to hydrogen/deuterium exchange or to enzymatic digestion and to identify through mass spectrometry peptides that are protected by the interaction. However, these methods are time-consuming and require specialized equipment and skills.

We have recently developed a method for determining the interaction regions in protein complexes, which allowed us to predict and validate the geometry of the assembly of β-arrestin with the receptor, c-Src, and the ERK signalling module (Raf, MEK, and ERK) [12]. In addition, results obtained from such an approach allow us to make hypotheses, which can be experimentally validated, for instance, on the mechanism of phosphorylation of residue T383 in β-arrestin upon activation of the receptor [13]. This method consists of two main steps. First, a computational method, based on an in-house protein–protein docking algorithm [14–16], allows determining four regions of the sequences of each partner possibly involved in the interaction. Second, these regions are used to design peptides that are used for refinement and experimental validation of the prediction.

This experimental validation can be conducted using various protocols. Although positive results using only one method are enough for the validation, interactions between a protein and a peptide are not easily detected. We give here three different possible validation methods, ranked in order of difficulty but also of sensitivity. The first method we describe here is GST-pulldown approach, which is used to visualize competition between the partner and a peptide, for binding to β-arrestin (Fig. 1a). If positive, the results of GST-pulldown validate the prediction of the interface.

However, GST-pulldown is not a very quantitative method and requires large quantities of both purified proteins. As an alternative, we suggest using homogenous time-resolved fluorescence (HTRF) to assess the competition (Fig. 2a). HTRF combines fluorescence resonance energy transfer technology (FRET) with time-resolved measurement (TR). In TR-FRET assays, a signal is generated

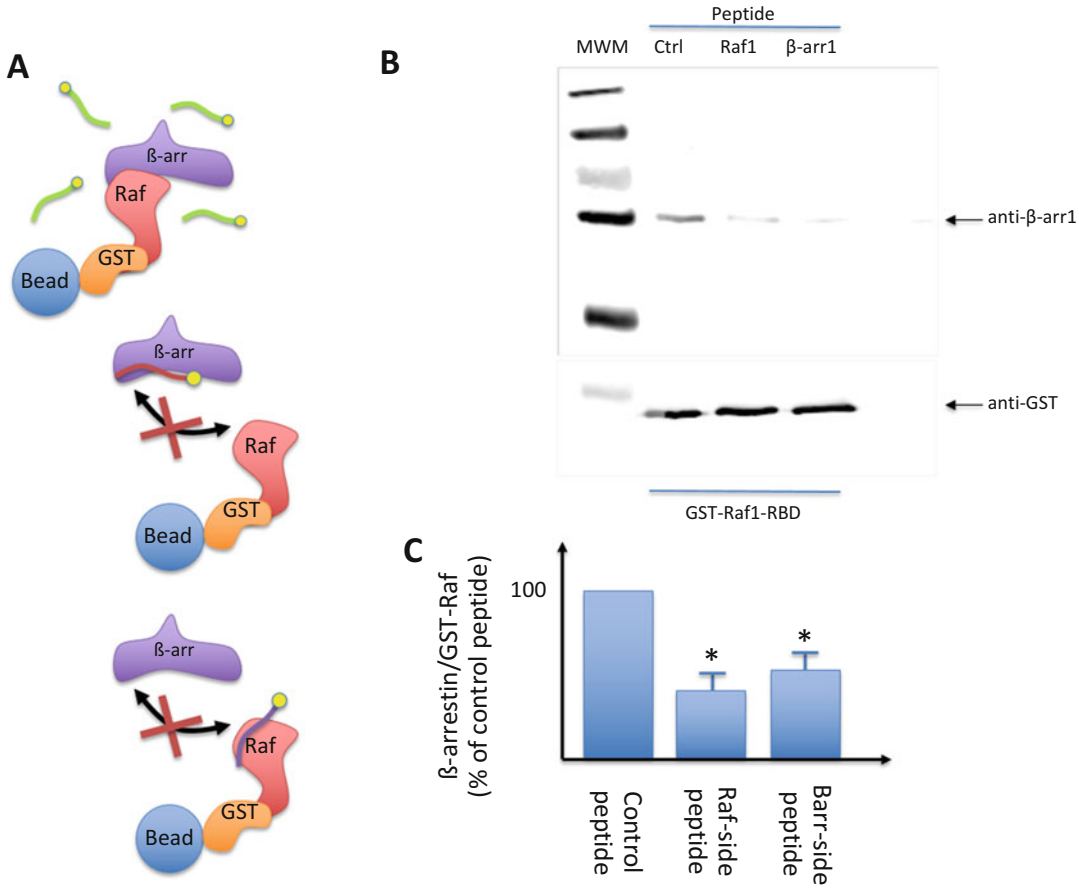


Fig. 1 (**a**) Principle of the GST-pulldown experiment with purified proteins. (**b**) Representative experiment to illustrate the disruption of the Raf1/β-arrestin 1 interaction by a competing peptide (73-ISPFEHQTY-81). In each condition, 25 ng of β-arrestin 1 are added, whereas GST-Raf1-RBD is not present in the last lane. The same membrane hybridized with an anti-GST antibody to monitor the pulled-down amount of GST-Raf-RBD is shown below. (**c**) Quantification of three independent experiments

through FRET between a donor (long-lived fluorescence) and an acceptor (short-lived fluorescence) molecule when in close proximity to each other (i.e., the distance between the two fluorophores is less than 1.8× the radius of Förster, i.e., <10 Å or 1 nm). Time delay (50–150 μs) between the initial light excitation and fluorescence measurement minimizes the contribution of all non-specific short-lived fluorescence emissions. Buffer and media interference is dramatically reduced by dual-wavelength detection, and the final signal is proportional to the extent of product formation. Specific fluorophores are used in HTRF forming different TR-FRET systems like europium cryptate donor (Eu^{3+}) or terbium donor (Tb^{2+}). These ions are not fluorescent on their own, since they need a light-collection device to be excited. HTRF technology has been applied to many antibody-based assays including GPCR

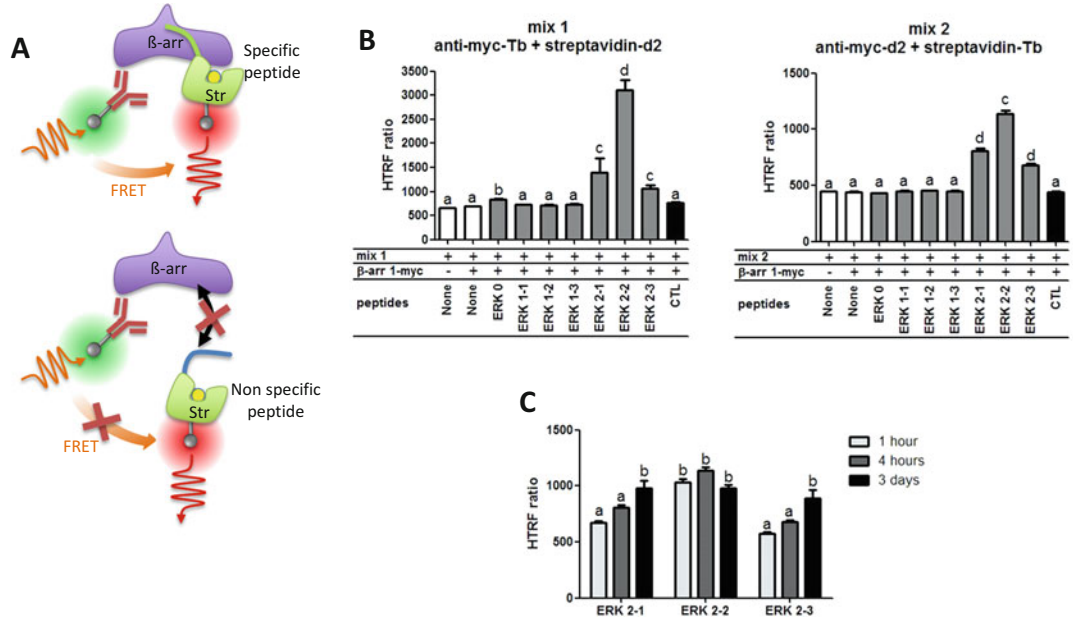


Fig. 2 (**a**) Principle of the HTRF experiment. (**b**) Quantification of three independent experiments showing β-arrestin 1 interaction with competing peptides after 3 h of incubation. Sequences of the peptides are given in **Note 9**. The control peptide is a portion of the sequence of the C5 complement protein. Different letters above the bars indicate statistically significant differences. (**c**) Quantification of three independent experiments showing β-arrestin 1 interaction with selected competing peptides after either 1 h, 3 h, or 3 days of incubation

signalling (cAMP and IP1), kinases, cytokines and biomarkers, bioprocess (antibody and protein production), as well as assays for protein–protein, protein–peptide, and protein–DNA/RNA interactions. Here, we describe how to measure FRET differences between two purified tagged proteins in the presence of competing peptides designed to interact with either β-arrestin or its protein partner.

If the affinity between β-arrestin and its partner is high, the affinity of the peptide might not be sufficient for competition. In that case, we have shown that biolayer interferometry can be used to evaluate the specificity of the peptide (Fig. 3a). Biolayer interferometry is very similar in its principles to surface plasmon resonance (SPR) but has the great advantage of being a non-fluidic system, which is easier to handle and maintain. It relies on the detection of the association of molecules on a surface at the tip of a biosensor, constituted mainly of an optic fiber [1]. This biosensor is first dipped in a well containing the first partner, which associates to the surface, and this association can be observed through the analysis of light reflected at the tip of the biosensor [2]. The biosensor can then be dipped in a second well containing the second partner, and the association with the first partner can be measured

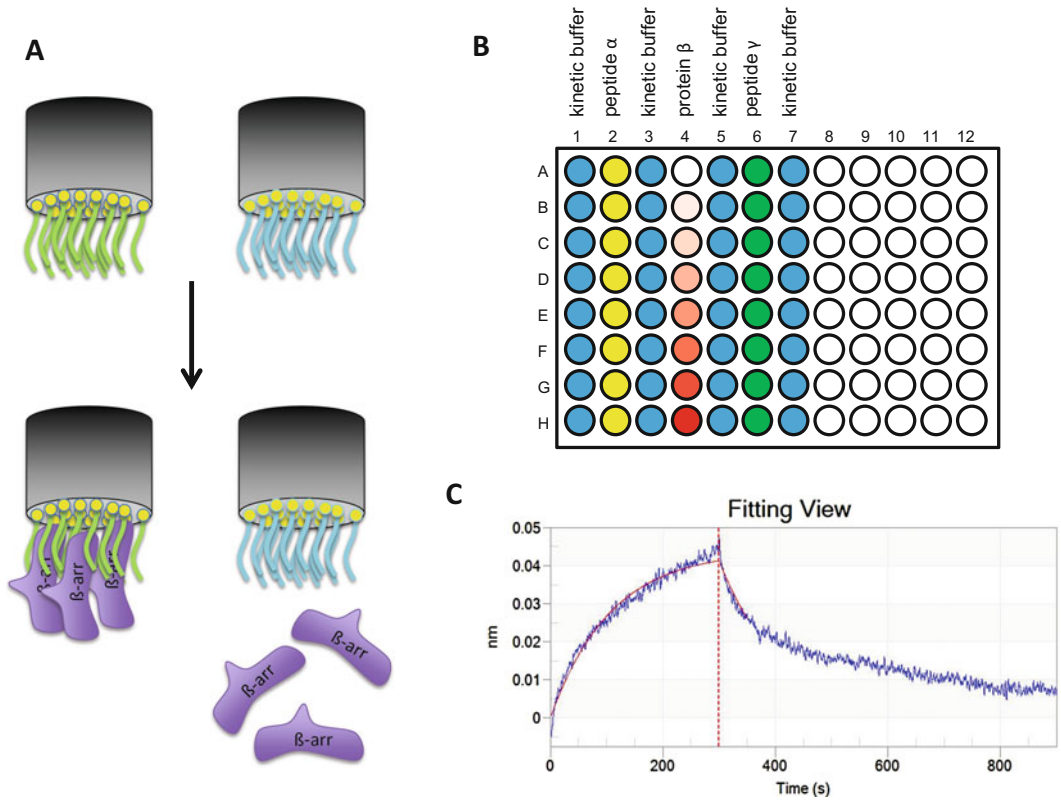


Fig. 3 (**a**) Principle of the interferometry experiment: biotinylated-specific peptide or control peptide binds to the streptavidin tip. β-arrestin then binds to the interfering peptide but not to the control peptide. (**b**) Sample plate scheme. Samples and buffer are loaded on the black 96-well plate as shown here. The peptides α and γ are prepared at one single concentration, whereas protein β is prepared in five concentrations. Well A4 contains only kinetic buffer and will be used as control. (**c**) Representative experiments to illustrate the observation by biolayer interferometry of the specific interaction between the competing peptide ERK2-3 and β-arrestin 1

using the same principle [3]. Finally, the biosensor can be dipped in a well containing only buffer, which allows monitoring the dissociation of the two partners. In our case, the first partner is the peptide designed to interfere with the association of β-arrestin with its partner, and biolayer interferometry is used to measure the association of β-arrestin with this peptide. We use biotinylated peptides, which can be loaded on streptavidin biosensors. The advantage is that the interaction affinity between biotin and streptavidin is very high, guaranteeing that the dissociation observed at **step 3** is that of the two loaded components and not the dissociation of the first component from the biosensor.

2 Materials

Unless otherwise mentioned, all chemicals are from Sigma Aldrich.

2.1 GST Glutathione S-Transferase (GST)-Pulldown

Plasmids and bacteria: GST-Raf1-RBD expressed from pGEX-2T was generously provided by Dr. Véronique Fafeur (Pasteur Institute, Lille). The Raf1-RBD (Ras-binding domain) corresponds to amino acids 51 to 131 of Raf1 and is the minimum domain required for binding to Ras-GTP. The pGEX-2T plasmid (GE Healthcare, Buckinghamshire, UK) was used as a negative control. C(6His)-tagged human β-arrestin 1 was from Gentaur (San Jose, CA, USA). Chemo-competent NEB-5α bacteria were from New England (Biolabs, Ipswish, MA, USA). Agar (LB-Agar Lennox) plates and L-broth (LB-medium Lennox powder), both purchased at MP Biomedicals, Illkirch, France, contained 100 μl/ml ampicillin (stock solution 100 mg/ml).

1. Lysis buffer used for protein production in *E. coli*: 250 mM NaCl, 10 mM $MgCl_2$, 10 mM EDTA, 1% Triton, 250 μg/ml lysozyme, 10 mM DTT, 1 mM PMSF, 3.4 U DNAse I, 1× protease and phosphatase inhibitor cocktail II (Thermo Fisher Scientific Inc. Waltham, MA, USA), in phosphate-buffered saline (PBS). This buffer has to be prepared extemporaneously and kept on ice until use.
2. Buffers used for GST (glutathione S-transferase)-pulldown. (a) Fusion protein-binding buffer: 10 mM Tris–HCl pH 8.0, 100 mM NaCl, 0.5% NP40, 20 mM EDTA, 1 mM PMSF or 1× protease, and phosphatase inhibitor cocktail II. (b) HNTG protein–protein interaction buffer: 20 mM Hepes, pH 7.9, 50 mM KCl, 2.5 mM $MgCl_2$, 1 mM DTT, 10% glycerol, 1× protease, and phosphatase inhibitor cocktail II. If prepared in advance, omit the protease/phosphatase inhibitors in the stock solutions.
3. Laëmmli buffer 2× was prepared with 8% SDS, 5% β-mercaptoethanol, 10% glycerol (w/v), 32 mM Tris–HCl pH 6.8, 0.01% bromophenol blue, and stored at room temperature. Western blot blocking solution was made with PBS/0.1 Tween 20 with 5% bovine serum albumin.
4. Polyclonal anti-β-arrestin primary antibody, diluted 1:2000, was from Abcam, Cambridge, England. IRDye Alexa fluor 680-labelled secondary antibody, diluted 1:15,000, was from Licor, Lincoln, NE, USA. Anti-GST antibody, diluted 1:500, was from Life Technologies, Carlsbad, CA, USA.
5. Competing peptides, synthesized by Genecust Laboratories (Dudelange, Luxembourg), were designed following prediction of the docking interface, as described above in Subheading 3.1.

2.2 Homogeneous Time-Resolved Fluorescence (HTRF)

Prepare all solutions (purified myc-β-arrestin1 (0.180 μg/μl, OriGene #TP321737) and ERK peptides (100 μg/μl)) in PBS(1×)-Tween 20 0.1% at 4 °C, and store purified proteins at −80 °C and acceptor- and donor-fused antibodies and peptides at −20 °C. Prepare all reagents in 384-well plate for a final volume of 20 μl which contains 10 μl of 2× purified protein ($[\text{myc-β-arrestin1}]_{\text{initial}} = 0.4$ ng/μl), 5 μl of 4× peptide ($[\text{ERK peptide}]_{\text{initial}} = 50$ mM), and 5 μl of 4× HTRF donor-coupled antibody ($[\text{α-c-myc Tb cryptate}]_{\text{initial}} = 30$ ng/μl, Cisbio) and acceptor-coupled antibody ($[\text{streptadivin-D2}]_{\text{initial}} = 1000$ ng/μl, Cisbio).

1. Prepare 10 ml of PBS(1×)-Tween 20 0.1%: add 1 ml of PBS 10× to 8.9 ml of water, and then add 100 μl of Tween 20. Mix gently to homogenate solution and store at 4 °C.
2. Gently thaw purified proteins on ice.
3. Dilute lyophilized peptide in DMSO, work on ice, and store at −20 °C.
4. Use white flat low volume 384-well plate to work with 20 μl final volume.
5. Settings measurements are defined by using Mikrowin 2010 software, and relative energy transfer rate of each condition is measured on microplate reader MITHRAS^2 LB 943 (Berthold technologies GmbH and Co.Kg, Germany).

2.3 Interferometry

1. 96-Well black plates, without lid (ref # 1608130, Greiner Bio-One, Kremsmünster, Austria).
2. Kinetic buffer 10× (ref #18-1092, 50 ml, Pall forteBio, Fremont, CA, USA).
3. SA (streptavidin) biosensors (Pall ForteBio, Fremont, CA, USA).
4. Octet RED96 system (Pall ForteBio, Fremont, CA, USA).
5. Octet software 9.0 version (Pall ForteBio, Fremont, CA, USA).
6. Biotinylated peptide α (=ligand, relevant peptide), stock suspension at 50 mM in dimethylsulfoxide (DMSO).
7. Protein β (=analyte, β-arrestin in our example), stock suspension at 1 μg/μl.
8. Biotinylated peptide γ (nonrelevant ligand), stock suspension at 50 mM in DMSO.

3 Methods

3.1 Predicting the Possible Interaction Regions and Designing Validation Peptides

1. Get the structure files corresponding to the two interacting partners, for example, from RCSB (http://www.rcsb.org) (*see* **Notes 1** and **2**).
2. If the files contain more than one chain, for example, if the atomic coordinates correspond to a homo-multimer, or if the structures have been determined in complex with another partner, remove irrelevant chains from file. Heteroatoms should also be removed. If the partner is constituted of more than one chain (e.g., an antibody, comprising heavy and light chains), it should be renumbered as a single chain (*see* **Note 3**).
3. Choose the partner that will not move (usually designated as the "receptor") and the partner that will move around the receptor partner (designated as the "ligand"). This choice does not change the prediction. However, all the proposed docking poses will be superimposed on the receptor partner. Consequently, if you are more interested on the interface on one of the partners, choose it as receptor. If you are interested in both interfaces, choose the smallest partner as ligand; the computations will be a bit faster.
4. Run PRIOR (*see* **Note 4**).
5. PRIOR outputs a file named "peptides.txt," which is a list of peptides. From our benchmarks, one of the first four peptides does belong to the interface, and the three others are often part of the interface also. Thus, it is recommended to consider using the four top-ranked peptides.
6. Each peptide computed by PRIOR is 15 residues long. Each peptide should be used for validation but also a peptide starting and ending three residues upstream and a peptide starting and ending three residues downstream. Indeed, we have often observed that the computed peptide might not be soluble, but the upstream and/or downstream peptides are. Thus, designing three peptides for each predicted interacting residue stretch increases the chance to have at least one peptide suitable for experimental validation (*see* **Note 5**).

3.2 GST-Pulldown

1. *Producing GST-Raf1-RBD fusion protein in E. coli.*
   (a) On day 1, transform competent NEB-5α bacteria with either a pGEX-2T plasmid encoding GST-Raf1-RBD or an empty plasmid encoding GST alone, which is used as a control. Spread bacteria on agar plates containing 100 μg/ml ampicillin, and incubate overnight (ON) at 37 °C.

(b) On day 2, amplify bacteria by picking one colony into 25 ml L-broth containing 100 μg/ml Ampicillin. Incubate ON at 37 °C in a shaking incubator at 200 rpm.

(c) On day 3, dilute the 25 ml of culture into 225 ml LB/Amp, and grow 3 h at 37 °C at 200 rpm. 10 ml of the 250 ml culture are stored at 4 °C until **step 1d** as a control of the non-induced condition. In the remaining 240 ml, induce protein expression by adding 2.4 ml EtOH (1% final concentration) + 600 μl IPTG (250 μM final concentration), and grow bacteria for 3 h at 37 °C in a shaking incubator at 200 rpm.

(d) Proceed with induced and non-induced bacteria lysis on ice. Centrifuge bacteria culture at 2500 × *g* for 30 min at 4 °C, in Nalgene bottles. Recover the pellet and centrifuge the supernatant again for 20 min. Both pellets should be recovered and pooled in lysis buffer (500 μl for 10 ml of culture), in a 15-ml Falcon tube. Incubate ON at 4 °C on a rotating wheel. The next day, the lysates are sonicated three times for 30 s on ice, centrifuged for 1 h at 12,000 × *g*, and filtered on 0.22 μm filters. Aliquots of non-purified GST-fusion protein controls (60 μl for the induced condition and 12.5 μl for the non-induced condition) are diluted in equal volumes of 2× Laëmmli buffer (v/v) and stored at −20 °C until use (*see* **Note 6**).

2. In vitro *protein–protein interaction*.

(a) Preparation of Glutathione Sepharose 4B beads. Pipette 20 μl of slurry beads (50% in EtOH) per ml of initial bacteria culture. Centrifuge the beads at 500 × *g* for 5 min, resuspend them in 10 ml PBS, and incubate at 4 °C on a rotating wheel for 1.5 h. Centrifuge the beads again at 500 × *g* for 5 min and resuspend in an equal volume of PBS.

(b) Purification of the fusion protein. Incubate the whole bacteria lysate with 4.8 ml of slurry beads prepared in Subheading 3.2, **step 2a**, and with 200 μl for the non-induced condition at 4 °C on a rotating wheel for 30 min. Centrifuge at 500 × *g* for 5 min, and then wash the beads twice with PILB. Beads are next saturated with 5 ml of 10% BSA under rotation at 4 °C for 10 min, washed once in 1 ml PILB, and centrifuged at 500 × *g* for 5 min before removing the supernatant. Beads can be used immediately, once extensively dried for 30 min at 37 °C. Alternatively, they can be stored as 50 μl dried aliquots at −20 °C for future use, after first resuspending them in PILB and centrifuging them again at 500 × *g* for 5 min.

(c) The reaction mix comprises 25 ng of recombinant human His-tagged β-arrestin 1, 50 µl of dried beads coated with either GST-Raf1-RBD or GST, and 0.5 mM (*see* **Note 7**) of one of the competing peptides or control peptide (Fig. 1a). These quantities correspond to a β-arrestin/peptide molar ratio of 10 to 1. The volume is completed to 1 ml with HNTG buffer, and the reaction mix is placed at 4 °C on a rotating wheel for 1 h (*see* **Note 8**). The beads are then washed six times with 1 ml HNTG (each time, centrifuge at 500 × *g* for 5 min).

(d) Competing peptides cover amino acids 30–38 of human β-arrestin 1 (HIDLVEPVD) or amino acids 65–74 (KQRTVVNVRN) on Raf1. The control peptide corresponds to amino acids 69–77 (DVLGLSFRK) of β-arrestin 1, a region that is outside of the predicted Raf1/β-arrestin 1 interface.

3. After the last centrifugation, dried beads are resuspended in 2× Laëmmli buffer (v/v), boiled at 100 °C for 30 min, and centrifuged for 10 min at 12,000 × *g*. Recover the supernatants (avoid pipetting beads), and load them onto 10% SDS-PAGE gels. After the transfer of the resolved proteins onto nitrocellulose membrane, dip the latter in 10 ml of blocking solution for 1 h at RT, and then incubate the membrane ON with a polyclonal anti-β-arrestin primary antibody and then with IRDye Alexa fluor 680-labelled secondary antibody, all diluted in blocking buffer. Protein-loading homogeneity is monitored by stripping, washing, and reprobing membranes with a polyclonal anti-GST antibody against GST-Raf1-RBD.

3.3 HTRF

Carry out all procedures on ice to preserve protein and peptide stability.

1. Peptide-based validation of the protein partner interaction area. Several peptides are designed at the interface region of each partner. The protocol given here allows testing the specific interaction of the peptides belonging to the interface region of one partner with the second partner. This protocol is illustrated here for the interaction of ERK peptides with β-arrestin 1 (Fig. 2a–c).

(a) Dilute β-arrestin 1 to 2 ng/µl in PBS(1×)-0.1% Tween 20, and dispense 5 µl per well in a low bottom 384-well plate.

(b) Dilute the ERK peptides to 2 mM in PBS (1×)-0.1% Tween 20 and dispense 10 µl per well.

(c) Cover the plate with adhesive and aluminum foils and incubate overnight at 4 °C under smooth agitation.

(d) Mix 3 ng of the donor-coupled antibody (or protein) and 50 ng of the acceptor-coupled antibody (or protein) in 5 μl and dispense in the well.

(e) Incubate 1 h at room temperature and keep the plate several days at 4 °C (*see* **Notes 10–13**).

2. Open microplate reader MITHRAS^2 LB 943 (Berthold Technologies GmbH and Co. Kg, Germany) and Mikrowin 2010 software.
3. The reader performs two sequential readings at 620 nm (donor) and 665 nm (acceptor) emission wavelengths. In mean windows of Mikrowin 2010 software, click on "Instrument" in menu bar, and then in "Excitation filter slide"; introduce bar with excitation filter 620 nm. Then click in "Emission filter slide," and introduce bar with emission filter 665 nm.
4. Load a predefined protocol HTRF by clicking on "Open Template" tab in mean window. Select TR-fluorescence and then HTRF Tb_red_348.par file.
5. Define measurements' sequence parameters in "Option" tab.
6. A dialog box opens with two tabs: Samples and Measurement,

   First click on "Samples," and enter parameters of plate format:

   (a) In plate type: Berthold 384-No33505.

   (b) In plate mode: Measurement.

   (c) In Measure order: By Rows and click on Meander

   Then select wells for measurements
   Second to features of the measurement operation, click on "Measurement". Three columns appear. Left column describes the settings of the chosen operation. Check that preselect steps of measurement are selected: "Delay," "Skake," "Lumi.Label," "Lumi.kinetic," "Fluor.kinetic," and "Fluor.kinetic."
   In middle column, double click in "HTRF-Tb-red" to verify parameters:

   (d) Counter time: 1.00 s.

   (e) Counter: photon.

   (f) Use: filter.

   (g) Reading position: top.

   (h) Aperture TRF filter: 384.

   (i) Excitation filter: 340 × 26 HTRF Tb cryptate.

   (j) Excitation optic: default.

   (k) Emission filter: 620 × m10 Eu cryptate.

   (l) Cycle time: 2000 μs.

   (m) Delay time: 50 μs.

(n) Reading time: 400 μs.

(o) Click second measurements.

(p) Excitation filter: 340 × 26 HTRF Tb cryptate.

(q) Emission filter: 665 × m7uv XL665, APC.

(r) Operation mode: By plate.

7. Before to start reading, give name of your experiment in "Plate ID" in the toolbar.
8. Click "START"; introduce your plate in the reader.
9. The live data measurement can be displayed by clicking on "measurement."
10. Calculate energy transfer rate (*see* **Note 13**).

3.4 Interferometry

1. Dilute the biotinylated peptides α and γ (called "ligands"), in 1× kinetic buffer to the determined concentrations (*see* **Notes 14** and **15**). 200 μl per well are needed.
2. Dilute the protein β (called "analyte") in kinetic buffer. Five association curves (i.e., five concentrations of the analyte) are necessary to measure a reliable Kd (*see* **Note 16**). One well must be left empty, i.e., with no analyte, only kinetic buffer.
3. Load the 200 μl of protein solutions or kinetic buffer in a black plate according to Fig. 3b.
4. Soak two columns of biosensors in 200 μl of kinetic buffer in a black plate positioned under the sensor tray.
5. Open the Octet Data Acquisition 9.0 software, open a new experiment wizard, and enter your plate scheme in "plate definition."
6. In "assay definition," set the experiment up as follows (Fig. 3b):

(a) Set a 60 s baseline in column 1.

(b) Set a 600 s loading step in column 2.

(c) Set a 60 s baseline in column 1.

(d) Set a 60 s baseline in column 3.

(e) Set a 600 s association in column 4.

(f) Set a 600 s dissociation in column 3.

(g) Click on "new assay." The following steps will appear in a different color.

(h) Set a 60 s baseline in column 5.

(i) Set a 600 s loading step in column 6.

(j) Set a 60 s baseline in column 5.

(k) Set a 60 s baseline in column 7.

(l) Set a 600 s association in column 4.

(m) Set a 600 s dissociation in column 7.
All the steps are performed at 30 °C and under 1000 rpm shaking.

7. In "sensor assignment," locate the two biosensor columns, containing peptides α and γ, as they appear in the sensor tray. The two columns should appear in two different colors, the same colors as the steps before. By right-clicking on the second biosensor column (the one loaded in the nonrelevant peptide γ), select "reference."
8. Start reading.
9. Open the Data Analysis 9.0 software, and load your experiment in "data selection."
10. Each curve must be corrected twice: first by subtracting the curve obtained from the wells without protein β (line A according to Fig. 3b) and second by subtracting for each curve obtained on the relevant peptide (α) its counterpart on the nonrelevant peptide (γ). To do so, in "processing," go to the **step 1** part, and click on "sensor selection." in the "sensor tray," the biosensors should appear as sample sensors in the column 1 and reference sensors in column 2. If not, change their settings by right-clicking on them. In the "sample plate map," right-click on the "no analyte" well, and set it as a reference sensor as well. Be sure that the selection boxes next to the reference sensor column and the non-analyte well are selected.
11. In "processing," go to **step 2**. Select "subtraction" and "double reference." The subtraction calculation formula should appear in the box.
12. In "processing," go to **step 3**. Select "Align Y axis" on "association."
13. Click on "Process data."
14. In "processed data," select the fitting model corresponding to your protein sample (typically the 1:1 model). The analysis must be performed for all the curves at once. To do so, select "global analysis" and "by color" (it implies that all the curves should appear in the same color; to do so, select them all, right-click, and select a random color). The Kd and other parameters are shown in the table (*see* **Notes 17–19**, Fig. 3c).

4 Notes

1. The list of PDB files corresponding to a given protein appears on the UniProt page of the protein, in the "Structure section." If there is more than one choice, the structure corresponding to the largest region should be chosen. In case there are

multiple files corresponding to this criterion, the one with the lowest resolution should be preferred. Finally, read carefully the corresponding Protein Data Bank (http://www.rcsb.org [17]) page, in order to see if the structure contains ligands, inhibitors, glycosylations, etc.

2. If the 3D structure of one of the partners has not been determined, it is possible to use the structure of a very close homologue. This is the case for β-arrestins1 and 2: the 3D structure of the human proteins has not been determined but only those of the bovine homologues. However, the only sequence differences between human and bovine proteins lie in the C-terminal tails, which are not present in the 3D structures. Consequently, the bovine structures can be used.
3. To remove chains and heteroatoms, PyMol software (https://www.pymol.org/) can be used.
4. At this step, PRIOR can be replaced by another protein–protein docking method, but there will be no automated peptide design. In that case this can be done manually: from the predicted complex 3D structure, list the amino acids in each partner that are involved in the interaction. For each stretch of residues predicted to be at the interface, design a 15-aa long peptide by extending this stretch in both directions (toward the N- and C-term). This procedure can also be applied for an "educated-guess" of the interface regions.
5. Regarding the design of peptides, the rules given in "Methods" should be applied with discernment, and some exceptions should be raised (Fig. 4):
   (a) If the computed peptide starts at position 1 of the sequence, no upstream peptide should be used. Conversely, if the computed peptide ends at the last residue of the partner, no downstream peptide should be used.
   (b) It sometimes happens that the computed peptide corresponds, in the 3D structure, to a sequence stretch whose central part is buried, which means that the two extremities are predicted to belong to the interface region. In that case, either the peptide should be ignored, or two different peptides should be generated by extending upstream and downstream, in order to define 15 residue-long peptides whose central regions are exposed and correspond to the extremities of the original peptide.
   (c) If the peptide corresponds to a helical region, it should be ignored. The reason is that a 15 residue-long peptide will only exceptionally fold as a helix.
   (d) Although there is no absolute rule to predict the solubility of a peptide, you should avoid sequences starting or

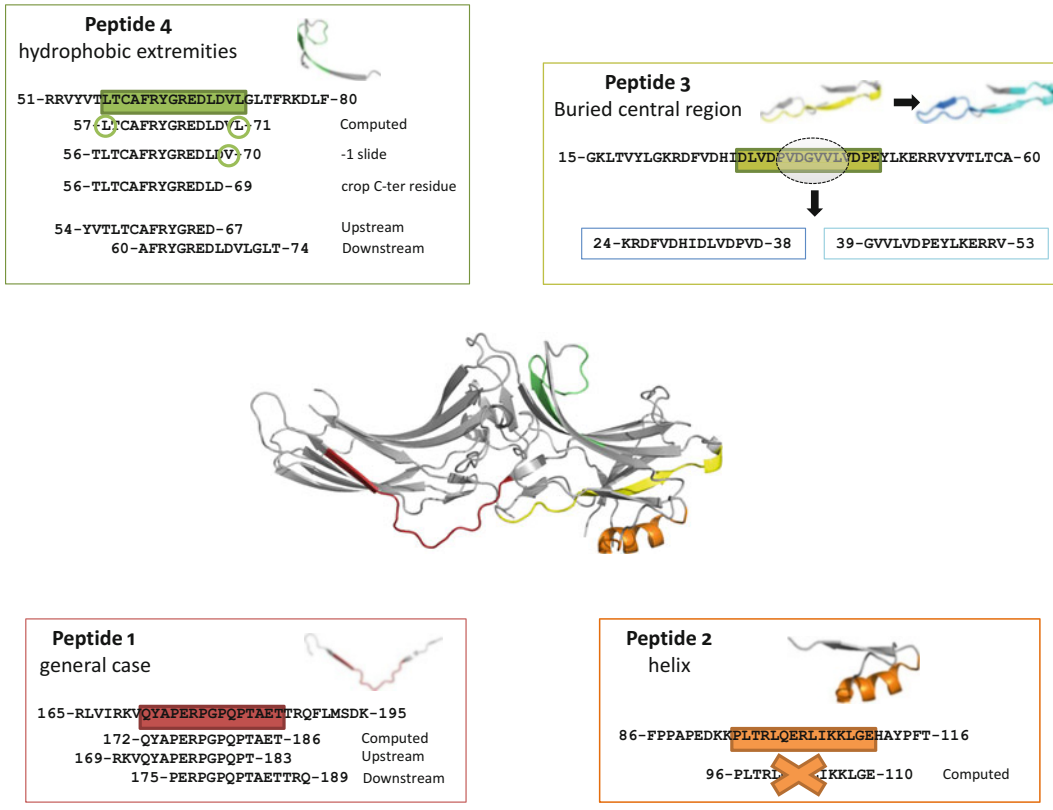


Fig. 4 Principles for refining the design of peptides. *See* text for details

ending with hydrophobic amino acids. If the computed peptide, or the upstream/downstream peptide, starts or ends with hydrophobic amino acids, try shifting upstream or downstream. Alternatively, the peptides can be shortened. The affinity having a tendency to decrease with the length of the peptide, the short peptides tend to be less favorable than longer ones. However, here also there is no prediction rule, and sometimes very nice results can be obtained with eight residue-long peptides.

6. Each step of the fusion protein production and binding to the glutathione beads can be monitored by SDS-PAGE 10% and Coomassie blue staining, by comparing induced and non-induced conditions, as well as purified and non-purified conditions. Serial dilutions of BSA can be used as a standard to estimate the amount of purified GST-Raf1-RBD.
7. We assayed several concentrations of competing peptide, and an inhibitory effect was visible from 0.5 mM. At the same concentration, no effect of the control peptide is observed.
8. β-arrestins are "sticky" proteins. Hence, when investigating β-arrestin interaction partners in cell lysates, only a 5-min

interaction time is enough, in order to avoid non-specific binding. However, with recombinant purified protein, this time had to be extended to 1 h.

9. ERK peptide sequences:

erk-antibarr-0	ISPFEHQTY
erk-antibarr-1.1	RVAIKKISPFEHQTY
erk-antibarr-1.2	IKKISPFEHQTYCQR
erk-antibarr-1.3	ISPFEHQTYCQRTLR
erk-antibarr-2.1	IRDILRASTLEAMRD
erk-antibarr-2.2	ILRASTLEAMRDVYI
erk-antibarr-2.3	ASTLEAMRDVYIVQD

10. As initial concentrations of purified protein are often lower, calculate how much ng of protein you need for a triplicate. Then, prepare an intermediate solution at 1:10 with PBS (1×)-Tween 0.1%, for each protein in a final volume of 50 µl or 20 µl. From 1:10 solutions, prepare mix of both proteins and adjust the final volume with PBS(1×)-Tween 0.1% to deposit 20 µl or 10 µl in 1 well of a 96-well plate or a 384-well plate, respectively.
11. To verify that HTRF-coupled antibodies recognize specifically tagged proteins, prepare conditions with an irrelevant antibody. Also, to make sure that there is no cross talk between secondary antibodies, prepare triplicate wells with only antibodies. Finally, to subtract medium background, prepare triplicate of PBS(1×)-Tween 20 only.
12. Preincubation allows the peptides to associate with the proteins. This association might be perturbed by the antibodies used for detection since the affinities of the peptides for the proteins are low (usually in the high micromolar range), whereas the affinities of antibodies binding to their targets are very high. Do not forget to prepare each condition with and without peptides. Since some complexes may gain in stability over time, it is recommended to keep the plate at 4 °C and make repeated measures along 3–4 days (Fig. 2c).
13. After plate reading, results are present in an Excel table were two sequential readings at 620 nm and 665 nm emission wavelengths are performed. The ratio of the fluorescence intensities 665/620 nm (acceptor/donor) enables the calculation of Delta F, which represents the relative energy transfer rate for each sample. Finally, to subtract medium background, prepare triplicate of PBS(1×)-Tween 20 only.

14. Start by setting the loading in an independent experiment. It is preferable that the loading curves remain linear (not reaching a plateau) as oversaturation of the biosensor is likely to induce the loading of a non-specific second layer of protein or peptide that will dissociate during the following baseline step. It is also possible to stop the loading before the plateau appears. Proper loading control consists in the absence of loading of the same protein in its non-biotinylated form and at the same concentration.
15. If possible, set the loadings of the relevant peptide and of the nonrelevant peptide, so they reach the same light deviation.
16. Make a preliminary run to determine the analyte concentration range. Typically, prepare four to five concentration points, in serial log dilutions (dividing concentration by ten at each dilution), starting at ten times the expected Kd. Select the range in which clear association curves are visible while not overspending your sample.
17. Interferometry allows measuring the dissociation constant of a protein complex (Kd), even for the medium-high affinities of signalling modules. The present methodology describes the analysis of the association between a peptide and a protein. This type of complex has a very low affinity, and since the measurement of the Kd requires five association curves of the protein over the peptide, the quantity of protein necessary may be high (up to milligrams). You may however observe the interaction between the peptide and the protein at one single concentration, even if it does not provide a Kd.
18. This methodology can also be used to measure the interaction between the two partner proteins. In that case, peptide α should be replaced by the biotinylated partner of β-arrestin.
19. It is important to appreciate that it may be difficult to visualize the interaction between two partners when their molecular weight is more than 100-fold different. This drawback can be overcome when the smallest of the two proteins is loaded on the biosensor. This is why it is important here to load the peptide on the biosensor and not the protein.

Acknowledgments

This publication was funded with support from the French National Research Agency under the program "Investissements d'avenir" Grant Agreement LabEx MabImprove: ANR-10-LABX-53, ANR (Contract no ANR-2011-1619 01), ANR GPCRnet, MABSILICO, and "ARD2020 Biomédicament" grants from Région Centre (32000593 APR Biomedicament).

References

1. Crepieux P, Poupon A, Langonne-Gallay N et al (2017) A comprehensive view of the β-arrestinome. Front Endocrinol 8:32
2. Kiel C, Verschueren E, Yang J-S et al (2013) Integration of protein abundance and structure data reveals competition in the ErbB signaling network. Sci Signal 6:ra109
3. Kim PM, Lu LJ, Xia Y et al (2006) Relating three-dimensional structures to protein networks provides evolutionary insights. Science 314:1938–1941
4. Kiel C, Vogt A, Campagna A et al (2011) Structural and functional protein network analyses predict novel signaling functions for rhodopsin. Mol Syst Biol 7:551
5. Kar G, Gursoy A, Keskin O (2009) Human cancer protein-protein interaction network: a structural perspective. PLoS Comput Biol 5: e1000601
6. Wang X, Wei X, Thijssen B et al (2012) Three-dimensional reconstruction of protein networks provides insight into human genetic disease. Nat Biotechnol 30:159–164
7. Cunningham BC, Wells JA (1989) High-resolution epitope mapping of hGH-receptor interactions by alanine-scanning mutagenesis. Science 244:1081–1085
8. Forsström B, Axnäs BB, Stengele K-P et al (2014) Proteome-wide epitope mapping of antibodies using ultra-dense peptide arrays. Mol Cell Proteomics 13:1585–1597
9. Hansen CS, Østerbye T, Marcatili P et al (2017) ArrayPitope: automated analysis of amino acid substitutions for peptide microarray-based antibody epitope mapping. PLoS One 12:e0168453
10. Opuni KF, Al-Majdoub M, Yefremova Y et al (2016) Mass spectrometric epitope mapping. Mass Spectrom Rev 9999:1–13
11. Wei H, Mo J, Tao L et al (2014) Hydrogen/deuterium exchange mass spectrometry for probing higher order structure of protein therapeutics: methodology and applications. Drug Discov Today 19:95–102
12. Bourquard T, Landomiel F, Reiter E et al (2015) Unraveling the molecular architecture of a G protein-coupled receptor/β-arrestin/Erk module complex. Sci Rep 5:10760
13. Cassier E, Gallay N, Bourquard T et al (2017) Phosphorylation of β-arrestin2 at Thr383 by MEK underlies β-arrestin-dependent activation of Erk1/2 by GPCRs. Elife 6:e23777
14. Bourquard T, Bernauer J, Azé J et al (2009) Comparing Voronoi and Laguerre tessellations in the protein-protein docking context, presented at the Voronoi diagrams, 2009. ISVD'09. In: Sixth international symposium on Voronoi diagrams
15. Azé J, Bourquard T, Hamel S et al (2011) Using Kendall-τ meta-bagging to improve protein-protein docking predictions. In: Pattern recognition in bioinformatics. Berlin Heidelberg, Springer, pp 284–295
16. Bourquard T, Bernauer J, Azé J et al (2011) A collaborative filtering approach for protein-protein docking scoring functions. PLoS One 6:e18541
17. Berman HM, Westbrook J, Feng Z et al (2000) The Protein Data Bank. Nucleic Acids Res 28:235–242



Chapter 13

Workflow Description to Dynamically Model β-Arrestin Signaling Networks

Romain Yvinec, Mohammed Akli Ayoub, Francesco De Pascali, Pascale Crépieux, Eric Reiter, and Anne Poupon

Abstract

Dynamic models of signaling networks allow the formulation of hypotheses on the topology and kinetic rate laws characterizing a given molecular network, in-depth exploration, and confrontation with kinetic biological data. Despite its standardization, dynamic modeling of signaling networks still requires successive technical steps that need to be carefully performed. Here, we detail these steps by going through the mathematical and statistical framework. We explain how it can be applied to the understanding of β-arrestin-dependent signaling networks. We illustrate our methodology through the modeling of β-arrestin recruitment kinetics at the follicle-stimulating hormone (FSH) receptor supported by in-house bioluminescence resonance energy transfer (BRET) data.

Key words β-Arrestins, Dynamic models, Biochemical reaction network, Parameter identification, Data fitting, Model selection

1 Introduction

β-Arrestins have long been recognized to play a major role in G protein-coupled receptor (GPCR) desensitization and internalization. They are also known to transmit signals of agonist-activated GPCRs to promote G protein-independent signaling [1–3]. β-Arrestin-mediated signaling has been reported to impact gene expression, transcription [4], and translation [5]. β-Arrestins serve as multi-protein scaffolds, connecting many partners [6], defining different pathways that act at different time and spatial scales [7, 8]. It is important to better understand β-arrestin signaling networks since it could lead toward the development of strategies, including the development of biased agonists (e.g., discriminating between G protein-dependent and β-arrestin-dependent signaling), with promising therapeutic implications [8–14].

Mark G. H. Scott and Stéphane A. Laporte (eds.), *Beta-Arrestins: Methods and Protocols*, Methods in Molecular Biology, vol. 1957, https://doi.org/10.1007/978-1-4939-9158-7_13, © Springer Science+Business Media, LLC, part of Springer Nature 2019

The complexity of β-arrestin-mediated cellular regulation motivates the use of mathematical models that take into account its dynamic (*see* **Note 1**). Dynamic biochemical reaction network models, presented in this chapter, allow formulation of hypotheses on molecular networks linked to β-arrestins, by explicitly integrating detailed knowledge on signal transduction. The first impact of such framework is to reveal potential alternatives or conflicting signaling mechanisms that have been hypothesized in the literature. Subsequently, iterative confrontations of model and data facilitate hypotheses rejection or acceptance. Finally, this methodology can be used to predict the behavior of unobserved quantities: concentration of molecules, parameter values, etc. For further information, readers can refer to reviews and papers dealing with applications of GPCR signaling modeling [15–19].

At the very beginning of the modeling pipeline, one has to gather existing biological knowledge from the literature. In light of the available information, and according to the specific biological questions that are being addressed, the modeler decides the level of precision of the dynamic model. Hence, which molecules of a particular signaling sub-network are taken into account and how the reactions between molecules should be represented will drive the choice of a particular mathematical framework. The nature and amount of available data to be confronted with the model outputs are also of primary importance. We would like to emphasize that the use of time series experimental data, which is becoming more and more favored due to the development of bioluminescence resonance energy transfer (BRET) or fluorescence resonance energy transfer (FRET) technologies [20], is clearly a major improvement for quantitative dynamic modeling [17–19]. Using perturbation experiments, which allow the observation of the system under different biological conditions, also clearly improves model selection.

Once a model has been defined, the modeler uses various tools to perform model analysis and numerical simulations, in order to gain knowledge on the behavior of the model outputs but also to assess the impact of the model inputs and parameters (initial concentrations, reaction rates, etc.). Next, using an appropriate statistical description of the data, the modeler performs data fitting, with the aid of optimization algorithms, in order to assess the validity of the model. Parameter identifiability analysis, model selection, and model predictions are major steps that provide key additional insight on the model's robustness and ability to accurately capture biological mechanisms. Of course, iterative model refinements and validation experiments are necessary to cement biological findings. We provide a graphical outline of the workflow in Fig. 1. For specific applications of various modeling strategies, readers can refer to useful published reviews [15, 21].

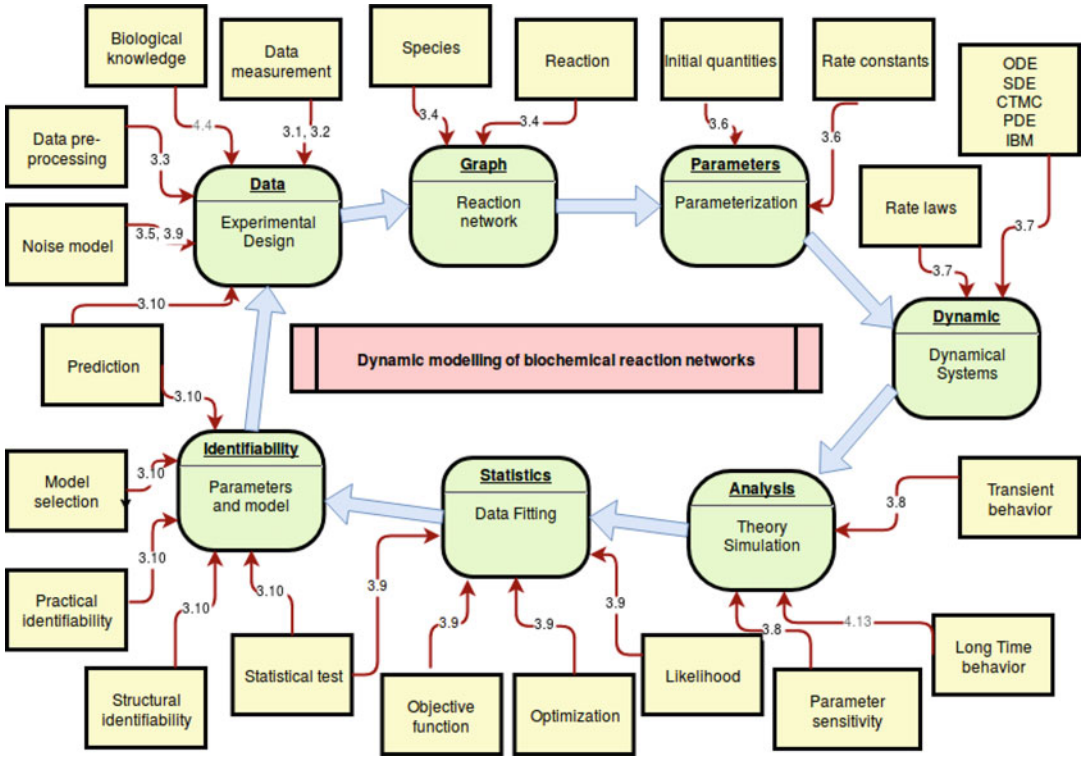


Fig. 1 Main steps of dynamical modeling of biochemical reaction networks. On each red arrow, we indicate the corresponding section in the main text. Note that this diagram is not exhaustive, and more interactions between each step should be represented (in particular, as we explain in the main text, if the data fitting is not accurate enough, one needs to come back to either experimental design, reaction network construction, or parameterization)

2 Materials

2.1 Software Packages

We list below a few standard software systems we routinely use while modeling dynamic reaction systems.

1. To represent a reaction network diagram, we use Cell Designer [22] running on a standard laptop. *See* example in Fig. 4.
2. To run model simulations, explore model behavior, and run some data fitting optimization, we use COPASI [23] running on a standard laptop.
3. To perform extensive data fitting optimizations and parameter identifiability identification analysis, we use Data2Dynamics (or D2D) (*see* [24]), running on a standard laptop, with MATLAB (R2010 or newer). The results on our example presented in this chapter were obtained with D2D; *see* Figs. 5, 6, and 7.

4. To perform extensive data fitting optimizations using global optimization algorithms, we use an in-house software HYPE (in preparation).

2.2 Plasmids

1. pcDNA3.1-hFSHR-Rluc8 (from A. Hanyaloglu, Imperial College, London, UK).
2. pcDNA3.1-yPET-β-arrestin 2 (from M.G. Scott, Institut Cochin, Paris, France).

2.3 Cell Culture and Transfection

1. Human embryonic kidney (HEK293-FT) cells (Thermo Fisher Scientific, Massachusetts, USA).
2. Cell culture dishes (Corning Life Sciences, Tewksbury, MA, USA).
3. DMEM supplemented with 10% v/v fetal bovine serum, 4.5 g/l glucose, 100 U/ml penicillin, 0.1 mg/ml streptomycin, and 1 mM glutamine.
4. Trypsin-EDTA solution.
5. Phosphate-buffered saline 1× without calcium and without magnesium supplemented with 10 mM HEPES.
6. Transfection reagent: Metafectene PRO (Biontex, Munchen, Germany).
7. Multichannel pipette—8 and 12 channels (Thermo Fisher Scientific, Massachusetts, USA).

2.4 BRET Measurements

1. 96-Well white microplates, flat-bottom, high binding, sterile (Greiner Bio-One, Courtaboeuf, France).
2. Coelenterazine h—250 μg (Interchim, Montluçon, France).
3. Recombinant human follicle-stimulating hormone (hFSH) (FollMerck-Serono, Darmstadt, Germany).
4. Mithras^2 LB 943 plate reader (Berthold Technologies GmbH and Co. Wildbad, Germany) for BRET measurements.

3 Methods

The following modeling methods are illustrated with kinetic data obtained from cells displaying β-arrestin recruitment to the human follicle-stimulating hormone receptor (hFSHR) stimulated with seven different doses of hFSH. To assess this in live cells and in real time, we used BRET technology as previously reported [12, 25] and described below.

3.1 Cell Transfection

1. HEK293 cells are grown until 50% of confluence (10×10^6 cells) in complete medium (DMEM supplemented with 10% v/v fetal bovine serum, 4.5 g/l glucose, 100 U/ml penicillin,

0.1 mg/ml streptomycin, and 1 mM glutamine) before their transient transfection with the plasmids encoding the different BRET sensors using Metafectene PRO following the manufacturer's protocol.

2. 5 μg of plasmid encoding FSHR-Rluc8 used as BRET donor and 5 μg of plasmid encoding yPET-β-arrestin 2 used as BRET acceptor are mixed and resuspended in 1 ml of serum-free DMEM.
3. In parallel 50 μl of Metafectene PRO are resuspended in 1 ml of serum-free DMEM.
4. The two mixes (plasmids and Metafectene PRO) are first pre-incubated separately for 5 min at room temperature.
5. Then the plasmid solution is mixed with Metafectene PRO mix, and the final solution (~2 ml) is incubated for 20 min at room temperature.
6. During the incubation of the transfection solution, cells are washed twice with PBS 1×, detached with 3 ml of trypsin-EDTA, and resuspended to 10×10^6 cells in a final volume of 18 ml of the complete medium.
7. After 20 min of incubation, the transfection solution (~2 ml) is mixed with 18 ml of cells in complete medium. This allows filling the whole 96-well plate with transfected cells using 200 μl per well.
8. Finally, 200 μl of plasmids + cells mix is distributed and seeded into each well of 96-well plate corresponding to 10^5 cells/well and is cultured for 48 h at 37 °C and 5% CO_2 before BRET assays.

3.2 BRET Measurements

1. Forty-eight hours after transfection, cells are first washed with 100 μl/well of PBS 1×.
2. Cells are then resuspended in 60 μl/well of PBS-HEPES 10 mM.
3. hFSH is prepared 5× in PBS-HEPES 10 mM at different doses for final concentrations of 0.0128, 0.064, 0.32, 1.6, 8, 40, and 200 nM.
4. Coelenterazine h (stock solution 1 mM) is first prepared 5× (25 μM) in PBS-HEPES 10 mM and kept on ice and protected from light.
5. For BRET measurements, to each 60 μl/well of cells in PBS-HEPES 10 mM, 20 μl/well coelenterazine h 5× (5 μM final) is added, followed by injection of 20 μl/well of either PBS (vehicle-treated cells) or FSH (FSH-treated cells) prepared 5× in PBS-HEPES 10 mM at different doses as mentioned above.

6. Importantly, in order to avoid any kinetic delay between the different wells, a single well for each vehicle-treated and FSH-treated cells is read at a time, and this is performed in independent quadriplicates.

3.3 Data Pre-processing

1. The raw data are obtained as light emission at both 480 ± 20 nm and 530 ± 25 nm for each well including vehicle-treated (control) and FSH-treated cells. The Mikrowin 2010 software of the Mithras^2 LB 943 plate reader automatically calculates the conventional BRET ratio of 530 ± 25 emission over 480 ± 20 emission for each well and at every reading time point.
2. Since our focus is on FSH-promoted β-arrestin 2 recruitment, the data are then transformed to "Induced_BRET" values by subtracting the 530/480 ratio of vehicle-treated cells from its corresponding ratio of FSH-treated cells. This subtraction is done at each reading time point, as described previously [20, 25, 26]. Our "Induced_BRET" data are shown in Fig. 2.
3. To remove any replicate bias effect, we normalize them by a constant shift value so that all replicates for a given dose are as close as possible to each other (*see* **Note 2**). In Fig. 3, we show the final data used in subsequent modeling steps.

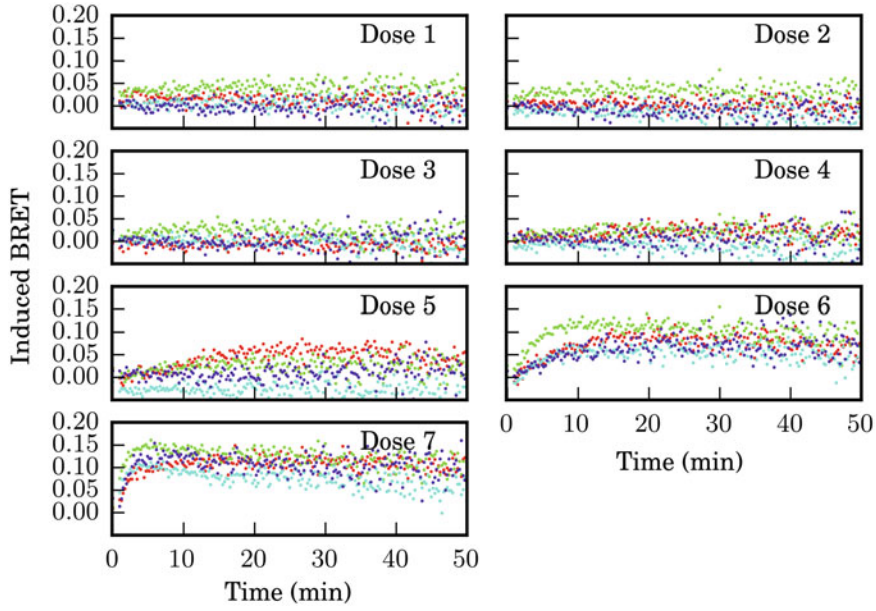


Fig. 2 Induced_BRET measurements for the recruitment of β-arrestin 2 at the FSHR after injection of a dose of FSH. Each of the four replicates, for the seven FSH doses, is plotted against time measurement (from $t = 0$ to $t = 50$). Dose 1 = 0.0128 nM; dose 2 = 0.064 nM; dose 3 = 0.32 nM; dose 4 = 1.6 nM; dose 5 = 8 nM; dose 6 = 40 nM; dose 7 = 200 nM

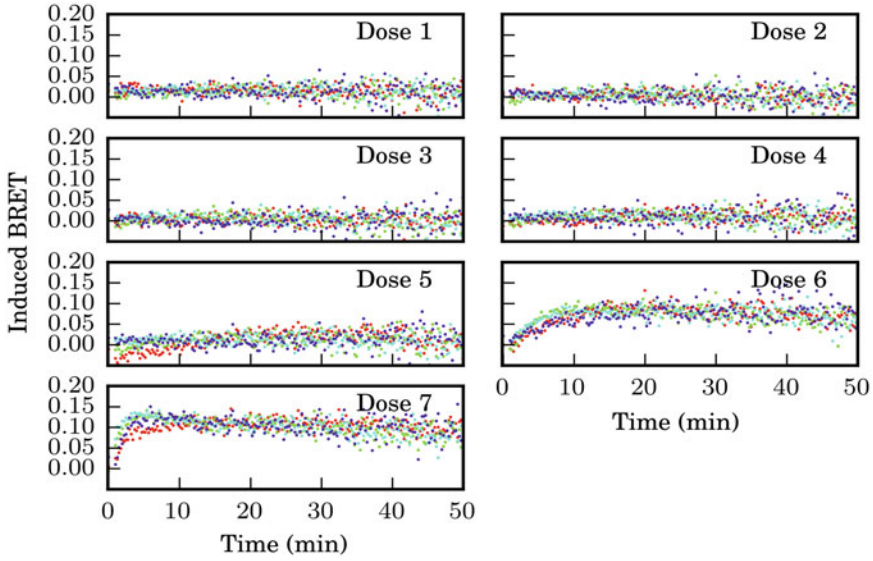


Fig. 3 Normalized Induced_BRET measurements for the recruitment of β-arrestin 2 at the FSHR after injection of a dose of FSH. The same as Fig. 2 but with normalization within replicates to cancel any replicate bias (*see* Subheading 3.3 and **Note 2**)

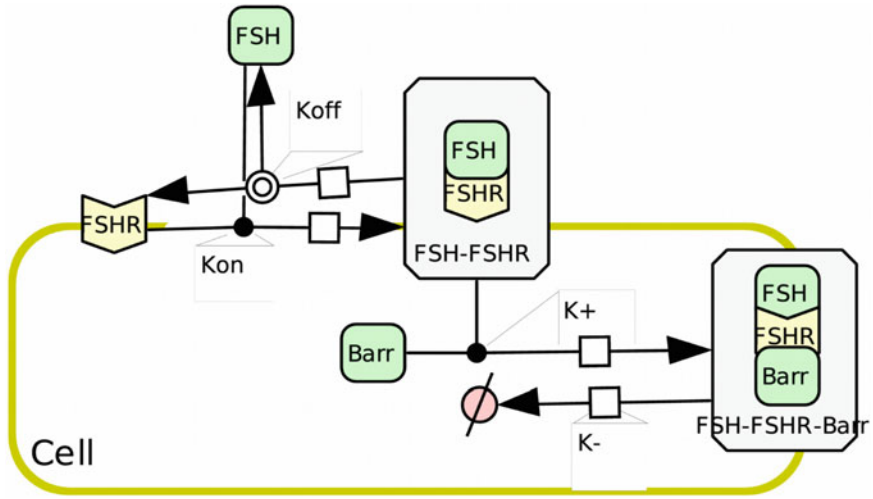


Fig. 4 Reaction network of a model for β-arrestin recruitment at the FSHR. We include five species, namely, FSH, FSHR, FSH-FSHR, β-arrestin, FSH-FSHR-β-arrestin, and four reactions (FSH + FSHR → [FSH-FSHR], [FSH-FSHR] → FSH + FSHR, β-arrestin + [FSH-FSHR] → [FSH-FSHR-β-arrestin], [FSH-FSHR-β-arrestin] → ∅) with rate constants, respectively, k_{on}, k_{off}, k^{+}, and k^{-}

3.4 Species and Reaction List

1. Create and visualize a reaction network model using diagram editor software such as Cell Designer (*see* Fig. 4). The following two steps are the key elements of a reaction network model (*see* **Notes 3** and **4**) and may be performed by successive iterations while comparing the model to the data (*see* Subheading

3.9). Competing hypotheses can be formulated at this step by dealing in parallel with different reaction network models (*see* **Note 5**).

2. Define a list of molecules or species of interest to include in the model. Input variables, (partially or completely) controlled by the experimentalist, and output variables, measured by the experimentalist, should obviously be included. Intermediate molecules (enzymes, complex assemblies, etc.) are taken into account according to the specific biological questions addressed (*see* **Note 6**). In our example, we choose a list composed of five distinct species, representing various states of three molecules (FSH, FSHR, [FSH − FSHR], β-arrestin, [FSH-FSHR-β-arrestin]). In the modeling context, this list is known as the state variables.
3. Define a list of reactions between the species. These reactions should exactly define the stoichiometry of each species in each reaction. In our example, we include four reactions:

$$\mathrm{FSH} + \mathrm{FSHR} \rightarrow [\mathrm{FSH} - \mathrm{FSHR}]$$

$$[\mathrm{FSH} - \mathrm{FSHR}] \rightarrow \mathrm{FSH} + \mathrm{FSHR}$$

$$\beta - \mathrm{arrestin} + [\mathrm{FSH} - \mathrm{FSHR}] \rightarrow [\mathrm{FSH} - \mathrm{FSHR} - \beta - \mathrm{arrestin}]$$

$$[\mathrm{FSH} - \mathrm{FSHR} - \beta - \mathrm{arrestin}] \rightarrow \emptyset$$

Hence, we have chosen to ignore GRK-mediated phosphorylation steps, and the internalization process is only represented as a sink reaction for the [FSH-FSHR-β-arrestin] complex (*see* **Note 7**).

3.5 Experimental Conditions and Observed Variables

1. Enumerate the experimental conditions and the measured data that will be compared to the kinetic model. In our example, we have seven conditions, corresponding to seven different doses for the input concentrations of FSH. In each of these experimental conditions, we measured a BRET signal, which is transformed by a pre-processing step as an Induced_BRET signal (*see* Subheadings 3.2 and 3.3).
2. Define the functions linking species of the model and measured data, including possible noise terms, coming from error measurements (*see* Subheading 3.9 and **Note 3**). In our example, we choose the relation

$$\mathrm{Induced\_BRET} = kf \times [\mathrm{FSH} - \mathrm{FSHR} - \beta - \mathrm{arrestin}] + \varepsilon,$$

where ε is the noise, defined as a Gaussian variable of mean 0 and unknown variance σ^2, and kf is an unknown proportional constant.

3.6 Parameter List

1. Once the reaction network and measured variables have been fully specified, we define the complete parameter set used in the model. For this, we assign to each state variable (i.e., a species

of the reaction network) a parameter that specifies its initial quantity (its value at the starting experimental time, e.g., $t = 0$). The initial concentrations are denoted in our example by

$$(\text{Init\_FSH}, \text{Init\_FSHR}, \text{Init\_}[\text{FSH} - \text{FSHR}], \text{Init\_}\beta - \text{Arrestin}, \text{Init\_}[\text{FSH} - \text{FSHR} - \beta - \text{Arrestin}]).$$

Similarly, we assign to each reaction of the network a parameter that specifies its rate constant (*see* Subheading 3.7). In our example, we denote the rate constants by k_{on}, k_{off}, k^+, and k^- (*see* Fig. 4).

2. For each experimental condition, one kinetic model (together with its observed variables) is constructed from the reaction network, its parameters, and the data/model relationship. Hence, each model has a set of initial quantities for the dynamical variables, a set of reaction rates for the reactions, and a set of measurement parameters for the observed variables. Note that in our example, we use the same reaction network for our seven experimental conditions, but it does not necessarily need to be the case in more general settings. Each of our 7 models has 11 parameters:

   Five initial quantities: (Init_FSH, Init_FSHR, Init_[FSH-FSHR], Init_β-Arrestin, Init_[FSH-FSHR-β-Arrestin])$_{\text{condition } i}$, $i = 1 \ldots 7$.

   Four kinetic rates: $(k_{on}, k_{off}, k^+, k^-)_{\text{condition } i}$, $i = 1 \ldots 7$.

   Two measurement parameters: $(kf, \sigma^2)_{\text{condition } i}$, $i = 1 \ldots 7$.

3. According to the experimental conditions, specify which parameters should have common values between any two conditions. The modeler thus may take into account possible perturbation experiments, where, for instance, some protein expression has been externally modified by the experimentalist (silencing RNA, overexpression, chemical inhibitor; *see* **Note 8**). In our example, because we deal with different doses of FSH, we take different values for the initial concentration of FSH for each condition, (Init_FSH) $_{\text{condition } i}$, but we assume that all remaining initial quantity parameters (Init_[FSH-FSHR], Init_[FSH-FSHR-β-arrestin], Init_FSHR, and Init_β-arrestin), as well as all rate constants (k_{on}, k_{off}, k^+, k^-), and all measurement parameters (kf, σ^2) have common values across conditions (because the same transfection protocol was used for all experiments; *see* Subheading 3.1).

4. In each experimental condition, specify whether the initial quantity for each state variable should be 0, a given known value, or a free parameter (i.e., an unknown value that will be found during the data fitting procedure at Subheading 3.9; *see*

Note 9). In our example, we use the known input dose injected by the experimentalist for the initial quantity of FSH, $(\text{Init\_FSH})_{\text{condition } i}$, and we consider that [FSH-FSHR] and [FSH-FSHR-β-arrestin] are not present initially, so that Init_[FSH-FSHR] = 0 and Init_[FSH-FSHR-β-arrestin] = 0 (we do not take into account any constitutive activity). Finally, the last two initial quantities Init_FSHR and Init_β-arrestin are free parameters and have identical values across the seven experiments.

5. Repeat the previous step for rate constants and measurement parameters. In our example, the rate constants (k_{on}, k_{off}, k^+, k^-) and measurement parameters (kf, σ^2) are free parameters and have identical values in the seven experiments (*see* **Note 10**).

3.7 Dynamic Rule

1. At this step, the modeler must choose a mathematical framework to simulate the time evolution of the molecules in the reaction network. There are essentially three choices. These choices must be made in compliance with the type of measured data. First, the modeler chooses to use discrete numbers or continuous concentrations to represent molecule abundance. Second, one chooses a stochastic or deterministic description (*see* **Note 3**). Third, the modeler specifies whether the spatial environment should be taken into account and, in this case, what mechanisms govern species displacements (Brownian motion in a continuous space, transitions between discrete compartments, etc.). No spatial effect is taken into account when one assumes that the reaction network takes place in a single well-mixed compartment (*see* **Note 11**). Also, note that when the order of magnitude of the number of molecules is believed to be large, it is advised to adopt a continuous deterministic formulation rather than a discrete stochastic one, for computational efficiency [27] (it is also mathematically justified).
2. The above three choices lead the modeler to adopt one of these mathematical descriptions: petri nets, continuous time Markov chain (CTMC), stochastic differential equation (SDE), individual-based model (IBM), partial differential equation (PDE, reaction-diffusion equations), or ordinary differential equations (ODE). The reader can refer to [15, 21] for further details. Here, for simplicity, and because it is the most common approach justified in standard cell culture experiments, we adopt the formalism of ordinary differential equations.
3. The modeler must finally choose how to represent reaction rate laws. In the ordinary differential equation context, we need to associate to each reaction a function that defines its velocity. For any reaction, its rate law is a function of the concentration of the reactants. The rate laws give a nonnegative number

representing the speed of that reaction, which will impact the variation of both reactants and products. The higher this rate is, the faster the reactants are consumed and the products generated. The gold standard choice for the rate laws is given by the law of mass action, which says that the rate of a reaction is proportional to the concentration of its reactants to the power of their stoichiometry (*see* **Note 12**). The proportional constant is the rate constant we assigned to each reaction in Subheading 3.6.

3.8 Model Analysis and Simulation

1. As the reader may have noticed, dynamical models of biochemical reaction networks have a clear well-defined mathematical structure, deriving essentially from the species and reaction lists or topological model (*see* **Note 3**). As such, in practice, the modeler does not need to explicitly write down the equations governing the time evolution, neither to code a numerical scheme to simulate these equations. Indeed, most software (*see* Subheading 2.1) in this field requires only as input the ingredients of the previous Subheadings 3.4, 3.5, 3.6, and 3.7.
2. According to the focus of the model and its objective, a first step to analyze it is given by the study of the long-time behavior: steady-state analysis, stability, and bifurcation. The objective of such theoretical analysis is to be able to predict, according to the parameter values, whether the molecule abundances will converge toward steady values as time goes to infinity, or will disappear or keep increasing, or continuously oscillate. It is out of the scope of this methodological chapter to detail this theory (*see* **Note 13**).
3. When we are interested in transient behaviors, or when the reaction network is too complex to perform theoretical analysis, one needs to perform numerical simulation. The modeler thus needs to identify a given set of parameters (initial quantities, rate constants, measurement parameters) to run a time course of species abundance. Many software packages allow such numerical exploration; we can refer, for instance, to Cell Designer or COPASI (*see* Subheading 2.1; *see* also **Note 14**).
4. A particularly useful way to numerically explore a model is to try to understand its parameter sensitivity. The objective is to explore the effect of changing a given parameter value on the observable variables. This notion is known as local parameter sensitivity, and it is defined mathematically as the first-order derivative of the observable variables with respect to the parameters. Although it is relatively easy to calculate (it can be calculated together with the solution of the ODEs), it has the disadvantage to be a local notion and hence will depend on the particular parameter set used, which is, at this step, still unknown! COPASI allows a systematic exploration of local

parameter sensitivity. More sophisticated tools exist to define a notion of global sensitivity and rely on sampling parameter sets on a given range of values [28].

3.9 Statistical Model and Data Fitting

1. To define a statistical procedure for data fitting, the first step is to specify an observation model (or measurement model, *see* **Note 3**). The most common choice is an additive Gaussian noise of mean zero and constant variance, which are well suited, for instance, to the analysis of fluorescence measurement. We have used this choice, as already specified in the data/model relationship in Subheading 3.5. In some applications, multiplicative log-normal noise may be a better choice (if the noise is asymmetric or higher for higher measured values). When we suspect the existence of outliers, Laplace distributed noise is shown to be robust [29]. For other statistical models adapted to stochastic or PDE models, we refer to [30].
2. When the noise model has been defined, an objective function is defined through the notion of Likelihood (L): a function of the parameter that gives the conditional probability of observing the data, given the value of the model parameters. This conditional probability is directly linked to the choice of the error model defined at the previous step. In the statistical framework, we call the "frequentist approach" the process of finding the parameter sets that maximize the likelihood (*see* **Note 15**). However, for practical computing performance, one usually prefers to minimize $-\log(L)$. For instance, the additive Gaussian noise model leads to minimize the standard weighted sum of squares. For more complex objective functions, we refer again to [29].
3. We then use an optimization algorithm to find possible parameter sets that minimize the objective function. Unfortunately, in concrete applications, the objective function is a nonlinear and non-convex function, for which there is no gold standard method to find the global minimum. There are actually a plethora of choices to perform such tasks. We find that multi-start deterministic optimization based on random initial parameter values and gradient descent-like methods, like D2D [24], performs well. We also use global optimization methods combining two well-established techniques, namely genetic algorithm and CMA-ES (HYPE, in preparation). *See* [31, 32] for other popular choices.
4. All numerical methods require initial parameter values to perform the optimization procedure or a range to search in (or an initial probability distribution in the Bayesian context; *see* **Note 15**). Thus, the modeler specifies such values using order of magnitudes that are compatible with the biological knowledge. Conservative choices will look for sufficiently large parameter

ranges (to make sure to find an optimal parameter set, at the price of increasing computational cost). In our example, we used wide initial ranges of 10–20 logs (*see* **Note 3**).

5. Once enough optimization routines have been performed to presumably reach the optimal solution (*see* **Note 16**), the modeler must decide whether the solution is acceptable or if the model should be modified to yield a better fit (and thus potentially back to Subheading 3.4). To make this decision, we use qualitative and quantitative information. Of course, visual inspection of the best fit is of importance. Final value of the objective function, if properly normalized (HYPE, in preparation), can be used, as well as convergence curves [24]. The modeler may also use a residual test to assess the validity of both the kinetic model and the error model. Using a chi-squared or Kolmogorov-Smirnov test, we may test the adequacy of the difference between the data to the model with the probability distribution used for the error model. Finally, goodness of fit criteria may be used to assess for lack-of-fit or over-fitting.

   In our example, we show the best fit together with residual test in Figs. 5 and 6, respectively. As demonstrated by Fig. 5, the model provides a satisfactory fit for the higher doses. The lower doses show a moderate discrepancy between model and data, as confirmed by residual plots and Kolmogorov-Smirnov

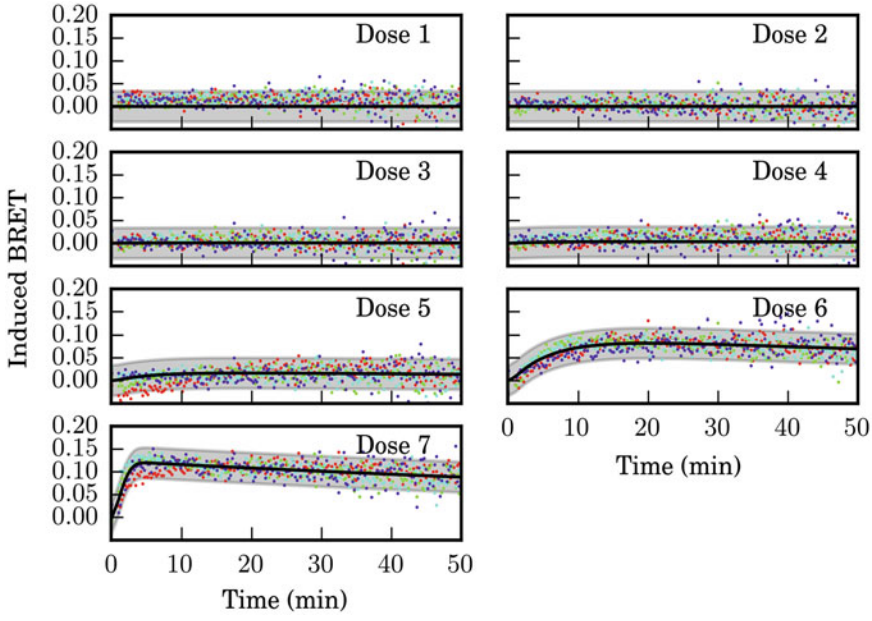


Fig. 5 Data fitting of the Induced_BRET. The black line plots the deterministic dynamic model (*see* reaction network in Fig. 4), and the gray-shaded area corresponds to the error measurement model ($\pm 1.96\sigma$). The color-dotted points are the normalized Induced_BRET measurements (the same as Fig. 3)

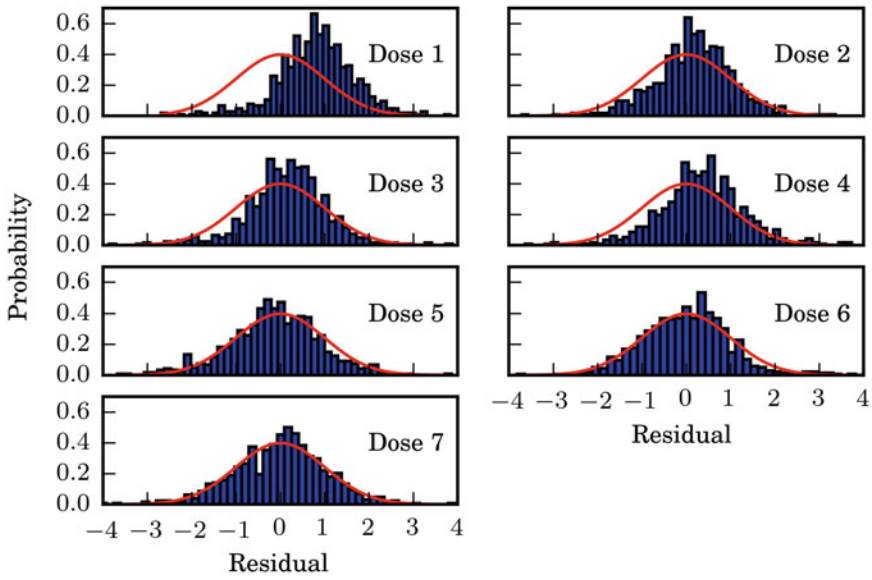


Fig. 6 Histograms of the residuals, obtained from the data fitting of Fig. 5. The *p*-values obtained from a Kolmogorov-Smirnov test (with mean 0 and variance 1 normal distribution) are, respectively, $<1 \times 10^{-16}$, 7.3×10^{-15}, 3.2×10^{-12}, $<1 \times 10^{-16}$, 0.006, 0.1, and 0.12 (for doses 1–7). Thus, normality test is accepted for the higher doses 6 and 7, and the test confirmed the visual shift of the residual for the lower doses

test (*see* Fig. 6). This bias could be removed by taking into account basal activity, for instance.

3.10 Parameter Identifiability: Model Selection

1. Theoretical (or structural) identifiability analysis aims at finding whether the optimization given by the data-fitting problem, assuming perfect time-resolved data and no data error measurement, has a unique solution or not. A model is not structurally identifiable if two distinct parameter sets give exactly the same observable values. For simple to moderately complex models, several methods exist to assess structural (non-) identifiability [33–35]. It is advised to perform such analysis before running computationally expensive numerical optimization procedures, as structural identifiability analysis may reveal over-parameterization (*see* **Note 3**) and can greatly simplify the numerical search. In such case, re-parameterization has to be considered (*see* **Note 16**). In our example, the structural identifiability analysis did not identify any over-parameterization. For practical efficiency, we used time and concentration adimentionalization (*see* **Note 3**) in order to make most of the unknown parameters dimensionless. We used Init_FSHR and k^- as reference for concentration and time units, respectively, and defined all other concentrations and kinetic rates relatively to both Init_FSHR and k-parameters.

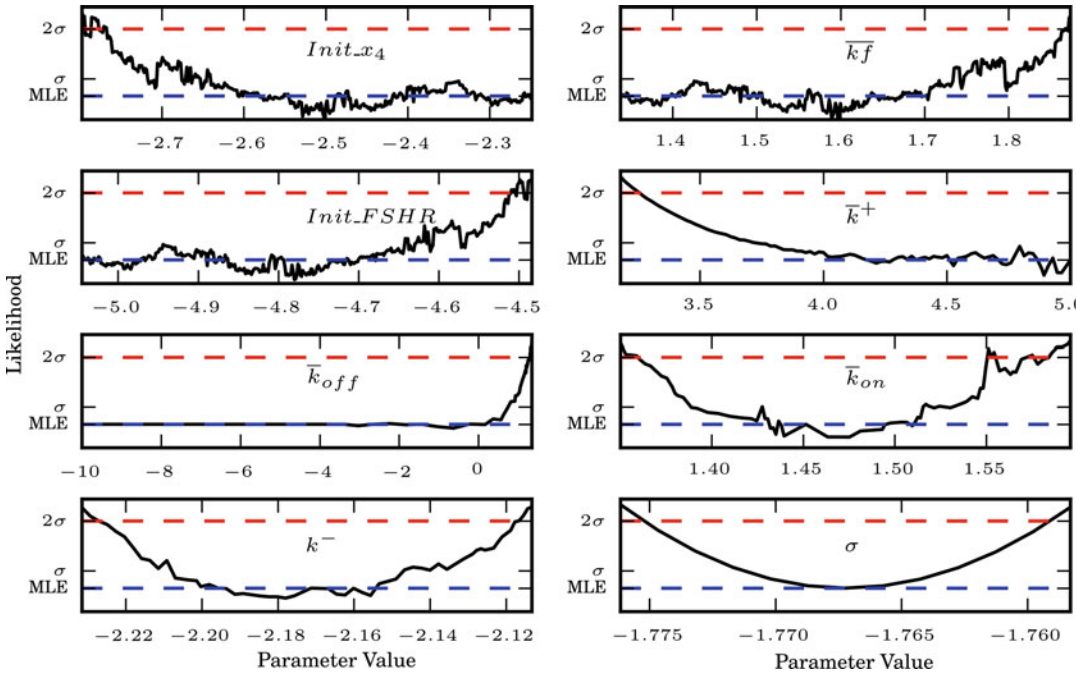


Fig. 7 Profile likelihood estimates for each parameter. In each subplot, we show the likelihood value around the optimized parameter set (black curve), the optimal likelihood value obtained during the optimization (dashed blue line), and the likelihood threshold value giving the 95% confidence interval for each parameter. Parameter values are in log scale

2. A complementary useful approach is given by the practical identifiability. Based on local evaluation of the objective function, it allows to give confidence interval to the best parameter values (if it is identifiable) or to shed light on non-identifiability, given the data, by revealing parameter combination that leads to similar objective function value. Of importance, this method is not restricted to parameter values but can be extended to any model output [36–38]. In our example, practical identifiability analysis performed with D2D revealed that most parameters are not practically identifiable (Fig. 7), suggesting that more data are needed (more doses or different measurements like number of free receptors or number of complex ligand receptors, for instance).
3. Often, the modeler is confronted to several alternative hypotheses for the biochemical reaction networks to represent a given set of data, either due to several competing biological hypotheses or in the course of the iterative search of the model that best fits the data. Again, several criteria may be used to choose one or another model. A useful standard statistical test to choose the appropriate number of parameters in nested models is given by the likelihood ratio test. Other quantities such as

AIC (Akaike information criterion) or BIC (Bayesian information criterion) are often used to perform model selection [39].

4. Finally, once a satisfactory model has been selected, the modeler may use non-observable variables or different simulated experimental conditions to perform model predictions. To confirm these predictions, additional experiments are performed. In the case of inadequacy with the model predictions, the iterative confrontation of models to data continues (again, back to Subheading 3.4).

4 Notes

1. We emphasize that this chapter is concerned with dynamic models, which have to be clearly distinguished with equilibrium models widely used in pharmacology [40]. Dynamic models assess time-response relationships, while equilibrium models in pharmacology assess dose-response relationships.
2. Data processing: We use a simple linear model as follows. Denote by Induced_BRET(t,j) the induced BRET signal measured at time t and replicate j, we assume that Induced_BRET(t,j) = $N(m(t,j), \eta^2)$, where the mean is decomposed into two effects: $m(t,j) = m\_t + s\_j$. Thus, we model the induced BRET signal as a Gaussian variable of mean $m(t,j)$ and constant variance η^2. The mean of replicate j is given by a time-dependent mean, shared by all four replicates, plus a replicate-dependent shift value given by s_j. Coefficients η^2, m_t, and s_j are estimated using the standard lm function in *R*. Finally, to normalize the Induced_BRET signal, we subtract from each replicate its shift value s_j.
3. Additional mathematical notes are provided for the interested reader, at the weblink http://yvinec.perso.math.cnrs.fr/Publi/RY_17_betarrestin_review_math_notes.pdf
4. Reaction network construction: Manual curation of the literature and biological knowledge should be taken into account in order to decide the relevance of intermediate partner molecules. Biomodel databases and pathway repositories may help to guide the modeler by starting from existing models. For a complete list, *see* Pathguide (http://www.pathguide.org). To look for protein interactions, good references to start with include BioGRID (https://thebiogrid.org/), STRING (https://string-db.org/), HIPPIE (http://cbdm-01.zdv.uni-mainz.de/~mschaefer/hippie/), or WikiPathways (http://www.wikipathways.org/index.php/WikiPathways). To look for existing models, *see*, for instance, Biomodels (https://www.ebi.ac.uk/biomodels-main/). Note that SBML (http://

sbml.org/Main_Page) is a standard language to share signaling network models.

5. We would like to emphasize the differences between an interaction or influence graph and a reaction network. In an influence graph, two molecules are linked if they interact with each other, but the mechanism is not specified (it could be a catalysis, or a complex formation, or other indirect mechanisms, etc.), in contrary to a reaction network. Often, one has a reasonable idea of the interaction graph, but several alternative reaction network models can be derived from it.
6. We designed an automatic procedure to complete existing signaling network models that could not explain the given observations [17, 41]. Structural modeling of multi-protein complex assemblies (docking) can also help in identifying partners and specific mechanisms [42, 43].
7. The use of the symbol $\emptyset$ does not necessarily mean that the species undergo a kind of degradation reaction but rather that we do not wish to track in detail which subsequent reaction the species [FSH-FSHR-β-arrestin] undergoes. In a similar manner, spontaneous formation of a species A, out of an environment not modeled in detail, will be represented by a reaction $\emptyset \rightarrow A$.

   Also, it is possible to model a reaction where the reactant is not consumed by also putting the species in the product side. For instance, transcription/translation processes are often modeled via reactions of the form DNA $\rightarrow$ DNA + RNA, RNA $\rightarrow$ RNA + Protein. A catalysis reaction may also be represented in this manner.
8. The advantage of using perturbation experiments is both to challenge the model (using a different range of behavior) and to increase the amount of data while not excessively increasing the number of parameters. We emphasize that the precise representation of the effect of a perturbation experiment is a modeling choice. As a rule of thumb, we choose to consider that all initial molecule concentrations may vary between two conditions when silencing RNA or overexpression of a given molecule is used, because such modification usually occurs before the actual start of the experiment (a given external input stimulus is applied at time $t = 0$, for instance). In contrary, when a specific chemical inhibitor is used, we modify only the initial concentration of its target and consider that all other initial concentrations are not affected and thus remain the same. When the reaction rate is believed to be affected by a perturbation experiment (for instance, if some enzyme not specifically modeled are shut down or overexpressed), we

choose to modify the reaction rate by an extra multiplicative factor compared to the control experiment.

9. Some initial quantities can also be fixed using an equilibrium hypothesis. Depending on the experimental protocol, before the experiment actually starts (time of input stimulus, for instance), we may consider that the variables are in equilibrium between each other. In such a case, initial quantity parameters can be expressed as a function of rate constants and other known initial quantities. For example, assuming that no FSH is present prior to injection by the experimentalist, this implies in our setting that Init_[FSH-FSHR] and Init_[FSH-FSHR-β-arrestin] both equal zero.
10. For complicated experimental design, we advise the use of a graphical network representation for each experimental condition, annotated by the particular parameter set used for this condition.
11. The single well-mixed compartment assumption of either continuous time Markov chain or ordinary differential equation formalism is clearly an approximation for live cell experiments. This approximation is often accepted in applications and can be mathematically justified through homogenization techniques [44].
12. Other possible choices not discussed here are given by Michaelis-Menten or Hill kinetics (which need more than one parameter per reaction but usually fewer species and reactions; *see* [45]).
13. Exploiting the structure of biochemical reaction networks, a theory that goes back to the seminal works of [46–48] allows to derive sufficient conditions on the reaction network structure to guarantee specific long-time behavior, irrespectively of its parameter values. This theory has recently received lots of attention; *see* [49–53]. Of practical importance for the modeler, one may, for instance, automatically check whether a reaction network satisfies some key properties to assess its long-time behavior. *See*, for instance, [54, 55].
14. For more theoretical information on the numerical simulations, the reader can refer to [27, 28].
15. Alternative approaches not discussed here: the Bayesian approach search for the complete probability distribution of the parameters, according to the likelihood and prior information on parameter values. *See* [56] for more details.
16. There are many tricks in parameter estimation that are mostly dictated by computing performance and numerical robustness. (a) It is often advised to adimentionalize the model. By doing so, only a few parameters carry physical units (mol, s, etc.),

while the remaining ones are defined as relative values and do not carry any units. (b) In top of adimentionalization, re-parameterization can occasionally reveal some identifiable parameter combinations and is thus worth considering. (c) Looking for parameter values in log scale allows the exploration of a larger state space in a computationally efficient manner and is more adapted to biological data. (d) Deciding when to stop a numerical search for a given model and a given parameterization is also nontrivial. Standard stopping criteria include the number of numerical evaluations of the objective function, the objective function value, the relative changes of the objective function between successive steps, and/or the relative changes of the parameters between successive steps.

References

1. Reiter E, Lefkowitz RJ (2006) GRKs and β-Arrestins: roles in receptor silencing, trafficking and signaling. Trends Endocrinol Metab 17(4):159–165
2. DeWire SM, Ahn S, Lefkowitz RJ, Shenoy SK (2007) β-Arrestins and cell signaling. Annu Rev Physiol 69(1):483–510
3. DeFea K (2008) β-Arrestins and Heterotrimeric G-proteins: collaborators and competitors in signal transduction. Br J Pharmacol 153 (S1):S298–S309
4. Ma L, Pei G (2007) β-Arrestin signaling and regulation of transcription. J Cell Sci 120 (2):213–218
5. Musnier A, Blanchot B, Reiter E, Crépieux P (2010) GPCR signalling to the translation machinery. Cell Signal 22(5):707–716
6. Crépieux P, Poupon A, Langonné-Gallay N, Reiter E, Delgado J, Schaefer MH, Bourquard T, Serrano L, Kiel C (2017) A comprehensive view of the β-Arrestinome. Front Endocrinol 8:32
7. Lohse MJ, Hofmann KP (2015) Spatial and temporal aspects of signaling by G-protein coupled receptors. Mol Pharmacol 88 (3):572–578
8. Reiter E, Ayoub MA, Pellissier LP, Landomiel F, Musnier A, Tréfier A, Gandia J, De Pascali F, Tahir S, Yvinec R, Bruneau G, Poupon A, Crépieux P (2017) β-Arrestin Signalling and bias in hormone-responsive GPCRs. Mol Cell Endocrinol 449:28–41
9. Kenakin T (2014) Quantifying biased β-Arrestin signaling. Handb Exp Pharmacol 219:57–83
10. Evron T, Peterson SM, Urs NM, Bai Y, Rochelle LK, Caron MG, Barak LS (2014) G protein and β-Arrestin signaling bias at the ghrelin receptor. J Biol Chem 289 (48):33442–33455
11. Flavie L, Gallay N, Jégot G, Tranchant T, Durand G, Bourquard T, Crépieux P, Poupon A, Reiter E (2013) Biased signalling in follicle stimulating hormone action. Mol Cell Endocrinol 382(1):452–459
12. Ayoub MA, Yvinec R, Jégot G, Dias JA, Poli SM, Poupon A, Crépieux P, Reiter E (2016) Profiling of FSHR negative allosteric modulators on LH/CGR reveals biased antagonism with implications in Steroidogenesis. Mol Cell Endocrinol 436:10–22
13. Riccetti L, Yvinec R, Klett D, Gallay N, Combarnous Y, Reiter E, Simoni M, Casarini L, Ayoub MA (2017) Human luteinizing hormone and chorionic gonadotropin display biased Agonism at the LH and LH/CG receptors. Sci Rep 7(1):940
14. Reiter E, Ahn S, Shukla AK, Lefkowitz RJ (2012) Molecular mechanism of β-Arrestin-biased Agonism at seven-Transmembrane receptors. Annu Rev Pharmacol Toxicol 52 (1):179–197
15. Linderman JJ (2009) Modeling of G-protein-coupled receptor signaling pathways. J Biol Chem 284(9):5427–5431
16. Heitzler D, Crépieux P, Poupon A, Clément F, Fages F, Reiter E (2009) Towards a systems biology approach of G protein-coupled receptor signalling: challenges and expectations. C R Biol 332(11):947–957
17. Poupon A, Reiter E (2014) Computational models to decipher cell-signaling pathways. In: Cellular endocrinology in health and disease. Elsevier, Amsterdam, pp 269–284

18. Ayoub MA, Yvinec R, Crépieux P, Poupon A (2016) Computational modeling approaches in gonadotropin signaling. Theriogenology 86(1):22–31
19. Reiter E, Yvinec R, Crépieux P, Poupon A (2016) Coupling of recognition and effect in GPRC signaling computational modelling approaches. In: Encyclopedia of the molecular life sciences. In press, London
20. Pfleger KDG, Seeber RM, Eidne KA (2006) Bioluminescence resonance energy transfer (BRET) for the real-time detection of protein-protein interactions. Nat Protoc 1 (1):337–345
21. Kinzer-Ursem T (2013) GPCR models in neuroscience in molecular and diffusion modeling. In: Encyclopedia of computational neuroscience, 1–7. Springer, New York
22. Kitano H, Funahashi A, Matsuoka Y, Oda K (2005) Using process diagrams for the graphical representation of biological networks. Nat Biotechnol 23(8):961–966
23. Hoops S, Sahle S, Gauges R, Lee C, Pahle J, Simus N, Singhal M, Xu L, Mendes P, Kummer U (2006) COPASI—a COmplex pathway SImulator. Bioinformatics 22(24):3067–3074
24. Raue A, Steiert B, Schelker M, Kreutz C, Maiwald T, Hass H, Vanlier J, Tönsing C, Adlung L, Engesser R, Mader W, Heinemann T, Hasenauer J, Schilling M, Höfer T, Klipp E, Theis F, Klingmüller U, Schöberl B, Timmer J (2015) Data2Dynamics: a modeling environment tailored to parameter estimation in dynamical systems. Bioinformatics 31(21):3558–3560
25. Ayoub MA, Landomiel F, Gallay N, Jégot G, Poupon A, Crépieux P, Reiter E (2015) Front Endocrinol 6:130
26. Ayoub MA, Zhang Y, Kelly RS, See HB, Johnstone EKB, McCall EA, Williams JH, Kelly DJ, Pfleger KDG (2015) Functional interaction between angiotensin II receptor type 1 and chemokine (C-C motif) receptor 2 with implications for chronic kidney disease. PLoS One 10(3):e0119803
27. Higham DJ (2008) Modeling and simulating chemical reactions. SIAM Rev 50(2):347–368
28. Goulet D (2016) Modeling, simulating, and parameter fitting of biochemical kinetic experiments. SIAM Rev 58(2):331–353
29. Maier C, Loos C, Hasenauer J (2017) Robust parameter estimation for dynamical systems from outlier-corrupted data. Bioinformatics 33(5):718–725
30. Hasenauer J, Jagiella N, Hross S, Theis FJ (2015) Data-driven modelling of biological multi-scale processes. arXiv:1506.06392
31. Gábor A, Banga JR (2015) Robust and efficient parameter estimation in dynamic models of biological systems. BMC Syst Biol 9(1):74
32. Egea JA, Henriques D, Cokelaer T, Villaverde AF, MacNamara A, Danciu DP, Banga JR, Saez-Rodriguez J (2014) MEIGO: an open-source software suite based on Metaheuristics for global optimization in systems biology and bioinformatics. BMC Bioinformatics 15 (1):136
33. Chis OT, Banga JR, Balsa-Canto E (2011) Structural Identifiability of systems biology models: a critical comparison of methods. PLoS One 6(11):e27755
34. Saccomani MP (2013) Structural vs practical Identifiability in system biology. In: IWBBIO, pp 305–313
35. Villaverde AF, Barreiro A, Papachristodoulou A (2016) Structural Identifiability of dynamic systems biology models. PLoS Comput Biol 12 (10):e1005153
36. Raue A, Kreutz C, Maiwald T, Bachmann J, Schilling M, Klingmüller U, Timmer J (2009) Structural and practical Identifiability analysis of partially observed dynamical models by exploiting the profile likelihood. Bioinformatics 25(15):1923–1929
37. Raue A, Schilling M, Bachmann J, Matteson A, Schelke M, Kaschek D, Hug S, Kreutz C, Harms BD, Theis FJ, Klingmüller U, Timmer J (2013) Lessons learned from quantitative dynamical modeling in systems biology. PLoS One 8(9):e74335
38. Raue A, Karlsson J, Saccomani MP, Jirstrand M, Timmer J (2014) Comparison of approaches for parameter Identifiability analysis of biological systems. Bioinformatics 30 (10):1440–1448
39. Kirk P, Thorne T, Stumpf MPH (2013) Model selection in systems and synthetic biology. Curr Opin Biotechnol 24(4):767–774
40. Kenakin T (2004) Principles: receptor theory in pharmacology. Trends Pharmacol Sci 25 (4):186–192
41. Rougny A, Yamamoto Y, Nabeshima H, Bourgne G, Poupon A, Inoue K, Froidevaux C (2015) Completing signaling networks by Abductive reasoning with perturbation experiments. In: ILP (late breaking papers), pp 95–100
42. Bourquard T, Landomiel F, Reiter E, Crépieux P, Ritchie DW, Azé J, Poupon A (2015) Unraveling the molecular architecture of a G protein-coupled receptor/β-Arrestin/Erk module complex. Sci Rep 5:10760
43. Cassier E, Gallay N, Bourquard T, Claeysen S, Bockaert J, Crépieux P, Poupon A, Reiter E,

Marin P, Vandermoere F (2017) Phosphorylation of β-Arrestin2 at Thr383 by MEK underlies β-Arrestin-dependent activation of Erk1/2 by GPCRs. Elife 6:e23777

44. Pavliotis GA, Stuart AM (2008) Multiscale methods: averaging and homogenization. In: Texts applied in mathematics. Springer, New York, p 53
45. Gillespie DT, Sanft KR, Petzold LR (2011) Legitimacy of the stochastic Michaelis Menten approximation. IET Syst Biol 5(1):58–69
46. Horn F (1972) Necessary and sufficient conditions for complex balancing in chemical kinetics. Arch Ration Mech Anal 49(3):172–186
47. Horn F, Jackson R (1972) General mass action kinetics. Arch Ration Mech Anal 47(2):81–116
48. Feinberg M (1972) Complex balancing in general kinetic systems. Arch Ration Mech Anal 49 (3):187–194
49. Othmer H (1980) The interaction of structure and dynamics in chemical reaction networks. In: Modelling of chemical reaction systems. Springer-Verlag, New York, pp 1–19
50. Gunawardena J (2003) Chemical reaction network theory for in-silico biologists. Notes available for download at http://jeremygunawardena.com/papers/crnt.pdf
51. Angeli D (2009) A tutorial on chemical reaction network dynamics. Eur J Control 15 (3):398–406
52. Anderson DF, Kurtz TG (2015) Stochastic analysis of biochemical systems. In: Stochastics in biological systems. Springer International Publishing, New York, pp 1–2
53. Carden J, Pantea C, Craciun G, Machiraju R, Mallick P (2016) Mathematical methods for modeling chemical reaction networks. BioRxiv:070326
54. Ellison P, Feinberg M, Ji H Chemical Reaction Network Toolbox. Available for download at http://www.crnt.osu.edu/CRNTWin
55. Donnell P, Banaji M, Marginean A, Pantea C (2014) CoNtRol: an open source framework for the analysis of chemical reaction networks. Bioinformatics 30(11):1633–1634
56. Raue A, Kreutz C, Theis FJ, Timmer J (2012) Joining forces of Bayesian and Frequentist methodology: a study for inference in the presence of non-Identifiability. Philos Trans A Math Phys Eng Sci 371(1984):20110544



Chapter 14

Proteomic Analysis of the β-Arrestin Interactomes

Yang Zhao and Kunhong Xiao

Abstract

Protein–protein interaction is crucial to protein function and cellular signaling. A number of approaches were developed and applied to characterize protein–protein interactions in the past decades. In recent years, mass spectrometry (MS)-based proteomic methods have emerged as powerful tools to identify protein binding partners in a global and high-throughput manner. In this chapter, we describe the proteomic methods used to characterize the whole sets of proteins associated with β-arrestins (β-arrestin interactomes). The method starts with co-immunoprecipitation (co-IP) of β-arrestin signaling complexes from cells followed by protease digestion and LC/MS/MS analysis (liquid chromatography/tandem mass spectrometry) of proteins in the β-arrestin signaling complexes. To investigate changes in the amounts of binding partners under different conditions, we also describe a SILAC (stable isotope labeling by amino acids in cell culture) method to obtain quantitative information for β-arrestin interactomes.

Key words β-Arrestin, Mass spectrometry, LC/MS, LC/MS/MS, Proteomics, Quantitative proteomics, SILAC, Stable isotope labeling by amino acids in cell culture, Interactome, Proteome, GPCR

1 Introduction

Inside a cell, numerous cellular functions are primarily achieved through protein–protein interactions, via the formation of transient or stable protein complexes. Therefore, characterization of binding partners of a protein is critical to understand the functions and signaling networks of this protein within the cell. In the past decades, numerous methodologies have been developed to identify binding partners of a target protein and to characterize protein–-protein interactions. These methods include traditional co-immunoprecipitation followed by Western blotting analysis [1], label transfer [2–4], yeast two-hybrid screen [5–7], phage display [8–10], in vivo cross-linking of protein complexes using photoreactive amino acid analogs [11], tandem affinity purification (TAP) [12, 13], strep-protein interaction experiment (SPINE) [14–16], and proximity ligation assay (PLA) [17, 18]. These methods have been widely used to study protein–protein interactions and provided valuable information to understand protein functions

Mark G. H. Scott and Stéphane A. Laporte (eds.), *Beta-Arrestins: Methods and Protocols*, Methods in Molecular Biology, vol. 1957, https://doi.org/10.1007/978-1-4939-9158-7_14, © Springer Science+Business Media, LLC, part of Springer Nature 2019

and biological processes. In recent years, following the completion of the human genome project and the advance in the fields of mass spectrometry (MS) and proteomics, MS-based proteomic methods to identify protein binding partners have emerged as powerful tools to characterize protein–protein interactions inside a cell [19–27]. MS-based proteomic approaches are high-throughput and global and provide opportunities to characterize the whole set of proteins that interact with a target protein at a given time (interactome).

β-Arrestins 1 and 2 are ubiquitously expressed and fundamental to the regulation of G protein-coupled receptor (GPCR)-mediated signaling [28–30]. In addition to their well-characterized roles in GPCR desensitization and internalization, recent evidence suggests that β-arrestins also function to facilitate a number of intracellular signaling processes, including the activation of the extracellular-regulated kinases, the C-jun terminal kinase, and the apoptosis signal-regulating kinase 1 [31–34]. The multifaceted nature of the β-arrestins and their universal influence on GPCR regulation and signaling rely on the fact that β-arrestins can serve as adaptors and scaffolds for a variety of binding partners in the cell. Using different traditional methods, a number of binding partners of β-arrestins were identified [29, 35]. These binding partners include signaling molecules such as Src, ERK1/2, JNK3, p38, and AKT and endocytic proteins such as clathrin, AP-2, *N*-ethylmaleimide-sensitive fusion protein (NSF), ARF6, and its guanine nucleotide exchange factor ARNO. In addition, it was discovered that β-arrestins interact with a number of other receptor proteins such as TGFβ III receptor, IGF1 receptor, nicotinic cholinergic receptor, and Notch [29]. With more and more binding partners being identified, it was appreciated that much broader roles of β-arrestins are not currently known. The identification of β-arrestin binding partners and their changes under different conditions in a global and high-throughput manner is therefore needed. Accordingly, we have initiated an approach utilizing techniques and strategies of MS-based proteomics to study β-arrestin interactomes [36].

As a robust and sensitive screening method, β-arrestin interactome analysis can be performed qualitatively and quantitatively. The qualitative β-arrestin interactome analysis starts with co-immunoprecipitation (co-IP) of β-arrestins and their binding partners (β-arrestin signaling complexes) in cells (e.g., HEK293 cell) stably overexpressing either Flag-tagged β-arrestin1 or 2 (Fig. 1a). After the β-arrestin signaling complexes have been pulled down via co-IP, all proteins in the complexes are digested by a protease (usually trypsin) to generate a pool of peptides. Liquid chromatography/tandem mass spectrometry (LC/MS/MS) analysis of these peptides followed by database search and data processing can then

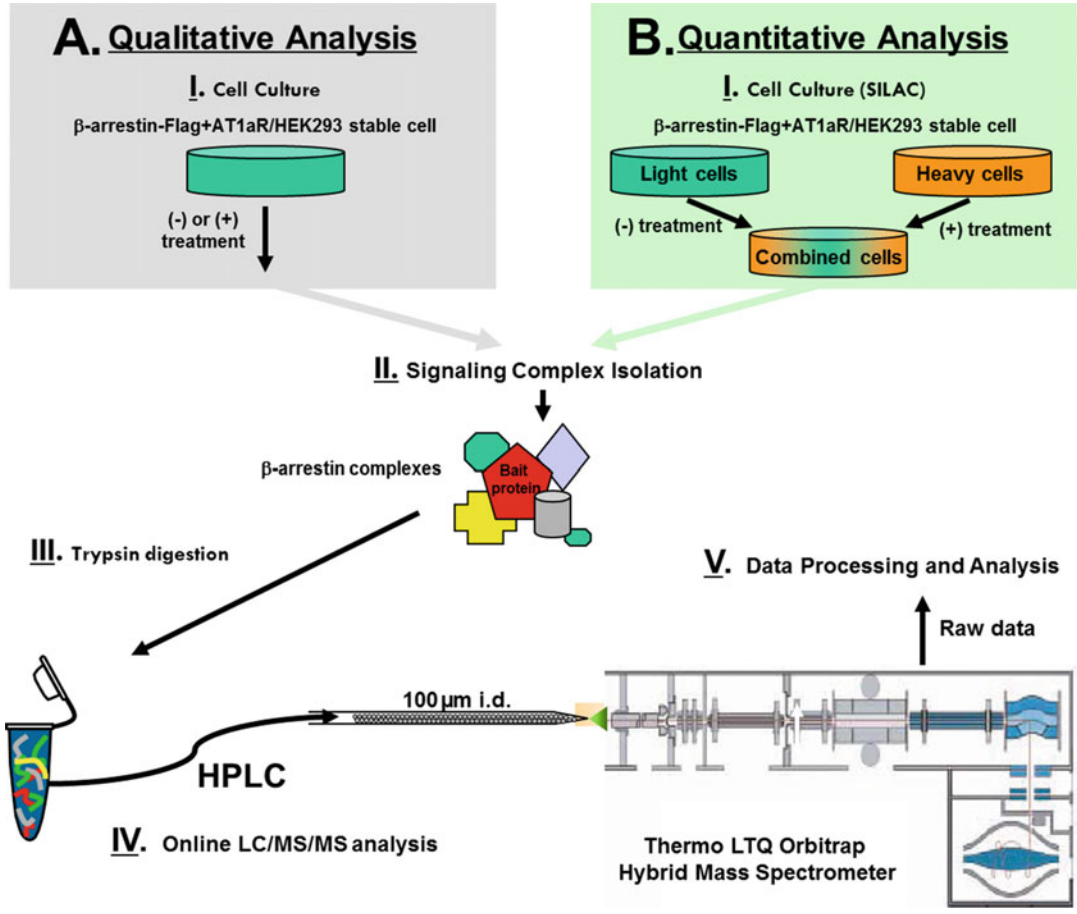


Fig. 1 Overview of qualitative and quantitative β-arrestin interactome analyses. (**a**) The experimental procedures for qualitative analysis of β-arrestin interactomes. HEK293 cells stably overexpressing HA-AT1aR and β-arrestin 1-FLAG or β-arrestin 2-FLAG are cultured and treated with or without 100 nM angiotensin II (left-top panel, Procedure I). Treated and untreated cells are harvested individually for the follow-up experiments. (**b**) The experimental procedures for quantitative analysis of β-arrestin interactomes. The quantitative analysis is usually achieved through the stable isotopic labeling (e.g., ^{13}C and ^{15}N) of one of the samples for comparison to an unlabeled sample. A metabolic stable isotope labeling strategy called SILAC (stable isotope labeling of amino acid in cell) is frequently used. In the experiment described in this figure, the stable isotope labeled "heavy" cells were treated with agonist (100 nM angiotensin II), whereas the unlabeled "light" cells serve as control without agonist treatment (right-top panel, Procedure I). Equal numbers of "light" and "heavy" cells were mixed after agonist treatment. The mixed cells were subjected to the follow-up experiments. After cell culture and harvest, experimental procedures (Procedures II–III) for qualitative and quantitative β-arrestin interactomes are the same, except for some MS instrument settings and database search and processing parameters during LC/MS/MS and data analysis (Procedures IV–V)

resolve all the proteins in β-arrestin signaling complexes and uncover the β-arrestin interactomes.

β-Arrestin interactome analysis can also be performed quantitatively to study changes in the amounts of binding proteins under different conditions. Quantitative interactome analysis involves

quantitative proteomics strategies such as SILAC (stable isotope labeling by amino acids in cell culture) and TMT (tandem mass tag). In this chapter, we will only describe the SILAC-based method. In SILAC-based β-arrestin interactome analysis, the cell line stably overexpressing Flag-tagged β-arrestins (either 1 or 2) is cultured side by side using different media (Fig. 1b). The conditions for these two cell cultures are almost identical, except in one condition, regular medium ("light medium") is used, whereas in the other condition, lysine and arginine in the medium ("heavy medium") are replaced by stable isotope-coded lysine and arginine (usually L-lysine-[$^{13}C_6$, $^{15}N_2$] and L-arginine-[$^{13}C_6$,$^{15}N_4$]). During cell growth, the stable isotope-coded lysine and arginine will be incorporated into proteins in the heavy medium. We can use one cell population (e.g., "heavy cells") as the experimental group to perform treatment and the other one (e.g., "light cells") as the non-treatment control group. During the experiments, the light and heavy cells are mixed together at 1:1 ratio and then subjected to co-immunoprecipitation and trypsin digestion. Since trypsin cleaves proteins at the C-termini of lysine and arginine, all tryptic peptides will have two isoforms ("light peptide" and "heavy peptide"). The light peptide is from the light cells (i.e., the control cells), and the heavy peptide is from the heavy cells (i.e., the treated cells). The corresponding light and heavy peptides are biologically and chemically identical but with different masses. This difference in masses can be detected by mass spectrometry leading to two peaks (i.e., a doublet) for each peptide. The peak ratio for the light and heavy peptides reflects the relative amount of each peptide or corresponding β-arrestin binding protein between the treatment and control group.

In this chapter, we describe the mass spectrometry-based proteomic methods used to characterize the β-arrestin interactomes as modulated by a model seven-transmembrane receptor, the angiotensin II type 1a receptor (AT1aR). These methods can be adopted to characterize the β-arrestin interactomes as modulated by other GPCRs.

2 Materials

2.1 Cell Culture and Treatment for Qualitative β-Arrestin Interactome Analysis

1. Human embryonic kidney (HEK293) cell line stably overexpressing HA-AT1aR and β-arrestin 1-FLAG or β-arrestin 2-FLAG (*see* **Note 1**).
2. Fetal bovine serum.
3. Penicillin/streptomycin.
4. Corning® culture dishes (D × H; 150 mm × 25 mm).
5. Angiotensin II (Sigma, St. Louis, MO).

6. Dulbecco's modified Eagle's medium (DMEM).
7. PBS.

2.2 Cell Culture and Treatment for Quantitative β-Arrestin Interactome Analysis

1. HEK293 cell line stably overexpressing HA-AT1aR and β-arrestin 1-FLAG or β-arrestin 2-FLAG.
2. Penicillin/streptomycin.
3. Corning® culture dishes (D × H; 150 mm × 25 mm).
4. Angiotensin II (Sigma, St. Louis, MO).
5. SILAC Media:
   (a) *Reagents*:
   - Custom-ordered DMEM powder without arginine, lysine, and leucine (Gibco, Formula # 03-5080EB) (Gibco/Invitrogen, Carlsbad, CA).
   - L-Lysine-[$^{13}C_6$, $^{15}N_2$] (Cambridge Isotope Laboratories, Andover, MA).
   - L-Arginine-[$^{13}C_6$,$^{15}N_4$] (Cambridge Isotope Laboratories, Andover, MA).
   - Dialyzed FBS (Hyclone) (Thermo Scientific, Waltham, MA).

   (b) *"Light" SILAC Medium*:

   To prepare 1 liter SILAC light medium, dissolve 13 grams custom-ordered DMEM powder, 104 mg L-leucine, 100 mg L-proline, 3.7 g $NaHCO_3$, and 3.12 g of HEPES in 900 mL of sterile deionized H_2O; adjust pH to 7.2; then add 100 mL dialyzed FBS, 1 mL of 25 mg/mL regular L-lysine (L-lysine-[$^{12}C_6$, $^{14}N_2$]), 1 mL of 25 mg/mL regular L-arginine (L-arginine-[$^{12}C_6$,$^{14}N_4$]), 1% penicillin/streptomycin, 150 μg/mL G418, and 150 μg/mL Zeocin; finally filter the medium using sterile bottle-top filter system (0.22 μm, 1000 mL, Fisher Scientific) (*see* **Notes 2–5**).

   (c) *"Heavy" SILAC Medium:*

   To prepare 1 L SILAC heavy medium, dissolve 13 g custom-ordered DMEM powder, 104 mg L-leucine, 100 mg L-proline, 3.7 g $NaHCO_3$, and 3.12 g of HEPES in 900 mL of H_2O; adjust pH to 7.2; then add 100 mL dialyzed FBS, 1 mL of 25 mg/mL stable isotopic coded L-lysine-[$^{13}C_6$, $^{15}N_2$], 1 mL of 25 mg/mL stable isotopic coded L-arginine-[$^{13}C_6$,$^{15}N_4$], 1% penicillin/streptomycin, 150 μg/mL G418, and 150 μg/mL Zeocin; finally filter the medium using sterile bottle-top filter system (0.22 μm, 1000 mL, Fisher Scientific) (*see* **Notes 2–5**).

2.3 Isolation of β-Arrestin Signaling Complexes from HEK293 Cells

1. Sorvall RC-6 Plus superspeed centrifuge and SS-34 rotor (Fisher Scientific, Pittsburgh, PA).
2. Anti-FLAG M2 affinity agarose beads.
3. Protein-G plus/Protein A Agarose Suspension.
4. 50 mL conical sterile polypropylene centrifuge tubes.
5. 30 mL plastic centrifuge tubes (uncapped) for SS-34 rotor.
6. Glycerol.
7. Glycerol lysis buffer: 50 mM HEPES, 0.5% NP-40, 150 mM NaCl, 10% glycerol, 2 mM EDTA. The following protease and phosphatase inhibitors can be added to the lysis buffer. Protease inhibitors: 10 μg/mL trypsin inhibitor, 17.4 μg/mL PMSF, 157 μg/mL benzamidine, 1 μg/mL pepstatin, 5 μg/mL aprotinin, and 5 μg/mL leupeptin. Phosphatase inhibitors: 50 nm microcystin-LR, 40 mg/100 mL NaF, and 18 mg/100 mL Na vanadate.
8. Wash buffer I: 20 mM Tris–HCl, pH 8.0, 100 mM NaCl, 1 mM EDTA, and 0.1% dodecyl-β-D-maltoside (DDM).
9. Wash buffer II: 20 mM Tris–HCl, pH 8.0, 100 mM NaCl, and 1 mM EDTA.
10. 2,4,6-Trichloroanisole (TCA) (Sigma, St. Louis, MO) (*see* **Note 6**).

2.4 SDS-PAGE Separation of β-Arrestin Signaling Complexes and In-Gel Trypsin Digestion

1. Four to twenty percent (4–20%) SDS-PAGE gels.
2. Brilliant Blue G-Colloidal Concentrate.
3. Axygen maximum recovery microcentrifuge tubes 1.7 mL.
4. Sequencing grade modified trypsin (Promega, Madison, WI).
5. 1,4-Dithiothreitol (DTT).
6. Iodoacetamide (IAA).
7. Ammonium bicarbonate.
8. Speed-Vac, vortex and benchtop microcentrifuge.

2.5 Tryptic Digest Clean-Up by Stage-Tip

1. 3 M Empore™ C18 SPE extraction disks (Sigma, St. Louis, MO).
2. GPS-L250 tips.
3. Acetonitrile (ACN).
4. Trifluoroacetic acid (TFA) (*see* **Note 6**).
5. Formic acid (FA) (*see* **Note 6**).
6. Methanol.

2.6 Liquid Chromatography/ Tandem Mass Spectrometry (LC/MS/MS) Analysis

1. A LC/MS/MS system for bottom-up proteomics, for example, a Thermo Scientific Orbitrap XL mass spectrometer coupled with a Waters nanoACQUITY Ultra Performance LC (UPLC) System (*see* **Note 7**).
2. Acetonitrile and LC/MS grade.
3. H_2O and LC/MS grade.
4. Trifluoroacetic acid (TFA) (*see* **Note 6**).
5. Formic acid (FA) (*see* **Note 6**).
6. 75μm × 150mm BEH C18 column (Waters, Milford, MA).

2.7 Database Search, Data Filtering, and Peptide/Protein Quantification

1. SEQUEST or other database search engines.
2. Proteome Discoverer, MaxQuant, and/or Vista program.

2.8 Postsearch Data Analysis and Bioinformatics Analysis

1. Osprey Network Visualization System (http://biodata.mshri.on.ca/osprey/).
2. Lists2Networks software system (http://www.lists2networks.org).
3. Ingenuity® Systems software (https://analysis.ingenuity.com/ipawst/public/ipatest.jsp).

3 Methods

3.1 Cell Culture and Treatment for Qualitative β-Arrestin Interactome Analysis

1. Culture ten (10) 150 mm culture dishes of HEK293 cells stably overexpressing HA-AT1aR and β-arrestin 1-FLAG or β-arrestin 2-FLAG in DMEM supplemented with 10% (v/v) fetal bovine serum and 1% penicillin/streptomycin, 150 μg/mL G418, and 150 μg/mL Zeocin (*see* **Note 8**).
2. When cells reach ~80% confluency, serum-starve cells for 4 h.
3. Treat cells with or without 100 nM angiotensin II for 5 min at 37 °C.
4. After treatment, wash cells twice with ice-cold PBS.
5. Scrape cells from the dishes, transfer to a 50 mL conical tube, and spin down the cells. The cell pellets are ready for lysis and β-arrestin signaling complex isolation (*see* Subheading 3.3)

3.2 Cell Culture and Treatment for Quantitative β-Arrestin Interactome Analysis

1. Maintain HEK293 cells stably overexpressing HA-AT1aR and β-arrestin 1-FLAG or β-arrestin 2-FLAG in SILAC "light" (e.g., DMEM medium containing "light" L-lysine-[$^{12}C_6$, $^{14}N_2$] and L-arginine-[$^{12}C_6$,$^{14}N_4$]) and "heavy" (e.g. DMEM medium containing "heavy" L-lysine-[$^{13}C_6$, $^{15}N_2$] and L-

arginine-[$^{13}C_6$,$^{15}N_4$]) media side by side for at least six doublings (*see* **Note 4**).

2. Expand cells to five (5) 150 mm culture dishes of "light" labeled cells and five (5) 150 mm culture dishes of "heavy" labeled cells.
3. When cells reach ~80% confluency, serum-starve for 4 h.
4. Treat the "heavy" labeled cells with 100 nM angiotensin II for 5 min. The "light" labeled cells are used as control without treatment (*see* **Note 9**).
5. Wash the cells with 10 mL cold PBS, twice.
6. Scrape cells from dishes and mix equal number of angiotensin II treated "heavy" cells with untreated "light" cells.
7. Spin down cells in a 50 mL conical tube. The cell pellets are ready for lysis and β-arrestin signaling complex isolation (*see* Subheading 3.3)

After cell culture and harvest, experimental procedures for qualitative and quantitative β-arrestin interactomes are the same, except for some MS instrument settings and database search and processing parameters during LC/MS/MS and data analysis.

3.3 Isolation of β-Arrestin Signaling Complexes from HEK293 Cells

1. Add 1 mL ice-cold glycerol lysis buffer to each tube of cell pellet from Subheading 3.1, **step 5** (e.g., samples for qualitative β-arrestin interactomes) or Subheading 3.2, **step 7** (e.g., samples for quantitative β-arrestin interactomes). Ensure that protease inhibitors are added to the glycerol lysis buffer.
2. Lyse the cells by three freeze–thaw cycles.
3. Resuspend the cells in 20 mL ice-cold glycerol lysis buffer and dounce 20 times in small (~5 mL) Dounce homogenizer.
4. Lyse the cells by rotating in the cold room for 1–2 h.
5. Clarify cell lysate by centrifugation at 23,500 × *g* for 20 min in SS-34 rotor using the 30 mL plastic centrifuge tubes (uncapped).
6. Transfer the supernatant to a new 50 mL conical tube. Pre-clean the supernatant with Protein-G plus/Protein A Agarose Suspension (100 μL slurry) by incubating in the cold room for 1 h.
7. Spin down the Protein-G plus/Protein A agarose beads at 1800 × *g*, and transfer the pre-cleaned supernatant to a 1.5 mL microcentrifuge tube.
8. Add 100 μL slurry of pre-equilibrated anti-FLAG M2 affinity agarose beads to the supernatant. Incubate with tumbling in the cold room for 4 h.

9. Spin down the anti-FLAG M2 beads at 6000 × *g*. Discard the supernatant, and transfer the anti-FLAG M2 beads to a new 1.5 mL microcentrifuge tube.
10. Wash the anti-FLAG M2 beads with 1 mL wash buffer I for three times followed by three times wash with wash buffer II.
11. Elute the protein complex using one of the following procedures:
12. *Elution option 1*: Elute the β-arrestin signaling complexes with 300 μL of 0.1 M glycine-HCl, pH 3.5, three times. Pool the three (3) eluates in one tube. Re-equilibrate to neutral pH with 1 M Tris–HCl as soon as possible after elution.
13. *Elution option 2*: Elute the β-arrestin signaling complexes with 300 μL of 100 μg/mL Flag peptide in wash buffer II, three (3) times. Pool the three (3) eluates in one tube.
14. Precipitate the β-arrestin signaling complexes with 20% TCA. The precipitated β-arrestin complexes can be stored at −80 °C until mass spectrometry analysis is performed.

3.4 SDS-PAGE Separation of β-Arrestin Signaling Complexes and In-Gel Trypsin Digestion

1. Prepare 4–20% SDS-PAGE gels to separate proteins in β-arrestin signaling complexes. Tape the combs to create a large well if the sample volume is large.
2. Load the β-arrestin signaling complexes in the gel, and run the gel at 200 V for about 30–45 min (*see* **Note 10**).
3. After SDS-PAGE, fix the proteins in the gel for 1 h with a solution of 7% acetic acid in 40% (v/v) methanol.
4. Immediately before staining, combine four parts of the 1× Brillant Blue G-Colloidal working solution and 1 part methanol. Vortex vigorously for 1 min. Remove the fixing solution, and add 20–30 mL of the Brilliant Blue G-Colloidal stain to gel, and shake for 1–2 h (*see* **Notes 11** and **12**).
5. Remove the stain, and destain the gel by adding a solution of 10% acetic acid in 25% (v/v) methanol. Shake for 1 min.
6. Remove the destaining solution and wash the gel twice in 25% methanol.
7. Remove the 25% methanol and add double distilled water.
8. Excise gel lane containing the proteins of β-arrestin signaling complexes into 4–6 regions using a clean razor blade or scalpel.
9. Chop each gel slice into small pieces (approximately 1 mm cubes), and transfer to separate 1.7 mL Axygen maximum recovery microcentrifuge tubes.
10. Add 500 μL of HPLC grade water to each tube, and incubate at room temperature for 10 min with gentle vortexing.

11. Remove the HPLC grade water. Add 100–300 μL of 25 mM ammonium bicarbonate in 50% acetonitrile, and incubate 10 min with gentle vortexing. Remove the solution, and repeat this destain/wash step several times. The gel pieces should become small, hard, and opaque (*see* **Note 13**).
12. Do one final wash with 100–300 μL of 100% acetonitrile for 10 min. At this point the dehydrated gel slices should be small and white.
13. Aspirate the acetonitrile and dry the gel pieces in Speed-Vac for 5 min.
14. Reduction and alkylation of cysteine residues.
    (a) Add enough 10 mM DTT to cover the gel slices, and incubate at room temperature for 30 min.
    (b) Remove the DTT and the same volume of 55 mM iodoacetamide. Incubate in the dark at room temperature for 45 min.
    (c) Remove the iodoacetamide, and wash the gel slices with 25 mM ammonium bicarbonate for 10 min with shaking.
    (d) Remove the wash solution and dry the gel slices with 100 μL 100% acetonitrile.
15. Add enough 10 ng/μL trypsin (Promega, sequencing grade) in 25 mM ammonium bicarbonate, pH 8.0 (resuspend one tube of trypsin in 4 mL of ammonium bicarbonate) to cover the gel slices. Incubate overnight at 37 °C in a shaker.
16. To extract the tryptic peptides, add 100–200 μL acetonitrile to the gel pieces, and incubate 10 min with gentle vortexing.
17. Transfer tryptic peptide solution to fresh 1.7 mL Axygen maximum recovery microcentrifuge tubes.
18. Rehydrate the gel pieces with 30–60 μL HPLC grade water, and incubate for 10 min with gentle vortexing.
19. Add 100–200 μL acetonitrile again and incubate 10 min with gentle vortexing. Add this extraction to the tube with tryptic peptides.
20. Lyophilize tryptic extract to dryness in a Speed-Vac.

3.5 Tryptic Digest Clean-Up by Stage-Tip

1. Pack two to three (2–3) cookies of 3 M Empore™ C18 SPE extraction disk into pipette tip.
2. To clean the column, add 40 μL of methanol to each tip, and push out 90% of the methanol with a 50 mL syringe. Wait for 10 min, and then push out the remaining 10%.
3. To wet the column, add 40 μL 0.1% TFA/50% acetonitrile solution, and push out completely with the syringe.

4. To equilibrate the column, add 20 μL 0.1% TFA and push out. Repeat twice.
5. Reconstitute the tryptic peptides in 20 μL 0.1% TFA, check pH, and add more concentrate TFA to ensure that pH < 2. Vortex.
6. To bind the sample, load 40 μL of sample to the tip and push it through. Repeat twice.
7. Wash the column once with 40 μL 0.1% TFA.
8. To elute into a fresh tube, add 40 μL 0.1% TFA/50% acetonitrile and push through. Repeat twice using 20 μL 0.1% TFA/50% acetonitrile each time.
9. Lyophilize samples to dryness in a Speed-Vac.

3.6 Liquid Chromatography/Tandem Mass Spectrometry (LC/MS/MS) Analysis

The instrument setting described here is for Thermo Scientific LTQ Orbitrap XL (Thermo Fisher Scientific) online coupled with a Waters nanoACQUITY UPLC system.

1. Load peptide mixtures onto a 75 μm × 150 mm BEH C18 column (particle size 1.7 μm, Waters).
2. Separate peptides using on a Waters nanoACQUITY UPLC using a linear acetonitrile gradient of 5%–40% B over 60 min (0.4 μL/min; mobile phase A, 0.125% FA; mobile phase B, 80% acetonitrile, 20% water, 0.125% FA).
3. Operate the LTQ Orbitrap XL mass spectrometer at positive ESI mode with the following source parameters: spray voltage, 4.5 kV; capillary temperature, 275 °C; tube lens, 100 V; and sheath gas flow, 10 units.
4. Acquire data on the LTQ Orbitrap XL mass spectrometer in the data-dependent mode using the TOP10 strategy [37, 38]. In brief, a scan cycle is initiated with a full scan of high mass accuracy (m/z 350–1800; acquired in the Orbitrap at 6×10^4 resolution setting and automatic gain control (AGC) target of 10^6), which was followed by MS/MS scans (AGC target 5000; threshold 3000) in the linear ion trap on the ten (10) most abundant precursor ions. Selected ions are dynamically excluded for 30 s. Singly charged ions are excluded from MS/MS analysis.

3.7 Database Search, Data Filtering, and Peptide/Protein Quantification

Database searches are performed using SEQUEST or other search engines against an appropriate database, such as the last version of UniProt human database (http://www.uniprot.org/). Use different database search parameters for qualitative and quantitative β-arrestin interactome analyses. The parameters described here are database search parameters using the SEQUEST algorithm with the target-decoy database searching strategy [39].

1. Database search:
   (a) Qualitative β-arrestin interactome analysis: Submit all MS/MS spectra to the SEQUEST search engine against the latest version of UniProt human database and its reversed complement. Searches can be performed with the following parameters: full trypsin specificity, a mass tolerance of 80 ppm, static modifications of 57.02146 Da (carboxyamidomethylation) on cysteine, and dynamic modifications of 79.96633 Da (phosphorylation) on serine, threonine, and tyrosine, and 15.99491 Da (oxidation) on methionine.
   (b) Quantitative β-arrestin interactome analysis: Submit all MS/MS spectra to the SEQUEST search engine against the latest version of UniProt human database and its reversed complement. Searches can be performed with the following parameters: full trypsin specificity, a mass tolerance of 80 ppm, static modifications of acrylamidated Cys (+71.0371), and dynamic modifications of 79.96633 Da (phosphorylation) on serine, threonine, and tyrosine, 15.99491 Da (oxidation) on methionine, 10.00827 Da on arginine, and 8.01420 Da on lysine.
2. Data filtering: All peptide matches are filtered to include <1% matches to reverse sequences by restricting the mass tolerance window and setting thresholds for XCorr and dCn′ [40] (defined as the normalized difference between Xcorr values of the top-ranked candidate peptide and the next candidate with a different amino acid sequence). The target/decoy search strategy [39] permits the discovery of proper criteria (XCorr, dCn′, ppm) to exclude all reverse hits in the results.
3. Peptide and protein quantification: For SILAC-based quantitative β-arrestin interactome analysis, peptide and protein quantification can be performed using software packages, such as the Vista program [41], MaxQuant, and Proteome Discoverer. First, peptide quantification is achieved using precursor ion quantification mode to calculate the heavy-to-light (or stimulated-to-non-stimulated) abundance ratio (either area under the curve or peak height). These peptide abundance ratios are then converted to $\log_2$ ratios. For each protein, the $\log_2$ ratios for all the peptides identified for this protein are averaged to calculate a $\log_2$ ratio for the protein. This averaged $\log_2$ ratio can be converted back to an average abundance ratio as a report for the relative changes in the amounts of proteins associated with β-arrestin after agonist stimulation. Alternatively, the average abundance ratio can be further converted to fold of increase ([fold of increase = average abundance ratio] if the average Vista ratio is ≥1) or percentage of decrease (% of

decrease; [% of decrease = (1 − average abundance ratio) × 100%], if the average abundance ratio is <1).

3.8 Postsearch Data Analysis and Bioinformatics Analysis

1. Bioinformatics annotations: Bioinformatics annotations can be carried out automatically or manually using Human Protein Reference Database (http://www.hprd.org/) or UniProt (http://www.uniprot.org/) to collect the protein names, UniProt accession numbers, gene symbol, and subcellular locations.
2. Functional category and subcellular distribution analysis: Proteins can be organized into functional groups according to their GO (gene ontology) categories using the Osprey Network Visualization System [42] (http://biodata.mshri.on.ca/osprey/). Subsequently, their functional annotations can be cross-validated using the functional annotations in the Human Protein Reference Database and UniProt database. Additionally, the subcellular distribution information of proteins was also obtained from the Human Protein Reference Database and UniProt database.
3. Other bioinformatics analysis: The β-arrestin interactome data can be used for further bioinformatics analysis to construct signaling pathways and networks. For example, the protein in the β-arrestin interactomes can be submitted for KEGG (Kyoto Encyclopedia of Genes and Genomes) canonical pathway analysis and Ingenuity sub-network analysis (*see* **Notes 14** and **15**).

4 Notes

1. Two double stable cell lines were used to determine the interactomes of β-arrestin 1 and 2 [36]. These two double stable cell lines are (1) HA-AT1aR and β-arrestin 1-FLAG in HEK293 and (2) HA-AT1aR and β-arrestin 2-FLAG in HEK293. Plasmids pcDNA3.1-HA-AT1aR, pcDNA3-β-arrestin1-FLAG, and pcDNA3-β-arrestin2-FLAG have all been described previously [36, 43].
2. Adding additional glutamine may play with amino acid metabolism in a negative way for SILAC.
3. The purpose of addition of 100 mg/L of L-proline in the SILAC media is to reduce arginine→proline conversion during the metabolic labeling process [44].
4. The metabolic incorporation rate should be checked in the "heavy" labeled cells. The metabolic incorporation rate should be higher than 95% before expanding cells for experiments.
5. The final concentrations of L-lysine (regular or stable isotope coded) and L-arginine (regular or stable isotope coded) in

SILAC media are 25 mg/L. These concentrations are lower than those used in regular DMEM medium for two purposes: (1) to lower the cost for stable isotope-coded amino acids and (2) to lower the arginine→proline conversion.

6. TFA, FA, and TCA are harmful by inhalation. They can cause severe burns and should be handled in a fume hood.
7. LC/MS/MS analyses can be performed in any instrument setting that is sufficient for bottom-up shot-gun proteomics, for example, an Orbitrap XL, Velos, Elite, Fusion, QE, QE plus, QE HF, or QE HFx mass spectrometer from Thermo-Fisher Scientific or another high-resolution mass spectrometer system from other vendors.
8. Ten (10) 15 cm dishes of cells will be used for each condition.
9. The experiments can also be performed using the "light" labeled cells as experimental group and the "heavy" labeled cells as control group.
10. Stop the electrophoresis when the front dye reaches the middle of the separation gel. Running proteins all the way to the bottom of the gel will generate large gel slices, which are not easy to handle during the in-gel digestion step.
11. Prepare 1× Brilliant Blue G-Colloidal working solution by adding 800 mL of deionized water to the bottle labeled Brilliant Blue G-Colloidal Concentrate. Mix by inversion and store at 2–8 °C once diluted.
12. Do not keep the gel in the stain solution for too long to overstain the gel. The dye in the overstained gel is difficult to remove at the destaining stage during the in-gel digestion step.
13. Alternatively, add 1 mL 25 mM ammonium bicarbonate in 50% acetonitrile, and incubate for 1 h. Replace the destain/wash solution once or twice.
14. KEGG canonical pathway analysis can be performed using the Lists2Networks software system (http://www.lists2networks.org) [45]. Using the KEGG pathway gene set (http://www.genome.jp/kegg) from GSEA [46], proteins in the β-arrestin interactomes are computed to obtain overlap between proteins in the β-arrestin interactomes and proteins belonging to pathways in KEGG using the Fisher exact test (Fisher test $p < 0.05$ with Bonferroni correction).
15. Ingenuity sub-network analysis can be performed using Ingenuity® Systems software (https://analysis.ingenuity.com/ipawst/public/ipatest.jsp). The protein list in β-arrestin interactomes is submitted to Ingenuity Pathway Analysis, and sub-networks are generated using the Ingenuity network construction algorithm and the Ingenuity knowledgebase.

Acknowledgment

This work was supported, in part, by US National Institutes of Health grant no. HL-075443 Proteomics Core support to K.X. This publication was also made possible by seed funding support to K.X. from the Department of Pharmacology and Chemical Biology, the University of Pittsburgh and Vascular Medicine Institute, the Hemophilia Center of Western Pennsylvania, and the Institute for Transfusion Medicine.

References

1. E G (2002) Protein–protein interactions: a molecular cloning manual. Cold Spring Harbor Laboratory Press, Cold Spring Harbor, NY
2. Ilver D et al (1998) Helicobacter pylori adhesin binding fucosylated histo-blood group antigens revealed by retagging. Science 279 (5349):373–377
3. Kleene R, Classen B, Zdzieblo J, Schrader M (2000) SH3 binding sites of ZG29p mediate an interaction with amylase and are involved in condensation-sorting in the exocrine rat pancreas. Biochemistry 39(32):9893–9900
4. Liu B, Archer CT, Burdine L, Gillette TG, Kodadek T (2007) Label transfer chemistry for the characterization of protein-protein interactions. J Am Chem Soc 129 (41):12348–12349
5. Rajagopala SV, Uetz P (2009) Analysis of protein-protein interactions using array-based yeast two-hybrid screens. Methods Mol Biol 548:223–245
6. Causier B, Davies B (2002) Analysing protein-protein interactions with the yeast two-hybrid system. Plant Mol Biol 50(6):855–870
7. Joung JK, Ramm EI, Pabo CO (2000) A bacterial two-hybrid selection system for studying protein-DNA and protein-protein interactions. Proc Natl Acad Sci U S A 97(13):7382–7387
8. Suchanek M, Radzikowska A, Thiele C (2005) Photo-leucine and photo-methionine allow identification of protein-protein interactions in living cells. Nat Methods 2(4):261–267
9. Sidhu SS, Fairbrother WJ, Deshayes K (2003) Exploring protein-protein interactions with phage display. Chembiochem 4(1):14–25
10. Kokoszka ME, Kay BK (2015) Mapping protein-protein interactions with phage-displayed combinatorial peptide libraries and alanine scanning. Methods Mol Biol 1248:173–188
11. Pham ND, Parker RB, Kohler JJ (2013) Photocrosslinking approaches to interactome mapping. Curr Opin Chem Biol 17(1):90–101
12. Krogan NJ et al (2006) Global landscape of protein complexes in the yeast *Saccharomyces cerevisiae*. Nature 440(7084):637–643
13. Gavin AC et al (2006) Proteome survey reveals modularity of the yeast cell machinery. Nature 440(7084):631–636
14. Herzberg C et al (2007) SPINE: a method for the rapid detection and analysis of protein-protein interactions in vivo. Proteomics 7 (22):4032–4035
15. Muller VS, Jungblut PR, Meyer TF, Hunke S (2011) Membrane-SPINE: an improved method to identify protein-protein interaction partners of membrane proteins in vivo. Proteomics 11(10):2124–2128
16. Muller VS, Tschauner K, Hunke S (2013) Membrane-SPINE: a biochemical tool to identify protein-protein interactions of membrane proteins in vivo. J Vis Exp (81):e50810
17. Soderberg O et al (2006) Direct observation of individual endogenous protein complexes in situ by proximity ligation. Nat Methods 3 (12):995–1000
18. Jarvius M et al (2007) In situ detection of phosphorylated platelet-derived growth factor receptor beta using a generalized proximity ligation method. Mol Cell Proteomics 6 (9):1500–1509
19. Babu M et al (2012) Interaction landscape of membrane-protein complexes in *Saccharomyces cerevisiae*. Nature 489(7417):585–589
20. Havugimana PC et al (2012) A census of human soluble protein complexes. Cell 150 (5):1068–1081
21. Trahan C, Oeffinger M (2016) Targeted cross-linking-mass spectrometry determines vicinal interactomes within heterogeneous RNP complexes. Nucleic Acids Res 44(3):1354–1369

22. Hosp F et al (2015) A double-barrel liquid chromatography-tandem mass spectrometry (LC-MS/MS) system to quantify 96 Interactomes per day. Mol Cell Proteomics 14 (7):2030–2041
23. Baldwin RM, Bejide M, Trinkle-Mulcahy L, Cote J (2015) Identification of the PRMT1v1 and PRMT1v2 specific interactomes by quantitative mass spectrometry in breast cancer cells. Proteomics 15(13):2187–2197
24. Lambert JP et al (2013) Mapping differential interactomes by affinity purification coupled with data-independent mass spectrometry acquisition. Nat Methods 10(12):1239–1245
25. Doerr A (2012) Interactomes by mass spectrometry. Nat Methods 9(11):1043
26. Rees JS et al (2011) In vivo analysis of proteomes and interactomes using parallel affinity capture (iPAC) coupled to mass spectrometry. Mol Cell Proteomics 10(6):M110 002386
27. Isabelle M et al (2010) Investigation of PARP-1, PARP-2, and PARG interactomes by affinity-purification mass spectrometry. Proteome Sci 8:22
28. DeWire SM, Ahn S, Lefkowitz RJ, Shenoy SK (2007) Beta-arrestins and cell signaling. Annu Rev Physiol 69:483–510
29. Lefkowitz RJ, Rajagopal K, Whalen EJ (2006) New roles for beta-arrestins in cell signaling: not just for seven-transmembrane receptors. Mol Cell 24(5):643–652
30. Lefkowitz RJ, Whalen EJ (2004) Beta-arrestins: traffic cops of cell signaling. Curr Opin Cell Biol 16(2):162–168
31. Shenoy SK, Lefkowitz RJ (2003) Multifaceted roles of beta-arrestins in the regulation of seven-membrane-spanning receptor trafficking and signalling. Biochem J 375(Pt 3):503–515
32. Luttrell LM, Lefkowitz RJ (2002) The role of beta-arrestins in the termination and transduction of G-protein-coupled receptor signals. J Cell Sci 115(Pt 3):455–465
33. McDonald PH, Lefkowitz RJ (2001) Beta-Arrestins: new roles in regulating heptahelical receptors' functions. Cell Signal 13 (10):683–689
34. Miller WE, Lefkowitz RJ (2001) Expanding roles for beta-arrestins as scaffolds and adapters in GPCR signaling and trafficking. Curr Opin Cell Biol 13(2):139–145
35. Lefkowitz RJ, Shenoy SK (2005) Transduction of receptor signals by beta-arrestins. Science 308(5721):512–517
36. Xiao K et al (2007) Functional specialization of beta-arrestin interactions revealed by proteomic analysis. Proc Natl Acad Sci U S A 104 (29):12011–12016
37. Haas W et al (2006) Optimization and use of peptide mass measurement accuracy in shotgun proteomics. Mol Cell Proteomics 5 (7):1326–1337
38. Li X et al (2007) Large-scale phosphorylation analysis of alpha-factor-arrested Saccharomyces cerevisiae. J Proteome Res 6(3):1190–1197
39. Elias JE, Gygi SP (2007) Target-decoy search strategy for increased confidence in large-scale protein identifications by mass spectrometry. Nat Methods 4(3):207–214
40. Villen J, Beausoleil SA, Gerber SA, Gygi SP (2007) Large-scale phosphorylation analysis of mouse liver. Proc Natl Acad Sci U S A 104 (5):1488–1493
41. Bakalarski CE et al (2008) The impact of peptide abundance and dynamic range on stable-isotope-based quantitative proteomic analyses. J Proteome Res 7(11):4756–4765
42. Breitkreutz BJ, Stark C, Tyers M (2003) Osprey: a network visualization system. Genome Biol 4(3):R22
43. Luttrell LM et al (2001) Activation and targeting of extracellular signal-regulated kinases by beta-arrestin scaffolds. Proc Natl Acad Sci U S A 98(5):2449–2454
44. Bendall SC et al (2008) Prevention of amino acid conversion in SILAC experiments with embryonic stem cells. Mol Cell Proteomics 7 (9):1587–1597
45. Lu R et al (2009) Systems-level dynamic analyses of fate change in murine embryonic stem cells. Nature 462(7271):358–362
46. Subramanian A et al (2005) Gene set enrichment analysis: a knowledge-based approach for interpreting genome-wide expression profiles. Proc Natl Acad Sci U S A 102 (43):15545–15550

Part IV

Methods to Analyse Ligand Bias



Chapter 15

Quantitating Ligand Bias Using the Competitive Model of Ligand Activity

Edward L. Stahl, Frederick J. Ehlert, and Laura M. Bohn

Abstract

G protein-coupled receptors (GPCRs) can interact with both G proteins and β-arrestin proteins to propagate different signaling outputs. In some contexts, agonists may drive the receptor to preferentially engage one of these effectors over the other. Such "ligand bias" may present a means to impart pathway-selective signaling downstream of this class of receptors. In cases where physiological responses are mediated by diverse pathways, this could, in part, provide a means to refine GPCR therapeutics. Cell-based signaling assays are used to measure the potential for signaling bias in vitro, and these measures take into account potency, efficacy, and the overall capacity of the assay. However, narrow assay windows sometimes limit the confidence in estimating agonist activity, if a compound performs as a very weakly efficacious partial agonist. This lack of response in an assay hampers the ability to measure and compare potencies, and the degree of separation of an agonist's performance, between two assays. In this chapter, we describe in detail a method for the estimation of the relative activity of a partial agonist and provide a stepwise protocol for calculating bias when this case arises.

Key words G protein, β-Arrestin, Signaling, GPCR, Functional selectivity, Biased agonism, Operational model

1 Introduction

G protein-coupled receptors are seven-transmembrane spanning receptors that respond to both endogenous and exogenous ligands. Once a ligand binds to the receptor, the receptor can be "activated" or "inactivated, "terms that are reflective of what is turning on and off as well as the receptor's state prior to ligand engagement. Classically, we envision an agonist binding to the GPCR and promoting the coupling to a heterotrimeric G protein, promoting the exchange of GDP for GTP and the dissociation of the trimeric species, and subsequently stimulating the signaling cascade. GPCRs also couple to other effectors, including the ubiquitously expressed scaffolding proteins, the β-arrestins. Engagement of the receptor with a β-arrestin protein can have diverse effects, which

Mark G. H. Scott and Stéphane A. Laporte (eds.), *Beta-Arrestins: Methods and Protocols*, Methods in Molecular Biology, vol. 1957, https://doi.org/10.1007/978-1-4939-9158-7_15, © Springer Science+Business Media, LLC, part of Springer Nature 2019

can range from stabilizing signaling complexes to disrupting the interaction with G protein (reviewed in [1]). In this manner, GPCR-β-arrestin interactions could promote signaling toward some pathways while preventing further signaling via others.

Since β-arrestins and G proteins represent a highly proximal point of interaction with receptors, as well as a pivotal point in signal propagation, assays measuring an agonist's ability to engage both are often compared. Typical GPCR agonists will both produce G protein-mediated signaling and lead to β-arrestin recruitment to the receptor. However, some agonists promote one signaling pathway over another and such compounds may be what one would call a "biased agonist." Finding biased agonists becomes important when there is evidence that the desirable effects of a drug acting at a receptor are mediated by one pathway, while the adverse effects can be attributed to another pathway. Several excellent articles have been written on how to measure biased agonism [2–4]; in this book chapter we will focus on methodology for determining whether an agonist is biased when it produces very minimal efficacy in one of the signaling pathways being compared.

The term "bias" implies a comparison to a norm; it is important to establish what the normal response of the system is in the two assays that are to be compared. To obtain a set point for comparison within an assay, a "reference" agonist is chosen based on its ability to maximally stimulate the assay in question. The reference agonist should produce a maximal response in both assays being compared. In this manner, we are able to effectively normalize the effects of a test agonist to the effects of the reference agonist within an assay prior to comparing its performance between two assays (wherein effects and performance refer to both efficacy and potency). The most useful signaling assays are those in which the reference agonist produces a potent as well as maximally efficacious response, allowing for less potent agonists to be tested within a range that solubility and nonspecific effects can be avoided. It is important to keep in mind that, since the signaling effects of test compounds are being compared to the performance of a reference agonist, changing the reference agonist, or the cell-based assay, may change the bias attribute.

We analyze functional responses to determine how ligands interact with receptors. This strategy involves applying a theory that describes drug-receptor interactions and an analysis that addresses the unspecified relationship between receptor activation and the measured response. An early approach for addressing the latter problem involves applying drug-receptor theory to describe the relationship between equivalent tissue responses under different conditions (e.g., presence and absence of antagonist). An equivalent response implies an equivalent level of receptor activation, and the unknown relationship between response and receptor

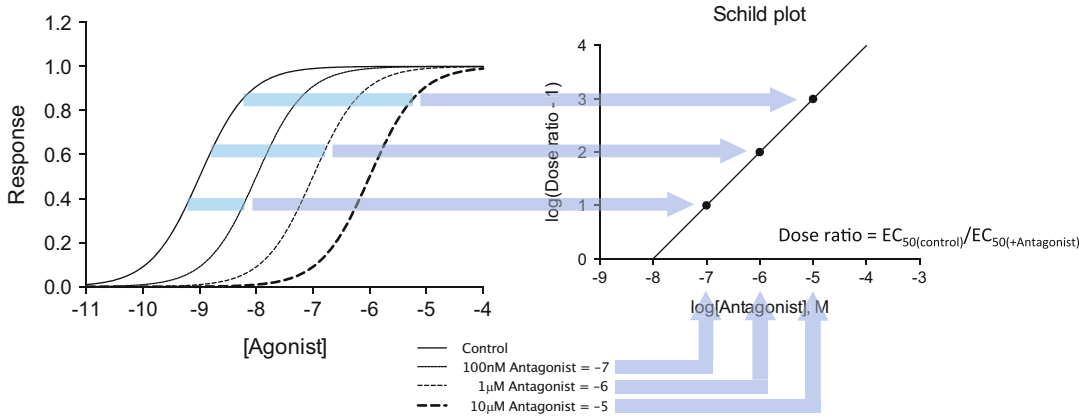


Fig. 1 *Producing a schild plot.* The Schild plot is produced by converting the degree of rightward shift, produced by the antagonist, into a linear relationship and plotting this relationship with respect to the log of the concentration of the antagonist. This figure presents an example of the process of producing and plotting these values

activation cancels out of the mathematical equality describing equivalent responses [5–7].

In the 1950s, H. O. Schild [5] used this approach to develop a method for estimating the dissociation constant of a competitive antagonist based on its ability to shift the concentration-response curve of an agonist. He showed that there is a linear relationship between the shift in the concentration-response curve produced by the competitive antagonist minus one (*shift*—1) and the concentration of the antagonist expressed relative to its dissociation constant. This can be seen graphically in the Schild plot where the dose ratio defines the degree of shift produced by the antagonist, in Fig. 1, and the *X-intercept* defines the antagonist's dissociation constant. A different expression of this effect is presented in Fig. 2 where the concentration of antagonist needed to produce 50% inhibition (the IC_{50}) depends on the concentration of agonist used to stimulate the response.

In a related approach, Stephenson defined the relationships between equiactive concentrations of a full agonist (A_1) and a partial agonist (P) and also between the full agonist (A_2) and a combination of concentrations of the full agonist (A_3) and partial agonist (P). This functional outcome is presented in a simplified form in Fig. 3. With the information from these studies, he was able to estimate the dissociation constant of the partial agonist (*see* **Note 1**) [7].

The relationship between receptor activation and response is described in the operational model as the product of intersecting hyperbolic functions [8]. In their regression equation, the function describing the formation of the agonist-receptor complex provides input to a second transducer function that generates the response.

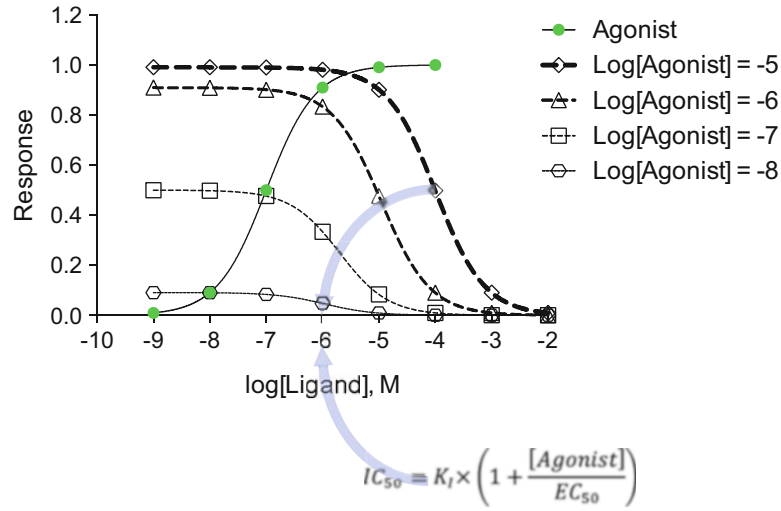


Fig. 2 *Determining antagonist affinity from inhibition curves*. The application of an agonist along with increasing concentrations of the antagonist permits the determination of the antagonist's affinity constant for the receptor. This is done, by applying the correction shown, to convert the IC_{50} into a K_I value (based on the concentration and EC_{50} of the agonist in the system)

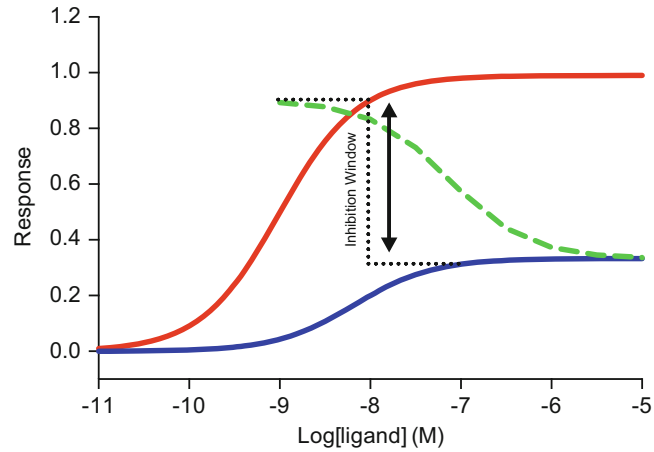


Fig. 3 *The experimental design for analyzing bias using the competitive method*. The effect of the reference agonist is presented as the most efficacious agonist. The partial agonist is only able to produce response to 0.4. The dotted curve indicates the window for the inhibition between the reference agonist and the partial agonist. The inhibition window and dotted curve describe the degree to which an agonist can displace the other agonist to change the maximum observed response

This approach accounts for nonlinear occupancy-response coupling and enables the investigator to estimate the pharmacological properties of the agonist by directly fitting the model to the observed

data. In the protocol described in this manuscript, we present a previously published method of quantitating the agonist activity of test ligands that can be applied to experimental data without prior knowledge of the occupancy-response relationship [9].

The method presented in this chapter involves measuring both the ability of the partial agonist to elicit responses and to antagonize the responses of a full agonist. This approach is specifically useful for ligands with relatively low E_{max} values. The concentration-response curves of such agonists are composed of small responses that often lack the requisite resolution to yield accurate parameters from nonlinear regression. Our approach circumvents this problem by measuring the partial agonist's ability to functionally antagonize the response produced by an ~EC_{80} of the reference agonist. The resulting competition curves span a larger range of agonist response values and yield more accurate parameters from the regression analysis. Additionally, we discuss several cases where the experimental evidence indicates that this method of analysis is not appropriate (**Note 2**). Finally, we present a simple method of plotting the difference in the relative activity of test agonists in different response pathways.

2 Materials

The methods of analysis in this chapter are designed and presented for GraphPad Prism version 6. These are also suitable for newer versions of Prism. The equations are also suitable for other software but may need changes to the syntax of the equation definition. A useful resource for understanding fitting with the operational method to analyze bias, in GraphPad Prism, is presented by van der Westhuizen et al. [10].

3 Methods

3.1 Producing Response Data Optimized to Apply the Competitive Bias Model

The experimental design for analyzing agonist activity and bias using the competitive bias model requires knowledge of the response pathways being investigated. In order to fit response data to the operational model, it is necessary to include a reference full agonist that produces a maximal response in all of the target pathways [2, 3]. This full agonist acts as a point of normalization to determine the sensitivity of the system. For example, the response produced by the reference agonist can be compared to a test agonist in two assay systems (assay 1 and assay 2). The results can then be interpreted as bias for assay 2 or low sensitivity of assay 1.

The standard method of bias analysis will produce a good quality estimate of the relative agonist activity, and bias, by using concentration-response data from a full reference agonist and test

agonists that produce moderate to full agonist activity [2, 3]. However, in the case where a test agonist is minimally efficacious in one system, the competitive approach is useful for establishing the effect of the test agonist on the receptor.

1. The experimental design for the competitive method begins by generating estimates of the concentration of a drug that gives half-maximal response (EC_{50}) and the maximal response (E_{Max}), for the reference agonist and each test agonist. The E_{Max} is a system-dependent parameter that needs to be determined in order to characterize the activity of each agonist in the experiment.
2. Based on the estimates of EC_{50} and E_{Max}, a concentration of the reference agonist should be selected that is high enough to establish an inhibition window for the test agonist to inhibit (Fig. 3). However, the selected concentration of the reference agonist cannot be excessively high or reversal of the response by the test agonist may not be possible in a reasonable concentration range. The selected concentration of the reference agonist should be co-applied with increasing concentrations of the test agonist to produce a concentration-inhibition curve for the test agonist.
3. Concentration-response curves of the reference agonist and test agonist should be produced at the same time as the concentration-inhibition curves discussed in the previous step. It is very common to normalize response data in order to compare data from different experiments. The analysis method presented here is well suited to normalized data as long as the data sets conform to a standard concentration-response relationship; a standard concentration-response relationship is one with an adequately defined baseline and maximal response as well as a sigmoidal response curve for each ligand in the response being measured.

3.2 Explanation of the Model and the Equations

Based on the concentration of the reference agonist chosen there will be a predictable rightward shift in the midpoint of the inhibition curve of the partial agonist. This produces two potential avenues of information to support the competitive nature of the two ligands. First, the distance on the abscissa between the midpoint of the partial agonist's stimulatory response curve and the midpoint of the partial agonist's inhibitory response curve is defined by the concentration of the full agonist that is to be inhibited. Second, as the concentration of partial agonist increases, its inhibitory and stimulatory curves should reach a shared asymptote if the full and partial agonists compete for the same site. The equations presented below originated in our previous publication [9] and can be used to produce best-fit values for this type of

Table 1
Parameter name, equation entry, and parameter definitions

Parameter name	Equation entry	Parameter definition
Top	Top	Maximum observed response produced in the system
Bottom	Bottom	Basal level of response of the system
$\mathrm{Log}R_{\mathrm{Reference}}$	Log$R$	The product of the τ and $K_{\mathrm{Reference}}$ parameters, of the reference agonist, from the operational model
$\mathrm{Log}K_{\mathrm{Test}}$	Log$K$BC	Log affinity constant of the test agonist
$\Delta\mathrm{Log}R_{(\mathrm{Test\text{-}Reference})}$	deltaLog$R$BC	The difference of the $\mathrm{Log}R_{\mathrm{Reference}}$ of the reference agonist and the Log$R$ of the test agonist

experimental data. These equations are adapted from the operational model of receptor signaling [8]. The parameter definitions for these equations are presented in Table 1.

For these studies, the reference agonist is fit with this equation:

$$\mathrm{Response} = \mathrm{Bottom} + \frac{E_{\mathrm{Max}}\text{-Bottom}}{1 + \left(\frac{1+10^{X}}{10^{(X+\mathrm{Log}R_{\mathrm{Reference}})}}\right)^{M}}$$

The test agonist in the Prism file is fit with a similar equation:

$$\mathrm{Response} = \mathrm{Bottom} + \frac{E_{\mathrm{Max}}\text{-Bottom}}{1 + \left(\frac{1+10^{A}+10^{(X\text{-}\mathrm{Log}K_{\mathrm{Test}})}}{10^{(A+\mathrm{Log}R_{\mathrm{Reference}})}+10^{\left(X+\mathrm{Log}R_{\mathrm{Reference}}+\Delta Log R_{(\mathrm{Test\text{-}Reference})}\right)}}\right)^{M}}$$

3.3 Entering the Data and Defining the Competitive Bias Model

1. In order to fit the data to the specific form of the model described, the data must be entered into the Prism data table in a specific order (Fig. 4). Following the experimental design instructions presented in the previous section, the X values for the data set should be expressed as the log of the molar concentration of the drug (e.g., 1 μM = −6). The resulting response data for the full reference agonist would be entered into column A of the data sheet. The response data for the test agonist concentration-response curve would be entered into column B of the data sheet. Finally, the concentration-inhibition curve data, produced by applying the test agonist on top of a defined concentration of the reference agonist, would be entered into column C of the data sheet. The concentration of the reference agonist used for inhibition should be entered in Group C. For example, in Fig. 4, Group C is titled "−8 Full Agonist + Test Agonist 1." This indicates that the concentration of reference agonist inhibited in this data set is −8 or 10 nM Full Agonist.

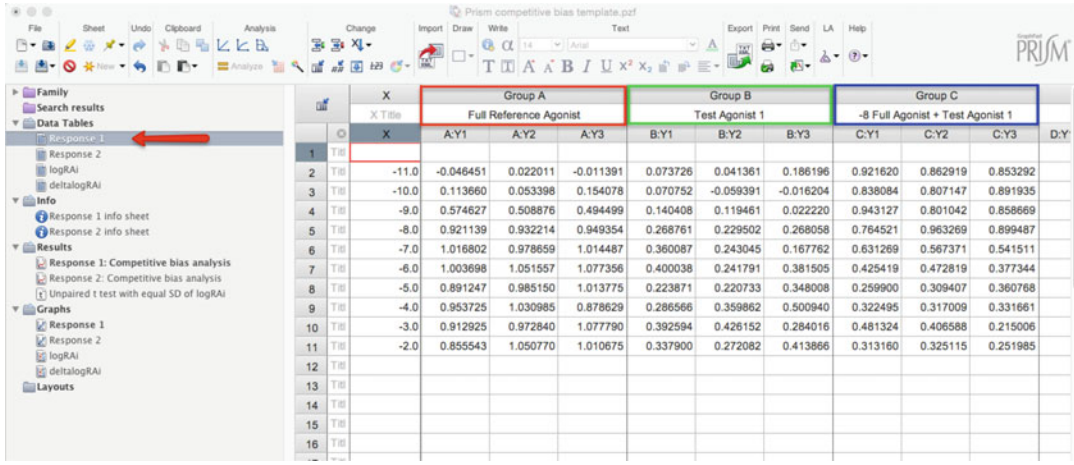


Fig. 4 *Orientation of data in Prism data sheet*. The orientation of the data on the Prism data sheet should be such that the reference agonist response data is inserted in Column A, the test agonist is in Column B, and the inhibition of the reference agonist by the test agonist is inserted in Column C. This orientation will permit the equation to appropriately handle the data as written

2. From the "Analysis" section, select Analyze and create a user-defined equation. Enter the text provided below into the equation definition section:

$$< \mathrm{A} > D = \left(\left(1 + \left(10^{(X)}\right)\right)/\left(10^{(X+\mathrm{Log}R)}\right)\right)$$
$$< \mathrm{B} > D = \left(1 + \left(10^{(X-\mathrm{Log}K\mathrm{BC})}\right)\right)/\left(10^{(X+\mathrm{Log}R+\mathrm{deltaLog}R\mathrm{BC})}\right)$$
$$< \mathrm{C} > D = \left(1 + \left(10^{(X-\mathrm{Log}K\mathrm{BC})}\right) + \left(10^{(A)}\right)\right)/\left(\left(10^{(A+\mathrm{Log}R)}\right) + \left(10^{(X+\mathrm{Log}R+\mathrm{deltaLog}R\mathrm{BC})}\right)\right)$$
$$Y = \mathrm{Bottom} + \left((E_{\max} - \mathrm{Bottom})/\left(1 + \left(D^{M}\right)\right)\right)$$

The equation is printed this way to define the column pair as Group B and Group C for the test ligand. The reason for this is that the test ligand data pair shares two parameter values that are only applied to those columns. To add additional columns (i.e., additional test ligands), a distinct column pair and the corresponding parameter definitions would need to be defined. For example, to fit two test agonists, lines <D> and <E> would need to be defined in the equation above. These additional lines include identical text to lines <B> and <C> *except* the parameters Log*K*DE and deltaLog*R*DE are defined in the new lines:

$$< \mathrm{D} > D = \left(1 + \left(10^{(X-\mathrm{Log}K\mathrm{DE})}\right)\right)/\left(10^{(X+\mathrm{Log}R+\mathrm{deltaLog}R\mathrm{DE})}\right)$$
$$< \mathrm{E} > D = \left(1 + \left(10^{(X-\mathrm{Log}K\mathrm{DE})}\right) + \left(10^{(A)}\right)\right)/\left(\left(10^{(A+\mathrm{Log}R)}\right) + \left(10^{(X+\mathrm{Log}R+\mathrm{deltaLog}R\mathrm{DE})}\right)\right)$$

More information on the specific steps for creating a user-defined model is available in the GraphPad Prism user guide [11].

3. Enter the initial parameter values by moving to the "Rules for Initial Values" tab:
   - Enter the initial parameter values for each of the parameters listed: Log*R*, Log*K*BC, A, deltaLog*R*BC, Bottom, E_{max}, and *M*. Depending on the type of data you are analyzing, these initial values may be useful:

     Set Log*R* to −1 × (Value of *X* at YMID)

     Set Log*K*BC to 1 × (Value of *X* at YMID)

     Set *A* to 1

     Set deltaLog*R*BC to 1

     Set Bottom to 1 × YMIN

     Set E_{max} to 1 × YMAX

     Set *M* to 1
4. Define the constraints that will be placed on the equation when fitting the data. It is reasonable to impose constraints similar to the ones presented below in order to analyze simple concentration-response data:
   The parameters *M*, Bottom, E_{max}, Log*K*BC, and deltaLog*R*BC can be constrained to "Shared value for all data sets".
   As a result of the specific experimental design being described in this text, one additional constraint must be applied to the model. The parameter A defines the concentration of the reference agonist that will serve as the starting point for producing the inhibition curve with the test agonist. For this purpose, the parameter A will be defined specifically for each column of data. Therefore, the parameter A should be constrained to be "Data set constant (=column title)" (*see* Subheading 3.3, **step 1**).
5. With the equation definition complete, Prism should be able to calculate the relative activity of each test agonist. The best-fit parameter values for the analysis will appear on a new analysis sheet, and curves for the analysis can be inserted onto the graph of the data. In the case where the experimental data cannot be fit by the equations, there is reason to suspect that a more complex mechanism is responsible (*see* **Note 3**).

3.4 Plotting ΔΔLogR, 95% Confidence Interval, and Calculating Bias Factor

1. The deltaLog*R*BC value for the test agonist is determined multiple times. These individual values can be used to determine if there is a difference in the mean deltaLog*R*BC value between responses. These calculations can be performed in Prism by creating a new column data sheet. The deltaLog*R*BC for each response should be entered in columns for Response 1 and Response 2 in the data sheet (Fig. 5).
2. Analyze the data using the *t* tests option under Column analyses. Specifically, the *t* test can be performed with the

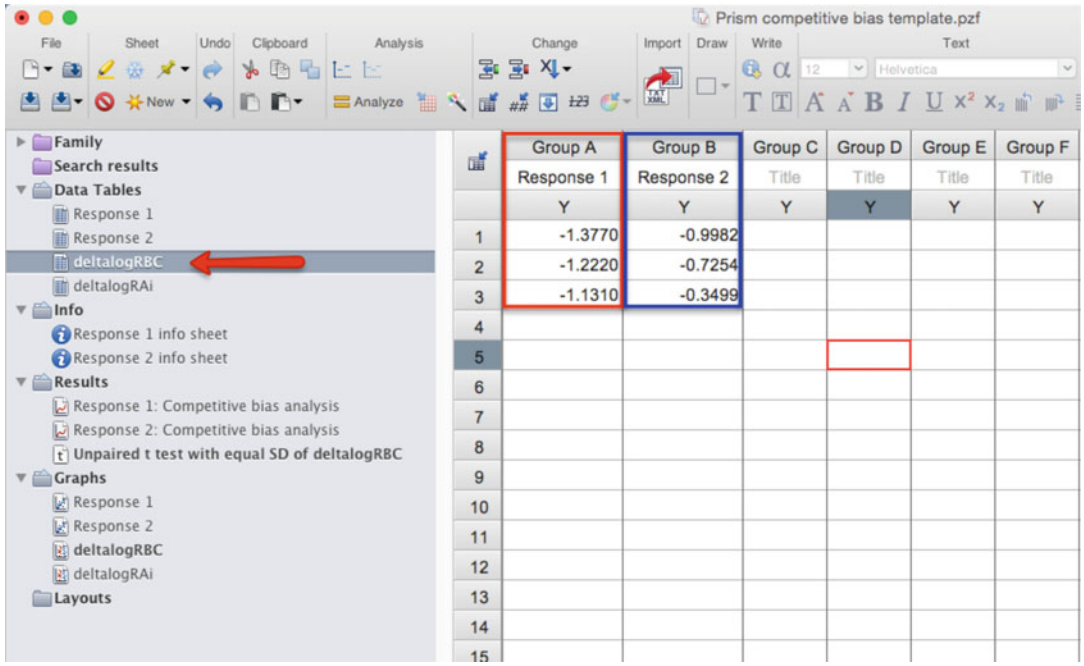


Fig. 5 *Entering ΔLogR values for comparison.* The ΔLog*R* values from multiple experiments can be entered into a column data sheet for analysis to produce the ΔΔLog*R*. Each column contains the series of ΔLog*R* values that result from the fit of individual experiments

selections indicated in Fig. 6. The results of this test present the difference of the deltaLog*R*BC values (ΔΔLog*R*; [4]). Also produced on this results sheet is the 95% confidence interval (CI) for the difference of means between the deltaLog*R*BC for Response 1 and the deltaLog*R*BC for Response 2.

3. The difference of the deltaLog*R*BC values and the 95% CI can then be copied onto a new column data sheet. On the corresponding graph for this new data sheet, plotting the median and range of the values will produce an image similar to Fig. 7. In this figure, the value for the median corresponds to the difference of means and the upper and lower edges of the box corresponds to the 95% CI for the difference of means. In this way, it is possible to graphically resent the ΔΔLog*R* or the bias of a ligand for one pathway or another.

4 Notes

1. In the simple case, the test ligand will produce the expected reversal of the response stimulated by the selected concentration of the reference agonist. This result is in agreement with a competitive interaction between the test ligand and the reference ligand at a shared binding site.

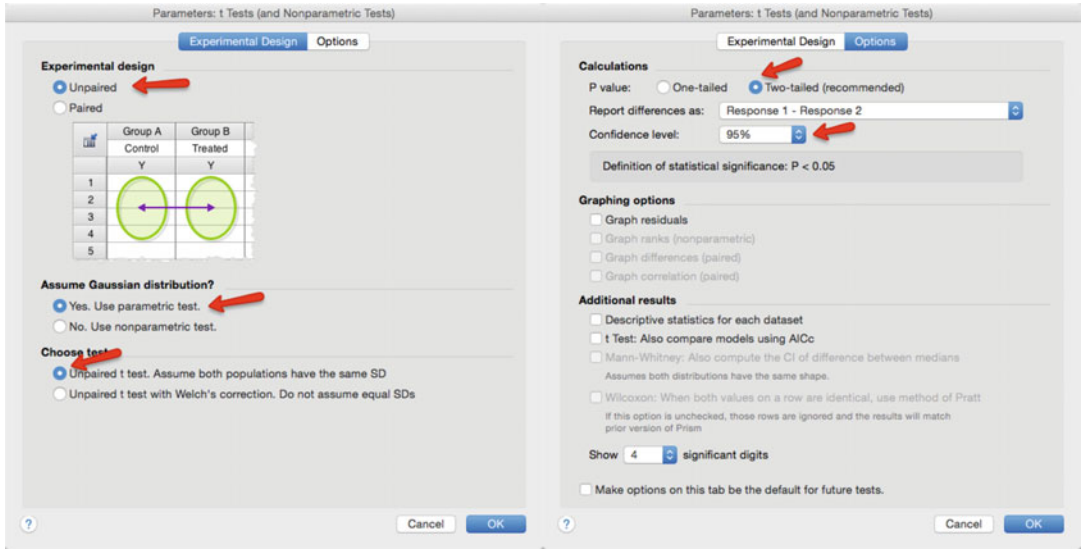


Fig. 6 *Producing the ΔΔLogR value*. The ΔΔLog*R* value is the result of the comparison of the means of the ΔLog*R* values entered in the table in Fig. 5. Using these settings in the *t*-test dialog box will produce the *difference of means* (with 95% confidence interval). This *difference of means* is the ΔΔLog*R* values used to estimate bias

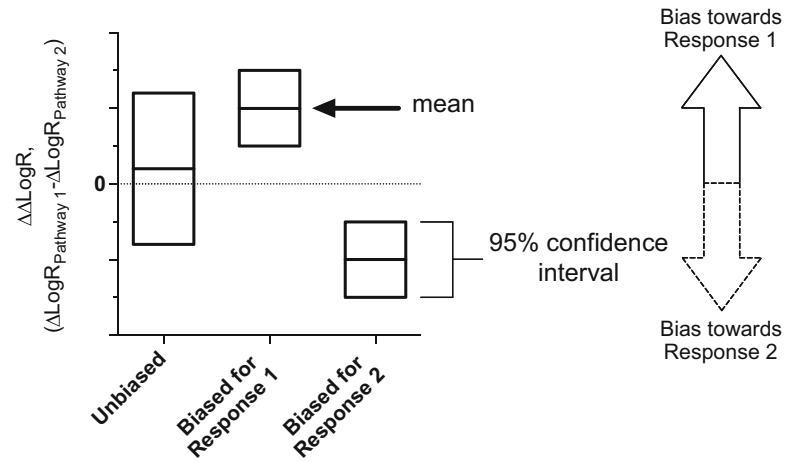


Fig. 7 *Plotting ligand bias*. The bias of a ligand can be plotted as the ΔΔLog*R* along with the upper and lower 95% confidence interval. This provides a graphical representation of ligand bias where the upper and lower limits of the boxes highlight the bias of a ligand. That is, the box does not overlap zero if the ligand is biased toward Response 1 or Response 2

2. There are a number of reasons that experimental data may not be well suited for this type of analysis. These cases are presented in Fig. 8. These three cases provide a partial list of the potential outcomes that may complicate the application of this method. It is worth presenting the cautionary note that this method is

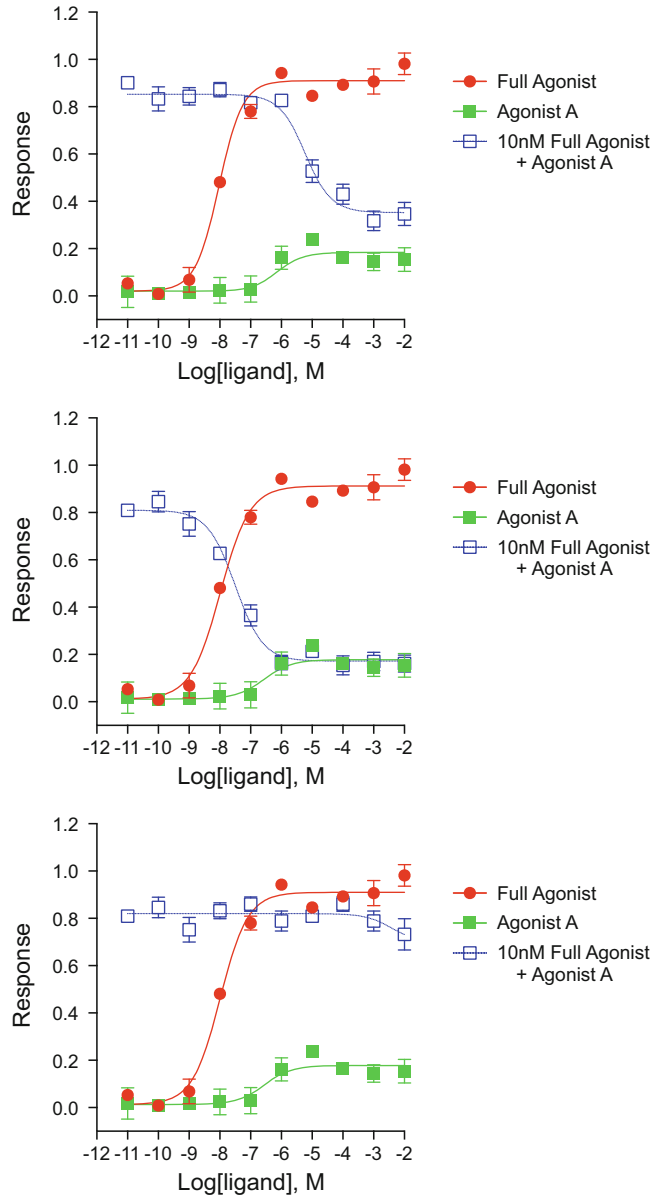


Fig. 8 Examples of complications using the competitive method of bias analysis. The first panel presents a distinct disagreement in plateau of response produced by test agonist in the absence and presence of reference agonist. The second panel presents the situation where the potency of the inhibition curve (IC_{50}) lies to the left of the potency of the stimulation curve (EC_{50}). The third panel presents little or no displacement of the full agonist by the partial agonist. Each of these scenarios suggests that a noncompetitive mechanism may be present and a more complex method might better suit the analysis of the data

suitable for analyzing competitive molecular interactions. If the analysis of experimental data with this approach produces a poor quality or ambiguous fit of the data, this may be an indication that the system needs to be optimized to produce more appropriate data. Alternatively, a different model may be more suitable for analyzing the experimental data set.

3. Additional experiments may be necessary to establish the specific reason why the experimental data was not adequately described by the competitive model. These additional experiments may provide valuable information to confirm or disprove the utility of this model or other models for analyzing the specific experimental data set [12, 13].

References

1. DeWire SM, Seungkirl A, Lefkowitz RJ, Shenoy SK (2007) β-Arrestins and cell signaling. Annu Rev Physiol 69:483–510
2. Ehlert FJ (2007) On the analysis of ligand directed signaling at G protein coupled receptors. NS Arch Pharmacol 377:549–577
3. Ehlert FJ, Griffin MT, Suga H (2011) Analysis of functional responses at G protein-coupled receptors: estimation of relative affinity constants for the inactive receptor state. JPET 338(2):658–670
4. Kenakin T, Watson C, Muniz-Medina V, Christopoulos A, Novick S (2012) A simple method for quantifying functional selectivity and agonist Bias. ACS Chem Neurosci 3 (3):193–203
5. Arunlakshana O, Schild HO (1959) Some quantitative uses of drug antagonists. Br J Pharmacol 48(14):48–58
6. Gaddum JH (1937) The quantitative effects of antagonistic drugs. J Physiol 89:7P–9P
7. Barlow RB, Scott NC, Stephenson RP (1967) The affinity and efficacy of onium salts on the frog rectus abdominis. Br J Pharmacol Chemother 31(1):188–196
8. Black JW, Leff P (1983) Operational models of pharmacological agonism. Proc R Soc Lond B Biol Sci 220(1219):141–162
9. Stahl EL, Zhou L, Ehlert FJ, Bohn LM (2015) A novel method for analyzing extremely biased agonism at G protein–coupled receptors. Mol Pharmacol 87(5):866–877
10. van der Westhuizen ET, Breton B, Christopoulos A, Bouvier M (2014) Quantification of ligand bias for clinically relevant beta2-adrenergic receptor ligands: implications for drug taxonomy. Mol Pharmacol 85 (3):492–509
11. "Entering a user-defined model into Prism." GraphPad Software, Inc. http://www.graphpad.com/guides/prism/6/curve-fitting/index.htm?reg_writing_models.htm. Accessed 1 May 2016.
12. Kenakin T, Christopoulos A (2013) Signalling bias in new drug discovery: detection, quantification and therapeutic impact. Nat Rev Drug Discov 12(3):205–216
13. Luttrell L, Kenakin T (2011) Refining efficacy: allosterism and bias in G protein-coupled receptor signaling. In: Luttrell L, Fergson S (eds) Signal transduction protocols, methods in molecular biology, vol vol. 756. Humana Press, Totowa, NJ

Part V

Methods to Study β-Arrestin Localization



Chapter 16

Methods to Investigate the Nucleocytoplasmic Shuttling Properties of β-Arrestins

Elodie Blondel-Tepaz, Thomas Guilbert, and Mark G. H. Scott

Abstract

β-Arrestins (β-arrs) were originally appreciated for the roles they play in the desensitization and internalization of G protein-coupled receptors (GPCRs). They are also now known to act as molecular scaffolds, providing control in multiple signalling pathways. Through their scaffolding properties, β-arrs dynamically regulate the activity and/or subcellular distribution of protein partners giving rise to an appropriate cellular response. There are two β-arr isoforms, namely, β-arr1 and β-arr2, which share high sequence homology and structural conservation. While the β-arrs often display conserved overlapping roles, decisive differences between the isoforms also exist. A striking example of this is the subcellular distribution of the β-arr isoforms. While β-arr1 is distributed both in cytoplasmic and nuclear compartments, β-arr2 displays an apparent cytoplasmic distribution. Both β-arrs are actively imported into the nucleus, but β-arr2 is constitutively exported by a leptomycin B-sensitive pathway due to a nuclear export signal in its C-terminus that is absent in β-arr1. β-arr2 therefore undergoes constitutive nucleocytoplasmic shuttling enabling the displacement of nuclear binding cargoes, such as Mdm2. Here, we describe methods to explore the differential nucleocytoplasmic shuttling capacities of the β-arrs.

Key words β-Arrestin, Nucleocytoplasmic trafficking, Nuclear export signal, Mdm2, p53

1 Introduction

Initially appreciated for the roles they play in the regulation of G protein-coupled receptors (GPCRs), the β-arrestins (β-arr1 and β-arr2) are also known to act as scaffolding platforms that control multiple signalling pathways [1, 2]. Through their scaffolding properties, β-arrs dynamically regulate the activity and/or subcellular distribution of protein partners giving rise to an appropriate cellular response [2–4]. While the β-arrs often display conserved overlapping roles, important differences between the isoforms also exist. As β-arr1 and β-arr2 share high sequence homology and structural conservation, these isoform-specific differences are often due to discrete molecular changes. For example, β-arr1 contains a phosphorylation site, in its C-terminal regulatory domain, at

Mark G. H. Scott and Stéphane A. Laporte (eds.), *Beta-Arrestins: Methods and Protocols*, Methods in Molecular Biology, vol. 1957, https://doi.org/10.1007/978-1-4939-9158-7_16, © Springer Science+Business Media, LLC, part of Springer Nature 2019

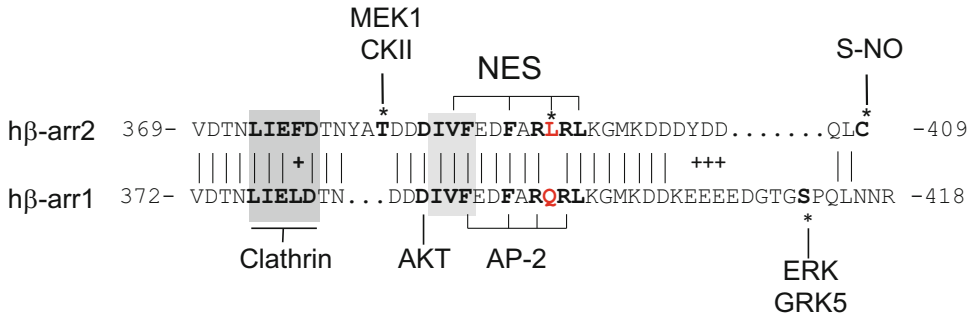


Fig. 1 Primary sequence comparison of the C-terminal regions of hβ-arr2 and hβ-arr1. Sequence alignment of the last 40 amino acids of human β-arr2 (top line) with human β-arr1 (bottom line). Functional residues conserved between β-arrs are indicated in bold. Isoform-specific functional residues are indicated in bold with an asterisk for β-arr2 and β-arr1. These include phosphorylation [5–8] and S-nitrosylation [17] sites that are implicated in GPCR-triggered signalling/trafficking events. The one amino acid difference that accounts for the presence of a NES in β-arr2 and its absence in β-arr1 is indicated in red [9, 10]. Grey shading indicates the clathrin-binding domain [18] and IVF motif that is involved in conformational change/endocytic function [19–21]. The residues implicated in AKT binding [22] and the AP-2 binding site are in bold [23, 24]

Ser412 that is absent in β-arr2 (Fig. 1). Phosphorylation of this site on β-arr1 by ERK or GRK5 plays a key role in the control of G protein-independent signalling to Src [5, 6]. Likewise, β-arr2 contains a carboxy-terminal phosphorylation site at Thr383 [7, 8] that is absent in β-arr1 (Fig. 1). MEK-dependent phosphorylation of this site is involved in GPCR-triggered β-arr-dependent ERK activation [7]. Perhaps one of the most striking differences is the subcellular distribution of the β-arr isoforms [9, 10]. Whereas β-arr1 presents a distribution between the nucleus and cytoplasm, β-arr2 shows an apparent cytoplasmic distribution at steady state. Both β-arrs are actively imported into the nucleus [9, 11], but β-arr2 is constitutively exported by a leptomycin B-sensitive pathway due to a nuclear export signal (NES) in its C-terminus (Fig. 1) that is absent in β-arr1 [9, 10]. This is due to a single amino acid change: Leu394 in human β-arr2 and Gln394 in human β-arr1 (Fig. 1). Substitution to the corresponding amino acid in the other isoform by mutagenesis (i.e., Leu394Gln in β-arr2 and Gln394Leu in β-arr1) results in "rewiring" of the distribution phenotype, with β-arr2ΔNES(Leu394Gln) accumulating in the nucleus and β-arr1+NES(Gln394Leu) displaying a prominent cytoplasmic localization [9, 10]. The nucleocytoplasmic shuttling function of β-arr2 serves to displace nuclear partners such as Mdm2, JNK3, and β-arr1 from the nucleus to the cytoplasm [9, 10, 12, 13]. In the case of Mdm2, its delocalization results in increased p53 stability in the nucleus and a p53-dependent cell cycle arrest in G_2/M [12] (Fig. 2). In contrast, following chronic stimulation of the β2-adrenergic receptor (β2-AR), nuclear β-arr1 scaffolds Mdm2 to p53, facilitating the ubiquitination and degradation of p53, which compromises genome integrity [14] (Fig. 2).

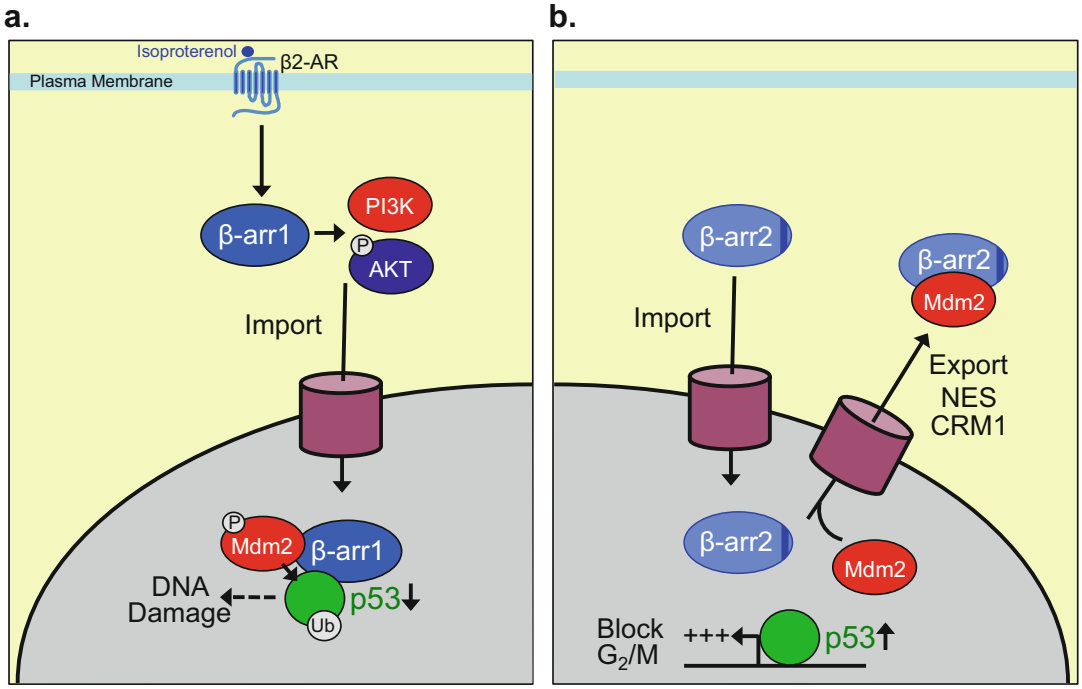


Fig. 2 Effects of β-arr1 and β-arr2 on the Mdm2/p53 signalling axis. (**a**) Following prolonged stimulation of the β2-AR, β-arr1 promotes AKT-mediated activation of Mdm2 (p-Mdm2). β-arr1 subsequently also acts as a nuclear scaffold promoting Mdm2 binding to p53, facilitating the ubiquitination and degradation of p53, which contributes to DNA damage [14]. (**b**) β-arr2 undergoes persistent nucleocytoplasmic shuttling at steady state due to active nuclear import and the presence of a NES in its regulatory C-terminal tail [9, 10]. This coupled with its oligomerization (not shown) permits the relocalization of Mdm2 from the nucleus to the cytoplasm, enhancing p53 levels/activity in the nucleus to promote a block in the cell cycle at G_2/M [12]

Here, we provide detailed methods to investigate β-arr nucleocytoplasmic shuttling function by (1) indirect immunofluorescence of native untagged proteins, (2) direct visualization of β-arr2 using YFP-tagged β-arr2, (3) nuclear binding partner Mdm2 displacement by β-arr2 in live cells using mCherry-tagged β-arr2 fusions and GFP-Mdm2, and (4) a one-hybrid genetic assay, using mLexA-GAL4AD-β-arr2 fusions in yeast cells to assess nuclear import.

2 Materials

2.1 Cell Lines and Yeast Strain

1. Human Embryonic Kidney 293-T (HEK-293 T) cell line.
2. HeLa human cervical cancer cell line.
3. *Saccharomyces cerevisiae* L40 reporter strain containing the two LexA-inducible genes, *HIS3* and *LacZ*.

2.2 Plasmids

1. Plasmids used for indirect immunofluorescence: pcDNA3.1-hβ-arr1, pcDNA3.1-hβ-arr1-Q394L(+NES), pcDNA3.1-hβ-arr2, pcDNA3.1-hβ-arr2-L394A(ΔNES) (*see* **Note 1**).
2. Plasmids used for direct fluorescence: pmCherry, pmCherry-hβ-arr2, pmCherry-hβ-arr2ΔNES, pYFP-hβ-arr2, pGFP-Mdm2.
3. The pNIA (Nuclear Import Assay) plasmids [15] containing modified LexA-Gal4AD (mLexA-Gal4AD) protein fusions (*see* **Note 2**): pNIA-VirE2 contains the agrobacterium protein VirE2 with no NLS; pNIA-IN contains the integrase gene from HIV-1, which is actively imported into the nucleus; pNIA-rβ-arr2 and pNIA-rβ-arr2ΔNES [9].

2.3 Cell Culture and Transfection

1. Dulbecco's modified Eagle's medium (DMEM), 4.5 g/L glucose, 4 mM glutamine, and 1 mM pyruvate, supplemented with 10% (v/v) fetal bovine serum, 100 U/mL penicillin, and 0.1 mg/mL streptomycin.
2. 0.05% Trypsin-EDTA solution.
3. Opti-MEM™ (Life Technologies).
4. Round 12 mm glass coverslips and 70% ethanol to sterilize them.
5. Six-well plates for cell culture.
6. GeneJuice® transfection reagent (Novagen).
7. Leptomycin B (LMB): LMB is dissolved in 70% methanol at a concentration of 90 μM (4500× stock solution) and stored at −20 °C.

2.4 Reagents for Imaging β-Arrs in Live Cells and by Indirect Immunofluorescence in Fixed Cells

1. DMEM without phenol red (DMEM w/o PR), containing 25 mM HEPES, for live cell imaging.
2. IBIDI μ-Slide 4 well ibiTreat: #1.5 polymer coverslip, tissue culture treated, sterilized, and IBIDI μ-Dish 35 mm, high Glass Bottom dishes (Biovalley) for live cell imaging.
3. 4% paraformaldehyde (PFA) (v/v).
4. Phosphate-buffered saline (PBS 1×).
5. PBS-1% bovine serum albumin (BSA) solution.
6. 50 mM NH_4Cl in PBS.
7. Triton X-100.
8. Mowiol mounting medium: 2.4 g Mowiol 4–88, 6 g glycerol, 6 mL of dH_2O, 12 mL 0.2 M Tris–HCl (pH 8.5), 2.5% DABCO. Add the Mowiol and glycerol together and mix, then add dH_2O and leave several hours at room temperature (RT). Add the Tris–HCl and heat to 50 °C with mixing, and clarify by centrifugation at 5000 × *g* for 10 min. Then add DABCO to reduce fluorescence fading. Prepare 1 mL aliquots and store at −20 °C (*see* **Note 3**).

9. Antibodies (Cell Signaling Technology): β-arr1 (D7Z3W) XP® rabbit monoclonal antibody, β-arr2 (C16D9) XP® rabbit monoclonal antibody.
10. 20 mM solution of Hoechst 33342, (2,5′-bi-1 h-benzimidazole, 2′-(4-ethoxyphenyl)-5-(4-methyl-1-piperazinyl)-trihydrochloride) or NucBlue® live ReadyProbes® Reagent (Molecular Probes) for live cell imaging.
11. Rhodamine-conjugated goat anti-rabbit immunoglobulin G.
12. Fluorescence inverted microscope Leica DMI6000 with sCMOS camera (ORCA flash 4.0 LT Hamamatsu) or equivalent.
13. Spinning disk confocal imaging system (CSU-X1, Yokogawa) based on an inverted Leica DMI6000 with a CoolSNAP HQ2 camera (Photometrics), equipped with a 63× PL APO OIL objective and a heated control chamber to maintain cells at 37 °C for live imaging during kinetic experiments, or equivalent.
14. Reverse-action tweezers (*see* **Note 4**).
15. Parafilm.
16. Glass slides.
17. MetaMorph 7.7.7 (Molecular Devices) and ImageJ 1.51 software (https://imagej.nih.gov/ij/) with StackReg plugin (http://bigwww.epfl.ch/thevenaz/stackreg/) for image analysis (*see* **Note 5**); in-house "TimeLapseCytoNucRatio" ImageJ routine (*see* **Note 6**); Prism software to plot data.

2.5 Yeast Culture, Transformation, and Assay Reagents

1. YPD: 10 g yeast extract/L, 20 g peptone/L and 20 g dextrose/L. Autoclave.
2. YPD agar (YPDA): as YPD supplemented with 20 g/L agar. Autoclave, and allow to cool to 55 °C before pouring plates.
3. Single and double dropout complete supplement mixture (CSM; MP Biomedicals). CSM-Trp and CSM-Trp-His.
4. DOBA dropout base with agar (DOBA) synthetic defined medium (MP Biomedicals). Add appropriate CSM dropout, autoclave, and cool to 55 °C before pouring plates.
5. Lithium buffer: 0.1 M LiAc, 10 mM Tris–HCl, 1 mM EDTA, pH 7.5. Autoclave.
6. 40% PEG-3350 (polyethylene glycol) prepared with sterile dH_2O. Warm to 50 °C to aid the PEG go into solution. Once cooled, filter sterilize.
7. Sonicated 10 mg/mL salmon sperm carrier DNA. Boil in water bath for 20 min and then cool on ice prior to use.
8. Replica plating tool with locking ring for use with 90 to 100 mm petri dishes (VWR International).

9. Sterile velveteen squares (15.2 cm × 15.2 cm) for replica plating of yeast (VWR International).
10. Sterile round nitrocellulose (NC) filter papers and 3 MM Whatman filter papers for β-galactosidase (β-gal) assay.
11. Z-buffer: 16.1 g/L $Na_2HPO_4{\cdot}7H_2O$, 5.5 g/L $NaH_2PO_4{\cdot}H_2O$, 0.75 g/L KCl, 0.246 g/L $MgSO_4{\cdot}7H_2O$. Adjust pH to 7.0 and autoclave. Store at room temperature for up to 1 year.
12. 100 mg/mL X-gal (5-bromo-4-chloro-3-indolyl-β-D-galactopyranoside) in N′-N′-dimethylformamide (DMF). Store at −20 °C.
13. 2-mercaptoethanol as 14.3 M pure liquid stock. Store at 4 °C.
14. Sterile 2 mm glass beads for plating yeast.

3 Methods

3.1 Detection of β-Arr Nucleocytoplasmic Shuttling by Immunofluorescence

1. Sterilize 12 mm round glass coverslips with 70% ethanol and let air-dry under the cell culture hood in a sterile culture dish.
2. Place two to four coverslips per well of a six-well plate (*see* **Note** 7). The number of cells seeded per well depends on each cell line, based on cell size and growth rate. In the case of HeLa cells, seed 150,000 cells per well of a six-well plate in 2 mL of complete DMEM.
3. The cells are subsequently cultured overnight in a cell culture incubator at 37 °C in a humidified atmosphere of 95% air, 5% CO_2. The cells should be about 40–50% confluent the day of the transfection. HeLa cells are transfected with 1 μg of plasmids encoding untagged hβ-arr1, hβ-arr1Q394L(+NES), hβ-arr2, and hβ-arr2ΔNES(L394A) per well of a 6-well plate using GeneJuice®. A ratio of 3 μL GeneJuice® to 1 μg of DNA is used. The transfection conditions should be determined empirically for each new experimental setup.
4. The following day, add LMB at a final concentration of 20 nM, or methanol vehicle control, to the cells and incubate for 1 h in the cell culture incubator.
5. Following the 1 h incubation period, aspirate the media and wash the cells twice with 1× cold PBS (2 mL/well).
6. Aspirate the PBS and immediately add 1 mL of 4% PFA to each well, for 15 min at RT to fix the cells.
7. Aspirate the fixative and rinse each well twice with 2 mL of PBS.
8. Add 1 mL of 50 mM NH_4Cl-PBS per well and incubate for 10 min to quench free aldehyde groups.
9. Aspirate the NH_4Cl-PBS solution and wash the wells twice with 1 mL of PBS.

10. To permeabilize the cells, add 1 mL 0.1% Triton X-100 (in PBS-1%BSA) to each well and wait for 15 min.
11. Prepare primary anti-β-arr1 and anti-β-arr2 antibodies (Subheading 2.4, **item 9**) by diluting 1 in 200 in PBS-1%-BSA blocking buffer.
12. Wash the wells twice with 1 mL of PBS-1%-BSA, incubating 5 min each time.
13. Cut a square of Parafilm, and secure in the bottom of a humidified chamber using tape (*see* **Note 8**).
14. Deposit a 40 μL drop of diluted anti-β-arr1 or anti-β-arr2 antibody per coverslip to be assessed on the Parafilm square.
15. Use tweezers to remove the coverslip from the well, remove excess fluid on tissue paper (to avoid further antibody dilution) and place gently with cells facing down on the drop of antibody.
16. Incubate for 1 h at RT or overnight at 4 °C.
17. Gently lift the coverslips up from the Parafilm with the tweezers, and place cell side up in the wells of the six-well plate containing 1 mL PBS-1%-BSA.
18. Wash the cells twice with 1 mL of PBS-1%-BSA, incubating 5 min each time.
19. Deposit a 40 μL drop of the secondary rhodamine-conjugated goat anti-rabbit IgG antibody diluted 1 in 500 in PBS-1% BSA on a clean piece of Parafilm.
20. As in **step 15**, remove excess fluid on the coverslip with tissue paper and place it gently with cells facing down on the drop of secondary antibody.
21. Incubate for 1 h at RT in the dark.
22. Gently lift the coverslips up from the Parafilm with the tweezers and place cell side up in the wells of the six-well plate containing 1 mL PBS-1% BSA.
23. Wash the cells twice with 1 mL of PBS-1% BSA, incubating 5 min each time.
24. Wash the cells with 1 mL of PBS, incubating 5 min.
25. Incubate 5 min with Hoechst 33342 diluted 1 in 12,000 in PBS.
26. Wash the cells twice with 1 mL of PBS, incubating 5 min each time.
27. Apply 5 μL of Mowiol-based mounting medium directly on a clean glass slide.
28. Take the coverslips from the six-wells, drain excess fluid, and mount one by one on the drops of mounting medium. Remove excess mounting medium gently with tissue paper. Mowiol-based mounting medium will harden with time (*see* **Note 9**).

29. Acquire fluorescence images with an inverted Leica DMI6000 microscope equipped with a 63× immersion oil objective and sCMOS camera or equivalent microscope system. Excitation and emission filters with 340–380 nm band-pass excitation, 400 nm dichroic mirror, 450–490 nm band-pass emission (for Hoechst), and 530–560 nm band-pass excitation, 565 nm dichroic mirror, and 572–647 nm band-pass emission (for rhodamine).
30. Images are acquired with MetaMorph, with binning set at one, exported as 16-bit TIFF files, and analyzed using ImageJ. Representative images are shown in Figs. 3 and 4 (*see* **Note 10**).

3.2 Live Cell Kinetic Imaging of YFP-β-Arr2 Distribution

1. Seed HeLa cells at a density of 50,000 cells per IBIDI μ-dish 35 mm, high Glass Bottom dish in 2 mL of complete DMEM.

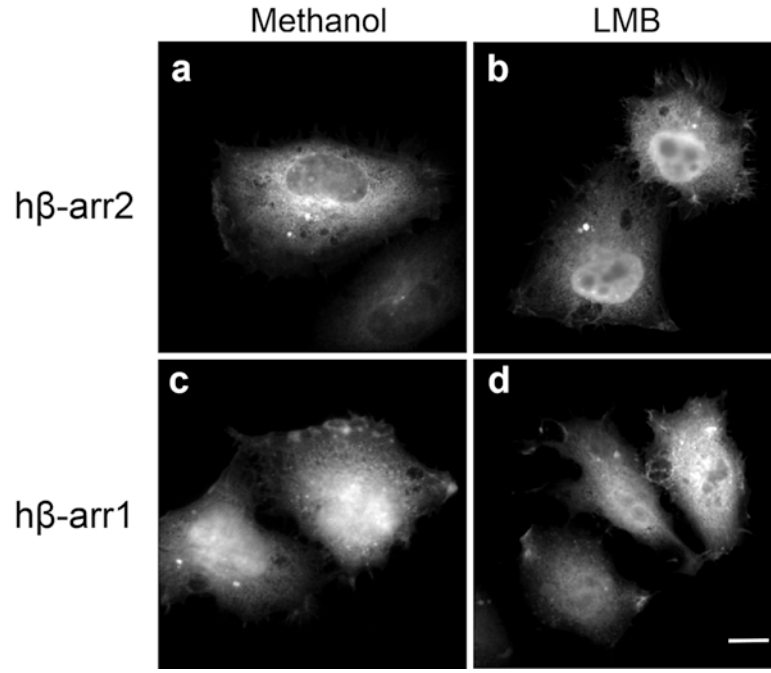


Fig. 3 LMB reveals constitutive nucleocytoplasmic shuttling of human β-arr2. HeLa cells transiently transfected with plasmids encoding untagged hβ-arr2 (**a** and **b**) or hβ-arr1 (**c** and **d**) were incubated with methanol (vehicle control) (**a** and **c**) or 20 nM LMB (**b** and **d**) during 1 h at 37 °C, then fixed and processed for fluorescence microscopy. β-arrs were detected using rabbit monoclonal anti-β-arr1 or anti-β-arr2 antibodies, followed by goat anti-rabbit IgG antibody conjugated to rhodamine. The cells were observed using an epifluorescence microscope. Scale bar, 10 μm

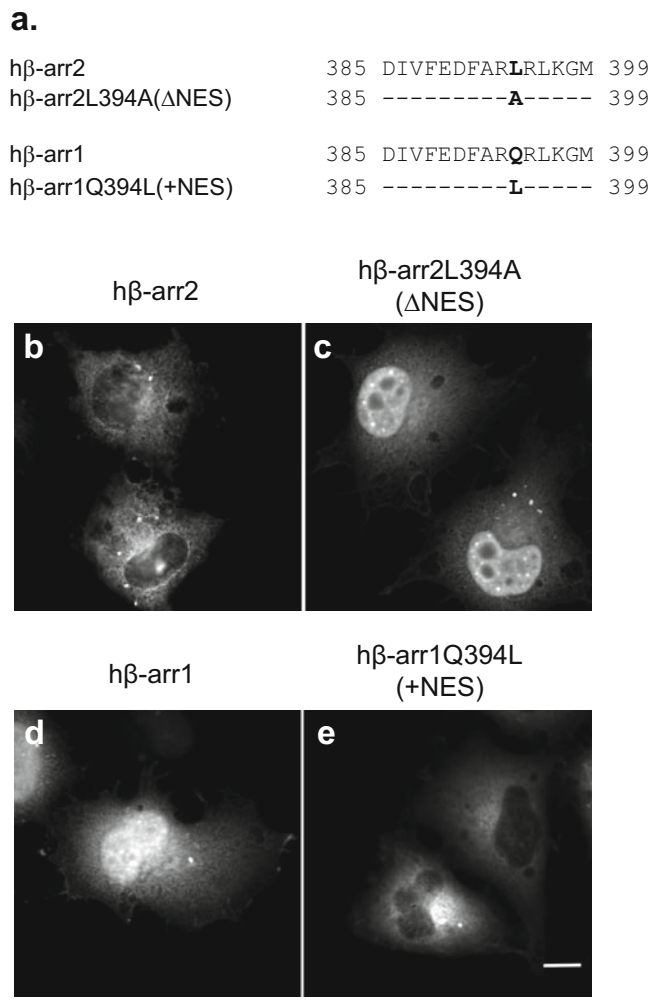


Fig. 4 Mutagenesis of individual amino acids to engineer nuclear export loss of function in human β-arr2 and nuclear export gain of function in human β-arr1. (**a**) The 385/399 region from hβ-arr2 is compared with the corresponding 385/399 region from hβ-arr1. Residues that have been replaced by Ala (A) or Leu (L) are indicated. HeLa cells expressing plasmids encoding untagged hβ-arr2 (**b**), hβ-arr2ΔNES (**c**), hβ-arr1 (**d**), or hβ-arr1Q394L (**e**). β-arrs were detected using rabbit monoclonal anti-β-arr1 or anti-β-arr2 antibodies, followed by goat anti-rabbit IgG antibody conjugated to rhodamine. The cells were observed using an epifluorescence microscope. Scale bar, 10 μm

2. Cells are subsequently incubated overnight and then transfected as described in Subheading 3.1, **step 3** with 1 μg of plasmid encoding YFP-hβ-arr2.
3. The day after the transfection, turn on the temperature control devices of the heated microscope chamber at least 6 h before any data acquisition, to ensure that all parts of the microscope are equilibrated to 37 °C.

4. Deposit a small drop of preheated immersion oil on the objective 5–10 min before installing the cells contained in the dish on the microscope stage.
5. Prepare cells for imaging. Carefully aspirate the media and wash the cells once with 1 mL of preheated DMEM w/o PR, containing 25 mM HEPES. Aspirate again and then gently overlay the cells with 2 mL of the same medium. Install the dish without the lid on the microscope stage.
6. Acquire images with a spinning-disk confocal microscope equipped with a 63× oil objective, an appropriate light source, and filter set for the fluorescent protein of choice (*see* Subheading 2.4, **item 13**). Excitation for GFP measurement uses 491 nm laser, coupled with 500 nm dichroic mirror, and 506–545 nm band-pass emission filter.
7. Find a cell or a group of cells that have been adequately transfected. Select an image plane through the cell center that provides good definition of the nucleus and surrounding cytoplasm.
8. Initiate image acquisition in time-lapse mode and take images every 3 min.
9. After the first couple of control images, add LMB very carefully just above the cells, in a 20 μL volume, to give a final concentration of 20 nM. Image cells for 90 min (*see* **Note 11**). Figure 5a shows a representative time-lapse experiment.
10. Images are acquired with MetaMorph with binning set at two, exported as 12-bit TIFF files, and analyzed using ImageJ.

3.3 Image Analysis of YFP-β-Arr2 Nucleocytoplasmic Partitioning Using a Homemade ImageJ Routine

The aim of this ImageJ routine is to quantify the relative levels of YFP-hβ-arr2 fluorescence distributed between the cytoplasm and nucleus as a function of time in the presence of LMB. StackReg plugin is needed (*see* **Note 5**).

1. Launch the "TimeLapseCytoNucRatio" macro (*see* **Note 6**), and select the folder containing raw time-lapse image data (TIFF files), one image per time acquisition. A recursive alignment of the stack images is automatically processed. Subsequently, the maximum and minimum intensity projection images are generated.
2. Place the first background circle on the image background around the cells. This step is repeated twice to determine a mean background level.
3. Now, indicate the number of cells to be analyzed in the field.
4. Using the maximum intensity projection image, manually trace cell outline of the first cell to be analyzed. Click OK.

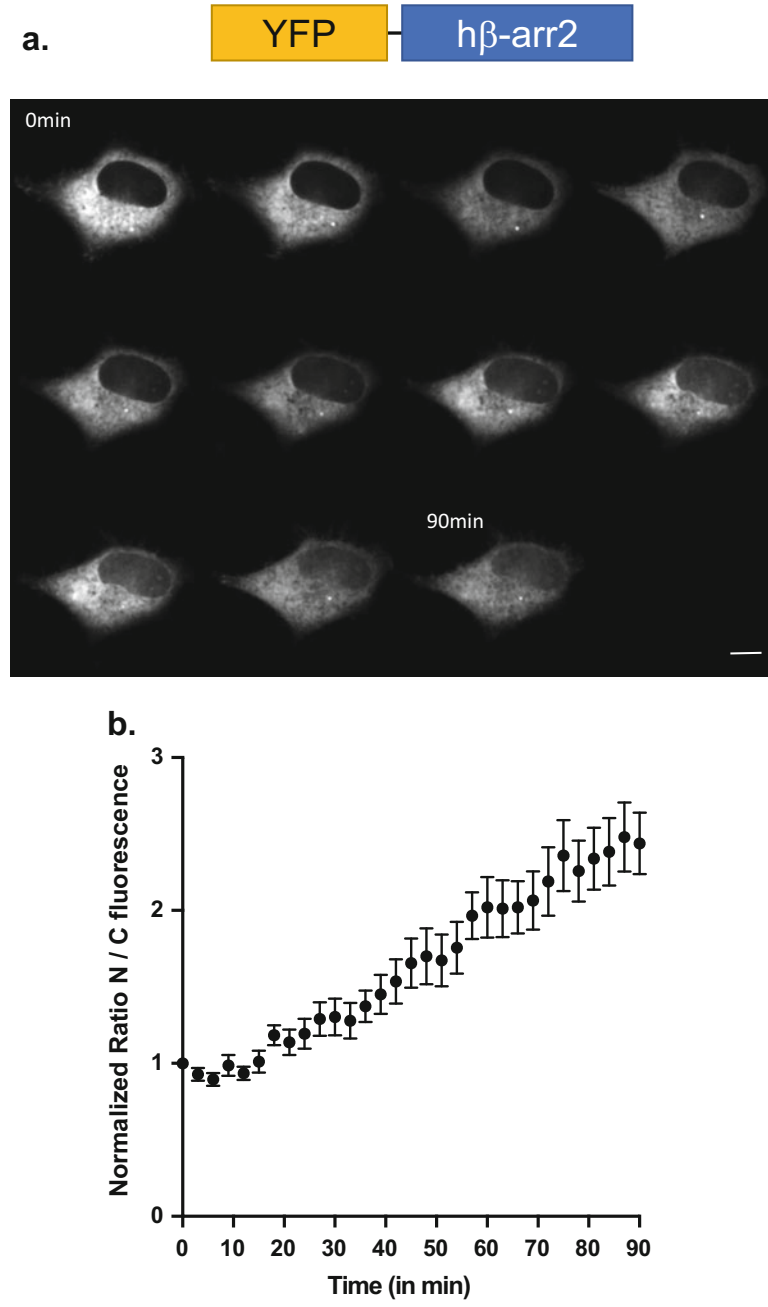


Fig. 5 Kinetic of human β-arr2 nuclear accumulation in the presence of LMB in live cells (**a**) Schematic representation of YFP-hβ-arr2 construct. Direct visualization of YFP-hβ-arr2 nuclear accumulation in a live HeLa cell in the presence of 20 nM LMB. Images were acquired every 3 min over a 90-min period, using a spinning disk confocal microscope equipped with a 37 °C heated control chamber. Images every 9 min are displayed. Scale bar, 10 μm. (**b**) Quantification of nine cells using the ImageJ plugin described in Subheading 3.3. Data represent mean ± SEM

5. Using the minimum intensity projection image, manually trace cell outline of the nucleus of the same cell. Click OK. The analysis of this cell is now finished.
6. Manually adjust the cell and nucleus regions of interest on the individual images in the stack. This ensures the outlines are the best possible fit over the course of the time lapse.
7. Repeat **steps 4–6** for all cells to be analyzed in this field.
8. Average intensities measured from **steps 2**, **4**, and **5** (time-lapse images) are automatically calculated and saved for each cell as a text file in the same folder as selected in **step 1**. Subtract the mean background from the cytoplasmic (cyto) and nuclear (nuc) values. The ratio of nuclear to cytoplasmic fluorescence can then be calculated using the background-subtracted values. Figure 5b shows the quantification of nine cells using this method plotted using Prism.

3.4 Monitoring GFP-Mdm2 Cytoplasmic Redistribution by mCherry-β-Arr2 in Live Cells

1. Plate HEK-293 T cells at a density of 25,000 cells per well of a μ-Slide 4-well ibiTreat in 700 μL of complete DMEM.
2. Cells are transfected as described in Subheading 3.1, **step 3** with 0.25 μg of plasmids encoding mCherry, mCherry-hβ-arr2 wt, or mCherry-hβ-arr2ΔNES and 0.05 μg of GFP-Mdm2 (*see* **Note 12**).
3. Twenty-four hours after transfection, prepare the cells for imaging. Add 50 μL of NucBlue® Live ReadyProbes® Reagent per well directly in the media, and incubate for 5 min in the cell culture incubator.
4. Aspirate the media carefully and wash the cells once with 700 μL of preheated DMEM w/o PR containing 25 mM HEPES. Aspirate again and add 700 μL of the same media (*see* **Note 13**).
5. Install the cells contained in the μ-Slide on the microscope stage.
6. Acquire images with a spinning disk confocal microscope as described in Subheading 2.4, **item 13**. For DAPI measurement, use 405 nm laser excitation, 405 nm dichroic mirror, and 417–477 nm band-pass emission filters; for GFP, use 491 nm laser excitation, 500 nm dichroic mirror, and 506–545 nm band-pass emission filters; and for mCherry measurement, use 561 nm laser excitation, 568 nm dichroic mirror, and 573–637 nm band-pass emission filters.
7. Images are acquired with MetaMorph with binning set at two, exported as 12-bit TIFF files, and analyzed using ImageJ. GFP-Mdm2 and Cherry/Cherry-β-arr2 images are shown in Fig. 6a and corresponding line traces performed using ImageJ in Fig. 6b.

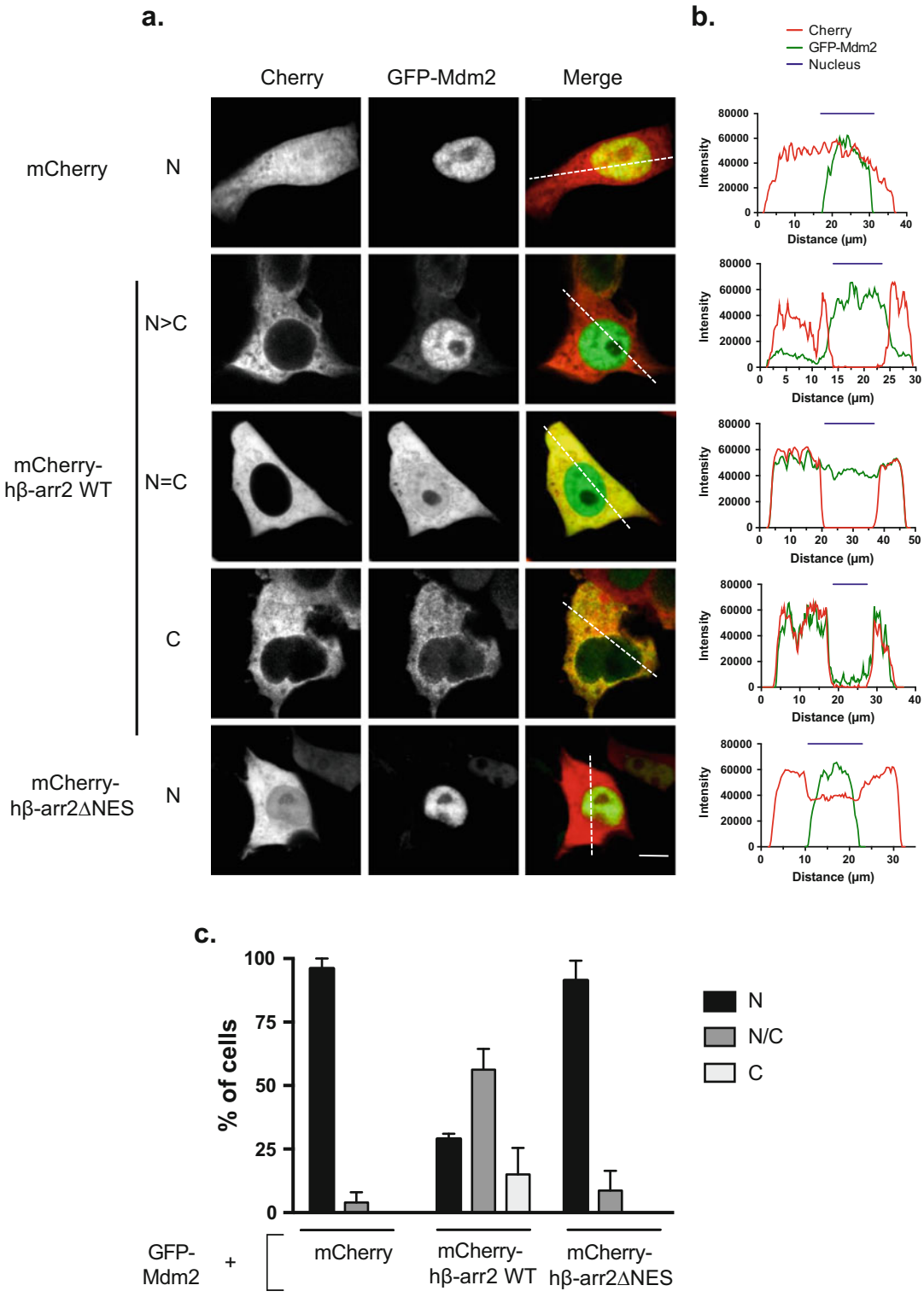


Fig. 6 Monitoring Mdm2 cytoplasmic relocalization by human β-arr2. (**a**) Live HEK cells expressing mCherry, mCherry-hβ-arr2, or mCherry-hβ-arr2ΔNES (left column) and GFP-Mdm2 constructs (middle column) were directly imaged in IBIDI μ-Slide multi-well dishes using a spinning disk confocal microscope. Merged images

8. GFP-Mdm2 displacement can be scored manually by counting the number of co-transfected Cherry/GFP-Mdm2 or Cherry-hβ-arr2/GFP-Mdm2 expressing cells with a nuclear (N) Mdm2 distribution, a partial cytoplasmic (N/C) Mdm2 distribution, and completely displaced (C) Mdm2 distribution as shown in Fig. 6c (*see* **Note 14**) [12].

3.5 Yeast Transformation for Nuclear Import Assay

1. Inoculate 50 mL of YPD, in a 500 mL conical flask, with L40 yeast (*see* **Note 15**) and incubate overnight at 30 °C with agitation (180 rpm).
2. The following day, dilute the saturated culture to an optical density (OD 600 nm) of 0.2 in a volume of 100 mL YPD.
3. Agitate at 30 °C (180 rpm) for 2–3 h until OD 600 nm is between 0.5 and 0.6, indicating log-phase growth.
4. Decant culture into sterile 50 mL tubes and centrifuge at 2200 × *g* at RT for 5 min.
5. Discard supernatant and wash/pool pellets from both tubes with 50 mL lithium buffer.
6. Centrifuge 2200 × *g* at RT for 5 min.
7. Discard supernatant.
8. Resuspend yeast pellet in 2 mL lithium buffer.
9. Agitate at 30 °C (180 rpm) for 1 h.
10. In 1.5 mL Eppendorf tubes, prepare the following for each transformation: 100 μg salmon sperm carrier DNA, 500 ng of pNIA plasmid (Fig. 7a) to be tested, 500 μL of 40% PEG 3350, and 100 μL of competent yeast from **step 9**.
11. Vortex Eppendorf tubes 1–2 s and incubate at 30 °C for 30 min.
12. Heat shock at 42 °C for 25 min.
13. Centrifuge at 13,000 rpm 5 s in a microcentrifuge.
14. Aspirate supernatant.
15. Wash yeast with 1 mL YPD.
16. Centrifuge at 13,000 rpm 5 s in microcentrifuge.
17. Repeat **steps 14–16**.
18. Aspirate, leaving 100 μL of supernatant above the yeast pellet.

Fig. 6 (continued) shown in right column. Scale bar, 10 μm. (**b**) Line traces generated in ImageJ of the corresponding traces in the merged images shown in (**a**) with Cherry and GFP intensities displayed in red and green, respectively. The nuclear area is defined with the horizontal blue line. (**c**) Manual quantification of nuclear (N), cytosolic (C), or partially displaced Mdm2 localization (N/C). Bars indicate the percentage of cells in each category. 80–100 cells were quantified for each experimental condition

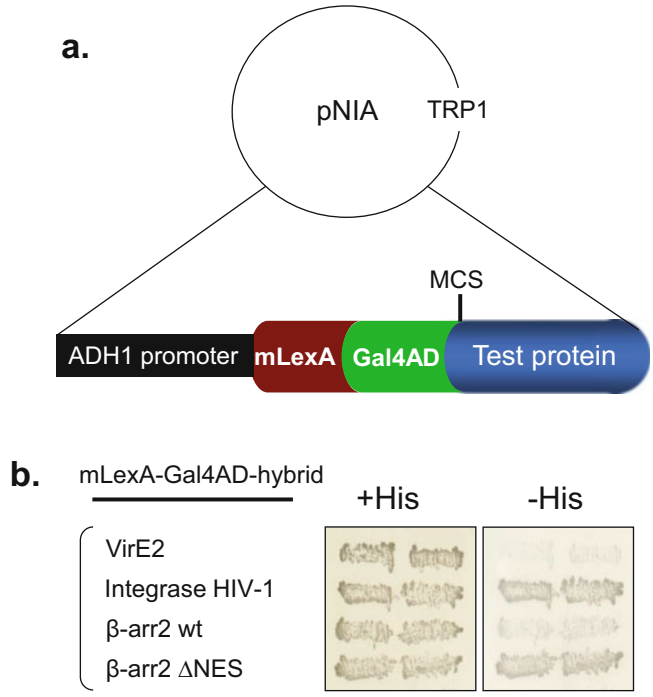


Fig. 7 Monitoring β-arr2 nuclear import using a one-hybrid genetic assay in yeast cells. (**a**) Schematic representation showing the triple-fusion protein expressed from the pNIA plasmid. It contains a modified form of the bacterial LexA protein lacking its intrinsic NLS (mLexA; *see* **Note 2**), the activation domain of the yeast gal4p (Gal4AD), and the protein to be tested for nuclear import. The plasmid also contains the ADH1 promoter to drive fusion expression, the TRP1 gene to allow yeast growth on minimal medium without tryptophan, and the multiple cloning site (MCS), containing *SmaI*, *BamHI*, *SalI*, and *PstI* restriction sites. (**b**) The L40 yeast reporter strain containing the indicated constructs was assessed for histidine auxotrophy. Transformants were patched on selective medium with histidine (−Trp+His) and subsequently replica plated on medium lacking histidine (−Trp–His). Growth in the absence of histidine indicates nuclear localization of the chimeric protein. Nuclear import can also be assessed using a β-gal assay (*see* Subheading 3.6, **steps 9–14**)

19. Resuspend pellet in the residual YPD supernatant, and pipette onto DOBA-Trp plates.
20. Spread yeast using sterile glass beads (about 10 beads/plate).
21. Place plates in a 30 °C incubator for 48–72 h.
22. When colonies are visible, proceed to Subheading 3.6.

3.6 Nuclear Import Auxotrophic and β-Gal Assays

1. Streak yeast colonies from Subheading 3.5, **step 22** in a patch on DOBA-Trp plates using a sterile pipette tip. This can be done in duplicate or triplicate. Mark top and bottom of plate with a marker pen for orientation.
2. Place plates in a 30 °C incubator overnight.
3. The next day prepare a DOBA-Trp and a DOBA-Trp-His plate for the histidine auxotrophy assay. For the β-gal assay, prepare a DOBA-Trp plate with a sterile round NC filter placed on the agar gently and rolled over with a sterile pipette to remove air bubbles. This will facilitate regular yeast growth onto the filter paper following replica plating.
4. Remove the plate with the patched yeast from the incubator.
5. Block a sterile velveteen square on the replica-plating tool using the locking ring to create an even surface.
6. Press the plate with the patched yeast gently but firmly onto the velveteen square. An impression of the yeast patches should be observed.
7. Replica plate the yeast onto the plates prepared in Subheading 3.6, **step 3** in the following order: DOBA-Trp plate with filter, DOBA-Trp-His and then DOBA-Trp.
8. Incubate plates at 30 °C. Monitor yeast growth on the DOBA-Trp (control) and DOBA-Trp-His (auxotrophic assay for nuclear import) plates over the next 2–3 days. Growth on DOBA-Trp-His plates indicates nuclear accumulation (Fig. 7b).
9. Once yeast have grown on the DOBA-Trp plate with NC filter (2–3 days), prepare Z-buffer containing 1 mg/mL X-Gal and 39 mM 2-mercaptoethanol for the *LacZ* reporter gene assay/β-gal assay.
10. For each plate to be tested, place a circle of 3 MM Whatman filter paper in the bottom of an empty petri dish. Aliquot 3 mL of Z-buffer/X-gal/2-mercaptoethanol into each dish, in a chemical hood.
11. The nitrocellulose filter, on which the yeast have grown, is then removed from the DOBA-Trp agar plate using a pair of long tweezers and lowered into a container with liquid nitrogen for 10 s. This permeabilizes the yeast.
12. The filter paper is then removed and warmed to room temperature (1–2 min).
13. Place the nitrocellulose filter paper gently yeast side up in the petri dish on the 3 MM filter paper with Z-buffer/X-gal/2-mercapoethanol mix, avoiding generating air bubbles.
14. Leave until the blue colour is observed (usually 1–4 h). Blue colour indicates nuclear accumulation [9].

4 Notes

1. QuikChange site-directed mutagenesis was used to introduce the hβ-arr2ΔNES (L394A) and hβ-arr1+NES (Q394L) mutations.
2. Gal4AD lacks a NLS, whereas the bacterial LexA protein is thought not to have evolved such a signal. LexA was found however to contain a short stretch of basic residues that may function as a NLS [15]. A modified LexA (mLexA) was therefore created carrying R157G and K159E amino acid substitutions, within the pNIA vector, and this was found to abrogate nuclear import driven by LexA in the LexA-Gal4AD-VirE2 fusion. The mLexA-Gal4AD chimera therefore allows nuclear import capacity of the fused test protein alone to be assessed.
3. Thawed Mowiol mounting medium can be kept for several weeks at 4 °C.
4. When processing multiple coverslips, we use reverse-action tweezers, which are normally closed. This is helpful as they maintain pressure on the coverslip without any pressure required from the operator.
5. The purpose of the StackReg ImageJ plugin is to align/match a stack of image slices.
6. To obtain the "TimeLapseCytoNucRatio" macro, send an email to thomas.guilbert@inserm.fr or mark.scott@inserm.fr.
7. For HEK-293 T cells, pre-coating of coverslips with poly-L-ornithine, poly-L-lysine, or type I collagen can be performed to improve cell adherence.
8. To make a humified chamber, simply take a 150 mm petri dish, with the secured Parafilm in place on the bottom, and then tape some folded tissue paper that has been moistened with water to the underside of the lid.
9. The coverslip can be sealed on the slide with transparent nail polish. Slides can be kept for several months at 4 °C in the dark.
10. HeLa cells are shown here, but similar results have been shown in many cell types including mouse embryonic fibroblasts, HEK, melanoma M2/A7 cell lines [16], lung adenocarcinoma H1299 cells [12], and osteosarcomal Saos2 cells [10].
11. If the cells start to move out of focus, readjust the focal plane between two points of the time lapse.
12. We have found a 5:1 ratio of β-arr2 to partner plasmid DNA works well to follow cytoplasmic displacement of nuclear β-arr2-binding partners. This has been used in our hands to successfully monitor JNK3 [9] and β-arr1 [13] displacement in addition to Mdm2 [12].

13. Cells could also be fixed at this point, as described in Subheading 3.1, **step 6**. After fixation, add 500 μL 1× PBS or IBIDI mounting medium to retard photobleaching.
14. The partial cytoplasmic (N/C) localization of GFP-Mdm2 is composed of two subcategories: N > C, where GFP-Mdm2 is displaced in the cytoplasm but is found more concentrated in the nucleus, and N = C, where GFP-Mdm2 is equally distributed between both compartments. These distributions are shown in Fig. 6a, panel rows 2 and 3.
15. Streak yeast on YPDA every week to have a fresh stock available. Once colonies have grown at 30 °C, store the plate at 4 °C. For longer-term storage, glycerol stocks can be prepared. For this, scrape half of the L40 yeast colonies from a YPDA plate, using a sterile bacterial loop, and transfer into 1 mL of 25% glycerol/YPD in a sterile cryovial tube. Store at −80 °C.

Acknowledgments

This work was supported by the Fondation ARC pour la Recherche sur le Cancer, Ligue Contre le Cancer (comité de L'Oise), the Who am I? laboratory of excellence (grant ANR-11-LABX-0071) funded by the "Investments for the Future" program operated by the French National Research Agency (grant ANR-11-IDEX-0005-01), CNRS, and INSERM. ETB was supported by a doctoral fellowship from the French Ministry of Research and the Fondation ARC. We also thank Jean Liotard and the Institut Cochin Imaging (IMAG'IC) and sequencing platforms (GENOMIC), for technical assistance.

References

1. Dewire SM, Ahn S, Lefkowitz RJ, Shenoy SK (2007) Beta-arrestins and cell signaling. Annu Rev Physiol 69:483–510
2. Gurevich VV, Gurevich EV (2014) Overview of different mechanisms of arrestin-mediated signaling. Curr Protoc Pharmacol 67.:Unit 2 10:11–19
3. Peterson YK, Luttrell LM (2017) The diverse roles of arrestin scaffolds in G protein-coupled receptor signaling. Pharmacol Rev 69 (3):256–297
4. Enslen H, Lima-Fernandes E, Scott MG (2014) Arrestins as regulatory hubs in cancer signalling pathways. Handb Exp Pharmacol 219:405–425
5. Luttrell LM, Ferguson SS, Daaka Y, Miller WE, Maudsley S, Della Rocca GJ, Lin F, Kawakatsu H, Owada K, Luttrell DK, Caron MG, Lefkowitz RJ (1999) Beta-arrestin-dependent formation of beta2 adrenergic receptor-Src protein kinase complexes. Science 283(5402):655–661
6. Barthet G, Carrat G, Cassier E, Barker B, Gaven F, Pillot M, Framery B, Pellissier LP, Augier J, Kang DS, Claeysen S, Reiter E, Baneres JL, Benovic JL, Marin P, Bockaert J, Dumuis A (2009) Beta-arrestin1 phosphorylation by GRK5 regulates G protein-independent 5-HT4 receptor signalling. EMBO J 28(18):2706–2718
7. Cassier E, Gallay N, Bourquard T, Claeysen S, Bockaert J, Crepieux P, Poupon A, Reiter E, Marin P, Vandermoere F (2017) Phosphorylation of beta-arrestin2 at Thr383 by MEK underlies beta-arrestin-dependent activation of Erk1/2 by GPCRs. elife 6:e23777

8. Kim YM, Barak LS, Caron MG, Benovic JL (2002) Regulation of arrestin-3 phosphorylation by casein kinase II. J Biol Chem 277 (19):16837–16846
9. Scott MG, Le Rouzic E, Perianin A, Pierotti V, Enslen H, Benichou S, Marullo S, Benmerah A (2002) Differential nucleocytoplasmic shuttling of beta-arrestins. Characterization of a leucine-rich nuclear export signal in beta-arrestin2. J Biol Chem 277(40):37693–37701
10. Wang P, Wu Y, Ge X, Ma L, Pei G (2003) Subcellular localization of beta-arrestins is determined by their intact N domain and the nuclear export signal at the C terminus. J Biol Chem 278:11648–11653
11. Hoeppner CZ, Cheng N, Ye RD (2012) Identification of a nuclear localization sequence in beta-arrestin-1 and its functional implications. J Biol Chem 287(12):8932–8943
12. Boularan C, Scott MG, Bourougaa K, Bellal M, Esteve E, Thuret A, Benmerah A, Tramier M, Coppey-Moisan M, Labbe-Jullie C, Fahraeus R, Marullo S (2007) Beta-arrestin 2 oligomerization controls the Mdm2-dependent inhibition of p53. Proc Natl Acad Sci U S A 104(46):18061–18066
13. Storez H, Scott MG, Issafras H, Burtey A, Benmerah A, Muntaner O, Piolot T, Tramier M, Coppey-Moisan M, Bouvier M, Labbe-Jullie C, Marullo S (2005) Homo- and hetero-oligomerization of beta-arrestins in living cells. J Biol Chem 280(48):40210–40215
14. Hara MR, Kovacs JJ, Whalen EJ, Rajagopal S, Strachan RT, Grant W, Towers AJ, Williams B, Lam CM, Xiao K, Shenoy SK, Gregory SG, Ahn S, Duckett DR, Lefkowitz RJ (2011) A stress response pathway regulates DNA damage through beta2-adrenoreceptors and beta-arrestin-1. Nature 477(7364):349–353
15. Rhee Y, Gurel F, Gafni Y, Dingwall C, Citovsky V (2000) A genetic system for detection of protein nuclear import and export. Nat Biotechnol 18(4):433–437
16. Scott MG, Pierotti V, Storez H, Lindberg E, Thuret A, Muntaner O, Labbe-Jullie C, Pitcher JA, Marullo S (2006) Cooperative regulation of extracellular signal-regulated kinase activation and cell shape change by filamin A and beta-arrestins. Mol Cell Biol 26 (9):3432–3445
17. Ozawa K, Whalen EJ, Nelson CD, Mu Y, Hess DT, Lefkowitz RJ, Stamler JS (2008) S-nitrosylation of beta-arrestin regulates beta-adrenergic receptor trafficking. Mol Cell 31 (3):395–405
18. Krupnick JG, Goodman OB Jr, Keen JH, Benovic JL (1997) Arrestin/clathrin interaction. Localization of the clathrin binding domain of nonvisual arrestins to the carboxy terminus. J Biol Chem 272(23):15011–15016
19. Han M, Gurevich VV, Vishnivetskiy SA, Sigler PB, Schubert C (2001) Crystal structure of beta-arrestin at 1.9 A: possible mechanism of receptor binding and membrane translocation. Structure (Camb) 9(9):869–880
20. Milano SK, Pace HC, Kim YM, Brenner C, Benovic JL (2002) Scaffolding functions of arrestin-2 revealed by crystal structure and mutagenesis. Biochemistry 41(10):3321–3328
21. Burtey A, Schmid EM, Ford MG, Rappoport JZ, Scott MG, Marullo S, Simon SM, McMahon HT, Benmerah A (2007) The conserved isoleucine-valine-phenylalanine motif couples activation state and endocytic functions of beta-arrestins. Traffic 8(7):914–931
22. Bjorgo E, Solheim SA, Abrahamsen H, Baillie GS, Brown KM, Berge T, Okkenhaug K, Houslay MD, Tasken K (2010) Cross talk between phosphatidylinositol 3-kinase and cyclic AMP (cAMP)-protein kinase a signaling pathways at the level of a protein kinase B/beta-arrestin/cAMP phosphodiesterase 4 complex. Mol Cell Biol 30(7):1660–1672
23. Schmid EM, Ford MG, Burtey A, Praefcke GJ, Peak-Chew SY, Mills IG, Benmerah A, McMahon HT (2006) Role of the AP2 beta-appendage hub in recruiting partners for clathrin-coated vesicle assembly. PLoS Biol 4 (9):e262
24. Laporte SA, Oakley RH, Holt JA, Barak LS, Caron MG (2000) The interaction of beta-arrestin with the AP-2 adaptor is required for the clustering of beta 2-adrenergic receptor into clathrin-coated pits. J Biol Chem 275 (30):23120–23126



Chapter 17

Monitoring β-Arrestin 2 Targeting to the Centrosome, Basal Body, and Primary Cilium by Fluorescence Microscopy

Anahi Molla-Herman, Kathryn M. Davis, Kirk Mykytyn, and Alexandre Benmerah

Abstract

Primary cilia (PC) are microtubule-based organelles that behave like a cellular antenna controlling key signaling pathways during development and tissue homeostasis. The ciliary membrane is highly enriched for G protein-coupled receptors (GPCRs), and PC are a crucial signaling compartment for this large receptor family. Downstream effectors of GPCR signaling are also present in cilia, and evidence obtained by our labs and others demonstrated that β-arrestin (βarr) family members are differentially recruited to PC and have investigated the role of GPCR activation in this process. In this chapter, we provide methods based on fluorescence microscopy on fixed or live cells suitable for investigating targeting and recruitment of βarrs at PC.

Key words Centrosome, Basal body, Primary cilia, Arrestin, Cellular signaling

1 Introduction

Primary cilia (PC) are antenna-like structures on the surface of most quiescent cell types in vertebrates that control key signaling pathways during development and tissue homeostasis [1]. PC dysfunctions linked to mutations in genes encoding for ciliary proteins have been shown to give rise to a growing number of genetic disorders known as ciliopathies [2].

PC are assembled from the mother centriole of the centrosome (Fig. 1), the major microtubule-organizing center in interphasic cells, which also plays a critical role in the organization of the mitotic spindle during mitosis [3]. The centrosome is composed of two centrioles, the mother, which presents specific appendages, and the daughter. During ciliogenesis, the mother centriole docks onto cellular membranes through its distal appendages, and the microtubule doublets from its distal end will extend wrapped into the ciliary membrane to form the axoneme [4]. The transition fibers formed by the distal appendages together with the transition

Mark G. H. Scott and Stéphane A. Laporte (eds.), *Beta-Arrestins: Methods and Protocols*, Methods in Molecular Biology, vol. 1957, https://doi.org/10.1007/978-1-4939-9158-7_17, © Springer Science+Business Media, LLC, part of Springer Nature 2019

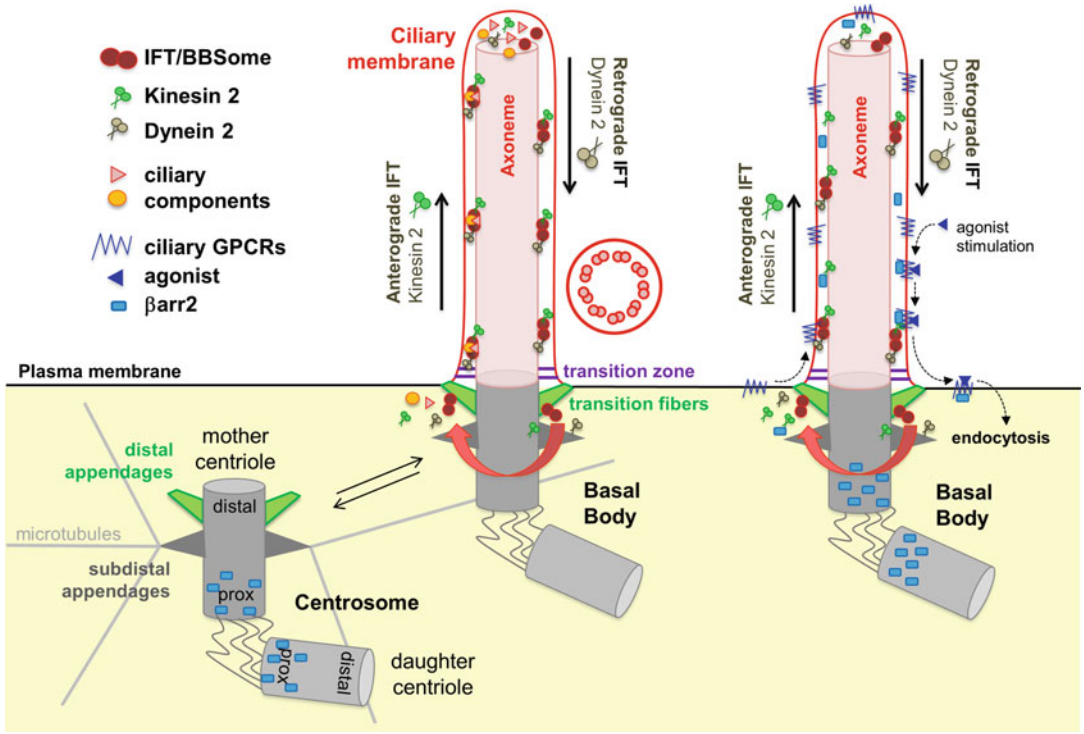


Fig. 1 Organization of centrosome and primary cilium. The centrosome in interphasic cells is composed of two centrioles (mother and daughter). The mother is characterized by the presence of the subdistal appendages on which microtubules are anchored and of distal appendages which are required for docking onto cellular membranes during ciliogenesis. Ciliogenesis of primary cilia occurs in quiescent or terminally differentiated G_0 cells in which the centrosome docks onto membranes and becomes the basal body. The axoneme is composed of nine doublets of microtubules extended from the mother centriole. The ciliary membrane presents a specific composition, thanks to the presence of the transition zone and of transition fibers which act as filter/diffusion barriers and prevent free exchange between the cilium compartment and the rest of the cell. Ciliogenesis and transport in and out of the cilium requires specific machinery, called IFT, which mediates anterograde and retrograde transport. The ciliary membrane is highly enriched in GPCRs. GPCRs are imported into and exported out of cilia through mechanisms involving IFT, the BBSome, and βarr2. Stimulation of ciliary GPCRs by their agonist induces βarr2 recruitment to activated GPCRs and potentially facilitates the association with retrograde IFT/BBSome for ciliary export

zone form a barrier similar to the nuclear pores and limit exchanges between the cytoplasm and ciliary compartment [5]. Therefore, all ciliary components (membrane and soluble proteins) must be transported through this barrier by a specific process called IFT (intraflagellar transport). This highly conserved machinery mediates both anterograde and retrograde transport of cargos along the axoneme with the help of both kinesin II and cytoplasmic dynein microtubule-based motors. This bidirectional transport allows the entry of molecules into the ciliary compartment as well as their exit, allowing both recycling of the transport machinery and the release of signaling intermediates to the cell body [6].

A striking observation is that PC are highly enriched for GPCRs that play key roles in their sensory/signaling abilities. This includes rhodopsin in the outer segment of photoreceptors (a modified PC) and odor receptors in ciliated olfactory neurons as well as smoothened (smo) during Hh signaling in various cell types and somatostatin receptor subtype 3 (Sstr3) and others in neurons [7, 8]. Cilia are also highly enriched for downstream signaling components of GPCRs including G proteins and adenylate cyclases [7]. The fact that βarrs are key regulators of GPCRs at the plasma membrane drove several groups to investigate their potential functions at PC. Indeed, the role of visual arrestin in the regulation of rhodopsin within the outer segment was previously well established. Early observations pointed to a role of βarr2 in the desensitization of odor receptors within cilia on olfactory neurons [9]. Ciliary localization of βarrs, and especially of βarr2, was confirmed by two further studies, which also identified them as partners of KIF3A [10, 11], a subunit of the dimeric anterograde IFT motor kinesin II (*see* above). These studies also indicated potential functions of βarrs in the transport of smo to PC [11] as well as in ciliogenesis [10]. More recently, a series of interesting studies shed some light on the function and regulation of βarr in cilia. First, global analysis of ciliary proteins by proximity labeling revealed that βarr2 is exported from cilia through the action of the BBSome [12], a complex working together with IFT to regulate trafficking of cargos, including GPCRs, in and out of cilia [7, 8] (Fig. 1). Second, βarrs [13] and again especially βarr2 [14, 15] were found to be required for the activation-induced elimination of GPCRs from cilia. Interestingly, in the case of Sstr3, activation by the agonist induces a rapid translocation of βarr2 into the cilium [14], further confirming that βarr2 likely acts as an adaptor connecting activated GPCRs to the IFT/BBSome machinery for ciliary exit similarly as it does with internalization from the plasma membrane through clathrin-coated pits [16].

Besides these observations linking βarrs to ciliary functions, βarr2 [10] and βarr1 [17] were also found at the centrosome in cycling cells, as well as at the basal body of ciliated quiescent cells, in which they colocalize with centriolar markers. Interestingly, βarrs were shown to bind to α-tubulin and to be required somehow for centriole duplication and/or cytokinesis [17]. These data suggest that βarrs might be involved in cilia-independent functions at the centrosomes, which remain to be investigated.

Here, we provide different methods for investigating the steady state and dynamic recruitment to centrosome/basal body and cilia in RPE1 and IMCD cells, which are cell lines commonly used in laboratories worldwide to study ciliogenesis, as well as in primary neurons.

2 Materials

2.1 Cells and Cell Culture Media

1. RPE1, a human retinal pigment epithelial cell line that stably expresses human telomerase reverse transcriptase (hTERT-RPE1; Clontech Laboratories, Inc.; ATCC CRL4000™).
2. HeLa, epithelial cervix carcinoma (ATCC CCL-2™).
3. HeLa stably expressing centrin-GFP (M. Bornens, Institut Curie, Paris, France).
4. mIMCD-3 (IMCD), mouse medulla/collecting duct epithelial cell line (ATCC CRL-2123™).
5. Mouse hippocampal neurons cultured from newborn (P0) pups.
6. Culture media for cell lines: Dulbecco's modified Eagle's medium DMEM-F12 1:1 GlutaMAX supplemented with antibiotics (100 U/mL penicillin and 100 mg/mL streptomycin) and 10% fetal bovine serum (FBS) for basic RPE1 cell culture conditions or with 0.5% FBS for low serum-containing media. DMEM supplemented with 10% FBS for HeLa cells. DMEM-F12 1:1 supplemented with 10% FBS for IMCD cell culture conditions.
7. Ciliation media: culture media with low serum (0.5% FBS).
8. Neurobasal-A medium (ThermoFisher Scientific) containing B-27 supplement (ThermoFisher Scientific), 0.5 mM GlutaMAX, insulin-transferrin-sodium selenite (ITS, Sigma-Aldrich), 50 μg/mL gentamicin, and Hibernate A low-fluorescence medium (BrainBits) for cultured neurons.
9. Transfection media for RPE1 cells: Opti-MEM (ThermoFisher Scientific) supplemented with 0.5% FBS.

2.2 Buffers, Solutions for Fluorescence Microscopy, and Drugs

1. 1× phosphate-buffered saline (PBS), pH 7.4.
2. 1× phosphate-buffered saline with Ca^{2+} and Mg^{2+} (PBS (Ca/Mg)), pH 7.4.
3. Fixation solution: 4% paraformaldehyde (PFA).
4. Permeabilization buffer for HeLa and RPE1 cells: 0.1% Triton X-100, 1 mg/mL BSA in PBS. Buffer should be passed through a sterile filter (0.2 μm) to avoid cellular contamination for long-term storage (*see* **Note 1**).
5. Permeabilization buffer for IMCD cells: 0.3% Triton X-100, 10 mg/mL BSA, 4% donkey serum, and 0.02% sodium azide in PBS (*see* **Note 2**).
6. Blocking buffer for HeLa and RPE1 cells: 1 mg/mL BSA in PBS.

7. Blocking buffer for IMCD cells: 10 mg/mL BSA, 4% donkey serum, and 0.02% sodium azide in PBS.
8. Quenching solution: 50 mM NH_4Cl in PBS.
9. Mounting media for HeLa and RPE1 cells: PBS-glycerol mix (1:1) using the SlowFade Light Antifade Kit containing DAPI from Molecular Probes (ThermoFisher Scientific).
10. Mounting media for IMCD cells: Immu-Mount (ThermoFisher Scientific).
11. Microtubule-depolymerizing solutions: Nocodazole (Sigma). 10 μM for immediate depolymerization (1 h). 1 μM for cell cycle synchronization (24 h).
12. Microtubule-stabilizing solution: 10 μM Taxol (paclitaxel).
13. 10 μM somatostatin-14 (Phoenix Pharmaceuticals).

2.3 Equipment

1. Cells are grown in an incubator under standard growth conditions (37 °C and 5% CO_2).
2. Cells are seeded on 12 mm glass coverslips (No. 1, NeuVitro).
3. For HeLa and RPE1 cells, coverslips are mounted on plain glass microscope slides (1 mm, Pearl). For IMCD cells, coverslips are sandwiched between microscope cover glass (No. 1; ThermoFisher Scientific) and a microscope slide.
4. 6- or 24-well cell culture plates.
5. 8-well μ-slide, Ibidi.
6. μ-Dish 35 mm, high Glass Bottom, Ibidi. Neurons were plated on 35 mm glass-bottomed (No. 1.5) dishes (MatTek) that had been coated with 40 μg/mL poly-D-lysine.
7. Electroporation is performed in 0.4 cm gap Gene Pulser/MicroPulser cuvettes (Bio-Rad).
8. Epifluorescence microscopy: Axiovert 100 M (Zeiss) with a micromax camera (Princeton Instruments) driven by Metamorph (Molecular Devices).
9. Confocal microscopy: TCS SP2 AOBS from Leica for FRAP studies in HeLa cells and TCS SP8 from Leica for imaging of IMCD cells.
10. Life-cell confocal microscopy: Andor Revolution WD spinning disk confocal imaging system (Andor Technology plc) controlled by Metamorph and equipped with a Nikon TiE inverted microscope with Perfect Focus System (Nikon Instruments), Andor iXon Ultra 897 back-illuminated EMCCD camera, ASI XY piezo-Z motorized stage (Applied Scientific Instrumentation), Yokogawa CSU-W1 confocal scanning unit (Yokogawa Electric Corporation), and solid-state lasers. OkoLab Bold Line stage-top incubator to control temperature and humidity.

11. Software for image analysis: Metamorph (Molecular Devices), ImageJ (https://imagej.nih.gov/ij/), Photoshop (Adobe Systems Inc.), and Application Suite X (Leica).

2.4 Antibodies, Staining Reagents, Plasmids, Conjugates, and Transfection Reagents

1. Primary antibodies (species, reference number, and dilution are indicated):
   (a) βarr2: rabbit pan-arrestin (abcam, ab2914; 1:100) or goat anti-β-arrestin 2 (abcam, ab31294; 1:500).
   (b) Pericentrin: Rabbit polyclonal (abcam, ab4448), centrosomal marker (1:1000).
   (c) γ-Tubulin: mouse monoclonal antibody against γ-tubulin (clone GTU-88), Sigma, centrosomal marker (1:1000).
   (d) α-Tubulin: mouse monoclonal antibody clone DM1A (T9026), sigma, microtubule marker (1:1000).
   (e) Acetylated α-tubulin (Ac.tub), mouse monoclonal antibody clone 6-11B-1 (Sigma, T7451) marker for stable microtubules (1:10,000).
   (f) Flag: rabbit polyclonal antibody from Sigma (F7425) (1:500).
   (g) Myc: mouse monoclonal antibody clone 9E10 from Santa Cruz Biotechnology (sc-40) (1:400).
2. Secondary antibodies:
   (a) Alexa^{350}-conjugated donkey anti-mouse IgG (Invitrogen, A10035) (1:600).
   (b) Alexa^{350}-conjugated donkey anti-rabbit IgG (Invitrogen, A10039) (1:600).
   (c) Alexa^{488}-conjugated donkey anti-mouse IgG (Invitrogen, A21202) (1:600).
   (d) Alexa^{488}-conjugated donkey anti-rabbit IgG (Invitrogen, A21206) (1:600).
   (e) Alexa^{488}-conjugated donkey anti-goat IgG (Invitrogen, A11055) (1:600).
   (f) Alexa^{546}-conjugated donkey anti-goat IgG (Invitrogen, A10036) (1:1000).
   (g) Alexa^{568}-conjugated donkey anti-goat IgG (Invitrogen, A11057) (1:600).
   (h) Alexa^{568}-conjugated donkey anti-mouse IgG (Invitrogen, A10037) (1:600).
   (i) Alexa^{647}-conjugated donkey anti-mouse IgG (Thermofisher, A-31571) (1:600).
   (j) Alexa^{647}-conjugated donkey anti-rabbit IgG (Thermofisher, A-31573) (1:600).

3. Expression plasmids (available from our laboratories upon request):
   (a) βarr1-GFP, βarr2-GFP, and βarr2-cherry were provided by Mark Scott and Stefano Marullo (Institut Cochin, Paris) and previously described in [10].
   (b) Centrin-GFP was provided by Dr. Michel Bornens (Institut Curie, Paris) [18].
   (c) Rat wild-type smoothened (smo) cloned into pcDNA3 (Invitrogen) was provided by Dr. J. Coulombe (Institut de Neurobiologie, Gif-sur-Yvette, France). Flag-tagged constitutively active form of smo (smo*) was generated according to Taipale et al. [19] and described previously in [10].
   (d) Mouse wild-type somatostatin receptor subtype 3 (Sstr3) was cloned into pcDNA3.1/Myc-His(-) (ThermoFisher) and pDsRed2-N (Takara Bio USA).
4. Transfection reagents: Fugene 6 (Promega), Genejuice (Novagen), and Lipofectamine LTX reagent with PLUS reagent (ThermoFisher). Cytomix transfection reagent: 120 mM KCl, 0.15 mM $CaCl_2$, 10 mM K_2HPO_4/KH_2PO_4, 25 mM Hepes, 2 mM EGTA, and 5 mM $MgCl_2$, pH adjusted to 7.6 with KOH, filter sterilized and stored at 4 °C.
5. Nuclear staining: 4′,6-diamidino-2-phenylindole dihydrochloride (DAPI) or DRAQ5.
6. Nail polish (Electron Microscopy Science).

3 Methods

3.1 Cell Cycle Synchronization in HeLa Cells

1. Set down four sterilized coverslips per well in a regular six-well plate under the hood. Add PBS and aspirate to make a vacuum between the coverslips and the plate (*see* **Note 3**).
2. 1.5×10^5 HeLa cells are seeded per well in 2 mL of culture media (Subheading 2.1, **item 6**) and cultured for 24 h (*see* **Note 4**).
3. In order to increase the number of mitosis to be analyzed per plate, HeLa cells are synchronized with 1 μM nocodazole treatment overnight (*see* **Note 5**).
4. Cell cycle arrest is further released by transfer into basic culture media.
5. Wash the cells twice with PBS (*see* **Note 6**).
6. Aspirate the PBS, and add fresh culture medium (2 mL per well in a six-well plate).
7. Cells are analyzed after 6 h or 12 h to observe mitotic events.

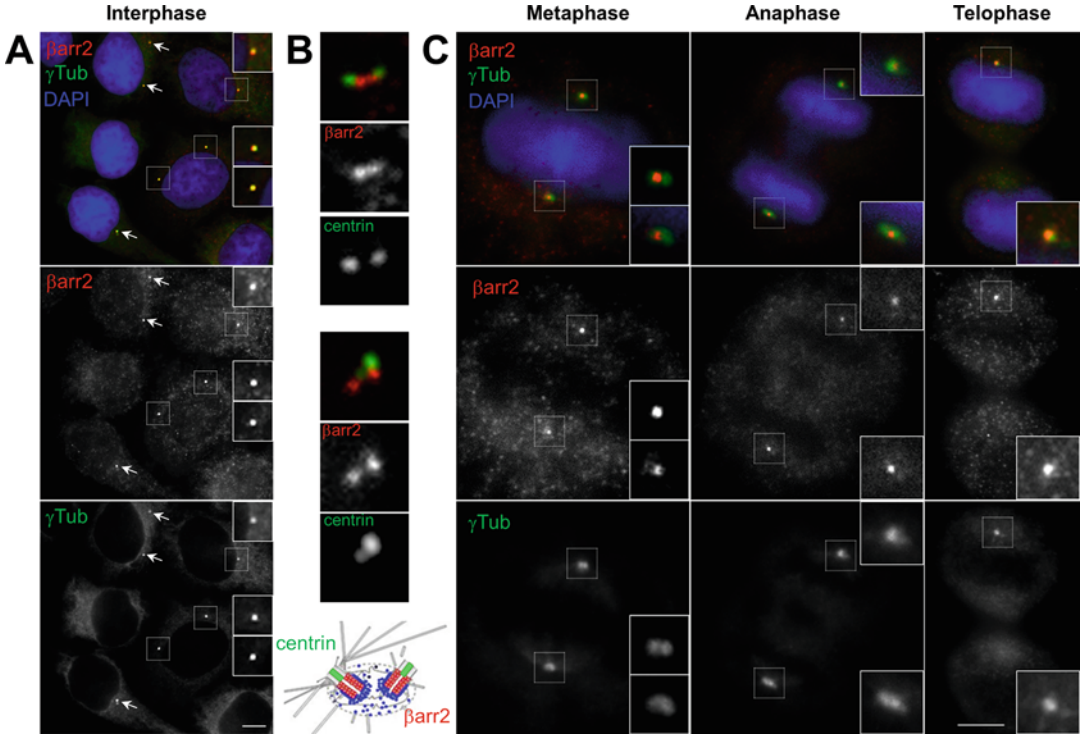


Fig. 2 Endogenous βarr2 is localized at the centrosome during the overall cell cycle. (**a**) Synchronized HeLa cells were fixed and stained for endogenous βarr2 (rabbit pan-arrestin (βarr2), red) and for γ-tubulin (γTub, green). DNA was stained with DAPI. Representative images of interphase and mitosis stages are shown. Arrows indicate representative γTub-stained centrosomes. Insets show higher magnifications of representative areas. (**b**) HeLa cells stably expressing a *centrin-GFP* were fixed and stained for endogenous βarr2 (goat anti-β-arrestin 2 (Abcam)) or transfected with plasmids encoding for the *βarr2-Cherry* fusion and then fixed and directly observed. The possible distribution of βarr2 within the centrioles is illustrated: centrin is localized at the distal regions of the centrioles (green). βarr2 is likely localized at the proximal region of the centrioles (red). Pericentrin is localized at the pericentriolar matrix around centrioles (blue). (**c**) Hela cells were synchronized, fixed, and stained for βarr2 and γTub. Different mitotic stages are shown. Insets show higher magnifications of representative centrosomal regions. Scale bars represent 5 μm

An example of endogenous βarr2 distribution in HeLa cells in interphase and mitosis (metaphase, anaphase, and telophase) is shown in Fig. 2. βarr2 is localized at the centrosome as shown by its colocalization with the centrosomal marker γ-tubulin (Fig. 2a, c). βarr2 sublocalization at the proximal ends of centrioles was confirmed using centrin as a marker of the distal ends (Fig. 2b).

3.2 Transfection of HeLa Cells with Plasmid DNA

1. Put four sterile (autoclaved) coverslips per well in a six-well plate. Add some PBS and aspirate to make a vacuum between the coverslips and the plate in order to make the coverslips stick to the bottom to avoid coverslip overlapping. Seed 2×10^5 cells per well for 24 h before transfection (*see* **Note 4**). Change the culture medium 2 h before transfection to have an optimal pH (*see* **Note 6**).

2. Prepare the transfection mix: For 1 μg of DNA, mix 100 μL of serum-free culture medium with 3 μL of GeneJuice. Vortex and let incubate for 5 min at RT. Add 1 μg of DNA. Incubate 10–15 min at RT for the liposome-DNA complexes to form.
3. Wash the cells twice with PBS (*see* **Note 6**).
4. Aspirate the PBS, and add fresh culture medium (2 mL per well in a six-well plate).
5. Add 100 μL of transfection mix per well (*see* **Note 4**).
6. Incubate the cells with the transfection mix for 24 h before fixation/immunofluorescence or live-cell imaging analysis.

An example of the differential distribution of transfected β-arrestin GFP fusions in HeLa cells is shown in Fig. 3. βarr2-GFP is localized at the centrosome as shown by its colocalization with the centrosomal marker pericentrin, whereas βarr1-GFP shows a cytoplasmic diffuse distribution similar to GFP (Fig. 3a).

3.3 Preparation of Cells for Immunofluorescence Microscopy in RPE1 and HeLa Cells

1. Wash the cells twice with room temperature (RT) PBS (*see* **Note 6**).
2. Fix the cells in 4% PFA for 20 min at 4 °C (by placing the plate on ice), followed by a 10-min incubation in quenching solution at RT.
3. Gently wash the cells twice with PBS always avoiding cell detachment (*see* **Note 6**).
4. Incubate the cells with primary antibodies in permeabilization buffer for 30–45 min at RT. Incubation can be made directly in the well; the minimal mix volume should then be 200 μL per well to avoid cell drying. To save antibodies, you can prepare a 40 μL drop containing the antibody/permeabilization mix on Parafilm® secured to the bench, and then gently invert your coverslip to put the cells in contact with the liquid. Do not forget to invert the coverslip again when you put it back in the well (*see* **Note 7**).
5. Wash the cells twice with blocking buffer at RT, and avoid cell detachment (*see* **Note 6**).
6. Incubate with secondary antibodies (mixed in blocking buffer) for 30 min at RT in the dark to preserve the fluorescence.
7. Wash once with blocking buffer and twice with PBS (*see* **Note 6**).
8. Lay down your cells on microscope slides in mounting medium (5 μL).
9. Add nail polish by putting small drops around the coverslip, and then complete the circle once the drops are dry (*see* **Note 8**).
10. Store at 4 °C and keep in the dark until observation.

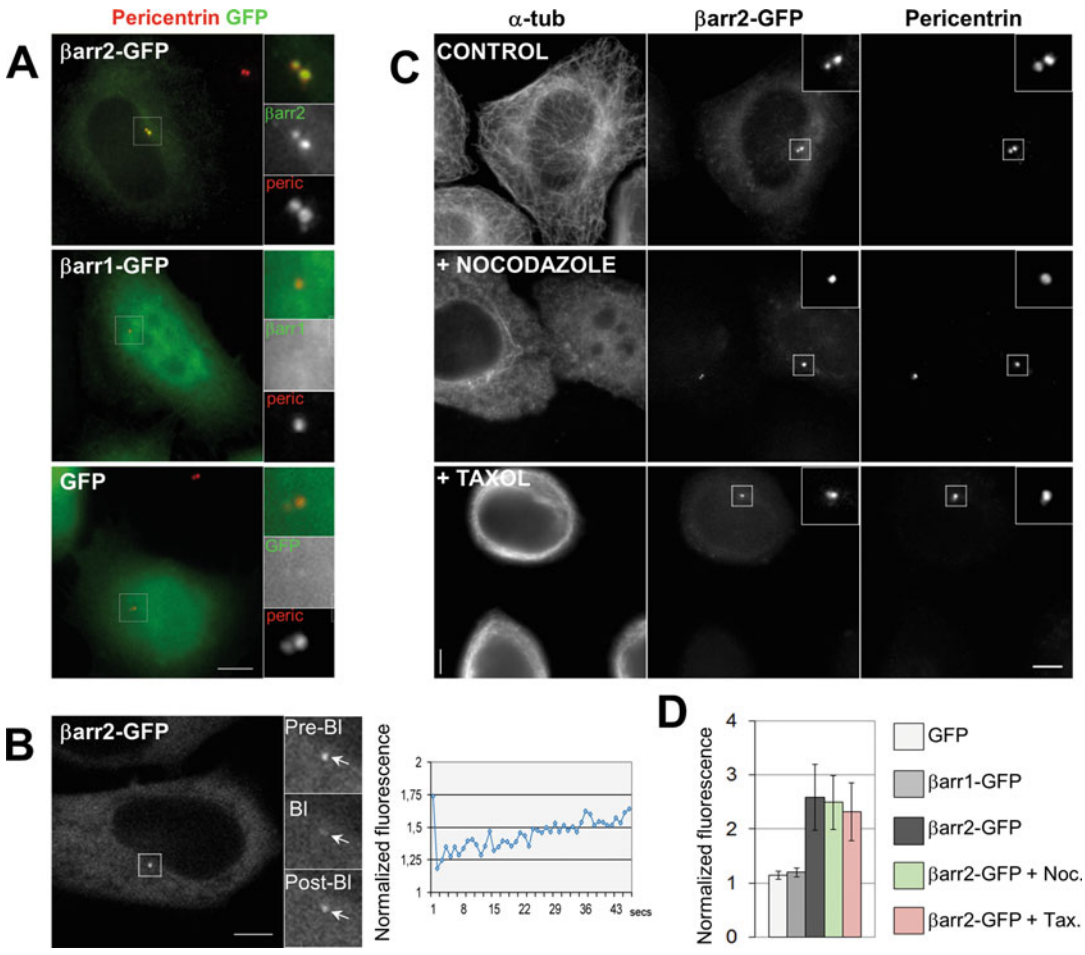


Fig. 3 βarr2 is targeted and enriched at the centrosome independently of microtubules. (**a**) HeLa cells were transfected with plasmids encoding for *βarr2-GFP* and *βarr1-GFP* or with *GFP* alone, fixed and stained for the centrosomal marker pericentrin. Insets show higher magnifications of centrosomal regions. (**b**) Live HeLa cells transiently expressing *βarr2-GFP* were treated for 1 h at 37 °C with nocodazole (10 μM) and then used for FRAP experiments. Images of a representative cell are shown. The centrosomal region was bleached twice. Insets show higher magnifications of the bleached region before bleaching (Pre-Bl), just after bleaching (Bl), and after bleaching (Post-Bl). Arrows indicate the analyzed *βarr2-GFP* stained centrosome. Fluorescence intensity of *βarr2-GFP* at the centrosome was normalized to cytoplasmic staining within an identical cytoplasmic region. (**c**) HeLa cells expressing *βarr2-GFP* were untreated (control) or treated with nocodazole or Taxol (10 μM) to depolymerize or stabilize microtubule network, respectively. Cells were fixed and stained for microtubules (α-tubulin) and for the centrosome (pericentrin). Insets show higher magnifications of centrosomal regions. (**d**) Centrosome-associated GFP fluorescence was quantified using a region defined by pericentrin staining and normalized to the cytoplasmic signal within the same cells. Values are the means (±2 SD) of at least 20 cells from 3 independent experiments. Scale bars represent 5 μm

3.4 Epifluorescence Microscopy in Fixed HeLa and RPE1 Cells

Pictures were acquired using a 63× objective (plan-apo; Zeiss) with a micromax camera (Princeton Instruments) driven by Metamorph. The final images are generated using ImageJ (https://imagej.nih.gov/ij/) and Photoshop (Adobe Systems Inc.).

3.5 Quantification of β-Arrestins Centrosomal Targeting in HeLa Cells: Role of Microtubules

1. Transfected HeLa cells are treated or not with nocodazole or Taxol (10 μM, 1 h).
2. Cells are subsequently fixed and stained as described in Subheading 3.3 with antibody against a centrosomal marker (pericentrin).
3. GFP signal at the centrosome is quantified from pictures using Metamorph (or ImageJ).
4. Pericentrin staining is used to define a region corresponding to the centrosome. The option "Auto-threshold for light objects" allows to transform the pericentrin staining into objects.
5. The pericentrin objects are then circled by selecting the option "Create regions around objects."
6. The resulting regions are then transferred to the GFP corresponding images, and the fluorescence intensity corresponding to GFP at the centrosome (CE) can be measured.
7. A region of the same size is selected outside the cell to measure the noise of the camera (CN) and another one in the cytoplasm (CY) of the same cell.
8. Normalized fluorescence at the centrosome was then calculated as follows: $NF = (CE - CN)/(CY - CN)$.

An example of quantitative analyses of GFP, βarr1-GFP, and βarr2-GFP localization at the centrosome in HeLa cells is shown in Fig. 3. These analyses show that βarr2-GFP is enriched at the centrosome compared to βarr1-GFP or GFP (Fig. 3a, d). Interestingly, the enrichment of βarr2-GFP at the centrosome is not affected by nocodazole or Taxol (Fig. 3c, d) showing that it is independent of microtubules.

3.6 βarr2 Dynamics at the Centrosome in HeLa Cells: Fluorescence After Photobleaching (FRAP)

1. 1×10^5 HeLa cells are seeded in Ibidi 8-well μ-slides.
2. After 24 h, cells are transfected with βarr2-GFP expressing plasmids as indicated in Subheading 3.2 (*see* **Note 9**).
3. The day after, βarr2 dynamics at the centrosome are analyzed using FRAP (fluorescence recovery after photobleaching). Cells are treated or not with 10 μM nocodazole for 1 h at 37 °C and analyzed using a confocal microscope after excitation with a 488 nm laser line from an argon laser.
4. A centrosomal region (50 × 50 pixels) is exposed to two consecutive pulses of 1 s with 100% of laser intensity, and fluorescence recovery is analyzed for 90 s taking an image every 1.3 s. A cytoplasmic non-centrosomal region of the same size is also taken into account for quantification, and normalizations are performed as described in Subheading 3.5 (*see* **Note 10**).

5. Images are analyzed using Metamorph to quantify normalized fluorescence at the centrosome similarly as described in Subheading 3.5 except that the region corresponding to the centrosome is directly circled using Metamorph.

An example of analysis of the dynamics of βarr2-GFP at the centrosome by FRAP is shown in Fig. 3b. After photobleaching, βarr2-GFP signal at the centrosome is rapidly and almost fully recovered indicating that the localization of βarr2 at the centrosome results from a dynamic exchange between a centrosomal and a cytoplasmic pool.

3.7 Induction of Ciliogenesis in RPE1 Cells

1. Set down one sterile coverslip per well in a regular 24 well plate under the hood.
2. To optimize cell culture and transfection steps, fix your coverslips to the bottom of the wells by filling each well with 0.5 mL of PBS, and then aspirate it with a 200 μL pipette tip to create a vacuum between the coverslip and the plate.
3. Seed 2.5×10^5 cells per well, and grow them in RPE1 culture conditions for 24 h (*see* **Note 4**).
4. Wash the cells twice in PBS (*see* **Note 6**).
5. Add ciliation media (0.5% FBS) for 24–48 h to allow primary cilia formation.
6. Monitor the efficiency of primary cilia formation by staining with acetylated α-tubulin antibody (you should obtain ~80% of ciliated cells) (*see* **Note 11**).

3.8 Transfection of Cells with Plasmid DNA in RPE1 Cells

1. Seed 1×10^5 cells per well in a 24-well plate containing a coverslip per well, and grow them for 24 h as indicated in Subheading 3.7.
2. Prepare the transfection mix. For four wells, mix 1 μg of DNA with 100 μL of Opti-MEM and 3 μL of Fugene 6.
3. Wash the cells twice with PBS (Ca^{2+}/Mg^{2+}) avoiding cell detachment (*see* **Note 6**).
4. Aspirate the PBS, and add 500 μL of low serum-containing Opti-MEM (0.5% FBS) to each well (*see* **Note 6**).
5. Add 25 μL of transfection mix per well (*see* **Note 4**).
6. Incubate the cells with transfection mix for 24 h before fixation/immunofluorescence or live-cell imaging analysis.

An example of RPE1 cell expressing endogenous βarr2 at the primary cilia is shown in Fig. 4a. Primary cilia are enriched with GPCRs (G protein-coupled receptors) as shown by the localization of a constitutively active form of smoothened (Smo*) at PC in Fig. 4b. Interestingly, exogenous βarr2-GFP is not present at the axoneme in the absence of Smo*(Ø) but is highly enriched at the

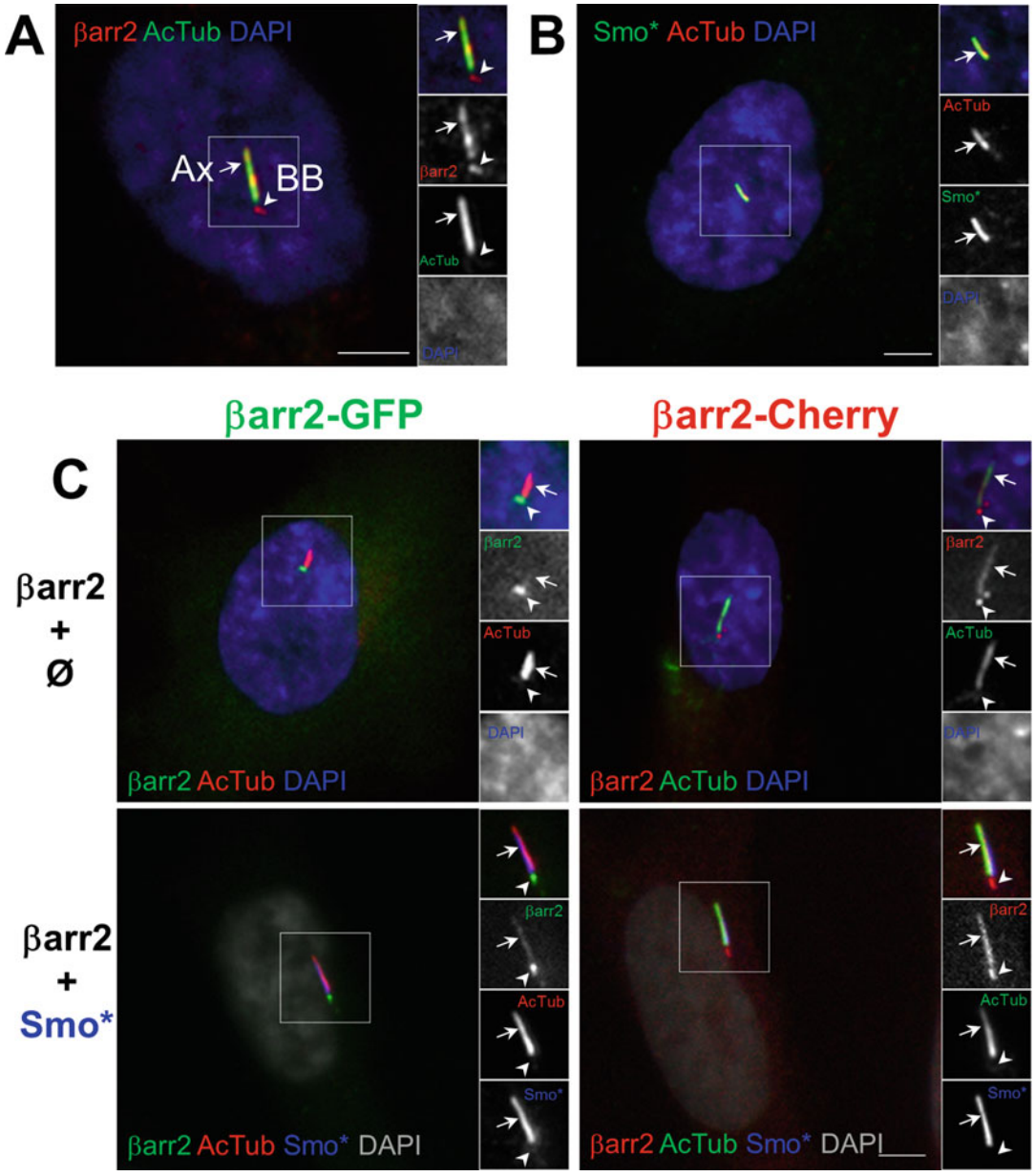


Fig. 4 βarr2 is found in the axoneme and basal body of primary cilia. (**a**) Confluent RPE1 cells were serum-starved for 24 h and then fixed and stained for acetylated α-tubulin (AcTub, green), which is highly enriched in primary cilia (axoneme (Ax)) and for endogenous βarr2 (rabbit pan-arrestin (Abcam), red). Arrows and arrowheads indicate AcTub-stained axonemes and βarr2-stained basal bodies (BB), respectively. (**b**) RPE1 cells transfected with a plasmid encoding for a Flag-tagged active form of smoothened (Smo*, green) were serum-starved for 24 h after transfection and then fixed and stained for AcTub (red) and Flag (Smo*, green). (**c**) RPE1 cells transfected with plasmids encoding either βarr2-GFP (left panels, green) or βarr2-Cherry (right panels, red) fusions alone (upper panels) or together with Flag-tagged Smo* (lower panels) were serum-starved for 24 h after transfection and then fixed and stained for either AcTub (upper panels) or for AcTub and Flag (Smo*, lower panels). Insets show higher magnifications of representative areas. Scale bars represent 5 μm

basal body. In the presence of Smo*, βarr2-GFP signal is more present at the axoneme (Fig. 4c, left panels). To further confirm these results, we used another fluorescence tag (Cherry), observing that βarr2-Cherry is localized at the axoneme and the basal body in the absence of Smo* and is more enriched at the axoneme in the presence of Smo* (Fig. 4c, right panels).

3.9 Transfection of IMCD Cells with Plasmid DNA

1. Prepare the electroporation mix and place it on ice. For each transfection, combine a total of 10 μg of DNA (5 μg of βarr2-GFP + 5 μg of Sstr3Myc) with 400 μL cytomix containing freshly added 2 mM ATP and 5 mM glutathione.
2. Resuspend 5×10^6 IMCD cells in 400 μL cytomix, pipette into a cuvette on ice, and electroporate using the following settings: 320 V, 950 μF, ∞ Ω, and 4 mm.
3. Resuspend the cells in fresh IMCD medium and plate onto a 60 mm dish with coverslips placed on the bottom.
4. Wash and refeed the cells 16–24 h after transfection.

3.10 Sstr3-Mediated Ciliary Recruitment of βarr2-GFP in IMCD Cells

1. After 40–48 h, set down one coverslip per well in a regular 24-well plate containing 1 mL of fresh IMCD medium. Let the cells recover for approximately 1 h in a tissue culture incubator.
2. Allow the glass vial containing lyophilized somatostatin-14 (SST) to warm up to room temperature for at least 20 min before resuspending it in water to a final concentration of 1 mM. Reconstituted SST should be stored in the glass vial at 4 °C and is effective for at least 1 month.
3. Add 10 μL of water (vehicle) or SST to each well, for a final concentration of 10 μM SST, and return the plate to the incubator for 20 min.

3.11 Preparation of IMCD Cells for Immunofluorescence Microscopy

1. Aspirate the media and fix the cells in 4% PFA for 15 min at RT.
2. Permeabilize the cells in permeabilization buffer for 10 min at RT.
3. Wash the cells once with blocking buffer for 5 min at RT. Incubate the cells with primary antibody in 250 μL blocking buffer for 16–24 h at 4 °C.
4. Wash the cells three times with blocking buffer for 5 min, each time, at RT. Incubate the cells with secondary antibody and nuclear stain in 250 μL blocking buffer for 1 h at RT in the dark.
5. Wash the cells three times with blocking buffer for 5 min at RT.
6. Place the coverslips facedown in 1–2 drops of mounting medium on a microscope cover glass. Cover with a microscope slide and turn over. The cells should be directly beneath the cover glass.

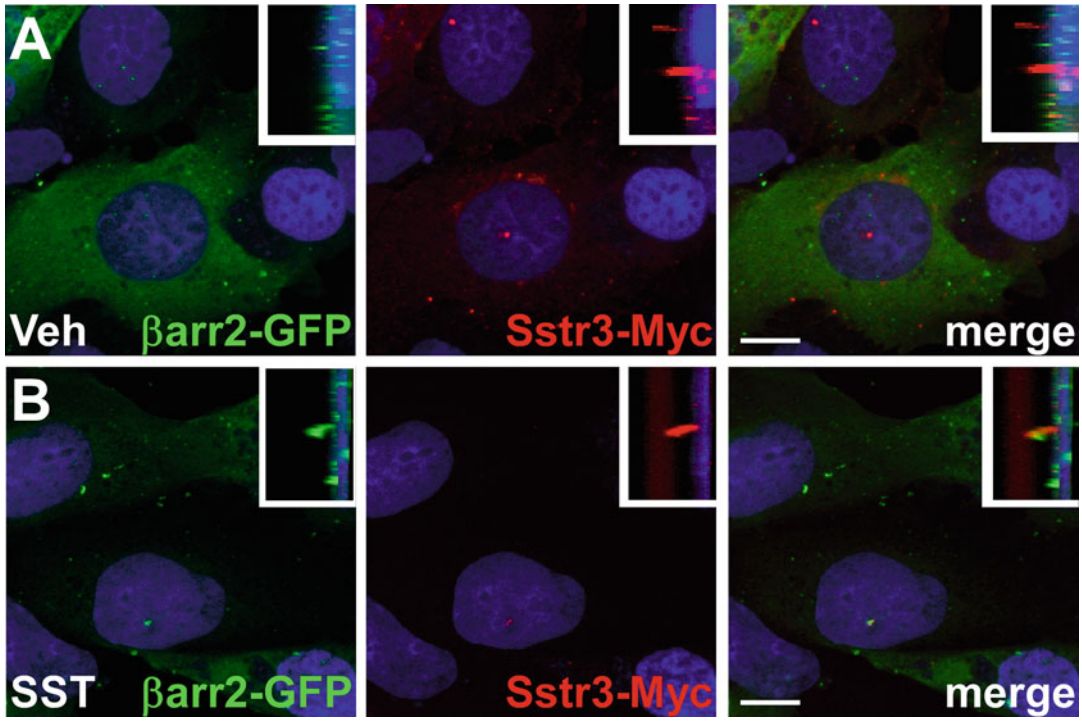


Fig. 5 βarr2-GFP is recruited into cilia in IMCD cells in response to somatostatin treatment. IMCD cells expressing βarr2-GFP and Sstr3-Myc were treated with vehicle (Veh) (**a**) or 10 μM somatostatin (SST) (**b**) for 20 min, fixed, and labeled with an antibody to detect Myc. Insets show side views of the cilia. Nuclei were stained with DRAQ5. Scale bars represent 10 μm

3.12 Fluorescence Microscopy of IMCD Cells

Image cells that are positive for βarr2-GFP and Sstr3-Myc, and capture multiple focal planes (Z-stack) spaced at ~0.3 μm intervals. The GFP, Myc, and DRAQ5 are excited with the 488, 552, and 638 nm laser lines, respectively.

Representative images of βarr2-GFP localization in IMCD cells expressing Sstr3-Myc in cilia are shown in Fig. 5. After 20 min of vehicle treatment, βarr2-GFP remains localized throughout the cytoplasm, but is not detected within cilia (Fig. 5a). After 20 min of 10 μM SST treatment, βarr2-GFP shows robust ciliary localization (Fig. 5b), suggesting that βarr2-GFP localizes to cilia in response to Sstr3 activation.

3.13 Transfection of Hippocampal Neurons with Plasmid DNA

1. To plate hippocampal neurons on glass-bottomed dishes, resuspend pelleted neurons from the hippocampus of one mouse in 1 mL of Neurobasal-A medium, and slowly pipette the cells onto the glass surface until the medium resembles a blister and covers the entire glass surface (*see* **Note 12**). Gently place the plate in a tissue culture incubator, and allow the neurons to adhere for approximately 2 h. Once the neurons

have adhered, add 2 mL of additional Neurobasal-A medium to completely cover the bottom of the dish.

2. On the day of transfection (we normally transfect on day 6), pipette virtually all the media from the dish into a sterile tube, and keep it at 37 °C (*see* **Note 13**).
3. Prepare the transfection mix. For each glass-bottomed dish, mix 1 μg of DNA (500 ng of βarr2-GFP + 500 ng of Sstr3DsRed) with 1 μL of PLUS reagent in 200 μL of Opti-MEM, and incubate for 5 min at RT. After 5 min, add 1.5 μL of Lipofectamine LTX reagent, mix, and incubate for an additional 30 min at RT.
4. Pipette the transfection mix over the neurons, and place the dish back in the incubator. After 2–4 h, add back the original conditioned media recovered in step Subheading 3.13, **step 2**.
5. Incubate the cells with transfection mix for 16–24 h before live-cell imaging analysis.

3.14 Live-Cell Imaging of Sstr3-Mediated Recruitment of βarr2-GFP in Hippocampal Neurons

1. Prior to imaging the cells, replace the media with 2 mL of Hibernate A low-fluorescence medium supplemented with B-27, glutaMAX, and ITS (*see* **Note 14**).
2. Image neurons expressing βarr2-GFP and Sstr3-DsRed. Acquire Z-stacks of the red and green fluorescence sequentially at 30 s intervals for 10 min using a 0.2 μm step size and a 100×/1.4NA PlanApo VC oil immersion objective. The GFP and DsRed2 are excited with the 488 nm and 561 nm laser lines, respectively.
3. Add somatostatin (20 μL of 1 mM stock solution) directly to the 2 mL of medium in the dish with a pipette, and continue acquiring Z-stacks sequentially for 10 min.

An example of SST treatment of a hippocampal neuron expressing βarr2-GFP and Sstr3-DsRed is shown in Fig. 6. Before SST treatment (t0), βarr2-GFP is enriched at the base of the cilium but is not detected within the cilium. βarr2-GFP localization in the cilium is detected within 2 min (t2) of SST treatment and is more robustly detected after 8 min (t8).

In conclusion, our experiments utilizing fixed and living cells indicate that exogenous βarr2 is enriched at the base of cilia expressing exogenous Sstr3 but is not detectable within the ciliary compartment. However, upon agonist addition, βarr2 is rapidly recruited into cilia where it likely interacts with Sstr3 to modulate receptor signaling and/or trafficking.

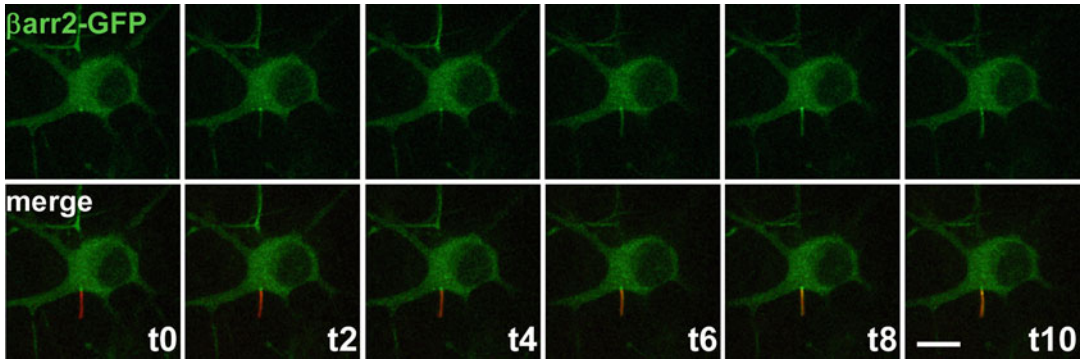


Fig. 6 βarr2-GFP is recruited into cilia in hippocampal neurons in response to somatostatin treatment. Live hippocampal neurons expressing βarr2-GFP and Sstr3-DsRed2 were treated with 10 μM somatostatin (SST) and imaged for 10 min. Elapsed time (t) in min of SST treatment is indicated in the lower right corner of each panel. Each image is a maximum intensity projection of a Z-stack that encompassed the entire cell body and cilium. Upper panels show the green channel (βarr2-GFP), and lower panels show both the green and red (Sstr3-DsRed) channels. Scale bar represents 10 μm

4 Notes

1. Permeabilization buffer should be stored at −20 °C in aliquots and thawed and kept at 4 °C upon use.
2. The addition of sodium azide prevents contamination and allows the buffer to be stored at 4 °C.
3. This step is important to stick the coverslips to the bottom of the wells and to avoid their overlap.
4. Move gently your plate in perpendicular directions in order to disperse cells or the transfection mix in the wells. Avoid circular movements; otherwise, generated vortex will deposit cells or the transfection medium mostly in the middle of the well.
5. This overnight treatment with nocodazole will depolymerize microtubules and will therefore arrest mitotic cells in G_2/M phase.
6. To avoid cell detachment, do not put directly the new medium onto the cells but slowly along wells' walls. Never aspirate the liquid directly over the coverslips, but lean the plate toward you, and use a 200 μL pipette tip to aspirate the medium along the wells' walls.
7. In case of doubt about the coverslip orientation, cells' covered surface can be observed on by holding it with the forceps and by exposing it to a source of light or by making a little scratch on the surface.
8. This step is required when using mounting media which do not dry (glycerol based). Avoid small holes that will favor oil

contact with mounting media and the cells. Avoid coverslip movements on the slide; otherwise, the cells will detach.

9. Do not forget to adapt the transfection mix to the volume of the used wells.
10. The centrosome can move in the horizontal and/or vertical axis during acquisition.
11. The antibody against acetylated α-tubulin allows visualization of stable MTs and, in addition to the axoneme of primary cilia, will also stain other stabilized MT such as cytoplasmic MTs (cell type dependent), mitotic spindle, and intercellular bridges. If cytoplasmic staining with this antibody is too strong, then avoid visualization of cilia; other ciliary markers can be used (Arl13b, glutamylated tubulin (GT335)).
12. Glass-bottomed dishes are manufactured by drilling a hole in the bottom of a plastic 35 mm tissue culture dish and covering the hole by attaching a glass coverslip to the outside of the dish. Thus, a shallow well is formed in the middle of the dish which will retain the medium containing cells over the glass surface.
13. Neurons are sensitive to media changes, and this conditioned media will be added back to the neurons. Ensure that a small amount of media is retained in the glass-bottomed well to prevent the neurons from drying out. This reduction in volume at the beginning of the transfection appears to facilitate the delivery of the DNA to the neurons and increases the transfection efficiency.
14. Hibernate medium allows the neurons to be maintained at 37 °C in ambient CO_2.

References

1. Ishikawa H, Marshall WF (2011) Ciliogenesis: building the cell's antenna. Nat Rev Mol Cell Biol 12:222–234
2. Mitchison HM, Valente EM (2016) Motile and non-motile cilia in human pathology: from function to phenotypes. J Pathol 241:294–309
3. Bornens M (2012) The centrosome in cells and organisms. Science 335:422–426
4. Benmerah A (2013) The ciliary pocket. Curr Opin Cell Biol 25:78–84
5. Takao D, Verhey KJ (2016) Gated entry into the ciliary compartment. Cell Mol Life Sci CMLS 73:119–127
6. Lechtreck KF (2015) IFT-cargo interactions and protein transport in cilia. Trends Biochem Sci 40:765–778
7. Schou KB, Pedersen LB, Christensen ST (2015) Ins and outs of GPCR signaling in primary cilia. EMBO Rep 16:1099–1113
8. Mykytyn K, Askwith C (2017) G-protein-coupled receptor signaling in cilia. Cold Spring Harb Perspect Biol
9. Dawson TM, Arriza JL, Jaworsky DE, Borisy FF, Attramadal H, Lefkowitz RJ, Ronnett GV (1993) Beta-adrenergic receptor kinase-2 and beta-arrestin-2 as mediators of odorant-induced desensitization. Science 259:825–829
10. Molla-Herman A, Boularan C, Ghossoub R, Scott MGH, Burtey A, Zarka M, Saunier S, Concordet J-P, Marullo S, Benmerah A (2008) Targeting of beta-arrestin2 to the centrosome and primary cilium: role in cell proliferation control. PLoS One 3:e3728

11. Kovacs JJ, Whalen EJ, Liu R, Xiao K, Kim J, Chen M, Wang J, Chen W, Lefkowitz RJ (2008) Beta-arrestin-mediated localization of smoothened to the primary cilium. Science 320:1777–1781
12. Mick DU, Rodrigues RB, Leib RD, Adams CM, Chien AS, Gygi SP, Nachury MV (2015) Proteomics of primary cilia by proximity labeling. Dev Cell 35:497–512
13. Pal K, Hwang S-H, Somatilaka B, Badgandi H, Jackson PK, DeFea K, Mukhopadhyay S (2016) Smoothened determines β-arrestin-mediated removal of the G protein-coupled receptor Gpr161 from the primary cilium. J Cell Biol 212:861–875
14. Green JA, Schmid CL, Bley E, Monsma PC, Brown A, Bohn LM, Mykytyn K (2016) Recruitment of β-Arrestin into neuronal cilia modulates somatostatin receptor subtype 3 ciliary localization. Mol Cell Biol 36:223–235
15. Nager AR, Goldstein JS, Herranz-Pérez V, Portran D, Ye F, Garcia-Verdugo JM, Nachury MV (2017) An actin network dispatches ciliary GPCRs into extracellular vesicles to modulate signaling. Cell 168:252–263.e14
16. Kang DS, Tian X, Benovic JL (2014) Role of β-arrestins and arrestin domain-containing proteins in G protein-coupled receptor trafficking. Curr Opin Cell Biol 27:63–71
17. Shankar H, Michal A, Kern RC, Kang DS, Gurevich VV, Benovic JL (2010) Non-visual arrestins are constitutively associated with the centrosome and regulate centrosome function. J Biol Chem 285:8316–8329
18. Piel M, Meyer P, Khodjakov A, Rieder CL, Bornens M (2000) The respective contributions of the mother and daughter centrioles to centrosome activity and behavior in vertebrate cells. J Cell Biol 149:317–330
19. Taipale J, Chen JK, Cooper MK, Wang B, Mann RK, Milenkovic L, Scott MP, Beachy PA (2000) Effects of oncogenic mutations in smoothened and patched can be reversed by cyclopamine. Nature 406:1005–1009

Part VI

Methods to Study Conformational Change of β-Arrestin



Chapter 18

A Mass Spectrometry-Based Structural Assay for Activation-Dependent Conformational Changes in β-Arrestins

Yang Zhao and Kunhong Xiao

Abstract

β-Arrestins are key regulation proteins for G protein-coupled receptors (GPCRs) signaling. Experimental evidence suggests that β-arrestins undergo conformational changes concomitant with binding to activated, phosphorylated GPCRs. We developed a mass spectrometry-based structural proteomic assay to monitor conformational changes associated with the activation of β-arrestins. This assay utilizes synthesized phosphopeptides mimicking phosphorylated C-terminal tails of GPCRs to activate β-arrestins. The activation-dependent conformational changes of β-arrestins are revealed using limited proteolysis coupled with both SDS-PAGE and mass spectrometry analysis. As an in vitro β-arrestin activation assay, this mass spectrometry-based structural method can be adapted as a simple but useful tool to study the nature and extent of conformational changes of β-arrestins downstream of different receptors as well as β-arrestin conformations associated with different functions, such as desensitization, internalization, and signaling.

Key words 7TMR, GPCR, GPCR phosphorylation, Phosphopeptide, Arrestin, β-Arrestin, Mass spectrometry, Proteomics, Limited proteolysis, Matrix-assisted laser desorption/ionization-time-of-flight mass spectrometry, MALDI-TOF MS

1 Introduction

Fundamental to the regulation of G protein-coupled receptors (GPCRs) are a group of proteins known as the β-arrestins [1–3]. The β-arrestins are unique in their ability to regulate GPCRs in that they can function to facilitate the processes of both receptor desensitization and internalization while simultaneously scaffolding additional signaling proteins [1–5]. Studies involving mutagenesis and biochemical and biophysical analysis suggest that β-arrestin undergoes conformational changes concomitant with binding an activated, phosphorylated GPCR [6–30]. A better comprehension of the nature and extent of conformational changes associated with the activation of β-arrestins is crucial to

Mark G. H. Scott and Stéphane A. Laporte (eds.), *Beta-Arrestins: Methods and Protocols*, Methods in Molecular Biology, vol. 1957, https://doi.org/10.1007/978-1-4939-9158-7_18, © Springer Science+Business Media, LLC, part of Springer Nature 2019

understand GPCR function and signaling, in particular with regard to recently discovered β-arrestin-mediated GPCR signaling modes.

In sharp contrast with the multiplicity of GPCRs, arrestins are a small family of proteins. There are only four known subtypes of arrestin: visual arrestin (arrestin 1), cone arrestin (arrestin 4), β-arrestin 1 (arrestin 2), and β-arrestin 2 (arrestin 3) [2, 31]. Visual arrestin and cone arrestin are expressed primarily in the retina and the pineal gland; they are almost exclusively involved in visual signaling. β-Arrestins 1 and 2 are ubiquitously expressed throughout the body and are fundamental to the regulation of GPCR-mediated signaling. In recent years, the X-ray crystal structures of visual arrestin, cone arrestin, β-arrestin 1, and β-arrestin 2 in different inactive and active states have been solved, revealing significant homology of the four arrestin isoforms [19, 21–23, 25, 32–39]. The overall structure of arrestin is an elongated molecule with two domains (N- and C-domain), connected through a 12-residue linker region. The most distinctive feature for arrestin structure is that of a hydrogen-bonded polar core, embedded between the N- and C-domains at the fulcrum of the molecule, which stabilizes the overall conformation [19, 21–23].

Although the recently resolved X-ray crystal structures of active forms of arrestins provided insight into the overall structural mechanism of arrestin activation [24, 25, 36, 39, 40], they are static and may not fully represent the precise structures of arrestins and their conformational changes in vivo. Other complementary biochemical and biophysical approaches are also useful to reveal details of the dynamic conformational changes of arrestins [29, 30]. For example, arrestin conformational change was first predicted by Hofmann and coworkers in the 1980s, on the basis of a high Arrhenius activation energy for the binding of visual arrestin to rhodopsin [18]. The idea of a conformational change in visual arrestin was further supported by Hargrave and others via biochemical and biophysical studies, including limited proteolysis [11, 16, 28]. Their data provides evidence that visual arrestin can undergo a conformational rearrangement in the presence of a phosphorylated peptide simulating the phosphorylated C-terminal tail of rhodopsin. Using a synthetic phosphorylated peptide mimicking the phosphorylated C-terminal tail of the vasopressin type II receptor (V_2R), we previously demonstrated conformational changes in both β-arrestins 1 and 2 [26, 27]. This β-arrestin activation assay involves using limited proteolysis to monitor the changes in solvent accessibilities of some key residues for β-arrestin structure and activation. Both SDS-PAGE and matrix-assisted laser desorption/ionization-time-of-flight mass spectrometry (MALDI-TOF MS) were used as readouts for limited proteolysis. The results obtained from these mass spectrometry-based studies [26, 27] were later confirmed by the X-ray crystallization structure of the V_2R8p-β-arrestin 1 complex [25]. Although this method is a

low-resolution structural approach, it is simple and straightforward and can be easily adapted to study conformational changes of β-arrestins activated by other phosphopeptides or phosphorylated GPCRs. In addition, more detailed and precise measurements of limited proteolytic peptides using more sensitive mass spectrometers will provide further structural information for β-arrestin activation and signaling.

2 Materials

2.1 Phosphopeptide Design and Synthesis

1. Phosphopeptide V_2R8p (also called V_2Rpp): ARGR**pT**PP**pS**LGPQDE**pSC**p**T**p**T**A**pS**p**S**p**S**LAKDTSS, with the phosphorylated residues shown as pT and pS and bolded. V_2R8p is synthesized by the Peptide Synthesis Core of Tufts University using an ABI 431 Peptide Synthesizer.
2. Control nonphosphopeptide V_2Rnp: ARGRTPPSLGPQDESCTTASSSLAKDTSS. V_2Rnp is synthesized by the Peptide Synthesis Core of Tufts University using an ABI 431 Peptide Synthesizer.
3. Preparative HPLC.

2.2 β-Arrestin Protein Sample Preparation

1. Wild-type β-arrestin 1 cDNA construct.
2. Wild-type β-arrestin 2 cDNA construct.
3. pGEX4T1 expression vector.
4. pGEX4T3 expression vector.
5. *E. coli* strain BL21 (DE3) pLysS.
6. Luria-Bertani (LB) broth.
7. LB agar plate.
8. Ampicillin.
9. Isopropyl-1-thio-β-D-galactopyranoside (IPTG).
10. Tris base.
11. Sodium chloride (NaCl).
12. Calcium chloride ($CaCl_2$).
13. 1,4-Dithiothreitol (DTT).
14. (Ethylenedinitrilo)tetraacetic acid (EDTA).
15. Ethylene glycol-bis(2-aminoethylether)-*N,N,N′,N′*-tetraacetic acid (EGTA).
16. Phenylmethanesulfonyl fluoride (PMSF).
17. Benzamidine.
18. Thrombin protease (Sigma).

19. Glutathione Sepharose 4B GST-tagged protein purification resin (GE Healthcare Life Sciences).
20. Heparin Sepharose 6 Fast Flow affinity resin (GE Healthcare Life Sciences).
21. SP Sepharose High Performance resin (GE Healthcare Life Sciences).
22. Superdex 75 10/300 GL size exclusion chromatography column (GE Healthcare Life Sciences).
23. ÄKTAFPLC system (GE Healthcare Life Sciences).
24. SDS-PAGE apparatus.
25. Liquid nitrogen.
26. 5 mL HiTrap Mono-Q column.
27. Binding buffer (B-buffer) (25 mM Tris–HCl, pH 8.5, 150 mM NaCl, 2 mM DTT, 2 mM EDTA, 2 mM EGTA, 1 mM PMSF, and 0.2 mg/mL benzamidine).
28. Column buffer 1 (C-buffer 1) (25 mM Tris–HCl, pH 8.5, 150 mM NaCl, 2.5 mM $CaCl_2$, 2 mM DTT).
29. Column buffer 2 (C-buffer 2) (25 mM Tris–HCl, pH 8.5, 150 mM NaCl, 2.5 mM $CaCl_2$, 2 mM DTT, 0.05% n-octyl-β-D-glucopyranoside (OG)).
30. Dilution buffer 1 (D-buffer 1) (25 mM Tris–HCl, pH 8.5, 2 mM DTT).
31. Dilution buffer 2 (D-buffer 2) (25 mM Tris–HCl, pH 8.5, 2 mM DTT, 0.05% OG).
32. Elution buffer 1 (E-buffer 1) (25 mM Tris–HCl, pH 8.5, 150 mM NaCl, 2 mM DTT).
33. Dialysis buffer 2 (DIA-buffer 2) (25 mM Tris–HCl, pH 8.5, 50 mM NaCl, 2 mM DTT, 2 mM EDTA, 2 mM EGTA, 0.05% OG).

2.3 Activation of β-Arrestin by V_2Rpp

1. V_2R8p: ARGR**pT**PP**pS**LGPQDE**pS**C**pTpTA**p**S**p**S**p**S**LAKDTSS.
2. V_2Rnp: ARGRTPPSLGPQDESCTTASSSLAKDTSS.
3. Peptide-dissolving buffer: 25 mM Tris–HCl, pH 8.0, and 150 mM NaCl.
4. 1 M NaOH.

2.4 Limited Tryptic Proteolysis

1. N-Tosyl-L-phenylalanine chloromethyl ketone (TPCK)-treated trypsin (Sigma).
2. Trifluoroacetic acid (TFA).
3. Liquid nitrogen or dry ice.
4. 1.7 mL Axygen microcentrifuge tubes.

5. 2× SDS-PAGE sample buffer (80 mM Tris–HCl, pH 6.8, 2% SDS, 10% glycerol, 0.0006% bromophenol blue, 0.1 M DTT).

2.5 SDS-PAGE Analysis

1. 4–20% SDS-PAGE gel (Invitrogen).
2. SDS-PAGE apparatus.
3. Acetic acid.
4. Methanol.
5. Brilliant blue G-Colloidal Concentrate (B2025, Sigma).
6. Double-distilled water.
7. Bio-Rad Universal Hood Gel Doc system.

2.6 MALDI-TOF MS Analysis

1. Sinapinic acid (SA) (Sigma).
2. Acetonitrile.
3. Trifluoroacetic acid (TFA).
4. Methanol.
5. C18 ZipTip® pipette tips (Millipore).
6. Stainless steel MALDI sample plate (Applied Biosystems).
7. Voyager-DE Biospectrometry Workstation (Applied Biosystems).
8. ProteinProspector program (http://prospector.ucsf.edu/).

3 Methods

3.1 Phosphopeptide Design and Synthesis

1. The phosphopeptide V_2R8p (or V_2Rpp) is designed based on the C-terminal sequence of the human V_2R which is ARGRTPPSLGPQDESCTTASSSLAKDTSS with eleven (11) potential phosphorylation sites. To synthesize the V2R8p, eight (8) phosphorylated residues are incorporated in a 29 mer phosphopeptide. The three most distal C-terminal residues "TSS" are not replaced with phosphorylated amino acids due to technical difficulties during peptide synthesis. The final sequence for V_2R8p is ARGR**pT**PP**pS**LGPQ-DE**pS**C**pTpTA**p**S**p**S**p**S**LAKDTSS, with the phosphorylated residues shown as pT and pS in bold type.
2. The corresponding nonphosphopeptide V_2Rnp is also synthesized as a control. The sequence of the V_2Rnp is ARGRTPPSLGPQDESCTTASSSLAKDTSS.
3. Both V_2R8p and V_2Rnp are purified by preparative HPLC.

3.2 β-Arrestin Protein Sample Preparation

3.2.1 β-Arrestin 1 Protein Purification

The step-by-step protocol described below is based on our previous work [26].

1. Wild-type β-arrestin 1 is subcloned into a pGEX4T1 vector to express GST-tagged β-arrestin 1 (i.e., GST-β-arrestin 1). Confirm cDNA by sequencing.
2. Transform GST-β-arrestin 1 DNA construct into *E. coli* strain BL21 (DE3) pLysS using conventional method.
3. After transformation, spread the cells onto an LB agar plate containing 100 μg/mL ampicillin, and incubate the plate at 37 °C overnight.
4. Pick up a single colony from the LB agar plate, and inoculate into 10 mL LB broth containing 100 μg/mL ampicillin. Incubate at 37 °C overnight with shaking at 200 rpm.
5. Inoculate 800 mL of LB media with 10 mL of overnight cell culture, and grow initially at 37 °C until the OD_{600} reaches 0.6–0.8.
6. Lower the temperature to 25 °C, and induce GST-β-arrestin 1 expression with 100 μM IPTG for 16 h.
7. Harvest the cells by centrifugation at 4500 × *g* for 30 min.
8. Resuspend bacterial cell pellet in binding buffer (B-buffer) to give 10% slurry (*w/w*).
9. Lyse the cells by freeze-thaw followed by sonicating the cell suspension in binding buffer by ten short pulses of 10 s with intervals of 30 s for cooling (*see* **Note 1**).
10. Centrifuge the cell lysate at 18,000 × *g* for 30 min, and filter the supernatant through a 0.8 μm membrane.
11. Load the clarified supernatant onto a glutathione-Sepharose (GS) column (Pharmacia or GE Healthcare) by gravity, and wash the column with 20 column volumes of column buffer 1 (C-buffer 1) (*see* **Note 2**).
12. Resuspend the GST-β-arrestin 1 bound GS resin in two column volumes of C-buffer 1.
13. Add thrombin protease (10 unit/L of cell culture) to cleave the GST protein tag, and start thrombin digestion at 4 °C for 16 h with gentle agitation of the GS resin.
14. Collect the flow through, and wash the GS resin with two volumes of B-buffer 1.
15. Pool the wash with the initial flow through. The NaCl concentration is diluted dropwise to 50 mM using dilution buffer 1 (D-buffer 1).
16. Load the cleaved β-arrestin 1 onto a 5 mL HiTrap Mono-Q column, and elute the β-arrestin 1 protein with a 50–500 mM linear NaCl gradient.

17. Fractions are analyzed by SDS-PAGE, and the β-arrestin 1-containing fractions are pooled and concentrated to 25 mg/mL.
18. Load the concentrated β-arrestin 1 onto a Superdex 75 10/300 GL size exclusion chromatography column, and elute the protein in elution buffer 1 (E-buffer 1).
19. Analyze β-arrestin 1-containing fractions by SDS-PAGE and Coomassie staining, pool the fractions with more than 95% purity, and concentrate protein to 5–25 mg/mL.
20. Flash freeze β-arrestin 1 protein in liquid nitrogen, and store at −80 °C (*see* **Note 3**).

3.2.2 β-Arrestin 2 Protein Purification

The step-by-step protocol described below is based on our previous work [27].

1. Wild-type β-arrestin 2 is subcloned into a pGEX4T3 vector to express GST-tagged β-arrestin 2 (i.e., GST-β-arrestin 2). Confirm cDNA by sequencing.
2. Transform GST-tagged β-arrestin 2 DNA construct into *E. coli* strain BL21 (DE3) pLysS.
3. Follow steps similar to those for β-arrestin 1 purification in Subheading 3.2.1, **step 3–11**.
4. Resuspend the GST-β-arrestin bound GS resin in two column volumes of column buffer 2 (C-buffer 2) (*see* **Note 4**).
5. Add thrombin protease (10 unit/L of cell culture) to cleave the GST protein tag, and start thrombin digestion at 4 °C for 16 h with gentle agitation of the GS resin.
6. Collect the flow through, and wash the GS resin with two volumes of C-buffer 2.
7. Pool the wash with the initial flow through, and dilute with dilution buffer 2 (D-buffer 2) to a final NaCl concentration of 50 mM.
8. Load the sample on a Heparin Sepharose column, and elute the β-arrestin 2 protein with a 50–350 mM linear NaCl gradient.
9. Pool fractions containing β-arrestin 2 proteins, and dialyze overnight against dialysis buffer 2 (DIA-buffer 2).
10. After dialysis, load the sample onto a SP Sepharose High Performance column, and elute β-arrestin 2 with a 50–350 mM linear NaCl gradient in the dialysis buffer.
11. Analyze fractions by SDS-PAGE, pool the fractions with more than 95% purity, and dialyze overnight against D-buffer 2.
12. Concentrate the purified protein to 5–10 mg/mL, flash freeze in liquid nitrogen, and store at −80 °C (*see* **Note 5**).

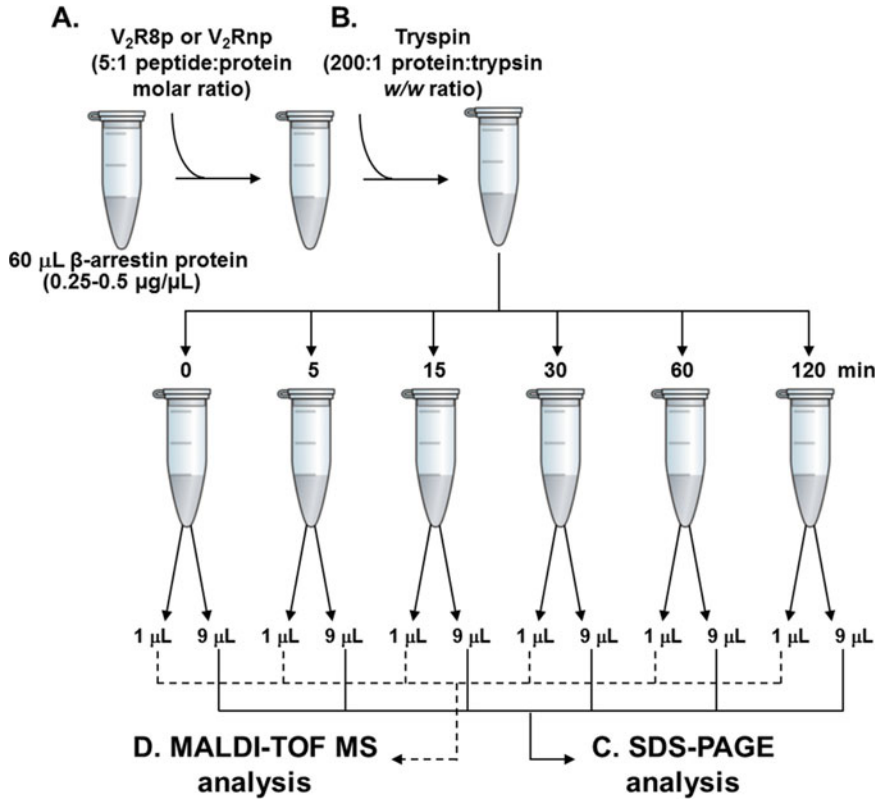


Fig. 1 Experimental procedures for the mass spectrometry-based structural assay for activation-dependent conformation changes in β-arrestins. (**a**) Activation of β-arrestin 1 or 2 by addition of 5:1 molar ratio excess (peptide-to-β-arrestin) of phosphopeptide V2R8p. V2Rnp is used as a control. (**b**) Trypsin at 100–5000:1 (β-arrestin-to-trypsin) ratio is added to the peptide-β-arrestin mixture to start the limited tryptic proteolysis reaction. The limited proteolysis reaction is quenched at different time points (e.g., 0, 5, 15, 30, 60, and 120 min). (**c**) At each time point, 1 μL (~0.25–0.5 μg of β-arrestin 1 or 2) of limited proteolysis mixture is removed for MALDI-TOF analysis. (**d**) Meanwhile, 9 μL (~2.25–4.5 μg of β-arrestin 1 or 2) of limited proteolysis mixture is removed for SDS-PAGE analysis

3.3 Activation of β-arrestin by V_2R8p (Fig. 1A)

1. Dissolve V_2R8p and V_2Rnp in 25 mM Tris–HCl, pH 8.0, 150 mM NaCl.
2. Adjust the pH of peptides with 1 M NaOH to 8.0.
3. Adjust the concentration of peptides to 1 mM with 25 mM Tris–HCl, pH 8.0, 150 mM NaCl.
4. Dilute β-arrestin (1 or 2) protein in 25 mM Tris–HCl, pH 8.0, 150 mM NaCl to a final concentration of 5–10 μM (~ 0.25–0.50 mg/mL or 0.25–0.50 μg/μL).
5. Transfer appropriate amount of β-arrestin (1 or 2) protein to a microcentrifuge tube at room temperature. If six (6) time points are used for limited tryptic proteolysis, transfer 60 μL diluted protein to the microcentrifuge tube.

6. Mix peptides (e.g., V_2R8p or V_2Rnp) with β-arrestin (1 or 2) protein at a 5:1 molar ratio (peptide to protein), and incubate the mixture at room temperature for 30 min (*see* **Note 6**).

3.4 Limited Tryptic Proteolysis (Fig. 1B)

1. Add an appropriate amount (usually 100–5000:1 *w/w* ratio of protein/trypsin) of N-tosyl-L-phenylalanine chloromethyl ketone (TPCK)-treated trypsin to the peptide-β-arrestin mixtures, and start limited proteolysis (*see* **Note 7**).
2. Incubate the limited proteolysis samples at 37 °C for different time points, for example, 0, 5, 15, 30, 60, and 120 min (*see* **Note 8**).
3. At each time point, quickly remove 1 μL (~0.25–0.5 μg of β-arrestin 1 or 2) from the limited proteolysis reaction to a microcentrifuge tube with 5 μL 1% TFA to quench the trypsin digestion. Flash freeze the microcentrifuge tube in liquid nitrogen, and store at −80 °C until MALDI-TOF analysis (*see* **Note 9**).
4. Meanwhile, quickly remove 9 μL (~2.25–4.5 μg of β-arrestin 1 or 2) from the limited proteolysis reaction to another microcentrifuge tube containing 9 μL of 2× SDS-PAGE buffer, and boil the sample for 5 min to quench the tryptic digestion.
5. After samples are collected for all planned time points, perform MALDI-TOF and SDS-PAGE analysis individually.

3.5 SDS-PAGE Analysis (Fig. 1C)

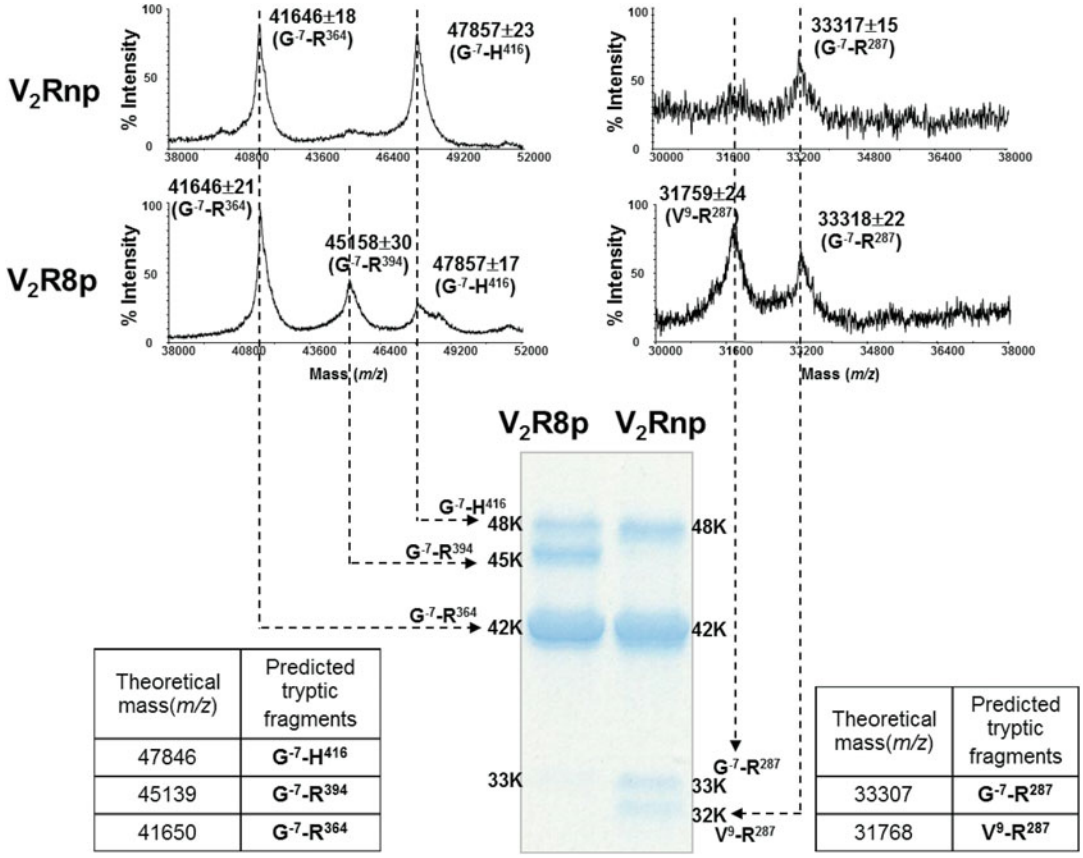
1. Load the samples on a 4–20% SDS-PAGE gel to determine the effects of peptides on the digestion pattern of β-arrestins (1 or 2) (*see* **Note 10**).
2. Run the gel at 200 V for about 30–45 min.
3. When gel electrophoresis is done, fix the proteins in the gel for 1 h with a solution of 7% acetic acid in 40% (*v/v*) methanol.
4. Immediately before staining, combine four parts of the 1× Brilliant Blue G-Colloidal working solution and one part methanol. Vortex vigorously for 1 min. Remove the fixing solution, and add 20–30 mL of the Brilliant Blue G-Colloidal stain to gel, and shake for 1–2 h (*see* **Note 11**).
5. Remove the stain, and destain the gel by adding a solution of 10% acetic acid in 25% (*v/v*) methanol. Shake for 1 min.
6. Remove the destain solution and wash the gel twice in 25% methanol.
7. Remove the 25% methanol and add double-distilled water.
8. Capture images of the gel using a Bio-Rad Universal Hood Gel Doc system or other gel image systems.

3.6 MALDI-TOF MS Analysis (Fig. 1D)

1. Remove the microcentrifuge containing 6 μL flash frozen limited tryptic proteolysis products (from Subheading 3.4, **step 3**) from −80 °C freezer, and thaw on ice.
2. Prepare matrix sinapinic acid (SA) as a saturated, aqueous solution that contains 45% acetonitrile and 0.1% TFA.
3. Add 6 μL SA matrix solution to 6 μL flash frozen limited tryptic proteolysis products. Vortex.
4. Deposit 0.5–1 μL of the sample matrix mixture on the MALDI-TOF sample plate (*see* **Note 12**).
5. Allow samples to air-dry at room temperature and then subject to MALDI-TOF analysis.
6. Collect MALDI-TOF mass spectra on a Voyager-DE Biospectrometry Workstation (Applied Biosystems) in the linear mode using a nitrogen laser (337 nm). Mass spectra are collected in the positive ion mode using an acceleration voltage of 25 kV and a delay of 900 ns. The grid voltage, guide wire voltage, low mass gate, and laser intensity are optimized to 92.5%, 0.15%, 10,000.0 *m/z*, and 2580 units, respectively. Each mass spectrum collected is the mean of 100–500 laser shots (*see* **Note 13**).

3.7 Data Analysis and Interpretation

1. Use SDS-PAGE gels to compare the limited tryptic proteolysis patterns of β-arrestin in the presence of V_2R8p and V_2Rnp. Estimate the masses of limited tryptic proteolysis fragments using molecular weight standards (Fig. 2; β-arrestin 2 is used in Fig. 2 to show data analysis procedures) (*see* **Note 14**).
2. Perform a theoretical MALDI-TOF MS analysis of the molecular masses for all potential tryptic proteolytic fragments for β-arrestin using a ProteinProspector program (http://prospector.ucsf.edu/prospector/cgi-bin/msform.cgi?form=msdigest) (*see* **Note 15**).
3. Use MALDI-TOF MS spectra obtained to compare the experimental molecular mass (*m/z*) of each limited proteolytic fragment with the theoretical masses (*m/z*) predicted by ProteinProspector program, and list all the candidate fragments with theoretical masses (*m/z*) within the standard deviations (Fig. 2).
4. Assign the limited proteolysis fragments shown on SDS-PAGE gels using experimental molecular mass (*m/z*) of each limited proteolytic fragment and the theoretical masses (*m/z*) predicted by ProteinProspector program (Fig. 2). The limited proteolytic fragments with only one possible theoretical mass (*m/z*) within standard deviation are assigned to individual proteolytic fragments directly. The fragments with more than one possible theoretical mass (*m/z*), which cannot be distinguished



Theoretical mass(*m/z*)	Predicted tryptic fragments
47846	G^{-7}-H^{416}
45139	G^{-7}-R^{394}
41650	G^{-7}-R^{364}

Theoretical mass(*m/z*)	Predicted tryptic fragments
33307	G^{-7}-R^{287}
31768	V^{9}-R^{287}

Fig. 2 Assignment of the limited tryptic proteolytic fragments of β-arrestins. The limited tryptic proteolytic fragments of β-arrestin 2 are analyzed by both SDS-PAGE (bottom and middle panel) and MALDI-TOF MS (top panels). The effects of V_2R8p on limited tryptic proteolysis of β-arrestin 2 can be revealed on SDS-PAGE gel by distinct limited proteolysis patterns of β-arrestin 2 in the presence of V_2R8p and V_2Rnp. The masses of limited tryptic proteolysis fragments are first estimated using molecular weight standards on SDS-PAGE gels. In order to assign each proteolytic fragment of β-arrestin 2, the sequence of β-arrestin 2 is subjected to a theoretical tryptic digestion using a ProteinProspector program. The theoretical masses (*m/z*) of the tryptic proteolytic fragment candidates within the standard deviation of the experimental mass (*m/z*, averaged) of each fragment are selected and listed (bottom, left, and right panels). The limited proteolytic fragments with only one possible theoretical mass (*m/z*) within standard deviation are assigned to individual proteolytic fragments directly. The proteolytic fragments with more than one possible theoretical mass (*m/z*), which cannot be distinguished by MALDI-TOF MS, can be assigned by coupling the MS data with N-terminal sequencing, a Western blot analysis with antibodies that recognize different domains of β-arrestins

by MALDI-TOF MS, are assigned by coupling the MS data with N-terminal sequencing, Western blot analysis with antibodies that recognize different domains of β-arrestins, or other methods (*see* **Notes 16–18**).

5. Use limited proteolysis data of β-arrestins obtained above to delineate solvent accessibility profiles of key residues that

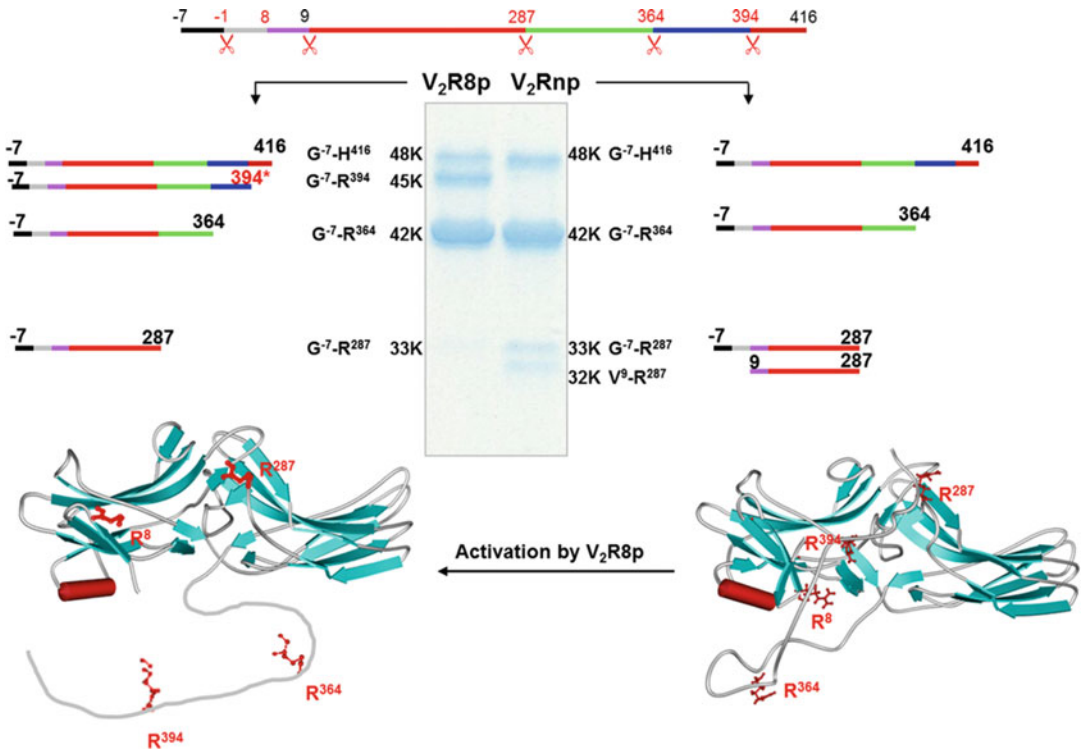


Fig. 3 Interpretation of limited proteolysis data using structural models of activation-dependent conformational changes in β-arrestins. Several key tryptic cleavage sites (e.g., $R,^{8}$ R^{287}, R^{364}, and R^{394}) of β-arrestin 2 are indicated on the top. The image of a SDS-PAGE gel is shown in the middle to demonstrate distinct limited proteolysis patterns of β-arrestin 2 in the presence of V_2R8p and V_2Rnp. The amino acid assignment of each band is labeled and illustrated on both sides of the SDS-PAGE gel image. On the bottom is a schematic model of activation-dependent conformational changes of β-arrestin 2 upon V_2R8p binding. Binding of V_2R8p leads to the release of the C-terminus from the core of the β-arrestin 2, as indicated by exposure of R^{394}, which was previously inaccessible because it is hidden in the polar core residue. Meanwhile, V_2R8p binding leads to a rearrangement of the N-terminus of β-arrestin 2, as indicated by the shielding of a previously accessible cleavage site, residue R^{8}

undergo significant changes in the presence of phosphopeptide V_2R8p.

6. Reveal the nature and extent of conformational changes of β-arrestins induced by V_2R8p binding and activation (Fig. 3; β-arrestin 2 is used to show data interpretation).

4 Notes

1. Cells can be lysed using different approaches, including sonication, cell cracker (Microfluides), or French press.
2. Protease inhibitors, such as PMSF and benzamidine, should be removed before thrombin digestion.

3. Protein purity is estimated using SDS-PAGE analysis against known BSA standards. Typical yield for β-arrestin 1 is about 5 mg/L of cell culture.
4. GST-tagged β-arrestin 2 protein is soluble at high concentration without detergents. However, protein aggregation/precipitation was observed after overnight thrombin digestion of the GST-tagged β-arrestin 2 protein. Addition of 0.05% n-octyl-β-D-glucopyranoside (OG) was found to prevent aggregation/precipitation of β-arrestin 2 proteins. This phenomenon was not observed during β-arrestin 1 purification.
5. Protein purity is estimated using SDS-PAGE analysis against known BSA standards. Typical yield for β-arrestin 2 is about 1 mg/L of cell culture.
6. Experiments with different V_2R8p to β-arrestin molar ratios showed that ratios of a large range (from 1:1 to 100:1) have similar effects on limited proteolysis of β-arrestin.
7. A 100–5000:1 *w/w* ratio of protein/trypsin is suggested for limited tryptic proteolysis. However, the optimized ratio should be determined by pilot experiments.
8. Limited tryptic proteolysis can also be performed at room temperature. The amount of trypsin and the limited proteolysis time points can be different when proteolysis temperature changes.
9. The TFA lowers the pH of the limited proteolysis solution and quenches the trypsin digestion reaction.
10. 4–20% SDS-PAGE gel is suggested. However, other SDS-PAGE gels can also be used.
11. Brilliant Blue G-Colloidal stain solution is suggested. However, other SDS-PAGE gel stain methods can also be used.
12. The methods for preparing MALDI-TOF plate can be different from the procedures described here. Please refer to appropriate MALDI-TOF plate preparation manuals and test different MALDI-TOF plate preparation methods to obtain the best MALDI signals.
13. Optimal MALDI-TOF instrumental parameters should be determined by experiments. Cytochrome c and carbonic anhydrase can be used as internal calibrants for data calibration. For each limited tryptic proteolytic fragment, the mean of the experimental molecular mass (m/z) is determined, and a standard deviation is calculated from multiple independent experiments.
14. Different molecular weight standards or markers should be used to estimate the masses of limited tryptic proteolysis fragments.

15. Parameter setting can allow two (2) maximum missed cleavages and with methionine oxidation as a variable modification. The average (av) *m/z* values should be used to compare with the experimental *m/z* values.
16. For N-terminal sequencing, limited proteolytic fragments are subjected to SDS-PAGE analysis. The proteolytic fragments are electrotransferred to a polyvinylidene difluoride membrane and stained by Coomassie Blue R-250. The stained protein bands of interest are excised and subjected to N-terminal sequencing.
17. If a limited proteolytic fragment cannot be distinguished by MALDI-TOF MS, Western blot analysis with an antibody that recognizes the predicted domain of β-arrestin can help to confirm the prediction and assignment.
18. One can use mass spectrometers with higher mass accuracy and higher resolution to obtain more precise masses of limited proteolytic fragments to facilitate the fragment assignments.

Acknowledgment

This work was supported, in part, by US National Institutes of Health grant no HL-075443 Proteomics Core support to K.X. This publication was also made possible by seed funding support to K.X. from the Department of Pharmacology and Chemical Biology, the University of Pittsburgh and Vascular Medicine Institute, the Hemophilia Center of Western Pennsylvania, and the Institute for Transfusion Medicine.

References

1. Ferguson SS, Zhang J, Barak LS, Caron MG (1998) Molecular mechanisms of G protein-coupled receptor desensitization and resensitization. Life Sci 62:1561–1565
2. Luttrell LM, Lefkowitz RJ (2002) The role of beta-arrestins in the termination and transduction of G-protein-coupled receptor signals. J Cell Sci 115:455–465
3. Pierce KL, Luttrell LM, Lefkowitz RJ (2001) New mechanisms in heptahelical receptor signaling to mitogen activated protein kinase cascades. Oncogene 20:1532–1539
4. Luttrell LM, Daaka Y, Lefkowitz RJ (1999) Regulation of tyrosine kinase cascades by G-protein-coupled receptors. Curr Opin Cell Biol 11:177–183
5. McDonald PH, Lefkowitz RJ (2001) Beta-Arrestins: new roles in regulating heptahelical receptors' functions. Cell Signal 13:683–689
6. Gurevich VV, Gurevich EV (2003) The new face of active receptor bound arrestin attracts new partners. Structure (Camb) 11:1037–1042
7. Hofmann KP (1999) Signalling states of photoactivated rhodopsin. Novartis Found Symp 224:158–175.; discussion 175–180
8. Raman D, Osawa S, Weiss ER (1999) Binding of arrestin to cytoplasmic loop mutants of bovine rhodopsin. Biochemistry 38:5117–5123
9. Sippel KC, DeStefano JD, Berson EL, Dryja TP (1998) Evaluation of the human arrestin gene in patients with retinitis pigmentosa and stationary night blindness. Invest Ophthalmol Vis Sci 39:665–670
10. Rim J, Oprian DD (1995) Constitutive activation of opsin: interaction of mutants with

rhodopsin kinase and arrestin. Biochemistry 34:11938–11945
11. Puig J et al (1995) Synthetic phosphopeptide from rhodopsin sequence induces retinal arrestin binding to photoactivated unphosphorylated rhodopsin. FEBS Lett 362:185–188
12. Gurevich VV, Benovic JL (1993) Visual arrestin interaction with rhodopsin. Sequential multisite binding ensures strict selectivity toward light-activated phosphorylated rhodopsin. J Biol Chem 268:11628–11638
13. Palczewski K, Riazance-Lawrence JH, Johnson WC Jr (1992) Structural properties of arrestin studied by chemical modification and circular dichroism. Biochemistry 31:3902–3906
14. Kotake S, Hey P, Mirmira RG, Copeland RA (1991) Physicochemical characterization of bovine retinal arrestin. Arch Biochem Biophys 285:126–133
15. McDowell JH et al (1999) Sulfhydryl reactivity demonstrates different conformational states for arrestin, arrestin activated by a synthetic phosphopeptide, and constitutively active arrestin. Biochemistry 38:6119–6125
16. McDowell JH et al (2001) Activation of arrestin: requirement of phosphorylation as the negative charge on residues in synthetic peptides from the carboxyl-terminal region of rhodopsin. Invest Ophthalmol Vis Sci 42:1439–1443
17. Palczewski K, Pulvermuller A, Buczylko J, Hofmann KP (1991) Phosphorylated rhodopsin and heparin induce similar conformational changes in arrestin. J Biol Chem 266:18649–18654
18. Schleicher A, Kuhn H, Hofmann KP (1989) Kinetics, binding constant, and activation energy of the 48-kDa protein-rhodopsin complex by extra-metarhodopsin II. Biochemistry 28:1770–1775
19. Han M, Gurevich VV, Vishnivetskiy SA, Sigler PB, Schubert C (2001) Crystal structure of beta-arrestin at 1.9 A: possible mechanism of receptor binding and membrane translocation. Structure (Camb) 9:869–880
20. Schubert C et al (1999) Visual arrestin activity may be regulated by self-association. J Biol Chem 274:21186–21190
21. Hirsch JA, Schubert C, Gurevich VV, Sigler PB (1999) The 2.8 A crystal structure of visual arrestin: a model for arrestin's regulation. Cell 97:257–269
22. Milano SK, Pace HC, Kim YM, Brenner C, Benovic JL (2002) Scaffolding functions of arrestin-2 revealed by crystal structure and mutagenesis. Biochemistry 41:3321–3328
23. Granzin J et al (1998) X-ray crystal structure of arrestin from bovine rod outer segments. Nature 391:918–921
24. Shukla AK et al (2014) Visualization of arrestin recruitment by a G-protein-coupled receptor. Nature 512:218–222
25. Shukla AK et al (2013) Structure of active beta-arrestin-1 bound to a G-protein-coupled receptor phosphopeptide. Nature 497:137–141
26. Nobles KN, Guan Z, Xiao K, Oas TG, Lefkowitz RJ (2007) The active conformation of beta-arrestin1: direct evidence for the phosphate sensor in the N-domain and conformational differences in the active states of beta-arrestins 1 and −2. J Biol Chem 282:21370–21381
27. Xiao K, Shenoy SK, Nobles K, Lefkowitz RJ (2004) Activation-dependent conformational changes in {beta}-arrestin 2. J Biol Chem 279:55744–55753
28. Palczewski K, Buczylko J, Imami NR, McDowell JH, Hargrave PA (1991) Role of the carboxyl-terminal region of arrestin in binding to phosphorylated rhodopsin. J Biol Chem 266:15334–15339
29. Xiao K, Chung J, Wall A (2015) The power of mass spectrometry in structural characterization of GPCR signaling. J Recept Signal Transduct Res 35:213–219
30. Xiao K, Sun J (2017) Elucidating structural and molecular mechanisms of beta-arrestin-biased agonism at GPCRs via MS-based proteomics. Cell Signal 41:56–64
31. Shenoy SK, Lefkowitz RJ (2003) Multifaceted roles of beta-arrestins in the regulation of seven-membrane-spanning receptor trafficking and signalling. Biochem J 375:503–515
32. Sutton RB et al (2005) Crystal structure of cone arrestin at 2.3A: evolution of receptor specificity. J Mol Biol 354:1069–1080
33. Zhan X, Gimenez LE, Gurevich VV, Spiller BW (2011) Crystal structure of arrestin-3 reveals the basis of the difference in receptor binding between two non-visual subtypes. J Mol Biol 406:467–478
34. Granzin J et al (2012) Crystal structure of p44, a constitutively active splice variant of visual arrestin. J Mol Biol 416:611–618. https://doi.org/10.1016/j.jmb.2012.01.028
35. Kim YJ et al (2013) Crystal structure of pre-activated arrestin p44. Nature 497:142–146
36. Kang Y et al (2015) Crystal structure of rhodopsin bound to arrestin by femtosecond X-ray laser. Nature 523:561–567. https://doi.org/10.1038/nature14656

37. Zhang J et al (1997) Molecular mechanisms of G protein-coupled receptor signaling: role of G protein-coupled receptor kinases and arrestins in receptor desensitization and resensitization. Receptors Channels 5:193–199
38. Granzin J, Stadler A, Cousin A, Schlesinger R, Batra-Safferling R (2015) Structural evidence for the role of polar core residue Arg175 in arrestin activation. Sci Rep 5:15808
39. Chen Q et al (2017) Structural basis of arrestin-3 activation and signaling. Nat Commun 8:1427
40. Zhou XE et al (2017) Identification of phosphorylation codes for arrestin recruitment by G protein-coupled receptors. Cell 170:457–469 e413



Chapter 19

Probing Arrestin Function Using Intramolecular FlAsH-BRET Biosensors

Erik G. Strungs, Louis M. Luttrell, and Mi-Hye Lee

Abstract

Information contained in the structure of extracellular ligands is transmitted across the cell membrane through allosterically induced changes in G protein-coupled receptor (GPCR) conformation that occur upon ligand binding. These changes, in turn, are imprinted upon intracellular effectors like arrestins and help determine which of its many functions are performed. Intramolecular fluorescein arsenical hairpin (FlAsH) bioluminescence resonance energy transfer (BRET), in which both the fluorescence donor and acceptor are contained within the same protein, can be used to report on activation-induced changes in protein conformation. Here, we describe a method using a series of *R*luc-arrestin3-FlAsH-BRET biosensors to measure stimulus-induced changes in arrestin conformation in live cells. Each *R*luc-arrestin3-FlAsH-BRET construct contains an N-terminal *Renilla* luciferase fluorescence donor that excites a fluorescent arsenical targeted to a different position within the protein by mutational insertion of a tetracysteine tag motif. Changes in net BRET upon GPCR stimulation can thus be viewed from multiple vantage points within the protein and used to develop an arrestin3 "conformational signature" that is receptor- and ligand-specific. This method can be used to determine how differences in GPCR and ligand structure influence information transfer across the plasma membrane and to classify GPCRs and/or ligands based on their capacity to induce different arrestin3 activation modes.

Key words Arrestin, Bioluminescence resonance energy transfer (BRET), Fluorescent arsenical, G protein-coupled receptor (GPCR), Ligand efficacy, Signal transduction

1 Introduction

Despite their relatively simple architecture, arrestins perform remarkably diverse roles in cells [1]. The non-visual arrestins, arrestin2 and 3 (β-arrestin1 and 2, respectively), for example, are able to recognize and bind hundreds of different activated GPCRs and are integral to the control of GPCR desensitization, sequestration, and intracellular trafficking. At the same time, they can interact with and localize dozens of cargo proteins, including signaling pathway intermediates that influence the tonic level of pathway activity and in some cases confer GPCR-dependent regulation. Importantly, these actions are influenced by multiple factors,

Mark G. H. Scott and Stéphane A. Laporte (eds.), *Beta-Arrestins: Methods and Protocols*, Methods in Molecular Biology, vol. 1957, https://doi.org/10.1007/978-1-4939-9158-7_19, © Springer Science+Business Media, LLC, part of Springer Nature 2019

among them cell background, the GPCR to which the arrestin has bound, and the structure of the ligand, suggesting that, like receptors, arrestins can adopt conformationally discrete activation modes that specify the functions(s) they will perform.

But how does it work? High-resolution x-ray crystallography has provided atomic level structural information on arrestins alone and in complex with rhodopsin [2–6]. While these "static" structures provide critical details about the conformational rearrangements that occur upon arrestin activation, they are unable to capture the kinetics of the process or explain how receptor and ligand structure impose their effects on arrestin function. A useful approach to addressing these questions involves fluorescence or bioluminescence resonance energy probes (FRET or BRET). BRET is a phenomenon that results from non-radiative energy transfer between an enzymatically activated luminescent substrate donor and a fluorophore acceptor. BRET occurs only when the donor and acceptor are in extremely close proximity (typically <10 nM) and changes in observed BRET are generally interpreted as movement of the donor and acceptor relative to each other. BRET was initially employed to examine regulated protein-protein interactions, e.g., arrestin recruitment to a GPCR [7]. In this setting, the donor, e.g., *Renilla* luciferase (*R*luc), and acceptor, e.g., yellow fluorescent protein (YFP), are appended to distinct proteins. Due to the proximity requirement for energy transfer to occur, increases in intermolecular BRET can be interpreted as a protein-protein interaction. Alternatively, conformational shifts within a protein can be observed using an adaptation known as intramolecular BRET, in which both donor and acceptor are appended to a single protein, e.g., *R*luc-arrestin-YFP [8]. In this case, changes in BRET may reflect a number of things including, but not limited to, conformational shifts within the protein of interest, steric interference of the donor and acceptor by recruitment of binding partners, or changes in the subcellular environment of the reporter.

A limitation of intramolecular BRET or FRET using conventional donor-acceptor pairs is that relatively large donor and acceptor proteins must be either appended to the N- and C-terminus of the protein of interest or inserted within the protein itself, potentially interfering with its function [8, 9]. A less disruptive approach is to employ a small membrane-permeant fluorescein derivative with two arsen-(III) substituents (fluorescein arsenical hairpin binder or FlAsH) as the acceptor along with either cyan fluorescent protein or *R*luc as the FRET or BRET donor, respectively. The FlAsH acceptor can then be targeted to multiple sites within the protein by mutational insertion of a small tetracysteine tag motif [10]. Intramolecular FlAsH-FRET or BRET has been used to report on activation-dependent conformational changes in arrestin3 [11, 12], as well as to characterize the temporal

relationships between GPCR-arrestin binding (measured by intermolecular FRET) and the conformational rearrangements that accompany arrestin activation (measured by intramolecular FlAsH-FRET) [12]. Here, we describe a method using a series of *R*luc-arrestin3-FlAsH-BRET biosensors to measure stimulus-induced changes in arrestin conformation in live cells. The change in BRET observed from multiple vantage points within the protein can be used to develop an arrestin3 "conformational signature" that is receptor- and ligand-specific and to classify GPCRs and/or ligands based on their capacity to induce different arrestin3 activation modes [11].

2 Materials

2.1 Design and Validation of Arrestin3 FlAsH-BRET Biosensors

1. The series of six *R*luc-arrestin3-FlAsH expression plasmids employed here were constructed by inserting a cDNA sequence encoding the tetracysteine motif, C–C–P–G–C–C, immediately following amino acid residues 77, 140, 171, 225, 263, and 410 of rat arrestin3 (*see* Fig. 1a) into the previously described pcDNA3.1-*R*luc-arrestin3 plasmid [13]. Constructs were prepared using a modification of the precise gene fusion polymerase chain reaction (PCR) method of Yon and Fried [14]. For each construct, two PCR steps were performed using the primer sets shown in Table 1. The first step was to generate two PCR fragments using the primer pairs: *R*lucHindF/FlashR and FlashF/*R*lucApalR. One PCR product contained a *HindIII* restriction site at the 5′ end and the C–C–P–G–C–C FlAsH motif at the 3′ end, while the other contained the complementary FlAsH sequence at the 5′ end and an *ApaI* restriction site at the 3′ end. A second PCR step was used to fuse the two fragments using three primers, *R*lucHindF, FlashR, and *R*lucApalR, and the two PCR fragments as template DNA. The resultant full-length arrestin3 PCR product containing the FlAsH motif insert was digested with *HindIII* and *ApaI* and cloned into the parent pcDNA3.1-*R*luc-arrestin3 plasmid to generate the *R*luc-arrestin3-FlAsH1-6 expression plasmids. All constructs were verified by dideoxynucleotide sequencing. As shown in Fig. 1b, the resultant *R*luc-arrestin3-FlAsH mutants enable monitoring BRET between the N-terminal *R*luc donor and a fluorescent arsenical acceptor located at various positions within N- and C-terminal globular domains of arrestin3 (*see* **Note 1**).
2. Confirmation that insertion of the tetracysteine motif does not compromise arrestin3 function was obtained by measuring intermolecular BRET between each *R*luc-arrestin3-FlAsH construct and the GPCR of interest bearing a C-terminal YFP

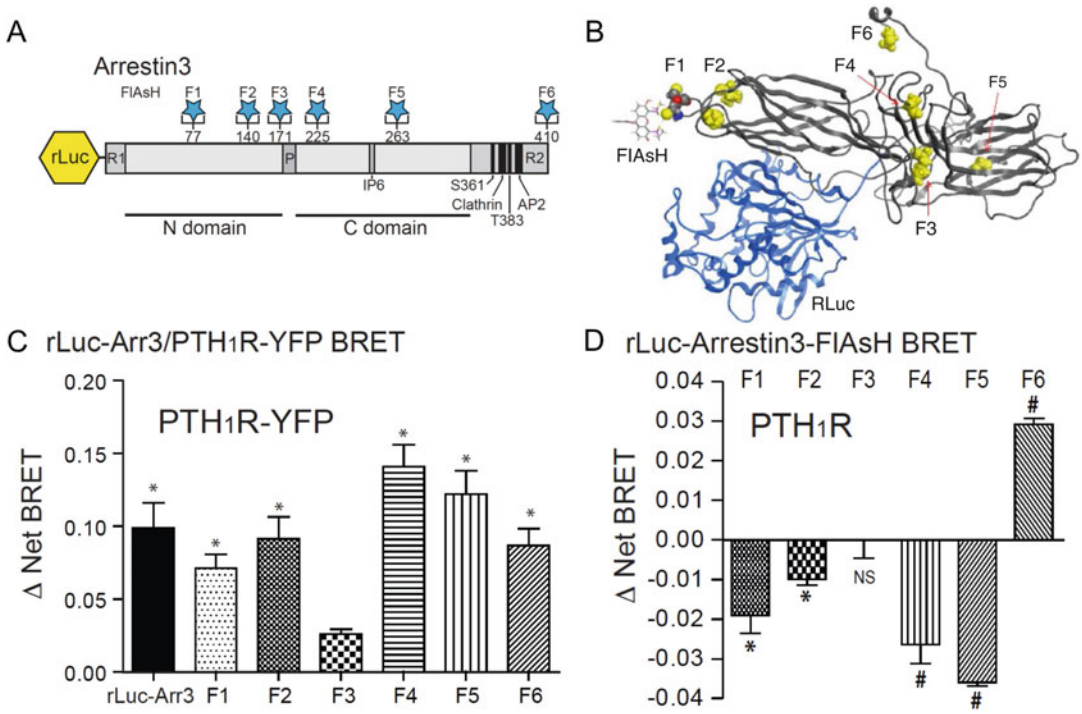


Fig. 1 Construction, validation, and use of arrestin3 FlAsH-BRET biosensors. (**a**) Linear representation of a panel of six *R*luc-arrestin3-FlAsH-BRET reporters (F1–F6) constructed by inserting the tetracysteine motif, C–C–P–G–C–C, following amino acid residues 77, 140, 171, 225, 263, and 410 of *R*luc-arrestin3. The location of each FlAsH motif is shown in relation to the globular N and C domains of arrestin3, as well as the clathrin and adapter protein 2 (AP2) binding sites and reported phosphorylation sites (Ser^{361} and Thr^{383}) in the arrestin3 C-terminal regulatory (R2) domain. (**b**) Three-dimensional computational model of *R*luc-arrestin3-FlAsH1-6 showing the spatial orientation of the six tetracysteine motifs as yellow space-filling molecules relative to the *R*luc moiety. The FlAsH molecule is depicted as bound to the F1 site. The structure of the N-terminal *Renilla* luciferase is shown in blue. The position of the *R*luc is highly flexible in this model and was manually placed for ease of representation. (**c**) Typical intermolecular BRET results demonstrating the efficiency of ligand-dependent recruitment of *R*luc-arrestin3-FlAsH1-6 to the $hPTH_1R$. The bar graph depicts mean ± SEM of independent biological replicates ($n = 3$). (**d**) Representative intramolecular *R*luc-arrestin3-FlAsH1-6 BRET signature produced by interrogating the hPTH(1-34) stimulated $hPTH_1R$ with each of the six biosensors shown in panel A. The bar graph depicts mean ± SEM of independent biological replicates ($n = 5$). In panels **c** and **d**; *$p < 0.05$, #$p < 0.005$ greater or less than vehicle-stimulated control. NS?

tag (*see* **Note 2**). These assays are performed in the absence of the fluorescent arsenical to permit measurement of BRET between the FlAsH mutant *R*luc-arrestin3 and GPCR-YFP, and change in net BRET (Δ Net BRET) is compared with that of the unmodified parent *R*luc-arrestin3 construct. Fig. 1c shows the comparison of the Δ Net BRET between *R*luc-arrestin3 and each of six *R*luc-arrestin3-FlAsH constructs upon recruitment to the type 1 human parathyroid hormone receptor ($hPTH_1R$). Note that five of the FlAsH constructs (F1, F2, F4, F5, and F6) produce a BRET signal similar to the

Table 1
Primer sequences used to generate *R*luc-arrestin3-FlAsH1-6

Primer	Sequence
RlucHindF	ATCAAGCTTGCGTTACCGGATCCATGGGTGAA
RlucApaIR	AACGGGCCCTCTAGACTAGCAGAACTGGTCA
FlAsH1F	GGATCCTGTCGATGGTTGTTGTCCTGGTTGTTGTGTGGTGCTTGTGGATC
FlAsH1R	GATCCACAAGCACCACACAACAACCAGGACAACAACCATCGACAGGATCC
FlAsH2F	GAGGACACAGGGAAGTGTTGTCCTGGTTGTTGTGCCTGTGGAGTAGAC
FlAsH2R	GTCTACTCCACAGGCACAACAACCAGGACAACACTTCCCTGTGTCCTC
FlAsH3F	GCTTATCATCAGAAAGTGTTGTCCTGGTTGTTGTGTACAGTTTGCTCCTG
FlAsH3R	CAGGAGCAAACTGTACACAACAACCAGGACAACACTTTCTGATGATAAGC
FlAsH4F	CCACGTCACCAACAATTGTTGTCCTGGTTGTTGTTCTGCCAAGACCGTCA
FlAsH4R	TGACGGTCTTGGCAGAACAACAACCAGGACAACAATTGTTGGTGACGTGG
FlAsH5F	AGCTTGAACAAGATGACCAGTGTTGTCCTGGTTGTTGTGTGTCTCCCAG TTCCACATT
FlAsH5R	AATGTGGAACTGGGAGACACACAACAACCAGGACAACACTGGTCATCTTG TTCAAGCT
FlAsH6R	ACGGGCCCTCTAGACTAACAACAACCAGGACAACAGCAGAACTGGTCATC

control, while one construct (F3) does not generate a significant signal (*see* **Note 3**).

2.2 Cell Culture and Transfection

1. pcDNA3.1-*R*luc-arrestin3-FlAsH1-6 expression plasmids (Addgene; Plasmids #74129, #74130, #74131, #74132, #74133, #74134).
2. cDNA expression plasmid encoding the GPCR of interest without a fluorescent tag.
3. HEK293 cells (ATCC; CRL1573).
4. Minimum essential medium (MEM) without additives.
5. MEM supplemented with 10% fetal bovine serum (FBS) and 1% antibiotic/antimycotic solution.
6. FuGENE® HD transfection reagent (Promega Corporation).
7. 10 cm sterile tissue culture plates or 75 cm^2 tissue culture flasks.
8. Six-well sterile tissue culture plates.
9. Sterile 1.5 mL clear polypropylene microfuge tubes with snap caps.

2.3 Intramolecular FlAsH-BRET

1. Dulbecco's phosphate-buffered saline (DPBS).
2. DPBS containing 2 mM EDTA.
3. Hank's balanced salt solution (HBSS) with 1.26 mM calcium and 0.9 mM magnesium and without phenol red.
4. TC-FlAsH™ In-Cell Tetracysteine Tag Detection Kit (Life Technologies Corp.). Each kit contains sufficient reagents for approximately 360 96-well plate wells. The FlAsH-EDT_2 labeling reagent is supplied as an 800× solution. To avoid repeated freeze-thaw cycles, store the FlAsH-EDT_2 labeling reagent in 5–10 μL aliquots in microfuge tubes at −20 °C in the dark (*see* **Note 4**). BAL wash buffer is supplied as a 100× concentrate and is stored at 4 °C. BAL wash buffer should be diluted to 1× in HBSS at room temperature just before use.
5. BRET buffer: 1 mM $CaCl_2$, 140 mM NaCl, 2.7 mM KCl, 900 μM $MgCl_2$, 370 μM NaH_2PO_4, 5.5 mM D-glucose, 12 mM $NaHCO_3$, 25 mM HEPES, pH 7.4.
6. Coelenterazine *h* (NanoLight Technology): Prepare 2.2 mM stock solution by dissolving 10 mg coelenterazine in a solution of 10 mL absolute ethanol and 200 μL 5 N HCl. Store 1.0 mL aliquots in black microfuge tubes at −80 °C.
7. GPCR ligand stocks as appropriate for the experiment.
8. TempAssure PCR 8-tube strips or clear round bottom 96-well plates for dispensing ligands and coelenterazine.
9. Opaque white 96-well plates for BRET assay.
10. 8-Channel multichannel pipettes (1–20 μL).
11. Berthold Technologies Tristar 3 LB 941, Molecular Devices i3× Multi-Mode Detection Platform, or similar instrument with 485 nm excitation and 525–585 emission filters (*see* **Note 5**).
12. Microsoft Excel®, GraphPad Prism®, or similar spreadsheet software for data calculation, graphing, and statistical analysis.

3 Methods

3.1 Cell Culture and Transfection

1. Maintain HEK293 cells in 10 cm tissue culture plates or 75 cm^2 flasks using MEM supplemented with 10% fetal bovine serum and 1% antibiotic/antimycotic solution (*see* **Note 6**).
2. On Day 1, passage 90% confluent HEK293 cells into six-well tissue culture plates at a seeding density that will attain approximately 50% confluence within 24 h. Each individual well of a six-well plate will yield sufficient cells for six wells of a 96-well plate. For small experiments, one or two wells of six-well plate can be transfected with each reporter. Transfecting two wells

with each reporter allows identically transfected cells to be labeled with FlAsH-EDT_2 labeling reagent for intramolecular FlAsH-BRET or left unlabeled for determining background BRET (*see* Subheading 3.2, **step 8**).

3. On Day 2, transfect 50% confluent cells with one *R*luc-arrestin3-FlAsH expression plasmid along with the GPCR of interest.
4. For each transfection, combine 94 μL of plain MEM with 6 μL of FuGENE® HD transfection reagent in a sterile plastic 1.5 mL microfuge tube. Vortex to mix and pulse in a microfuge. Allow to stand for 5 min at room temperature.
5. Add 1.0–1.5 μg of cDNA expression plasmid encoding the untagged GPCR of interest, e.g., pCMV6-$hPTH_1R$, and 100–300 ng of one *R*luc-arrestin3-FlAsH expression plasmid to each tube (*see* **Note 7**). Flick tubes to mix and pulse in a microfuge. Allow to stand at room temperature for 15 min.
6. Add the transfection mixtures to each well of a six-well plate, and return cells to the tissue culture incubator. Allow cells to incubate at 37 °C overnight.
7. On Day 3, aspirate and discard medium from cells. Replace with 2 mL/well of MEM containing 10% FBS and antibiotic/antimycotic, and return cells to incubator. Allow cells to incubate at 37 °C overnight. Cells will be labeled on Day 4 after attaining 90% confluence.

3.2 FlAsH Labeling the Tetracysteine Tag

1. On Day 4, aspirate growth medium from cells and discard. Wash monolayers 1× with DPBS to remove serum.
2. Detach cells by adding 1 mL of DPBS containing 2 mM EDTA to each well. Gently pipette cells and transfer to 1.5 mL microfuge tubes.
3. Centrifuge at 3000 × *g* in a microcentrifuge for 3 min to pellet cells. Aspirate and discard the supernatant. Resuspend the cell pellet in 500 μL of HBSS. Gently triturate several times to disperse cells.
4. Add 0.67 μL (2.5 μM final concentration) of FlAsH-EDT_2 labeling reagent from the TC-FlAsH™ In-Cell Tetracysteine Tag Detection Kit to each microfuge tube. Gently invert tubes 4–5 times to mix. Incubate at room temperature in the dark for 30 min (*see* **Note 8**).
5. Centrifuge at 3000 × *g* for 3 min to pellet cells. Aspirate and discard the labeling medium. Resuspend cells by gentle trituration in 1 mL of room temperature 1× BAL wash buffer diluted from the 100× stock with HBSS.
6. Centrifuge at 3000 × *g* for 3 min to pellet cells. Aspirate and discard the wash buffer. Resuspend cells in 650 μL of BRET

buffer, gently triturating several times to ensure cells are evenly dispersed.

7. Transfer 100 μL of cells suspended in BRET buffer per well of an opaque white 96-well plate (approximately 1.5×10^5 cells/well) as needed for the experiment (*see* **Notes 9** and **10**). After preparing the experimental plate, wrap it in aluminum foil, and maintain it in the dark at room temperature until ready to perform the experiment.
8. To determine background BRET, it is necessary to prepare cells from identically transfected wells following Subheading 3.2, **steps 1–7**, except for omitting the FlAsH-EDT_2 labeling reagent from Subheading 3.2, **step 4**. The background BRET ratio is that measured in the absence of the fluorescence acceptor, which in this case is achieved by omitting the fluorescent bi-arsenical (*see* Subheading 3.5, **step 2**).

3.3 Preparing the Drug Plate

1. Prepare vehicle and ligand solutions during the 30 min FlAsH labeling period.
2. Dilute ligand stocks to 12× desired final concentration in BRET buffer (*see* **Note 11**). Prepare non-stimulated controls using the same dilution of ligand vehicle in BRET buffer.
3. Aliquot ~15 μL of 12× ligand per experimental well into PCR tube strips or round bottom 96-well drug plates, whichever is more convenient. Stimulations will be carried out using a multichannel pipettor to transfer ligand one row at a time, so the drug plate must be laid out in a grid corresponding to the layout of the experimental plate (*see* **Note 12**).

3.4 Intramolecular FlAsH-BRET Assay

1. Just before use, dilute the 2.2 mM stock coelenterazine solution to 12× desired final concentration (60 μM) in BRET buffer. Once added to the cell plate, the final coelenterazine concentration will be 5 μM. Transfer the 12× solution into PCR tube strips or round bottom 96-well drug plates for dispensing with a multichannel pipettor.
2. Using an appropriate multi-mode plate reader, verify *R*luc-arrestin3-FlAsH expression and tetracysteine tag labeling by measuring TC-FlAsH fluorescence with an excitation wavelength of 485 nm and emission wavelength of 535 nm.
3. Using a multichannel pipettor, transfer 10 μL of 12× ligand from the PCR tube strips or round bottom 96-well drug plate to the corresponding wells in the experimental plate. Pipette up and down several times to ensure mixing. Change pipette tips between rows to avoid mixing ligands or cells expressing different reporters.
4. Allow cells to preincubate with ligand for 0–10 min at room temperature before adding coelenterazine (*see* **Notes 13** and **14**).

5. Using a multichannel pipettor, transfer 10 μL of coelenterazine solution from the PCR tube strips or round bottom 96-well drug plate to the corresponding wells in the experimental plate. Pipette up and down several times to ensure mixing. Change pipette tips between rows to avoid mixing ligands or cells expressing different reporters.
6. Return the experimental plate to the plate reader, and allow 2 min for the *R*luc emission to stabilize, and then record six consecutive 1 s readings of *R*luc (485 nm) luminescence and TC-FlAsH fluorescence (530 nm; YFP setting) at 1 min intervals. Total read time in 5 min, beginning 2 min after the addition of coelenterazine.

3.5 Data Analysis and Interpretation

1. The BRET ratio is the TC-FlAsH fluorescence signal (530 nm) over the Rluc signal (485 nm) measured simultaneously. This ratio is automatically calculated by the software of multi-mode plate readers and exported as a Microsoft Excel spreadsheet.
2. Determine the Δ Net BRET for each ligand-stimulated condition relative to vehicle-stimulated in the same experiment. For each well, the mean of the six consecutive reads is calculated to obtain the average BRET ratio. The Net BRET ratio for each well is then calculated by subtracting the background BRET ratio measured in cells in the same experiment that lack the BRET acceptor, i.e., were not labeled with FlAsH-EDT_2, from the mean BRET ratio observed in FlAsH-EDT_2 labeled cells. The Δ Net BRET is then obtained by dividing the Net BRET ratio obtained in stimulated cells by the Net BRET ratio measured in cells exposed to vehicle only. This ratio represents the fractional change in BRET occurring upon ligand stimulation and is typically ±0.01–0.05 using our *R*luc-arrestin3-FlAsH reporters. If duplicate or triplicate wells are used, a coefficient of variance (CV) can be determined, and the mean Δ Net BRET technical replicates on the plate can be used as a datum for determining the mean Δ Net BRET across multiple biological replicates of the experiment (*see* **Note 15**).
3. The GPCR-specific "conformational signature" of activated arrestin3 can be displayed graphically by plotting the Δ Net BRET observed upon ligand stimulation for each of the six *R*luc-arrestin3-FlAsH reporters as in Fig. 1d (*see* **Note 16**).

4 Notes

1. This technique is adaptable to other allosterically regulated proteins, e.g., GPCRs themselves [15]. In selecting the site for insertion of the tetracysteine motif, it is helpful to take advantage of x-ray crystallographic structures if available

(Fig. 1b). Optimal sites would be in flexible regions of the protein that might be expected to move upon activation and away from key structural elements necessary for protein folding and stability. Since arrestin activation is associated with displacement of the C-terminus and an approximately 20° rotation of the N and C domains relative to one another [4, 6], we chose to place tetracysteine motifs near the C-terminus and at sites predicted to be on the surface of the N and C domains away from known sites of GPCR interaction.

2. *R*luc luminescence cannot be visualized with sufficient resolution using microscopy equipment available to most laboratories, and cells loaded with FlAsH-EDT_2 may fluoresce diffusely upon direct excitation, making direct visualization of their recruitment to an activated GPCR difficult. We chose to validate that FlAsH mutant arrestins are functional by quantifying the efficiency of intermolecular BRET between each *R*luc-arrestin3-FlAsH construct and an agonist-activated YFP-tagged GPCR, here the $hPTH_1R$.
3. In our experiments, we chose to include the F3 construct, which is poorly recruited to GPCRs, as an internal negative control.
4. The FlAsH-EDT_2 labeling reagent is a bi-arsenical compound and toxic. Wear appropriate personal protective equipment when handling, and discard used solutions as specified by your institutional guidelines for toxic waste.
5. The method described here is for BRET measurements performed using a Berthold Technologies Tristar 3 LB 941 but is readily adaptable to other instruments. Note that intramolecular Δ Net BRET signals are often small, on the order of 1–5%, so the plate reader must have sufficient sensitivity and stability to perform reliable measurements.
6. Any readily transfectable cell line and transient transfection protocol can be used once optimized. The method described here has been optimized for HEK293 cells transfected using FuGENE® HD.
7. The optimal ratio of GPCR and *R*luc-arrestin3-FlAsH expression plasmids needs to be determined empirically. Since the Δ Net BRET observed upon stimulation reflects the "population average" change in arrestin conformation, the most consistent results are obtained when experiments are performed in relative receptor excess, such that at steady state the maximum attainable fraction of *R*luc-arrestin3-FlAsH reporter is receptor-bound. We recommend performing two test transfections: (1) transfect a fixed amount of *R*luc-arrestin3-FlAsH reporter plasmid (200 ng) and increasing amounts of GPCR plasmid (0.1–1.5 μg) to determine the quantity of GPCR cDNA at

which the Δ Net BRET signal plateaus; and (2) transfect a fixed amount of GPCR plasmid (1.0–1.5 μg) and increasing amounts of *R*luc-arrestin3-FlAsH reporter plasmid (10–500 ng) to determine the quantity of reporter plasmid that gives the most reproducible Δ Net BRET signal. In the latter case, as quantity of *R*luc-arrestin3-FlAsH reporter plasmid is decreased, the Δ Net BRET will become greater, but BRET signal intensity will decrease leading to more variability. In our hands, 100–300 ng of *R*luc-arrestin3-FlAsH reporter plasmid per well produces the most consistent and robust Δ Net BRET signals.

8. The optimum final concentration of FlAsH-EDT_2 labeling reagent may vary from 1 to 10 μM and labeling time from 30 to 60 min. For labeling *R*luc-arrestin3-FlAsH proteins in detached HEK293 cells, we find that using 2.5 μM final concentration FlAsH-EDT_2 labeling reagent and labeling for 30 min give consistent results.
9. The optimal cell number per well will vary somewhat between different plate readers and should be determined empirically in pilot assays.
10. For a simple experiment, e.g., generating an *R*luc-arrestin3-FlAsH-BRET signature in response to agonist exposure, we might transfect two wells of a 6-well plate with each pcDNA3.1-*R*luc-arrestin3-FlAsH1-6 expression plasmid along with the receptor of interest. Following the protocol above, each transfected well provides enough transfected cells for six wells of a 96-well plate. Combining cells from two identically transfected wells provides sufficient material to label half with FlAsH-EDT_2 labeling reagent to measure intramolecular FlAsH-BRET, while the other half is processed identically except for omitting the labeling reagent to measure background BRET. Cells expressing the reporters would be arrayed in a 6 row × 8 column grid on a single 96-well plate, with each row representing a different *R*luc-arrestin3-FlAsH construct and each column representing a ligand or vehicle treatment. The first two columns are for unlabeled vehicle-treated cells (background BRET), and the next six columns are for labeled vehicle- and agonist-treated cells (FlAsH-BRET). We recommend using at least two adjacent wells for each ligand-reporter condition (technical replicates) per plate so that a coefficient of variance (CV) can be determined for quality control.
11. Since the most consistent *R*luc-arrestin3-FlAsH-BRET profiles are obtained when the maximum fraction of reporter is GPCR-bound, stimulations are usually carried out at saturating ligand concentration. It may be helpful to perform an initial ligand

concentration-response curve to determine the ligand concentration that gives the maximum Δ Net BRET signal. In the example shown here, hPTH(1–34) stock (0.1 mM in sterile distilled water) was diluted to 1.2 μM in BRET buffer (12× final concentration) to yield a final ligand concentration of 0.1 μM in the assay well.

12. Depending on the experiment, e.g., performing concentration-response curves, it may be more practical to prepare ligands in a 96-well drug plate. If using a microplate reader equipped with auto-injectors, it will be necessary to prepare both ligands and coelenterazine in 96-well plates.
13. Both the time and temperature of ligand stimulation are relevant variables and should be determined empirically. Since coelenterazine should be added just prior to reading, when performing a time course experiment, stagger the addition of drug to the wells, and add coelenterazine to all wells simultaneously. In our hands, the Net BRET ratios produced by *R*luc-arrestin3-FlAsH reporters are stable from 2 to 10 min after ligand stimulation, and we routinely preincubate for 3 min with ligand before adding coelenterazine (5 min ligand exposure before reading).
14. We have also performed ligand stimulations at 37 °C to determine whether incubation temperature affected the *R*luc-arrestin3-FlAsH-BRET profile. For stable arrestin-binding GPCRs [16], e.g., the PTH_1R, temperature has no significant effect on the profile, even though incubation at 37 °C allows the GPCR-arrestin complexes to exit the plasma membrane and transit to early endosomes.
15. In our hands the observed Δ Net BRET for GPCR-stimulated change in *R*luc-arrestin3-FlAsH-BRET is reproducible enough that five to six biological replicates are sufficient to discern effects of ±0.01 with $p < 0.05$.
16. It should be evident that an *R*luc-arrestin3-FlAsH1-6 BRET profile is not a "conformational signature" per se in that changes in intramolecular BRET reflect both changes in the distance/orientation of the donor and acceptor fluorophores due to conformational rearrangement and steric effects generated by arrestin interaction with its receptor and non-receptor binding partners. Thus, it is not possible to ascribe the *R*luc-arrestin3-FlAsH-BRET signal at a given position to specific conformational shifts or engagement of binding partners. The utility of the method is in comparing/classifying the effects of different ligand/GPCR complexes on the arrestin3 signature. For example, we have found that features of the signature are conserved between receptors with similar arrestin binding/signaling characteristics and that the Δ Net BRET at

selected positions correlates with downstream arrestin function, e.g., "class A" versus "class B" trafficking [16] and arrestin-dependent ERK1/2 activation, suggesting that *R*luc-arrestin3-FlAsH-BRET probes can predict arrestin function based on the ligand-induced conformational signature [11].

Acknowledgments

This work was supported by National Institutes of Health Grants R01 DK055524 (LML), R01 GM095497 (LML), Department of Veterans Affairs Merit Review Grant I01 BX003188 (LML), and the Research Service of the Charleston, SC Veterans Affairs Medical Center. The contents of this article do not represent the views of the Department of Veterans Affairs or the United States Government.

References

1. Peterson YK, Luttrell LM (2017) The diverse roles of arrestin scaffolds in G protein-coupled receptor signaling. Pharmacol Rev 69:256–297
2. Han M, Gurevich VV, Vishnivetskiy SA, Sigler PB, Schubert C (2001) Crystal structure of beta-arrestin at 1.9 A: possible mechanism of receptor binding and membrane translocation. Structure 9:869–880
3. Zhan X, Gimenez LE, Gurevich VV, Spiller BW (2011) Crystal structure of arrestin-3 reveals the basis of the difference in receptor binding between two non-visual subtypes. J Mol Biol 406:467–478
4. Shukla AK, Manglik A, Kruse AC, Xiao K, Reis RI, Tseng WC, Staus DP, Hilger D, Uysal S, Huang LY, Paduch M, Tripathi-Shukla P, Koide A, Koide S, Weis WI, Kossiakoff AA, Kobilka BK, Lefkowitz RJ (2013) Structure of active β-arrestin-1 bound to a G-protein-coupled receptor phosphopeptide. Nature 497:137–141
5. Kim YJ, Hofmann KP, Ernst OP, Scheerer P, Choe HW, Sommer ME (2013) Crystal structure of pre-activated arrestin p44. Nature 497:142–146
6. Kang Y, Zhou XE, Gao X, He Y, Liu W, Ishchenko A, Barty A, White TA, Yefanov O, Han GW, Xu Q, de Waal PW, Ke J, Tan MH, Zhang C, Moeller A, West GM, Pascal BD, Van Eps N, Caro LN, Vishnivetskiy SA, Lee RJ, Suino-Powell KM, Gu X, Pal K, Ma J, Zhi X, Boutet S, Williams GJ, Messerschmidt M, Gati C, Zatsepin NA, Wang D, James D, Basu S, Roy-Chowdhury S, Conrad CE, Coe J, Liu H, Lisova S, Kupitz C, Grotjohann I, Fromme R, Jiang Y, Tan M, Yang H, Li J, Wang M, Zheng Z, Li D, Howe N, Zhao Y, Standfuss J, Diederichs K, Dong Y, Potter CS, Carragher B, Caffrey M, Jiang H, Chapman HN, Spence JC, Fromme P, Weierstall U, Ernst OP, Katritch V, Gurevich VV, Griffin PR, Hubbell WL, Stevens RC, Cherezov V, Melcher K, Xu HE (2015) Crystal structure of rhodopsin bound to arrestin by femtosecond X-ray laser. Nature 523:561–567
7. Charest PG, Bouvier M (2003) Palmitoylation of the V2 vasopressin receptor carboxyl tail enhances beta-arrestin recruitment leading to efficient receptor endocytosis and ERK1/2 activation. J Biol Chem 278:41541–41551
8. Charest PG, Terrillon S, Bouvier M (2005) Monitoring agonist-promoted conformational changes of beta-arrestin in living cells by intramolecular BRET. EMBO Rep 6:334–340
9. Vilardaga JP, Bünemann M, Krasel C, Castro M, Lohse MJ (2003) Measurement of the millisecond activation switch of G protein-coupled receptors in living cells. Nat Biotechnol 21:807–812
10. Hoffmann C, Gaietta G, Bünemann M, Adams SR, Oberdorff-Maass S, Behr B, Vilardaga JP, Tsien RY, Ellisman MH, Lohse MJ (2005) A FlAsH-based FRET approach to determine G protein-coupled receptor activation in living cells. Nat Methods 2:171–176
11. Lee M-H, Appleton KM, Strungs EG, Kwon JY, Morinelli TA, Peterson YK, Laporte SA, Luttrell LM (2016) The conformational signature of activated arrestin3 predicts its

trafficking and signaling functions. Nature 531:665–668

12. Nuber S, Zabel U, Lorenz K, Nuber A, Milligan G, Tobin AB, Lohse MJ, Hoffmann C (2016) FRET-based β-arrestin biosensors reveal a rapid, receptor-dependent activation/deactivation cycle in living cells. Nature 531:661–664
13. Perroy J, Adam L, Qanbar R, Chenier S, Bouvier M (2003) Phosphorylation-independent desensitization of GABA(B) receptor by GRK4. EMBO J 22:3816–3824
14. Yon J, Fried M (1989) Precise gene fusion by PCR. Nucleic Acids Res 17:4895
15. Devost D, Sleno R, Pétrin D, Zhang A, Shinjo Y, Okde R, Aoki J, Inoue A, Hébert TE (2017) Conformational profiling of the AT1 angiotensin II receptor reflects biased agonism, G protein coupling, and cellular context. J Biol Chem 292:5443–5456
16. Oakley RH, Laporte SA, Holt JA, Caron MG, Barak LS (2000) Differential affinities of visual arrestin, beta arrestin1, and beta arrestin2 for G protein-coupled receptors delineate two major classes of receptors. J Biol Chem 275:17201–17210

Part VII

Methods to Study Roles of β-Arrestins in Physiopathology



Chapter 20

Methods to Study the Roles of β-Arrestins in Meningococcal Signaling

Zoé Virion, Stefano Marullo, and Mathieu Coureuil

Abstract

Neisseria meningitidis is a Gram-negative diplococcus restricted to humans that causes severe septicemia and/or meningitidis. Initial adhesion to human endothelial cells is mediated through the interaction of type IV pili with the hetero-oligomeric complexes formed by the human receptors CD147 and the β2-adrenergic receptor. Interaction with this complex heterodimer activates a β-arrestin-biased signaling pathway leading to actin polymerization and accumulation of ezrin and ezrin-binding partners. These signaling events promote the formation of cell plasma membrane protrusions in endothelial cells, which are crucial for *N. meningitidis* colonies to resist shear stress and colonize blood vessels. Here we provide detailed protocols to evaluate the role of β-arrestins in actin and ezrin signaling downstream of G protein-coupled receptor activation.

Key words β-Arrestins, β2-Adrenergic receptor, *Neisseria meningitidis*, Membrane protrusion

1 Introduction

Neisseria meningitidis is a Gram-negative diplococcus restricted to humans that causes severe septicemia and/or meningitis. The ability of meningococci to interact with endothelial cells is essential in meningococcal pathogenesis [1, 2]. Initial bacterial adhesion is mediated by the interaction of meningococcal type IV pili (TFP), which are protruding filaments made of polymeric pilins. Two components of the pili, the pilin PilE and PilV, bind to the adhesion receptor CD147, also known as EMMPRIN/Basigin [3]. Following this first contact, *N. meningitidis* TFP interact with the β2-adrenergic receptor (β2AR), an event facilitated by the fact that CD147 and the β2AR form constitutive hetero-oligomeric complexes in human cells [4]. Binding to the β2AR activates a biased signaling pathway, involving β-arrestins, not G protein activation, which ultimately leads to actin polymerization and accumulation of ezrin and ezrin-binding proteins below bacterial colonies and in host cell membrane protrusions that surround the bacteria

Mark G. H. Scott and Stéphane A. Laporte (eds.), *Beta-Arrestins: Methods and Protocols*, Methods in Molecular Biology, vol. 1957, https://doi.org/10.1007/978-1-4939-9158-7_20, © Springer Science+Business Media, LLC, part of Springer Nature 2019

[5]. These protrusions are key factors of meningococcal infection and blood vessel colonization, since they enhance the cohesion of growing bacterial microcolonies and the stability at the apical surface of capillary endothelial cells under the shear stresses caused by the bloodstream.

To analyze the role of β-arrestins during *N. meningitidis* infection, we used two different approaches: we studied the role of β-arrestins during the infection of endothelial cells, and we set up a reconstituted model of meningococcal infection in HEK293 cells. Here we describe the methods used to study the role of β-arrestins as signal transducers, downstream of the TFP/β2AR complex, leading to the formation of ezrin/actin-enriched membrane protrusions. These methods may be commonly used for studying the role of β-arrestins downstream of G protein-coupled receptor (GPCR) activation.

2 Materials

2.1 Cell Lines and Bacteria

1. *N. meningitidis* serogroup C strain 8013 (namely, 2C4.3) and its SiaD defective derivative that is non-encapsulated and expresses Opa protein [6].
2. HCMEC/D3 human cerebral microvascular endothelial cells [7].
3. The human embryonic kidney 293-T (HEK293-T) cell line.

2.2 Plasmids and siRNAs

1. Small-interfering RNAs targeting human β-arrestin-1 (5′-AAAGCCUUCUGCGCGGAGAAU-3′), human β-arrestin-2 (5′-GGCUUGUCCUUCCGCAAAGAC-3′) [8], and GRK2 (5′-AAGAAGUACGAGAAGCUGGAGUU-3′) and control off-target siRNA (5′-GATAAGGTGCTGCGTGGACCC-3′).
2. Coding regions for human β-arrestin-1, human β-arrestin-2, human ADRB2- (β2-adrenergic receptor; β2AR), human angiotensin II type 1 receptor (AT1R) inserted into the pEGFPN1 plasmid [5].
3. β-Arrestin-2ΔSrc-GFP mutant (P91G, P93D, P94R, P97L), which cannot interact with Src PH-3 domain, was prepared by site-directed mutagenesis using human β-arrestin-2-GFP as template [5].
4. Sequences for β-arrestin-1, human β-arrestin-2 were introduced in the pCMV-Tag3A plasmid [9].
5. The coding region of human CEACAM-1 was introduced into the pCDNA3.1 plasmid [10].

2.3 Cell Culture and Transfection Reagents

1. GCB agar (Difco) plates containing Kellogg's supplements: 0.2 μg/ml thiamine, 0.45% D(+) glucose, 12 μM $Fe(NO_3)_3$ $9H_2O$, 2 mg/ml glutamine. When required add 5 μg/ml chloramphenicol [11].
2. HCMEC/D3 medium: EBM-2 medium (Lonza) supplemented with 5% heat-inactivated FBS, 1.4 mM hydrocortisone, 5 mg/ml ascorbic acid, 10 mM HEPES and 1 ng/ml b-FGF, 100 U/ml penicillin, and 0.1 mg/ml streptomycin.
3. Dulbecco's modified eagle medium (DMEM) containing high glucose, supplemented with 5% heat-inactivated FBS, 1 mM L-glutamine, 100 U/ml penicillin, and 0.1 mg/ml streptomycin.
4. Opti-MEM (Gibco).
5. Phosphate-buffered saline.
6. Trypsin-EDTA solution.
7. Type I rat tail collagen.
8. Polylysine 0.01% solution.
9. Amaxa Nucleofactor Kit for Huvec (Lonza).
10. Lipofectamine 2000 (Invitrogen).

2.4 Immunofluorescence Assay

1. 10× phosphate-buffered saline (PBS) solution.
2. A 16% paraformaldehyde (PFA) solution is diluted along with 10× PBS the day of experiment to obtain fresh 4% PFA/1× PBS solution.
3. Glass coverslips (12 mm diameter, 0.1 mm thickness).
4. Triton X100 solution.
5. Bovine serum albumin, fraction V.
6. 4′,6′-Diamidino-2-phenylindole hydrochloride (DAPI).
7. Alexa-546 conjugated phalloidin (Invitrogen).
8. Mowiol Tris-MWL-4-88.
9. We used LEICA SP5 confocal microscope.

2.5 Antibodies

1. Rabbit polyclonal anti-β-arrestin-1/2, D24H9 rabbit monoclonal antibody (Cell Signaling).
2. Mouse monoclonal anti-GRK2 clone C5/1.1 (Upstate).
3. Rabbit polyclonal anti-actin (Sigma-Aldrich).
4. Anti-mouse IgG (H + L) and anti-rabbit IgG (Life technologies).
5. (H + L) coupled to horse radish peroxidase (Jackson ImmunoResearch Laboratories).

6. Rabbit polyclonal serum anti-ezrin (Gift of Dr. P Mangeat CNRS, UMR5539, Montpellier, France). Alternatively rabbit polyclonal antibody anti-ezrin (Cell Signaling).

3 Methods

3.1 Culture of *Neisseria meningitidis* and Cell Infection

The same protocol can be used for all cell infection experiments. Cells are infected with bacteria, grown up to the exponential phase in the corresponding cell culture media, at multiplicity of infection (MOI) of 50 (*see* **Note 1**). Cells are washed to remove non-adherent bacteria and limit medium acidification.

1. A frozen aliquot of *Neisseria meningitidis* is seeded on GCB agar plates the day before infection.
2. The day of infection, resuspend bacteria in the cell culture medium (without antibiotics) that have been used for the culture. After adjustment of the OD_{600} to 0.05, bacteria are incubated under constant agitation (150 RPM) at 37 °C in a 5% CO_2 incubator for 2 h or until OD_{600} reaches 0.2.
3. In the meantime, wash the cells twice with fresh culture medium without antibiotics, and wash them again 30 min later with cell culture medium without antibiotics.
4. Add bacteria to the cells at a MOI of 50, and leave them without agitation for 30 min at 37 °C in a 5% CO_2 incubator.
5. Wash the cells twice with fresh culture medium without antibiotics, and incubate the cells for 2 additional hours to allow the growth of *N. meningitidis* colonies before subsequent procedures.

3.2 Studying β-Arrestins During Meningococcal Infection of Endothelial Cells

To investigate the role of β-arrestins in signaling pathways elicited by meningococcal infection of human endothelial cells, we use two complementary approaches:

1. siRNAs are used to inhibit β-arrestin-1, β-arrestin-2, or the G protein-coupled receptor kinase 2 (GRK2) expression. The GRK family specifically phosphorylates agonist-activated GPCRs, leading to their desensitization. Phosphorylation of agonist-activated GPCRs by GRKs provides docking sites for β-arrestins. Since inhibition of GRKs prevents β-arrestin translocation to activated GPCRs, the inhibition of a signaling pathway involving β-arrestins after GRK knockdown strongly supports the involvement of an upstream GPCR involvement.
2. We also use a dominant-negative (DN) approach based on the expression of a β-arrestin-2 mutant unable to bind Src (βarr-Δ Src). The recruitment and activation of Src downstream of the β2AR were reported to be mediated by both β-arrestin-1 [12]

and β-arrestin-2 [5]. A dominant-negative effect caused by the expression β-arrestin-2 deficient in Src binding indicates the involvement of this tyrosine kinase in the investigated process and a mechanistic role of β-arrestin-2 in Src activation downstream of GPCR.

The effects of both β-arrestin knockdown and DN experiments are studied by assessing the ability of *N. meningitidis* to recruit cytoskeletal proteins (such as ezrin and actin) and to promote the formation of membrane protrusions at the site of adhesion under bacterial colonies. In these experiments actin filaments are stained with phalloidin, and ezrin enrichment is revealed by using immunostaining.

3.2.1 Inhibition of Signaling Proteins in HCMEC/D3 Cells Using SiRNA

1. Seed endothelial hCMEC/D3 cells at a density of 25×10^3 cells per cm^2 in flasks coated with 5 mg/cm^2 rat tail collagen type I.
2. Once the cells have reached 90–95% confluence, trypsinize cells, and prepare 100 μl aliquots containing 1×10^6 cells in suspension in Nucleofector solution of the Amaxa Huvec Nucleofactor® Kit.
3. Add 100 nM of specific (*see* **Note 2**) or control siRNAs to the nucleofactor cell mixture, and transfer it into a Nucleofector cuvette avoiding air bubbles.
4. Nucleofection is achieved by applying the Nucleofector® program U-002 (in a "Huvec-old" Nucleofector® I device).
5. After nucleofection, add immediately 500 μl of cell culture medium to the cuvette, and dispatch the mixture into four different 2 cm^2 wells containing collagen-coated coverslips.
6. The next day, wash the cells twice, and incubate them for 2 additional days before the anticipated experiments.
7. Three days after nucleofection, infect the cells as described above in Subheading 3.1. Measure the inhibition of the expression of the targeted protein by SDS-PAGE and Western blot experiments.

3.2.2 Expression of Dominant-Negative β-Arrestin-2 in HCMEC/D3 Cells

1. Cells are processed as in Subheading 3.2.1 except that 2 μg of plasmid DNA coding for β-arrestin-2ΔSrc-GFP or β-arrestin-2-GFP is added to the Nucleofector suspension.
2. After nucleofection, cells are dispatched into four different 2 cm^2 wells containing collagen-coated coverslips.
3. Cells are infected the day after nucleofection (*see* Subheading 3.1).

3.2.3 Immunofluorescence Assay and Analysis of Bacteria-Induced Signaling in Host Cell

1. After infection (*see* Subheading 3.1), fix cells in 4% PFA for 15–20 min.
2. Wash slides three times for 5 min with PBS.
3. Permeabilize the cells with 0.1% Triton X-100 in PBS for 10 min.
4. Wash the slides three times for 5 min with PBS 0.1% bovine serum albumin (PBS-BSA), and incubate in PBS-BSA for additional 20 min.
5. For the analysis of ezrin enrichment under bacterial colonies, fixed cells are incubated with anti-ezrin antibodies (*see* **Note 3**). For the visualization of polymeric actin, primary antibodies are not necessary.
6. Wash the slides three times for 5 min with PBS 0.1% bovine serum albumin (PBS-BSA).
7. Incubate the cells for 1 h with goat anti-rabbit IgG conjugated to Alexa Fluor to reveal anti-ezrin antibodies. In the same mix, DAPI is added at 1 μg/ml (*see* **Note 4**) to stain nuclei and bacteria. To reveal polymeric actin, Alexa Fluor-coupled phalloidin is added instead at a final dilution of 1/100.
8. Wash the slides three times with PBS.
9. Mount the slides with Mowiol.
10. Stained cells are then analyzed directly under confocal microscope by counting the recruitment of labeled actin or immunolabeled ezrin at the site of bacterial adhesion as shown in Fig. 1. At least 50 bacterial colonies are analyzed per coverslip. This experiment is performed two to three times in triplicate. Results are expressed as the number of recruitment events per 100 colonies. This strategy has been automated by the laboratory of Guillaume Duménil; details may be found in Soyer et al. [13].

3.3 A Reconstitution Model to Investigate β-Arrestins Downstream of a Specific GPCR Using a Gain of Function Approach

Neisseria meningitidis activates β-arrestins downstream of pili-bound β2AR. To dissect this signaling pathway, we use HEK293 cells that are known not to express β2AR receptor and to express low levels of endogenous β-arrestins [9] (*see* **Note 5**). Since *N. meningitidis* does not adhere to HEK293 cells via TFP, we also transfected CEACAM-1 receptor in cells [14]. This receptor allows the adhesion of meningococci expressing OpaB adhesin. With this approach, cells that are not competent for adhesion and signaling of *N. meningitidis* can be turned into a permissive phenotype via the expression of exogenous proteins. HEK293 cells reconstituted with the β2AR and β-arrestins recapitulate meningococcal-promoted signaling, leading to ezrin and/or actin recruitment, provided that initial bacterial adhesion can occur (*see* **Note 6**) (Fig. 2). Angiotensin II type 1 receptor (AT1R) is used as negative control (*see* **Note 7**).

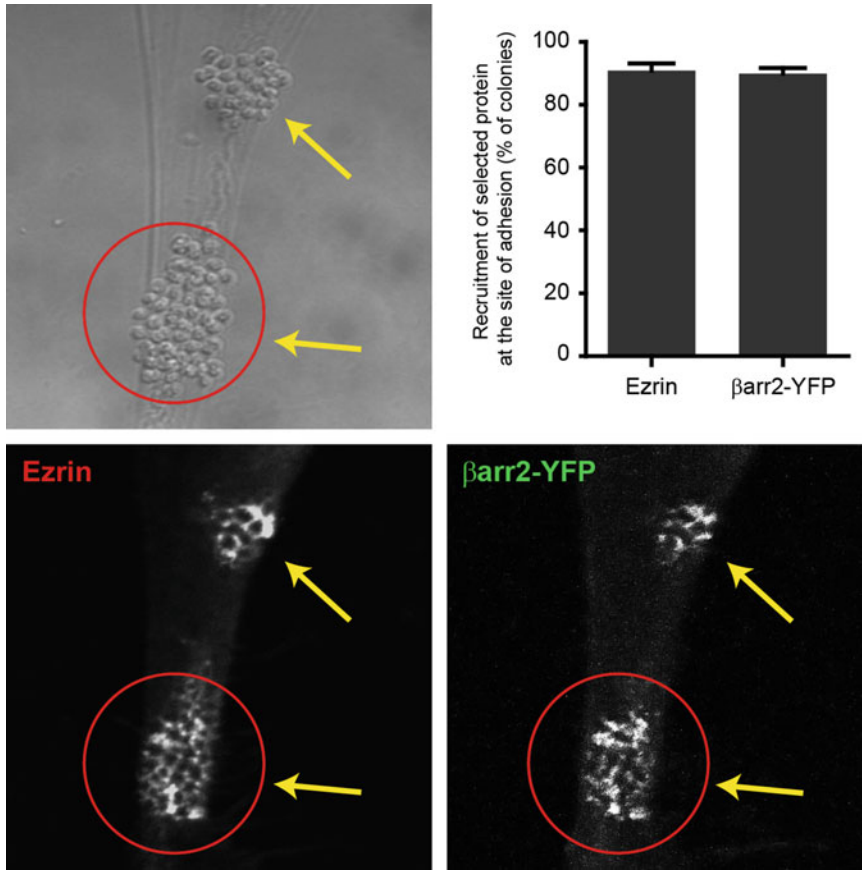


Fig. 1 Recruitment counting strategy. Cells transfected with the β-arrestin-2-YFP containing plasmids were infected, fixed, and immunostained for ezrin. Arrows indicate colonies that adhere to YFP-expressing cells. The percentage of colonies associated with protein recruitment is indicated on the graph

3.3.1 HEK293 Cell Transfection with Plasmids for GPCRs, β-Arrestins, and Adhesion Molecules

1. The day before transfection, seed HEK293 cells at a density of 10^5 cells per cm^2 in 24-well plates containing glass coverslips coated with polylysine (*see* **Note 8**).
2. Twenty-four hours later, prepare two mixes separately for each well: Mix (A) consists of 1 μl lipofectamine 2000 in 50 μl Opti-MEM; mix (B) consists of 0.2 μg of each plasmid DNAs (*see* **Note 9**).
3. Mix A and B by carefully pipetting up and down, and incubate for 20 min at room temperature.
4. In the meantime, remove the culture medium from the wells containing the cells, and add 400 μl of fresh complete DMEM in each well.

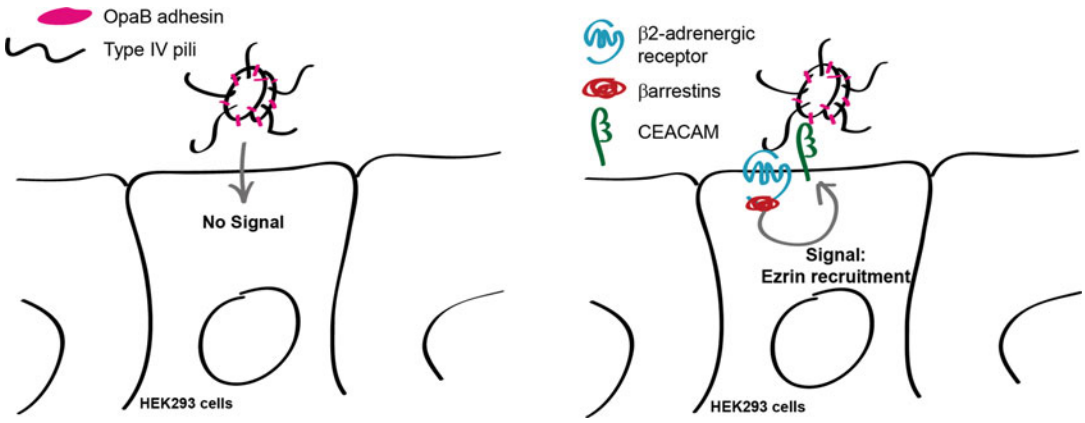


Fig. 2 Transfection strategy of HEK293 cells. TFP-dependent recruitment of ezrin in HEK-293 cells requires the expression of β2AR and βarrs and adhesion of meningococci via OpaB/CEACAM interaction

5. Add the mix A + B to the cells.
6. After 6 h, replace the medium and incubate overnight.
7. The day after transfection, proceed for infection using non-encapsulated *N. meningitidis* (*see* Subheading 3.1).

3.3.2 Analysis of Infected Cells

1. Fix the cells in 4% PFA as described in Subheading 3.2.3.
2. Actin staining is difficult to analyze in confluent HEK293 cells; we recommend using ezrin staining to determine meningococcus-promoted signaling.
3. Recruitment of ezrin at the site of bacterial adhesion is quantified as explained in Subheading 3.2.3 (Fig. 2).

4 Notes

1. Fifty bacteria per cell are classically used for *N. meningitidis* infection, since approximately 1 to 10% of total bacteria adhere to human cells. To estimate the density of bacteria, consider that 1 OD_{600} corresponds to 10^9 bacteria. The number of cells seeded in each cell is determined by cell counting.
2. HCMEC/D3 cells express both β-arrestin-1 and -2. The simultaneous inhibition of both proteins can be achieved by using a mix of siRNA targeting either transcript. The actual level of inhibition is determined in cell lysates (RIPA buffer) by SDS-PAGE and Western blot, comparatively of controls (cells treated with control siRNA).
3. Ezrin antigenicity is high. Commercial anti-ezrin antibodies are generally used at a dilution of 1/500 (usually, the concentration of Cell Signaling antibodies is not indicated).

4. Bacteria and cell DNA are revealed by a low concentration of DAPI, which allows clear discrimination in the same acquired image.
5. This strategy was convenient to study the β2AR. However, this model may be easily transposed to the study of any GPCR in CRISPR/Cas9 knockout HEK293 cells, which are easily obtained using vectors that have been deposited at Addgene (for instance, lentiCRISPR V2: https://www.addgene.org/52961/) [15].
6. HEK293 cells do not support *N. meningitidis* adhesion. Given that TFP-mediated adhesion and signaling are two independent events [16], we confirmed that transfection of the β2AR in these cells did not restore bacterial adhesion [5]. Type IV pili are the only bacterial attributes capable of promoting adhesion of capsulated *N. meningitidis*. Yet, non-encapsulated strains can interact with host cells via Opa proteins, which recognize CEACAM (carcinoembryonic antigen-related cell adhesion molecules) [10]. Being devoid of CEACAMs, HEK293 cells need to be transfected with a plasmid encoding CEACAM-1 and subsequently infected with a non-encapsulated strain.
7. The experiment described in Subheading 3.3 allows the study of GPCR/β-arrestins signaling in conditions where most of the β-arrestin-dependent signaling events depend on transfected GPCRs. However it is important to carefully control the specificity of the signal in non-transfected cells or in cells expressing only the exogenous receptor or only the exogenous β-arrestin.
8. Wash the coverslips once with 70% ethanol and let dry. Soak the coverslips in 0.01% polylysine solution for 2 h at room temperature. Wash once the coverslips with PBS.
9. It is important to adapt the quantity of vector used in order to express the same final amount of GPCR and β-arrestins. Moreover, one should control that proteins are not excessively expressed, since overexpression cause accumulation in the endoplasmic reticulum or in the Golgi apparatus.

References

1. Join-Lambert O, Lecuyer H, Miller F, Lelievre L, Jamet A, Furio L, Schmitt A, Pelissier P, Fraitag S, Coureuil M, Nassif X (2013) Meningococcal interaction to microvasculature triggers the tissular lesions of purpura fulminans. J Infect Dis 208 (10):1590–1597. https://doi.org/10.1093/infdis/jit301
2. Coureuil M, Lecuyer H, Bourdoulous S, Nassif X (2017) A journey into the brain: insight into how bacterial pathogens cross blood-brain barriers. Nat Rev Microbiol 15(3):149–159
3. Bernard SC, Simpson N, Join-Lambert O, Federici C, Laran-Chich MP, Maissa N, Bouzinba-Segard H, Morand PC, Chretien F, Taouji S, Chevet E, Janel S, Lafont F, Coureuil M, Segura A, Niedergang F, Marullo S, Couraud PO, Nassif X, Bourdoulous S (2014) Pathogenic Neisseria meningitidis utilizes CD147 for vascular colonization. Nat Med

4. Maissa N, Covarelli V, Janel S, Durel B, Simpson N, Bernard SC, Pardo-Lopez L, Bouzinba-Segard H, Faure C, Scott MGH, Coureuil M, Morand PC, Lafont F, Nassif X, Marullo S, Bourdoulous S (2017) Strength of Neisseria meningitidis binding to endothelial cells requires highly-ordered CD147/beta2-adrenoceptor clusters assembled by alpha-actinin-4. Nat Commun 8:15764
5. Coureuil M, Lecuyer H, Scott MG, Boularan C, Enslen H, Soyer M, Mikaty G, Bourdoulous S, Nassif X, Marullo S (2010) Meningococcus hijacks a beta2-adrenoceptor/beta-arrestin pathway to cross brain microvasculature endothelium. Cell 143 (7):1149–1160
6. Nassif X, Lowy J, Stenberg P, O'Gaora P, Ganji A, So M (1993) Antigenic variation of pilin regulates adhesion of Neisseria meningitidis to human epithelial cells. Mol Microbiol 8 (4):719–725
7. Weksler BB, Subileau EA, Perriere N, Charneau P, Holloway K, Leveque M, Tricoire-Leignel H, Nicotra A, Bourdoulous S, Turowski P, Male DK, Roux F, Greenwood J, Romero IA, Couraud PO (2005) Blood-brain barrier-specific properties of a human adult brain endothelial cell line. FASEB J 19(13):1872–1874
8. Scott MG, Pierotti V, Storez H, Lindberg E, Thuret A, Muntaner O, Labbe-Jullie C, Pitcher JA, Marullo S (2006) Cooperative regulation of extracellular signal-regulated kinase activation and cell shape change by filamin A and beta-arrestins. Mol Cell Biol 26(9):3432–3445
9. Storez H, Scott MG, Issafras H, Burtey A, Benmerah A, Muntaner O, Piolot T, Tramier M, Coppey-Moisan M, Bouvier M, Labbe-Jullie C, Marullo S (2005) Homo- and hetero-oligomerization of beta-arrestins in living cells. J Biol Chem 280(48):40210–40215
10. Virji M, Watt SM, Barker S, Makepeace K, Doyonnas R (1996) The N-domain of the human CD66a adhesion molecule is a target for Opa proteins of Neisseria meningitidis and Neisseria gonorrhoeae. Mol Microbiol 22 (5):929–939
11. Kellogg DS Jr, Cohen IR, Norins LC, Schroeter AL, Reising G (1968) Neisseria gonorrhoeae. II. Colonial variation and pathogenicity during 35 months in vitro. J Bacteriol 96(3):596–605
12. Luttrell LM, Ferguson SS, Daaka Y, Miller WE, Maudsley S, Della Rocca GJ, Lin F, Kawakatsu H, Owada K, Luttrell DK, Caron MG, Lefkowitz RJ (1999) Beta-arrestin-dependent formation of beta2 adrenergic receptor-Src protein kinase complexes. Science 283(5402):655–661
13. Soyer M, Charles-Orszag A, Lagache T, Machata S, Imhaus AF, Dumont A, Millien C, Olivo-Marin JC, Dumenil G (2014) Early sequence of events triggered by the interaction of Neisseria meningitidis with endothelial cells. Cell Microbiol 16(6):878–895
14. Billker O, Popp A, Gray-Owen SD, Meyer TF (2000) The structural basis of CEACAM-receptor targeting by neisserial Opa proteins. Trends Microbiol 8(6):258–260. discussion 260-251
15. Sanjana NE, Shalem O, Zhang F (2014) Improved vectors and genome-wide libraries for CRISPR screening. Nat Methods 11 (8):783–784
16. Merz AJ, Enns CA, So M (1999) Type IV pili of pathogenic Neisseriae elicit cortical plaque formation in epithelial cells. Mol Microbiol 32 (6):1316–1332



Chapter 21

Methods to Investigate the Roles for β-Arrestin-2 in Allergic Inflammatory Airway Disease

Akhil Hegde and Julia K. L. Walker

Abstract

Spatial and temporal control of gene expression using cre/loxP technology is a major methodological advance for biomedical research. The ability to alter gene expression after an in vivo disease model has been established and allows researchers the opportunity to examine the impact of that gene on the perpetuation of a disease, a mechanistic insight that is arguably more therapeutically relevant than developmental mechanisms.

We used the cre/LoxP technology in mice to show that β-arrestin-2, a gene previously shown to be required for the development of the asthma phenotype, is also required for the perpetuation of, at least, the airway hyperresponsiveness characteristic of that phenotype. Here we describe stepwise methods for the activation of the cre-loxP technology and induction of murine allergic inflammatory airway disease. We comment on the unanticipated problems encountered, which we speculate were a result of interactions between the allergen and β-arrestin-2 gene (*Arrb2*) regulation and the effect of tamoxifen on the asthma phenotype. The issues encountered here may be generally applicable to cre/loxP utilization in inflammatory disease models, especially if the gene of interest is associated with the inflammatory cascade.

Key words β-Arrestin-2, Allergic asthma, Airway hyperresponsiveness, Mice, OVA, Inducible knockout, Tamoxifen

1 Introduction

β-Arrestins (β-arrestin-1 and 2), ubiquitously expressed intracellular proteins, regulate seven-transmembrane receptor (7TMR) signaling by terminating G protein-dependent signaling events and transducing alternate signaling pathways [1, 2]. Given the integral role for 7TMRs in normal physiology and pathophysiology, β-arrestins have been implicated in the process of inflammation [3] as well as many diseases including cardiovascular disease [4], cancer [5, 6], and asthma [7, 8].

β-Arrestin-knockout (KO) mice have provided a valuable tool with which to examine the importance of β-arrestins in the development of various disease models; however, of equal or greater therapeutic interest are the mechanisms by which diseases continue

Mark G. H. Scott and Stéphane A. Laporte (eds.), *Beta-Arrestins: Methods and Protocols*, Methods in Molecular Biology, vol. 1957, https://doi.org/10.1007/978-1-4939-9158-7_21, © Springer Science+Business Media, LLC, part of Springer Nature 2019

and/or advance. The advent of cre/loxP technology has afforded researchers spatiotemporal control over the transcription or excision of murine genes of interest [9–12] making possible the examination of potential involvement of genes/proteins in disease perpetuation. For example, we showed, using KO mice, that β-arrestin-2 is essential for the development of the asthma phenotype [8]. Subsequently, using cre/loxP mice (R26-CreERT2/β arr2$^{flx/flx}$), we demonstrated that β-arrestin-2 is also required for the continuation of asthma-like characteristics in mice [7].

The subject of this report describes the methods that can be used to establish allergic inflammatory airway disease in mice and activate the cre/loxP. In addition, we describe the methodological challenges we encountered including delayed reduction of lung β-arrestin-2 protein expression and slight dampening effects of tamoxifen on the inflammatory phenotype.

2 Materials

Prepare all reagents at room temperature and store as indicated below. Tamoxifen is a hazardous substance that requires careful handling and disposal. Handle tamoxifen powder exclusively in the chemical fume hood by pre-weighing a lidded container and adding the powder in the fume hood. Don appropriate personal protective equipment (PPE) to protect yourself. Change gloves frequently and wash hands after removing gloves. After injection of tamoxifen, place the needle and syringe into a contaminated sharps bin without recapping.

2.1 Tamoxifen Solution

20 mg/ml tamoxifen in corn oil. Tamoxifen is purchased as a powder. The solvent for tamoxifen is corn oil. Weigh 20 mg of tamoxifen and dissolve in 1 ml of corn oil. Shake on a rocking platform shaker at room temperature until tamoxifen is completely dissolved in corn oil. Store at −20 °C (*see* **Note 1**).

2.2 OVA for Sensitization

0.1 mg/ml ovalbumin (OVA) and 20 mg/ml alum in normal saline. OVA is albumin from chicken egg white. Grade V is desired and available from Sigma-Aldrich Corp. OVA is prepared on the day of injection as follows: OVA stock solution aliquot, which is prepared by dissolving 10 mg OVA in 1 ml normal saline and stored at −20 °C (*see* **Note 2**), is to be taken out of the freezer and thawed. From this 10 mg/ml stock solution aliquot of OVA, take 1 μl into a tube, add 50 μl of alum and 49 μl of normal saline, shake vigorously using a vortex, and use within 3 h for injection.

2.3 OVA for Aerosol Challenge

10 mg/ml OVA in normal saline. For aerosol delivery of OVA, make a 1% (w/v) OVA solution. Weigh 10g of OVA (Grade V) and dissolve it in 1000 ml of normal saline. Shake well at room

temperature; make sure OVA is completely dissolved by visually checking, and store at −20 °C (*see* **Note 3**). Starting on day 21, challenge the mice with "OVA for aerosol challenge" by pouring 200 ml of the 1% (w/v) OVA solution into a Six-Jet Atomizer (TSI Inc., St. Paul, MN, USA) and activating three jets for 1 h. Each jet produces approximately 0.2 μm particles and particle concentrations greater than 10^7 particles per cm^3.

2.4 Immunoblot

1. Novex® Tris–Glycine gels (4–20).
2. PVDF membrane (pore size 0.45 μm, 7 cm × 8.4 cm).
3. Tris-buffered saline containing Tween-20 (TBS-T): 137 mM NaCl, 20 mM Tris–HCl, pH 7.4, 0.1% Tween-20. Store at room temperature.
4. RIPA (radioimmunoprecipitation assay) lysis buffer: 50 mM Tris–HCl, pH 7.8, 150 mM NaCl, 5 mM EDTA, 10 mM NaF, 1% NP-40, 0.5% Na-deoxycholate, 0.1% SDS.
5. 2× Laemmli Sample Buffer containing β-mercaptoethanol at 710 mM.
6. Tris–glycine running buffer: 10× concentration is 30 g Tris base, 144 g glycine, 10 g SDS. Bring to 1 L with water. Dilute to 1× with water prior to use in electrophoresis.
7. Semi-Dry Transfer buffer: 5.8 g Tris–Cl (Trizma), 2.9 g glycine, 0.37 g SDS in water. Bring to 800 ml with water and add 200 ml methanol.
8. Protease inhibitors: 1 mM PMSF, 5 μg/ml leupeptin, 10 ng/μl benzamidine, 0.7 μg/ml pepstatin A, 10 μg/ml aprotinin.
9. Blocking solution: 5% nonfat dry milk in TBS-T. Store at 4 °C for 1 week or prepare fresh.
10. A2CT: In house polyclonal antibody, a generous gift from Professor Robert J. Lefkowitz. Antibodies against β-arrestin-2 are also available commercially (e.g.,, Santa Cruz Biotechnology, Catalogue number sc-13140; Abnova, Catalogue number H00000409-M01, etc.) (*see* **Note 4**).
11. HRP-conjugated anti-rabbit IgG (ECL anti-rabbit IgG, Horseradish Peroxidase-Linked Species-Specific Whole antibody).
12. Chemiluminescent detection system (Pierce SuperSignal West Femto reagent).
13. Signal assessed using densitometry GeneTools program (SynGene, Frederick, MD, USA).
14. Stripping buffer.
15. To assess protein loading use β-actin primary antibody.

2.5 Conditional (Inducible) β-Arrestin-2 Knockout Mice (R26-CreERT2/β arr2$^{flx/flx}$)

Mice with β-arrestin-2 gene are flanked by loxP sites (βarr2$^{flx/flx}$) and the global promoter Rosa-26 (R26) to express the fusion protein between estrogen receptor (ER) and Cre recombinase (R26-CreERT2) [7]. These conditional β-arrestin-2 mice and their littermate cre-negative control mice (βarr2$^{flx/flx}$) can be used to control the spatiotemporal deletion of β-arrestin-2 expression (*see* **Note 5**).

2.6 Methacholine for Asthma Phenotype Measurement

Use 1000 μg/ml methacholine (Sigma-Aldrich) in saline for the preparation of various dilutions.

3 Methods

3.1 Conditional (Inducible) Knockout of β-Arrestin-2

1. Inject tamoxifen solution (20 mg/ml) intraperitoneally (i.p.) at 75 mg/kg every day for 5 days into mice [7] that are at least 6 weeks old (*see* **Note 6**).
2. Inject 3.75 μl/g body weight of corn oil i.p. every day for 5 days into control mice. These mice control for potential effects of the tamoxifen vehicle on the phenotype. Observe mice to ensure no ill effects of i.p. injection.

3.2 OVA Model of Asthma

Ovalbumin (OVA) can be used to induce allergic inflammatory airway disease (asthma model) in mice.

1. Sensitize the mice to the allergen OVA by single i.p. injections of "OVA for sensitization" solution (refer to Subheading 2.2) at 100 μl per mouse on day zero and day 14 (*see* **Note 7**).
2. Starting on day 21, challenge the mice with "OVA for aerosol challenge" (refer to Subheading 2.3). The OVA aerosol challenge is to be repeated on three consecutive days per week.
3. Inject control mice with saline i.p. (100 μl) on day 0 and day 14 and expose to saline aerosol on three consecutive days per week similar to OVA sensitization and challenge, until the day of the phenotype assessment. These mice control for potential effects of aerosol exposure on the phenotype.
4. Assess asthma phenotype 24 h after the last OVA or saline aerosol challenge (*see* **Notes 8** and **9**). For details on asthma phenotype assessment consult [8, 13]. Briefly, measure airway responsiveness in a terminally anesthetized and tracheotomized mouse by i.v. injecting escalating doses of the bronchoconstrictor methacholine (MCh) (0–400 μg/kg) and ventilating the mouse using a tracheal cannula attached to a computer-controlled ventilator. Tracheal pressure is used to calculate Newtonian resistance (R_n), an indicator of airway luminal diameter that represents resistance of the central airways, by using the forced oscillation technique, an invasive method that

measures lung impedance (flexiVent, SCIREQ, Montreal, PQ, Canada). At termination of lung mechanics measurements, mice are saline-lavaged through the tracheal cannula, and bronchoalveolar lavage fluid is used for total and differential cell counts. To evaluate cellular inflammation and airway mucin content, stained 5-μm-thick sections of 4% paraformaldehyde-fixed and paraffin-embedded lungs are scored according to standard histologic criteria.

3.3 Assessment of the Tissue Deletion of β-Arrestin-2 by Immunoblot

1. Prepare whole cell lysate of the lung by homogenizing a small piece of lung (10–20 mg) in RIPA lysis buffer with protease inhibitors, inversion rotate for 30 min at 4 °C, centrifuge for 30–60 min at 4 °C at the maximum speed in a table top centrifuge, and collect the supernatant. Store the supernatant cell lysate at −80 °C until use.
2. Thaw and mix (25 μg) cell lysate from above with equal volume of 2× Laemmli Sample Buffer. Load sample onto 4–20% Novex® Tris–Glycine gels and electrophorese for 3–4 h (*see* **Note 10**) using 1× tris–glycine running buffer. Transfer proteins to PVDF membranes for immunoblotting: pre-wet filter paper and PVDF membrane with semi-dry transfer buffer. Onto the semidry transfer apparatus, layer in the following order: moistened filter paper, PVDF membrane, electrophoresed gel, and moistened filter paper. Connect the top portion of the semi-dry transfer apparatus; run the transfer at constant current (0.278 Amp) for 1 h at room temperature. Never reuse the transfer buffer.
3. Remove membrane from transfer apparatus. Wash the membrane for 5 min three times with gentle agitation in normal saline. Block the PVDF membranes overnight with gentle agitation at 4 °C in blocking solution which contains TBS-T and 5% nonfat dry milk.
4. Remove the membrane from the milk, and wash the membrane for 5 min three times with gentle agitation in TBS-T. Incubate the PVDF membrane with primary A2CT antibody (or other commercial β-arrestin-2 antibody, refer to Subheading 2.4, **item 10**) in TBS-T for 2 h at room temperature with gentle agitation. A2CT is diluted 1:2000 in TBS-T and has a tenfold higher affinity for β-arrestin-2 over β-arrestin-1.
5. Remove and save the primary antibody at 4 °C for subsequent use. Wash the membranes with TBS-T for 5 min 3 times with gentle agitation.
6. Incubate the washed membrane with secondary antibody for 2 h at room temperature. Secondary antibody is HRP-conjugated anti-rabbit IgG is diluted 1:500 in TBS-T.

7. Wash the membranes with TBS-T for 5 min three times with gentle agitation to remove excess secondary antibody, and detect the protein by chemiluminescence.
8. Quantitate each immunoblot band by densitometry using the GeneTools program (SynGene, Frederick, MD, USA).
9. Strip antibodies by incubating the membrane with Pierce Western Stripping Buffer for 15 min at 50 °C. Wash three times with normal saline and block overnight according to Subheading 3.3, **step 3**.
10. To evaluate amount of protein loaded per lane, follow Subheading 3.3, **steps 4–8** except substitute β-actin primary antibody and appropriate secondary antibody for A2CT antibody.

4 Notes

1. Tamoxifen should be handled carefully while weighing to avoid creating powder dust or aerosol. Tamoxifen is a hazardous substance, and the person handling it should wear appropriate PPE such as gloves, masks, laboratory safety glasses or splash goggles, long-sleeved lab coats, and closed toe footwear. Aerosols may be produced during any open handling of tamoxifen powder or during open manipulations of suspensions. All unused portions of tamoxifen along with the container must be disposed of as hazardous chemical waste. Additional quantities of tamoxifen can be weighed and dissolved in corn oil (100 mg/5 ml), and the aliquots can be stored at −20 °C for 1 week. Always use a 5 ml pipet to measure corn oil as it is very viscous and difficult to accurately measure the volume. It takes a couple of hours to dissolve tamoxifen completely in corn oil on a shaker; be patient, warming is not necessary. After thawing the tamoxifen solution, if it is not clear, slight warming in a water bath at 37 °C will help dissolve tamoxifen. As far as possible, use tamoxifen solutions within 1 week of preparation. Tamoxifen is sensitive to light, so protect tamoxifen solutions from light by covering with aluminum foil.
2. Prepare OVA stock solution (10 mg/ml) by dissolving 10 mg OVA in 1 ml of normal saline. Once dissolved, transfer about 10 μl of OVA stock solution into small tubes, and store the aliquots (10 mg/ml) at −20 °C.
3. OVA dissolves slowly in normal saline. Thus the OVA for aerosol solution should be shaken well manually (vortex is not needed) and kept aside for 1 h to make sure the dissolution is complete. Alternatively, let the weighed amount of OVA sit on the appropriate volume of normal saline in a bottle, keep aside for a couple of hours without shaking at room

temperature, and OVA will dissolve completely. OVA for aerosol solution can be frozen at −20 °C and must be used within 1 week of preparation. Freezing and thawing the OVA solution three times within that week to take out about 200 ml for each aerosol challenge will not affect the quality of the OVA solution.

4. Antibody against β-arrestin-2 is also available commercially but must be tested for selectivity to β-arrestin-2 over β-arrestin-1 or extend the time of gel electrophoresis so that good separation of the two β-arrestin proteins occurs.
5. Requests for R26-CreERT2/βarr2$^{flx/flx}$ mice can be submitted to Dr. Wei Chen, Dept. of Medicine, Duke University Medical Center, Durham, NC 27710, USA. Email: w.chen@dm.duke.edu.
6. If you are not familiar with the method of i.p. injection, request instruction/training from a veterinarian or other IACUC-approved personnel. Proper training is required by law. Mouse body weight should be monitored to make sure the dose of tamoxifen is tolerated and no adverse reactions are occurring. No drastic weight loss, no pain or bleeding at the site of injection, no distress, and no lack of grooming should be observed in mice that tolerate tamoxifen treatment.
7. Alum adjuvant is used in the "OVA for sensitization" solution to sensitize the mice to the protein allergen (OVA). Use a 1 ml syringe to accurately measure the alum volume required for the "OVA for sensitization" solution. To avoid the settling of alum particles, frequently mix the "OVA for sensitization" solution between injections. OVA for sensitization should be prepared fresh on the day of injection and used within 3 h.
8. The time required for deletion of β-arrestin-2 from the tamoxifen-treated β-arrestin-2 conditional knockout mouse is tissue specific. In our preliminary experiments, the mice are treated with tamoxifen every day for 5 days, and the tissue is collected 2, 5, and 7 days after the last dose of tamoxifen, which was d7, d10, and d12 of the protocol. For significant deletion of β-arrestin-2, it requires 7 days from the last dose of tamoxifen for lungs and a few days less for the spleen and bone marrow (Fig. 1). However these mice were not sensitized or challenged with the allergen OVA. For the OVA-sensitized and OVA-challenged mice, at least 12 days from the end of tamoxifen injection are required to reduce lung expression of β-arrestin-2 to low levels (Fig. 4 in [7]). This is substantially longer than the other tissues assessed including the bone marrow and spleen [7]. The unexpected delay in ablation of β-arrestin-2 expression is likely a result of interactions between the allergen-sensitization and–challenge protocol and

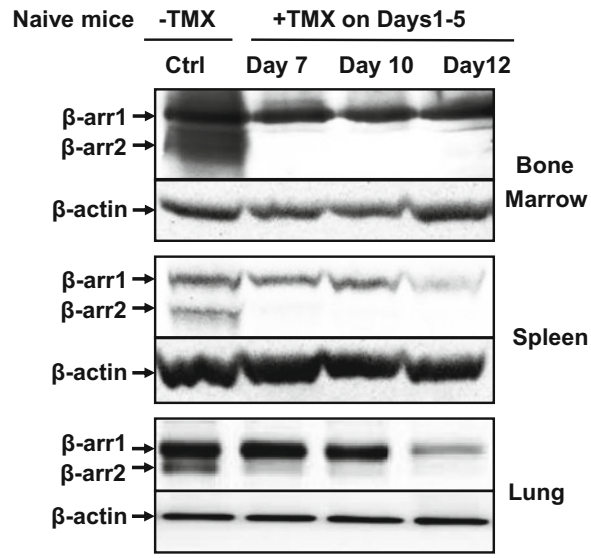


Fig. 1 Changes in tissue β-arrestin-2 protein levels with time in conditional β-arrestin-2 knockout mice (R26-CreERT2/βarr2$^{flx/flx}$) treated with or without tamoxifen. The mice were treated with tamoxifen daily for 5 days (on days 1, 2, 3, 4, and 5). Immunoblots of the bone marrow (upper panel), spleen (middle panel), and lung (lower panel) were obtained 2, 5, and 7 days after the last dose of tamoxifen (on days 7, 10, and 12 of the protocol). A2CT antibody was used to detect β-arrestin-1 and β-arrestin-2. β-actin immunoblot was used as a control for protein loading and can be used for correcting β-arrestin-2 levels of expression by densitometry. The first lane was loaded with a mixture of purified rat β-arrestin-1 and β-arrestin-2 as a positive control

β-arrestin-2 gene regulation since the OVA treatment is associated with elevated β-arrestin-2 expression in the lung. Altered tamoxifen dosing schedules and/or experimental protocols may need to be employed in studies where the treatment enhances expression of the gene of interest.

9. Another consideration related to the use of tamoxifen to activate cre-recombinase is that tamoxifen has been shown to elicit both pro- and anti-inflammatory effects in vivo [14–16]. Thus, researchers must take this into consideration to ensure that any inflammatory phenotype to be assessed is appropriately robust, even in the face of potential tamoxifen-mediated modulation of the phenotype.
10. Difficulty observing β-arrestin-2 bands on immunoblots, due to poor antibody specificity for β-arrestin-2 over β-arrestin-1, can be somewhat overcome by achieving good separation of the two β-arrestin signals. Gel electrophoresis should be run slowly for about 4 h in a cold room. If electrophoresis is conducted at too high voltage or at room temperature, the integrity of the gel will be compromised due to overheating.

Electrophoresis instructions are as follows: for the first 20 min, set voltage to 50 V, and then increase voltage to 100 V for 2 h followed by 125 V for 70–100 min. Use Bio-Rad Kaleidoscope marker to help visualize the separation of proteins of molecular weight in the range of β-arrestins (~46–47 kDa). Essentially electrophorese the gel until the orange marker (30 kD) has run off the gel.

Acknowledgments

We thank Minyong Chen who conducted the immunoblot in Fig. 1. This work was supported by NIH grant R01 AI110007 to J.K.L.W.

References

1. Lefkowitz RJ, Shenoy SK (2005) Transduction of receptor signals by beta-arrestins. Science 308:512–517
2. Lefkowitz RJ, Whalen EJ (2004) β-Arrestins: traffic cops of cell signaling. Curr Opin Cell Biol 16:162–168
3. Sharma D, Parameswaran N (2015) Multifaceted role of β-arrestins in inflammation and disease. Genes Immun 16:499–513
4. Kim J, Zhang L, Peppel K, Wu J-H, Zidar DA et al (2008) β-Arrestins regulate atherosclerosis and neointimal hyperplasia by controlling smooth muscle cell proliferation and migration. Circ Res 103:70–79
5. Buchanan FG, Gorden DL, Matta P, Shi Q, Matrisian LM et al (2006) Role of β-arrestin 1 in the metastatic progression of colorectal cancer. Proc Natl Acad Sci U S A 103:1492–1497
6. Fereshteh M, Ito T, Kovacs JJ, Zhao C, Kwon HY et al (2012) β-Arrestin2 mediates the initiation and progression of myeloid leukemia. Proc Natl Acad Sci U S A 109:12532–12537
7. Chen M, Hegde A, Choi YH, Theriot BS, Premont RT et al (2015) Genetic deletion of β-Arrestin-2 and the mitigation of established airway hyperresponsiveness in a murine asthma model. Am J Respir Cell Mol Biol 53:346–354
8. Walker JK, Fong AM, Lawson BL, Savov JD, Patel DD et al (2003) Beta-arrestin-2 regulates the development of allergic asthma. J Clin Invest 112:566–574
9. Copeland NG, Jenkins NA, Court DL (2001) Recombineering: a powerful new tool for mouse functional genomics. Nat Rev Genet 2:769–779
10. Murray SA, Eppig JT, Smedley D, Simpson EM, Rosenthal N (2012) Beyond knockouts: cre resources for conditional mutagenesis. Mamm Genome 23:587–599
11. Schwenk F, Baron U, Rajewsky K (1995) A cre-transgenic mouse strain for the ubiquitous deletion of loxP-flanked gene segments including deletion in germ cells. Nucleic Acids Res 23:5080–5081
12. Van Duyne GD (2015) Cre Recombinase. Microbiol Spectr 3
13. Walker JKL, Kraft M, Fisher JT (2012) Assessment of murine lung mechanics outcome measures: alignment with those made in asthmatics. Front Physiol 3:491
14. Behjati S, Frank MH (2009) The effects of tamoxifen on immunity. Curr Med Chem 16:3076–3080
15. Cai Y, Zhou J, Webb DC (2012) Estrogen stimulates Th2 cytokine production and regulates the compartmentalisation of eosinophils during allergen challenge in a mouse model of asthma. Int Arch Allergy Immunol 158:252–260
16. Riffo-Vasquez Y, Ligeiro de Oliveira AP, Page CP, Spina D, Tavares-de-Lima W (2007) Role of sex hormones in allergic inflammation in mice. Clin Exp Allergy 37:459–470



Chapter 22

Methods to Study Roles of β-Arrestins in the Regulation of Pancreatic β-Cell Function

Stéphane Dalle, Safia Costes, Gyslaine Bertrand, and Magalie A. Ravier

Abstract

Novel findings reveal important functional roles for β-arrestin 1 and β-arrestin 2 in the regulation of insulin secretion, β-cell survival, and β-cell mass plasticity not only by glucose but also by G-protein-coupled receptors, such as the glucagon-like peptide-1 (GLP-1) and the pituitary adenylate cyclase-activating polypeptide (PACAP) receptors or GPR40, or tyrosine kinase receptors, such as the insulin receptor. Here, we describe experimental protocols to knock down β-arrestins by small interference RNA, to follow subcellular localization of β-arrestins in the cytosol and nucleus of the insulinoma INS-1E rat pancreatic β-cell line, and to analyze β-arrestin protein expression by Western blot using INS-1E cells and isolated mouse or human pancreatic islets. We also provide details on how to genotype β-arrestin 2 knockout (*Arrb2*$^{-/-}$) mice and to evaluate β-arrestin-mediated roles in β-cell mass plasticity and β-cell signaling using immunocytochemistry on pancreatic sections or on primary dispersed β-cells from wild-type mice and *Arrb2*$^{-/-}$ mice.

Key words Pancreatic β-cell, Small interference RNA, Subcellular fractionation, Western blot, Genotyping, Immunocytochemistry, Immunofluorescence, β-Arrestins

1 Introduction

Type 2 diabetes is a major public health issue with worldwide increasing incidences. It is the most prevalent form of diabetes that accounts for ~90% of all diabetic subjects. Typically recognized as a metabolic disease with disrupted glucose metabolism, type 2 diabetes is characterized by abnormally prolonged high blood glucose levels [1]. This chronic hyperglycemia is considered as a consequence of the complex heterogeneous nature, of polygenic origin, and of the illness, which combines insulin resistance in peripheral tissues (failure of insulin action) and impaired insulin secretion from pancreatic β-cells. Although the relative importance of each of these disorders in the etiology of type 2 diabetes has been disputed, both are necessary for the development of the disease, which appears, even in the case of severe insulin resistance, only

Mark G. H. Scott and Stéphane A. Laporte (eds.), *Beta-Arrestins: Methods and Protocols*, Methods in Molecular Biology, vol. 1957, https://doi.org/10.1007/978-1-4939-9158-7_22, © Springer Science+Business Media, LLC, part of Springer Nature 2019

when an impaired insulin secretion exists [2, 3]. Moreover, a progressive decrease in β-cell mass has been reported in patients with type 2 diabetes [2, 4]. Together, these evidences support the notion that β-cells play a central role in the etiology of type 2 diabetes. Therapeutic strategies designed to protect and to preserve a functional pancreatic β-cell mass are therefore essential to fight diabetes.

Pancreatic β-cell proliferation, survival, and secretion are well described to be regulated by signaling pathways linked to glucose, G-protein-coupled receptors (GPCRs), such as the glucagon-like peptide-1 (GLP-1), the pituitary adenylate cyclase-activating polypeptide (PACAP) receptors, or GPR40, and tyrosine kinase receptors (TKRs), such as the insulin receptor. Novel findings, including those from our group, reveal important functional roles for β-arrestin 1 (ARRB1) and β-arrestin 2 (ARRB2) in the regulation of insulin secretion, β-cell survival, β-cell proliferation, and β-cell mass plasticity [5–15]. This chapter details various step-by-step methods that we routinely use in the laboratory to investigate the roles of β-arrestins (ARRBs); in particular, we detail how (1) to evaluate levels of ARRB expression, (2) to analyze subcellular localization of ARRBs, (3) to knock down *Arrbs* by small interference RNA approaches in β-cells, (4) to genotype *Arrb2* knockout ($Arrb2^{-/-}$) mice, and (5) to evaluate ARRBs roles in β-cell signaling and β-cell mass plasticity using immunocytochemistry on pancreatic sections or on primary dispersed β-cells from wild-type mice and $Arrb2^{-/-}$ mice.

2 Materials

Prepare all the solutions with ultrapure water. Keep the reagents at room temperature (unless indicated otherwise). Follow the regulation for waste disposal.

2.1 Arrb Knockdown by Small Interference RNA in INS-1E Cells

2.1.1 Silencers Used and Preparation (Life Technologies)

Arrb1 Silencer® Select siRNA (5 nmol, Catalog reference s129662), *Arrb2* Silencer® Select siRNA (5 nmol, Catalog reference s129664), and Silencer® Select Negative Control No. 1 siRNA (5 nmol, Catalog reference 4390843). Briefly, centrifuge the tube to ensure that the dried siRNA is at the bottom of the tube. Resuspend the 5 nmol siRNA using 100 μl of nuclease-free water provided for a final concentration of 50 μM. Store at −20 °C until use.

2.1.2 Reagents

Lipofectamine® 3000, Opti-MEM® Medium, and RPMI medium (all Life Technologies).

2.2 Protein Extraction and Immunoblots from INS-1E Cells and Islets

Keep the solutions and materials at 4 °C.

2.2.1 Protein Extraction

1. 50 mM Tris–HCl buffer (pH 7.5): In a glass beaker, mix 250 ml of water and 3.03 g of Tris-base. Once the mixture is homogenized, adjust the pH to 7.5 by adding hydrochloric acid (HCl). Make up the volume to 500 ml and store at 4 °C.
2. 1 M NaCl buffer: In a glass beaker, mix 90 ml of water and 5.84 g of NaCl. Make up the volume to 100 ml and store at 4 °C.
3. 100 mM dithiothreitol (DTT): In 10 ml of water, mix 154 mg of DTT. Make aliquots of 500 μl and store at −20 °C.
4. 1 M sodium fluoride (NaF): In 10 ml of water, mix 419.9 mg of NaF. Make aliquots of 500 μl and store at −20 °C.
5. 100 mM sodium orthovanadate (Na_3VO_4): In 10 ml of water, mix 184 mg of Na_3VO_4. Make aliquots of 500 μl and store at −20 °C.
6. Protease inhibitor cocktail powder (Catalog reference P2714-1BTL, Sigma): Resuspend the powder in 10 ml of water (10× solution). Make aliquots of 100 μl and store at −20 °C.
7. Nonidet P-40 (NP-40) or IGEPAL® (Sigma).
8. Pre-Buffer: In a glass beaker, mix 191 ml of water with 240 ml of 50 mM Tris–HCl, pH 7.5, 90 ml of 1 M NaCl, and 1.04 ml of 1 M $MgCl_2$. Keep at 4 °C.
9. Cell lysis buffer: 0.5% NP-40, 20 mM Tris–HCl, pH 7.5, 150 mM NaCl, 2 mM $MgCl_2$, 1 mM DTT, 5 mM NaF, and 1 mM Na_3VO_4. In 43.5 ml of pre-buffer, mix 250 μl of NP-40, 500 μl of 100 mM DTT, 250 μl of 1 M NaF, and 500 μl of 100 mM Na_3VO_4. Make aliquots of 900 μl and store at −20 °C. When needed, extemporaneously add 100 μl of protease inhibitors (10× solution) to this 900 μl aliquot.
10. Mini-centrifuge.
11. Phosphate-buffered saline (PBS).
12. Plastic scraper.
13. Ice.

2.2.2 Protein Assay

1. Bicinchoninic Acid solution (Catalog reference B9643, Sigma).
2. Copper (II) sulfate pentahydrate 4% solution (Catalog reference C2284, Sigma).
3. Protein standard solution, 2 mg/ml bovine serum albumin (BSA).
4. 96-well plates.
5. Spectrophotometer.
6. Water bath.

2.2.3 Immunoblots

1. NuPAGE® LDS sample buffer (4×) (Novex, Catalog reference NP007, Life Technologies).
2. NuPAGE® sample reducing agent (10×) (Catalog reference NP004, Life Technologies).
3. Boiling recipients.
4. Running buffer: Mix 950 ml of water with 50 ml of NuPAGE® MES SDS Running Buffer (20×) (Catalog reference NP0002, Life Technologies).
5. NuPAGE® Novex 4–12% Bis-Tris Gel 1.0 mm (Life Technologies).
6. NuPAGE® Antioxidant (Catalog reference NP005, Life Technologies).
7. SeeBlue® Plus2 Pre-stained Protein Standard (Catalog reference LC5925, Life Technologies).
8. Methanol.
9. Transfer buffer: Mix 375 ml of water with 25 ml of NuPAGE® Transfer Buffer (20×) (Catalog reference NP0006-1, Life Technologies) and 100 ml of methanol.
10. FluoroTrans® polyvinylidene difluoride (PVDF) membrane 0.2 μm.
11. Blotting tweezer to hold the PVDF membrane.
12. Blotting roller.
13. Orbital Shaker.
14. Small containers where the membrane can fit with 10 ml liquid.
15. Restore™ Western Blot Stripping Buffer (21059, Life Technologies).
16. 10× TBS: 200 mM Tris–HCl, pH 7.6, 1.37 M NaCl buffer. In 800 ml of water, dissolve 48.2 g of Tris-base and 160 g of NaCl. Once the mixture is homogenized, adjust the pH to 7.6 by adding hydrochloric acid (HCl). Make up the volume to 2 l and store at room temperature.
17. Tween® 20.
18. Washing solution (TBS-T): 1× TBS, 0.1% Tween® 20. Dilute 100 ml of 10× TBS in 800 ml of water. Add 1 ml of Tween® 20 and make up the volume up to 1 l. Store at room temperature.
19. Blotting-grade blocker, nonfat dry milk (Bio-Rad).
20. Blocking solution: TBS-T, 5% milk: Weigh 2.5 g of milk, and mix gently with 40 ml of TBS-T in a beaker with the help of a stirrer. Make up the volume to 50 ml with TBS-T and store at 4 °C for up to two days.

21. Primary antibodies: Anti-ARRB2 mouse monoclonal antibody (Catalog reference ab54790, Abcam) and anti-ARRB1 mouse monoclonal antibody (Catalog reference 610551, Becton Dickinson).
22. Secondary antibody: Goat Anti-Mouse IgG (H + L) horseradish peroxidase enzyme (HRP) conjugate.
23. Immobilon Western Chemiluminescent HRP substrate (Millipore).
24. Transparent plastic sheet protector.
25. Plastic bag sealer.
26. Chemiluminescence imaging system.
27. ImageJ software for blot analysis.

2.3 Cytoplasmic and Nuclear Protein Extraction

1. NE-PER Nuclear and Cytoplasmic Extraction Reagents (Catalog reference 78833, Life Technologies).
2. Halt Protease Inhibitor Cocktail 100× (Catalog reference 78425, Life Technologies).
3. Cytoplasmic Extraction Reagent I (CERI) solution: 500 μl of CERI +5 μl Halt Protease Inhibitor Cocktail (100×).
4. Nuclear Extraction Reagent (NER) solution: 100 μl NER + 1 μl Halt Protease Inhibitor Cocktail (100×).
5. Phosphate-buffered saline (PBS).
6. Mini-centrifuge.
7. Vortex.

2.4 Genotyping of Arrb2 Knockout Mice

1. KAPA mouse genotyping kit (KK7301 or KK7302).
2. PCR-grade water.
3. Primers for our mice (*see* Subheading 3.4) are Arrb2WT-forward GATCAAAGCCCTCGATGATC (intron 2), Arrb2KO-forward GCTAAAGCGCATGCTCCAGA (Neomycin), and Arrb2-reverse ACAGGGTCCACTTTGTCCA (exon 3). Arrb2WT-forward and Arrb2KO-forward are specific for the wild-type and knockout allele, respectively, while the primer Arrb2-reverse ACAGGGTCCACTTTGTCCA is common for both wild type and knockout. Amplicon lengths are 605 bp and 300 bp for Arrb2WT and Arrb2KO alleles, respectively.
4. 25 mM $MgCl_2$.
5. 50× TAE. In 300 ml of water, dissolve 96.8 g of Tris-base and 1.48 g of EDTA. Add 22.84 ml of glacial acetic acid. Adjust pH to 8.2 by adding glacial acetic acid. Make up the volume to 400 ml and store at room temperature.

6. 1% (w/v) agarose gel in TAE containing 0.2–0.5 μg/ml ethidium bromide.
7. 0.5 ml tubes.
8. PCR tubes.
9. Mini-centrifuge.
10. Cycler for PCR (Mastercycler, thermocycler, etc.).
11. Ice.
12. Heating block or water bath.

2.5 Immunocytochemistry on Pancreatic Sections from Arrb2$^{-/-}$ Mice

1. Phosphate-buffered saline containing Ca^{2+}/Mg^{2+} (PBS).
2. Tween® 20. Prepare 0.05% Tween in PBS.
3. 37% formaldehyde solution (Sigma). Prepare 4% formaldehyde solution in PBS.
4. Absolute ethanol.
5. 70% ethanol (500 ml) for Subheading 3.5.1.
6. 90% and 70% ethanol (200 ml each) for Subheading 3.5.3.
7. Xylene.
8. Citrate buffer pH 6. Prepare 200 ml of 1× citrate buffer.
9. Milli-Q water.
10. 1% BSA in PBS.
11. Primary antibodies of interest. Here are the antibodies used in Fig. 4: Guinea pig anti-insulin antibody (Abcam, 1/200 in 1% BSA in PBS) and mouse anti-glucagon antibody (Sigma-Aldrich, 1/400 in 1% BSA in PBS).
12. 4′,6-Diamidino-2-phenylindole (DAPI) to stain nuclei.
13. Secondary antibodies of interest. Here are the antibodies used in Fig. 4: Cy3 AffiniPure Donkey Anti-Guinea Pig antibody (Jackson ImmunoResearch, 1/500 in 1% BSA in PBS), Alexa Fluor® 488 AffiniPure Donkey Anti-Mouse antibody (Jackson ImmunoResearch, 1/500 in 1% BSA in PBS).
14. Mowiol® 4–88: Weigh 6 g of glycerol and add 2.4 g of Mowiol. Mix with a magnetic stirrer for at least 3 h. Add 6 ml of Milli-Q water and mix with a magnetic stirrer overnight.

    Add 12 ml of Tris–HCl 0.2 M, pH 8.5. Mix with a magnetic stirrer 1 h at room temperature.

    Incubate 20 min at 50 °C. Mix gently during the incubation period. Transfer into a 50 ml tube. Centrifuge at 20 °C at 5000 × *g* during 15 min. Make 500 μl aliquots in 1.5 ml tube and store at −20 °C.
15. Flat embedding cassettes (Catalog reference 410-02S Klinipath).

16. Sponge for embedding cassettes (Catalog reference F/PP15–8010 Microm Microtech).
17. Microscope slides.
18. Microscope cover slips (24 mm × 60 mm).
19. Dako Pen or any water-repelling pen.
20. Immunocytochemistry racks.
21. Opaque plastic or metallic box with a sealed lid.
22. Fluorescence microscope. The model used to generate the images was an Axio Imager microscope (Zeiss).

2.6 Immunocytochemistry on Dispersed Pancreatic Islet Cells from *Arrb2*$^{-/-}$ Mice

1. Phosphate-buffered saline containing Ca^{2+}/Mg^{2+} (PBS).
2. 37% formaldehyde solution. Prepare 4% formaldehyde solution by diluting in PBS.
3. 100 mM glycine in PBS from 1 M stock. 1 M stock: 0.75 g in 10 ml, pH 8.5 with NaOH.
4. 10% FBS in PBS.
5. 0.2% Triton in PBS.
6. 3% BSA in PBS.
7. Parafilm M®.
8. Microscope cover slips (15 or 18 mm diameter).
9. Microscope slides.
10. Opaque plastic or metallic box with a sealed lid.
11. Primary antibodies of interest. Here are the antibodies used in Fig. 5: Guinea pig anti-insulin antibody (Abcam, 1/200 in 1% BSA in PBS) and rabbit antibody raised against our protein of interest (1/150 in 1% BSA in PBS).
12. Secondary antibodies of interest. Here are the antibodies used in Fig. 5: Alexa Fluor® 488 AffiniPure donkey Anti-Guinea Pig antibody (Jackson ImmunoResearch, 1/5000 in 1% BSA in PBS), Cy3 AffiniPure Donkey Anti-Rabbit antibody (Jackson ImmunoResearch, 1/6000 in 1% BSA in PBS).
13. Mowiol® 4–88: Prepare as in Subheading 2.5, **item 14**.

3 Methods

3.1 Arrb Knockdown by Small Interference RNA in INS-1E Cells

1. Seed the INS-1E cells to be 60–80% confluent at transfection (i.e., 800,000 INS-1E cells per well in six-well plates).
2. The next day, dilute Lipofectamine 3000 in Opti-MEM Medium: 3.3 μl Lipofectamine in 110 μl Opti-MEM.
3. Dilute siRNA in Opti-MEM Medium. For a 50 nM siRNA final concentration in the well: 1.2 μl siRNA in 118.8 μl Opti-MEM.

4. Add 110 µl of diluted siRNA to 110 µl of diluted Lipofectamine.
5. Incubate for 5 min.
6. During this time, rinse wells with Opti-MEM Medium. Add 800 µl of Opti-MEM Medium per well.
7. Add 200 µl siRNA-lipid complex to INS-1E cells (total volume per well is 1 ml). Incubate cells at 37 °C.
8. 24 h after transfection, replace Opti-MEM Medium with 2 ml of complete RPMI culture medium.
9. Lyse for protein extraction (*see* Subheading 3.2) or perform immunocytochemistry (*see* Subheading 3.6) of INS-1E cells 48 h or 72 h after transfection.

3.2 Protein Extraction and Immunoblots from INS-1E Cells and Islets

Detailed protocols from our lab to isolate the islets of Langerhans [15, 16] have already been published. In this section, we have described procedures that we have already used for ARRBs and other proteins of interest [8, 9, 15, 17].

3.2.1 Protein Extraction

Pre-chill down the material to be used and keep everything on ice.

1. Aspirate culture medium (from culture dishes for INS-1E cells, or from 1.5 ml tubes for islets).
2. Rinse twice with cold PBS.
3. Add 110 µl lysis buffer per well (for INS-1E cells in 6-well plates) or 30 µl lysis buffer per 100 islets. Lyse for 10 min on ice.
4. Scrape cells with a plastic scraper and collect the lysate into 1.5 ml tube. For the islets only: sonicate the sample at low power, three times for 5 s on ice.
5. Centrifuge for 10 min at 10,621 × *g* at 4 °C in mini-centrifuge to remove cellular debris, and transfer the supernatant into 1.5 ml tubes.
6. Keep the samples at −80 °C until subsequent protein assay determination using bicinchoninic acid solution (BCA) and immunoblotting.

3.2.2 Protein Assay

Protein determination by the Bicinchoninic Acid (BCA) method was performed according to the manufacturer's instructions.

3.2.3 Immunoblots

Run INS-1E cell or islet lysates (35–40 µg of protein) in a NuPAGE® Novex 4–12% Bis-Tris gel. Transfer the proteins from the gel to a PVDF membrane (*see* **Notes 1** and **2**). All procedures can be done at room temperature unless specified otherwise.

1. Place the PVDF membrane in a dish, and add the blocking solution until it covers the membrane. Shake gently for 1 h at room temperature on an orbital shaker.
2. Prepare the solution containing primary antibody by adding anti-ARRB1 or anti-ARRB2 antibodies in new blocking solution. Use 8 μl of antibody to 2 ml of blocking solution (1/250).
3. Place the membrane in a small plastic bag. Add the antibody solution and seal the plastic (*see* **Note 3**). Incubate overnight shaking gently on the orbital shaker in cold room.
4. Discard the antibody solution.
5. Wash the membrane three times for 5 min in washing solution under gentle agitation.
6. Discard the washing solution.
7. Prepare the solution containing the secondary antibody in new blocking solution. Use 1 μl of antibody to 2 ml of blocking solution (1/2000).
8. Place the membrane in a small plastic bag. Add the secondary antibody solution and seal the plastic. Incubate 1 h shaking gently on the orbital shaker at room temperature.
9. Wash the membrane three times for 5 min in washing solution under gentle agitation.
10. Apply the Immobilon Western Chemiluminescent HRP substrate as indicated by the manufacturer and incubate for 1 min.
11. Place the membrane between a transparent plastic sheet protector.
12. Proceed to signal detection using a chemiluminescence imaging system (Fig. 1).

3.3 Cytoplasmic and Nuclear Protein Extraction

Pre-chill down the material to be used and keep everything on ice.

1. Aspirate culture medium from INS-1E cells plated in six-well plates.
2. Rinse once with cold PBS.
3. Add 1 ml of cold PBS to each well.
4. Scrap the cells with a plastic scraper and collect the cells into 1.5 ml tube.
5. Centrifuge for 1 min at 2655 × *g*, in a mini-centrifuge, at 4 °C to pellet the cells.
6. Carefully remove and discard the supernatant, leaving cell pellet as dry as possible.
7. Add 100 μl of ice-cold CERI solution to the pellet. Resuspend the cells.

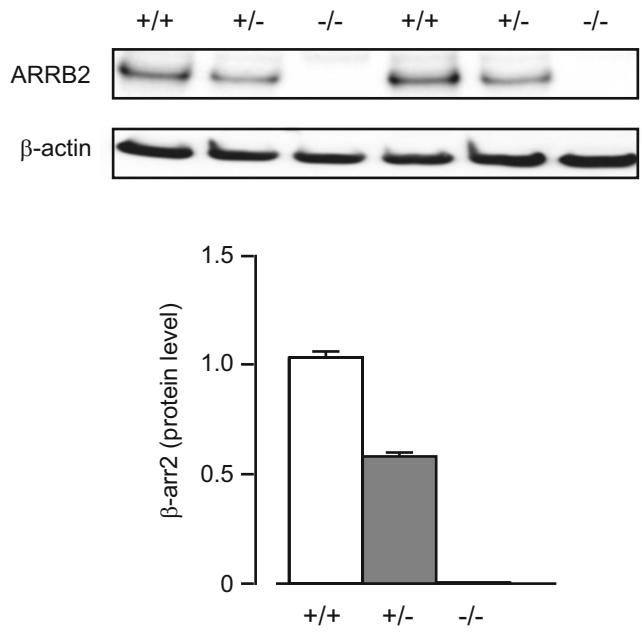


Fig. 1 ARRB2 protein expression in *Arrb2*$^{+/+}$, *Arrb2*$^{+/-}$, and *Arrb2*$^{-/-}$ mice. Representative immunoblots and quantitative analysis by densitometry using ImageJ of Arrb2 protein from *Arrb2*$^{+/+}$, *Arrb2*$^{+/-}$ and *Arrb2*$^{-/-}$ mice. Reproduced from [9] with permission from Springer

8. Vigorously vortex the tube on the highest setting for 15 s.
9. Incubate the tube on ice for 10 min.
10. Add 5.5 μl of ice-cold Cytoplasmic Extraction Reagent II (CER II) solution to the tube.
11. Vortex the tube on the highest setting for 5 s.
12. Incubate the tube on ice for 1 min.
13. Vortex the tube on the highest setting for 5 s.
14. Centrifuge for 5 min, in a mini-centrifuge, at 20,817 × *g* at 4 °C.
15. Transfer the supernatant (cytoplasmic extract) to a clean tube, and keep the sample at −80 °C until immunoblot analysis.
16. Rinse the insoluble (pellet) fraction, which contains nuclei, with 100 μl of CERI solution.
17. Vortex the tube on the highest setting for 8 s.
18. Centrifuge for 5 min at 20,817 × *g* at 4 °C.
19. Discard the supernatant.
20. Suspend the pellet fraction in 28 μl of ice-cold NER solution.
21. Vortex the tube on the highest setting for 15 s.

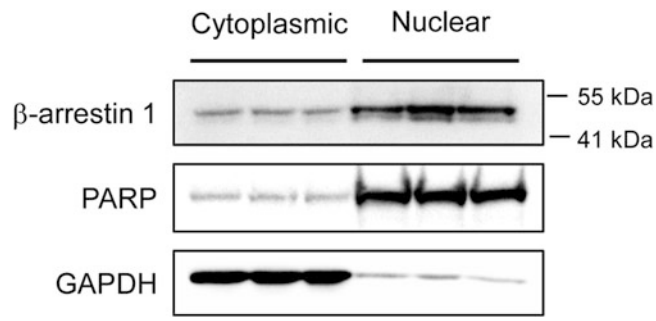


Fig. 2 Detection of β-arrestin 1 in cytoplasmic and nuclear fractions from INS-1E cells. INS-1E cells were subjected to subcellular fractionation. Cytoplasmic and nuclear fractions resolved by SDS-PAGE and immunoblotted with anti-β-arrestin 1, anti-GAPDH (loading control for cytoplasmic fraction), and anti-PARP antibody (loading control for nuclear fraction)

22. Place the sample on ice and continue vortexing for 15 s every 10 min, for a total of 40 min.
23. Centrifuge the tube for 10 min, in a mini-centrifuge, at 20,817 × *g* at 4 °C.
24. Transfer the supernatant (nuclear extract) to a clean tube, and keep the sample at −80 °C until immunoblot analysis (*see* Subheading 3.2.3). Figure 2 illustrates a typical ARRB1 immunoblot image obtained after cytoplasmic and nuclear protein extraction.

3.4 Genotyping of *Arrb2*$^{-/-}$ Mice

Our original *Arrb2* heterozygous mice were obtained from Dr. Robert J. Lefkowitz (Duke University Medical Center, Durham, NC, USA). *Arrb2*$^{-/-}$ mice under different strain are available from the Jackson Laboratory (www.jax.org/mouse-search?searchTerm=arrb2). As already reported [9] our mice were subsequently backcrossed onto C57BL/6 J background (Charles River, Lyon, France). *Arrb2*$^{-/-}$ mice and their wild-type littermate (*Arrb2*$^{+/+}$) are generated by breeding heterozygous animals in our EOPS animal facility at the Institut de Génomique Fonctionnelle, Montpellier, France. Animals are housed in standard conditions with a 12 h light/dark cycle, stable temperature (22 ± 1 °C), controlled humidity (55 ± 10%), and water and food ad libitum.

DNA extraction and PCR can be performed using classical techniques (*see* **Note 4**). In the laboratory we use a slightly adapted protocol from KAPA mouse genotyping kit (www.kapabiosystems.com).

3.4.1 DNA Extraction

1. Warm up the heating block (or water bath) to 75 °C.
2. Prepare a mix for the extraction. For each extraction tube: 44 μl PCR-grade water, 5 μl express extract buffer (vortex before

adding), and 1 μl express extract enzyme (never vortex, mix with pipette).

3. Add 50 μl of the mix on mouse tail or ear tissue.
4. Incubate for 10 min at 75 °C (during this step cells are lysed, nucleases and proteins degraded, and DNA released).
5. Incubate for 5 min at 95 °C (to inactivate the thermostable KAPA express extract protease).
6. Incubate the samples on ice (2–3 min to cool down the samples).
7. Vortex for 2–3 s, centrifuge at high speed, with a mini-centrifuge, for 1 min, and transfer 40 μl of supernatant to fresh 0.5 ml tubes or alternatively use immediately the sample for PCR.

3.4.2 PCR Reaction

1. Prepare a mix containing for each sample reaction (protocol slightly adapted from KAPA mouse genotyping kit): 3.625 μl PCR-grade water, 0.25 μl $MgCl_2$ (from 25 mM stock), 0.625 μl of 10 μM primer *Arrb2*WT-forward, 0.625 μl of 10 μM primer *Arrb2*KO-forward, 0.625 μl of 10 μM primer *Arrb2*-reverse, and 6.25 μl KAPA2G fast genotyping mix (do not vortex, mix by hand). Prepare four extra tubes for the mix to have control lanes (1 WT, 1 KO, 1 H_2O only, and 1 extra).
2. Add 0.5 μl of extracted DNA in PCR tubes.
3. Add 12 μl of the PCR mix to samples.
4. Make a short spin of samples in a mini-centrifuge.
5. Run the PCR, repeating **steps b–d** below for 35 cycles:
   (a) 95 °C, 3 min.
   (b) 95 °C, 15 s.
   (c) 58 °C, 15 s.
   (d) 72 °C, 30 s.
   (e) 72 °C, 7 min.
   (f) 4 °C.
6. Load samples on agarose gel (1% in TAE) containing ethidium bromide, and run for 45 min at 100 V (Fig. 3).

3.5 Immunocytochemistry on Pancreatic Sections from *Arrb2*$^{-/-}$ Mice

In this section we have described the procedure that we have used in Ravier et al. *Diabetologia* [9] (*see* **Note 5**).

3.5.1 Pancreas Setting into Cassettes

1. Sacrifice the animal by cervical dislocation according to your animal care institutionally approved procedures.
2. Locate the pancreas and immediately harvest.

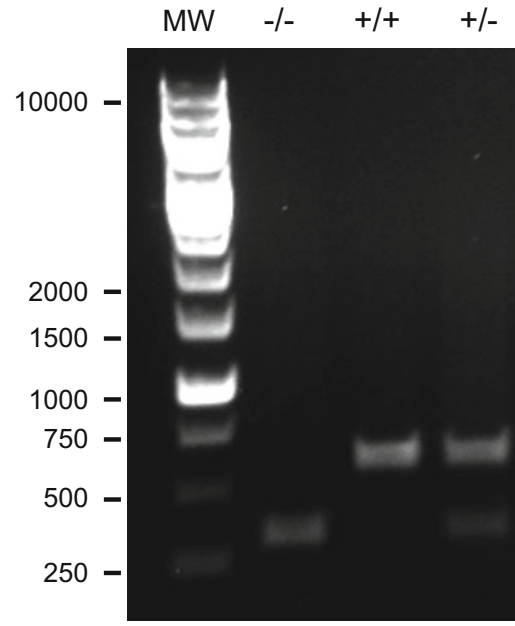


Fig. 3 Genotyping of *Arrb2*$^{+/+}$, *Arrb2*$^{+/-}$, and *Arrb2*$^{-/-}$ mice. Mouse genotyping was performed by DNA extraction and PCR as described in Subheading 3.4. Samples were loaded on an agarose gel (1% in TAE) containing ethidium bromide, and run for 45 min at 100 V. MW: Molecular weight. Amplicon lengths are 605 bp and 300 bp for *Arrb2*$^{+/+}$ and *Arrb2*$^{-/-}$ alleles, respectively. Reproduced from [9] with permission from Springer

3. Spread into flat embedding cassette with fixed lid containing a PBS humidified sponge.
4. At this stage you can also weigh the pancreas. This step is required if you want to assess the pancreatic islet or β-cell mass.
5. Place a second PBS humidified sponge, and close the cassette.
6. Place the cassette in 4% formaldehyde under a fume hood, and leave 20–24 h under stirring at room temperature.
7. Wash two times with PBS, each time for 5 min.
8. Wash with 70% ethanol to dehydrate the pancreas and store at 4 °C.

3.5.2 Dehydration and Paraffinizing of the Pancreas

For this step, our samples are processed by the RHEM facility in Montpellier (https://www.rhem.cnrs.fr/) for final steps of dehydration and paraffin embedding. The pancreas is longitudinally sectioned through pancreatic head-to-tail axis (4 μm thick). We use three pancreatic sections per mouse, separated by at least 100 μm. Detailed protocols can be found elsewhere (www.protocolsonline.com/histology/sample-preparation/paraffin-processing-of-tissue).

3.5.3 Deparaffinizing and Rehydrating Pancreatic Sections

1. Place slides (pancreatic sections) in an immunocytochemistry rack.
2. Wash with xylene for 10 min under a fume hood.
3. During this washing step, prepare 200 ml of 1× citrate buffer, pH 6. It has to be freshly prepared. Warm up the solution directly in a proper immunocytochemistry rack (98 °C, water bath).
4. At the end of **step 2**, wash with a second bath of xylene for 5 min.
5. Wash with absolute ethanol (99.9%) for 5 min.
6. Wash with 90% ethanol for 5 min.
7. Wash with 70% ethanol for 5 min.
8. Rehydrate with Milli-Q water for 5 min.

3.5.4 Antigen Retrieval and Immunohistochemical Staining

Day 1

1. Place the slides in the citrate buffer rack, pH 6, that has been prepared in Subheading 3.5.3, **step 3**, and incubate for 30 min at 98 °C.
2. Leave the citrate buffer rack to cool down for 30 min at room temperature.
3. Remove the slides from the rack, drain for few seconds, and wipe around the section with tissue paper to remove the citrate buffer.
4. Use a water-repelling pen such as Dako Pen to draw a circle around the pancreatic section.
5. Place the slides horizontally in a humidified chamber (*see* **Note 6**).
6. Cover pancreatic slices with the blocking buffer (PBS with 1% BSA), and leave for 30 min at room temperature.
7. Drain slides and wipe around the sections with tissue paper.
8. Add primary antibodies diluted in PBS with 1% BSA to cover the entire pancreatic section.
9. Shut the lid of the box and keep at 4 °C overnight.

Day 2

10. Drain slides and wash three times in Tween 0.05% in PBS, each time for 10 min at room temperature.
11. From now on, the following steps should be performed with as little exposure to light as possible.
12. Add secondary antibodies and DAPI (to stain nuclei) diluted in PBS with 1% BSA (1/1000) to cover the entire pancreatic section.

13. Shut the lid of the box and keep at room temperature for 45 min.
14. Drain slides and wash two times in Tween 0.05% in PBS, each time for 10 min at room temperature.
15. Wash with PBS for 10 min at room temperature.
16. Wash with Milli-Q water for 10 min at room temperature.
17. Mount slides with Mowiol or any other mounting agent recommended for fluorescence (Dako Glycergel, DABCO, VECTASHIELD, etc.) (*see* **Note 7**). Place a drop (~40 μl) of mounting medium on the slide (*see* **Note 8**), and put a glass cover slip on the top.
18. Let slides dry at 4 °C overnight in the dark before examining the cells under a fluorescence microscope. Figure 4 illustrates a typical immunocytochemistry experiment observed in sections from *Arrb2*$^{+/+}$and *Arrb2*$^{-/-}$ mouse pancreas.
19. After imaging, slides mounted in Mowiol can be stored at −20 °C and can be reimaged several months after, depending on the stability of antibodies.

3.6 Immunocytochemistry on Dispersed Pancreatic Islet Cells from *Arrb2*$^{-/-}$ Mice

A detailed protocol to prepare dispersed islet cells has already been published [16]. Compared to immunocytochemistry on pancreatic sections, this protocol allows to stimulate the cells with drugs or to re-express our protein of interest (ARRB2) by adenoviral infection of pancreatic β-cells (Fig. 5). In this section, we have described the procedure that we currently use in our lab [18] (*see* **Note 9**).

Day 1

1. If cells are expressing a fluorescent protein, such as GFP, from now, the following steps should be performed with as little exposure to light as possible.
2. Fix cells with 3.7% formaldehyde in PBS containing Ca^{2+}/Mg^{2+} at room temperature for 20 min. If you plan doing an immunofluorescence experiment against a phosphorylated protein, you should add 80 mM NaF (to protect from phosphatases).
3. Wash cells with PBS for 5 min.
4. Wash cells with 100 mM glycine in PBS for 5 min (*see* **Note 10**).
5. Wash cells with blocking buffer 10% FBS in PBS for 5 min.
6. Wash cells twice with PBS.
7. Permeabilization of cells with 0.2% Triton in PBS for 20 min.
8. Wash cells three times with PBS.
9. Wash cells with blocking buffer with 3% BSA in PBS at room temperature for 15 min.

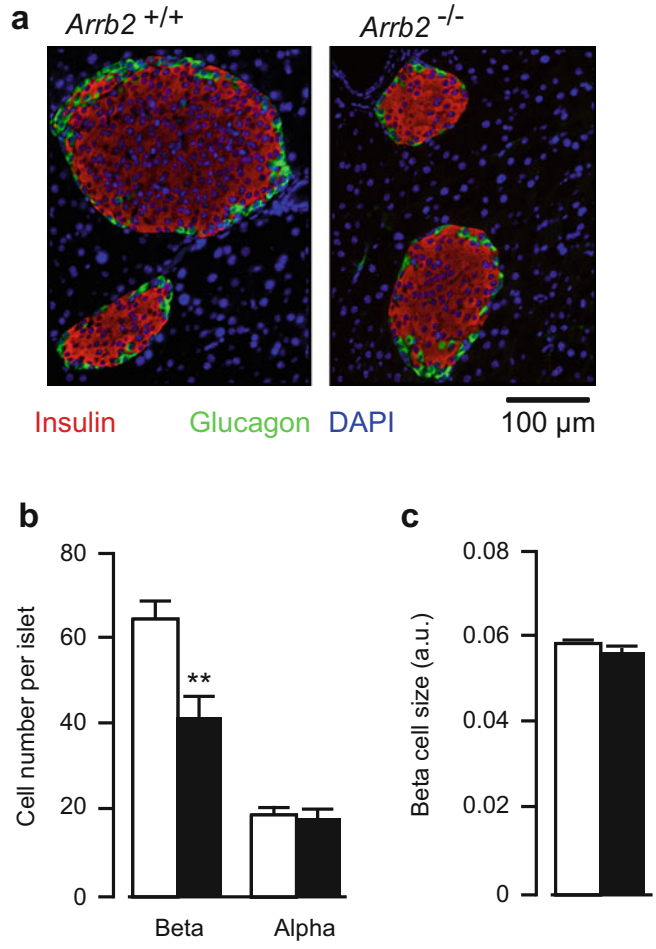


Fig. 4 Immunocytochemistry on dispersed islet cells from *Arrb2*$^{-/-}$ mice that re-express ARRB2. (**a**) Representative immunofluorescence staining of insulin and glucagon from a pancreatic section. Nuclei have been labeled with DAPI. Quantification of beta and alpha cell number per islet (**b**) and beta cell size (**c**) within the islets from *Arrb2*$^{+/+}$ vs. *Arrb2*$^{-/-}$ mice, using the calibrated ImageJ analysis program. $^{**}p < 0.01$ compared with *Arrb2*$^{+/+}$ mice. White, *Arrb2*$^{+/+}$, black, and *Arrb2*$^{-/-}$. Reproduced from [9] with permission from Springer

10. Drain the cover slip and wipe around the sections with tissue paper.
11. On Parafilm M® placed in a humidified chamber (*see* **Note 6**), for a 15 mm diameter cover slip, add 60 µl of primary antibody in 3% BSA in PBS (*see* **Notes 8** and **11**).
12. Place the cover slip inverted on the Parafilm M®, cells facing the primary antibody/Parafilm M® (*see* **Note 12**).
13. Shut the lid of the box and incubate overnight at 4 °C in the dark.

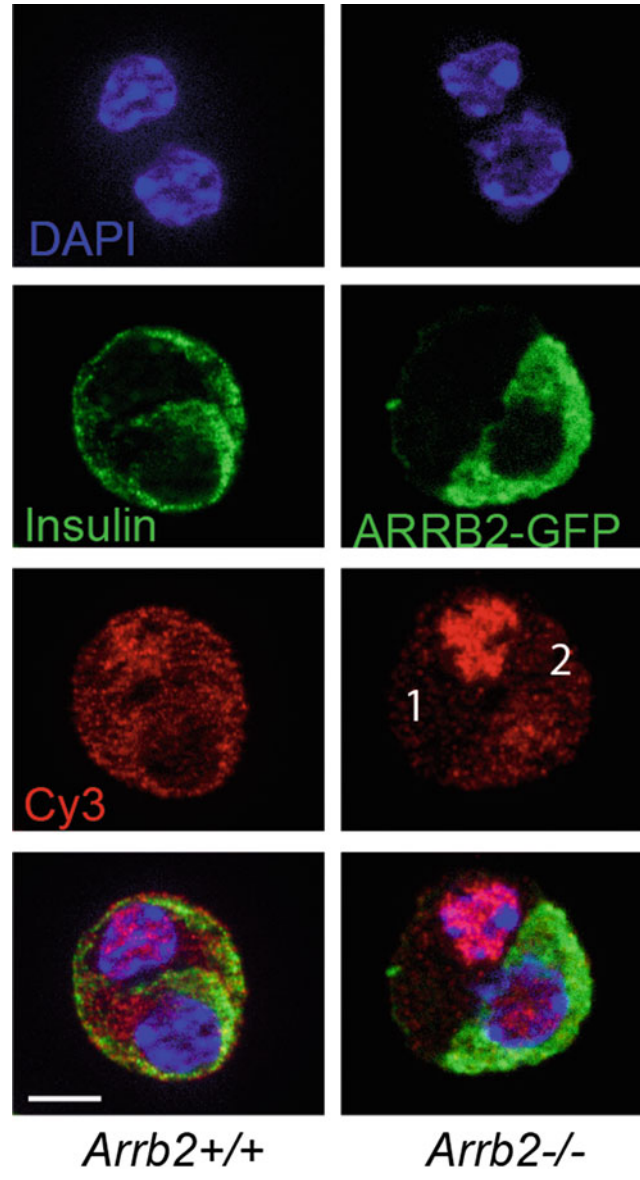


Fig. 5 Immunocytochemistry on dispersed islet cells from *Arrb2*$^{-/-}$ mice that re-express ARRB2. *Arrb2*$^{+/+}$ mouse β-cells were immunostained for insulin, and our protein of interest was immunostained in red. When ARRB2 expression was restored (ARRB2-GFP) in *Arrb2*$^{-/-}$ β-cells, it reduced the fluorescence intensity of our protein of interest in the nucleus (compare cell 1 with cell 2 or *Arrb2*$^{+/+}$ mouse β-cells). Scale bar, 5 μm

Day 2

14. Wash cells three times with PBS, each time for 10 min.

    From now, the following steps should be performed with as little exposure to light as possible if it was not already required in **step 1** from day 1.

15. On Parafilm M® placed in a humidified chamber (*see* **Note 6**), for a 15 mm diameter cover slip, add 60 µl of secondary antibody and DAPI (to stain nuclei) diluted in PBS with 3% BSA (1/1000) (*see* **Notes 8** and **11**).
16. Place the cover slip inverted on the Parafilm M®, cells facing the secondary antibody/Parafilm M® (*see* **Note 12**).
17. Shut off the lid of the box and incubate for 1 h at room temperature in the dark.
18. Wash cells three times with PBS, each time for 10 min.
19. Drain the cover slip and wipe around the sections with tissue paper.
20. Mount slides with Mowiol or any other mounting agent recommended for fluorescence (Dako Glycergel, DABCO, VECTASHIELD, etc.) (*see* **Note 7**). Place a drop (~20 µl) of mounting medium on the slide (*see* **Note 8**), and put a glass cover slip on the top.
21. Let slides dry at 4 °C overnight in the dark before examining the cells under a fluorescence microscope. Figure 5 illustrates a typical immunocytochemistry observed in dispersed islet cells from *Arrb2*$^{-/-}$ mice.
22. After imaging, slides mounted in Mowiol can be stored at −20 °C and can be reimaged several months after, depending on the stability of antibodies.

4 Notes

1. PVDF membranes need to be activated in methanol for 30 s before use.
2. It is important to handle the membrane with blotting tweezers and to keep it wet at all time.
3. Verify that you don't have bubbles at the interface between your membrane and the antibody solution.
4. Commercially available kits from several companies can be found elsewhere: www.quantabio.com/accustart-ii-pcr-genotyping-kit; www.systembio.com/genome-engineering-ez-genotyping-kit; www.neuvitro.com/rapid-genotyping-system.htm. Mice are genotyped by PCR using genomic DNA isolated from tail, but DNA isolated from ear can also be used.
5. Other detailed protocols can be found elsewhere: www.abcam.com/protocols/immunocytochemistry-immunofluorescence-protocol; www.cellsignal.com/contents/resources-protocols/immunofluorescence-general-protocol/if.

6. Usually we place humidified tissue paper at the bottom of an opaque plastic or metallic box with a sealed lid.
7. The mounting medium prevents dehydration, optimizes the refractive index for microscopy, prevents photobleaching, and preserves samples for long-term storage.
8. Avoid making bubbles. Burst bubbles with a thin needle or remove with the pipette.
9. Other similar detailed protocols can be found elsewhere: www.abcam.com/protocols/immunocytochemistry-immunofluorescence-protocol; www.cellsignal.com/contents/resources-protocols/immunofluorescence-general-protocol/if.
10. Glycine will bind free aldehyde groups that occur with fixative such as formaldehyde. This step will reduce the background due to non-specific binding of primary and secondary antibodies.
11. This procedure reduces the volume of the antibody that has to be used.
12. Check that you don't have bubbles at the interface between your cells and the antibodies.

References

1. DeFronzo RA (1988) Lilly lecture 1987. The triumvirate: beta-cell, muscle, liver. A collusion responsible for NIDDM. Diabetes 37 (6):667–687
2. Butler AE, Janson J, Bonner-Weir S, Ritzel R, Rizza RA, Butler PC (2003) Beta-cell deficit and increased beta-cell apoptosis in humans with type 2 diabetes. Diabetes 52(1):102–110
3. Leibowitz G, Kaiser N, Cerasi E (2009) Balancing needs and means: the dilemma of the beta-cell in the modern world. Diabetes Obes Metab 11(Suppl 4):1–9
4. Rahier J, Guiot Y, Goebbels RM, Sempoux C, Henquin JC (2008) Pancreatic beta-cell mass in European subjects with type 2 diabetes. Diabetes Obes Metab 10(Suppl 4):32–42
5. Dalle S, Ravier MA, Bertrand G (2011) Emerging roles for beta-arrestin-1 in the control of the pancreatic beta-cell function and mass: new therapeutic strategies and consequences for drug screening. Cell Signal 23 (3):522–528
6. Kong KC, Butcher AJ, McWilliams P, Jones D, Wess J, Hamdan FF, Werry T, Rosethorne EM, Charlton SJ, Munson SE, Cragg HA, Smart AD, Tobin AB (2010) M3-muscarinic receptor promotes insulin release via receptor phosphorylation/arrestin-dependent activation of protein kinase D1. Proc Natl Acad Sci U S A 107(49):21181–21186
7. Lin Z, Zhao Y, Song L, Mu K, Zhang M, Liu H, Li X, Zhao J, Wang C, Jia W (2016) Deletion of beta-Arrestin2 in mice limited pancreatic beta-cell expansion under metabolic stress through activation of JNK pathway. Mol Med 22:74–84
8. Quoyer J, Longuet C, Broca C, Linck N, Costes S, Varin E, Bockaert J, Bertrand G, Dalle S (2010) GLP-1 mediates antiapoptotic effect by phosphorylating bad through a beta-arrestin 1-mediated ERK1/2 activation in pancreatic beta-cells. J Biol Chem 285 (3):1989–2002
9. Ravier MA, Leduc M, Richard J, Linck N, Varrault A, Pirot N, Roussel MM, Bockaert J, Dalle S, Bertrand G (2014) Beta-Arrestin2 plays a key role in the modulation of the pancreatic beta cell mass in mice. Diabetologia 57 (3):532–541
10. Sonoda N, Imamura T, Yoshizaki T, Babendure JL, Lu JC, Olefsky JM (2008) Beta-Arrestin-1 mediates glucagon-like peptide-1 signaling to insulin secretion in cultured pancreatic beta cells. Proc Natl Acad Sci U S A 105 (18):6614–6619

11. Talbot J, Joly E, Prentki M, Buteau J (2012) Beta-Arrestin1 mediated recruitment of c-Src underlies the proliferative action of glucagon-like peptide-1 in pancreatic beta INS832/13 cells. Mol Cell Endocrinol 354(1–2):65–70
12. Zhang M, Zhu Y, Mu K, Li L, Lu J, Zhao J, Huang X, Wang C, Jia W (2013) Loss of beta-arrestin2 mediates pancreatic-islet dysfunction in mice. Biochem Biophys Res Commun 435 (3):345–349
13. Zhu L, Almaca J, Dadi PK, Hong H, Sakamoto W, Rossi M, Lee RJ, Vierra NC, Lu H, Cui Y, McMillin SM, Perry NA, Gurevich VV, Lee A, Kuo B, Leapman RD, Matschinsky FM, Doliba NM, Urs NM, Caron MG, Jacobson DA, Caicedo A, Wess J (2017) Beta-arrestin-2 is an essential regulator of pancreatic beta-cell function under physiological and pathophysiological conditions. Nat Commun 8:14295
14. Mancini AD, Bertrand G, Vivot K, Carpentier E, Tremblay C, Ghislain J, Bouvier M, Poitout V (2015) Beta-Arrestin recruitment and biased agonism at free fatty acid receptor 1. J Biol Chem 290 (34):21131–21140
15. Broca C, Quoyer J, Costes S, Linck N, Varrault A, Deffayet PM, Bockaert J, Dalle S, Bertrand G (2009) Beta-Arrestin 1 is required for PAC1 receptor-mediated potentiation of long-lasting ERK1/2 activation by glucose in pancreatic beta-cells. J Biol Chem 284 (7):4332–4342
16. Ravier MA, Rutter GA (2010) Isolation and culture of mouse pancreatic islets for ex vivo imaging studies with trappable or recombinant fluorescent probes. Methods Mol Biol 633:171–184
17. Rivera JF, Costes S, Gurlo T, Glabe CG, Butler PC (2014) Autophagy defends pancreatic beta cells from human islet amyloid polypeptide-induced toxicity. J Clin Invest 124 (8):3489–3500
18. Michele Leduc JR, Costes S, Muller D, Varrault A, Compan V, Mathieu J, Tanti J-F, Pagès G, Pouyssegur J, Bertrand G, Dalle S, Ravier MA (2017) ERK1 is dispensable for mouse pancreatic beta cell function but is necessary for glucose-induced full activation of MSK1 and CREB. Diabetologia 60 (10):1999–2010



Chapter 23

Methods to Investigate β-Arrestin Function in Metabolic Regulation

Bing Luan, Jian Zhao, and Gang Pei

Abstract

Type II diabetes is one of the most serious worldwide public health problems, and its hallmark is insulin resistance, obesity associated with chronic inflammation, and defective islet β-cell function. β-Arrestins play important roles in diabetes pathogenesis through scaffolding insulin-induced AKT activation in the liver, suppressing peroxisome proliferator-activated receptor-γ-mediated adipogenesis and inflammatory responses in adipose tissue and through promoting GLP-1-induced insulin secretion in the islet. The current chapter provides detailed protocols for both in vitro and in vivo studies of the function of β-arrestins associated with type II diabetes.

Key words β-Arrestins, Insulin resistance, Obesity, Inflammation, Insulin secretion

1 Introduction

Insulin resistance, a hallmark of type II diabetes, is a defect of insulin in stimulating insulin receptor signaling [1]. Upon stimulation by insulin, the insulin receptor recruits and phosphorylates insulin receptor substrate proteins, leading to activation of the phosphatidylinositol-3-OH kinase (PI(3)K)-Akt pathway. Activated Akt phosphorylates downstream kinases and transcription factors, thus mediating most of the metabolic actions of insulin such as suppression of glucose output in liver and stimulation of glucose uptake in adipose tissue [2, 3]. β-Arrestins competitively inhibit insulin-induced ubiquitination and degradation of IRS-1, which improves insulin-stimulated Akt activation [4]. In addition, β-arrestins can also scaffold Src and Akt to form a signal complex that is a prerequisite of full Akt activation via Src phosphorylation [5] (Fig. 1). Here, we describe the principal methods to investigate the function of β-arrestins in insulin-stimulated AKT activation as well as metabolic actions of insulin in liver and adipose tissue. Primary hepatocytes and primary adipocytes provide invaluable tools to investigate β-arrestin function in vitro. While detection of

Mark G. H. Scott and Stéphane A. Laporte (eds.), *Beta-Arrestins: Methods and Protocols*, Methods in Molecular Biology, vol. 1957, https://doi.org/10.1007/978-1-4939-9158-7_23, © Springer Science+Business Media, LLC, part of Springer Nature 2019

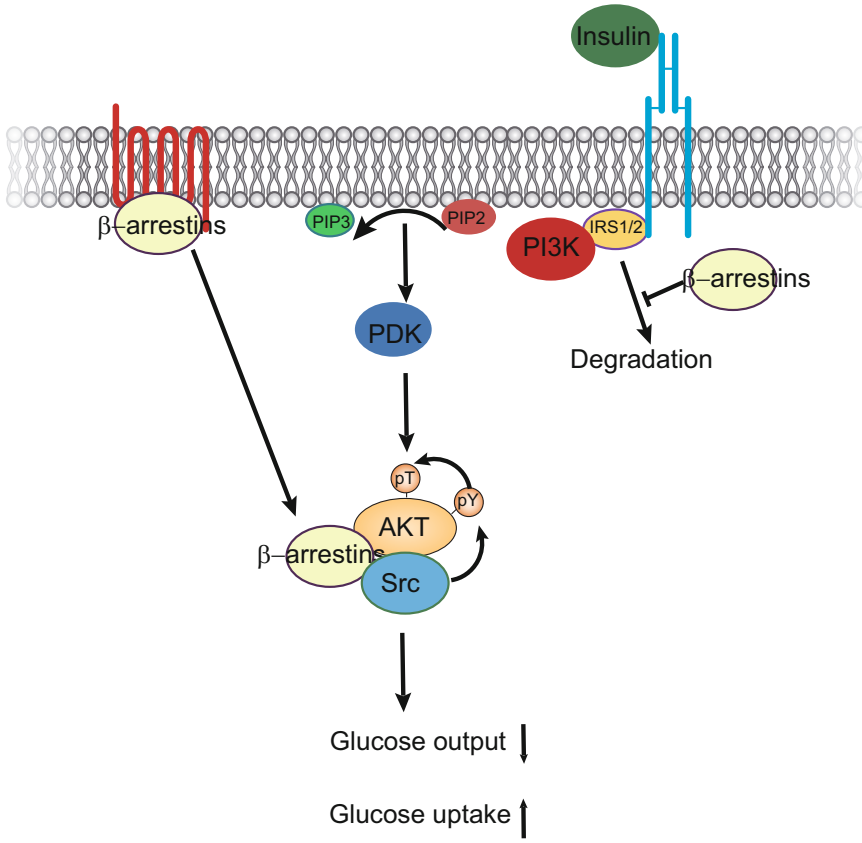


Fig. 1 β-Arrestins promote insulin signaling. β-Arrestins inhibit insulin-induced ubiquitination and degradation of IRS-1 and scaffold a Src-Akt complex to promote insulin signaling

glucose production within primary hepatocytes as well as glucose uptake in primary adipocytes directly demonstrates the functional output of β-arrestins, insulin signal pathway detection by immunoblot, immunoprecipitation, and real-time PCR reveals the molecular mechanisms underlying β-arrestin-mediated influence on insulin signaling in different tissues. Most importantly, glucose tolerance test, insulin tolerance test, pyruvate tolerance test, as well as metabolic cage studies using β-arrestins knockout mice and β-arrestins overexpression mice further unmask the important in vivo role of β-arrestins under physiological and pathological conditions.

Obesity is regarded as the major risk factor for insulin resistance, type II diabetes, and various cardiovascular diseases. An abnormal accumulation of adipocytes, the infiltration of macrophages into adipose tissue, and enhanced systemic inflammation are the major pathological features of obesity [6]. β-Arrestin1 represses diet-induced obesity through repression of adipogenesis and inflammatory responses via its interaction with peroxisome proliferator-activated receptor-γ [7, 8] (Fig. 2). We also provide

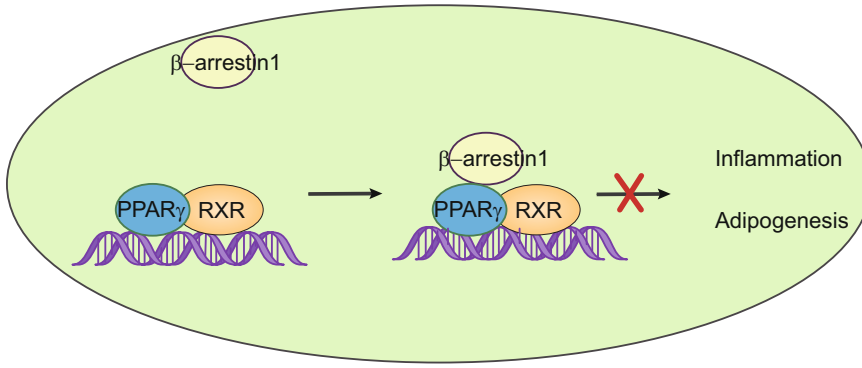


Fig. 2 β-Arrestin1 inhibits adipogenesis and inflammation via PPARγ. β-Arrestin1 represses adipogenesis and adipose inflammatory responses via its interaction with PPARγ

protocols of adipocyte differentiation and macrophage isolation as well as Oil Red O staining and F4/80 macrophage staining to investigate β-arrestin function in adipogenesis and macrophage-induced inflammation both in vitro and in vivo.

β-Cell failure, characterized by decreases in insulin secretion and β-cell mass, is a key feature of type II diabetes. β-Cell function and mass are controlled by glucose and hormones/neurotransmitters that activate G protein-coupled receptors such as the glucagon-like peptide-1 (GLP-1) receptor or receptor tyrosine kinases such as insulin receptor. β-Arrestins promote glucose-induced insulin secretion through GLP-1 [9]. Meanwhile, β-arrestins are also required for β-cell mass plasticity through insulin signaling [10] (Fig. 3). Protocols for islet isolation with methods to measure glucose-induced insulin secretion and β-cell mass by immunofluorescence are also discussed in detail in this chapter.

Taken together, β-arrestins have emerged as important signaling adaptors in type II diabetes, and further investigation of β-arrestins function in metabolic regulation will perhaps reveal new potential therapeutic possibilities and consequences for drug screening.

2 Materials

2.1 *Mice*

β-Arrestin1-knockout and β-arrestin2-knockout mice were kindly provided by R. J. Lefkowitz (Duke University Medical Center). β-Arrestin1-transgenic and β-arrestin2-transgenic mice were generated as described [11]. C57BL/6J mice and *db/db* mice were purchased from Shanghai Laboratory Animal Center (Shanghai, China) and were adapted to colony cages with 12 h light/dark cycle in a temperature-controlled environment with free access to water and standard irradiated rodent diet (5% fat; Research Diet, D12450, New Brunswick, NJ, USA). For high-fat diet (HFD) studies, 6-week-old mice were maintained on HFD (60% fat; Research Diets, D12492) for 12 weeks.

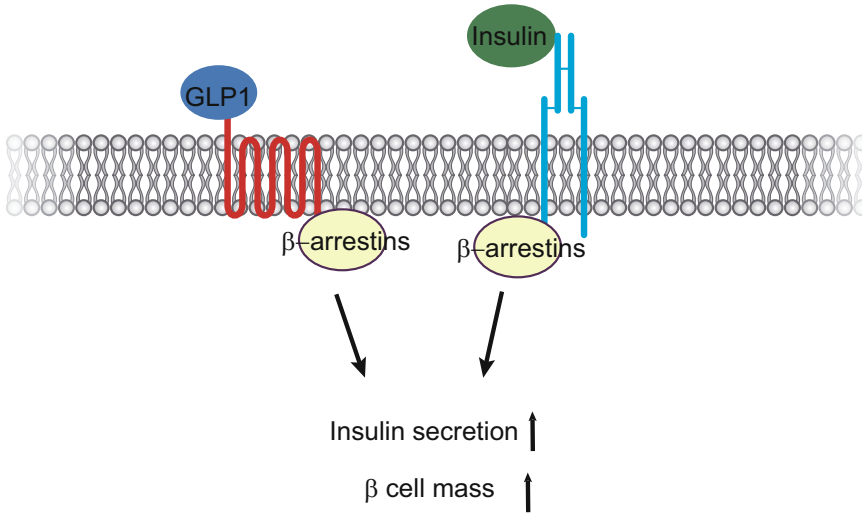


Fig. 3 β-Arrestins promote insulin secretion and β cell mass. β-Arrestins promote GLP-1-induced insulin secretion and insulin-stimulate β-cell mass plasticity

2.2 Primary Hepatocytes Preparation

1. HBSS: 0.25 nM EGTA in HBSS (Thermo Fisher Scientific #14175095, Waltham, MA, USA), 50 mL per mouse.
2. Collagenase: 5 mM $CaCl_2$, 12 mg collagenase (type IV) (Sigma #C5138, St. Louis, MO, USA) in HBSS, 50 mL per mouse.
3. DBF M199: 0.2% BSA, 2% FBS in M199 medium (Thermo Fisher Scientific #11150-067, Waltham, MA, USA).

2.3 Primary Adipocytes Preparation

1. HEPES buffer (pH 7.4): 1.5 mM D-glucose, 2.2% BSA, 135 mM NaCl, 2.2 mM $CaCl_2$, 1.25 mM $MgSO_4$, 0.45 mM KH_2PO_4, 2.17 mM Na_2HPO_4, 10 mM HEPES.
2. Collagenase (Type I) (Sigma #C0130, St. Louis, MO, USA): Dissolve 1.25 mg collagenase type I powder in 1 mL of HEPES buffer.

2.4 Islet Isolation

1. Isolation buffer: HBSS containing 10 mM HEPES, 1 mM $MgCl_2$, 5 mM glucose, pH 7.4.
2. Washing buffer: Isolation buffer containing 1 mM $CaCl_2$.
3. Collagenase (Type P) (Sigma #11213857001, St. Louis, MO, USA): 0.8 mg/mL collagenase (type P) in isolation buffer.

2.5 Glucose Production in Hepatocytes and Glucose Uptake in Adipocytes

1. Reaction buffer: Dissolve 80 mg $MgCl_2$, 40 mg NADP, 24 mg ATP, in 24 mL 0.1 M Tris, pH 8.5.
2. KRH buffer: 25 mM HEPES-NaOH, pH 7.4, 120 mM NaCl, 5 mM KCl, 1.2 mM $MgSO_4$, 1.3 mM $CaCl_2$, 1.3 mM KH_2PO_4.

2.6 Immunoprecipitation and Immunoblot

1. Cell lysis buffer (RIPA buffer): 50 mM Tris–HCl, pH 7.5, 150 mM NaCl, 0.5% BSA, 1% NP-40.
2. 5× running buffer: 15.1 g Tris, 94 g glycine, 5 g SDS; add water to 1 L.
3. 10× Tris/glycine buffer: 58 g Tris, 29 g glycine; add water to 1 L.
4. Transfer buffer: 100 mL 10× Tris/glycine buffer, 200 mL methanol; add water to 1 L.
5. 10× TBST: 12.1 g Tris, 40 g NaCl, 1% Tween-20, adjust pH to 7.6; add water to 0.5 L.
6. Sample buffer: 50 mM Tris–HCl pH 7.4, 2% SDS, 5% β-mercaptoethanol, 10% glycerol, 0.01% bromophenol blue.

2.7 Glucose-Induced Insulin Secretion

1. Krebs-Ringer bicarbonate HEPES buffer (KRBH): 129 mM NaCl, 5 mM $NaHCO_3$, 4.8 mM KCl, 1.2 mM $KH2PO_4$, 1.2 mM $MgSO_4$, 2.5 mM $CaCl_2$, 2.8 mM glucose, 10 mM HEPES, and 0.1% BSA at pH 7.4.

3 Methods

3.1 Assessing the In Vitro Function of β-Arrestins on Insulin Sensitivity

Primary hepatocyte, adipocyte, macrophage, and islet provide valuable tools to investigate the in vitro function of β-arrestins in different metabolic tissues.

3.2 Primary Hepatocyte Preparation

1. Prepare and prewarm HBSS, collagenase (type IV), and media (*see* **Note 1**).
2. Anesthetize mice with 50 mg/kg Nembutal.
3. Set up and perfuse the whole perfusion pump system (peristaltic pumps, Harvard Apparatus, Holliston, MA, USA) with warm HBSS.
4. Tape and open mice, expose portal vein, punctuate it with shield winged needle, fix the needle with clamps, turn on the peristaltic pump motor at 6 mL/min through the portal vein for a couple of minutes, and make sure that liver is turning white.
5. Pause motor and perfuse with collagenase.
6. Cut the liver and put it in HBSS (50 mL).
7. Filter the cells (Nylon mesh 350 nm pore size, Small Parts, Inc. CMN-0350).
8. Centrifuge at 50 × *g* for 3 min, wash with DBF, and then centrifuge another 3 min.

9. Resuspend the cells, check viability by trypan blue (0.4%) staining (10 μL cells (approximately 10^4 cells) + 10 μL dye).
10. Plate cells in DBF medium. 2 h later, replace media with M199 (*see* **Note 2**).

3.3 Primary Adipocyte Preparation

1. Sacrifice animals. Dissect epididymal fat depots.
2. Mince fat tissues with scissors in HEPES buffer (*see* **Note 3**).
3. Digest adipose tissue fragments in the HEPES buffer with collagenase (Type I) at 37 °C with vigorous shaking for 60 min.
4. Dilute the resulting cell suspension in 20 mL HEPES buffer.
5. Filter diluted cell suspension with 400 μm nylon mesh to remove undigested tissues.
6. Wash filtrate three times with 10 mL HEPES buffer and centrifuge at 2500 × *g* for 10 min. The supernatant contains adipocytes and the pellet contains stromal vascular (SVF) cells.
7. Suspend isolated adipocytes or SVF in 10 mL 1% FBS-DMEM, and incubate at 37 °C for 40 min.
8. Isolated adipocytes (1.5 mL of 2:1 ratio of packed cells to medium) are then plated on 500 μL collagen-coated 6-well plates (*see* **Note 4**).

3.4 Bone Marrow-Derived Macrophage Isolation

1. Plate L929 cells in 10 cm plate for 7 day and collect the supernatant.
2. Filter through a 0.45 μm filter and store aliquots frozen at −20 °C (L929-conditioned medium).
3. Sacrifice animals. Expose the hind legs and remove all muscle tissue from the bones.
4. Separate the femur and tibia by cutting at the knee joint. Flush the bones with 10 mL 10% FBS-DMEM using a 5 mL syringe and a 25 gauge needle.
5. Pipette the bone marrow cells up and down to bring the cells into single-cell suspension.
6. Pass the cells through a cell strainer, and wash the strainer with another 5 mL 10% FBS-DMEM.
7. Count the bone marrow cells, and plate the cells in L929-conditioned medium for 2 h (*see* **Note 5**).
8. Wash cells twice with 5 mL PBS and add fresh L929-conditioned medium.
9. Differentiate cells for 7 days.

3.5 Islet Isolation

1. Sacrifice animals. Remove the bowel to the left side of the open mouse, and expose the pancreas and common bile duct.

2. Place a clamp on either side of the small intestine, where the bile duct drains, leaving a small pocket for collagenase solution to enter the intestine.
3. Inflate the pancreas through the bile duct with a 30 g needle and 5 mL syringe containing 3 mL of cold collagenase (type P) solution, starting at the gall bladder.
4. Quickly remove the pancreas from the body, and place it in a siliconized vial containing 2 mL of collagenase solution.
5. Seal each vial and place it into a 37 °C water bath for 10–20 min. Shake the vial vigorously.
6. Filter diluted cell suspension through a large sterile sink strainer into a sterile 1000 mL beaker, and forcefully pipette off the screen with washing buffer on ice.
7. Wash filtrate three times with HEPES buffer, and centrifuge at 2500 × *g* for 10 min.
8. Centrifuge at 400 × *g* for 1 min, wash with washing buffer, and then centrifuge another 1 min.
9. Resuspend the pellet in 7 mL of Ficoll, density 1.108, by vortexing vigorously. Layer on top of each density of Ficoll 2 mL of each of the remaining densities in this order: 1.096, 1.069, and then 1.037.
10. Centrifuge for 15 min at 600 × *g* at 4 °C with no break.
11. Pick islets from the second layer using spoid (sterile plastic eyedropper). Transfer all collections to a 50 mL conical tube containing 25 mL of ice-cold buffer.
12. Wash three times with washing buffer.
13. Resuspend islets in 20 mL RPMI-1640 (containing 10% FCS and 10 U/mL penicillin and 100 μg/mL streptomycin, HEPES, MEM-NEAA), and mix gently.

3.6 Glucose Production in Hepatocyte

1. Treat hepatocytes with insulin for 30 min, and then add forskolin or glucagon for 6 h.
2. Change media to 4 mL RPMI without glucose + 1 mM lactate + 10 mM sodium pyruvate. Incubate for 1 h (*see* **Note 6**).
3. Collect 2 mL media in 10 mL tubes; add 50 μL 40% perchloric acid to precipitate protein and freeze at −20 °C, if needed.
4. Add 100 μL media control or sample to 900 μL reaction buffer. Mix well and transfer to cuvette.
5. Add 5 μL glucose-6-phosphate dehydrogenase (Roche #10190454103, 1000 U/mL). Mix and incubate at room temperature (RT) for 10 min, and read background absorbance at 340 nm (DO1).

6. Add 5 μL hexokinase (Roche #11119796103, 1500 U/mL). Mix and incubate at RT for 15 min. Read absorbance at 340 nm (DO2).
7. Calculation:
$$\frac{((DO2-DO1)\text{sample}-(DO2-DO1)\text{control})\times\text{dilution}\times\text{total volume}}{6.22\times10^6\ \text{ml/mole}\times\text{number of cells per incubation}}.$$
8. Normalize the readings to the total protein content.

3.7 Glucose Uptake in Adipocyte

1. Incubate adipocytes with serum free DMEM for 3 h.
2. Incubate in 1 mL of Krebs-Ringer HEPES buffer with 200 nM insulin for 20 min with or without treatments.
3. Add 1 μCi of 2-deoxy-D-[2,6-3*H*]-glucose and 0.1 mM 2-deoxy-D-glucose to each well for 10 min.
4. Wash cells three times with KRH buffer.
5. Lyse cells in 1 mL of RIPA buffer.
6. Detect ^{3}H-glucose content in 8 mL of scintillation cocktail using a liquid scintillation counter.

3.8 Insulin Signaling Detection by Immunoprecipitation and Immunoblot

3.8.1 Immunoprecipitation

1. For adherent cells, pour off media and rinse plates twice with ice-cold PBS.
2. Scrape adherent cells from dishes. Centrifuge scraped adherent or suspension cells (300 × *g*), and wash pellet once with PBS plus protease inhibitors cocktail (Sigma #S8820, St. Louis, MO, USA).
3. Resuspend cell pellet in lysis buffer plus the protease inhibitors (*see* **Note 7**). Incubate on ice for 10 min. Centrifuge at 12,000 × *g* for 10 min at 4 ° C.
4. Carefully remove the supernatant and transfer to a new tube (*see* **Note 8**).
5. Preclear chromatin by adding normal rabbit (or mouse) IgGs with protein A (or G) beads. Use 10–20 μL of protein A beads for every 1×10^6 cells of starting material (*see* **Note 9**).
6. Incubate on a rotating platform at 4 °C for 60 min. Centrifuge at 1500 × *g* for 5 min.
7. Transfer supernatant to a clean tube, and set aside a volume equal to 10% of your samples for later use as a total input control. Sample volumes should be between 200 and 500 μL. Add ~1 μg of antibody to each sample (*see* **Note 10**).
8. Incubate on a rotating platform at 4 °C for at least 4 h. Overnight is better.
9. Add 40–50 μL of protein A beads to each sample (slurry mixture of 50% beads in suspension). Incubate on the rotating platform at 4 °C for 1–2 h.
10. Centrifuge samples at 4 °C, 1500 × *g* for 1–2 min.

11. Remove supernatant and wash pellets five times with 1 mL of cold lysis buffer. For each wash, incubate samples on a rotating platform for 10 min at 4 °C, and then centrifuge at 1500 × *g* for 1 min at 4 °C (*see* **Note 11**).
12. After the last wash, centrifuge and remove the last traces of buffer.
13. Add protein loading buffer to the protein beads, and boil at 100 °C for 5 min before loading on SDS-PAGE gel.

3.8.2 Immunoblot

1. Clean glass plates and lock the sandwich to the casting stand.
2. Prepare the separating/resolving gel solution, and mix by inverting the tube. Check the table for the exact loading amount (*see* **Note 12**).
3. Slowly add the separating gel solution (10% as an example: 3.3 mL 30% acrylamide/bis-acrylamide, 2.5 mL 1.5 M TRIS pH 8.8, 0.1 mL ammonium persulfate, 0.004 mL TEMED, 4 mL water to 10 mL final volume) to the sandwich along an edge of one of the spacers.
4. Cover the top of the gel with a layer of 100% ethanol.
5. Allow the gel to polymerize (*see* **Note 13**).
6. Pour off the ethanol layer, rinse with water, and take off excess water.
7. Prepare the stacking gel solution and mix it by inverting the tube.
8. Apply the stacking gel solution along an edge of one of the spacers.
9. Insert a 10- or 15-well comb into the layer of stacking gel solution.
10. Allow the stacking gel solution to polymerize.
11. Make up 1 L of 1× Tris-glycine-SDS running buffer (5× lab stock).
12. Prepare the sample and load the gel.
13. Assemble the gel cassette (*see* **Note 14**), push the gel plates all the way down, and then lock them.
14. Fill up the inner chamber (*see* **Note 15**) and add to half full in the outer chamber.
15. Carefully take off the comb, lift straight up.
16. Rinse out the wells.
17. Load the gel (20 μL).
18. Put on the lid and run the gel (1–2 h) at 80 V for ~0.5 h until the bromophenol blue migration line reaches the separating gel and switch to 120 V for appropriate time (*see* **Note 16**).

19. While running, prepare polyvinylidene fluoride (PVDF) membrane with blue wrap paper. Wet the membranes in methanol for 20 s.
20. Transfer the membrane to transfer buffer for 10 min.
21. Cut four sheets of Whatman 3 MM filter paper exactly the same dimensions as the separating gel (two sheets per gel).
22. Place filter paper soaked in transfer buffer for 10 min.
23. Assemble transfer sandwich. Remove all the bubbles between membrane and filter paper by gently rolling a pipette over the surface of membrane, gel, and filter paper. Keep gel and membrane wet.
24. Carefully place the upper filter paper and white lid side so that the gel and membrane do not move.
25. Place the cassette in the transfer apparatus (black side facing the black side).
26. Add a frozen-ice bowl in the apparatus, then fill the chamber with transfer buffer, and transfer at 400 mA for 120 min.
27. While transferring, prepare TBST and 5% milk/TBST (2.5 g milk in 50 mL TBST in 50 mL tube).
28. Disassemble, immediately place membrane into 10 mL 5% milk/TBST.
29. Block for 20 min with gentle shaking.
30. Add primary antibody in 5% BSA/TBST (*see* **Note 17**).
31. Incubate 1–2 h at RT or overnight at 4 °C.
32. Washing: 1 × 15 min in TBST rocking (one wash is enough).
33. Dilute the horseradish peroxidase (HRP)-labeled second antibody with 5% milk/TBST.
34. Incubation: Incubate the membrane for 45 min to 1 h at RT rocking.
35. Wash as in **step 37**, three times.
36. Mix an equal volume of detection solution 1 (4 °C) with detection solution 2 (black and white caps; Pierce™ ECL Western Blotting Substrate # 32106) to sufficiently cover the membranes.
37. Place membrane protein side up. Add the detection reagent to the protein side of the membrane.
38. Incubate for 1 min at room temperature.
39. Transfer membrane onto a sheet protector protein side up, cover it. Gently smooth out air pockets.
40. Place the blots, protein side up, in the film cassette, and tape up to secure.

41. Turn off the lights in the dark room and under red light carefully place an autoradiography film on top of the membranes, close the cassette, and expose for different time, starting with 10 s.
42. Develop the film (*see* **Note 18**).
43. Store the membrane in TBST at 4 °C until the further use.

3.9 Target Gene Expression by Real-Time PCR

3.9.1 RNA Extraction (Adapted from TRIzol® Reagent Manual from Life Technologies)

Tissues

1. To homogenize samples (*see* **Note 19**), add 1 mL TRIzol Reagent per 50–100 mg of tissue sample (*see* **Note 20**).
2. Homogenize sample using a homogenizer (SCILOGEX D160 Homogenizer as an example).

Adherent Cells

Cell Lysis

1. Remove growth media from culture dish.
2. Add 1 mL TRIzol Reagent directly to the cells in the culture dish per 10 cm^2 of culture dish surface area (*see* **Note 21**).
3. Lyse the cells directly in the culture dish by pipetting the cells up and down several times.

Suspension Cells

1. Harvest cells by centrifugation (300 × *g*) and remove media.
2. Add 0.75 mL of TRIzol Reagent per 0.25 mL of sample (5–10 × 10^6 cells).
3. Lyse cells in sample by pipetting up and down several times.

Phase Separation

1. Incubate the homogenized sample at RT for 5 min.
2. Add 0.2 mL of chloroform per 1 mL of TRIzol Reagent, and shake tube vigorously by hand for 15 s.
3. Incubate for 2–3 min at RT and centrifuge the sample at 12,000 × *g* for 10 min at 4 °C.
4. Remove the aqueous phase and place in to a new tube (*see* **Note 22**).

RNA Isolation

1. Add 0.5 mL 100% isopropanol and Incubate at RT for 10 min.
2. Centrifuge at 12,000 × *g* for 10 min at 4 °C.
3. Remove the supernatant and wash the pellet with 1 mL 75% ethanol twice.
4. Vortex briefly and centrifuge at 12,000 × *g* for 10 min at 4 °C.
5. Vacuum and air dry the RNA pellet (*see* **Note 23**).
6. Resuspend the RNA pellet in RNase-free water (*see* **Note 24**).

3.9.2 Reverse Transcription (Adapted from SuperScript First-Strand Synthesis System Manual from Life Technology)

1. Prepare the following RNA/primer mixture in each tube: 0.5 mg Total RNA; Random primer 3 μL (50 ng/mL), 1 μL 10 mM dNTP mix; complete to 10 μL with RNase-free H_2O.
2. Incubate the samples at 65 °C for 5 min and then place on ice for at least 1 min.
3. Prepare the reaction master mixture. For each reaction add the following: 2 μL 10× RT buffer; 4 μL 25 mM $MgCl_2$; 2 μL 0.1 M DTT; 1 μL RNAase OUT.
4. Add the reaction mixture to the RNA/primer mixture, mix briefly, and then place at RT for 2 min.
5. Add 1 μL SuperScript II RT to each tube, mix, and incubate at 25 °C for 10 min.
6. Incubate the tubes at 42 °C for 30 min, heat inactivate at 70 °C for 15 min, and then set on ice.
7. Store the cDNA at −20 °C until use for real-time PCR.

3.9.3 Real-Time PCR

1. Normalize the primer concentrations, and mix gene-specific forward and reverse primer pair. Each primer (forward or reverse) concentration in the mixture is 0.5 μM.
2. Set up the experiment and the following PCR program on Roche LightCycler® 96 (Table 1).
3. Prepare the following mixture in each optical tube (Table 2).

   Add 5 μL template DNA for a total volume of 20 μL.
4. Analyze the real-time PCR result with the lightCycler Software. Analyze the dissociation curve for primer specificity.

3.10 Assessing the In Vivo Function of β-Arrestins on Insulin Sensitivity

Glucose tolerance test (GTT), insulin tolerance test (ITT), pyruvate tolerance test (PTT), indirect calorimetry by metabolic cages, glucose-induced insulin secretion, and section staining are wildly used to investigate the in vivo metabolic function of β-arrestins.

3.11 GTT, ITT, and PTT

3.11.1 GTT

1. Mice are placed in a clean cage and fasted overnight (14–16 h) with free access to water.
2. The tip of the tail is gently cleaned with an isopropyl alcohol wipe. With a sterile scalpel blade, a small incision is made at the tip of the tail of freely moving mice. Glucose is measured from a 5–10 μL drop of blood using a glucometer (One Touch Ultra Glucometer (Johnson & Johnson, New Brunswick, NJ, USA) as an example).
3. Mice are given an intraperitoneal injection of sterile glucose (2 mg/g body weight) and are returned to their home cage. Blood glucose is periodically measured (every 15–30 min) for 2 h following the injection.
4. At the end of the procedure, the bleeding is stopped with wound stop powder.

Table 1
PCR program, recommended by Roche

Program name	Cycles	Analysis mode
Pre-incubation	1	None
Target (°C)	Acquisition mode	Hold
95	None	5 min
Amplification	45	Quantification
Target (°C)	Acquisition mode	Hold
95	None	10 s
60	None	10 s
72	Single	10 s
Program name	**Cycles**	**Analysis mode**
Melting curve	1	Melting curves
Target (°C)	Acquisition mode	Hold acquisitions
95	None	5 s
65	None	1 min
97	Continuous	5 per °C
Program name	**Cycles**	**Analysis mode**
Cooling	1	None
Target (°C)	Acquisition Mode	Hold
40	None	30 s

Table 2
PCR reaction mix, recommended by Roche

Reagent	Final concentration	Volume (μL)/reaction
Water		1
Primer-forward (5 μM stock)	0.5 μM	2
Primer-reverse (5 μM stock)	0.5 μM	2
LightCycler 480 SYBR green I master	1×	10
	Total	15

3.11.2 ITT

1. Ad libitum or 6-h-fasted mice are used for this procedure. The tip of the tail is gently cleaned with an isopropyl alcohol wipe. With a sterile scalpel blade, a small incision is made at the tip of the tail of freely moving mice.
2. Glucose is measured from a 5–10 μL drop of blood using a glucometer. Mice are given an intraperitoneal injection of insulin (0.75–2 mU/g body weight) and are returned to their home cage (*see* **Note 25**).
3. Blood glucose is periodically measured (every 15–30 min) for 2 h following the injection. At the end of the procedure, the bleeding is stopped with wound stop powder.

3.11.3 PTT

1. Mice are placed in a clean cage and fasted overnight (14–16 h) with free access to water.
2. The tip of the tail is gently cleaned with an isopropyl alcohol wipe. With a sterile scalpel blade, a small incision is made at the tip of the tail of freely moving mice. Glucose is measured from a 5–10 μL drop of blood using a glucometer.
3. Mice are given an intraperitoneal injection of sodium pyruvate dissolved in PBS (2 mg/g body weight) and are returned to their home cage. Blood glucose is periodically measured (every 15–30 min) for 2 h following the injection.
4. At the end of the procedure, the bleeding is stopped with wound stop powder.

3.12 Metabolic Cages (Indirect Calorimetry)

1. Oxygen consumption, carbon dioxide production, heat production, locomotor activity, feeding, and drinking rates are measured from individually housed mice using a LabMaster System (TSE) or Columbia system.
2. Mice are transferred from their home cage to a new clean cage bottom. A lid fitted with air inlets and outlets, a food basket, and a water bottle are attached to the cage (*see* **Note 26**).
3. Mice are housed in the metabolic cages for measurement of metabolic parameters for 3–5 days. Mice are checked daily. Food and water are replenished as required. Mice are fed the same diet that they are being studied with, except that the pellets are manufactured as a 0.5 to 1 g pellet to accommodate the size of the food basket.
4. At the end of the experiment, mice are returned to a home cage. The food baskets, water bottles, and lids are washed with water and disinfected with Clidox followed by 70% isopropyl alcohol.

3.13 H&E Staining, Oil Red O Staining, and F4/80 Staining

3.13.1 Specimen Preparation

Cultured Cell (Seeded on Slides in 35 mm Plate)

1. Aspirate medium from the 35 mm well, and then cover cells to a depth of 2–3 mm with 4% formaldehyde in PBS (w/v) for 15 min at RT.
2. Aspirate fixative, and rinse three times in PBS for 5 min each.

Paraffin Sections (*see* **Note 27**)

1. Incubate sections in three washes of xylene for 5 min each.
2. Incubate sections in two washes of 100% ethanol for 10 min each.
3. Incubate sections in two washes of 95% ethanol for 10 min each.
4. Rinse sections twice in distilled water for 5 min each.
5. Antigen Unmasking (*see* **Note 28**).

   For Citrate: Bring slides to a boil in 10 mM sodium citrate buffer pH 6.0, and then maintain at a sub-boiling temperature (approximately 90 °C) for 10 min. Cool slides on bench top for 30 min.

   For EDTA: Bring slides to a boil in 1 mM EDTA pH 8.0 followed by 15 min at a sub-boiling temperature. No cooling is necessary.

Frozen Sections

1. Fix frozen tissue with 2–4% formaldehyde in PBS (w/v) for 15 min at RT.
2. Rinse slides three times in PBS for 5 min each.

3.14 H&E Staining

1. Wash sections briefly in distilled water.
2. Stain in Hematoxylin solution for 5 min.
3. Wash in running tap water for 5 min.
4. Differentiate in 1% acid alcohol for 30 s.
5. Wash running tap water for 1 min.
6. Bluing in 0.2% ammonia water or saturated lithium carbonate solution for 30 s to 1 min.
7. Wash in running tap water for 5 min.
8. Rinse in 95% alcohol, 10 dips.
9. Counterstain in eosin solution for 30 s to 1 min.
10. Dehydrate through 95% alcohol 2 changes of absolute alcohol, 5 min each.
11. Clear in 2 changes of xylene, 5 min each.
12. Mount with xylene-based mounting medium.

3.14.1 Oil Red O Staining

1. Add 2 mL of PBS to wash the cells or sections and remove PBS completely (*see* **Note 29**).
2. Add 2 mL of 10% formalin (RT) and incubate for 10 min at RT.
3. Discard formalin and add 2 mL fresh formalin. Incubate for at least 1 h or longer (*see* **Note 30**).
4. Remove formalin with a pipette.
5. Wash cells with 2 mL of distilled water twice.
6. Wash cells with 2 mL of 60% isopropanol for 5 min at RT.
7. Let the cells dry completely at RT. If possible, use a hairdryer to dry.
8. Add 1 mL of Oil Red O working solution and incubate at RT for 10 min.
9. Remove Oil Red O solution and immediately add distilled water. Wash the cells four times with distilled water.
10. Acquire images under the microscope for analysis (*see* **Note 31**).
11. Remove all the water and let dry.
12. Elute Oil Red O dye by adding 1 mL of 100% isopropanol, and incubate for 10 min with gently shaking.
13. Pipette the isopropanol with Oil Red O up and down several times to ensure that all Oil Red O is in the solution.
14. Transfer the solution to a 1.5 mL eppendorf tube.
15. Measure OD at 500 nm using 100% isopropanol as blank.

3.14.2 F4/80 Staining (Immunohistochemistry)

1. Wash sections in distilled water three times for 5 min each at RT.
2. Incubate sections in 3% hydrogen peroxide for 10 min.
3. Wash sections in H_2O twice for 5 min each.
4. Wash sections in wash buffer for 5 min.
5. Block each section with 100–400 μL blocking solution for 1 h at RT.
6. Remove blocking solution, and add 100–400 μL F4/80 antibody (Abcam #ab6640) diluted in recommended antibody diluent to each section. Incubate overnight at 4 °C.
7. Remove antibody solution, and wash sections in wash buffer three times for 5 min each.
8. Add 100–400 μL of biotinylated secondary antibody (Vector Labs, #BA-9400), diluted in TBST as per the manufacturer's recommendation, to each section. Incubate 30 min at RT.

9. Prepare avidin-biotin complex (ABC) reagent (Vector Labs, #PK-6100) according to the manufacturer's instructions, and incubate solution for 30 min at RT.
10. Remove secondary antibody solution, and wash sections three times with wash buffer for 5 min each at RT.
11. Add 100–400 μL ABC reagent to each section and incubate for 30 min at RT.
12. Remove ABC reagent and wash sections three times in wash buffer for 5 min each.
13. Add 100–400 μL 3,3′-diaminobenzidine (DAB) substrate (Vector Labs, #SK-4100) to each section, and monitor staining closely.
14. As soon as the sections develop, immerse slides in distilled water.
15. If desired, counterstain sections in hematoxylin.
16. Wash sections in distilled water two times for 5 min each.
17. Incubate sections in 95% ethanol two times for 10 s each.
18. Repeat in 100% ethanol, incubating sections two times for 10 s each.
19. Repeat in xylene, incubating sections two times for 10 s each.
20. Mount coverslips.

3.15 Glucose-Induced Insulin Secretion

3.15.1 In Vitro

1. Batches of 20–30 cultured islets were placed in 96-well plates.
2. Flick media from plate. Blot briefly on paper towel.
3. Add 150 μL of KRBH+2 mM glucose to each well (multichannel preferred). Add to the side of the well.
4. Repeat **steps 3** and **4**.
5. Rest cells for 2 h in the tissue culture incubator.
6. Repeat **steps 3**–**5**.
7. Incubate for 1 h in the tissue culture incubator.
8. Remove 50 μL of supernatant taking care not to disturb the bottom of the well. Spin at 1500 × *g* for 5 min at 4 °C. Take 25 μL of the supernatant off and freeze at −20 °C.
9. Repeat **step 3**.
10. Add in KRBH+20 mM glucose.
11. Repeat **steps 8** and **9**.
12. To get total insulin, add 100 μL of lysis buffer.
13. Detect insulin levels using Mouse Insulin ELISA kit (Mercodia Mouse Insulin ELISA # 10-1113-01).

3.15.2 In Vivo

1. Anesthetize mice with 50 mg/kg Nembutal.
2. Right jugular vein and left carotid artery were catheterized.
3. 10 μL D-glucose dissolved in saline was rapidly injected at a dose of 0.10, 0.25, or 0.75 g/kg.
4. Continuous infusion of glucose (20 or 40 g/dL) or saline was begun at a rate of 1.0–2.0 μL/min.
5. Plasma glucose was measured at 5 min intervals for 90 min.
6. The rate of glucose infusion was adjusted according to the glucose values to maintain glucose levels at baseline, 11.1, 16.7, or 30 mmol/L.
7. Blood samples were taken in heparinized tubes at 0, 1, 5, 20, 50, 70, and 90 min and immediately centrifuged; afterward the plasma was separated and stored at −20 °C for analysis.
8. Plasma insulin was determined by ELISA.

3.16 Immunofluorescence of Islet β-Cell

1. Block pancreas section in blocking buffer for 60 min.
2. While blocking, prepare antibodies (anti-insulin antibody, Dako A0564; anti-glucagon antibody, Abcam ab82270; anti-Somatostatin antibody, Santa Cruz sc7819) by diluting it in antibody dilution buffer as indicated by the manufacturer's datasheet.
3. Aspirate blocking solution; apply diluted primary antibody and incubate overnight at 4 °C (*see* **Note 32**).
4. Rinse three times in PBS for 5 min each.
5. Incubate section in fluorescein-conjugated secondary antibody (Alexa Fluor 647 Donkey Anti-mouse, Yesen #34113ES60; Alexa Fluor 594 Donkey Anti-Guinea pig, Jackson #706-585-148; Alexa Fluor 488 Donkey Anti-Goat, Jackson #705-545-003). Diluted in antibody dilution buffer for 1–2 h at RT in dark.
6. Rinse three times in PBS for 5 min each time.
7. Mount the coverslip onto slides with mounting reagent (VECTASHIELD Antifade Mounting Medium with DAPI, Vector Labs #H-1200).
8. Acquire images under the microscope for analysis (*see* **Note 33**).

4 Notes

1. Prewarm to 38 °C.
2. Do not extend the time as debris and dead cells will also attach to the plate.

3. The tissues should be cut as small as possible to improve the efficiency of digestion.
4. SVF cells could proliferate for 2–4 passages and could be stored in nitrogen for further use.
5. 2 h is enough for myeloid cells such as monocytes to attach to the plate.
6. It is better to use RPMI without phenol red.
7. The final volume of cell lysis buffer should be sufficient so that there are no clumps of cells.
8. At this point, cell lysis can be snap frozen in liquid nitrogen and stored at −80 °C for up to several months.
9. If you're using rabbit antibodies, use Protein A beads; if using mouse monoclonal antibodies, use Protein G beads.
10. The amount of antibody you need to use will be determined empirically.
11. Efficient washing is critical to reduce background. If background becomes an issue, transfer the beads to a different tube in between washes. Try to remove as much buffer as possible after each wash without aspirating the protein A beads.
12. Use 10–12.5% gels for 30–60 kDa proteins. If the molecular weight of proteins interested is 70–200 kDa, use 5–10% gel, whereas 12–40 kDa proteins use 14–15% gels.
13. Verify the leftover in the tube first, before continuing.
14. Be sure that gel combs are facing the module or face inside; if only one gel is used, be sure to use the dam on the other side.
15. Make sure it does not leak; if it does, dissemble and push the gel plates all the way down and then close it.
16. Varies with the protein of interest.
17. The amount of antibody (both first and second) will need to be determined empirically. Follow the antibody datasheet recommendations for reference.
18. Expose different time to obtain the desire density of signals.
19. Do not wash cells before addition the TRIzol Reagent to avoid increased chance of mRNA degradation.
20. Process or freeze tissue samples immediately upon collection.
21. Add 0.5 mL TRIzol Reagent for a 35 mm dish, 1 mL for a 60 mm dish, or 2 mL for a 100 mm dish.
22. Avoid drawing any of the interphase or organic layer, which contains DNA and proteins, into the pipette when removing the aqueous phase.
23. The pellet may be invisible; however, still proceed to washing it.

24. Do not allow the RNA to dry completely, because the pellet will lose it solubility.
25. Determine the amount of insulin according to the body weight. Overdose of insulin will cause hypoglycemia and death of the mice. Inject glucose (2 mg/g body weight) immediately if sign of hypoglycemia occurs.
26. Allow mice to accommodate to the new environment for 24–48 h before collecting data.
27. Do not allow slides to dry at any time during this process.
28. Follow product datasheet recommendations for the unmasking solution.
29. Use frozen section for Oil Red O staining.
30. Samples can be kept in formalin for a couple of days before staining. Wrap with parafilm and cover with aluminum foil to prevent cells from drying.
31. For best results, examine specimens immediately.
32. Using primary antibodies directly conjugated with Alexa Fluor fluorochromes will greatly shorten the procedure without influence on the signal dramatically.
33. For best results, examine specimens immediately using appropriate excitation wavelength of your fluorochrome-conjugate antibody. For long-term storage, store slides flat at 4 °C, protected from light.

References

1. Taniguchi CM, Emanuelli B, Kahn CR (2006) Critical nodes in signalling pathways: insights into insulin action. Nat Rev Mol Cell Biol 7 (2):85–96
2. Biddinger SB, Kahn CR (2006) From mice to men: insights into the insulin resistance syndromes. Annu Rev Physiol 68:123–158
3. Burgering BM, Coffer PJ (1995) Protein kinase B (c-Akt) in phosphatidylinositol-3-OH kinase signal transduction. Nature 376 (6541):599–602
4. Usui I, Imamura T, Huang J, Satoh H, Shenoy SK, Lefkowitz RJ et al (2004) Beta-arrestin-1 competitively inhibits insulin-induced ubiquitination and degradation of insulin receptor substrate 1. Mol Cell Biol 24(20):8929–8937
5. Luan B, Zhao J, Wu H, Duan B, Shu G, Wang X et al (2009) Deficiency of a beta-arrestin-2 signal complex contributes to insulin resistance. Nature 457(7233):1146–1149
6. Hotamisligil GS (2006) Inflammation and metabolic disorders. Nature 444(7121):860–867
7. Zhuang LN, Hu WX, Zhang ML, Xin SM, Jia WP, Zhao J et al (2011) Beta-arrestin-1 protein represses diet-induced obesity. J Biol Chem 286(32):28396–28402
8. Zhuang LN, Hu WX, Xin SM, Zhao J, Pei G (2011) Beta-arrestin-1 protein represses adipogenesis and inflammatory responses through its interaction with peroxisome proliferator-activated receptor-gamma (PPARgamma). J Biol Chem 286(32):28403–28413
9. Sonoda N, Imamura T, Yoshizaki T, Babendure JL, Lu JC, Olefsky JM (2008) Beta-Arrestin-1 mediates glucagon-like peptide-1 signaling to insulin secsretion in cultured pancreatic beta cells. Proc Natl Acad Sci U S A 105 (18):6614–6619
10. Ravier MA, Leduc M, Richard J, Linck N, Varrault A, Pirot N et al (2014) Beta-Arrestin2 plays a key role in the modulation of the pancreatic beta cell mass in mice. Diabetologia 57 (3):532–541
11. Shi Y, Feng Y, Kang J, Liu C, Li Z, Li D et al (2007) Critical regulation of CD4+ T cell survival and autoimmunity by beta-arrestin 1. Nat Immunol 8(8):817–824



Chapter 24

Methods to Investigate the Role of β-Arrestin Signaling in Parkinson's Disease

Nikhil M. Urs

Abstract

β-Arrestin function has largely been investigated in cell culture-based systems. Here we describe methods to investigate β-arrestin2 signaling in vivo by developing novel mouse models and viral methods to overexpress β-arrestin2 in the mouse brain. The methods and concepts described here are in the context of Parkinson's disease (PD) and developing automated in vivo drug screening platforms.

Key words Arrestins, Parkinson's disease, Dyskinesias, Screening tool

1 Introduction

Parkinson's disease (PD) is a progressive neurodegenerative disorder characterized by dopamine (DA) neuron degeneration and severe motor deficits. The primary treatment for PD symptoms is the DA precursor, L-DOPA. However, after a few years of L-DOPA treatment, most PD patients develop side effects known as L-DOPA-induced dyskinesias (LIDs). LIDs are hypothesized to manifest as a result of supersensitivity of DA receptors [1, 2]. We have previously shown that deletion of β-arrestin2 exacerbates, whereas overexpression ameliorates LIDs or abnormal involuntary movements (AIMs) in various animal models [3]. In particular, we have developed a novel model of AIMs using the DA transporter (DAT) knockout mice called DA-deficient DAT KO or DDD model [4]. The DDD model is generated by using DAT-KO mice, which have deficits in vesicular DA storage and rely solely on de novo synthesis of DA by tyrosine hydroxylase (TH) to maintain their ambient but low levels of tissue DA. Systemic treatment of DAT-KO mice with α-methyl-*p*-tyrosine (AMPT), an irreversible pharmacological inhibitor of TH, results in acute and complete depletion of their pre-synaptic DA stores accompanied by akinesia, tremor, and rigidity that can be acutely and completely reversed by

Mark G. H. Scott and Stéphane A. Laporte (eds.), *Beta-Arrestins: Methods and Protocols*, Methods in Molecular Biology, vol. 1957, https://doi.org/10.1007/978-1-4939-9158-7_24, © Springer Science+Business Media, LLC, part of Springer Nature 2019

L-DOPA. AIMs have largely been characterized in toxin-based rodent models of PD involving unilateral lesioning of DA neurons using 6-hydroxydopamine (6-OHDA), and these AIMs are measured manually by a blinded observer [5, 6]. Although blinded, such measures are prone to observer bias and can lead to inconsistent reporting of observations. The DDD model, which is a bilateral model of DA depletion and uses automated measures of locomotor activity and AIMs, thus represents a facile and unbiased model for quantifying behavior. The DDD model can be used as a screening tool for β-arrestin biased or unbiased compounds with anti-dyskinesia and/or antiparkinsonian activity. Using the DDD model, we have established an automated screening tool and screened several compounds that have been used in the clinic as anti-dyskinetic drugs. Here, we describe methods to setup the DDD model and perform an anti-dyskinesia drug screen. In addition, we describe brief methods to virally overexpress β-arrestin2 in the striatum of mouse brains and test its effect on L-DOPA-induced behaviors.

2 Materials

2.1 Animals

2- to 4-month-old, age- and sex-matched dopamine transporter knockout (DAT–KO) mice (Source: Laboratory of Dr. Marc Caron, Duke University or Jackson laboratories Stock No: 022301).

2.2 Activity Monitors

Any automated beam break based activity monitor. We use the VersaMax analyzer and activity monitors (Version 1.4B) from Accuscan instruments Inc. (now Omnitech Inc.). The activity monitors connect to a standard computer with the Accuscan VersaMax plug and play software (Version 3.0.0.1). The activity monitor detects both horizontal and vertical beam breaks. Omnitech also has an upgraded software for these monitors called Fusion and may be purchased separately from the vendor.

2.3 Drugs and Solutions

Prepare all drugs fresh on the day of the experiment.

1. Pharmacological grade saline (Patterson Veterinary).
2. α-Methyl-DL-tyrosine methyl ester HCl (AMPT) (Sigma) 125 mg/kg intraperitoneal (*i.p.*) (*see* **Note 1**). Make a 25 mg/ML solution in saline, and inject 5 μl/gm of mouse weight, i.e., *150 μl*, for a 30 gm mouse.
3. L-DOPA methyl ester HCl (Sigma) 20 mg/kg (*i.p.*) or subcutaneous (*s.c.*). Make a 4 mg/ML solution in saline and inject 5 μl/gm of mouse weight.

4. Benserazide (Sigma) 10 mg/kg *i.p.* Make a 2 mg/ML solution in the L-DOPA solution above. Benserazide is a peripheral amino acid decarboxylase inhibitor and is used to prevent conversion of L-DOPA to DA in peripheral tissues and maximize CNS levels of L-DOPA.

Drugs used for anti-dyskinesia screen.

5. Rapamycin (LC laboratories) 4 mg/kg *i.p.*
6. Yohimbine (Sigma) 10 mg/kg, *i.p.*
7. Amantadine (Sigma) 30 mg/kg *s.c.*
8. Eltoprazine (Tocris) 10 mg/kg *i.p.*
9. Buspirone (Sigma) 5 mg/kg *i.p.*

Drugs for stereotaxic surgeries.

10. Meloxicam (Patterson Veterinary) 5 mg/kg *s.c.*

2.4 Stereotaxic Frame and Viral Vectors

We recommend the stereotaxic frames from Kopf with an anesthesia nose adaptor, for surgical viral injections. Adeno-associated virus (AAV) vectors containing the βarr2 gene can be generated in-house or from viral vector core facilities. The βarr2 gene can be tagged with GFP or have a bicistronic cassette with GFP. We use an EF1-α-βarr2-myc-p2A-mCerulean construct [3].

3 Methods

3.1 The DDD Model of PD Symptoms and Dyskinesias

1. To generate the DDD model, inject DAT-KO mice with 125 mg/kg AMPT *i.p.* The DAT-KO mice are hyperactive to begin with but injecting AMPT will deplete these mice of DA (DDD) [4]. DA depletion is almost 100% after 1 h. At this stage, the mice represent a model of PD symptoms showing akinesia and tremor, and this effect lasts for approximately 12 h.
2. Place the mice in the activity monitor chambers upon injection of AMPT, and record the baseline activity. Both horizontal and vertical activity recordings are required for data analyses.
3. After 1 h of baseline recording, remove the mice from the chambers, and inject them with L-DOPA/Benserazide (20/10–50/25 mg/kg, *i.p.*) to assess recovery of motor symptoms. Place the mice back in the activity monitor chambers, and record their activity for another 2 h (Fig. 1a) (*see* **Note 2**).
4. To assess the role of βarr2 in L-DOPA-induced behaviors, cross the DAT-KO and βarr2KO mice [7] to generate DAT/βarr2 double KO mice. Deletion of βarr2 (Fig. 1b, DDD/βarr2KO) causes a significant reduction in their forward locomotor activity. However, the DDD/βarr2KO mice now switch to vertical activity (*see* **Note 3**).

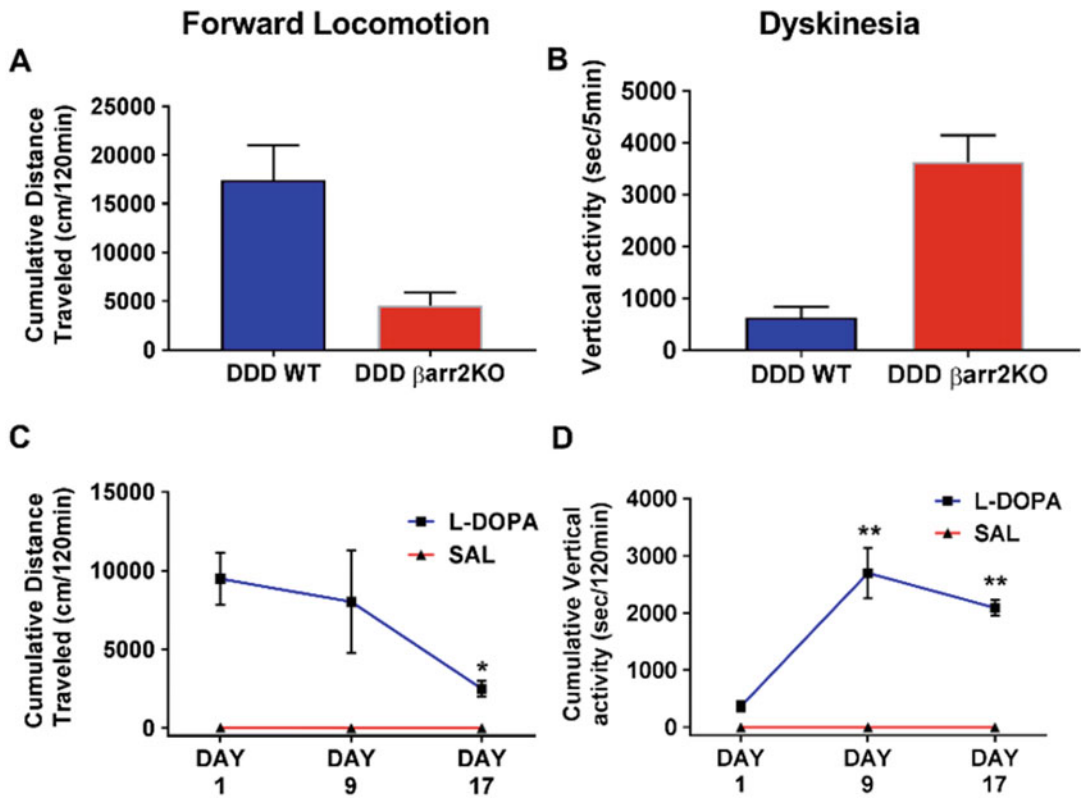


Fig. 1 Barr2 deletion or chronic L-DOPA modifies locomotion and dyskinesias in a DDD mouse model of PD. All mice were injected with AMPT (DDD) and 60 min later followed by L-DOPA/Benserazide (50/12.5 mg/kg, i.*p.*) and activity recorded for 120 min. (**a**) DDD/βarr2KO mice show a reduced L-DOPA locomotor response as assessed by total cumulative distance traveled, while (**b**) DDD/βarr2KO mice show increased cumulative vertical activity (3-paw dyskinesia) upon L-DOPA treatment ($n = 8$). Chronic L-DOPA exposure (**c**) reduces forward locomotion, while it (**d**) increases vertical activity/3-paw dyskinesia in DDD mice ($n = 8$). *$p < 0.05$, **$p < 0.01$ compared to day 1

5. To induce clinically relevant dyskinetic behaviors or AIMs in the DDD mice, inject with AMPT followed by L-DOPA/Benserazide once a day for 1–2 weeks chronically (Fig. 1c and d). Drug administration and activity recording for the chronic regime is the same as the acute regime but done over multiple days (*see* **Note 4**).
6. To setup an anti-dyskinesia drug screen, first inject AMPT and record baseline activity. After 1 h, inject test compounds acutely or chronically along with L-DOPA/Benserazide, and record horizontal and vertical activity for 2 h (*see* **Note 5**). As a control, inject known anti-dyskinetic compounds (e.g., eltoprazine, buspirone, and amantadine [5, 8]) to test their effect on locomotor activity and dyskinesias (Fig. 2) (*see* **Note 6**).
7. Thus, the DDD model can be used as a robust, unbiased, and blinded automated screening platform for anti-dyskinesia

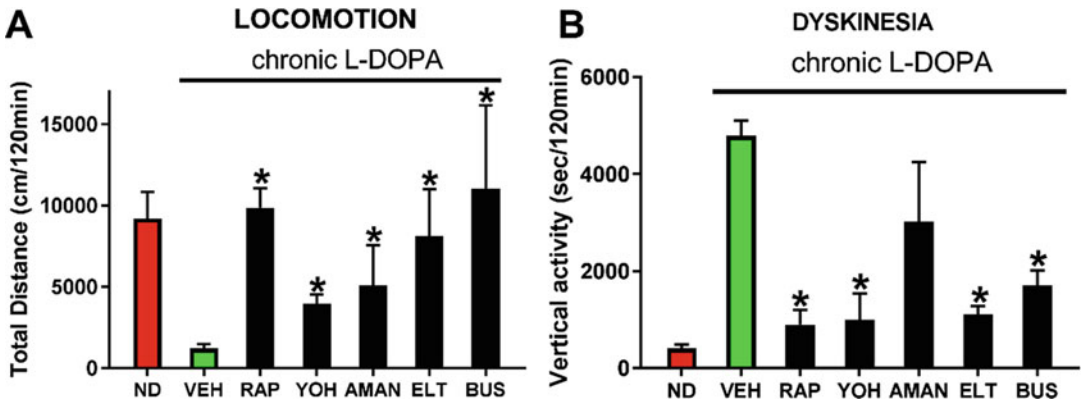


Fig. 2 DDD mice as a behavioral screening tool. DAT-KO mice were treated with AMPT followed by L-DOPA/Benserazide treatment (25/12.5 mg/kg, *i.p.*) either acutely (non-dyskinetic *[ND], red bars*) or chronically daily for 12 days and their activities recorded. On day 12, mice were preinjected with vehicle (VEH), rapamycin (RAP, 4 mg/kg *i.p.*), yohimbine (YOH, 10 mg/kg i.p), amantadine (AMAN, 30 mg/kg s.c.), eltoprazine (ELT, 10 mg/kg *i.p.*), or buspirone (BUS, 5 mg/kg i.p.) and their (**a**) forward locomotion or (**b**) vertical activities recorded for 120 min.*$p < 0.05$, compared to VEH using one-way ANOVA (Bonferroni *post-hoc* tests)

drugs. This screening platform can also be used to test β-arrestin biased compounds for their antiparkinsonian and anti-dyskinetic ability.

3.2 Stereotaxic Surgeries for Viral Transduction

1. To study the effects of βarr2 overexpression on L-DOPA-induced locomotor activity and dyskinesias, stereotaxically inject (*see* **Note 7**) DDD mice with an AAV vector, encoding for the βarr2 gene, in the striatum bilaterally.
2. First, place the mouse in the anesthesia induction chamber filled with 3–4% vaporized isoflurane and check anesthetic depth by a toe-pinch reflex. Upon induction of anesthesia, shave the fur from the surgical site with a generous border (at least 1 cm when possible) to avoid contaminating the incision site. Shave the fur in a location separate from the surgical area.
3. Place the mice on the stereotaxic frame (Kopf) with an anesthesia nose cone (1–2% isoflurane maintenance). Inject the mice with pharmacological grade saline (*s.c.*) for hydration and meloxicam (5 mg/kg *s.c.*) for preemptive analgesia. Clean the surgical site with a germicidal scrub, being careful to scrub from the center of the surgical site toward the periphery. Germicidal scrub and rinse combinations include a 4% chlorhexidine scrub followed by a warmed sterile saline rinse (preferred) or, povidone-iodine scrub followed by a 70% isopropyl alcohol rinse. Perform, at least three alternating preparations of germicidal scrub and rinse. Drape the area with sterile drapes to prevent contaminants from entering the surgical field.

4. Stabilize and level the head of the mouse using non-rupture ear bars, and disinfect the skin on the head with Nolvasan/betadine solution. Using a fresh scalpel, make a straight incision on the skin (between eyes and ears) to expose the skull, and clean the exposed skull of connective tissue. Clean the skull surface with sterile saline.
5. Level the mouse head using bregma and lambda as reference points.
6. Using a drill attached to the stereotaxic frame, drill holes bilaterally in the skull at the coordinates AP, +1.1, ± ML 1.7, DV −2.9 and AP, −0.3 ML, ±2.2, DV, −3.0, relative to bregma. Then, using an injector-needle assembly (*see* **Note 8**) attached to the stereotaxic frame, inject 0.5–1.0 μl of AAV bilaterally, at a rate of 0.2 μl per min. After injection, allow the needle tip to sit in the tissue for 5 min to allow for additional dispersion.
7. After injection, close the scalp incision using wound clips, and place the mice in cages placed on a warming pad set to 37–39 Celsius to recover from the surgery.
8. Let the mice recover for 2 weeks to allow for viral expression of βarr2. After the 2-week recovery period, test the mice in the chronic L-DOPA paradigm (Subheading 3.1) (*see* **Note 9**).

4 Notes

1. The dose of AMPT of 125 mg/kg is ideal because it allows the mice to briefly recover from their parkinsonian phenotype for feeding and drinking and drastically reduces the mortality rate of the DDD mice.
2. Data in Fig. 1 are presented as cumulative activity for the post-L-DOPA injection period of 2 h.
3. The activity monitors record movement using horizontal or vertical beam breaks. Horizontal beam breaks record total distance traveled in cm, which represents the normal locomotor activity of the mouse upon L-DOPA injection, i.e., anti-parkinsonian activity. The vertical beam breaks observed with the DDD/βarr2KO mice records activity when it is standing upright on its hind-paws with rapid forelimb movements and tongue protrusions, which represents dyskinesias or AIMs [3].
4. For the chronic paradigm locomotor test, activity is recorded every alternate day. On the days that the activity is not recorded, the DDD mice are injected with AMPT followed by L-DOPA/Benserazide and returned to their home cages. Therefore, dyskinesias are induced either by acute L-DOPA in DDD/βarr2KO mice or by chronic L-DOPA in DDD/WT mice.

5. Drugs can be injected daily during dyskinesia acquisition or on the last day of the screen once dyskinesias have already been established.
6. For the anti-dyskinesia screen in Fig. 2, data are presented as cumulative activity for the post-L-DOPA injection period of 2 h.
7. Isoflurane gas anesthesia is recommended for the DAT-KO mice over ketamine/xylazine for stereotaxic injections.
8. The injector-needle assembly can be either a *Neuros* Hamilton syringe with a 33-gauge needle or the Drummond Nanoject III with a pulled glass capillary needle.
9. Again, the DDD model can be used as a screening platform for gene therapy candidates as anti-dyskinesia or antiparkinsonian treatments.

Acknowledgments

I would like to thank the Michael J. Fox Foundation (grant #11764) for their support in this project. I would also like to thank Dr. Marc Caron, in whose lab this work was conducted.

References

1. Gerfen CR, Miyachi S, Paletzki R, Brown P (2002) D1 dopamine receptor supersensitivity in the dopamine-depleted striatum results from a switch in the regulation of ERK1/2/MAP kinase. J Neurosci 22(12):5042–5054
2. Porras G, Berthet A, Dehay B, Li Q, Ladepeche L, Normand E, Dovero S, Martinez A, Doudnikoff E, Martin-Negrier ML, Chuan Q, Bloch B, Choquet D, Boue-Grabot E, Groc L, Bezard E (2012) PSD-95 expression controls L-DOPA dyskinesia through dopamine D1 receptor trafficking. J Clin Invest 122(11):3977–3989. https://doi.org/10.1172/JCI5942659426
3. Urs NM, Bido S, Peterson SM, Daigle TL, Bass CE, Gainetdinov RR, Bezard E, Caron MG (2015) Targeting beta-arrestin2 in the treatment of L-DOPA-induced dyskinesia in Parkinson's disease. Proc Natl Acad Sci U S A 112(19):E2517–E2526. https://doi.org/10.1073/pnas.1502740112
4. Sotnikova TD, Beaulieu JM, Barak LS, Wetsel WC, Caron MG, Gainetdinov RR (2005) Dopamine-independent locomotor actions of amphetamines in a novel acute mouse model of Parkinson disease. PLoS Biol 3(8):e271. doi:05-PLBI-RA-0272R3. https://doi.org/10.1371/journal.pbio.0030271
5. Lundblad M, Andersson M, Winkler C, Kirik D, Wierup N, Cenci MA (2002) Pharmacological validation of behavioural measures of akinesia and dyskinesia in a rat model of Parkinson's disease. Eur J Neurosci 15(1):120–132. doi:1843
6. Lundblad M, Picconi B, Lindgren H, Cenci MA (2004) A model of L-DOPA-induced dyskinesia in 6-hydroxydopamine lesioned mice: relation to motor and cellular parameters of nigrostriatal function. Neurobiol Dis 16(1):110–123. https://doi.org/10.1016/j.nbd.2004.01.007S0969996104000178
7. Bohn LM, Gainetdinov RR, Lin FT, Lefkowitz RJ, Caron MG (2000) Mu-opioid receptor desensitization by beta-arrestin-2 determines morphine tolerance but not dependence. Nature 408(6813):720–723. https://doi.org/10.1038/35047086
8. Lundblad M, Usiello A, Carta M, Hakansson K, Fisone G, Cenci MA (2005) Pharmacological validation of a mouse model of l-DOPA-induced dyskinesia. Exp Neurol 194(1):66–75



Chapter 25

Methods to Investigate β-Arrestin-1/β-Catenin Signaling in Ovarian Cancer Cells

Laura Rosanò, Roberta Cianfrocca, and Anna Bagnato

Abstract

Endothelin-1 (ET-1), which acts through the endothelin A receptor (ET_AR) or ET_BR, belonging to the large family of G-protein coupled receptors (GPCR), is involved in physiopathological processes, such as cancer. In epithelial ovarian cancer, a pervasively activated ET-1/ET_AR axis drives different steps of tumor progression and confers drug resistance. In this malignancy, one major aspect associated with the ET_AR signaling machinery resides in the fact that this receptor may use β-arrestin-1 (β-arr1) function to spatially and temporally activate key oncogenic pathways. This results in specificity of ET-1/ET_AR signal transduction mechanisms and downstream signaling pathways. As such, β-arr1 has been recognized as an important signal transducer involved in multiple cross talks with other signaling pathways, including those activated by tyrosine kinase receptors. The interaction with diverse sets of partners positions β-arr1 as a critical regulator of GPCR signal transduction and permits the integration of ET_AR-mediated signals with other cytoplasmic or nuclear inputs. In particular, the scaffolding function of β-arr1 provides an essential link in translating ET_AR function by altering β-catenin localization and function, promoting β-catenin-related transcriptional activity and gene transcription relevant to tumor progression. This chapter outlines the methodologies for the measurement of β-arr1/β-catenin protein interactions and functional activity in tumor cells.

Key words Endothelin-1, Endothelin A receptor, β-Arrestin1, β-Catenin, Immunoprecipitation, Chromatin immunoprecipitation (ChIP), Cell transfection, Reporter plasmid

1 Introduction

The endothelin (ET) family refers to three structurally related small bioactive peptides, ET-1, ET-2, and ET-3, and two G protein-coupled receptors (GPCR), endothelin receptor type A (ET_AR) and B (ET_BR) [1, 2]. During the last decades, a plethora of data demonstrated that the activation of ET_AR by endogenous ET-1 cooperates with intrinsic signaling networks of ovarian cancer to promote tumorigenesis and cancer progression [3]. In ovarian cancer cells, ET_AR plays multiple roles, acting as a regulator of cell motility, invasion, metastasis, and drug response, making it an exciting druggable vulnerability in this malignancy [3]. In an autocrine or paracrine fashion, dysregulated activation of ET_AR by ET-1

Mark G. H. Scott and Stéphane A. Laporte (eds.), *Beta-Arrestins: Methods and Protocols*, Methods in Molecular Biology, vol. 1957, https://doi.org/10.1007/978-1-4939-9158-7_25, © Springer Science+Business Media, LLC, part of Springer Nature 2019

is crucial for the selective and precise modulation of cancer-associated signaling pathways, including that of MAPK, NF-κB, β-catenin, PI3K/Akt, and Rho GTPase, associated with their functional expression levels and subcellular localization. Of particular interest are the findings that, although G proteins function as transducers of ET_AR activation triggering a well-defined set of intracellular signaling cascades, several oncogenic pathways are mediated by noncanonical functions of β-arrestin1 (β-arr1), acting as an adaptor/scaffold to restrict signaling to different cellular compartments [4]. β-arr1 is a member of a small family of proteins that are involved in GPCR signal termination and receptor trafficking [5, 6]. However, important studies have demonstrated novel functions of β-arr1 as a signal mediator recruiting non-G-protein effectors in multiprotein complexes, through its ability to act as a multifunctional adaptor capable of finely modulating multiple signaling pathways involved in tumor progression, driven by GPCR but also by other non-GPCR pathways [4, 6]. β-arr1 directly interacts with proteins displaying various functions and localizations, including nuclear proteins [4, 6]. In particular, β-arr1 function can regulate spatiotemporal nuclear translocation, and the direct positioning of proteins involved in epigenetic modifications on their target gene promoters [7–10]. In this context, recent findings delineated more nuanced aspects of ET-1 signaling, highlighting that ET_AR activation might exhibit sustained and persistent signaling of intracellular pathways depending on the interaction with β-arr1 [11–18]. One of the major oncogenic signaling nodes triggered by ET_AR/β-arr1 interaction is that of β-catenin. Indeed, ET_AR activation by ET-1 recruits β-arr1 to the receptor, eliciting one set of actions operating in the cytoplasm to stabilize β-catenin, which culminates in its subsequent accumulation in the nuclear compartment, generating signaling patterns at specific nuclear β-catenin/T-cell factor 4 (TCF4) transcriptional activity locations to regulate epigenetic modifications and gene transcription [11, 13, 15, 18]. The consequence is that its specific target genes can be "turned on" by favoring the dissociation of histone deacetylase 1 (HDAC1) and the recruitment of p300 acetyltransferase (HAT). This highlights β-arr1-driven gene expression as an additional level of fine-tuned regulation of signaling driven by ET-1 in cancer [13, 15]. Because β-arr1 functions as a hub determining cell fate on the base of which partner(s) it engages, biochemical methodologies for measuring protein-protein and DNA-protein interactions described in this chapter represent an interesting and general approach to study the different interactions of β-arr1, which serves as a platform on which regulatory transcriptional complexes could be built to regulate different outcomes. In this chapter, we describe in detail the methodology to analyze β-arr1 and β-catenin interaction in the cytosolic and nuclear compartments in response to ET_AR activation by using (a) a

co-immunoprecipitation (IP) assay to evaluate the physical association between endogenous β-arr1 and β-catenin/TCF4 complex in the cytosol and in the nuclei, demonstrating that ET_AR co-opts β-arr1 to regulate β-catenin nuclear localization; (b) a reporter gene assay to measure the effects of β-arr1/β-catenin nuclear association on β-catenin/TCF4 transcriptional activity; and (c) chromatin IP (ChIP) and re-ChIP assays to analyze the selective enrichment of β-arr1 with β-catenin and TCF4 at specific gene promoters together with epigenetic modifiers, such as p300 HAT. These techniques can be used for the characterization of a common mechanism used by β-arr1 as a nuclear interactor competent to activate the expression of downstream target genes and also perhaps any upstream regulators of nuclear function of β-arr1. The advantage of these techniques is that they allow the investigator to examine in tumor cells stimulated with ET-1: (1) the specificity of β-arr1/protein interactions in the cytosol or in nuclear fractions; (2) how β-arr1 functions as a nuclear platform for epigenetic modifications, such as histone acetylation, and chromatin remodeling; and (3) how ET-1 receptor antagonists can affect β-arr1/protein interactions.

2 Materials

2.1 Cell Culture

1. Human ovarian serous adenocarcinoma HEY cells (ATCC).
2. RPMI 1640 medium.
3. Fetal bovine serum (FBS).
4. Penicillin-streptomycin.
5. Trypsin–HCl EDTA (0.05%).
6. Dulbecco's Phosphate-Buffered Saline (DPBS) with 9,5 mM (PO_4).
7. 150-mm tissue culture dishes.
8. 10-, 25-, and 50-mL sterile plastic serological pipets.
9. T75 tissue culture flasks.
10. Six-well cell culture plates.
11. Endothelin-1 (Bachem).
12. Endothelin-1 receptor antagonists: Zibotentan, ZD4054, N-(3-methoxy-5-methylpyrazin-2-yl)-2-(4-[1,3,4-oxadiazol-2-yl] phenyl) pyridine-sulfonamide, (AstraZeneca), is a selective ET_AR antagonist, and Macitentan (MAC), Opsumit, also N-(5-[4-bromophenyl]-6-{2-[5-bromopyrimidin-2-yloxy]ethoxy}pyrimidin-4-yl)-N′-propylsulfamide, is a dual ET_AR/ET_BR antagonist (Actelion Pharmaceuticals).

2.2 Co-Immunoprecipitation (Co-IP)

1. DPBS.
2. Tris–HCl Buffered Saline, pH 7.4 (TBS).
3. Blotting-grade blocker, nonfat dry milk.
4. NE-PER nuclear and cytoplasmic extraction reagents (Thermo Scientific).
5. Protein G or A-Agarose beads 50% slurry.
6. Protein A Peroxidase Conjugated (Thermo Scientific).
7. Primary antibodies against: β-Arr1 (K-16), β-catenin (E-5), TCF4 (H-125), tubulin (DM1A), and control immunoglobulin (IgG) (Santa Cruz Biotechnology).
8. Secondary antibodies: anti-goat-horseradish peroxidase (HRP), anti-rabbit-HRP, and anti-mouse-HRP.
9. DC Protein Assay kit (Bio-Rad).
10. Mini-PROTEAN TGX precast gels (10%) in Tris-glycine buffer (Bio-Rad).
11. 4× Laemmli protein sample buffer.
12. Precision plus protein standard (Bio-Rad).
13. Trans-Blot Turbo mini-size transfer stacks (Bio-Rad).
14. Trans-Blot Turbo Transfer System (Bio-Rad).
15. Clarity Western-enhanced chemiluminescence (ECL) substrate (Bio-Rad).
16. Photographic film for use with enhanced chemiluminescence (ECL) substrates for horseradish peroxidase (HRP) (CL-XPosure Film) (Thermo Fisher).
17. Image processing and analysis in JAVA (Image J) software.

2.3 Transfection and Luciferase Reporter Assay

1. DPBS.
2. Opti-MEM I medium.
3. Lipofectamine 2000 (Thermo Fisher Scientific).
4. TCF reporter plasmid (TOP-flash) containing 2 sets of 3 copies of the TCF-binding site (wild type) upstream of the thymidine kinase minimal promoter and luciferase open reading frame (Upstate Biotech).
5. TCF reporter plasmid (FOP-flash) containing two full and one incomplete copies of the TCF-binding site (mutated) followed by three copies in the reverse orientation, serving as a negative control to TOP-flash (Upstate Biotech).
6. Reporter vector designed for the expression of β-galactosidase in mammalian cells from the human cytomegalovirus immediate early gene promoter (pCMV-β-galactosidase vector) (Promega).

7. ON-TARGET plus Human ARRB1 siRNA-SMART pool (L-011971), containing four different siRNAs targeting β-arr1 (Dharmacon, Lafayette, USA).
8. ON-TARGET plus control nontargeting siRNA (D-001810) (Dharmacon).
9. 10 mM Na_2PO_4.
10. Chlorophenolred-β-D-galactopyranoside (CPRG).
11. Luciferase reporter gene assay kit (Promega).
12. Lysis buffer: 250 mM NaCl, 50 mM HEPES, pH 7.4, 1 mM EDTA, 1% Nonidet P-40, protease inhibitor cocktail tablets (Roche).
13. 96-well white fluorescence plates.
14. Microplate spectrophotometer, Multiskan FC (Thermo Scientific).
15. Luminometer, Glomax (Promega).

2.4 ChIP and Re-ChIP Assay with PCR Detection

Prepare all solutions using ultrapure water (Milli-Q Integral Water Purification Systems), sterile filter tips, and filter the solutions with either 0.22 μm or 0.45 μm filters. Prepare and store all reagents at room temperature (unless indicated otherwise).

1. DPBS.
2. 37% formaldehyde, Molecular Biology Reagent Grade.
3. Glycine 2.5 M: 18.767 g in 100 mL of water.
4. Protease inhibitors: 1 mM PMSF, 100 μM leupeptin, 0.3 μM aprotinin, 1 μM pepstatin A, and 10 μM bestatin.
5. Cell lysis buffer: 50 mM Tris–HCl, pH 8, 2 mM EDTA, pH 8, 0.1% NP40, 10% glycerol. Supplement with protease inhibitors before using.
6. Nuclei lysis buffer: 50 mM Tris–HCl, pH 8, 5 mM EDTA, pH 8, 1% SDS. Supplement with protease inhibitors before using.
7. Dilution buffer: 50 mM Tris–HCl, pH 8, 2 mM EDTA, pH 8, 200 mM NaCl, 0.5% NP40. Supplement with protease inhibitors before using.
8. Wash buffer: 20 mM Tris–HCl, pH 8, 2 mM EDTA, pH 8, 0.1% SDS, 1% NP40, 500 mM NaCl. Supplement with protease inhibitors before using.
9. Tris-EDTA based (TE) buffer: 10 mM Tris–HCl, pH 7.5, 2 mM EDTA, pH 8. Supplement with protease inhibitors before using.
10. Extraction buffer: TE buffer supplemented with 2% SDS.
11. Diagenode bioruptor sonicator.

12. Protein G-Agarose 50% slurry.
13. Salmon sperm DNA (Life technologies).
14. Proteinase K (Life technologies).
15. Antibodies against: β-arrestin-1 (K-16), β-catenin (E-5), p300 HAT (N-15), TCF4 (H-125), HDAC1 (H-51) and control IgG (Santa Cruz Biotechnology), AcH3, AcH4 (Upstate Biotechnology), AcH3(Lys 18), AcH3(Lys 27) (Millipore).
16. Dithiothreitol (DTT).
17. Qiagen QIAquick PCR purification kit.
18. Molecular biology agarose.
19. FluoroVue™ Nucleic Acid Gel Stain (10,000×) (Smobio).
20. Primers of selected β-catenin/TCF target gene promoters:
    (a) ET-1F: 5′-CAGCTTGCAAAGGGGAAGCG-3 and R: 5′- TCCGACTTTATTCCAGCCCC -3′.
    (b) CyclinD1 F: 5′-GAGCGCATGCTAAGCTGAAA-3′ and R: 5′-GGACAGACGGCCAAAGAATC-3.
    (c) MMP-2F: 5′-GAGGTCGCTTTCTTTGCCATCT -3′ and R: 5′-AGCGACTCCATCTTGAACAGG-3.
    (d) MMP-9F: 5′-CACTGTATCCTTGACCTTCTTTCTGG-3′ and R:5′-GCTTCCTCTCCCTGCTTCATCTG -3′.
    (e) Axin2 F: 5′-CTGGAGCCGGCTGCGCTTTGATAA-3′ and R: 5′-CGGCCCCGAAATCCATCGCTCTGA-3′.
21. Gel Image Capture System, Gel-Doc (Bio-Rad).

3 Methods

3.1 Cell Culture

1. These protocols take advantage of the property of human ovarian cancer cell HEY endogenously expressing ET_AR and β-arr1, and which are therefore highly sensitive for the detection of receptor activity following ET-1 agonist stimulation. Cells grow in RPMI 1640 medium supplemented with 10% FBS and 1× penicillin/streptomycin, in a humidified atmosphere of 5% CO_2 at 37 °C. To determine the effect of ET-1 or antagonist treatment, cells are serum-starved for at least 24 h prior to treatment to achieve quiescent conditions. Additional controls, such as the use of the drug vehicle, should be concomitantly used (*see* **Note 1**).
2. Cells are grown in serum-free medium with or without ET-1 (100 nM) and/or receptor antagonists, zibotentan or macitentan (1 μM). When ET-1 is used in combination with ET-1 receptor antagonist, the antagonist needs to be added 30 min before ET-1.

3.2 Co-Immunoprecipitation (IP) Assay

To identify binding partners of β-arr1, such as β-catenin, perform the co-IP technique, by using target protein-specific antibodies to capture proteins that are bound to a specific target protein. The principle of an IP is that an antibody (monoclonal or polyclonal) against a specific target protein forms an immune complex with that target in cell lysate. The immune complex is precipitated on a beaded support to which an antibody-binding protein is immobilized (such as Protein A or G), and any proteins not precipitated on the beads are washed away. The antigen is then eluted from the support and analyzed by gel electrophoresis, followed by western blot (WB) detection to verify its identity.

1. Before performing Co-IP assays, plate cells onto 150 mm dishes in growth medium and allow them to grow up to 80–90% of confluence. Then wash cells with DPBS, discard DPBS, add 2 mL Trypsin/EDTA solution and gently resuspend them in at least one equal volume of complete media. Recover the cells in a 15-mL tube, centrifuge cells at 270 × *g* for 5 min, at 4 °C.
2. Treat cells with ET-1 (100 nM) and/or either zibotentan or macitentan (1 μM) for 30 min.
3. For preparing nuclear and cytoplasmic fractions, use the NE-PER kit, a nuclear protein extraction method that involves simple, stepwise lysis of cells and centrifugal isolation of nuclear and cytoplasmic protein fractions. Follow the manufacturer's instructions. The NE-PER reagents efficiently solubilize and separate cytoplasmic and nuclear proteins into fractions with minimal cross-contamination or interference from genomic DNA and mRNA.
4. Determine the protein content of the extracts.
5. To reduce non-specific binding of proteins to beads, use preclearing to remove potentially reactive, non-specific components from a lysate sample prior to the IP. Take 300 μg in a final volume of 500 μL of nuclear and/or cytoplasmic fractions, add 30 μL beads, and incubate at 4 °C for 1–2 h under constant rotation.
6. Centrifuge at 15682 × *g*, in a microcentrifuge, for 1 min, at 4 °C, separate the beads from the cell lysate, and transfer the precleared lysate to a clean 1.5 mL tube. Save 10 μg in a final volume of 20 μL as an input control.
7. Simultaneously with **step 5**, incubate 40 μL beads with 2 μg of primary antibody or non-specific IgG, as negative control for any co-IP experiment. Prepare as follows: calculate the amount of beads needed for the total number of IP samples, and add the total amount of antibody or non-specific IgG; add DPBS up to a final volume of at least 500 μL, and rotate for 3 h at 4 °C.

8. Centrifuge at 15682 × *g*, in a microcentrifuge for 1 min, at 4 °C.
9. Transfer the same amount of pre-absorbed beads in the pre-cleared lysate (**step 5**), and rotate overnight at 4 °C.
10. The next day centrifuge at 15682 × *g*, for 1 min, at 4 °C, and wash three times with 1 mL of DPBS. Centrifuge at 15682 × *g*, for 1 min between washes. Remove supernatant carefully, and add 20 μL of 4× Laemmli sample buffer and vortex.
11. Heat the IP and input (plus 1× Laemmli sample buffer) samples to 95–100 °C for 5 min, and centrifuge for 1 min at 15682 × *g*, at room temperature. Load the sample along with precision protein standard on 10% SDS-PAGE gels, and transfer to nitrocellulose membrane.
12. Perform WB by using antibodies to β-arr1 (K-16) (1:200), β-catenin (E-5) (1:200), TCF4 (H-125) (1:200) diluted in 5% nonfat dry-milk in TBS buffer and the appropriate secondary conjugated antibody: anti-goat-HRP (1:5000), anti-rabbit-HRP (1:5000), and anti-mouse-HRP (1:2000) (*see* **Note 2**). Develop with ECL using CL-XPosure Films and quantify using an image program such as Image J.

3.3 Transfection and Luciferase Reporter Assay

Use the TOP-flash luciferase reporter assay (a plasmid containing the wild-type TCF-binding regions) to verify whether β-arr1/β-catenin interaction is linked to β-catenin-dependent TCF4 transcriptional activity.

1. The day before transfection, seed the cells at 1×10^5 cells/well (consider a triplicate for each point) into 6-well cell culture plates in complete RPMI 1640, and allow cells to grow up to 60% of confluence. Add three additional points to control the efficiency of β-arr1 silencing by WB.
2. Perform transfection by preparing two solutions: solution A, containing 3 μL of Lipofectamine 2000 in 250 μL of Opti-MEM medium for each well, and solution B containing 200 pmol of β-arr1 siRNA or non-targeting control siRNA in 250 μL of Opti-MEM medium for each well. After 5 min, mix the two solutions (A + B) and wait 15 min.
3. During the 15 min of waiting of **step 2**, change the culture medium using 1.5 mL/well of serum-free medium, and then add the transfection solution into each well by shaking gently. Put the cell culture plates back into the incubator at 37 °C under 5% CO_2 for at least 5 h, remove transfection mix from each well, and add 2 mL/well of serum-free medium (*see* **Note 1**), and grow cells in the incubator overnight.

4. The next day, perform the second transfection as in **steps 2** and **3**, and prepare two solutions as follow: solution A, containing 3 μL of Lipofectamine 2000 in 250 μL of Opti-MEM medium for each well, and solution B containing 1 μg of Top-Flash or Fop-Flash reporter plasmid, plus 0.25 μg of pCMV-β-galactosidase vector in 250 μL of Opti-MEM medium for each well (*see* **Note 3**).
5. Grow the cells with or without ET-1 and/or ET-1 receptor antagonists in serum free-media for an additional 24 h.
6. The next day, remove the media and wash the cells with 1 mL/well of DPBS.
7. Add 250 μL/well lysis buffer to wells where β-arr1 has been silenced to control the efficiency of silencing, and analyze by WB.
8. Add 250 μL/well of 1× cell lysis buffer provided in the luciferase assay kit, and scrape off the cells. Transfer into 1.5 mL tubes and centrifuge at 9279 × *g*, in a microcentrifuge for 5 min, at 4 °C.
9. To measure the β-galactosidase expression levels of transfected cells, required for normalizing the luciferase assay, transfer 70 μL/well of cell lysate into 96-well plates and add 130 μL/well of the following solution: 90 μL of 0.01 M Na_2PO_4, 10 μL of 30 mg/mL CPRG, and 100 μL of 1× DPBS. Incubate at 37 °C until the solution becomes reddish, and determine the absorbance at 540 nm using a microplate spectrophotometer.
10. To measure the luciferase expression levels of transfected cells, transfer 50 μL/well of cell lysate into a 96-well white fluorescence plate, and add 100 μL of luciferase substrate provided by the luciferase kit. Load the plate into the luminometer and measure the luminescence intensity.
11. To normalize the results, the relative luciferase activity in each well is obtained by dividing the luminescence intensity by the corresponding β-galactosidase intensity. Results are expressed as the ratio of TOP-Flash over FOP-Flash activity and represent values as mean of results of different independent experiments.

3.4 ChIP Assay

A powerful technique for identifying and analyzing in vivo interactions between specific proteins and genomic DNA regions, as well as to monitor the presence of histones with posttranslational modifications at specific genomic locations, is the ChIP assay. Briefly, cross-linked chromatin is sonicated to generate smaller DNA fragments, followed by immunoprecipitation with specific antibodies. After elution of the protein-DNA complexes from protein G-agarose beads, the samples are heated to reverse the covalent

cross-links and the DNA fragments are purified and analyzed by PCR or real-time PCR.

1. ChIP assays require copious amounts of starting material. Therefore, a minimum of 1×10^6 cells is recommended for each immunoprecipitation; however, the number of cells necessary to perform ChIP assays can be extended and empirically determined. In the proposed protocol, the cells are grown up to 80–90% confluence in 150-mm dishes (*see* **Note 4**).
2. Wash the cells with DPBS, then add 2 mL Trypsin/EDTA solution, gently resuspend in at least one equal volume of serum media, and recover the cells in a 15 mL tube.
3. Count the cells (a minimum of 5×10^6 cells are needed), and centrifuge at $270 \times g$ for 5 min, at 4 °C.
4. Resuspend the pellet with 10 mL DPBS. Cross-link the DNA to the proteins by incubating cells with 1% formaldehyde for 8 min at room temperature (mix gently by flipping the tube three times) (*see* **Note 5**).
5. Stop cross-link by adding glycine to a 125 mM final concentration. Gently mix by flipping the tubes.
6. Centrifuge at $270 \times g$ for 5 min, at 4 °C. Wash cells three times with 15 mL of cold DPBS, and resuspend cells in 1 mL of cold cell lysis buffer supplemented with protease inhibitors, and transfer to a 1.5 mL tube. Incubate 5 min on ice.
7. Centrifuge at $835 \times g$ in a microcentrifuge for 5 min, at 4 °C, and resuspend nuclei (which appear translucent) in 600 μL of cold nuclei lysis buffer supplemented with protease inhibitors. Keep samples on ice.
8. Sonicate chromatin. To obtain fragments between 300 and 500 bp, sonicate with high setting for intervals of 30 s "on" followed by 30 s "off" for a total of 10 min (Diagenode Bioruptor Sonicator) (*see* **Note 6**).
9. Centrifuge at $15682 \times g$, in a microcentrifuge for 10 min, at 4 °C, transfer the supernatant into a 15 mL tube, and dilute chromatin with 9 volumes of dilution buffer supplemented with protease inhibitors. (At this point the samples can be stored at −20 °C.)
10. Incubate chromatin for 1 h at 4 °C under constant rotation with 80 μL of previously blocked beads, prepared as follows: calculate the amount of protein G needed for the total number of samples, and add salmon sperm DNA to a final concentration of 1 mg/mL, and rotate for 2 h at 4 °C. Centrifuge at $15682 \times g$, in a microcentrifuge for 1 min, at 4 °C, wash three times with 1 mL of cold wash buffer, and resuspend the beads with cold wash buffer, to a final concentration of 50% (*see* **Note 7**).

11. Centrifuge the tubes containing precleared chromatin at 134 × *g*, for 5 min, at 4 °C, and gently divide chromatin into 1 mL aliquots per antibody. 300 μL aliquots are used for INPUT (5% of precleared chromatin), which is the fraction useful to normalize the starting material. These aliquots can be stored at 4 °C for up to 4 months.
12. Add 2 μg of primary antibody or non-specific IgG, used as the irrelevant antibody (IRR) for each ChIP reaction, and incubate overnight at 4 °C with constant rotation (*see* **Note 8**).
13. The next day, add 40 μL of 50% salmon sperm-saturated beads (*see* **step 10**) to the immunocomplexes, and incubate at 4 °C for 30 min with constant rotation.
14. Centrifuge at 15682 × *g*, for 1 min, at 4 °C, and wash seven times with 1 mL of washing buffer, rotating 1 min at 4 °C. Centrifuge at 15682 × *g*, for 1 min between washes. Carefully remove the supernatant, and wash three times with 1 mL TE as before.
15. Elute immunocomplexes by adding 100 μL of extraction buffer and incubating 5 min at 37 °C. Centrifuge at 15682 × *g*, for 1 min, at room temperature, and transfer the supernatant into a clean 1.5 mL tube. Repeat all for three times to obtain a final volume of 300 μL for each ChIP reaction.
16. Take the INPUT samples out of the freezer to process them as the immunocomplexes. Add 15 μL of 4 M NaCl to each sample (immunocomplexes and INPUT), and incubate for at least 4 h (or overnight) at 65 °C to reverse the cross-link.
17. Add 50 μg of proteinase K plus 6 μL of 0.5 M EDTA, pH 8, and 24 μL of 1 M Tris–HCl, pH 6.5, to each sample, and incubate at 50 °C for 1 h.
18. Extract DNA using the MiniElute purification Kit (Qiagen), following the manufacturer's instructions (*see* **Note 9**).
19. Elute DNA in 30 μL of sterile water, and proceed to PCR reactions (*see* Subheading 3.6).

3.5 Re-ChIP Assay

To evaluate the coexistence of different factors in a given genomic region, such as β-arr1/β-catenin with p300 HAT on specific β-catenin target genes, ChIP–reChIP assay must be performed, since ChIP assay alone is unable to distinguish between two factors coexisting in the same DNA region. A ChIP-reChIP experiment consists in performing a ChIP assay with two rounds of IP before DNA recovery, allowing to determine whether two given proteins localize at the same genomic region.

1. Perform the ChIP protocol above from **steps 1–14** of Subheading 3.4.
2. Remove supernatant and elute the immunocomplexes by incubation for 30 min at 37 °C in 25 μL of 10 mM DTT. Centrifuge at 15682 × *g*, for 1 min, at room temperature, to collect the beads at the bottom of the tube.
3. Isolate the supernatant in new 1.5 mL tubes, repeat **step 2**, and collect all the supernatant in the same 1.5 mL tube.
4. Dilute the recovered supernatant (~50 μL) 10 times with ChIP dilution buffer supplemented with protease inhibitors.
5. Proceed with a second immunoprecipitation reaction by adding 2 μg of antibodies against the protein of interest or with IgG control, and incubate overnight at 4 °C with constant rotation.
6. Continue with **step 13** of the Subheading 3.4 of the ChIP protocol.

3.6 Analysis of Immunoprecipitated DNA

To analyze isolated DNA, run qualitative or quantitative PCR with primers targeting the specific promoter regions of genes of interest. PCR results are normalized to the total chromatin (INPUT) samples. In our protocol, we use qualitative PCR, starting with 2 μL of each INPUT to determine the amount of related immunoprecipitated DNA (*see* **Note 10**). We select a set of β-catenin/TCF4-target genes, such as ET-1, Cyclin D1, Axin 2, Matrix metalloproteinase (MMP)-2 (used as negative control) and MMP-9, and run PCRs as follows:

1. Perform the reaction in a final volume of 25 μL, with 0.625 U of AmpliTaq DNA Polymerase, 1× PCR Buffer II and 2 mM of $MgCl_2$, plus 0.2 μM of forward primer, 0.2 μM reverse primer, and 0.2 mM of each dNTP.
2. Incubate reactions in a thermal cycler for 25–35 cycles at 58 °C (T_m), for 30 s at each cycle.
3. The PCR products (10 μL) are separated by electrophoresis in a 2.0% agarose gel containing nucleic acid gel staining (1:10,000). Images are acquired and quantified by gel image capture system (Gel-Doc, Bio-Rad).

4 Notes

1. Serum deprivation is a method to block all the signals triggered by the serum. In this quiescent state, cells can respond to a specific stimulation, such as ET-1. Additional controls, such as the use of drug vehicle, should be used: 5% acetic acid for ET-1 and 100% methanol for macitentan.

2. To obtain clean and specific WB signals for β-arr1, which run very close to heavy chain of IgG, use HRP-conjugated protein A instead of HRP-conjugated secondary antibody.
3. The transfection protocol, including the amounts of plasmid DNA and Lipofectamine, needs to be optimized for different cell lines. The transfection efficiency could be affected by a number of factors, such as the cell density, the quality of prepared plasmids, and the transfection duration.
4. The number of cells needed varies according to each cell type. Adjust cell number in order to obtain a good amount of chromatin, for at least five independent antibodies per sample, and keep the cell number constant in each sample of the same experiment.
5. The cross-link step should be optimized, since too little cross-linking will not sufficiently preserve the chromatin structure from sonication, and too much cross-linking will hamper the DNA fragmentation.
6. Optimal fragmentation can be achieved by testing various sonication conditions on chromatin, followed by DNA isolation and estimating the sonication efficiency by 1% agarose gel electrophoresis. Ideally, the bulk of the chromatin is sonicated to a length between 250 and 750 bp. For efficient fragmentation, sonication at low power, in combination with several pulses, is preferred over sonication at high power and few pulses, but conditions vary with the sonication device used. It is important to keep the chromatin sample cooled on ice during sonication. Sonicated chromatin can be stored at −80 °C for at least a few months.
7. Chromatin preclearance with adsorbed beads reduces unspecific background.
8. 3–4 μg of antibody is an optimum amount to assure efficient immunoprecipitation. Depending on the antibody, 2 μg could be sufficient. The IgG must be from the same species in which the antibody to target protein was generated. Because the anti-β-arr1 (K-16), sc-9182 (Santa Cruz Biotechnology), has been removed from trade, a good alternative is represented by anti-β-arr1 [E274], ab32099 (abcam). To evaluate the presence of chromatin modifiers, such as p300 HAT and HDAC1, or the levels of lysine residues susceptible to acetylation by p300 HAT in histone H3, use specific antibodies to p300 HAT, HDAC1, AcH3(Lys18), and AcH3(LysK27).
9. DNA extraction could be done with phenol-chloroform, followed by precipitation.
10. To determine sample amount to be used in the PCR reaction, first run a PCR with 2 μL of each INPUT, and adjust the

quantities loaded until obtaining equal signals. Gel-Doc image capture and analysis (Bio-Rad) are one of the systems available to analyze and quantify the PCR products.

References

1. Masaki T, Vane JR, Vanhoutte PM (1994) International Union of Pharmacology nomenclature of endothelin receptors. Pharmacol Rev 46:137–142
2. Nelson J, Bagnato A, Battistini B, Nisen P (2003) The endothelin axis: emerging role in cancer. Nat Rev Cancer 3:110–116
3. Rosanò L, Spinella F, Bagnato A (2013) Endothelin 1 in cancer: biological implications and therapeutic opportunities. Nat Rev Cancer 13:637–651
4. Peterson YK, Luttrell LM (2017) The diverse roles of arrestin scaffolds in G protein-coupled receptor signaling. Pharmacol Rev 69:256–297
5. Shenoy SK, Lefkowitz RJ (2011) β-Arrestin-mediated receptor trafficking and signal transduction. Trends Pharmacol Sci 32:521–533
6. Rosanò L, Bagnato A (2016) β-arrestin1 at the cross-road of endothelin-1 signaling in cancer. J Exp Clin Cancer Res 35:121–113
7. Purayil HT, Zhang Y, Dey A, Gersey Z, Espana-Serrano L, Daaka Y (2015) Arrestin2 modulates androgen receptor activation. Oncogene 34:3144–3151
8. Qin R, Li K, Qi X, Zhou X, Wang L, Zhang P et al (2014) β-Arrestin1 promotes the progression of chronic myeloid leukaemia by regulating BCR/ABL H4 acetylation. Br J Cancer 111:568–576
9. Zecchini V, Madhu B, Russell R, Pértega-Gomes N, Warren A, Gaude E, Borlido J et al (2014) Nuclear ARRB1 induces pseudohypoxia and cellular metabolism reprogramming in prostate cancer. EMBO J 33:1365–1382
10. Shenoy SK, Han S, Zhao YL, Hara MR, Oliver T, Cao Y, Dewhirst MW et al (2012) β-arrestin1 mediates metastatic growth of breast cancer cells by facilitating HIF-1-dependent VEGF expression. Oncogene 31:282–292
11. Rosanò L, Cianfrocca R, Masi S, Spinella F, Di Castro V, Biroccio A et al (2009) Beta-arrestin links endothelin A receptor to beta-catenin signaling to induce ovarian cancer cell invasion and metastasis. Proc Natl Acad Sci U S A 106:2806–2811
12. Cianfrocca R, Rosanò L, Spinella F, Di Castro V, Natali PG, Bagnato A (2010) Beta-arrestin-1 mediates the endothelin-1-induced activation of Akt and integrin-linked kinase. Can J Physiol Pharmacol 88:796–801
13. Rosanò L, Cianfrocca R, Tocci P, Spinella F, Di Castro V, Spadaro F et al (2013) β-Arrestin-1 is a nuclear transcriptional regulator of endothelin-1-induced β-catenin signaling. Oncogene 32:5066–5077
14. Cianfrocca R, Tocci P, Semprucci E, Spinella F, Di Castro V, Bagnato A et al (2014) β-Arrestin 1 is required for endothelin-1-induced NF-κB activation in ovarian cancer cells. Life Sci 118:179–184
15. Rosanò L, Cianfrocca R, Tocci P, Spinella F, Di Castro V, Caprara V et al (2014) Endothelin A receptor/β-arrestin signalling to the Wnt pathway renders ovarian cancer cells resistant to chemotherapy. Cancer Res 74:7453–7464
16. Semprucci E, Tocci P, Cianfrocca R, Sestito R, Caprara V, Veglione M et al (2016) Endothelin A receptor drives invadopodia function and cell motility through the β-arrestin/PDZ-RhoGEF pathway in ovarian carcinoma. Oncogene 35:3432–3442
17. Cianfrocca R, Tocci P, Rosanò L, Caprara V, Sestito R, Di Castro V et al (2016) Nuclear β-arrestin1 is a critical cofactor of hypoxia-inducible factor-1α signaling in endothelin-1-induced ovarian tumor progression. Oncotarget 7:17790–17804
18. Cianfrocca R, Rosanò L, Tocci P, Sestito R, Caprara V, Di Castro V et al (2017) Blocking endothelin-1-receptor/β-catenin circuit sensitizes to chemotherapy in colorectal cancer. Cell Death Differ 24(10):1811–1820. https://doi.org/10.1038/cdd.2017.121

INDEX

A

ADP-ribosylation factors (ARF) 15, 159, 160, 164–167, 170
Adrenergic receptor 3, 60, 95, 252, 325, 326
Agonist 4, 11, 59, 76, 93, 134, 159, 170, 195, 228, 235, 273, 318, 328, 398
Airway hyperresponsiveness 338
Allergic asthma 46
Angiotensin II type 1 receptor (AT1R) 12, 18, 20, 22, 25, 26, 32, 33, 35, 43, 44, 60–63, 65, 66, 85, 86, 88, 89, 160, 166, 326, 330
Antagonist 4, 34, 236–238, 395, 398, 401
Arrestin 3–5, 9–47, 59–81, 83–88, 93–102, 107–119, 121, 139–156, 159–175, 177–193, 195–213, 217–230, 251–268, 273, 293–306, 309–321, 325–333, 345–363, 365–391, 393–406

B

Basal body ..... v, 271–288
β2-adrenergic receptor (β2AR) 3, 60, 61, 63, 65, 66, 95–97, 122, 123, 129
β2-adrenoceptor 79
β-arrestin 1 ..... 4, 59, 74, 77, 97, 124, 170, 172, 179–181, 218, 228, 294, 295, 298–301, 305, 309, 326–328, 332, 355
β-arrestin 2 ..... 4, 59, 74, 77, 97, 124, 218, 228, 271–288, 294, 295, 299–305, 309, 326–329, 332, 335
β-arrestin interacting partner 159
β-arrestin partners 17, 35, 150, 153, 154, 177–193, 218
β-arrestin recruitment 63, 64, 84, 86, 198, 201, 236
β-arrestins (β-arrs) ..... v, vi, 3–5, 9–47, 59–81, 83–88, 93–102, 121–123, 127–129, 131, 133, 134, 139–156, 159–175, 177–193, 195–213, 217–230, 235, 236, 251–268, 293–306, 325–333, 345–363, 365–391, 393–406
β-catenin 28, 39, 393–406
Biased agonism 236
Biochemical reaction networks 196, 197, 205, 209, 212
Bioluminescence resonance energy transfer (BRET) ..... v, 32, 33, 59–68, 83–88, 93–102, 140, 141, 143, 151–154, 156, 196, 198–202, 207, 209, 309–321

C

Cell transfection 61, 62, 66, 84, 85, 97–99, 115, 122, 133, 134, 141, 160, 173, 198, 199, 254, 312, 314–315, 327, 331, 332
Cellular signaling 271
Centrosome ..... v, 271–288
Chromatin immunoprecipitation (ChIP) 395, 397–398, 401–404
Co-immunoprecipitation (Co-IP) 109, 127, 131, 140, 142, 145–148, 153, 155, 164, 166, 167, 218, 220, 394, 396, 399–401
Confocal microscopy 275
Cyclic adenosine monophosphate (cAMP) ..... v, 21, 36, 37, 72, 73, 77, 80, 122, 180

D

Data fitting 196, 197, 203, 206–208
Desensitization ..... v, 3, 4, 9–13, 21, 31, 36, 37, 46, 59, 69, 94, 121, 139, 195, 218, 273, 293, 309, 328
Dynamic models 196, 207, 209
Dyskinesias 385, 387–390

E

Endocytosis ..... v, 9, 10, 12–15, 18, 19, 24, 31, 36–39, 42, 43, 59, 61
Endosomes 12, 25, 31, 34, 36, 38, 43, 44, 59, 60, 64, 65, 320
Endothelin-1 ..... 23, 28, 395
Endothelin A receptor (ET_AR) 12, 18, 46, 393–395, 398
Enhanced bystander BRET (EbBRET) 59–68

F

Fluorescent arsenical 32, 311, 312, 316
Functional selectivity 235

Mark G. H. Scott and Stéphane A. Laporte (eds.), *Beta-Arrestins: Methods and Protocols*, Methods in Molecular Biology, vol. 1957, https://doi.org/10.1007/978-1-4939-9158-7, © Springer Science+Business Media, LLC, part of Springer Nature 2019

G

Genotyping 349, 350, 354–357
GGA3 ..... 160–162, 164–166
GPCR kinases (GRKs) 4, 11, 32, 34, 36, 37, 43, 93, 202, 328
GPCR phosphorylation 11, 15, 32, 36–38, 43, 44, 93, 328
G protein-coupled receptors (GPCR) 4, 9, 59, 69, 83, 93, 107, 139, 159, 169, 177, 195, 218, 235, 251, 273, 293, 309, 326, 346, 393
G proteins ..... v, 3–5, 9, 11, 25, 31–34, 37, 43, 60, 122, 139, 169, 235, 236, 273, 325, 394
Green fluorescent protein (GFP) 4, 60, 71, 73, 77, 79, 86, 110, 111, 116, 117, 133, 151, 153, 155, 173, 260, 262, 264, 279–281, 285, 286, 359, 387
GST pull-down 145–147, 150, 151

H

Heterodimerization 83

I

Immunocytochemistry 77, 81, 346, 350–352, 356–362
Immunofluorescence 253–258, 279, 282, 284, 330, 359, 360, 367, 382
Immunoprecipitation (IP) 123, 127–129, 134, 146, 148, 155, 161, 162, 167, 366, 369, 372–375, 399–402, 404, 405
Inducible knockout 338
Infection 70, 74, 76, 79, 80, 326, 328–330, 332, 359
Inflammation 23, 140, 339, 366, 367
Insulin resistance 345, 365, 366
Insulin secretion 346, 367–369, 376, 381–382
Interactome ..... v, 38, 217–230
Interface region 185, 190
Internalization 4, 9, 11–13, 15, 18, 20, 25, 42–44, 59–61, 67, 139, 159, 195, 202, 218, 273, 293

J

JNK3 activation 20, 108

L

Ligand efficacy 309
Limited proteolysis 294, 300–305
Liquid chromatography–mass spectrometry (LC-MS) 223
Liquid chromatography/tandem mass spectrometry (LC/MS/MS) 218, 219, 223, 224, 227, 230

M

Mass spectrometry (MS) ..... v, 139, 178, 218, 220, 223, 225, 227, 230, 293–306
Matrix-assisted laser desorption/ionization-time of flight mass spectrometry (MALDI-TOF MS) 294, 297, 302, 303, 306
Mdm2 ..... 10, 12, 24, 27–30, 35, 36, 38, 39, 126–128, 252–254, 262–264, 267, 268
Membrane blebbing 169–175
Membrane protrusions 27, 325, 329
Mice 4, 22, 25, 45, 46, 70, 76, 335–339, 341, 342, 346, 349–351, 354–362, 366, 367, 369, 376, 378, 382, 384–391
Mitogen-activated protein kinases (MAPKs) ..... v, 10, 13, 15, 19, 20, 35, 36, 38, 43, 108, 394
Model selection 196, 207–210
Muscarinic acetylcholine receptor 69

N

Neisseria meningitidis 35, 46, 325, 326, 328–330, 332, 333
Nuclear export signal (NES) 20, 24, 27, 35, 36, 39, 252, 253, 267
Nucleocytoplasmic trafficking v

O

Obesity 29, 46, 366
Operational model 237, 239, 241
Ovalbumin (OVA) 336–342

P

p53 ..... 10, 24, 30, 36, 252, 253
Pancreatic β-cell 46, 345–363
Parameter identification 197
Parkinson's disease (PD) ..... v, 24, 46, 385–391
Phosphodiesterases (PDEs) 21, 36, 37, 121, 127, 203, 206
Phosphopeptide 31, 295, 297, 300, 304
Plasma membrane (PM) 12, 21, 22, 24–26, 28, 30, 36–38, 44, 59, 60, 63, 65, 66, 159, 170, 173, 273, 320
Primary cilia (PC) 36, 38, 271–273, 282, 283, 288
Protein complex 43, 94, 178, 193, 217, 225
Protein kinase A (PKA) 3, 21
Protein-protein docking 178, 190
Protein-protein interactions 60, 107, 108, 127, 151, 182, 185, 186, 217, 218, 310
Proteome 13, 223, 228
Proteomics ..... v, 13, 38, 217–230

Q

Quantitative proteomics 219

R

Ral GDP dissociation stimulator (Ral-GDS)..... 169–175
Reporter plasmid..... 318, 396, 401

S

Scaffolds..... v, 9–47, 108, 121, 139, 140, 195, 218, 235, 251–253, 293, 365, 366, 394
Screening tool 386, 389
Seven-transmembrane receptor (7TMR) 220, 335
Signalling 4, 44, 59, 69, 93, 107, 169, 177, 179, 195, 217, 235, 255, 271, 293, 309, 325, 335, 365
Signalling selectivity/bias 5, 69
Signal transduction ..... v, 5, 10, 30, 35, 37, 140, 169, 196
Small interference RNA (siRNA)..... 29, 34, 71, 73, 74, 77, 79, 160, 163–166, 326, 328, 329, 332, 346, 351, 397, 400
Stable isotope labeling by amino acids in cell culture (SILAC) 219–221, 223, 228
Subcellular fractionation..... 355

T

Tamoxifen..... 336, 338, 340–342
Therapeutics ..... v, 5, 34, 40, 46, 47, 195, 335, 346, 367
Titration..... 95, 96, 98, 99, 118
Trafficking..... v, 4, 10, 12–13, 19, 25, 30, 39, 40, 43, 44, 59–68, 159–168, 252, 273, 286, 309, 321, 394
Transfection 61, 62, 66, 70, 71, 73, 74, 76, 77, 79, 80, 84, 85, 96–99, 101, 110, 111, 115, 117–119, 122, 126, 128, 133, 134, 141, 145, 146, 152, 153, 156, 160, 163, 164, 171, 172, 198, 199, 203, 254, 256, 259, 262, 274, 276–279, 282–288, 312, 314–315, 318, 327, 331–333, 351, 352, 396–397, 400–401, 405
Translocation 11, 28, 60, 170, 173, 175, 273, 328, 394

U

Ubiquitin (Ub)..... 12, 13, 24–25, 27, 35, 43, 44, 94–97, 128, 140
Ubiquitination..... 12, 13, 24, 25, 29, 35–38, 40, 42–44, 93–102, 126–128, 134, 252, 253, 365, 366

W

Western blot (WB)..... 94, 109, 110, 114, 115, 117, 123, 125, 127, 128, 133, 142, 147, 151, 154–156, 162, 163, 166, 182, 217, 303, 306, 329, 332, 348, 374, 399

Y

Yeast two-hybrid 140–143, 217